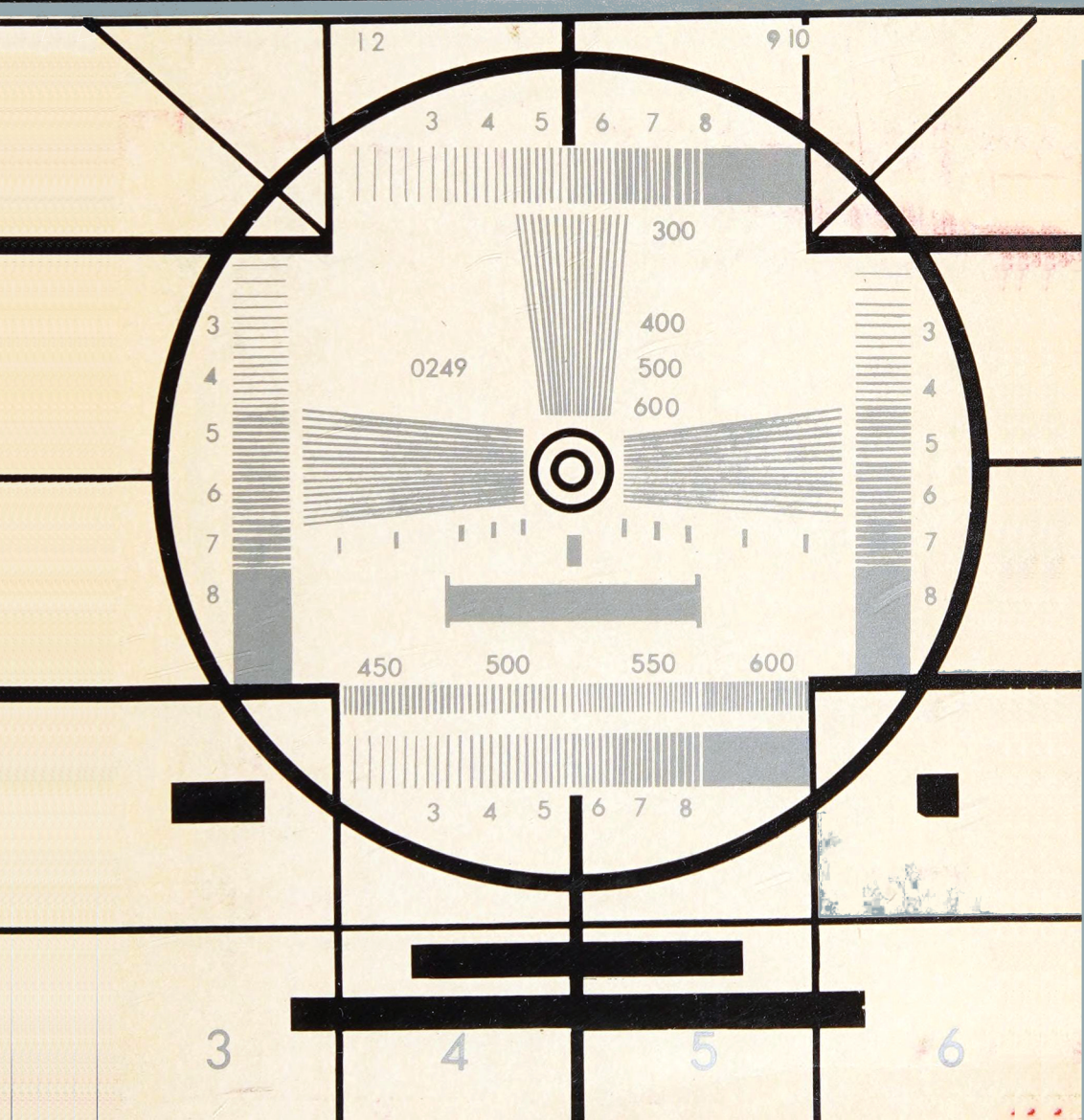
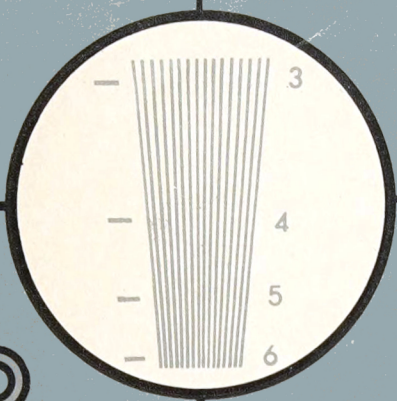


TELEVISION

V.F.SAMOYLOV, B.P.KHROMOV





450

| ||| |

500

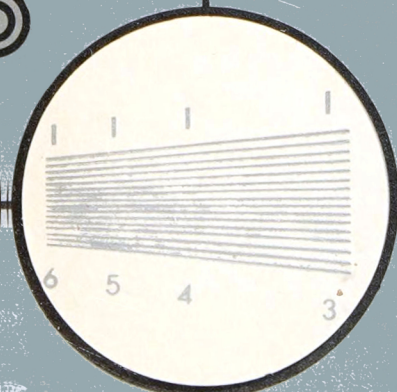
| ||| |

550

| ||| |

600

| ||| |





В. Ф. САМОЙЛОВ, Б. П. ХРОМОЙ

ТЕЛЕВИДЕНИЕ

ИЗДАТЕЛЬСТВО «СВЯЗЬ»

МОСКВА

V. F. SAMOYLOV,
TELEVISION

B. P. KHROMOY

Translated from the Russian
by

BORIS KUZNETSOV

MIR PUBLISHERS
MOSCOW

First published 1977

Revised from the 1975 Russian edition

The Greek Alphabet

Α α	Alpha	Ι ι	Iota	Ρ ρ	Rho ¹
Β β	Beta	Κ κ	Kappa	Σ σ	Sigma
Γ γ	Gamma	Λ λ	Lambda	Τ τ	Tau
Δ δ	Delta	Μ μ	Mu	Υ υ	Upsilon
Ε ε	Epsilon	Ν ν	Nu	Φ φ	Phi
Ζ ζ	Zeta	Ξ ξ	Xi	Χ χ	Chi
Η η	Eta	Ο ο	Omicron	Ψ ψ	Psi
Θ θ	Theta	Π π	Pi	Ω ω	Omega

The Russian Alphabet and Transliteration

А а	a	К к	k	Х х	kh
В в	b	Л л	l	Ц ц	ts
Б б	v	М м	m	Ч ч	ch
Г г	g	Н н	n	Ш ш	sh
Д д	d	О о	o	Щ щ	shch
Е е	e	П п	p	Ъ	''
Ё ё	e	Р р	r	Ы ы	y
Ж ж	zh	С с	s	Ь	'
З з	z	Т т	t	Э э	e
И и	i	У у	u	Ю ю	yu
Й й	y	Ф ф	f	Я я	ya

На английском языке

CONTENTS

INTRODUCTION	9
0.1. Analysis and Reproduction of Picture Information in Television	9
0.2. Brief History of Television	18
Chapter One. VISION, PHOTOMETRY, ILLUMINATION AND OPTICS	21
1.1. The Human Eye	21
1.2. Photometric Quantities and Units	24
1.3. Brief Outline of Optics	30
1.4. Selection of the Frame Frequency	37
1.5. Interlaced Scanning	41
1.6. Picture Luminance	43
1.7. Picture Contrast	45
1.8. Tonal Gradations	46
1.9. Picture Definition	49
1.10. Factors Affecting Picture Resolution	54
1.11. Aperture Distortion	56
Chapter Two. THE PICTURE TUBE	59
2.1. Picture-Tube Construction	59
2.2. Electron Beam Focusing	60
2.3. Electrostatic Focusing	61
2.4. Electromagnetic Focusing	67
2.5. Modulation of the Electron Beam	71
2.6. Factors Affecting Picture Contrast	74
2.7. Spectral Emission Characteristic of Screen Phosphors	77
2.8. Phosphor Persistence	77
2.9. Beam Deflection	79
2.10. Operation of an Electromagnetic Deflection Yoke	81
2.11. Construction of Deflection Yokes	85
2.12. Ion Spot	89
Chapter Three. SCANNING GENERATORS	92
3.1. Difference in Operation Between Vertical and Horizontal Scanning	92
3.2. Features of the Horizontal Scanning Generator	92
3.3. Tube Horizontal Output Stage	98
3.4. Line Sweep Driver Circuit (Sawtooth Generator)	110
3.5. Features of the Vertical Scanning Generator	113
3.6. Tube Vertical Output Stage	114
3.7. Vertical Output Stage Driver	118
3.8. Transistor Horizontal Scanning Generator	123
3.9. Transistorized Vertical Scanning Generator	126

Chapter Four. THE FREQUENCY SPECTRUM OF THE TELEVISION SIGNAL	128
4.1. Upper and Lower Boundaries of the Television Spectrum	128
4.2. Line Structure of the Television Spectrum	131
4.3. Spectrum of the D.C. Component	135
4.4. R. F. Spectrum for the Television Signal	137
Chapter Five. GENERATION OF THE TELEVISION SIGNAL	138
5.1. Standard Video Signal Waveform	138
5.2. Synchronizing Signal Generator	144
5.3. Pulse Shaper	152
Chapter Six. SYNCHRONIZATION OF SCANNING GENERATORS	156
6.1. Impulsive Synchronization	156
6.2. Block Diagram of the Impulsive Synchronization System	159
6.3. Separation of the Composite Synchronizing Signal from the Video Signal	161
6.4. Transistor Amplitude Separator	165
6.5. Separation of Horizontal from Vertical Sync Pulses	168
6.6. Inertia-Type Horizontal Synchronization	174
Chapter Seven. CAMERA TUBES	181
7.1. Basic Characteristics of Camera Tubes	181
7.2. Photoemission and Basic Laws	182
7.3. Spectral Response Characteristics of Photocathodes	183
7.4. Integral Sensitivity of Photocathodes	184
7.5. Nonstorage Camera Tubes	185
7.6. Storage-Type Camera Tubes	189
7.7. Potential of an Insulated Target	194
7.8. Iconoscope	199
7.9. Image Iconoscope	207
7.10. Camera Tubes Using a Low-Velocity Beam	210
7.11. Image Orthicon	216
7.12. Vidicon	224
7.13. Plumbicon	231
7.14. Monoscope	233
Chapter Eight. TELEVISION BROADCASTING	235
8.1. Expansion of TV Broadcasting	235
8.2. Equipment of a Program TV Centre	235
8.3. TV Cameras	242
8.4. Television Film Equipment	246
8.5. Amplification of the Video Signal in TV Cameras (Noise Compensation)	249
8.6. D.C. Restoration	257
8.7. Aperture Compensation	263
8.8. Gamma Correction	270
Chapter Nine. TELEVISION RECORDING	275
9.1. Role of Television Recording	275
9.2. Optical Recording	276
9.3. Magnetic Recording	279
9.4. Design Features of a Television Tape Recorder	286

Chapter Ten. TELEVISION RELAY SYSTEMS	296
10.1. Ways and Means of Extending the Coverage of Television Service	296
10.2. Radio Relay Systems	296
10.3. Cable Relay Systems	297
10.4. Satellite Relay Systems	301
Chapter Eleven. COLOUR TELEVISION	306
11.1. Colour Television Systems	306
11.2. Basic Facts from Colorimetry	306
11.3. Sequential Colour Television System	323
11.4. Simultaneous Colour Television Systems	326
11.5. Colour Picture Tube	330
11.6. Luminance Signal	336
11.7. Bandwidth of Fine Detail	339
11.8. Colour-Signal Band-Sharing	342
11.9. Colour-Difference Signals	345
11.10. NTSC Compatible Colour Television System	347
11.11. <i>I</i> - and <i>Q</i> -Signals	353
11.12. SECAM Colour Television System	354
11.13. Basic Parameters of the SECAM System	357
11.14. Block Diagrams of the SECAM Coder and Decoder	362
11.15. Operation of the Line-by-Line Switch and the Colour Identification Circuit	366
11.16. Delay Line	371
11.17. Basic Features of the PAL System	373
Chapter Twelve. TELEVISION TEST AND ALIGNMENT PROCEDURES	
12.1. Objectives of Test and Alignment Procedures in Television	378
12.2. Testing the Performance of a Receiver with a Test Pattern	379
12.3. Amplitude and Frequency Response Tests	382
12.4. Transient Response Tests	384
12.5. Testing the Video Channel for Amplitude Linearity	386
12.6. Colour Bar Chart Signal for Colour Television	389
Chapter Thirteen. LARGE-SCREEN TELEVISION SYSTEMS	392
13.1. Brief Outline of Existing Systems	392
13.2. Projection-Tube System	395
13.3. Light-Modulator Systems	398
13.4. Laser Television Projectors	401
Chapter Fourteen. INDUSTRIAL-INSTITUTIONAL TELEVISION	406
14.1. Tasks and Special Features of IIT	406
14.2. Advantages of 3-D Television	413
14.3. Stereoscopic Effect	413
14.4. Basic Arrangement of a Stereoscopic Television System	415
14.5. Transmission of 3-D Television Signals over Communication Lines	418

INTRODUCTION

0.1. Analysis and Reproduction of Picture Information in Television

Television, or the transmission of picture information over an electric communication channel, differs from the transmission of any other signals, say sound, in that it uses far more sophisticated techniques, apparatus and equipment. This book will take the reader through the whole sequence of the basic circuits and units that make up a television system, with proper attention to their interaction and characteristics. Before going into details, however, it is important to form a general idea about the principles underlying the organization of telecasts and define the importance of the individual units with regard to the overall system.

To repeat, television is the transmission and reception of motion pictures over electric communication channels. It is desired that the picture picked up by a television receiver, be a faithful reproduction of the scene televised (from a TV studio, a theatre, etc.). Any scene being televised has a wide range of specific features and qualities. It may contain a great number of colours, gradations of shade, coarse and fine details; motion may be present in a variety of forms and the objects making up the scene are usually in three dimensions.

The more faithful the received TV picture is, the more elaborate, expensive and bulky the TV equipment must be. On the other hand, among the important requirements for a TV system, and especially so for a telecasting system, are the utmost in simplicity, reliability and low cost. To simplify the physical facilities employed in telecasts, it is essential to determine which qualitative aspects are of secondary importance in the TV picture. It may be agreed that colour and 3-dimensional effect are second in importance to other aspects more vital to the information transmitted, such as definition and contrast. This is why, in the early days of television scientists and inventors limited themselves to finding methods for the transmission of two-dimensional black-and-white motion pictures with acceptable definition and contrast.

In the early 20th century when telecommunication and electronics were in their infancy, TV systems, primitive from the standpoint of the present day, were mechanical. Mechanical devices such as rotating discs, mirror drums and so on were used at both the sending and

receiving ends. Today, TV equipment is all-electronic; in both camera and picture tubes magnetic and electric fields cause electron beams to move practically free from inertia. The replacement of mechanical by electronic television has made it possible to reproduce a high-quality picture approaching the original scene in quality.

For an insight into the principles utilized in television, we shall take up a very simple case—the transmission of a two-dimensional black-and-white picture. The techniques used for the reproduction of colour and for the creation of the stereoscopic effect at present will be discussed elsewhere in the book.

For ease of presentation, we shall compare telecasts with sound transmission. In both cases, changes in the physical quantity chosen (sound pressure or light intensity) at the sending end are converted to changes in an electric quantity (current or voltage). In this way, the message to be conveyed is formed into a signal. It is to be noted, however, that there is a good deal of difference between a sound and a TV message. Among other things in transmitting a TV picture it is important, in addition to the instantaneous value of the physical quantity involved (light intensity), to locate the point associated with this intensity in the original scene. In other words, while a sound signal may be described by only a time function, $v_s = f_s(t)$, the TV signal (due to a two-dimensional black-and-white picture) is in principle a function of three dimensions: $v_{TV} = f_{TV}(t, x, y)$, where x and y are the coordinates of points in the picture plane.

Theoretically, a TV picture may have an infinite number of points (infinitesimal elements). Therefore, none of existing real communication channels would be able to pass this infinitely large information within a finite time interval. Nor is it required in practice. Because the resolution of the eye is limited, it will suffice to reproduce any scene by a finite number of finite elements. However, these elements must be sufficiently fine and their number must be sufficiently great for the eye not to discern (or nearly not to discern) the dot (discrete) structure of the picture received.

Obviously, the smaller the elements into which a picture is analysed (or scanned, in television parlance) and the greater the number of such elements, the more faithful the reproduced picture is. As an example, Fig. 0.1a shows a simple picture intended for transmission, while Fig. 0.1b, c and d shows the received pictures arranged as the number of picture elements increases. An increase in the number of picture elements improves picture definition and resolution of detail. In the Soviet Union, the TV picture is scanned into about 500,000 elements. If TV equipment is operating trouble-free, this figure is sufficient for the reproduction of a high-definition picture.

Thus, the pick-up device may be visualized as made up of a huge number of information sources (each corresponding to an element of

the scene being televised). Each of these sources must be connected to an appropriate reproducing element at the receiving end. In fact, this idea was at the basis of the *parallel* television system (Fig. 0.2a) first advanced by D. Kerry in 1875. The pick-up device in this case is a mosaic of photocells of which there are as many as picture elements. An image of the scene or subject-matter is projected onto the mosaic by an objective lens. Each cell is connected by a separate

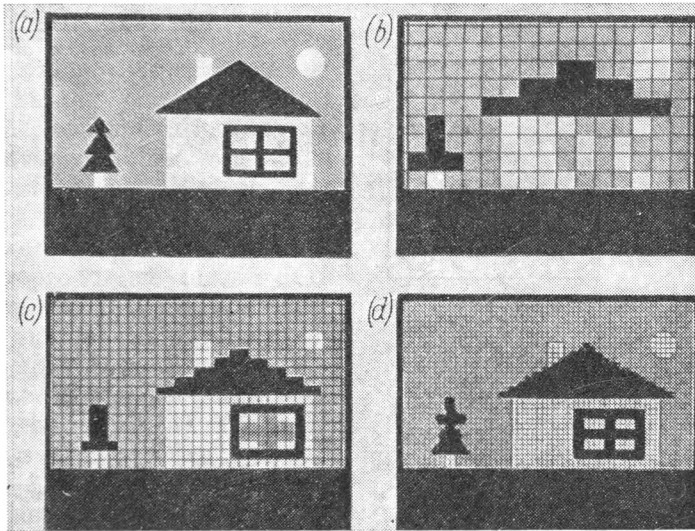


Fig. 0.1. Picture definition as a function of the number of picture elements (a) original scene; (b) 190-element picture; (c) 770-element picture; (d) 2100-element picture

wire in a multi-conductor cable to a corresponding controlled light source in the reproducing device, or screen (for simplicity, we have omitted power supplies and amplifiers normally needed for operation). Each light source is controlled to generate an amount of light proportional to that falling on the cathode of the respective photocell, that is, to the light intensity at the corresponding point of the scene.

Although theoretically possible, the parallel television system of Fig. 0.2a is impractical. For one thing, the connecting cable for present-day television would have to have about 500,000 conductors and could hardly be made at all. For another, a separate pick-up device would have to be provided for each receiving device. Obviously, with the many millions of TV sets now in use, this system would be entirely unsuitable.

These limitations were avoided in *sequential* television systems (Fig. 0.2b). They utilized the property of the eye known as persistence

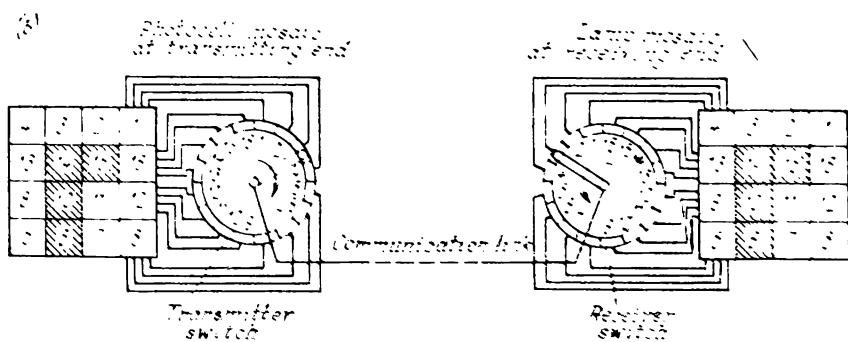
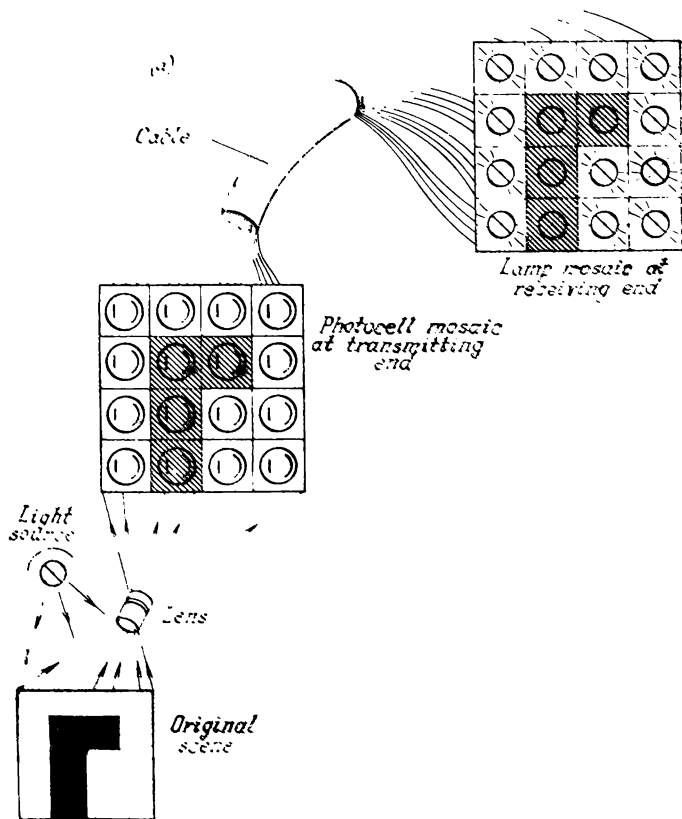


Fig. 0.2. Television systems
(a) parallel; (b) sequential

of vision (widely exploited in present-day electronic television). Owing to this property, a flashing light source would appear to emit light continuously, if the flashes occur in a sufficiently rapid succession. The system based on this property and shown in Fig. 0.2b was proposed in a variety of designs by A. de Paiva (1878), P. I. Bakhmetiev (1880), S. Bidwell (1881) and others. In this system, a commutator switch at the sending end connects the photocells of the mosaic in turn. The commutator switches of the pick-up device and of the reproducer must rotate in step and in time with each other; that is, at the same rotational speed the contact arms of the commutator switches must take up the same position at any time.

As a result, the light sources of the reproducing mosaic are turned on sequentially and generate an amount of light proportional to that received by the respective photocell from each point of the scene. If the commutator switches rotate at a sufficiently high speed, the flashes of the light sources produce an illusion of continuous light.

A major disadvantage of the system shown in Fig. 0.2b is the use of commutator switches with rubbing contacts. For one thing, the contacts wear away rapidly; for another, it is difficult techni-

cally to build a commutator switch that would have a sufficiently great number of contact segments. Big impetus to the development of mechanical television systems was given in 1884 when P. Nipkow of Germany invented his mechanical analyzer, now known as the Nipkow disc. It did away with the limitations of the earlier systems. In fact, the idea of analyzing a picture by scanning is still used by electronic television. In sketch form the construction of the Nipkow disc (for 15 scanning lines) is shown in Fig. 0.3. The light-weight aluminium disc has apertures numbered 1, 2, 3, . . . , which are arranged along a spiral in such a manner that every next aperture is nearer the disc centre by its height, y_1 . In front of the disc there is a fixed frame, $ABCD$, limiting the size of the picture. As the disc

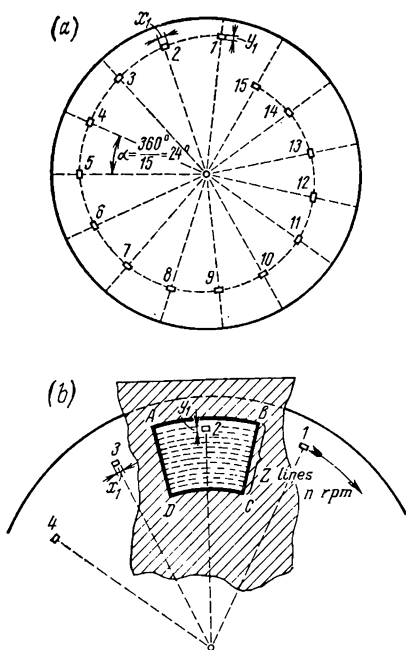


Fig. 0.3. Nipkow disc

is revolved, apertures, 1, 2, 3, . . . move within the frame along the paths called lines, so that only one aperture appears within the frame at a time. In this way, the scene within the frame (this portion of the scene is appropriately called a frame, too) is explored, or scanned, line after line. Obviously, there can be as many lines as there

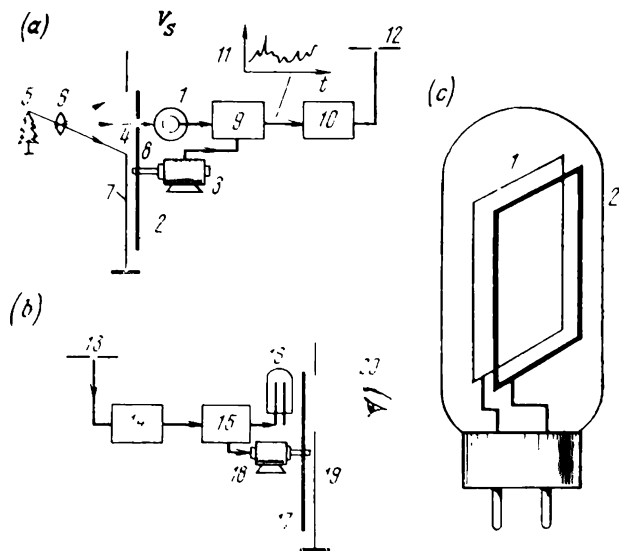


Fig. 0.4. Television system using a Nipkow disc

(a) transmitting scanner; (b) receiving scanner; (c) light source: 1—photocell; 2—Nipkow disc as analyzer; 3—electric motor; 4—image; 5—scene; 6—objective lens; 7—fixed frame; 8—aperture in Nipkow disc; 9—video amplifier; 10—radio transmitter; 11—signal oscillogram; 12—transmitting antenna; 13—receiving antenna; 14—radio receiver; 15—video amplifier; 16—light source; 17—Nipkow disc as synthesizer; 18—electric motor; 19—fixed frame; 20—observer's eye

are apertures in the disc. The width of a picture element is that of an aperture, x_1 . No sharp dilineation exists between the picture elements in this system.

The transmitting scanner (sometimes called an analyzer) and the receiving scanner (sometimes called a synthesizer) using Nipkow discs are shown in the functional diagrams of Fig. 0.4a and b. In the transmitting scanner, the Nipkow disc, 2, driven by an electric motor, 3, is placed in front of a photocell, 1. An objective lens, 6, throws an image, 4, of the scene, 5, onto a fixed frame, 7, placed next to the disc. Light from an element of the scene is concentrated by one of the apertures, 8, onto the cathode of the photocell. The video signal, as it is called, 11, emerging from the amplifier, 9, varies in time in exactly the same manner as the light intensity does in passing from one element to another.

In the receiving device, the video signal is amplified and applied to a flickering light source, 16, the instantaneous brightness of which is proportional to the instantaneous magnitude of the signal. The source may be a neon gas-discharge lamp (Fig. 0.4c) capable of varying its brightness at the rate of 10,000 to 15,000 per second with practically no time lag. In front of the light source, 16, is placed the receiving Nipkow disc, 17, driven by an electric motor, 18, in step and in time with the pick-up disc, 2. The observer, 20, sitting in front of the fixed frame, 19, watches a picture which is a combination of elements and lines.

The scanner using the Nipkow disc operates on what may be called the instantaneous-value (non-storage) principle. Each TV signal produced in this system utilizes only a negligible fraction of the total luminous flux from the entire scene the same instant it is generated. This "instantaneous" (non-storage) flux passes through an aperture to the photocell. The remainder is rejected by the disc without any use. Because of this such systems cannot produce a sufficiently bright, contrast and sharply defined picture. For example, the TV picture today has about 600 lines and 500,000 picture elements. To handle this information adequately, each hole in the Nipkow disc would have to be as small as $1/500,000$ part of the disc area. The light passing through this aperture to the photocell would be so negligible that the video signal would hopelessly be drowned in photocell and amplifier noise.

A high-quality picture can only be produced by electronic scanning means. A simplified schematic arrangement of an electronic scanner (for black-and-white television) is shown in Fig. 0.5a. The key element in this arrangement is a camera tube, 3, which converts light coming from the scene, 1, into an electric signal for transmission over a communication link. The camera tube of any type and construction has two key assemblies:

1. A photocathode, 4, which is a thin layer of a photo-emissive material, that is one capable of emitting electrons in response to incident light.

2. An electron gun, 6, to produce the scanning electron beam, 7. The gun includes a hot (thermionic) cathode, 5, which supplies electrons for the beam, and elements for beam pre-focusing. The envelope of the camera tube mounts a focusing magnet, 9, and deflection coils, 8. The magnet is shaped so as to set up a permanent magnetic field which provides the main focusing of the electron beam. The deflection coils are arranged in two pairs, each pair being energized with sawtooth currents so that they set up varying magnetic fields causing the electron beam to deflect horizontally (line deflection) and vertically (frame deflection). A lens, 2, throws an image of the scene, 1, onto the photocathode, 4, of the camera tube, 3. Incident

light causes the photocathode to emit electrons in quantities proportional to the light intensities of the picture elements. The photocathode is made semitransparent so that at least part of the incident light can pass onto the vacuum side (on the right in the diagram) and

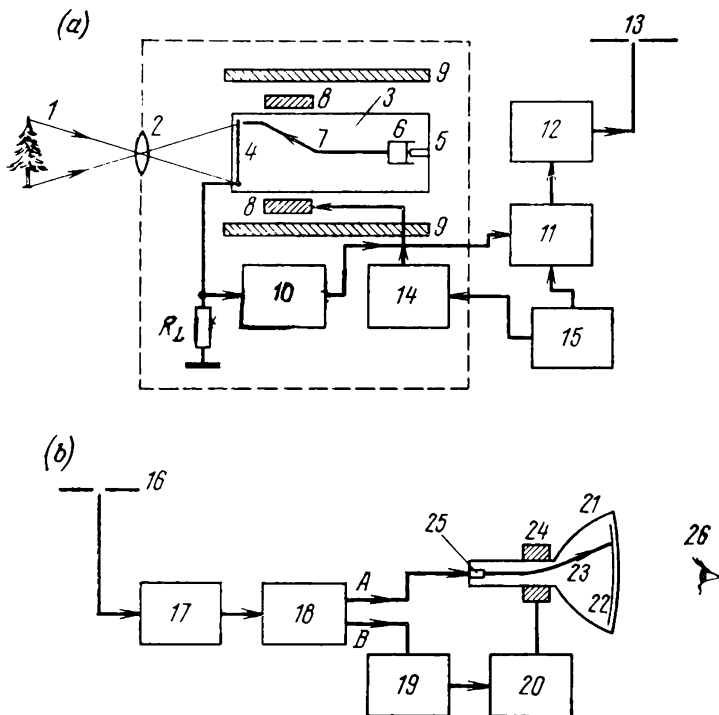


Fig. 0.5. Simplified block diagram of an electronic television system

(a) transmitting terminal; (b) receiving terminal; 1—scene being televised; 2—optical lens; 3—camera tube; 4—photocathode; 5—thermionic cathode; 6—electron gun; 7—electron beam; 8—deflection yoke; 9—focuser; 10—preamplifier; 11—main amplifier; 12—radio transmitter; 13—transmitting antenna; 14—sweep generator; 15—synchronizing generator; 16—receiving antenna; 17—radio receiver; 18—video amplifier; 19—sync pulse separator; 20—sweep generator; 21—picture tube; 22—phosphorescent screen; 23—electron beam; 24—deflection yoke; 25—modulator; 26—observer's eye

cause photoemission inside the tube. On breaking away from the photocathode, electrons leave on its surface positive potentials varying in magnitude in accordance with the light intensities of the respective scene elements. In this way, a charge image is produced on the vacuum side of the photocathode. The deflection coils cause the electron beam, 7, produced by the hot cathode, 6, to sweep rapidly from left to right (along the lines) and also, but more slowly, from top to bottom and retrace with a much slower sawtooth pattern, thereby

scanning the charge image on the surface of the photocathode, not unlike the Nipkow disc (see Fig. 0.3*b*). As the beam scans the charge image an alternating current flows through the load resistor, R_L . This is the video signal current the instantaneous value of which corresponds to the potential at each point of the charge image and, hence, to the light intensity of each scene element. The video signal is then amplified by units, 10 and 11, fed to the transmitter, 12, and radiated by an antenna, 13.

The line and frame sawtooth currents which energize the deflection coils and cause the beam to deflect are supplied by a sweep unit, 14. So that each line and frame scan will retrace and begin always at the same time and in the same position, the sweep unit is disciplined by synchronizing pulses supplied by a synchronizing generator, 15. This generator also furnishes synchronizing pulses which are embedded in the composite television signal in an amplifier, 11, to synchronize the sawtooth current generators of the deflection systems in the TV receivers. The components shown in Fig. 0.5*a* enclosed in the dashed box make up a TV camera which can be set up on a suitable mount to facilitate camera motion about the studio or to hold it fixed for film transmission.

The equipment used at the receiving end is shown in the block diagram of Fig. 0.5*b*. The antenna, 16, and the radio receiver, 17, are conventional units. The video amplifier, 18, has two outputs; one of them, *A*, applies a sufficiently strong video signal to the control electrode of the picture tube, 25, to control the intensity of the electron beam. From the other output, *B*, the video signal goes to unit 19 where synchronizing pulses are retrieved from the composite television signal. These pulses are then applied to the line and frame sweep generators, 20, to keep them running in synchronism and in phase with their counterparts in the camera tube. The electromagnetic field set up by the deflection system, 24, causes the electron beam, 23, of the picture tube to sweep from left to right (horizontal or line scan) and from top to bottom (vertical or frame scan) and then rapidly retrace. In so doing the beam strikes the phosphorescent screen, 22, applied to the vacuum side of the picture tube face, and causes it to phosphoresce with the intensity proportional to that of the electron beam. As a result, a television picture is formed.

In the Soviet Union, the commercial television picture has the following characteristics:

Vertical scan (or frame) frequency, n	25 fr/s
Lines per frame, Z	625
Aspect (width to height) ratio, $p = w/h$. . .	4/3

0.2. Brief History of Television

As is seen from the functional diagram of Fig. 0.5, a telecast involves three consecutive stages:

1. Light is converted to electric signals.
2. The electric signals are transmitted over a distance.
3. The received electric signals are converted to a visible image.

These processes have become feasible owing to advances in physics, radio engineering, optics and a number of other fields of science and technology. Television has become a practicable proposition owing to the discoveries and inventions made at the turn of the 20th century. Important contributions were made by Russian scientists, too. In 1888-1890, A.G. Stoletov carried out fundamental research in the field of photoelectricity. Later, the photo-electric effect would play an important role in television. Stoletov's work laid the foundation for the development of photo-electric devices. On May 7, 1895, A.S. Popov became the first man in the world to demonstrate a radio receiver in operation. Popov's invention marked the beginning of practical radio as a means of wireless communication. Next came along vacuum tubes, amplifiers and receivers, all of them giving impetus to electronic television system. In Russia, the early days of electronic television are associated with B.L. Rosing, a physicist. This outstanding scientist was the first to realize the limitations of mechanical television systems. As he wrote, "Attempts to build electrical telescopes based on the simple mechanics of material bodies, which yields under ordinary conditions so simple and, it would seem, feasible solutions must inevitably end up in failure... The cathode ray is the ideal inertia-free pen for which Nature itself has cut a niche in the receiver of the electrical telescope. It has a valuable property in that it can be bodily moved at whatever speed by means of an electric and magnetic field...". Rosing's inventions were centred round electronic television. On July 25, 1907, ten years after his first experiments, he applied for a privilege on his invention. A major distinction of Rosing's invention was the use of a cathode-ray device (not unlike the present-day picture tube) at the receiving end. Rosing took out patents for his invention in Russia, Great Britain and Germany. A public demonstration took place on May 9, 1911.

In the succeeding years, television developed mainly by way of improvements in the various pieces of equipment. Main emphasis was placed on camera tubes, that is devices which convert optical images into electric signals. In 1911, A.A. Campbell Swinton proposed the first camera tube operating by the "instantaneous (non-storage) principle" explained earlier. Between 1920 and 1930, several designs of this type of camera tube were proposed in various countries. In the

USSR, such tubes were developed by B.A. Grabovsky, V.I. Popov, N.G. Piskunov, A.A. Chernyshev and Yu.S. Volkov.

In the United States, F. Farnsworth came out with his dissector and in the Soviet Union G.V. Braude with his non-beam single-line tube. Because of the low sensitivity, both types were limited to the transmission of motion-picture films almost exclusively.

Non-storage tubes did not make much headway in television because their sensitivity was as low as that of mechanical television analyzers. A real breakthrough came with tubes which depended for their operation on the storage of charge. For the first time, this idea was stated clearly by Ch.F. Jenkins in the United States in 1928. This type of tube utilizes all of the light coming from the scene, because of which they have a higher sensitivity in comparison with non-storage tubes. Pioneers in the design of camera tubes operating by charge storage were K. Tihany of Hungary (1928), F. Anroto of Canada (1929), and A.P. Konstantinov of the USSR (1930). The first workable camera tube designed along these lines was built by S.I. Katayev of the Soviet Union in 1931. The invention had been preceded by studies into the physics of the processes accompanying the scanning of photoemissive surfaces by the electron beam and development work on techniques for the manufacture of multielement light-sensitive surfaces. In 1932, S.I. Katayev published a detailed description of his tube and a method for the manufacture of a mosaic photocathode. That was the world's first disclosure of a workable camera tube utilizing charge storage. In mid-1933, the laboratory of the All-Union Electrotechnical Institute made several experimental tubes of this type.

Outside the Soviet Union, work on the storage-type tube was conducted by V.K. Zworykin at the RCA laboratories. His work culminated in mid-1933 in a new type of television pick-up tube which he named the iconoscope. Zworykin's iconoscope did not differ from Katayev's tube in principle of operation, and Katayev's application filed in September 1931 preceded Zworykin's by a few months.

The invention of the storage television pick-up tube was an important milestone in the progress of television. The iconoscope was used for studio and motion-picture telecasts in all countries for over 20 years. It came as proof that high-quality television was round the corner and stimulated work on all-electronic television.

Another important invention dating back to the year 1933 was that by P.V. Shmakov and P.V. Timofeyev who proposed a new type of television pick-up tube which has come to be known as the image iconoscope. With a sensitivity higher than that of the iconoscope, the image iconoscope is still in service at some TV centres.

The first experimental telecast in the Soviet Union took place on October 1, 1931. The system was mechanical, with a 30-line, 12.5-frame picture. Higher resolution (180 lines) was shown by an operating

laboratory equipment of the electronic type developed under Ya. A. Ryftin in the Soviet Union in 1935. Experimental TV centres with still higher resolution were built in the Soviet Union in 1938 (in Leningrad with a 240-line picture and in Moscow with a 343-line image). Both centres had worked until the outbreak of the 1941-1945 war. Post-war years saw a rapid expansion of television broadcasting in the Soviet Union. Before long, TV centres were built in the capitals of all Union Republics and other major cities, employing television equipment with a 625-line image. Already in 1963, a total of 130 transmitting stations were in operation, serving between them about 10 million TV sets. On November 4, 1967, Europe's biggest TV centre fitted with the latest TV equipment went into operation in Moscow. In 1973, a total of 131 program TV centres and 1440 low- and high-power relay stations were operative, covering a territory with a population of 220 million and with a total number of over 55 million TV sets. Today, central programs are disseminated by a widespread network of radio-relay, cable and space links. In fact, the Soviet Union has the world's largest TV broadcasting system via communication satellites. The ORBITA network incorporating over 20 stations to receive TV signals from communication satellites was built in one year.

Regular colour TV broadcasts in the Soviet Union began on October 1, 1967. Since then, Soviet industry has acquired know-how for the manufacture of colour TV equipment and colour TV sets. At present, TV specialists in the Soviet Union are busy with further developments in colour TV, improvements in picture quality, and wider use of television in new fields of science and technology.

CHAPTER ONE

VISION, PHOTOMETRY, ILLUMINATION AND OPTICS

1.1. The Human Eye

In comparison with, say, radio broadcasts, telecasts use a far more elaborate equipment and techniques. This is why throughout the history of television every effort has been applied to find ways and means for simplifying it without detriment, as far as practicable, to the picture seen on the TV screen.

To avoid unnecessary complications in a TV system and to make it readily accessible to a wider TV audience, it is essential to define the limits of the necessary qualitative characteristics of the TV image—definition, contrast, etc., beyond which it would be useless to move. This involves knowledge of how to evaluate these characteristics, for one thing, and recognition of the fact that these limits are dictated by the limitations of the human eye and that the eye is in fact the instrument which measures these limits in the final analysis.

Here is in brief how the human eye is built. The eye is an almost perfect ball about 2.5 cm in diameter (Fig. 1.1). Most of its outer surface consists of a tough and fibrous coat called the *sclera*, 1, which protects the eyeball against injury. At the front, the sclera extends into a thin and transparent *cornea*, 2, acting as an entrance lens for the eye. Behind the cornea is the *iris*, 4, which can expand and contract (involuntarily to the human being) to adjust the size of the central opening in the iris, called the *pupil*, 5. In this way, adaptation takes place, that is, automatic adjustment of the amount of light that can enter the eye. Behind the iris is the “*crystalline*” *lens*, 3, a transparent elastic body biconvex in shape. The chamber in front of the lens and back of the cornea is filled with a watery fluid called the *aqueous humour*, 6. The chamber behind the lens contains a jelly called the *vitreous body* or *humour*, 7. Thus the optical system of the eye is made up of the cornea, aqueous humour, lens and vitreous humour. This system throws an image of the scene watched onto the *retina*, 8. The retina contains a huge number of the receptor cells of the eye, called rods and cones. Sharpest vision is obtained in a small region of the retina called the *fovea*, or *fovea centralis*, 10. The fovea appears as a small depression in the retina, just opposite the lens. The area around the fovea, called the *macula lutea*, 9, is covered by a yellow pigmented layer.

The curvature of the “crystalline” lens can be varied by the muscles enveloping the lens from all sides. In this way, the focal power of the lens is adjusted so as to adapt it to the viewing distance; this process is called *accommodation*.

The two kinds of receptor cells in the eye, the *rods* and the *cones*, differ in properties and in the functions served. The rods are more sensitive to light than the cones, but they cannot discern the colours. As a result, the visual sensations produced in the brain due to the action of the rods appear as untinted, gray tones. Less sensitive to

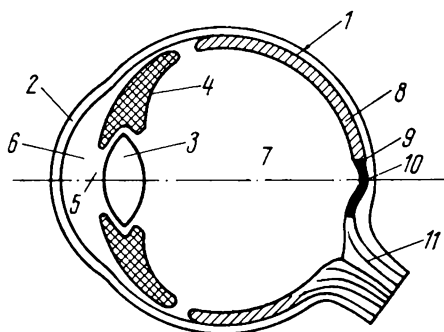


Fig. 1.1. The human eye

1—sclera; 2—cornea; 3—crystalline lens; 4—iris; 5—pupil; 6—aqueous humour; 7—vitreous body or humour; 8—retina; 9—macula lutea; 10—fovea centralis; 11—optic nerve

light, the cones have the remarkable property of differentiation between colours. There are three different kinds of cones, some sensitive to green, others to red, and still others to blue. Within the macula lutea, the predominant light-sensitive cells are the cones, and those around its periphery are the rods. The total number of rods is estimated at about 100 million, and that of cones at over 5 million.

At the rear is the exit through which the *optic nerve*, 11, leaves the eyeball. Within the eyeball the optic nerve divides into a multitude of nerve fibres. Within the fovea, each cone has its own fibre; on moving away from the fovea each fibre is now connected to two or three receptor cells, and at the periphery of the macula lutea each fibre serves a group of cones and rods. The total number of fibres in the optic nerve is about a million.

Whether or not the eye can resolve fine detail depends on where an image is formed on the retina. The resolving power of the eye is at its highest at the fovea. The limit of resolution, called the *acuity of vision*, is assessed in terms of the minimum angle ϕ within which two separate objects, say two black stripes (at *a* and *b* in Fig. 1.2a),

appear separately. Obviously, stripes a and b will be perceived as separate if their images, a' and b' , on the retina are separated by at least one light-sensitive cell. In such a case, the presence of an intermediate cell, c' , will produce in the brain the sensation that the stripes are separate. Experiments have shown that the acuity of vision

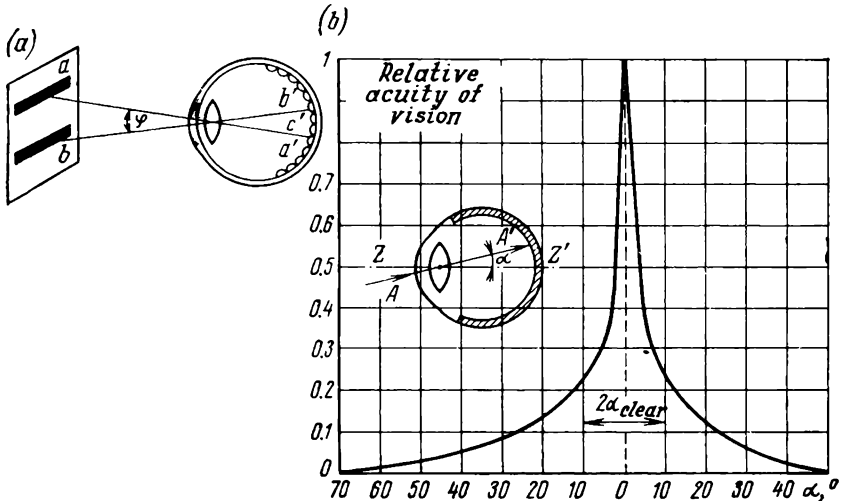


Fig. 1.2. Acuity of vision

(a) set-up for acuity determination; (b) acuity of vision as a function of viewing angle

depends on the brightness of the scene and that it increases with increasing brightness. At the brightnesses obtained on TV or motion-picture screens, the acuity of vision is about one minute of arc, or $1/60^\circ$. This figure may be used as a guide in various calculations.

As already noted, the density of nerve fibres falls off rapidly on moving away from the fovea towards the periphery of the macula lutea. The acuity of vision decreases in proportion. The plot of Fig. 1.2b shows the decrease in the acuity of vision as a function of the angle α formed by the optic axis ZZ' of the eye, passing through the centre of the crystalline lens and the fovea, and by the ray AA' radiating from the object viewed. As is seen, the acuity of vision falls off rapidly with increasing angle α . Setting the limit of decrease in the acuity of vision at 20%, the angle of clear vision will be $\alpha_{clear} = \pm 10^\circ$, or $2\alpha_{clear} = 20^\circ$. This figure indicates that objects outside this angle would appear blurred, and to perceive fine detail in them the observer would have to turn his eyes or even head.

The human eye responds differently to different colours (that is, to different wavelengths). The eye sees best at a wavelength of $\lambda_0 = 0.55 \mu\text{m}$, which corresponds to yellow-green colour. Thus, given the same intensity, the yellow-green region will be visible best of all other spectral regions. This property is called the relative luminous efficiency, or visibility, of monochromatic radiation. Its plot as a function of wavelength, $V(\lambda)$, appears in Fig. 1.3 (see the colour plate). At wavelengths of $\lambda_v = 0.38$ to $0.40 \mu\text{m}$ (which corresponds to violet) and $\lambda_r = 0.74$ to $0.77 \mu\text{m}$ (which corresponds to red), the relative visibility fall to practically zero. It is to be noted that the boundaries between the various colours in the diagram are shown arbitrarily. Actually, the colours change from one into another gradually.

1.2. Photometric Quantities and Units

We shall briefly dwell on four basic photometric quantities most often used in television: *luminous flux*, *luminous intensity*, *illumination*, and *luminance*.

The term light (or more accurately, visible light) applies to that part of the electromagnetic spectrum (radiant energy) which lies within the wavelength range from $\lambda_v = 0.38 \mu\text{m}$ to $\lambda_r = 0.77 \mu\text{m}$ and is perceived by the human eye. Two factors must be taken into account in evaluating the effect of luminous energy on the eye:

(1) the relative luminous efficiency, or relative luminosity, of monochromatic radiation, sometimes referred to as the visibility of radiation (see colour plate, Fig. 1.3);

(2) variations in the distribution density of radiant power at various wavelengths displayed by practical light sources (Fig. 1.4a):

$$\rho(\lambda) = dP/d\lambda \quad (1.1)$$

where $\rho(\lambda)$ = power density of electromagnetic radiation, $\text{W}/\mu\text{m}$

P = power of the light source, W

λ = wavelength, μm

Thus, the power, in watts, of visible light is given by an integral of the form:

$$P_{\text{light}} = \int_{\lambda_v}^{\lambda_r} V(\lambda) \rho(\lambda) d\lambda \quad (1.2)$$

Since $V(\lambda)$ is a dimensionless quantity, and $\rho(\lambda)$ is expressed in $\text{W}/\mu\text{m}$, P_{light} has the dimension of watts.

The power of visible light, as expressed in terms of its effect on the normal eye is called the *luminous flux*, F . The unit of the luminous flux is the lumen. The power of electromagnetic radiation has experimentally been found to be related to the luminous flux *at the peak of the visibility curve*, $\lambda_0 = 0.55 \mu\text{m}$, as

$$F_{\lambda_0} = 683 P_{\text{light}} \quad (1.3)$$

Relations (1.2) and (1.3) offer a means for determining, at least in principle, the luminous flux of any source as

$$F = 683 \int_{\lambda_v}^{\lambda_r} V(\lambda) \rho(\lambda) d\lambda \quad (1.4)$$

As an example of using Eq. (1.4), we shall calculate the luminous flux emitted by a white light source with a uniform distribution of radiant power with wavelengths (a light source for which $\rho(\lambda) = \text{constant}$ is called *equi-energetic*, Fig. 1.4b). If the radiant power is $P = 1 \text{ W}$ within the visible region of the spectrum (between $\lambda_v = 0.38 \mu\text{m}$ and $\lambda_r = 0.77 \mu\text{m}$), then the power density, $\text{W}/\mu\text{m}$, will be

$$\rho(\lambda) = dP/d\lambda = P/(\lambda_r - \lambda_v) = 1/(\lambda_r - \lambda_v) \quad (1.5)$$

Thus,

$$F_{\text{white}} = 683 \int_{\lambda_v}^{\lambda_r} V(\lambda) d\lambda / (\lambda_r - \lambda_v) = 683 / (\lambda_r - \lambda_v) \int_{\lambda_v}^{\lambda_r} V(\lambda) d\lambda \quad (1.6)$$

In Eq. (1.6), the integral is equal to the area under the relative visibility curve shown in Fig. 1.3.

For approximate calculations, we may replace the integral in Eq. (1.6) by an approximate sum:

$$F_{\text{white}} \approx 683 \frac{1}{n} \sum_{i=1}^n V_n$$

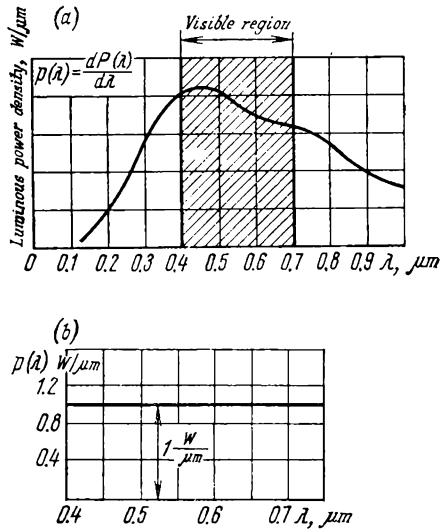


Fig. 1.4. Power distribution of light sources

(a) a source with an arbitrary power distribution; (b) a source of equal-energy white light

Relative Visi

n	1	2	3	4	5	6	7	8
$\lambda, \mu m$	0.4	0.42	0.44	0.46	0.48	0.50	0.52	0.54
V_n	0	0.02	0.05	0.10	0.18	0.35	0.70	0.94

The values of relative visibility, V_n (the ordinates of the plot in Fig. 1.3) are tabulated in Table 1.1, for n points on the x -axis.

Referring to Table 1.1,

$$n = 17$$

and

$$\sum_1^n V_n = 5.49$$

whence

$$V_{av} = \frac{1}{n} \sum_1^n V_n = 5.49/17 = 0.322$$

and the flux of white light emitted by the source with a power of one watt in the visible region of the spectrum is then

$$F_{white} \approx 683 \times 0.322 = 220 \text{ lumens}$$

Thus, we have got two equivalents of radiant energy and luminous flux:

for yellow-green colour: $\lambda_0 = 0.55 \mu m$, $V_0 = 1$, $1 \text{ W} = 683 \text{ lumens}$;
for white light: $\rho(\lambda) = \text{constant} \times 1 \text{ W} = 220 \text{ lumens}$.

To help the reader to visualize the lumen, the following values of luminous flux can be quoted.

(1) An ordinary incandescent lamp has a luminous efficiency of $K = 8$ to 15 lumens/W . A 100-watt lamp will emit a luminous flux of $F = 800$ to 1500 lumens .

(2) To produce a sufficiently bright image on a motion-picture screen with an area of $S = 6 \times 8 \text{ m} = 48 \text{ m}^2$, the cine projector should throw a luminous flux of $F = 8000 \text{ lumens}$ on the screen.

Luminous intensity, I , is the density of the luminous flux within a solid angle. Imagine a point source of light, A^* (Fig. 1.5). In the

* A point source of light is a source of radiant energy of dimension d negligible compared with the distance l to the surface on which the emitted light is incident. Usually, it is assumed that $l \geq 10 d$.

Table 1.1

bility Values

9	10	11	12	13	14	15	16	17
0.56	0.58	0.60	0.62	0.64	0.66	0.68	0.70	0.72
1.0	0.88	0.65	0.35	0.17	0.07	0.02	0.01	0.0

general case, a source emits different amounts of light in different directions. Let us determine the luminous intensity in, say, direction AB . To do so, we cut mentally a small area, dS , which is at right angles to the line AB . The solid angle* bounded by the outline of the area is defined as

$$d\omega = dS/(AC)^2 = dS/R^2 \quad (1.7)$$

and the light intensity is given by

$$I = dF/d\omega \quad (1.8)$$

where dF is the luminous flux passing through the elementary area dS or, which is the same, bounded by the solid angle $d\omega$.

The unit of luminous intensity is the candela. If a solid angle of one steradian encloses a uniformly distributed luminous flux of one lumen, the light intensity in that direction will be one candela.

The definition of the candela adopted internationally states: the magnitude of the candela is such that the luminance of a full radiator at the temperature of solidification of platinum is 60 candelas per centimetre. Practically, this is determined as follows. A specimen of chemically pure platinum is melted in a vessel, a slim refractory tube is immersed in the molten platinum and is allowed to come up to its temperature. As this happens, light is emitted by the internal surface of the tube through its open end. The intensity of the light emitted at the solidification point of platinum (2046.5 K) along the axis of the tube from an area of $1/60\pi = 0.0053 \text{ cm}^2$ is taken to be one candela. It is to be noted that the standard measure is the candela, and the lumen is a derived unit.

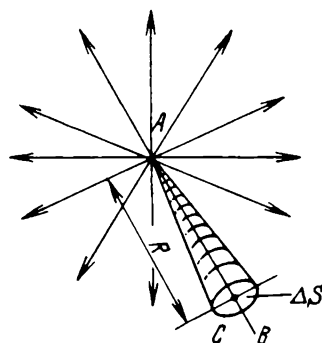


Fig. 1.5. Determination of luminous intensity

* A steradian is a solid angle whose vertex is at the centre of a sphere and which cuts out on that sphere an area equal to the square of its radius.

The average luminous intensity, I_{av} , of a point source of light is defined as the ratio of the total flux emitted, F_{tot} , to the total solid angle (in steradians), $\omega_{tot} = 4\pi R^2/R^2 = 4\pi$:

$$I_{av} = F_{tot}/4\pi \quad (1.9)$$

For example, a 100-watt lamp emitting a luminous flux of $F_{tot} = 800$ to 1500 lumens has an average luminous intensity of

$$I_{av, lamp} = F_{tot}/4\pi = (800 \text{ to } 1500)/4\pi = 60 \text{ to } 120 \text{ candelas}$$

When a luminous flux, F , reaches a surface, S , the average *illuminance* is

$$E_{av} = F/S \quad (1.10)$$

As often as not, different points on a surface are illuminated differently, and the need arises to define the illuminance of a surface element

$$E = dF/dS \quad (1.11)$$

where dF = luminous flux incident on a surface element

dS = area of that element

The unit of illuminance is the lux (lx), defined as the illuminance of an area of 1 square metre over which a luminous flux of 1 lumen is uniformly distributed. To help visualize this unit, several practical examples are listed in Table 1.2.

Table 1.2

Light receptor	Illuminance, lx
Motion-picture screen	40-200
Book at reading	20
TV studio	2000
Shadow in summer	1000
Sun-lit sea-beach in summer	100,000

Luminance, B , is defined as the ratio of light intensity to the surface emitting it. It is important to stress that, in contrast to illuminance, luminance is an attribute of a surface emitting or reflecting rather than receiving light.

Imagine a luminous elementary surface S (Fig. 1.6a). It is emitting a luminous flux the density of which depends on the direction of emission. Thus, light intensity is a function of direction. The observer's eye located at an arbitrary point M measures the area of

the surface S from its projection S_α . The apparent area of S , seen at an angle α , is given by

$$S_\alpha = S \cos \alpha \quad (1.12)$$

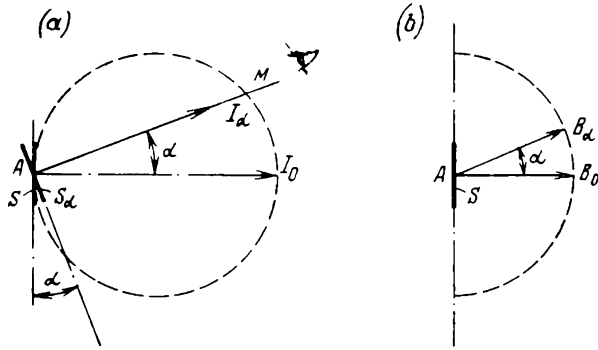


Fig. 1.6. Luminance of a surface obeying Lambert's law
(a) distribution of luminous intensity; (b) luminance distribution

Hence, the luminance B_α seen from point M will be given by

$$B_\alpha = I_\alpha / S_\alpha = I_\alpha / S \cos \alpha \quad (1.13)$$

For a direction at right angles to the luminous surface,

$$B_0 = I_0 / S \quad (1.14)$$

The unit of luminance is the candela per square metre (cd/m^2). A luminance of one cd/m^2 is produced by a luminous surface of one square metre in area and a light intensity of one candela in a direction normal to the surface.

According to the manner in which they are excited, surfaces may be self-luminous (such as the screen of a TV receiver, the filament of an incandescent lamp), and secondary which reflect or transmit part of incident light (motion-picture screens, bowls of lighting fixtures).

A few practical examples of luminance are listed in Table 1.3.

Many light sources (luminous surfaces) emit light which is distributed in accordance with *Lambert's cosine law*. Notably, the light emitted by a TV picture tube follows this law fairly accurately.

Figure 1.6a shows a side view of a luminous surface, S . The luminous intensity due to this surface depends on the angle α between the viewing direction and the normal to the surface. For the radiance from surfaces obeying Lambert's cosine law, the luminous (or light) intensity is proportional to the cosine of the angle

$$I_\alpha = I_0 \cos \alpha \quad (1.15)$$

where I_0 is the light intensity in the direction normal to the surface.

Table 1.3

Surface	Luminance, cd/m ²
Motion-picture screen	10-30
Picture-tube screen	40-80
Projection picture-tube screen	1 to $2 \cdot 10^4$
Burning match	$5 \cdot 10^3$
Incandescent lamp filament	$5 \cdot 10^6$ to 10^7
Electric arc	10^8 to $2 \cdot 10^8$
Sun	$1.5 \cdot 10^9$

A luminous surface with the luminous intensity obeying this law is said to be a *perfect or ideal diffuser*. For perfect diffusers, the tips of the luminous intensity vector, I_α , will lie on a sphere (on a circle in the plane of Fig. 1.6a) touching the surface at point A.

The apparent area of the surface S viewed at the angle α is given by Eq. (1.12). Thus, the luminance viewed at an angle α to the surface is

$$B_\alpha = I_\alpha / S_\alpha = (I_0 \cos \alpha) / (S \cos \alpha) = I_0 / S = B_0 \quad (1.16)$$

Equation (1.16) shows that for a perfect diffuse radiator the luminance is independent of the angle of view. Therefore, for perfect or ideal diffusers the luminance diagram is a circle with point A as centre (Fig. 1.6b). Incidentally, this is why the picture on a TV screen appears to have the same luminance, no matter where the observer may be sitting—in front of or sideways to the screen.

By relatively simple manipulations it can be shown that the total luminous flux emitted by a luminous surface of a hemi-sphere and obeying Lambert's cosine law will be

$$F_{tot} = \pi I_0 \quad (1.17)$$

where I_0 is the luminous intensity in the direction normal to the surface.

1.3. Brief Outline of Optics

Basic properties of lenses. An image of an illuminated or self-luminous object is produced on a screen, photographic or cine film, or the photocathode of a TV pick-up by a lens usually made up of several elements. Sometimes, for example in projection large-screen TV, use is made of spherical mirrors.

A single lens may be converging (positive) or diverging (negative). A beam of parallel rays passing through a converging lens is caused

to converge to a single point, F (Fig. 1.7a) called the *focus* of the lens and located on the lens's axis of symmetry, ZZ' , alternatively called the *optical axis*. A beam of parallel rays passing through a diverging lens (Fig. 1.7b) is caused to diverge. If this diverging cone of rays is mentally extended in the reverse direction, the point where

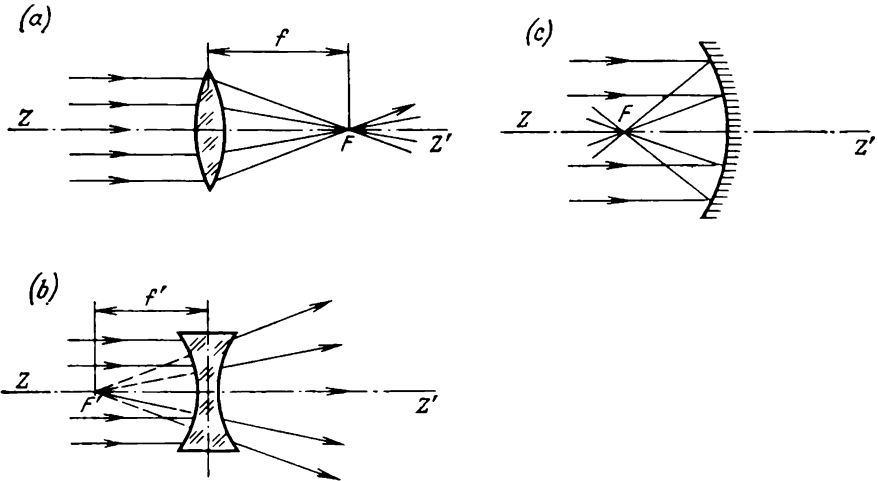


Fig. 1.7. Lenses and optical elements

(a) real focus F of a collective lens; (b) virtual focus F' of a diverging lens; (c) real focus F of a spherical mirror

the rays converge on the optical axis (actually, the place of convergence can only approximately be likened to a point) gives the so-called *virtual focus*, F' .

A spherical mirror can collect a beam of parallel rays to a single point, too (Fig. 1.7c). Here, too, the parallel rays are caused to converge to a single point called the focus, F , of the spherical mirror.

The distance from a lens to its focus is called the *focal length*, f (or f') of that lens, which is a very important characteristic.

If a beam of parallel rays be passed through a lens in the reverse direction, it will again converge to a single point on the optical axis, but on the opposite side. Thus, each lens has two foci and two focal lengths. For thin lenses, both focal lengths are the same.

A very important characteristic of a lens is its *focal power* φ ; it defines the converging or diverging effect of the lens. The focal power is the reciprocal of the focal length, f :

$$\varphi = 1/f \quad (1.18)$$

The shorter the focal length, the stronger the converging or diverging effect of the lens, that is, the greater its focal power φ .

The unit of focal power is the *diopter*. A focal power of one diopter is shown by a lens whose focal length is one metre.

It is assumed that converging (convex) lenses have a positive focal power and that diverging (concave) lenses have a negative focal power.

The optical power of a system made up of two thin lenses of any type and separated a small distance d apart is defined as

$$\varphi = \varphi_1 + \varphi_2 - d\varphi_1\varphi_2 \quad (1.19)$$

Aberrations of lenses. It may only approximately be assumed that the image produced by a lens is a true representation of the object,

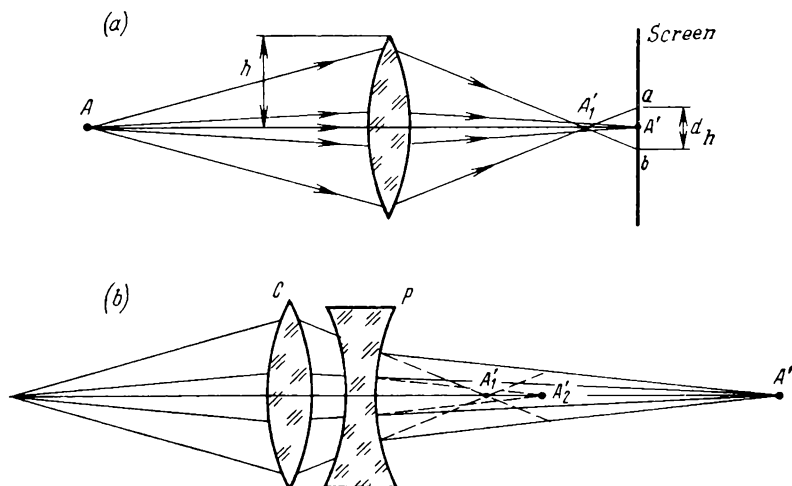


Fig. 1.8. Spherical aberration

(a) path of rays in spherical aberration; (b) correction of spherical aberration in a converging lens C by means of a diverging lens P

point for point. In fact, it is only the rays close to the optical axis of a lens (paraxial rays) that are collected to a single point. Peripheral rays, that is the rays incident on the lens away from its optical axis will converge to other points after passing through the lens, as shown in Fig. 1.8a.

If a viewing screen be placed so that point A' (an image of point A) appears on that screen, the image will appear surrounded by a halo, ab . If, apart from high-lights, the image has dark areas, they may be illuminated by the halos from adjacent high-lights. As a result, the image will be of low contrast, dull and lacking fine detail. Obviously, halos cause the image to appear out of focus and blurred.

This failure of the rays emerging from the same point on the object to converge to a single point after passing through a lens is called the *spherical aberration* of that lens. Spherical aberration is a very important shortcoming of lenses and mirrors. Quantitatively, the spherical aberration of a lens can be measured by the diameter of the halo, d_h . For a simple lens it can be found by the following approximate equation:

$$d_h = (a/f^2) h^3 \quad (1.20)$$

where h is the effective radius of the lens, f is its focal length, and a is the coefficient of spherical aberration, depending on the lens shape, refractive index of the lens material, and the relative position of the lens and object.

One of the methods for correcting spherical aberration is to narrow the effective diameter, or entrance pupil, of the lens, that is, the term h by placing an aperture stop in the beam path ("stopping down"). Obviously, an aperture stop will reduce the amount of light passing through the lens, that is, reduce the efficiency of the lens.

Another method of correcting spherical aberrations, which does not affect the amount of light entering the lens, is to use a combination of several elements. Figure 1.8*b* illustrates how this can be done by combining a converging lens C and a diverging lens D of appropriately matched characteristics. In this combination, the rays converge at a farther point (A' instead of A'_1 and A'_2), that is, the focal length is increased and the focal power is decreased. However, spherical aberration is minimized considerably.

Apart from spherical aberration, lenses and mirrors suffer from other forms of aberration affecting the rays off the lens axis. They, too, defocus and distort the image.

Among the aberrations affecting the rays off the lens axis are *coma*, *astigmatism* and *distortion*. In all of them, the cause of aberration is failure of the axes of symmetry of the light beam and lens to coincide (Fig. 1.9). A beam of light whose axis $A_1A'_1$ is off the optical axis ZZ' of the lens will fail to image at the same point after passage through the lens, even though it may be free from spherical aberration. Axial dissymmetry at small angles ω mainly causes what is known as *coma* because the rays passing through the outer zone form a cometlike image, *1*.

At large angles ω , *astigmatism* is predominant. In this case, in failing to image to a single point, the passing rays form an ellipse, *2*.

In the case of *distortion*, the image formed by a lens is geometrically dissimilar to the object. For example, the square grid of Fig. 1.10*a* may be imaged as shown in Fig. 1.10*b*, resulting in barrel distortion, or as in Fig. 1.10*c*, leading to pin-cushion distortion.

As with spherical aberration, the aberrations affecting off-axis rays can be corrected (reduced to an acceptable minimum) by com-

bining lenses having suitable radii or curvature, separation between elements, and refractive indexes.

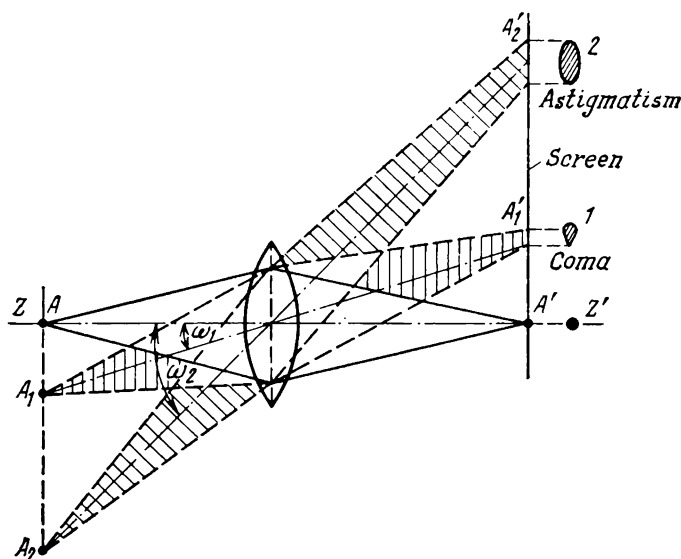


Fig. 1.9. Aberration of off-axis rays
1—coma; 2—astigmatism

Multi-element lenses. The lenses used in photographic, cine and TV cameras consist each of a multiplicity of simple lenses or elements, matched for various characteristics.

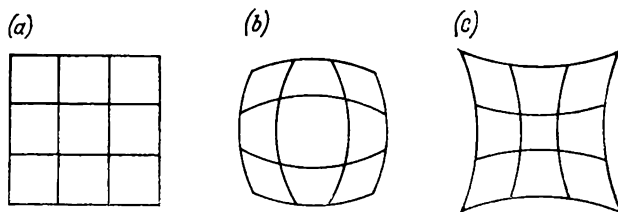


Fig. 1.10. Distortions
(a) original pattern; (b) barrel distortion (c) pin-cushion distortion

The characteristics for which the elements of a multi-element lens are matched are the radii of curvature, lens thickness, refractive indexes, separation between elements. When properly matched, the elements can reduce the aberrations of the composite lens to an ac-

ceptable minimum. Unfortunately, such lenses are fairly complex in design.

The efficiency of a multi-element lens, that is, its ability to form a sufficiently large and bright image, depends to a considerable degree on what is called the *speed of a lens*. Consider this point in greater detail.

Figure 1.11 shows how an image, $A'B'C'$, of a plane object, ABC , is formed by a lens, O . Select point B on the optical axis. Light

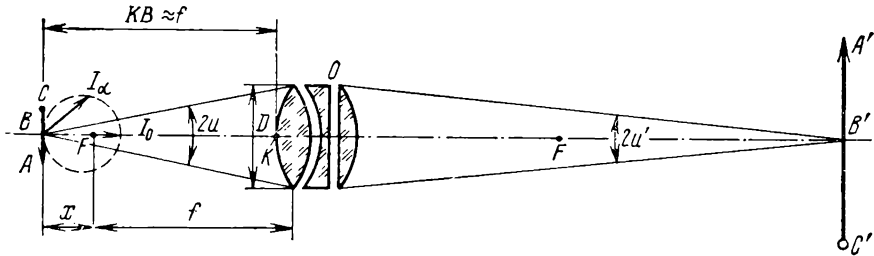


Fig. 1.11. Image formation by a lens

from this point is collected by the lens within an angle $2u$, called an *aperture angle*. If point B obeys Lambert's cosine law (see Sec. 1.2), the light intensity diagram will be a circle (dotted in Fig. 1.11) touching line ABC at point B . As is seen, if the aperture angle is not too large, the light intensity within it will vary insignificantly and be approximately equal to I_0 . At magnifications $\beta = 10$ to 20 , usually employed in TV optical systems, the length $x = 0.1f$ to $0.05f$, that is, $x \ll f$, and the distance KB from the object to the lens (object distance) may be assumed to be equal to the focal length, that is, $KB \approx f$. Then the solid angle enclosing the light beam radiating from the point and collected by the lens will be approximately given by

$$\omega_{entr} = (\pi D^2/4)/f^2 = (\pi/4) (D/f)^2 \quad (1.21)$$

where D is the diameter of the lens (or, more accurately, the diameter of its entrance pupil*).

The luminous flux F_{entr} emitted by point B and entering the lens is, in accordance with Eq. (1.8), defined by an integral of the form

$$F_{entr} = \int_{2u} I_{\alpha} d\omega$$

* As a rule, the entrance pupil of a multi-element lens is not equal to the diameter of the first element because the stops and mounts used inevitably reduce the clear or effective diameter, which is then called the entrance pupil.

Deeming the luminous intensity within the aperture angle $2u$ practically constant, $I_\alpha = \text{constant} = I_0$, we get

$$F_{entr} = I_0 \int_{2u} d\omega = I_0 \omega_{entr} = (\pi/4) I_0 (D/f)^2$$

After passage through a lens, some light is lost due to absorption by and reflection from the lens elements. As a result, the luminous flux, F_{ex} , emerging from the lens is smaller than F_{entr} , that is,

$$F_{ex} = \tau F_{entr} = (\pi/4) \tau I_0 (D/f)^2 \quad (1.22)$$

where τ is the transmittance of the lens.

As is seen from Eq. (1.22), the emerging luminous flux is affected by three characteristics of the lens: transmittance τ , effective lens (entrance pupil) diameter D , and focal length f . The ratio D/f is called the *reciprocal relative aperture* (reciprocal f -number) of a lens. The greater the reciprocal f -number, the greater the amount of light admitted by the lens, and the brighter the image formed. The square of the reciprocal f -number

$$A = (D/f)^2 \quad (1.23)$$

is called the *speed of a lens*.

The *total speed* of a lens is defined as

$$A_{tot} = \tau (D/f)^2 \quad (1.24)$$

It follows from Eq. (1.22) that the efficiency of a lens might be improved by increasing its reciprocal f -number. Unfortunately, an increase in D (or a decrease in f) would lead to an increase in aberration [see, for example, Eq. (1.20) where $h = D/2$]. To correct them, additional elements would have to be incorporated in the lens; this would, however, reduce τ , and render the lens more expensive and complex to make.

The efficiency, η , of a lens (in terms of luminous flux) is the ratio of the luminous flux, F_{ex} , emerging from the lens to the total luminous flux available from the source, $F_{tot} = \pi I_0$ [Eq. (1.17)]. Noting Eq. (1.22), we may write

$$\eta = F_{ex}/F_{entr} = F_{ex}/\pi I_0 = (\tau/4) (D/f)^2 \quad (1.25)$$

that is, the efficiency is decided by the total speed of the lens.

For photographic lenses, the f -number is about two. Assuming (from practical experience) that the transmittance of a lens is about 0.8, the efficiency will be

$$\eta = (\tau/4) (D/f)^2 = (0.8/4) (1/2)^2 = 0.05 = 5\%$$

That is, the lens utilizes as little as 5% of the light emitted by the object.

1.4. Selection of the Frame Frequency

Television uses the same technique for the transmission of moving objects as is used in motion-pictures. Basically, a series of individual still pictures differing in the phase of the motion and caught by the lens is transmitted (Fig. 1.12). When these stills are reproduced, the persistence of vision creates an illusion of a continuous motion.

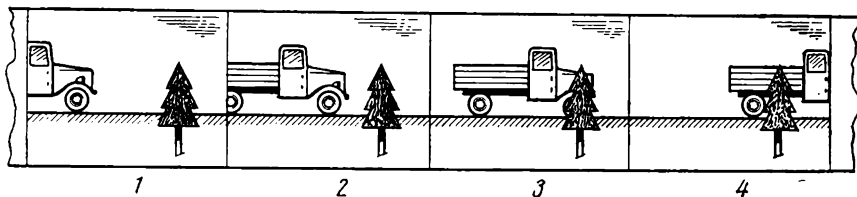


Fig. 1.12. Reproduction of motion by a sequence of stills

As the number of stills, or frames, shown every second is increased, the frequency spectrum needed for television signals has to be expanded. In order to minimize the frequency spectrum, or bandwidth, needed, the number of frames per second should be kept to a reasonable minimum at which the viewer would not notice the intermittent nature of the stills. Experiments show that this minimum is 10 to 15 frames per second (as the speed of the motion transmitted increases, it appears increasingly more jerky).

Thus, on the basis of experiments, the choice ought to be 10 to 15 frames per second. Unfortunately, at this frame frequency another unpleasant factor comes in, known as flicker, when the whole of the picture produces the sensation of a pulsating motion. To avoid this flicker effect, the frame frequency has to be increased three to three and a half times.

Quantitatively the frame frequency is related to what is known as the *critical flicker or fusion frequency*, or simply the critical frequency. An idea about this frequency can be gained from a simple experiment such as this. Place a rotating disc one half of which is made transparent in front of a lamp (Fig. 1.13a) and look at the lamp through the disc. As long as the disc is revolved slowly, the lamp will appear flickering. As the speed of the disc is increased, the individual flashes merge into one another, until the lamp appears to give up light continuously. The frequency of flashes at (or above) which the flicker effect disappears is called the critical flicker frequency, F_{cr} . It is mainly determined by the brightness and colour of the light source. The flicker effect is most severe with yellow-green light which shows the greatest visibility to the human eye.

The illusion of a continuous emission from a flashing light source is produced by the persistence of vision. This effect is illustrated in Fig. 1.13*b*. When a square pulse of light, B_m , excites the eye, an

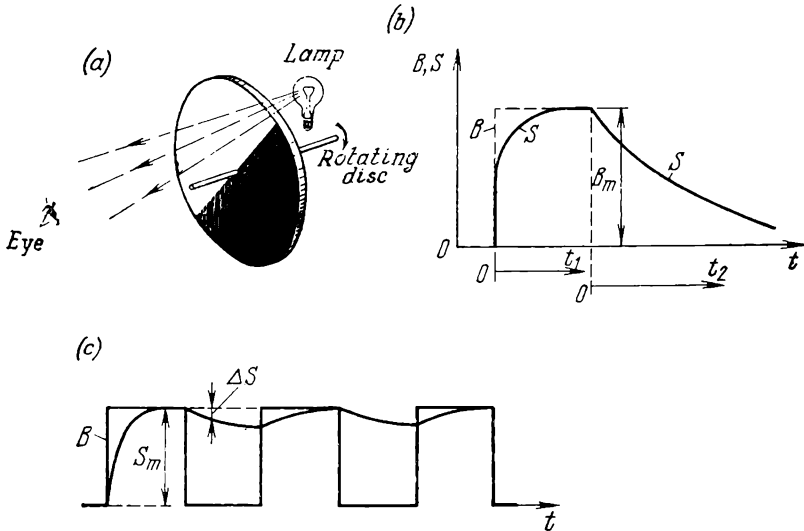


Fig. 1.13. Critical flicker or fusion frequency

(a) determination of the flicker frequency; (b) eye's response to a light pulse; (c) merger of individual responses to light pulses

appropriate response (apparent luminance), S , builds up exponentially

$$S_1 = S_m [1 - \exp(-t_1/\tau_1)] \quad (1.26)$$

rather than instantaneously.

When the light impulse ceases, the sensation of light in the brain decays likewise exponentially rather than at once:

$$S_2 = S_m \exp(-t_2/\tau_2) \quad (1.27)$$

Experiments have shown that $\tau_1 \ll \tau_2$, or that the response to a light impulse rises faster than the sensation decays after removal of the impulse. For an average human eye, the decay (or fall) time is $\tau_2 \approx 0.1$ to 0.15 s.

If light flashes follow at a sufficiently high rate (Fig. 1.13*c*), the fractional decay in luminance, $\Delta S/S_m$, between pulses will not exceed 2 to 5%, and the observer will not notice the individual flashes.

In motion-pictures and television, special importance is attached to the dependence of the critical frequency on luminance. As is

seen from Fig. 1.14, which is an experimental plot of the relation, the critical frequency rises with increasing luminance. In other words, at low screen luminance the frame frequency (also called frame-scan or vertical-scan frequency in television) may well be low without causing the flicker effect. This fact was utilized in the early years of television (1931-1937), when the luminance of TV screens was a few tenths of a candela per square metre (the screens were neon tubes). Accordingly, the frame-scan frequency was 12.5 per second. Today,

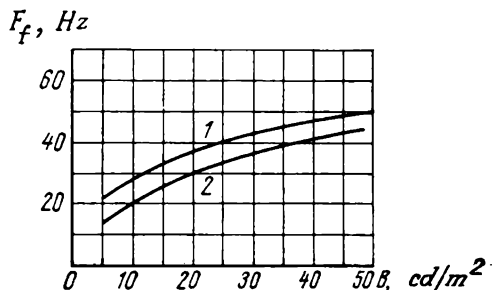


Fig. 1.14. Flicker frequency as a function of source luminance
1—disc-chopped lamp; 2—picture-tube screen

the luminance of the TV screen has increased hundreds of times. As is seen from the plot of Fig. 1.14, at a luminance of 30 to 40 cd/m^2 the frame-scan frequency must be 40 to 50 per second.

As a way of saving bandwidth, it might be possible to select the lowest limit of 40 frames per second. In broadcasting television, however, use is made of 50 frames per second which is the mains frequency. For one thing, this figure provides a margin over the critical frequency; for another, the frame-scan frequency can readily be locked to the frequency of the mains from which the equipment is energized at both the transmitting and receiving ends.

This synchronization (maintenance of equality between supply frequency and frame-scan frequency) is essential because it minimizes interference. This interference can affect the quality of the TV picture in two ways. Firstly, by breaking through the rectifier and filament circuits into the video amplifier of a TV receiver, it appears as horizontal bright and dark stripes (Fig. 1.15a). Secondly, by breaking through into the line sweep generator, it distorts the vertical edges of the picture (Fig. 1.15b). In a properly aligned TV receiver with properly synchronized supply and frame-scan frequencies, these two forms of interference are stationary and usually remain unnoticed or, at least, do not distract the viewer. If, on the other hand, the supply frequency and the frame-scan frequency differ even by a small amount, the interference will be moving. A moving disturbance, even a small

one, is more annoying than a large but stationary disturbance. This is why in broadcasting television the frame-scan frequency is chosen equal to the supply frequency. The equality is maintained by a suitable device provided at each TV centre.

It should be noted, however, that this synchronization has an adverse technical aspect, especially when TV programs are exchanged between cities or countries operating from different supply mains. For example, the distribution networks in Moscow and Kiev are not precisely maintained at the same frequency or phase. Therefore,

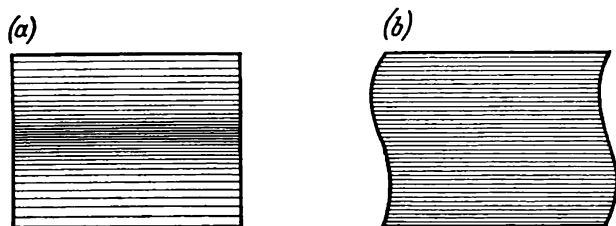


Fig. 1.15. Mains-induced interference on the TV screen
(a) horizontal dark and light stripes; (b) distortion of vertical edges

when a TV program is relayed from Kiev to Moscow or the other way round, it is not at all easy to lock the frame-scan frequency to supply frequency. As a result, moving disturbances inevitably appear on TV screens either in Moscow or in Kiev.

Because of this, the recent trend has been towards using other sources of synchronization. Synchronizing signals may be derived from a crystal-controlled master oscillator set up at a central TV station and relayed to the master oscillators at TV centres in other cities over a communication channel (cable or overhead) in order to hold them locked to the correct frequency. In such cases, however, the power units of TV receivers must be made to far more stringent standards in order to avoid pick-up from the supply mains, as this might produce moving disturbances.

If we compare a revolving disc masking a lamp (see Fig. 1.13a) and a TV screen, we shall see that they are two entirely different flashing sources of light. Light from the lamp is chopped abruptly, while that from the TV screen is continuous. Because of after-glow, a luminous line on the TV screen decays exponentially (Fig. 1.16a) rather than at once, after the electron beam comes off that line. To simplify our reasoning, we shall consider an empty raster (that is, one without any picture shown). Then the picture-tube screen will change its luminance as follows: the luminance will be a maximum on the line just left by the beam (line *AB* in Fig. 1.16b). Upwards of this line, the screen luminance will gradually decrease in accordance

with the plot of Fig. 1.16a. As the electron beam is scanned, the boundary AB will move downwards. At a low frame-scan frequency, the viewer will see a bright bar moving continuously from top to bottom. From experiments carried out on a sufficiently great number of observers, it has been found that for this moving luminous bar the critical flicker frequency depends on luminance as shown by curve 2 in the plot of Fig. 1.14. In this case, the critical frequency is

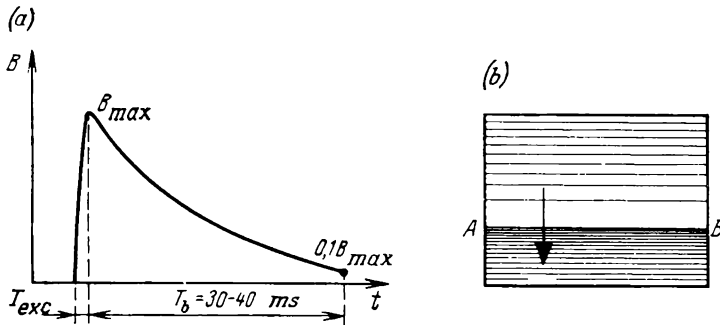


Fig. 1.16. Phosphor response to excitation by electrons
(a) persistence characteristic (T_{exc} = excitation time; T_b = decay time); (b) motion of highlight edge AB on the screen

the minimum frequency at which the viewer does not notice a moving bar on his TV receiver and the screen appears uniformly and continuously illuminated. From comparison of curves 1 and 2 in Fig. 1.14 we may conclude that the critical frequency for the TV screen is lower than that for the lamp masked by a revolving disc and that the flicker effect is easier to control. The latter advantage is due to the after-glow of the screen, as it moderates the flicker effect.

1.5. Interlaced Scanning

From the foregoing it might be concluded that the frame frequency for broadcasting television should be 50 frames per second. Unfortunately, a 625-line picture transmitted at this frame-scan frequency would require a bandwidth of over 12 MHz. Signals occupying a huge bandwidth like this are difficult to transmit without marked distortion as they pass through the transmission link, and difficult to process (detect and amplify) in a receiver before they are fed to the picture tube. Also, this would drastically reduce the number of TV channels that could be set up within the frequency band allocated to television.

One way to overcome this limitation is by means of *interlaced scanning*. This technique makes it possible to halve the frame-scan

frequency (and to narrow the bandwidth required in proportion), while retaining the picture quality (resolution, contrast, etc.), and to exceed the critical flicker frequency by a comfortable margin. In principle, interlaced scanning is not unlike a technique employed in motion-picture projection. As the reader probably knows, motion pictures are projected at a speed of 24 frames per second. Because, however, motion-picture screens have a brightness of a few tens of

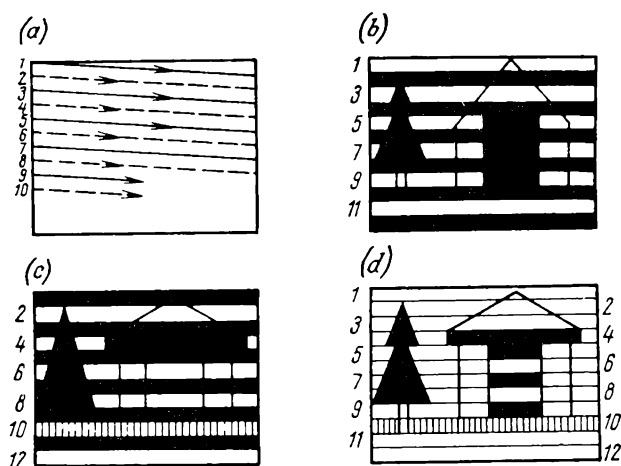


Fig. 1.17. Interlaced scanning

(a) interlace sequence; (b) odd field; (c) even field; (d) complete frame

cd/m², this frame-projection frequency is insufficient to exceed the critical frequency. To avoid the flicker, a cine projector has a rotating disc in front of the film gate aperture, called the flicker shutter, which interrupts the light passing through each frame twice during the time interval it is stationary in the film gate aperture. In this way, the spectator sees, as it were, twice as many frames (called fields) or, which is the same, the frame (or, rather, field) projection frequency is now 48 per second, which is enough to exceed the critical flicker frequency.

With interlaced scanning, there are two fields per frame, and each field scan is arranged to explore half the lines that make up a frame (by the USSR scanning standard, there are 625 lines per frame). The first field scan can explore, say, odd lines (1, 3, 5, etc.), the second field scan, even lines (2, 4, 6, etc.) (Fig. 1.17). This is done at 50 field scans per second. Frames, each made up of two fields, are thus scanned at the rate of 25 per second. Although each field explores only half the total lines in the image (312.5 lines), the persistence of vision produces an illusion that the viewer sees a full frame con-

taining 625 lines. Thus, by doubling the rate at which the picture is reproduced on the screen, interlaced scanning makes it possible to exceed the critical frequency with a sufficient margin without having to extend the bandwidth needed. Today, interlaced scanning is widely used both in the Soviet Union and abroad.

Thus, in order to lock rigidly the frame scan frequency to the power-source frequency, to operate above the flicker threshold, and to reduce the bandwidth required, the number of fields per second has been set at 50, which works out to a frame-scan frequency of 25 per second. It is to be noted that in Soviet TV usage the field scanning frequency is often called the frame scanning frequency, or simply the frame frequency. For example, it may be heard that the sawtooth frame scanning generator (actually, the field scanning generator) has a frequency 50 Hz.

1.6. Picture Luminance

If it is to be watched comfortably, without undue eye strain, the television picture must be sufficiently bright. A picture which is too low or too high in luminance is equally unpleasant to see.

From many years' practice with both motion pictures and telecasts, highlight luminance should normally be of the order of 40 to 60 cd/m². In a room with dimmed light, a luminance of 20 cd/m² will usually be sufficient. It is to be remembered that in a carefully curtained room the excessively bright TV screen produces the unpleasant sensation of a "gaping window" (a bright rectangle against the dark background). The picture appears more pleasant and quiet when a small external light is turned on.

The visual luminance of a TV screen as a flashing light source when flashes occur at a rate exceeding the critical flicker frequency is defined as the mean taken over a period:

$$B_{vis} = \frac{1}{T} \int_0^T B(t) dt \quad (1.28)$$

where B_{vis} = visual luminance of the screen

T = period of light impulses, equal to one frame time

$B(t)$ = instantaneous true luminance of a picture element

Equation (1.28) is known as the *Talbot law*.

The significance of Eq. (1.28) will be clear from reference to the plot of Fig. 1.18 which shows, with a degree of idealization, luminance impulses from a picture element. When in scanning the TV screen, it strikes this element, the electron beam gives rise to a radiance, $B(t)$, which attains a maximum value of luminance, B_m , in time T_{el} during which the element is scanned. After the beam moves

off this element, its radiance will decay almost exponentially:

$$B(t) = B_m \exp(-t/\tau) \quad (1.29)$$

Let us relate the maximum (impulse) luminance B_m to its average (visual) value, B_{vis} . By the Talbot law:

$$\begin{aligned} B_{vis} &= \frac{1}{T} \int_0^T B(t) dt = \frac{1}{T_f} \int_0^{T_f} B_m \exp(-t/\tau) dt = \\ &= B_m (\tau/T_f) [1 - \exp(-T_f/\tau)] \end{aligned} \quad (1.30)$$

where τ = screen after-glow time constant

T_f = frame period (the negligibly small $T_{el} \approx T_f/500,000$ may be ignored for simplicity)

An excessive after-glow time may cause the image of moving objects to appear blurred. It is permissible if the residual luminance

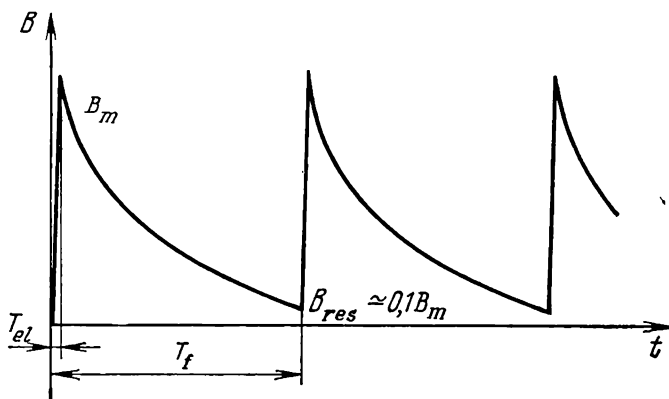


Fig. 1.18. Determining the luminance of a picture-tube screen

due to after-glow over a frame scan period does not exceed 5 to 10% of the initial value. Then, from Eq. (1.29),

$$(0.05 \text{ to } 0.1) B_m = B_m \exp(-T_f/\tau)$$

whence

$$T_f/\tau = 3 \text{ to } 2.3$$

Substituting these values in Eq. (1.30) gives

$$B_m = (2.6 \text{ to } 3.2) B_{vis}$$

or, on the average, $B_m \approx 3B_{vis}$. With an apparent (visual) luminance of $B_{vis} = 40 \text{ cd/m}^2$, the maximum luminance (at the point illuminated by the electron beam) will be $B_m = 120 \text{ cd/m}^2$.

1.7. Picture Contrast

The contrast of a TV picture has to do with the actual difference in luminance between the whitest and blackest portions of the picture. It is expressed in terms of the contrast ratio or range which is the ratio of the maximum to minimum luminance values in the picture:

$$\beta = B_{\max}/B_{\min} \quad (1.31)$$

The contrast range is a very important quality of the TV picture. It is not unlike the dynamic range of sound in radio. As the contrast range is increased, the picture quality is improved because it contains a greater number of gradations between highlights and shadows, and any noise stands out less conspicuously. A good contrast range makes the picture look more natural and detail more discernible. Ideally, the contrast range of the picture should be as close to that of the scene as possible. Unfortunately, a number of technical limitations impair the contrast range and contrast ratio of TV pictures.

An idea about the contrast range of some of the scenes most widely encountered in TV practice can be gleaned from Table 1.4 which quotes the respective contrast ratios.

Table 1.4

Scene	Contrast ratio
Landscape with highlights and shadows on a bright sunny day	1000
Average landscape	100
Artificially illuminated interior	20-60
Motion-picture screen	50-100
Good photograph	50-100
Fine detail in TV picture	5-8
Coarse detail in TV picture (2 to 5% or more of linear dimensions of the screen)	30-40

In television, it is customary to define the contrast ratio for fine and coarse detail separately. This is done because of some technical differences in the reproduction of each, to be discussed later on. For the time being it may be noted that the two contrast ratios may differ substantially.

A poor contrast range is to a great extent traceable to imperfections in the picture tube. The contrast range is also affected by the frequency and amplitude response of the various circuits in the television chain. Noise accompanying the television signal can affect the contrast, too, by adding a kind of veil and brightening the shadows.

1.8. Tonal Gradations

A television picture is mainly one of shades of gray. In addition to the lightest and darkest portions, it has a great many intermediate luminance values or tonal gradations. A picture having a great number of tonal gradations is more impressive, vivid and crisp and the edges of objects have a "sharpness" appearance. This is why it is important to reproduce the gradation of gray tones existing in the scene faithfully. Sometimes the television picture need not have the full range of tonal gradations of the original scene; for example, two extreme values of luminance, B_{\max} and B_{\min} , will suffice in the

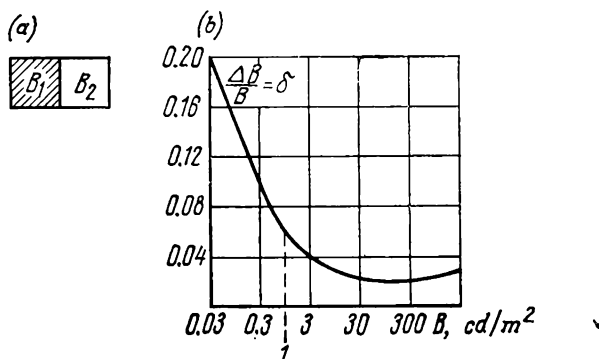


Fig. 1.19. Contrast sensitivity of the eye

(a) adjacent test fields differing in luminance; (b) contrast sensitivity as a function of luminance

transmission of titles and captions (black letters against a white background), engineering drawings and the like. An ample gradation of gray tones is essential, however, in the transmission of live programs, films, etc.

The transmission and reproduction of a wide tonal range imposes stringent requirements on TV equipment. It is important therefore to determine the minimal number of tonal gradations beyond which any increase would only complicate the equipment without any improvement in picture quality. As in many other cases, the only instrument which can set a reasonable limit for the maximum number of tonal gradations is the eye.

To begin with, we should determine the difference in luminance between two shades of gray which is just noticeable to the eye. Imagine two illuminated fields placed next to each other (Fig. 1.19a). These fields are presented to a group of spectators. At the beginning of the experiment, $B_1 = B_2$. Then, say, B_2 is gradually changed while B_1 is held constant. Independently of one another, the spectators

should tell when each just notices that B_2 differs from B_1 . In this way, we can determine the difference threshold

$$\Delta B = |B_2 - B_1| = \frac{\Delta B_1 + \Delta B_2 + \dots + \Delta B_n}{n}$$

just noticeable to the spectator between the two fields (here, ΔB_n stands for the individual reports of the spectators and n is the number of spectators).

Such experiments have been conducted more than once, and they have established beyond any doubt that the difference threshold, ΔB , depends on the initial value of B_1 . As B_1 is increased, $\Delta B = |B_2 - B_1|$ increases, too. An example will illustrate the point. The TV screen has a highlight luminance of 40 cd/m^2 . It should be changed (increased or decreased) by at least 0.8 cd/m^2 to make the change just noticeably different. That is, the eye would hardly notice any difference between a luminance of 40.8 cd/m^2 or 39.2 cd/m^2 and a luminance of 40 cd/m^2 . The luminance of an incandescent lamp is $5 \times 10^6 \text{ cd/m}^2$. A change of 0.8 cd/m^2 in its luminance would not be noticed by the eye at all. For the eye to just notice any change, ΔB should be $2.5 \times 10^5 \text{ cd/m}^2$ in this case.

The ratio $\Delta B/B$ is called Weber's fraction and the statement that this fraction is a constant independent of B

$$\Delta B/B = \delta \approx \text{constant} \quad (1.32)$$

is known as Weber's law,

where ΔB = difference threshold

B = initial luminance

δ = contrast sensitivity of the eye

The contrast sensitivity of the eye changes but little over a fairly wide range of luminance. A plot of the eye's contrast sensitivity as a function of luminance is shown in Fig. 1.19*b*. For the luminances normally associated with the TV screen (from 40 to 1 cd/m^2), the contrast sensitivity of the eye ranges between 0.05 and 0.02 , so that $\delta_{av} \approx 0.03$.

Now imagine a TV picture as consisting of stripes as shown in Fig. 1.20, such that the luminance of a next stripe differs from that of the preceding one by the difference threshold, ΔB , decided by the contrast sensitivity δ of the eye.

Let the contrast ratio, $\beta = B_{\max}/B_{\min}$, of the picture be specified in advance. The luminance of the first stripe is $B_1 = B_{\min}$, that of the second $B_2 = B_1 + \Delta B_1 = B_1 + \delta B_1 = B_1(1 + \delta)$, of the third $B_3 = B_2 + \Delta B_2 = B_2 + \delta B_2 = B_2(1 + \delta) = B_1(1 + \delta)^2$, and that of the m th stripe $B_m = B_1(1 + \delta)^{m-1}$.

Noting that $B_1 = B_{\min}$ and $B_m = B_{\max}$, we get

$$\beta = B_{\max}/B_{\min} = (1 + \delta)^{m-1}$$

whence

$$m = \frac{\ln \beta}{\ln (1 + \delta)} + 1$$

At $\delta \ll 1$ (in our example, $\delta = 0.02$ to 0.05), $\ln (1 + \delta)$ is about δ . Also, recalling that $\ln x = 2.3 \log_{10} x$, we get

$$m = \frac{2.3 \log_{10} \beta}{\delta} + 1 \quad (1.33)$$

The maximum number, m , of luminance-discrimination steps for the eye is directly proportional to the logarithm of the contrast ratio,

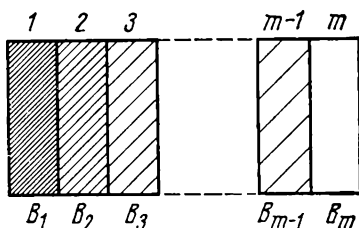


Fig. 1.20. Determining the number of tonal gradations

β , and inversely proportional to the contrast sensitivity, δ , of the eye.

Assuming that in television $\beta = 10$ to 40 and $\delta = 0.03$, we have

$$m = \frac{2.3 \log_{10} (10 \text{ to } 40)}{0.03} = 80 \text{ to } 130$$

or, on the average, about 100.

So far we have dealt with the difference in luminance just noticeable to the eye. Any change in luminance produces a sensation in the brain, which is described fairly accurately by Fechner's extension of Weber's law, and known as the Weber-Fechner law. It can be derived as follows. Formally, Weber's law, Eq. (1.32), may be re-written in terms of infinitesimal increments as

$$dS = dB/B \quad (1.34)$$

where dS is an infinitesimal change in the sensation. By integrating the left- and right-hand sides of Eq. (1.34), we get

$$\int_{S_0}^S dS = \int_{B_0}^B dB/B$$

that is,

$$S - S_0 = \ln (B/B_0) \quad (1.35)$$

where B_0 = initial luminance

B = changed luminance

S_0 = initial sensation

S = sensation due to changed luminance

Equation (1.35) expresses the Weber-Fechner law mathematically. It states that as the stimulus (luminance) is increased arithmetically, the sensation increases logarithmically.

Sensation is a psycho-physiological attribute and cannot therefore be accurately measured in quantitative terms. Although the equation is quantitative, its utility lies in the fact that it describes how the human being senses changes in luminance.

A plot of $S = f(B)$ based on Eq. (1.35) appears in Fig. 1.21. Fairly accurately verified by experiments, this plot shows that luminance and the sensation it causes in the human brain are not related in direct proportionality. As luminance is increased, the sensation increases at a progressively slower rate. This quality of vision is of

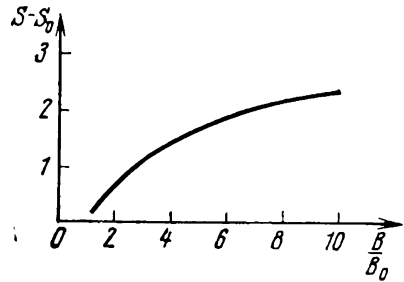


Fig. 1.21. Plot of the Weber-Fechner law

paramount importance to man in his day-to-day activities. This point can be illustrated by an example. The luminance just discernible by the human eye is $B_{\min} \approx 0.1 \text{ cd/m}^2$. The luminance of a dazzling light (as that of the filament in an incandescent lamp) is $B_{\max} = 10^7 \text{ cd/m}^2$. Thus, the contrast range is $B_{\max}/B_{\min} = 10^7 \div 10^{-1} = 10^8$. If the sensation were directly proportional to luminance, this range could hardly be accommodated by the brain. The property of vision described by the Weber-Fechner law compresses, as it were, this huge range in the brain. According to Eq. (1.35) the sensation changes only by a factor of 18:

$$\ln(10^7/10^{-1}) = 18.4$$

1.9. Picture Definition

The definition of a television picture has to do with the maximum number of fine details discernible in the image, provided the televised scene has a sufficient wealth of fine detail, too.

Definition is an important aspect of picture quality. With poor definition, the picture lacks crispness or sharpness; long and medium shots of faces become unrecognizable.

Above all, the definition of the television picture depends on the resolving power, or resolution, of the picture-imaging medium, that is,

its ability to discern and reproduce fine detail present in the televised scene. In turn the resolving power depends on the number of picture elements (or lines) chosen, the performance of camera and picture tubes, frequency and amplitude response of the amplifiers, transmitters, receivers, etc. A television equipment having a high resolving power will usually produce a more crisp or sharp picture.

Sometimes picture definition is separated into image-detail visibility (perception of fine detail) and sharpness (reproduction of image edge gradients). In fact, there are techniques and procedures for adjusting or controlling only, say, image-detail visibility or only

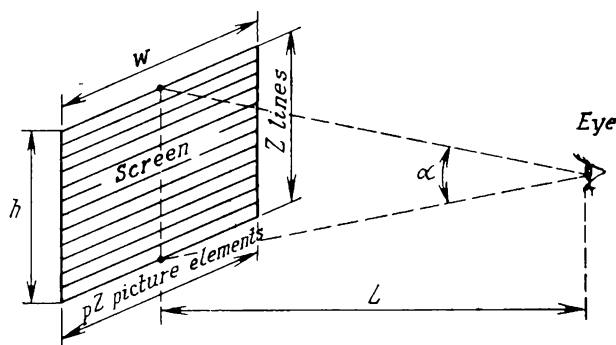


Fig. 1.22. Determining the maximum number of lines per frame

sharpness. In a conventional television system, however, an improvement or impairment in image-detail visibility will usually be accompanied by an improvement or impairment in the reproduction of image edge gradations. This is why it is only on rare occasions that definition may be divided into detail visibility and sharpness.

Reproduction of fine detail and edge gradations on a television screen is above all dependent on the number of picture elements, N , adopted by the scanning standard. For a given aspect ratio, $p = w/h$, where w is the width and h is the height of the picture (Fig. 1.22), the number of picture elements is uniquely related to the number of lines per frame, Z :

$$N = pZZ = pZ^2 \quad (1.36)$$

Obviously, the maximum number of fine detail is $N/2$, because any two white elements must be separated by a black one.

According to the Soviet scanning standard, $p = 4/3$ and $Z = 625$. Therefore, $N = (4/3)(625)^2 = 520.832$ elements. This is an idealized value of N in the sense that it does not take into account the fact that some lines are lost during vertical flyback or retrace and some elements are lost during horizontal flyback or retrace. In

practice, the retrace ratio defined as

$$\theta = t_2/T \quad (1.37)$$

where t_2 is the retrace interval and T is the scan or trace interval, is as follows:

(a) $\theta_v = t_{2v}/T_v = 1.5 \text{ ms} \div 20 \text{ ms} = 0.075$ for vertical or frame scanning*;

(b) $\theta_h = t_{2h}/T_h = (10 \text{ to } 14 \mu\text{s}) \div 64 \mu\text{s} = 0.16 \text{ to } 0.22$ for horizontal or line scanning.**

Because no information is transmitted about the televised scene during retrace, the true number, N_{true} , in terms of the ideal N can be expressed as

$$N_{true} = pZ(1 - \theta_h)Z(1 - \theta_v) = (1 - \theta_h)(1 - \theta_v)N \quad (1.38)$$

that is,

$$\begin{aligned} N_{true} &= (0.78 \text{ to } 0.84) \times 0.925 \times 520,832 \\ &= 375,780 \text{ to } 404,687 \text{ elements} \end{aligned}$$

On the average, N_{true} is about 400,000 elements.

The number N_{true} might be used to describe quantitatively the limit of resolution attainable in a television picture. However, a more convenient measure of resolution is the number of lines per standard frame. This choice is quite legitimate because the numbers of lines and elements per frame are uniquely related by Eq. (1.36). Therefore, when and if necessary, the true number of elements can be found from the known number of lines per frame. Prior to 1950, the standard number of lines per frame in the Soviet Union was 343 lines; today it is 625 lines.

It may be asked how many lines are needed to produce an image of satisfactory resolution. There is no unique answer to this question. The required number of lines per frame depends on the scene being televised, that is, on the amount of intermediate and fine detail it contains and the number of luminance gradations. An important factor also is whether the TV camera takes a long, medium or close shot of the scene. As an illustration, Table 1.5 presents some data

Table 1.5

Object televised	Minimum number of lines per frame required
Close-up of a face	120-150
Two or three persons at full height	250-300
Large number of people (a chorus, spectators at a stadium, etc.)	450-650

* Here, t_{2v} is the duration of the frame or vertical blanking pulse.

** $t_{2h} = 14 \text{ ms}$ is associated with picture tubes for which the aspect ratio is $p = 5/4$ (such as the Soviet-made 59JK2E).

taken from practice (in this table, the figures correspond to satisfactory picture resolution).

Because the scenes to be televised may be widely different and some of them may contain a great number of fine detail (such as crowds of spectators in a stadium), in designing a television system the greatest practicable number of lines per frame should be chosen. However, an increase in this number entails an increase in the frequency bandwidth needed, and this, in turn, causes complications in the design of television equipment.

In recent decades, emphasis has mainly been placed on increasing the number of lines per frame (so as to improve picture definition), which involved many problems, both theoretical and engineering. As a matter of historical record, the experimental TV system operated in the Soviet Union in the 1930s used a 30-line picture (mechanical scanning) and a bandwidth of about 6000 Hz. The electronic TV system commissioned in Moscow in 1937 used a 343-line picture and needed a bandwidth of 1,500,000 Hz. The TV system currently in operation in the Soviet Union uses a 625-line picture and needs a bandwidth of about 6,000,000 Hz.

Is a 625-line picture a reasonable limit or it will pay to improve picture definition through a greater number of lines per frame despite the increased complexity in television equipment? The answer to this question is decided by the properties of the human eye, above all by visual acuity (see Sec. 1.1). Visual acuity is determined by presenting to an observer a test object made up of two bright stripes (or dots) against a dark background (see Fig. 1.2a), which is set up at a progressively increased viewing distance.

As noted in Sec. 1.2 (see Table 1.3), under conditions of luminance existing on the TV screen, visual acuity is $\varphi = 1'$ (one minute of arc).

Basing ourselves on this figure, we can determine the maximum number of lines per frame beyond which it is senseless to go. The optimal viewing distance of a television image is three or four times the screen height, that is, $L = (3 \text{ to } 4) h$ (Fig. 1.22). From this viewing distance, the observer need not move his head to see all of the image. The viewing angle, α , is then such that the observer can take in the whole of the TV screen. This angle is

$$\alpha^\circ \approx (h/L) (180/\pi) = 1/(3 \text{ to } 4) (180/3.14) = 14^\circ \text{ to } 20^\circ$$

The raster (the alternating pattern of bright scanning and dark lines) will not appear consisting of individual lines if the separation between them (in angular units) does not exceed the visual acuity of the observer's eye. Thus, the maximum number of lines per frame is

$$Z_{\max} = \alpha/\varphi = (14 \text{ to } 20)/(1/60) = 840 \text{ to } 1200$$

From comparison of $Z = 625$ lines adopted in the USSR and $Z_{\max} = 1200$, it might appear that the maximum resolution is only half-utilized. Practically, this is not so, however. Experiments have shown that subjective picture resolution A (that is, one estimated by the human eye) does not increase in proportion to the number of lines per frame. This fact is illustrated by the plot of Fig. 1.23 which can be obtained as follows. The image produced by a television system having provisions for varying the number of lines and, as a result, objective resolution, is presented to a great number of observers. The unit of subjective resolution is the change in the number of lines which remains unnoticed by 75% of the observers. As is seen from the plot of Fig. 1.23, subjective resolution rises rapidly as long as the number of lines per frame is fairly low. At 500 to 600 lines, subjective resolution changes by an insignificant amount—a few per cent per hundred lines. That is, the increase in the number of lines per frame from 600 to 1000 will produce an improvement of as little as 5% in subjective resolution. As will be shown later (see Sec. 4.1), the frequency spectrum of the television signal is proportional to the square of line-

scan frequency. Because of this, an insignificant improvement in subjective resolution (by as little as 5%) would be accompanied by a substantial increase in the bandwidth needed: $1000^2/600^2 = 2.8$ times, that is, the required bandwidth would be about 18 MHz.

There are some other factors that govern the choice of the number of lines per frame. In determining Z_{\max} we assumed that the observers used all of their visual acuity, one minute of arc. In normal circumstances, however, people seldom use their full visual acuity. To begin with, viewing objects separated by one minute of arc would place too much strain on the eyes, and this strain would last for the duration of a TV program. Also, the contrast of fine detail in a TV image is low, and this reduces visual acuity, too. This is also true of scenes abundant in moving objects, because in viewing them the resolving power of the eye is drastically cut down. Last but not least, in television as in motion pictures the key object of a scene (say, the face of an actor) will usually be shown in a close-up for greater impressiveness or detail visibility.

In the light of the foregoing and also from the plot of Fig. 1.23, we may conclude that 625 lines per frame is a satisfactory choice for picture definition.

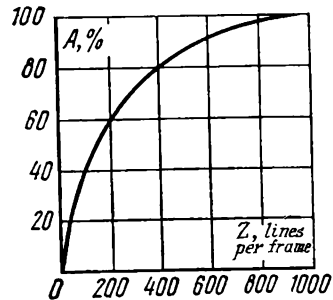


Fig. 1.23. Subjective picture resolution A as a function of the number of lines per frame Z

It is to be noted, however, that the television picture may sometimes appear to be of low quality even with 625 lines per frame. This happens not because the number of lines is insufficient, but because some elements in the television system show substandard performance, or because the receiver has a limited bandwidth, or the picture tube is of low quality, or the amplitude response of the system is unsatisfactory, or noise and interference is too strong.

As communications engineering advances, the time will come when it is attractive, both technically and economically, to use a greater number of lines per frame in broadcasting television. Today, there are special-purpose television systems (scientific, engineering, medical, etc.) where high picture definition is vitally important, and their number of lines per frame is substantially greater than that used in television broadcasting.

1.10. Factors Affecting Picture Resolution

In television, it is customary to differentiate between vertical resolution and horizontal resolution. This is because the television image has a line structure, and different technical factors affect the reproduction of fine detail horizontally (along the lines) and vertically (across the lines).

The arrangement of fine detail does not usually affect the visual acuity of the normal eye. Therefore, in designing a television equipment it is important to seek equality between horizontal and vertical resolution.

Horizontal resolution is mainly dependent on the bandwidth occupied by the received signal and on aperture distortion. Vertical resolution does not practically depend on bandwidth, but it is affected by the quality of interlaced scanning and the total number of lines per frame.

In investigations of vertical resolution, it is convenient to use a test chart as a set of black horizontal bars drawn against a white background (Fig. 1.24a). As a rule, the spacing between the black bars is equal to their width. With this test chart placed in front of a camera tube, we obtain an image of alternating black and white bars on its photocathode. As this striped test chart is moved away from the camera (and focus is readjusted as may be necessary), the bars in the image will progressively decrease in width, while their number per unit of frame height will increase. Finally, an instant comes when adjacent black and white bars fall on adjacent scanning lines. This is a limiting case, because if we move the test chart farther away, the bars can no longer be reproduced separately since the number of lines is finite. Thus, the maximum number of details or elements that can be accommodated vertically (the maximum vertical resolution $R_{V\max}$ is half the number of lines per frame (there are $Z/2$

white bars and $Z/2$ black bars), or

$$R_{V \max} = Z/2 \quad (1.39)$$

In practice, it never happens that so many black and white bars can be accommodated in the picture vertically. Suppose that the test chart is slightly moved up or down or that the camera is shifted a little up or down. This small displacement may cause the bars in the television picture to merge completely. Figure 1.24*b* illustrates a case where the black and white bars fall midway between scanning lines. The scanning beam of the camera tube will produce an averaged signal for each line, corresponding to gray (because now each line is half-white and half-black). On the receiver screen, a continuous gray field instead of separate bars will be seen (Fig. 1.24*c*). It appears that vertical resolution falls to zero.

The test-chart bars might partly merge if the scanning lines are tilted or bent, or caused to move by instability in the power sources, or differ in vertical density because of the nonlinearity of the vertical sweep, etc. This is why the number of lines per frame does not give an accurate measure of vertical resolution. With a smaller number of bars, the relative position of the horizontal bars and scanning lines affects vertical resolution less. This is why the practical vertical resolution is

$$R_V = (0.6 \text{ to } 0.7) R_{V \max} = (0.3 \text{ to } 0.35) Z$$

Horizontal resolution (along the lines) is investigated with the aid of a test chart on which vertical black bars are drawn against a white background (Fig. 1.24*d*). Obviously, moving this test chart up or down, left or right relative to the scanning lines will not cause any changes in the image reproduced. Thus, horizontal resolution is independent of the relative position of the image and scanning lines.

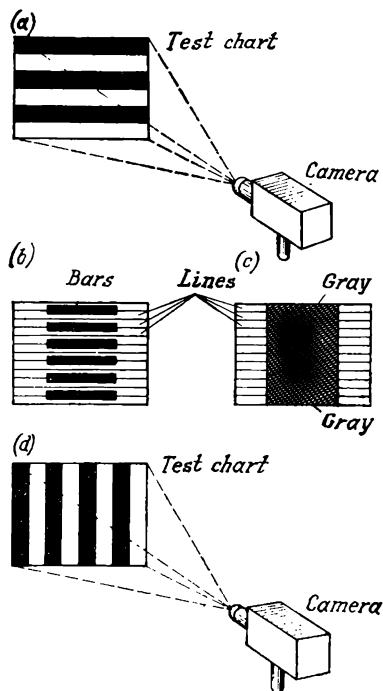


Fig. 1.24. Determination of TV picture resolution

(a) test chart for vertical resolution determination; (b) arrangement of bars of the test chart between picture lines; (c) complete loss of vertical resolution; (d) test chart for determining horizontal resolution

1.11. Aperture Distortion

As the test chart is moved away from the camera tube (and the focusing controls are adjusted as may be necessary), the width of and the spacing between the vertical bars in the television picture will decrease. Finally, at some definite distance, the bars will merge together to produce a continuous gray field.

This limitation on horizontal resolution is above all due to aperture distortion* and the finite bandwidth of the television signal. To

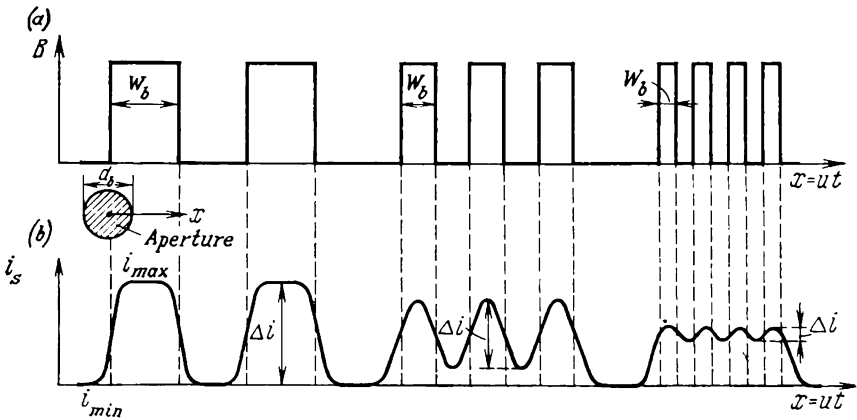


Fig. 1.25. Aperture distortion

(a) relation between luminance pulse (bar) width, W_b , and beam diameter d_b ; (b) amplitude of the television signal, Δi , as a function of aperture distortion

trace the effect of aperture distortion on horizontal resolution, we shall assume that the bandwidth is sufficiently broad not to cause frequency distortion in the image.

How aperture distortion comes about is shown in Fig. 1.25. Suppose that the luminance distribution along a scanning line is as shown in Fig. 1.25a (black and white bars alternate). The electron beam of the pick-up tube moves along the line and produces a television signal (Fig. 1.25b). If the beam diameter, d_b , is smaller than the bar width, W_b , the signal will have 100% modulation, that is, it will vary from i_{max} to i_{min} . If, on the other hand, the beam diameter exceeds the bar width, that is, $d_b > W_b$, the scanning beam will cover a black and some of a white bar at the same time. As a

* In electronic television, the aperture is the cross-sectional area of the electron beam at the point where it is incident on the photocathode of a pick-up tube or the screen of a picture tube.

result, the "black" signal will be brightened up, the "white" signal will be darkened, and the swing of the signal will be decreased. At $d_b = 2W_b$, the beam will cover both a black and a white bar at the same time, and the signal will degenerate to an unvarying "gray" component. In other words, to be capable of resolving fine detail along the scanning line, the electron beam should be sharply pointed. Otherwise, the fine detail occurring along the line will be lost. In a similar way, aperture distortion will cause a loss of image edge gradients (sharpness) (Fig. 1.26). This results in an area, $\alpha\beta$, where a dark element is no longer separated distinctly from a lighter one, and the image definition is spoiled.

Quantitatively, aperture distortion may be expressed in terms of the relative decrease in the signal due to fine detail (Fig. 1.25b):

$$K = \Delta i / (i - i_{\min}) \quad (1.40)$$

Figure 1.27a shows plots of aperture characteristics, $K = f(m)$, obtained experimentally for two most commonly used Soviet-made

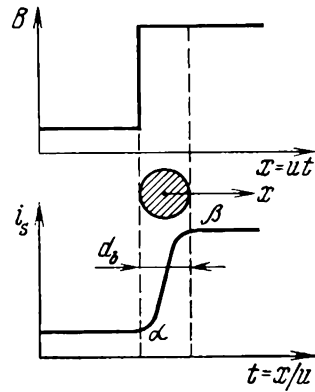


Fig. 1.26. Loss of image edge gradients (sharpness) due to aperture distortion

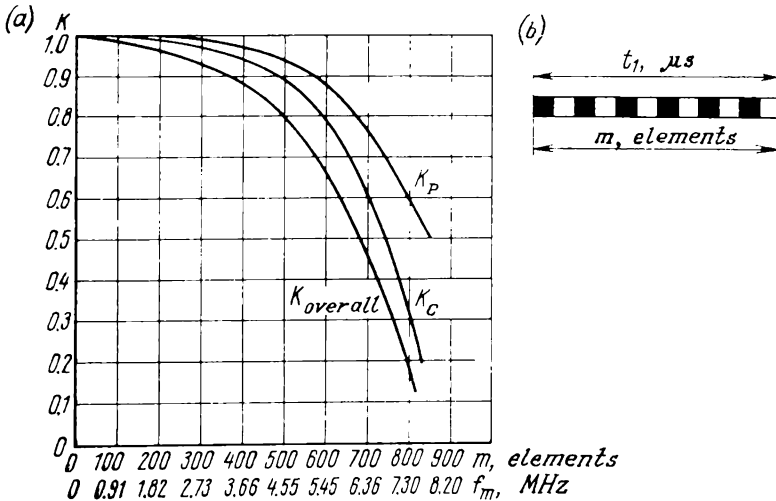


Fig. 1.27. Aperture distortion caused by the camera and picture tubes
(a) aperture characteristics; (b) relation between number of picture elements and their scanning rate

tubes (the ЛИ-201 camera tube and the 59ЛК2Б picture tube). In these plots, m is the number of elements along a line ($m/2$ black and $m/2$ white elements).

The overall aperture distortion is

$$K_{overall} = K_c K_p \quad (1.41)$$

It is seen from Fig. 1.27 that the signal amplitude is 40 to 20% of the maximum corresponding to the standard number of elements per line ($m = pZ = 700$ to 800).

The number of black-and-white elements occurring on a line, m , and the maximum rate, f_m , at which these elements can be scanned as the beam is deflected horizontally can be related in accordance with Fig. 1.27b, as

$$f_m = m/2t_h \quad (1.42)$$

where t_h is the horizontal scan time (usually, $t_h = 0.86T_h = 0.86 \times 64 = 55 \mu\text{s}$).

The values of f_m found by Eq. (1.42) are plotted as abscissa in the plot of Fig. 1.27a in addition to those of m .

CHAPTER TWO

THE PICTURE TUBE

2.1. Picture-Tube Construction

A television picture tube is a cathode-ray tube in which electrical signals are translated into a visible picture, or image, on a phosphorescent screen.

In sketch form, a television picture tube is shown in Fig. 2.1. Its structure essentially comprises an evacuated glass envelope, 1,

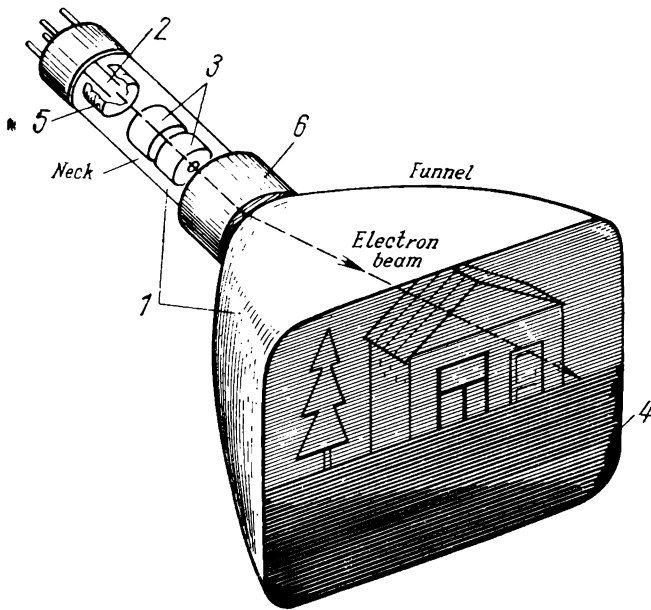


Fig. 2.1. Sketch of a picture tube

which encloses all the remaining elements and screen; an indirectly-heated thermionic cathode, 2, which emits electrons; an electron-optical system, 3, which focuses the electrons into a beam so that at the point where it is incident on the screen its diameter is not more

than the width of one scanning line (which is important for the reproduction of fine detail); a phosphorescent screen, 4, which is a thin coat of phosphor caused to fluoresce by impinging electrons. This coat of phosphor is deposited on the vacuum side of the nearly flat face of the envelope; a control electrode (or modulator), 5, to which the a.c. signal is applied to control (or modulate) the beam in intensity (current), thereby producing variations in screen luminance which correspond to those in the televised scene; and a deflection system, 6, which is put on the neck of the envelope close to its flaring portion. The system has two pairs of deflection coils (one each for horizontal and vertical deflection of the electron beam) which cause the beam to scan rapidly horizontally (line scanning) and at a relatively slower rate vertically (frame scanning). The deflection coils are enclosed in a cylindrical ferrite shield.

Soviet-made picture tubes bear type designations which read as follows:

type 47JK2B—a 47-cm-diagonal (or diameter) cathode ray picture tube, Model 2, white phosphor;

type 59JK3I—a 59-cm-diagonal cathode-ray picture tube, Model 3, colour.

The picture tube accomplishes three forms of beam control by means of electric and electromagnetic fields: (1) focusing; (2) deflection; and (3) intensity modulation. We shall now consider the three forms of control separately in turn.

2.2. Electron Beam Focusing

Both picture and camera (or pick-up) tubes may use any one of two types of focusing: (1) by means of an electrostatic field set up by metal cylinders and diaphragms enclosed within the neck of the tube envelope; usually the axis of symmetry of this field is the same as that of the tube; and (2) by means of an electromagnetic field set up by coils put around the neck of the tube; here, too, the axis of symmetry is the same as that of the tube.

Both electrostatic and electromagnetic focusing has merits and demerits of its own. A major advantage of electrostatic focusing is that it dissipates less power. Also, the elements of an electrostatic focusing system are smaller in size and simple to connect to the supply circuits of the TV set. It is important, too, that the system is insensitive to variations in supply voltage.

Electromagnetic focusing dissipates more power, the focusing coils take a good deal of copper wire to wind them, and the coils have to be enclosed in a steel shell. Because of this the resultant structure is bulky and heavy, with a weight of over one kilogram per coil. In operation, the temperature of the coil wire rises, and so does its resistance because of which the focusing current is reduced and focu-

sing is impaired. As a result, the receiver has to be fitted with a wire-wound rheostat to adjust focus from time to time.

In the Soviet Union, electromagnetic focusing was used in picture tubes manufactured immediately after the second world war (1947 to 1955). At present, broadcast TV sets use only electrostatic focusing. With it, there is no need for periodic focus adjustments and the receiver can be made smaller in size for the same screen size.

2.3. Electrostatic Focusing

In diagrammatic form, an electrostatic focusing system for a picture tube is shown in Fig. 2.2. It is seen to consist of two parts: (1) the main lens formed by the focusing anode, 3, and the main anode, 4; the associated electric field is marked by the dashed lines *a* and *b*;

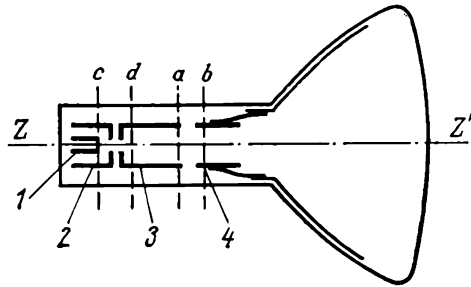


Fig. 2.2. Sketch of an electrostatically focused picture tube

(2) an immersion lens formed by the emitting surface of a thermionic cathode, 1, a control electrode, 2, and the focusing anode; the associated field is marked by the dashed lines *c* and *d*.

A rigorous mathematical description of electron lenses (both electrostatic and magnetic) leads to unwieldy and complex equations which cannot be used for the engineering design of these lenses with sufficient simplicity. Therefore, we shall dwell only on the basic features of focusing systems.

Consider the operation of the main lens shown in sketch form and on an exaggerated scale in Fig. 2.3a. On the inside, the bulb and part of the neck of the envelope are given a coat of aquadag, 1, a conductive graphite coating, which serves as the main anode of the picture tube. A high-tension voltage, V_a (relative to the cathode) is applied to the main anode via a terminal, 5, which passes through the glass and connects to the aquadag coat. The focusing anode, 3, is fed a direct voltage, V_f , such that $V_f < V_a$. The lens is formed by two coaxial cylindrical electrodes, 2 and 3. Electrode 2 is held in contact

with the aquadag coat by springs 4. The equipotential surfaces in the field set up between electrodes 2 and 3 are represented by curves $\alpha\beta\gamma$. The electrons emitted by the cathode form a diverging beam which is caused to move by the accelerating voltages V_f and V_a towards the screen. On passing through the focusing field $\alpha\beta\gamma$, the diverging

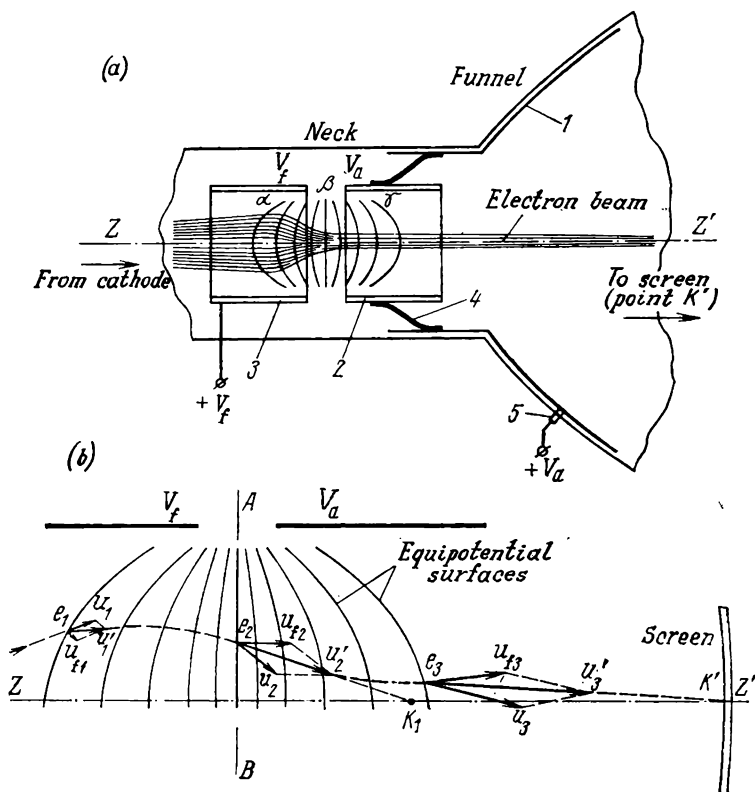


Fig. 2.3. Operation of the main lens in an electrostatic focusing system (a, b)
1—aquadag; 2—main (second) anode; 3—focusing electrode; 4—contact springs; 5—main-anode (ultor) terminal

beam turns into a converging one. By adjusting the voltage difference, $V_a - V_f$, it is possible to have the point of convergence, K' , fall on the surface of the phosphorescent screen.

In greater detail, the focusing action of the electrostatic field is explained in Fig. 2.3b. Each electron enters the focusing field (point e_1 on the projection of an equipotential surface) at velocity u_1 . For convenience, we recall one of the definitions of an equipotential surface: a free charged particle of zero mass and of zero initial velocity, when placed in an electric field, will travel along a path per-

pendicular to the equipotential surface. In our case, an electron of charge e has a mass m and an initial velocity u_1 . Interacting with the charge on the electron, the electric field imparts to it a new velocity component the vector of which, u_{f1} , is at right angles to the equipotential surface at point e_1 . The resultant velocity u_1 and, as a consequence, the direction in which the electron is travelling at point e_1 is the vector sum of u_1 and u_{f1} . It is seen from Fig. 2.3b that the velocity components u_f due to the focusing field cause the diverging

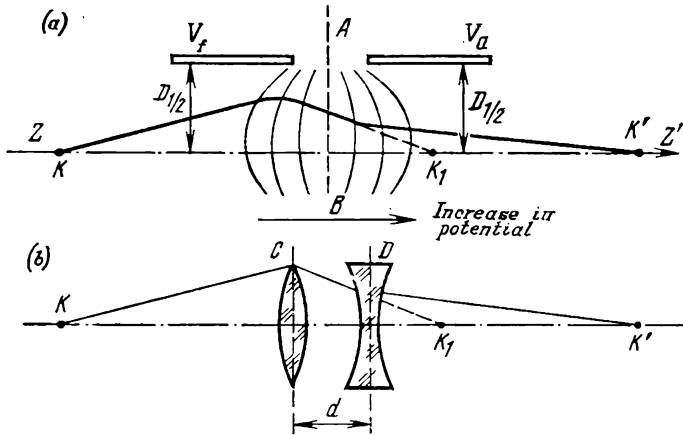


Fig. 2.4. Analogy between an electron and a light optical system
(a) electronic focuser; (b) light focusing system

paths of the beam electrons to converge (focus) on the axis ZZ' of the tube. As a result, on moving from left to right, the paths of electrons, e_1, e_2, \dots , tend to curve more and more towards the tube axis.

The line AB in Fig. 2.3b marks the position of the surface crossing the focusing field at the points where the perpendiculars to that surface are parallel to the tube axis. To the right of this surface the vectors of velocity u_f are directed away from the axis ZZ' ; that is, these components are now having a defocusing effect on the electron beam. Yet, on the whole, the optical system of Fig. 2.3b does focus the diverging electron beam into one converging towards the axis (at point K'). If there were no electric field on the right of the surface AB (which is physically unfeasible), the beam would converge at point K_1 which is closer to the focusing system than point K' . Because of the action exerted by the right-hand half of the field, this happens at a farther point, K' .

Figure 2.4 draws an analogy between an electron and a glass optical system. The partial field to the left of the surface AB (Fig. 2.4a) is

analogous to a collecting (converging) lens C (Fig. 2.4b), and the right-hand field, to a diverging lens, D . Using Eq. (1.25) from light optics, it can be shown that the system in the figure is, on the whole, a collecting (converging) one. The equation in question has the form

$$\varphi = \varphi_1 + \varphi_2 - d\varphi_1\varphi_2 \quad (2.1)$$

where φ = focal power of a two-element lens defined as $\varphi = 1/f$ where f is the focal length of the lens
 $\varphi_1 = 1/f_1$ = focal power of the first element
 $\varphi_2 = 1/f_2$ = focal power of the second element
 d = spacing between the lens elements

In electron optics it is proved that the focal power of an electron lens decreases with increasing potentials on its equipotential

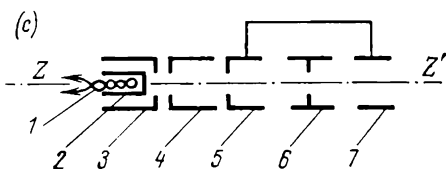
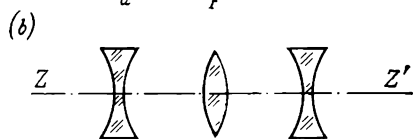
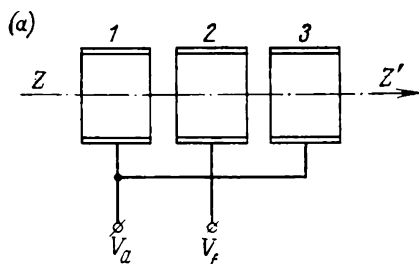


Fig. 2.5. Multi-element focusing systems (a) three-electrode focuser; 1, 3—main anode 2—focusing anode; (b) optical analog of the above system; (c) pentode electron gun: 1—heater; 2—thermionic cathode; 3—control electrode; 4—accelerating electrode; 5, 7—main anode; 6—focusing electrode

surfaces. Because the potentials (relative to the cathode) on the right of surface AB (Fig. 2.4a) are higher than those on the left, the focal power of the diverging lens in Fig. 2.4b will be lower than that of the converging lens, that is, $|\varphi_d| < \varphi_c$. On putting $|\varphi_d| = \alpha\varphi_c$ where $\alpha < 1$, and substituting φ_d and φ_c in Eq. (2.1), we get

$$\begin{aligned} \varphi &= \varphi_c - \alpha\varphi_c - d\varphi_c (-\alpha\varphi_c) \\ &= (1 - \alpha)\varphi_c + d\alpha\varphi_c^2 \end{aligned}$$

Because $1 - \alpha > 0$, the optical power of such a two-element lens is positive, and the whole system is a converging one.

It should be stressed that the presence of a diverging lens in the focusing system of Fig. 2.4 produces no detrimental effect; in fact, this is an advantage because it markedly reduces the spherical aberration of the entire system (see Fig. 1.12) by causing the electron paths to converge more accurately to the point K' on the screen.

The focusing system shows good performance when it has three electrodes instead of two (Fig. 2.5a). As is seen, the same voltage

is applied to electrodes 1 and 3. Such a system has a wider range of variables (diameters, electrode spacings, etc.) which may be matched so as to correct aberrations more effectively. Also, the middle (focusing) electrode, 2, maintained at a potential, V_f , which is below V_a , does not remove electrons from the beam. Owing to this, the current in the focusing electrode circuit is zero, and the entire system gives a more reliable and consistent performance.

An analogy between light and electron optics is shown in Fig. 2.5b. The electron-beam producing structure (usually called an *electron gun*) consisting of four electrodes (a cathode, control electrode, focusing electrode and main anode, Fig. 2.2) suffers from an unpleasant

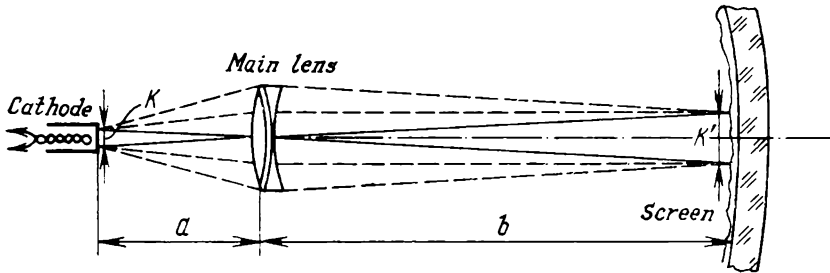


Fig. 2.6. Focusing system using a main lens alone

effect which consists in that a change in the voltage at the control electrode (done in order to modulate the beam in intensity) affects the quality of focus. For example, an increase in the beam current (producing a brighter spot on the screen) has a defocusing effect. As a result, the highlights suffer a loss in both resolution and sharpness in comparison with the lowlights. This limitation is markedly reduced in a five-electrode (pentode) electron gun. In diagrammatic form, a pentode electron gun is shown in Fig. 2.5c. As is seen, there is one more, accelerating, electrode, 4. This electrode usually maintained at $V_{accel} = 500$ to 800 V acts to equalize the quality of focus in both the bright and dark portions of the image.

Apart from the main focusing system examined above, all thermionic-cathode TV tubes (both camera and picture) use one more focusing device, called an immersion lens which sets up a field in close proximity to the thermionic cathode. The need for this type of lens may be explained as follows. Refer to Fig. 2.6 which shows an optical focusing system using only one main lens. For simplicity, we shall neglect its aberrations. An image of the cathode with a diameter K is projected by the main lens onto the screen as a circle of diameter K' with a magnification β defined as

$$\beta = K'/K = b/a \quad (2.2)$$

For ordinary picture tubes, $b \approx 3a$, that is, $\beta \approx 3$. In other words, the diameter of the electron beam at the point where it strikes the screen will be three times the cathode diameter. In practice, to obtain a beam current sufficient for the screen to give up the desired luminance, the emitting surface of the cathode must have a diameter $K \geq 1$ mm. Then the diameter of the luminous spot on the screen will be $K' = 3$ mm. However, K' must not exceed the width of a scanning line, or else it would cover adjacent lines, and this would impair picture definition.

As an example, we shall calculate the limit of spot diameter for the Soviet-made 59JK2E picture tube (Fig. 2.7) for which the

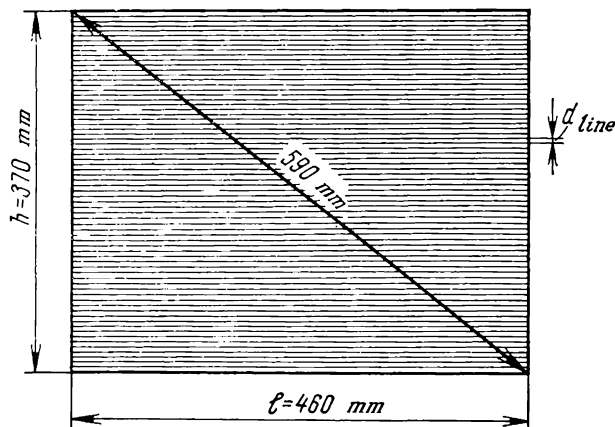


Fig. 2.7. Determining the limiting spot diameter

screen height is $h = 370$ mm, the number of lines per frame is $Z \approx 600$; the line width is $d_{line} = h/Z = 370/600 \approx 0.6$ mm.

Thus, if appropriate measures are not taken, the beam spot would cover $K'/d_{line} = 3/0.6 = 5$ lines at a time.

This drawback is eliminated by the use of an immersion lens. The optical train of this lens is shown in Fig. 2.8a. It contains a cathode, a control electrode (modulator), an accelerating electrode (in a pentode electron gun) or focusing electrode (in a tetrode electron gun). Since the difference in potential between the accelerating electrode and cathode is 600 to 800 V, and the spacing, l , between them is negligible (5 to 8 mm), the electric field set up in the immersion lens is of a considerable intensity, and its equipotential surfaces have the configuration shown by the dashed lines in the drawing. The electrons emitted by the thermionic cathode are compressed by this field into a narrow beam which has a characteristic neck called the crossover. The diameter K_1 of the crossover is a fraction

of that of the emitting surface, K , on the cathode. The main focusing system throws an image of the crossover onto the screen (Fig. 2.8b).

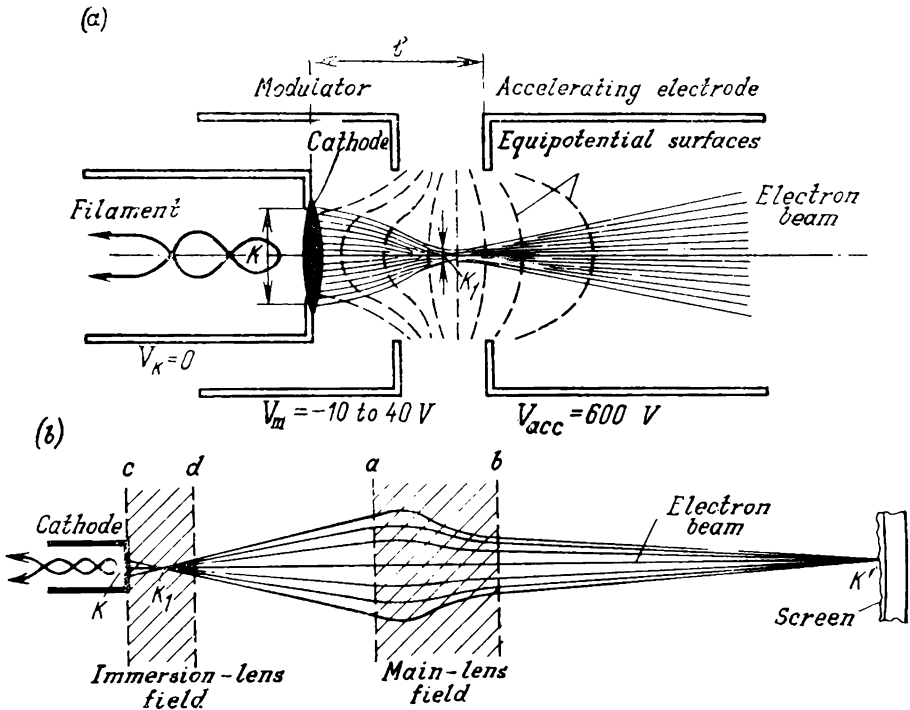


Fig. 2.8. Immersion lens

(a) optical train; (b) complete beam focusing system of a picture tube

As in the previous example, we shall calculate the required degree of beam compression in the immersion lens. Assuming that $K' = 0.6$ mm and having $K = 1$ mm and $\beta = 3$, we get

$$\beta_{i.l} = K/K' = \beta K/K'' = 3 \times 1/0.6 = 5$$

That is, an immersion lens will compress the electron beam to one-fifth of its original diameter.

2.4. Electromagnetic Focusing

In sketch form, a picture tube in which the electron beam is focused by the magnetic field of a suitably shaped coil is shown in Fig. 2.9a. The coil, called the focuser, is put on the neck, close to the deflection system or yoke. In this type of picture tube, there is no main

electrostatic lens, and use is therefore made of a simpler triode electron gun made up of elements 1, 2 and 3 which form an immersion lens.

The focuser is essentially in three parts (Fig. 2.9 *b*): a steel pole piece and end-plate or cheek, 1, a paper-base-laminate former, 2, on

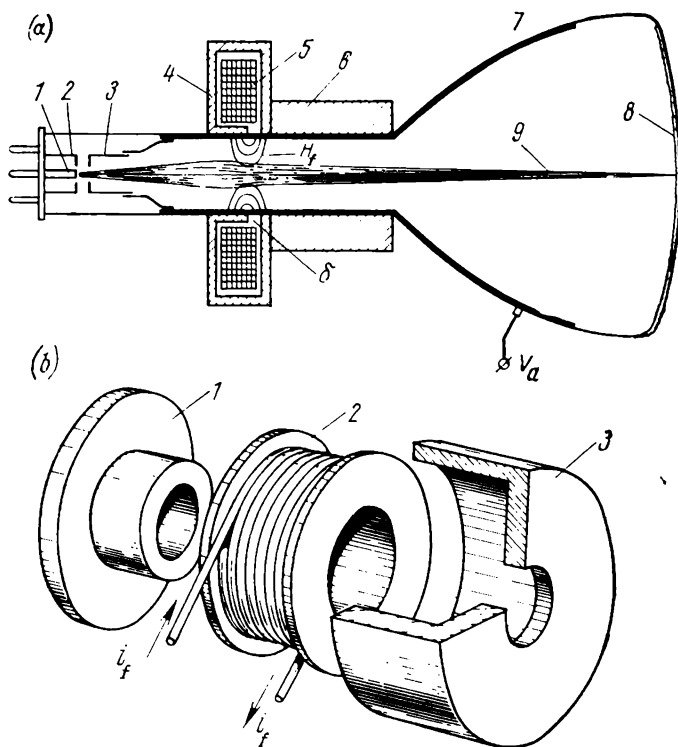


Fig. 2.9. Magnetic focusing by a short coil

(a) sketch of a coil-focused picture tube: 1—thermionic cathode; 2—control electrode; 3—main anode; 4—steel yoke shield; 5—focusing coil; 6—deflection yoke; 7—tube funnel; 8—phosphor screen; 9—electron beam; δ —magnetic air gap; H_f —focusing field; (b) focusing coil: 1—steel pole-piece and cheek; 2—paper-base-laminate former; 3—steel shield

which a coil is wound, and a steel shield, 3, which leaves a short circular air gap, δ (Fig. 2.9a), where the focusing magnetic field is concentrated.

For better insight into the operation of an electromagnetic focusing system, refer to Fig. 2.10. An electron moving along path AB which lies in plane I enters the magnetic field at point e with a velocity \bar{v} . The axis of symmetry, ZZ' , of the picture tube lies in the

same I -plane which also contains a line of force. The field intensity vector \bar{H} is directed along a line which is tangent to the line of force, $\alpha\beta$. The interaction between the velocity vector \bar{u} of the moving particle e and the field intensity vector \bar{H} is defined in terms of Lorentz's force as

$$\bar{F} = e[\bar{u}\bar{H}] \quad \text{or} \quad F = euH \sin \varphi$$

where φ = angle between the vectors \bar{u} and \bar{H}
 e = charge on the electron

Since the vector \bar{F} is defined by the vector product of \bar{u} and \bar{H} , it lies in the Q -plane normal to the I -plane. For convenience, we

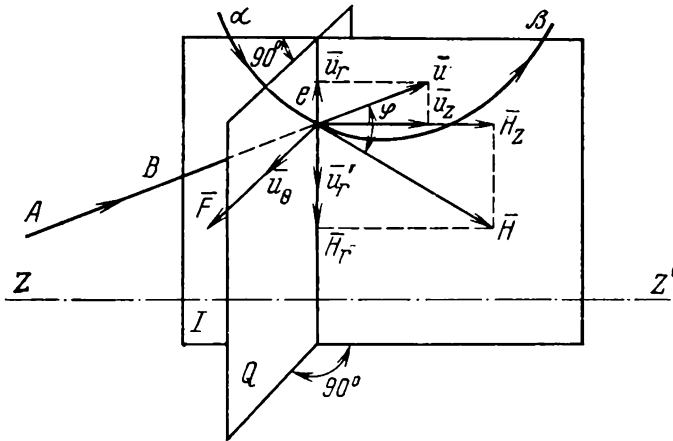


Fig. 2.10. Explaining operation of the focusing system

resolve the vectors \bar{u} and \bar{H} into components directed along the axis of the tube (\bar{u}_z and \bar{H}_z) and at right angles to it (\bar{u}_r and \bar{H}_r). Hence, we may conclude the following: (1) the vectors \bar{u}_z , \bar{H}_z and \bar{u}_r , \bar{H}_r do not interact because the sine of the angle between them is zero; (2) the vectors \bar{u}_z , \bar{H}_r and \bar{u}_r , \bar{H}_z do interact because the sine of the angle between them is a maximum (equal to unity).

The function of the focusing system is to compensate for the velocity component \bar{u}_r which causes the electron to depart from the axis ZZ' of the tube.

The direction in which the interaction force \bar{F} acts can be found by the right-hand rule (for electrons moving in a magnetic field) as follows: placing the fingers in the direction of the velocity vector \bar{u}_z , so that the field intensity vector \bar{H}_r enters the palm, the thumb

will indicate in the direction of the vector $\bar{F}_1 = e [\bar{u}_z \bar{H}_r]$ lying in the Q -plane normal to the I -plane. In the same manner, it can be shown that the force of interaction $F_2 = e [\bar{u}_r \bar{H}_z]$ between the vectors \bar{u}_r and \bar{H}_z is in the direction of the force \bar{F}_1 : $F = F_1 + F_2$.

Thus, the interaction between the velocity vector \bar{u} of the electron e and the field intensity vector \bar{H} causes the electron to leave

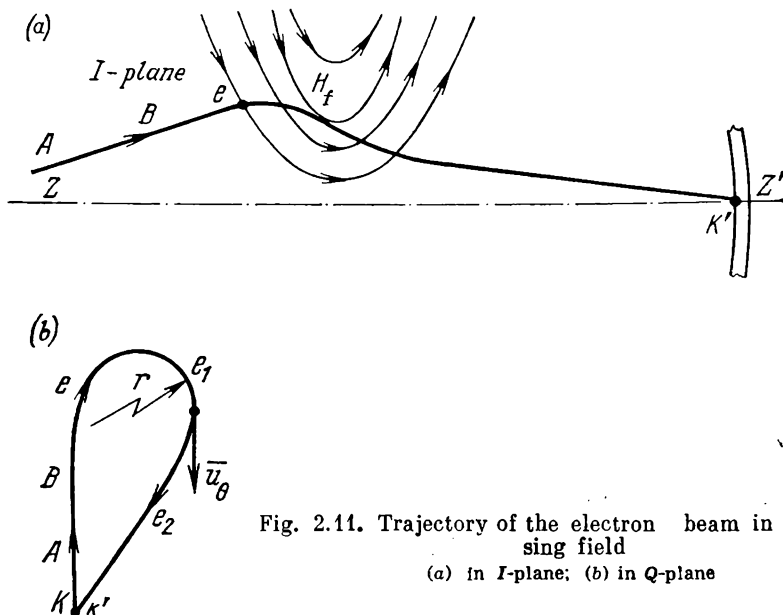


Fig. 2.11. Trajectory of the electron beam in the focusing field

(a) in I -plane; (b) in Q -plane

the I -plane. The force \bar{F} imparts to the electron a new velocity component, \bar{u}_θ , which causes the electron to move along a curve lying in the Q -plane normal to the I -plane.

The velocity vector \bar{u}_θ interacts with the intensity component vector \bar{H}_z and gives rise to a force $\bar{F}_r = e [\bar{u}_\theta \bar{H}_z]$ driving the electron path towards the axis ZZ' (the direction in which the force \bar{F}_r acts can likewise be determined by the right-hand rule). In turn, this force imparts to the electron a velocity component \bar{u}_r directed towards the axis ZZ' . To sum up, the beam is focused as a result of a consecutive compensation of the defocusing velocity component \bar{u}_r by the focusing component \bar{u}_r .

The projection of the resultant trajectory of the electron in the I -plane appears in Fig. 2.11a.

The rotating velocity components u_θ in planes normal to the I -plane impart to the electron an additional displacement in the Q -plane along the curves e , e_1 , e_2 , . . . , shown in Fig. 2.11b. This

figure shows the projection of the electron trajectory onto one of the Q -planes normal to the I -plane. In this plane, the electron traces out a curve the instantaneous radius of which is given by

$$r = (mu_0)/(eH_z)$$

where m and e are the mass and charge of an electron.

Since the velocity u_0 and the field intensity component H_z vary as the electron moves from cathode to screen, the radius of curvature, r , of the curve e, e_1, e_2, \dots will change too.

The position of the point K' where the electron trajectories converge can be controlled (so as to place the point of convergence precisely on the screen, that is, to adjust focus) by varying the current traversing the focusing coil.

2.5. Modulation of the Electron Beam

Control of the beam current with the voltage applied between the control electrode and cathode is often referred to as beam modulation. In its effect, the control electrode (modulator) in a picture tube is similar to the control grid in a radio tube, and it is called the control grid, too. The higher the negative voltage between the control grid and the cathode, the smaller the beam current. The effect of the voltage applied between the control grid and the cathode on the beam current can be explained by two factors. Firstly, this negative voltage, by repelling the electrons in the cathode space charge, causes them to move back towards the cathode. Secondly, the control-grid voltage changes the shape of the electric field set up by the immersion lens so that the effective emitting area of the cathode is reduced. Figure 2.12 shows the distribution of current density at the cathode surface determined experimentally for different control-grid potentials. As is seen, an increase in the negative voltage V_m at the control grid brings about a decrease in the cathode current density, $j_k = di_k/ds$, and reduces the effective cathode diameter, d_k .

The dependence of cathode current on control-grid voltage (control-grid characteristic) is described by an empirical equation of the form

$$i_k = A(V_m - V_b)^v \quad (2.3)$$

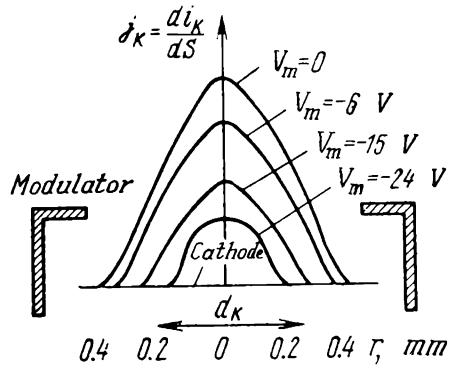


Fig. 2.12. Current density distribution at cathode surface for different modulator potentials

where A = proportionality factor

V_m = absolute control-grid voltage (relative to cathode)

V_b = blanking voltage causing the beam current to fall to zero

γ = exponent decided by the geometry and electric parameters of the electron gun (it usually ranges between 1.5 and 2.5)

The current i_b of the electron beam reaching the screen usually is smaller than the cathode current, i_k , because some of the electrons are intercepted by the accelerating electrode, focusing electrode

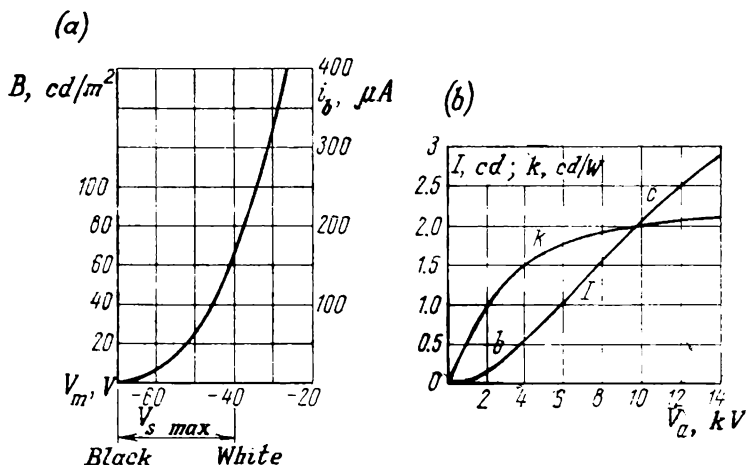


Fig. 2.13. Picture-tube characteristics

a) modulation characteristic; (b) light intensity and luminous efficiency as functions of main-anode (ultor) voltage

and other parts of the picture tube. However the beam current as such is difficult to separate from all other components, and in practice it is usual to quote the relation $i_k = f(V_m)$. In fact the two characteristics, $i_k(V_m)$ and $i_b(V_m)$, may be taken as being identical because the difference between i_k and i_b is negligible (Fig. 2.13a).

The beam electrons which bombard the phosphor on the picture-tube screen are highly energetic (over 10^4 eV). They cause the electrons of the phosphor atoms to move to higher energy levels. On jumping back, these excited electrons give up the additional energy imparted by the beam in the form of quanta of light. This process is called cathodoluminescence.

As the beam impinges on the phosphor, not all of its kinetic energy is converted to light. A good proportion is wasted as heat and, to a far smaller degree, is converted to X-rays. As a rule, the useful

luminous energy is not more than 10% of the total energy imparted by the electron beam.

The materials capable of cathodoluminescence, ordinarily called phosphors, are silicates, sulphides, oxides and phosphates of the metals zinc, cadmium, calcium, magnesium and beryllium. The efficiency of a phosphor can be improved and the desired colour of phosphorescence can be obtained by adding to it so-called activators in amounts as small as a few molecular per cent. The most commonly used activators are copper, silver and manganese.

A phosphor should be highly efficient in converting the energy of the electron beam to light, have a sufficiently long service life, a sufficiently long afterglow (or persistence) close to the duration of one image frame, the requisite colour of phosphorescence, and a sufficiently high secondary electron emission at high values of voltage at the main anode.

The light output of the screen of a picture tube is related to electron-beam power by the following expression:

$$I = ki_b V_a^n \quad (2.4)$$

where I = light output of the screen, cd|

k = proportionality factor

i_b = beam current, A

V_a = H.T. voltage at the main anode, V

n = exponent decided by the physical parameters of the phosphor (usually, $n = 1$ to 2)

A plot relating I to V_a based on Eq. (2.4) is shown in Fig. 2.13*b* for i_b = constant $\approx 10^{-4}$ to 1.5×10^{-4} A.

With an accuracy sufficient for practical applications, Eq. (2.4) can be approximated within the region *bc* by the equation of a straight line:

$$I = ki_b (V_a - V_0) \quad (2.5)$$

Since for existing picture tubes $V_0 = 1$ to 2 kV and $V_a = 10$ to 16 kV and more, $V_a \gg V_0$, and so

$$I \approx ki_b V_a = kP_a \quad (2.6)$$

where P_a is the beam power.

In this case, the factor $k = I/P_a$ takes on a simple practical meaning: it defines the luminous efficiency of a phosphor and is expressed in cd/W.

As is seen from the plot of Fig. 2.13*b*, for conventional picture tubes operating on an E.H. voltage of $V_a > 4$ to 6 kV the luminous efficiency k is practically constant and equal to 2 to 4 candelas per watt of beam power.

The luminance, B , of the screen can be found simply from Eqs. (1.13), (1.14) and (2.6):

$$B = I/S_{\text{screen}} = ki_b V_a / S_{\text{screen}} \quad (2.7)$$

where S_{screen} = surface area of the screen in m^2
 B = screen luminance in cd/m^2

As an example, for the Soviet-made 59JIK2B picture tube, $S_{screen} = hw = 0.37 \times 0.46 \text{ m}^2 = 0.17 \text{ m}^2$, $V_a = 16 \text{ kV}$, $i_b = 10^{-4} \text{ A}$ and $k = 4 \text{ cd/W}$, and the screen luminance is

$$B = ki_b V_a / S_{screen} = 40 \text{ cd/m}^2$$

(compare with Table 1.3 in Sec. 1.2).

Since, in accordance with Eqs. (2.4) and (2.7) the screen luminance is proportional to the beam current, i_b , we may lay off luminance as ordinate on the same plot of Fig. 2.13a. Sometimes, this plot is referred to as the light modulation characteristic of a picture tube.

In practice, the maximum beam current of a conventional picture tube is $i_{b \text{ max}} = 100 \text{ to } 150 \mu\text{A}$ (in which case, in accordance with Fig. 2.13a, the control-grid voltage is $V_{g \text{ max}} = -40 \text{ to } -45 \text{ V}$). A greater beam current would impair focus and there is a danger that the strong beam would burn through the phosphor. Thus, the working range of signal voltage, V_{sign} , in accordance with Fig. 2.13a, extends from -70 V (the darkest portion of the image) to -40 V (the brightest portion).

2.6. Factors Affecting Picture Contrast

The electron beam striking the phosphor causes it to emit light in two directions: outside, towards the viewer, and inside the envelope. Partly reflected from the internal coating of the envelope,

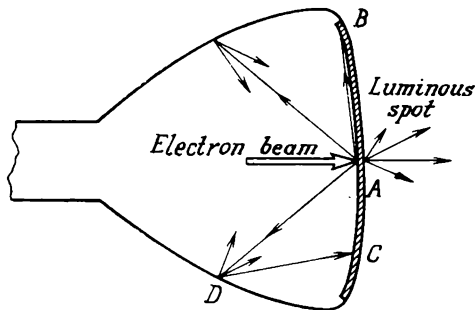


Fig. 2.14. Reduced picture contrast due to internally scattered light

the light rays are scattered and reach the screen again where they brighten up the darker portions of the image (for example, ray DC in Fig. 2.14), thereby reducing the contrast of the picture. A further impairment in picture contrast comes about because the face of the picture tube is made slightly convex to resist atmospheric pres-

sure, and this curvature enables some rays to go directly from high-lights to shadows (for example, ray AB).

Another cause of reduced picture contrast is halation. The effect of halation which affects mostly fine and medium detail is illustrated in Fig. 2.15*a*. The electron beam striking the screen at, say, point A excites the phosphor. Some of rays going out of this point travel forward, towards the viewer, and some are reflected at the interface between the glass and the air and go back to illuminate

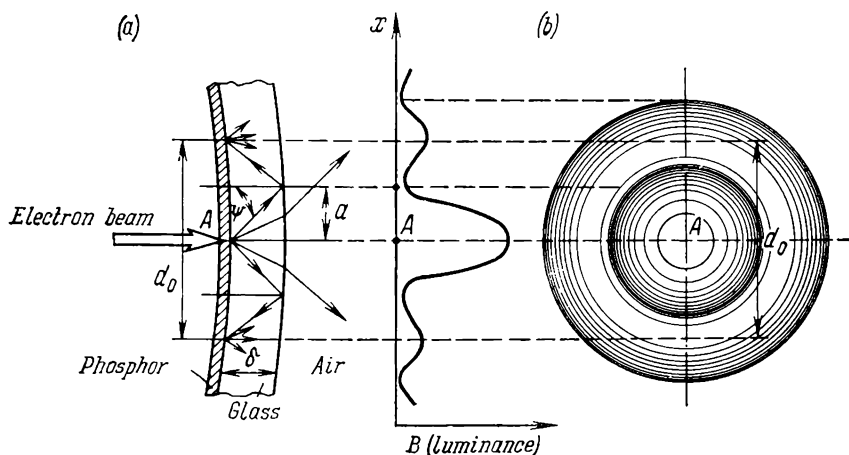


Fig. 2.15. Halation

(a) paths of rays in the tube face-plate; (b) luminance distribution

the phosphor around point A . As a result, the viewer can see a bright luminous spot surrounded by a less bright ring, the halo (Fig. 2.15*b*). The diameter of the halo, d_h , can be determined approximately, assuming that total internal reflection (TIR) takes place. If light is incident on the interface between the glass and the air at sufficiently great angles, it will be reflected totally, without crossing the interface. The angle ψ (Fig. 2.15*a*) at which this occurs is called the critical angle. For glass against air this angle is 42° . Using this figure and the construction in Fig. 2.15*a*, the diameter of the halo is then

$$d_h = 4a = 3.6\delta \quad (2.8)$$

where

$$a = \delta \tan 42^\circ = 0.9\delta$$

Of course, this is an approximate expression because the halo has no sharply defined edges. Recalling that the thickness of the screen glass is usually about $\delta = 5$ mm, the halo diameter will be $d_h = 3.6 \times 5 = 18$ mm. If the image has fine detail such as dark dots or

lines, they will be overlapped by halos from adjacent highlights, and their contrast will be drastically reduced. Obviously, halation can affect the contrast of detail from very fine to that measuring about $d_h/2 = 9$ mm. Similarly, halation impairs contrast in coarse detail by reducing the sharpness of edge gradients.

An effective way to improve contrast and luminance of the television picture is to deposit a thin film of aluminium on the vacuum side of the picture tube (Fig. 2.16a). The reflecting aluminium film is usually 0.05 to 0.5 μm thick. The electron beam accelerated at

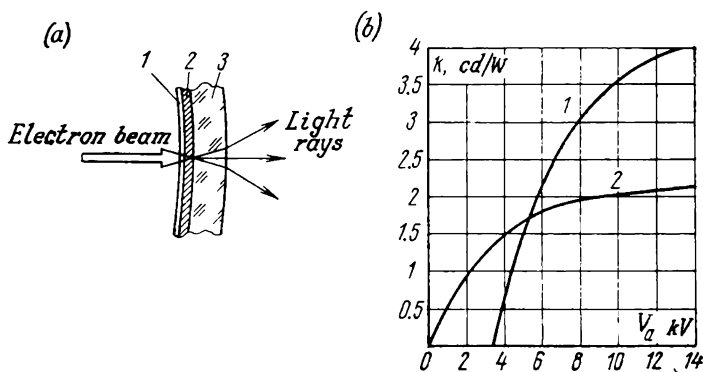


Fig. 2.16. Aluminized picture-tube screen

(a) detail of screen structure: 1—aluminium backing; 2—phosphor; 3—face-plate; (b) luminous efficiency as a function of anode voltage: 1—for aluminized screen; 2—for non-aluminized screen

6 kV and more (the anode voltage of the picture tube) penetrates this film readily and excites the phosphor. The aluminium film blocks light from passing inside the envelope, thereby improving the contrast of the picture appreciably. Also, this film acts as a mirror reflecting light towards the viewer. This practically doubles the luminance of the image.

The efficiencies of an aluminized, 1, and of a non-aluminized, 2, screen as a function of anode voltage are shown in the plot of Fig. 2.16b. At an anode voltage of 10 kV and more, the aluminized screen yields twice as much light per watt of beam power. Also, the aluminium film is opaque to the massive ions, thereby protecting the screen against damage by ion bombardment and the appearance of the cross-burn (to be discussed in greater detail in Sec. 2.11).

While improving the contrast of coarse detail as it removes back-lighting, the aluminium film does not practically reduce halation, and the contrast of fine detail remains low. One way to improve the contrast of fine detail is to use neutral-filter glass for the screen of the picture tube. This is done by adding appropriate ingredients to

the glass in the process of making to increase light absorption. The manner in which the filter glass operates to improve the picture contrast is explained in the diagram of Fig. 2.17. The incident light ray, I_1 , emitted by a luminous point A on the phosphor traverses a path, AB , in the filter glass. The interfering ray, I_2 , due to halation, has to traverse a markedly longer path, $ACDE$, in the filter glass, and is therefore absorbed more.

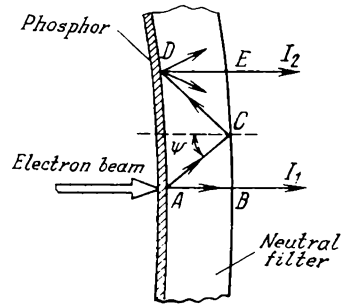


Fig. 2.17. Use of filter glass

2.7. Spectral Emission Characteristic of Screen Phosphors

Most often, phosphors for black-and-white picture tubes are made from a mechanical mixture of two components: (1) zinc sulphide and (2) zinc-cadmium sulphide. This mixture is activated with a few molecular per cent of silver which improves the luminous efficiency of the phosphor by a considerable amount. The activator also affects the colour of screen luminescence.

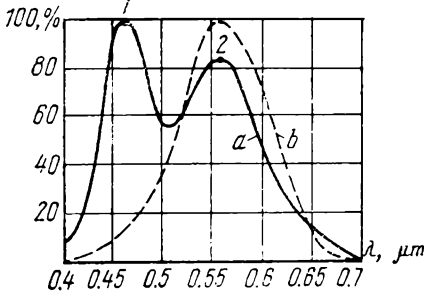


Fig. 2.18. Spectral emission characteristic of screen phosphors for black-and-white picture tubes

As an example, Fig. 2.18 shows the spectral emission characteristic of BM-5 phosphor for black-and-white picture tubes (chemical formula: $\text{ZnS} : \text{Ag} + \text{Zn}$, 47%; $\text{CdS} : \text{Ag}$, 53%).

This phosphor has a predominantly blue emission because peak 1 exceeds peak 2. As is seen from the plot of Fig. 2.18, the spectral emission characteristic a of BM-5 phosphor lies within the visibility curve b of the human eye, and this enhances luminous efficiency of the screen.

2.8. Phosphor Persistence

The plot of Fig. 2.19 shows variations in the luminance of a screen element with time (BM-5 phosphor is taken as an example). During the time interval, T_f , while it dwells on a screen element, the beam

causes it to fluoresce (curve LM). Then the beam moves on to the next element, the light given out by the previous element gradually decays (curve MN) and this is observed as persistence of light emission after excitation, or afterglow. The time interval during which

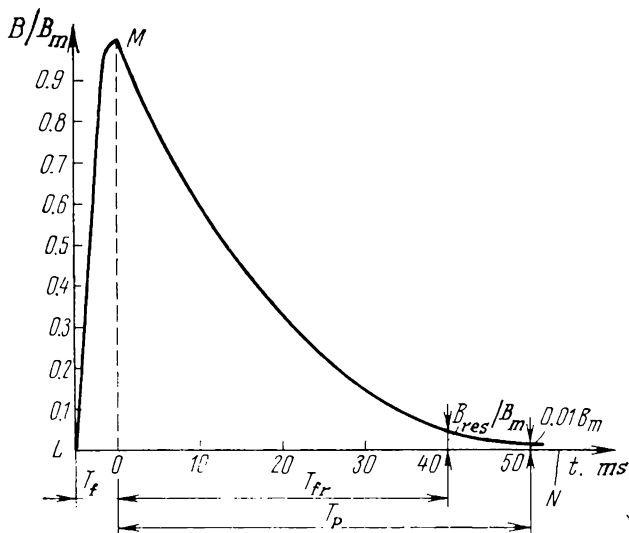


Fig. 2.19. Persistence characteristic of a phosphor

the luminance decays to 1% of its peak value after the beam has moved on is called the persistence time of the phosphor, T_p .

Phosphor persistence plays a positive part because it reduces flicker. However, excessive persistence causes the fast-moving parts of the image to appear smeared. Therefore, it is desirable that afterglow should decay completely within the time interval required to transmit one frame, $T_{fr} = 1/25 \text{ s} = 4 \times 10^{-2} \text{ s}$ (or two fields in the case of interlaced scanning). Experience shows that the smear of fast-moving objects becomes unnoticeable when the luminance carried over from the previous frame does not exceed 5%.

With an accuracy sufficient for practical needs, the decay characteristic (curve MN) may be approximated by an exponential relation of the form

$$B = B_m \exp(-t/\tau) \quad (2.9)$$

The time constant, τ , in the above expression depends on the physical and chemical characteristics of the phosphor. For БМ-5 phosphor, the persistence time, T_p , is about $5 \times 10^{-2} \text{ s}$. Once T_p is

known, the time constant τ can be determined from Eq. (2.9):

$$\tau = \frac{T_p}{\ln(B_m/0.01B_m)} = 5 \times 10^{-2} \div \ln 100 = 1.1 \times 10^{-2} \text{ s}$$

Substituting $\tau = 1.1 \times 10^{-2}$ and $T_{fr} = 4 \times 10^{-2}$ s in Eq. (2.9), we find that the screen luminance remaining at the end of frame transmission is

$$B_{res} = B_m \exp(-T_{fr}/\tau) = B_m \exp(-4 \times 10^{-2}/1.1 \times 10^{-2}) \approx 0.03B_m$$

which is acceptable.

2.9. Beam Deflection

The third form of beam control, beam deflection, has as its objective to move the beam horizontally (line deflection) and vertically (frame deflection). As it is deflected both vertically and horizontally, the beam synthesizes, or reproduces, the televised scene line by line and frame by frame as a television image (see Fig. 2.1).

The beam may be deflected either by plates (electrostatic deflection) or by coils (electromagnetic deflection). In the early years of television both forms were used. However, electrostatic deflection lost its importance with the advent of large-size picture tubes with great diagonal deflection (or bulb) angles. The deflection systems using plates, 1, and coils, 2, are compared in Fig. 2.20a. The plates are fed a sawtooth deflection voltage, V_d , and the coils are energized with a sawtooth deflection current, I_d .

An advantage of electromagnetic deflection is that the beam can be deflected through a fairly large diagonal angle (at present, $2\varphi_m \geq 110^\circ$) without causing appreciable beam defocusing. In electrostatic deflection, the limiting deflection angle, $2\varphi_e$, for which the beam defocusing is still tolerable does not practically exceed 30° . As is seen from Fig. 2.20a, the small deflection angle realizable in an electrostatically deflected picture tube makes the envelope bulky and heavy. In accordance with Fig. 2.20a, the tube length is $L \geq (D/2) \cot \varphi$. Assuming that the tube has a diagonal $D \geq 60$ cm, for an electrostatically deflected tube this will give

$$L_e = (D/2) \cot \varphi_e = (60/2) \cot 15^\circ = 110 \text{ cm}$$

and for a magnetically deflected tube,

$$L_m = (D/2) \cot \varphi_m = (60/2) \cot 55^\circ = 21 \text{ cm}$$

or

$$L_e/L_m = 110/21 = 5.25 \text{ times}$$

Mention should be made of one more drawback associated with electrostatic beam deflection: the amplitude of the deflection voltage, V_d , applied to the plates is about one-third of the anode voltage, V_a . At $V_a = 16$ kV, the deflection voltage is $V_d \approx 5$ kV.

Such a voltage is difficult to generate by economical circuits. This is why present-day TV receivers use solely picture tubes with magnetic beam deflection.

As picture-tube manufacture advanced, the tube envelope grew progressively shorter, the screen bigger in size, and its mass decrea-

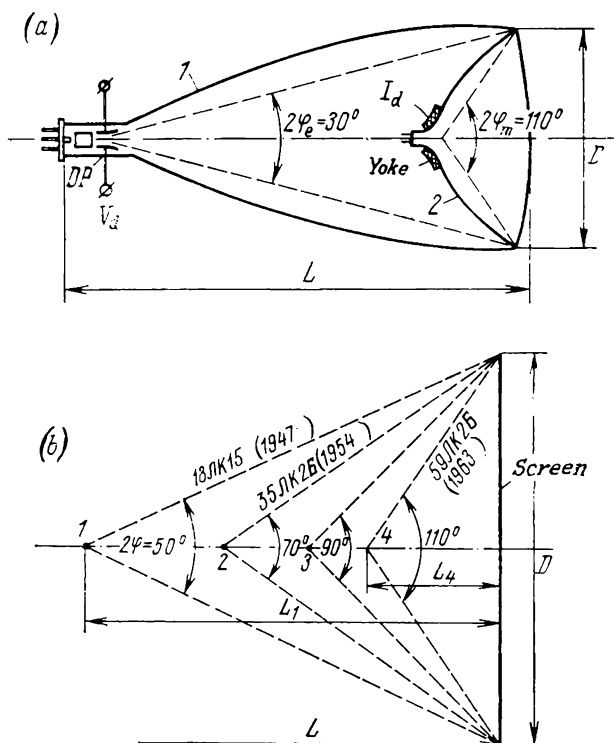


Fig. 2.20. Relative size of a picture tube as a function of deflection angle
(a) for 30-deg and 110-deg picture tubes; (b) relative length of magnetically deflected tubes for different deflection angles

sed. The increase in screen size made it necessary to increase the deflection angle. The manner in which the bulb angle, 2φ , increases with decreasing envelope length L and with the screen diagonal, D , held constant is illustrated in Fig. 2.20b. By 1963, the relative length of the picture tube had decreased to one-third of its size in 1947 (from $L_1 = 105$ cm to $L_2 = 35$ cm).

With a short picture tube, the TV receiver can be enclosed in a smaller cabinet and made more compact and handy, which is an advantage in the home.

2.10. Operation of an Electromagnetic Deflection Yoke

Two pairs of coils, or yokes, are used to deflect the beam in a magnetically deflected picture tube; one pair does so horizontally (a horizontal yoke) and the other pair vertically (a vertical yoke). As an example, Fig. 2.21*a* shows a sketch of the vertical yoke. The

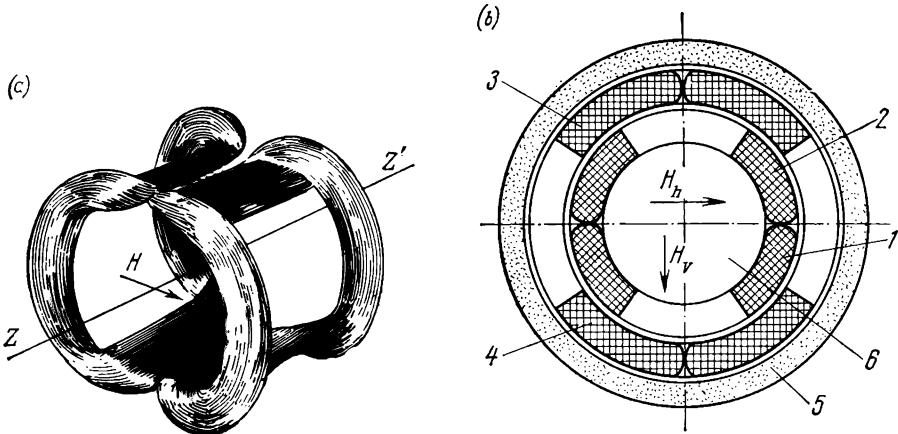


Fig. 2.21. Deflection yoke

(a) sketch of vertical deflection coils; (b) sectional view through deflection yoke: 1 and 2—horizontal deflection coils; 3, 4—vertical deflection coils; 5—ferrite shell; 6—tube neck

field intensity vectors are at right angles to the tube axis. Figure 2.21*b* shows a sectional view of the complete deflection yoke comprising the two pairs of coils and a ferrite shell or shield.

The manner in which the electron beam is deflected by a uniform magnetic field due to the deflection yoke of axial length a is shown in Fig. 2.22. In this figure, the magnetic lines of force are at right angles to the plane of the drawing and directed towards the reader. The effective length of the deflecting field is somewhat shorter than the geometrical length of the yoke. This difference is due to the edge effect, the design of the yoke ends, etc. The difference, however, is negligible, and for simplicity it may be assumed that the effective length of the deflecting field does not differ from axial yoke length.

On the neck, the deflection yoke must be placed as close to the flaring part (funnel) of the envelope as possible; otherwise, the electron beam deflected by the yoke would be intercepted by the neck, and shadows would form in the corners of the raster.

In present-day picture tubes, the tube face (screen) is made slightly convex—the radius of curvature, r , is two or three times the

radius of deflection, l (Fig. 2.22)*. If no measures were taken, the raster would be stretched at the edges in comparison with its central portion (this is known as symmetrical distortion).

Let us establish the relation between the intensity, H , of the deflecting magnetic field (or the current, i_y , in the deflection coils

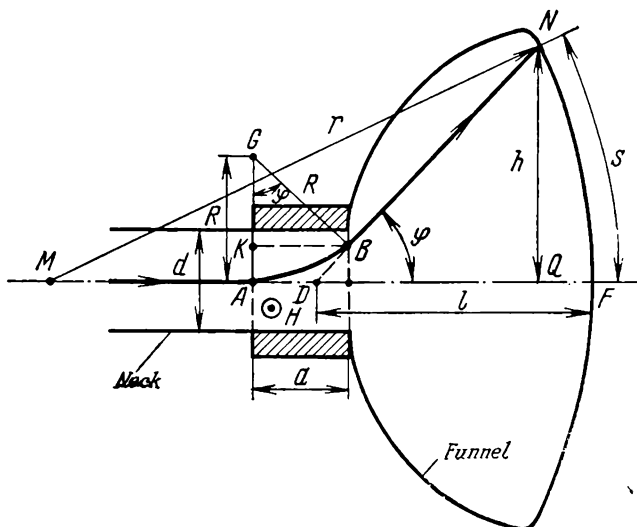


Fig. 2.22. Beam deflection in a picture tube
M—centre of curvature; D—centre of deflection; r —radius of curvature

proportional to that field intensity) and the deflection half-angle, φ . In a uniform magnetic field, the electron entering it with a velocity u moves along the arc of a circle whose radius is defined as

$$R = mu/eH \quad (2.10)$$

where m is the mass and e is the charge of the electron.

The velocity with which an electron moves in the magnetic field due to the deflection yoke is decided by the voltage, V_a , at the second anode:

$$u = \sqrt{2eV_a/m} \quad (2.11)$$

Substituting the expression for u from Eq. (2.10) into Eq. (2.11) gives

$$R = k_1 \sqrt{V_a}/H \quad (2.12)$$

* In large-screen picture tubes, the face is a function of several (two or three) spheres.

where

$$k_1 = \sqrt{2m/e} \quad (2.13)$$

From triangle *KBG* it follows that

$$a/R = \sin \varphi \quad (2.14)$$

Combining Eqs. (2.12) and (2.14), we obtain

$$\sin \varphi = k_2 H \quad (2.15)$$

where k_2 is a coefficient of proportionality between the sine of the deflection half-angle φ and the magnetic field intensity H :

$$k_2 = a/\sqrt{2mV_a/e} \quad (2.16)$$

Thus, in accordance with Eq. (2.15), the sine of the deflection half-angle in a uniform magnetic field is proportional to the deflection field intensity. Recalling that in any coil the magnetic field intensity is proportional to its ampere-turns, we may state that for a given number of turns the sine of the deflection half-angle is proportional to the yoke current, i_{dy} :

$$\sin \varphi = k_3 i_{dy} \quad (2.17)$$

For simplicity, we may put

$$x = \sin \varphi = k_2 H = k_3 i_{dy} \quad (2.18)$$

Thus, the parameter x may designate (on different scales) the sine of the deflection half-angle, the deflection field intensity, or the current in the deflection yoke.

To an observer at some distance from the TV screen, the deflection is not the true distance, s , on the screen, but its projection on a plane normal to the axis of the picture tube. In Fig. 2.22, this projection is marked h .

Using the designation of Fig. 2.22, we may write

$$NQ/DQ = h/\sqrt{r^2 - h^2} - (r - l) = \tan \varphi \quad (2.19)$$

Noting that

$$\tan \varphi = \sin \varphi / \sqrt{1 - \sin^2 \varphi} = x / \sqrt{1 - x^2}$$

we obtain from Eqs. (2.19) and (2.11)

$$h/l = x \sqrt{q^2 - (q-1)^2 x^2} - x(q-1) \sqrt{1 - x^2} \quad (2.20)$$

where the parameter

$$q = r/l \quad (2.21)$$

defined by the ratio of the radius of curvature to the radius of deflection gives a measure of screen convexity.

The dependence of beam deflection, h , across the screen on yoke current, $x = k_3 i_{dy}$, described by Eq. (2.20), is illustrated in Fig. 2.23a.

In this plot, $q = r/l = 2$ (which roughly applies to Soviet-made picture tubes).

Thus, the relation between h and x is nonlinear. It is the cause of symmetric raster distortions. The name symmetric implies that

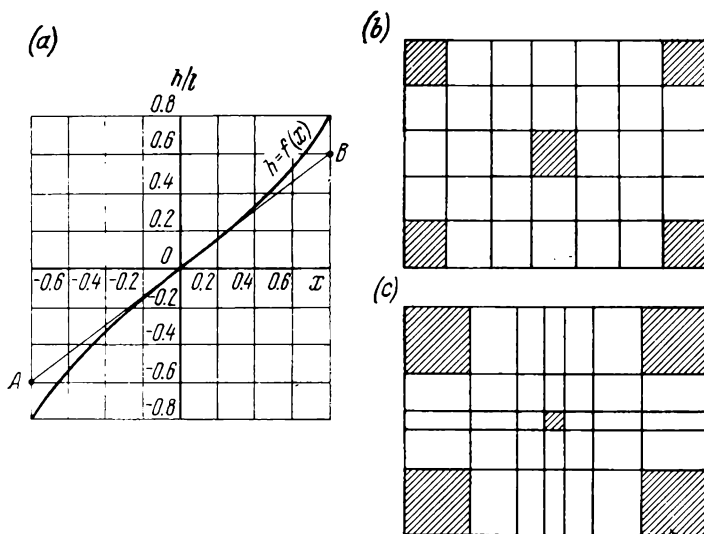


Fig. 2.23. Beam deflection as a function of magnetic field for flat screen (a) plot of the function; (b) undistorted pattern; (c) symmetrically distorted pattern

the raster is stretched at the edges symmetrically relative to its centre. Figure 2.23 illustrates symmetric distortion of the screen when a grid pattern is televised.

When the beam deflection across the screen is small ($x \ll 1$) it may be assumed that the relation $h = f(x)$ is linear (the line AB in Fig. 2.23a):

$$h/l \approx x \quad (2.22)$$

A measure of nonlinearity (coefficient of symmetric distortion) is the relative discrepancy between the linear relation, Eq. (2.22), and the nonlinear relation, Eq. (2.20):

$$\gamma = \frac{h_{(2.20)} - h_{(2.22)}}{h_{(2.22)}} = \sqrt{q^2 - (q-1)^2 x^2} - (q-1) \sqrt{1-x^2} - 1 \quad (2.23)$$

Noting Eq. (2.18), the relationship between the coefficient of symmetric distortion, γ , and the deflection half-angle, φ , may be expressed as

$$\gamma = \sqrt{q^2 - (q-1)^2 \sin^2 \varphi} - (q-1) \cos \varphi - 1 \quad (2.24)$$

The dependence of γ on φ for several values of q is plotted in Fig. 2.24. For present-day picture tubes with a wide deflection half-angle ($\varphi = 110^\circ/2$), symmetric distortion usually is 16 to 24%.

2.11. Construction of Deflection Yokes

From Eq. (2.14) it follows that, all other conditions being equal, the deflection half-angle φ increases with increasing yoke length. It would then appear that an increase in yoke length might enhance the sensitivity of the deflection yoke. However, if the yoke were made too long, shadows would appear in the corners of the raster (Fig. 2.25). Therefore, the optimum length of a *cylindrical deflection yoke* (for picture tubes with an abrupt change from neck to funnel, as shown in Fig. 2.22) is given by

$$\begin{aligned} a_h &= \frac{0.8d}{2} \cot \varphi_h/2 \\ a_v &= \frac{0.6d}{2} \cot \varphi_v/2 \end{aligned} \quad (2.25)$$

where d = neck diameter

φ_h = half-angle of horizontal deflection

φ_v = half-angle of vertical deflection

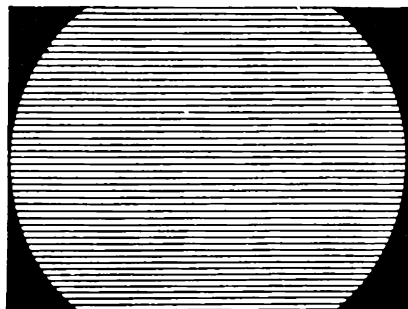


Fig. 2.25. Shadows in raster corners due to excessive length of deflection yoke

(50° and 70°). Their ends, E , are flared out to minimize their distorting effect on the field. The deflection yoke assembly has two yokes each having a pair of coils, one pair (the lower one, closer to the tube envelope) providing horizontal deflection, and the other (the upper one) vertical deflection. The magnetic lines of force of the horizontal and vertical deflection fields, H_h and H_v , must be at right angles to one another. To enhance the sensitivity of the deflection yoke, it is enclosed in a ferrite shell having low magnetic losses.

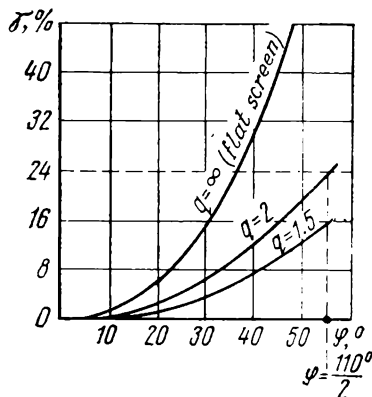


Fig. 2.24. Coefficient of symmetric distortion, γ , as a function of deflection angle φ for several values of screen curvature

Cylindrical deflection yokes (Fig. 2.26a) are employed in picture tubes with relatively small total deflection angles

Let us determine the relation between the ampere-turns and the deflection angle for one yoke. Figure 2.26b shows its cross-sectional view (the other is omitted for simplicity) and the iron shell around it. To minimize the geometric distortions of the raster, the deflection

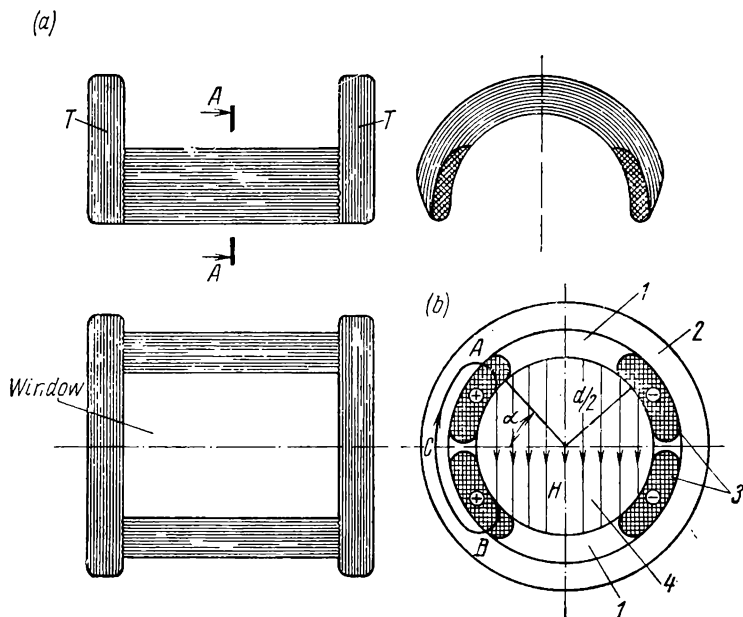


Fig. 2.26. Cylindrical deflection yoke

(a) external appearance; (b) sectional view; 1—window; 2—ferrite shell; 3—deflection coils; 4—picture-tube neck

field inside the tube neck must be as uniform as practicable. This is done by suitably arranging the coil turns.

The relation between the magnetic field intensity H and the ampere-turns, iw , producing this field is defined by the Ampere circuital law:

$$\oint_l H dl = 0.4\pi iw \quad (2.26)$$

where H is expressed in oersteds, i in amperes, and the sign \oint_l signifies that the summation is taken over a closed contour (of length l , in centimetres). In our case, l stands for a closed line of force.

With some idealization, one of the contours, $l = ABC$, is shown in Fig. 2.26b. The turns contributing to the ampere-turns in this case are those within the contour l . The iron shell has a permeability hundreds of times that of vacuum. Therefore, the magnetic field intensity within the shell is reduced by a factor of several hundred.

Because of this, in evaluating the integral, Eq. (2.26), we may neglect the part associated with the portion of the line of force within the

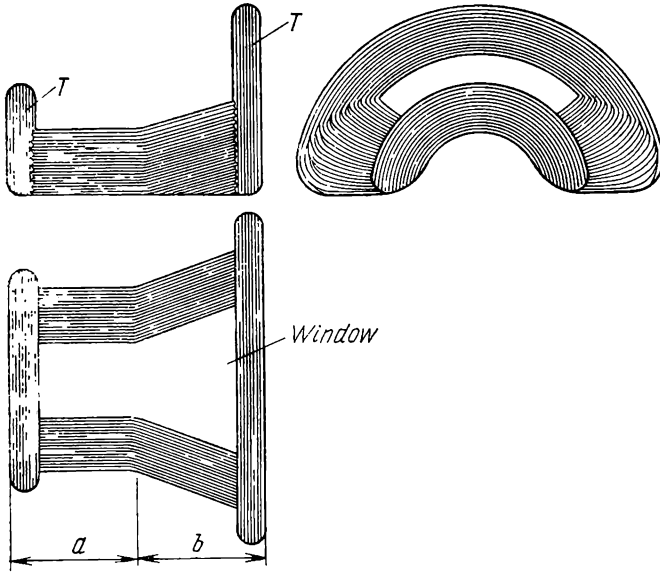


Fig. 2.27. Flared-out deflection yoke

shell. Also, the field within the area AB inside the tube neck must be uniform by definition, that is, $H = \text{constant}$ at any point inside the neck. Hence,

$$\oint_l H dl \approx H \int_A^B dl = Hd \sin \alpha = 0.4\pi iw_\alpha$$

and

$$iw_\alpha = (Hd/0.4\pi) \sin \alpha \quad (2.27)$$

where d is the neck diameter.

The total ampere-turns due to the yoke (for the line of force passing along the neck diameter, that is, at $\alpha = 90^\circ$) is

$$iw_{d_y} = Hd/0.4\pi \quad (2.28)$$

Substituting the expression for H from Eq. (2.28) into Eq. (2.15) and recalling that the electron charge is $e = 1.601 \times 10^{-19}$ C and the electron mass is $m = 9.109 \times 10^{-28}$ and that $1 \text{ V} = 10^8 \text{ CGSM}$, we obtain

$$iw_{d_y} = 2.7 (d/a) \sin \varphi \sqrt{V_r} \quad (2.29)$$

Thus, the deflecting ampere-turns are proportional to the sine of the deflection angle.

Equation (2.29), deduced under some idealization, yields a somewhat underestimated value of the necessary deflection ampere-turns in comparison with practical data. From practice, the following correction may be suggested

$$iw_{dy} = 2.7q (d/a) \sin \varphi \sqrt{V_a} \quad (2.30)$$

where $q_h \approx 1.4$ and $q_v \approx 1.2$.

The inductance (in henrys) of one pair of deflection coils can be determined with an accuracy sufficient for approximate calculations from the equation

$$L_{dy} = aw_{dy}^2 \times 10^{-8} \quad (2.31)$$

where a is the geometrical yoke length in cm and w_{dy} is the number of turns in the pair of coils.

In order to enhance deflection sensitivity, that is, to obtain a specified deflection angle with the least possible number of ampere-turns, the neck of a 110-degree picture tube is arranged to change into its funnel gradually (Fig. 2.27), and the yoke is built so that it partly covers this transition (Fig. 2.28). In this way, the geometric yoke length can be increased without any shadows appearing in the corners of the screen and, according to Eq. (2.30), the required deflection ampere-turns may be reduced in proportion. However, the deflection efficiency in the flaring part, b , will be reduced in comparison with that in the cylindrical portion, a , because the field intensity in the flaring part is reduced, too.

For tubes with a gradual neck-to-funnel transition, the number of deflecting ampere-turns is given by

$$iw_{dy} = 2.7q (d_1/a_{eq}) \sin \varphi \sqrt{V_a} \quad (2.32)$$

where

$$a_{eq} = a + b \frac{1 + d_1/d_2}{2} \quad (2.33)$$

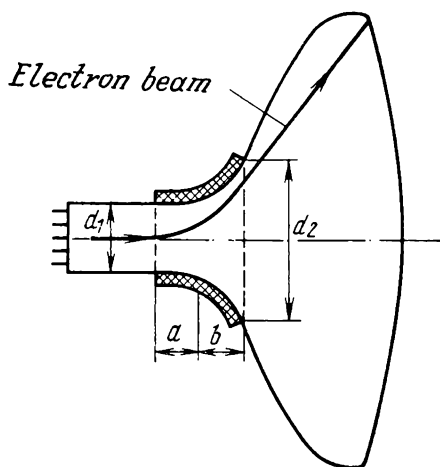


Fig. 2.28. Beam deflection in a picture tube with a gradual transition from neck to funnel

2.12. Ion Spot

As they fly towards the screen, the beam electrons collide with the gas molecules remaining in the evacuated envelope. As a result,

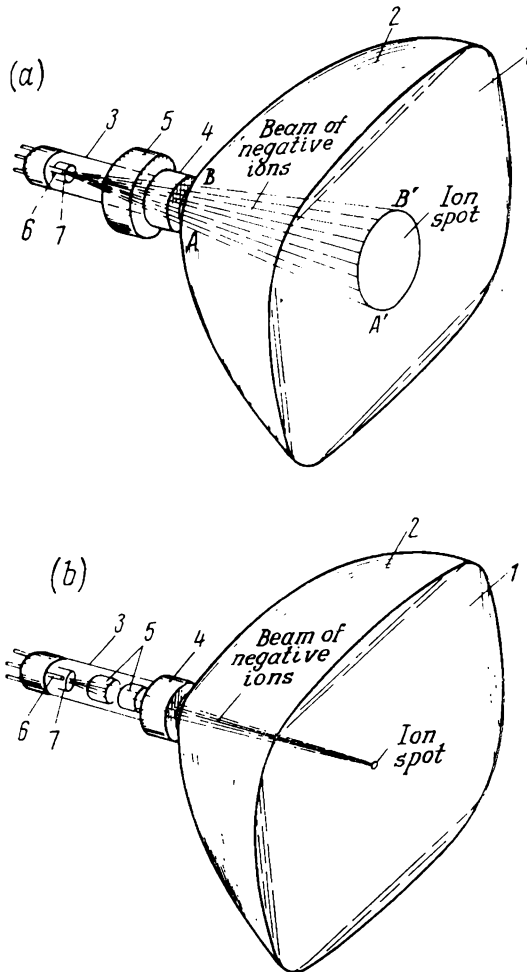


Fig. 2.29. Formation of the ion spot in (a) magnetically focused picture tube; (b) electrostatically focused picture tube
 1—screen; 2—funnel; 3—neck; 4—deflection yoke; 5—focuser; 6—thermionic cathode; 7—control electrode

the gas is ionized, and the *positive* ions that are formed are driven by the accelerating electric fields towards the cathode, that is, against

the stream of electrons. The bombardment of the cathode by positive ions causes it to emit *negative* ions. More massive than electrons, these negative ions are accelerated by the anode voltage of the picture tube and impinge on the screen with a considerable force. Gradually, ionic bombardment leads to the destruction of the phosphor.

As follows from Eq. (2.11), the magnetic focusing and deflecting fields have practically no effect on the trajectories of ions because their mass is thousands of times as great as that of electrons. Figure

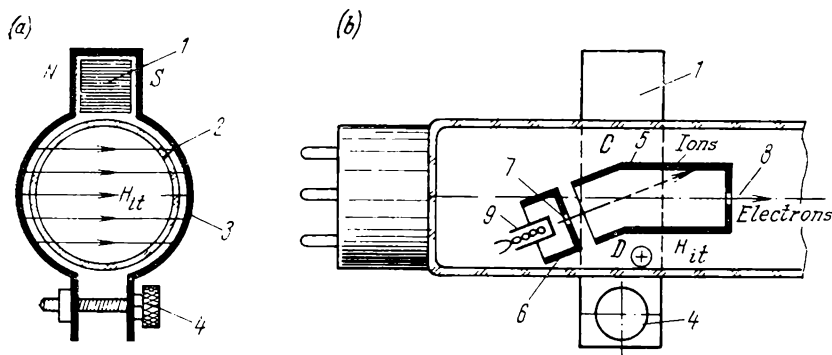


Fig. 2.30. Ion trap

1—ion-trap magnet; 2—tube neck; 3—pole pieces; 4—mounting screw; 5—focusing (or accelerating) electrode; 6—control electrode; 7—control-grid aperture; 8—focusing (accelerating) electrode aperture; 9—thermionic cathode

2.29a shows the beam of negative ions shaped within an electromagnetically focused, electromagnetically deflected picture tube. Liberated from the cathode as a divergent beam, the ions form on the screen a circular ion spot which is the projection of the circle *AB* at the transition of the tube neck to its funnel.

Electrostatic focusing is independent of the mass of beam particles. Therefore, in an electrostatically focused, electromagnetically deflected tube, the ions are focused to a central point on the screen (Fig. 2.29b). In this case, damage is caused to the central portion of the screen, known as ion burn.

In the older makes of picture tubes, ion traps were used as a precaution against ion-spot formation. In an ion-trap gun, a suitably shaped permanent magnet is put on the rear part of the neck (Fig. 2.30) so that the lines of force of this magnet are directed across the neck. The magnet can be adjusted, as may be necessary, for its position along and around the tube axis. The focusing or accelerating electrode, 5, depending on the construction of the electron gun used, which is close to the control electrode, 6, has a bend, *CD*. The electrons and negative ions liberated from the cathode are allowed

to pass through an apertured disc, 7, and enter the field, H_{it} , of the ion trap. The more massive ions which are not deflected by this field remain within electrode 5. The electrons are deflected by this field H_{it} , and pass through aperture 8 on towards the screen.

In the latest makes of picture tubes (47JK2B, 59JK2B and 61JK2B), there is no ion trap. Ion spot formation is prevented by the use of an aluminized screen backing 0.05 to 0.5 μm thick (see Fig. 2.16a). Electrons pass readily through the aluminium film and excite luminescence in the screen, while the massive ions are stopped.

CHAPTER THREE

SCANNING GENERATORS

3.1. Difference in Operation Between Vertical and Horizontal Scanning

In both camera and picture tubes, the electron beam is deflected horizontally (horizontal or line scan) and vertically (vertical or frame scan) by scanning (or sweep) generators which are suitable circuits supplying sawtooth current for the deflection coils. The horizontal (line) and vertical (frame) scanning generators substantially differ in both the principle of operation and the circuit configuration. This difference arises above all from the fact that the two types of sweep generator use different operating frequencies. In broadcast television, a typical horizontal scanning generator operates at $f_h = 15,625$ Hz and a typical vertical (frame) scanning generator at $f_v = 50$ Hz.

The a.c. currents and voltages supplied by a scanning generator drastically differ from sinusoidal. Including the 20th harmonic (which is practically enough for the pulse waveform to be reproduced faithfully), the maximum operating frequency of the horizontal scan generator is about $f_{\max, h} = 15,625 \times 20 \approx 300$ kHz. At this frequency, stray capacitances and eddy-current losses in magnetic cores become decisive. Because of this, the core of the output transformer must be made from a magnetic material having a high reluctance (this material usually is ferrite). In contrast, the top frequency of the vertical scanning generator is a mere $f_{\max, v} = 50 \times 20 = 1000$ Hz.

Therefore, the ordinary electrical-sheet steel used for audio-frequency transformers may well be used for the vertical output transformer.

The marked difference in operating frequency between horizontal and vertical scanning generators considerably affects the character of load on the output stage. For example, for the horizontal scanning generator the deflection yoke presents an inductive load. For the vertical scanning generator, the deflection yoke may be taken as being purely resistive in many theoretical and practical considerations.

3.2. Features of the Horizontal Scanning Generator

The simplest and very efficient horizontal output circuit is one with a two-way switch (Fig. 3.1). Referring to the diagram, L_y is the yoke inductance, C_r is the capacitor whose capacitance is deci-

ded by the retrace time interval, Sw is the switch (which may be the output tube or transistor) provided to switch the circuit between scan and retrace, R is the equivalent loss resistance (in the plate circuit of the output tube or the collector circuit of the output transistor, in the coils, cores, etc.), and E is the supply voltage. To

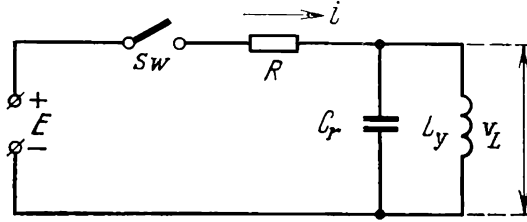


Fig. 3.1. Equivalent circuit of horizontal output circuit with a two-way switch

simplify the consideration of the circuit, we shall neglect the equivalent loss resistance, assuming that $R = 0$. Then closure of the switch Sw (the start of an active scan) will cause the direct voltage E to be applied across the yoke inductance L_y (the capacitor C_r will charge to E instantaneously) and the current i in the coils will rise linearly (portion AB in the plot of Fig. 3.2a):

$$\left. \begin{aligned} v_L &= L_y di/dt = E = \text{constant} = V_1 \\ i_L &= \frac{1}{L_y} \int_0^t v_L dt = Et/L_y \end{aligned} \right\} \quad (3.1)$$

At the instant corresponding to point B (Fig. 3.2a) the switch Sw opens and the current i which has reached the magnitude I_m by that time is directed into the retrace capacitor C_r . A resonant circuit, $L_y C_r$, is thus formed, and the current varies cosinusoidally during retrace, t_2 , (portion BCD in the plot of Fig. 3.2a):

$$i = I_m \cos \omega t$$

while the voltage across L_y during t_2 varies sinusoidally (portion $B'C'D'$ in the plot of Fig. 3.2b):

$$v_L = -\omega L_y I_m \sin \omega t = -V_{2m} \sin \omega t \quad (3.2)$$

At the end of retrace (point D) the switch Sw closes again, the supply source shunts the resonant circuit $L_y C_r$, and harmonic oscillations in it cease. Direct voltage is again impressed on L_y , and the current within the portion DEF (during scan, t_1) varies linearly. If we examine the portion DEF depicting the total change in current during the active scanning motion, we shall note that it consists of

two halves equal in area, namely the negative part BDE and the positive part EFG . During the second (positive) half of the active scan the current i flows from the supply source, through the closed switch into the horizontal yoke L_y . The negative sign of the portion DE signifies that now the current is flowing from the yoke back to

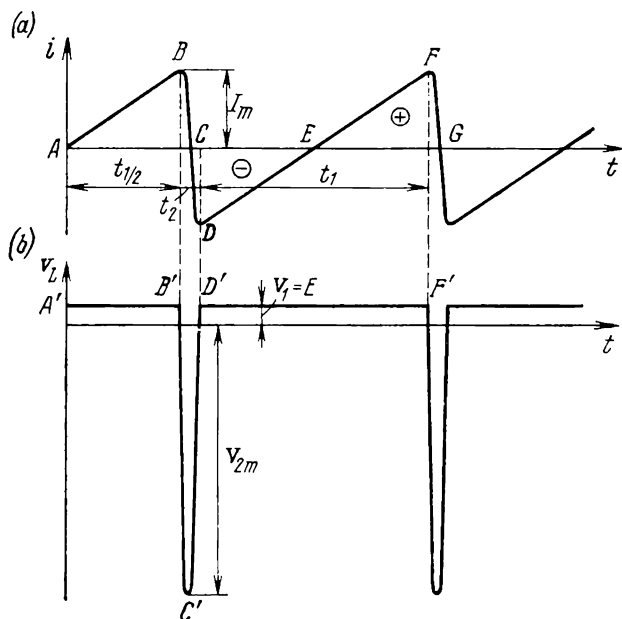


Fig. 3.2. Waveforms of deflection-yoke current and voltage
(a) yoke current; (b) pulse voltage

the supply source. Hence we may conclude that, firstly, the switch Sw must be capable of conducting current both ways (this is why we have called this circuit one with a two-way switch). Secondly, the idealized circuit under consideration draws no active power from the supply source because the energy $A_L = L_y I_m^2 / 2$ stored by the yoke during the second half of the active scan is wholly returned to the supply source during the first half of the active scan in the next cycle. Thus, the circuit carries no direct current component.

From the foregoing we may draw a conclusion of fundamental importance: no active power is needed to deflect the electron beam. In practice, however, the scanning generators are usually far from

perfection, and the losses associated with them result in the consumption of a considerable amount of active power (running into several tens of watts for wide-angle picture tubes).

Referring to the diagram of Fig. 3.1, we shall deduce some basic quantitative relations. As follows from the plot of Fig. 3.2, the retrace (flyback) time t_2 is equal to the half-period of free oscillations

$$t_2 = T_f/2 = \pi \sqrt{L_y C_r} \quad (3.3)$$

In scanning circuits built around tubes, the capacitance C_r is parasitic; it is formed by the output capacitance of the output tube, the capacitance of the output transformer windings, etc. In practice, this parasitic capacitance amounts to 80 to 120 pF.

During the active scanning motion, the voltage V_1 across the horizontal yoke L_y is practically equal to supply voltage

$$V_1 \approx E \quad (3.4)$$

(the difference between the two is the voltage drop across the series loss resistance). Referring to the plot of Fig. 3.2 again, the amplitude of deflecting current and the scan voltage V_1 can be related as follows. Assuming that the scan portion DEF is linear, we may write

$$V_1 = L_y di/dt = L_y 2I_m/t_1 \quad (3.5)$$

For a specified picture tube, Equations (2.30) and (2.32) uniquely define the necessary deflecting ampere-turns, $I_m w_y$. Using also Eq. (2.31), the scan voltage may be defined as

$$V_1 = a w_y \frac{2(I_m w_y)}{t_1} 10^{-8} \quad (3.6)$$

where a is the effective yoke length in cm.

In turn, when the deflecting ampere-turns, $I_m w_y$, are set in advance, the amplitude of deflecting current is defined by a simple relation

$$I_m = I_m w_y / w_y \quad (3.7)$$

A very important parameter which shows whether or not a given tube or transistor is suitable for use in the horizontal output stage is the retrace pulse voltage V_{2m} (Fig. 3.2b). The retrace pulse voltage ought not to exceed the safe value specified for that tube or transistor.

From Eqs. (3.2), (3.3) and (3.5), we get

$$V_{2m} = (\pi/2) V_1 (t_1/t_2) = 1.57 V_1 (t_1/t_2) \quad (3.8)$$

The suitability of the switch (output tube or transistor) for use in the horizontal scanning circuit is decided by two parameters: the maximum current I_m flowing through the closed switch (during scan) and the maximum voltage $V_m = V_{2m} + E$ arising across the open switch (during retrace). The product of the two quantities

characterizes the serviceability of the switch and is called its interrupting power:

$$P_{inter} = I_m (V_{2m} + E) = I_m V_m \quad (3.9)$$

Noting Eqs. (3.4) and (3.8), we may write

$$P_{inter} = I_m V_1 (1 + 1.57 t_1/t_2) \quad (3.10)$$

Multiplying the left- and right-hand sides of Eq. (3.6) by I_m gives

$$I_m V_1 = 2 \frac{a (I_m w_y)^2}{t_1} 10^{-8} \quad (3.11)$$

From comparison of Eqs. (3.10) and (3.11), we may connect the deflecting ampere-turns $I_m w_y$ and the interrupting power P_{inter} as

$$P_{inter} = 2a (1/t_1 + 1.57/t_2) (I_m w_y)^2 10^{-8} \quad (3.12)$$

Thus, for the specified yoke length a , and the specified scan and retrace times, t_1 and t_2 , the interrupting power is proportional to the square of the deflecting ampere-turns.

Data sheets for horizontal output tubes or transistors quote the maximum safe pulse current and voltage. Obviously, when selecting a tube or transistor for the horizontal output stage, the choice should be based on the following inequality:

$$I_{sw \max safe} V_{sw \max safe} \geq P_{inter} = I_m V_m \quad (3.13)$$

So far we have neglected the series loss resistance R in the circuit of Fig. 3.1. However this resistance has an adverse effect on the performance of the horizontal output stage. For one thing, this resistance causes the deflection current waveform to depart from

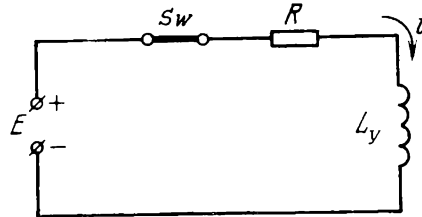


Fig. 3.3. Equivalent circuit of horizontal output circuit during scan, with regard for resistance

linearity during scan, which in turn results in geometric distortions, usually visible as picture stretching along the left-hand edge and compression along the right-hand edge. For another, this resistance leads to wastage of a considerable amount of active power.

Consider the effect of the series loss resistance R on the waveform of yoke current during scan. In this condition, the switch Sw is clos-

ed, and the capacitance C_r has a negligible effect. This condition may be depicted by the equivalent circuit of Fig. 3.3. In this circuit, L_y is charged by magnetic energy from the supply source E via the resistance R , and the current is varying exponentially:

$$i = (E/R) [1 - \exp(-t/\tau)] + A \quad (3.14)$$

where $\tau = L_y/R$ is the time constant of the circuit and A is the constant of integration.

During retrace (the switch Sw is open) the supply source E and the series loss resistance R are disconnected and a resonant circuit, $L_y C_r$, is formed, such that the current and voltage waveforms during retrace do not differ from those already examined. The current and voltage waveforms of the deflection yoke are shown in Fig. 3.4a and 3.4b, respectively. In contrast to the idealized case of Fig. 3.2 ($R = 0$), the scan current i has a convex bulge (nonlinearity), while the scan voltage v_1 decays towards the end of the scanning cycle rather than remains constant.

The nonlinearity of scan current can conveniently be assessed in terms of the so-called nonlinearity factor β :

$$\beta = \frac{|di/dt|_{t=0} - |di/dt|_{t=t_1}}{|di/dt|_{t=0}} \quad (3.15)$$

where $|di/dt|_{t=0}$ and $|di/dt|_{t=t_1}$ are the rates of change of current at the start and end of scan, respectively (see Fig. 3.4a).

Nonlinearity is nonexistent when the rate of change of current is the same at the start and end of scan, that is when $\beta = 0$. In the other extreme case, when di/dt falls from some value at the start of scan to zero at the end of scan, the nonlinearity β is 100%. Let us determine the dependence of the nonlinearity factor on the circuit

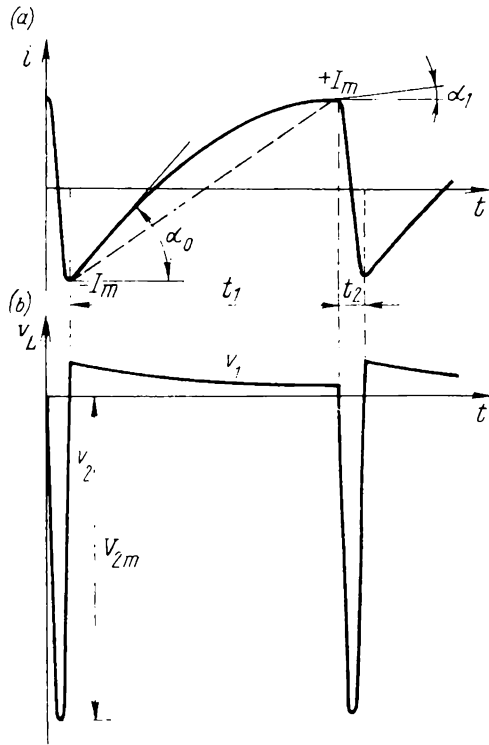


Fig. 3.4. Waveforms of yoke current and voltage in the circuit of Fig. 3.3
(a) yoke current; (b) pulse voltage

parameters (see Fig. 3.3). To begin with, we differentiate Eq. (3.14) with respect to time:

$$di/dt = (E/R) (1/\tau) \exp(-t/\tau) = (E/R) (R/L_y) \exp(-t/\tau)$$

whence

$$\begin{aligned} |di/dt|_{t=0} &= E/L_y \\ |di/dt|_{t=t_1} &= (E/L_y) \exp(-t_1/\tau) \end{aligned}$$

Substituting the above expressions for current in Eq. (3.15) gives

$$\beta = 1 - \exp(-t_1/\tau) \quad (3.16)$$

Since at $x \ll 1$, $1 - \exp(-x) \approx x$, for small linearities Eq. (3.16) may be replaced with the following approximate expression:

$$\beta \approx t_1/\tau = t_1 R/L_y \quad (3.17)$$

The above expression is more graphic than Eq. (3.16) in showing that an increase in R entails an increase in the nonlinearity β . At $R = 0$, nonlinearity is nonexistent. An increase in L_y also decreases the nonlinearity. Thus, in order to improve the linearity of the deflecting current, the time constant, $\tau = L_y/R$, must be increased.

3.3. Tube Horizontal Output Stage

Of the many millions of TV receivers now in use in the Soviet Union, only several tens of thousands use transistor horizontal scanning generators.

Transistor horizontal scanning generators offer obvious advantages over tube circuits, such as high economy of operation, reliability, and long service life. However, they suffer from disadvantages which prevent their use in the horizontal output stages of mains-operated stationary TV sets. These disadvantages include the high cost of good output transistors, high reject percentage in manufacture, and the relatively complex input circuit. Because of this, it still remains a practical necessity to study the operation of present-day horizontal output circuits built around tubes.

The output tube of a horizontal scanning generator performs two basic functions. Firstly, it acts as a switch to terminate the horizontal scan at the end of each line and to permit retrace. Secondly, provided its grid voltage is of an appropriate waveform, the output tube maintains the desired sawtooth current waveform during scan.

Consider the case where a linear current is produced during scan. For an ideal case where the plate current-grid voltage characteristic (Fig. 3.5) is a straight line, the necessary grid voltage waveform will be described by an equation of the form

$$v_g = at/g_m - I_0/g_m \quad (3.18)$$

where g_m = transconductance of the tube

I_0 = current at zero grid voltage

As follows from Fig. 3.2 and Eq. (3.8), the voltage pulse arising across the yoke L_y during retrace may run into several thousand volts in tube circuits. By Lenz's rule, the positive side of this voltage is applied to the plate of the output tube. Although the output tubes

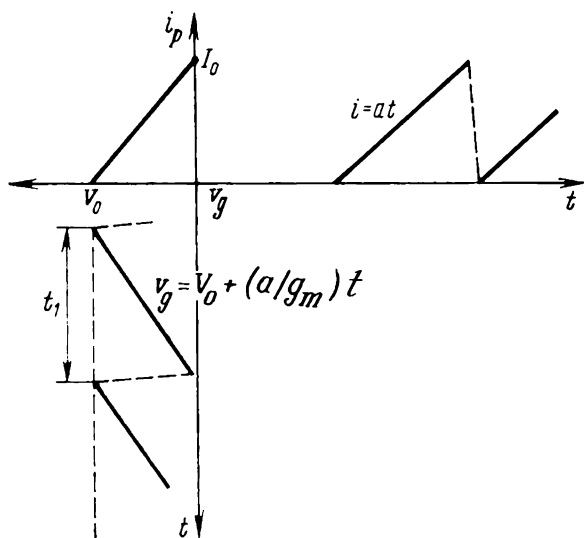


Fig. 3.5. Waveform of grid voltage and corresponding linear current

in line-scan circuits are usually tetrodes and pentodes which have a high plate dynamic resistance, the retrace voltage pulse is so high that the plate current-grid voltage curve is appreciably shifted to the left during retrace (Fig. 3.6).

For example, the retrace pulse voltage arising in a 110-degree horizontal output stage is $V_{2m} = 8$ kV. The 6II36C tube used here has an amplification factor of $\mu = 250$. The shift of the plate current-grid voltage curve to the left is

$$\Delta v_g = V_{2m}/\mu = 24 \text{ V}$$

Therefore, in order to cut off the tube during retrace, narrow rectangular pulses (V_{rect} in Fig. 3.6) have to be added to the sawtooth grid voltage.

Speaking of the necessary waveform for the grid voltage during scan (Figs. 3.5 and 3.6) we have ignored the effect of the parasitic capacitance C_r . Experience shows, however, that this capacitance

has a marked effect at the start of scan. The tube presents a considerable resistance during this time interval, and it is not able to shunt the oscillatory circuit made up of the equivalent inductance and the stray circuit capacitance (in practical circuits utilizing transformers, the equivalent inductance consists of the yoke inductance,

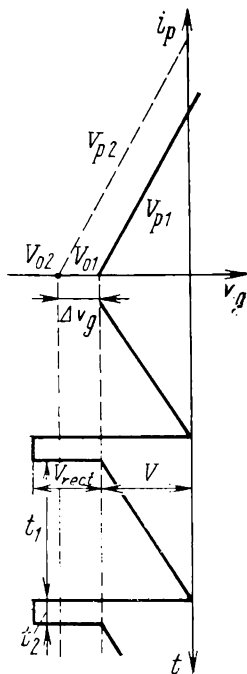


Fig. 3.6. Shift of the plate current-grid voltage curve of the output circuit tube and compensation of the shift by correcting pulse V_{rect}

L_y , reflected into the plate circuit of the output tube, and the parallel-connected inductance L_1 of the transformer primary). As a result, damped sinusoidal oscillations of voltage and current may exist not only during retrace, but also during the first half of scan, and superimpose on the fundamental current and voltage (Fig. 3.7). It is not until after one-third to one-half of the scan time, when the grid voltage rises so that the tube d.c. resistance falls to a value at which the oscillations in the resonant circuit become aperiodic

$$R \leq (1/2) \sqrt{L_{eq}/C_0} \quad (3.19)$$

(where R is the tube resistance, L_{eq} is the equivalent inductance in the plate circuit and C_0 is the parasitic shunt capacitance), that the current begins to rise almost linearly. Distortion of the current waveform like that shown in Fig. 3.7 causes an appreciable distortion at the left-hand edge of the raster which looks like a contracted accordion.

These unwanted oscillations at the start of scan can be suppressed by extending the horizontal output stage to include a sufficiently high-power damper diode which will shunt the resonant circuit at appropriate instants. The damper diode is connected in the line-scan circuit and its operating conditions are chosen so that the diode is conducting only during the first half of scan and has no effect during the second half of scan and retrace. Owing to its effectiveness, diode damping is a feature of all horizontal scanning circuits today.

In the older circuits where the picture tube screen and anode voltage were relatively small, the damper diode performed only one function — that of smoothing unwanted oscillations at the start of scan. In present-day circuits, it additionally about halves the current drawn from the supply source and boosts the direct voltage feeding the plate circuit of the output tube.

The average current through the damper diode is equal to the average current through the output tube and is somewhere between 50 and 100 mA. Thus, the damper diode must be of a sufficiently high power rating so as to stand up to the heavy voltage pulse during retrace. The horizontal scanning circuits of Soviet-made TV receivers usually employ special-purpose diodes such as types 6Ц10П, 6Д14П and 6Ц19П.

In a simplified form, the horizontal output stage containing a damper diode appears in Fig. 3.8a. The bias voltage, E_d , for the

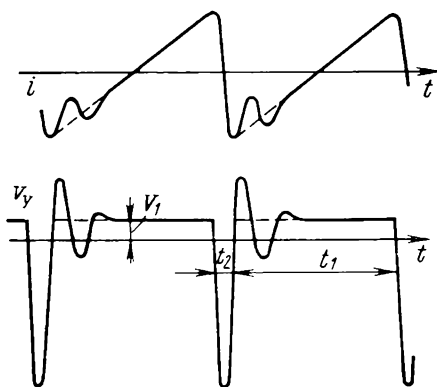


Fig. 3.7. Superimposition of damped sinewaves on main current and voltage during first half of scan

damper diode is usually chosen to be equal to that across the inductance L_{eq} during scan (Eq. 3.5):

$$E_d \approx V_1 = L_{eq} 2I_m / t_1$$

It is to be noted that this voltage is applied to the plate of the damper diode in negative polarity. In the absence of a damper diode the scan voltage across L_{eq} would contain a sinusoidal component, $\alpha\beta\gamma_0$ (Fig. 3.8c). In the presence of a damper diode, the very first peak of this voltage, α , exceeding the bias or delay voltage E_d of the diode renders it conducting, and the diode shunts the resonant circuit (curve *ab* in Fig. 3.8c). The resistance of the high-power diode is now so small that, once it becomes conducting, the effect of the distributed stray capacitance may be neglected. When this happens the damped resonant circuit includes L_{eq} , E_d and the diode resistance R_d ; this can be recognized as an aperiodic circuit. Owing to provision of a damper diode, no cosinusoidal damped oscillations appear in the deflecting current at the start of scan, and the deflection current becomes practically linear.

The above horizontal output stage in which the output tube and the damper diode operate at the same time and for the entire scan interval was used in small-screen, narrow-angle TV receivers. With

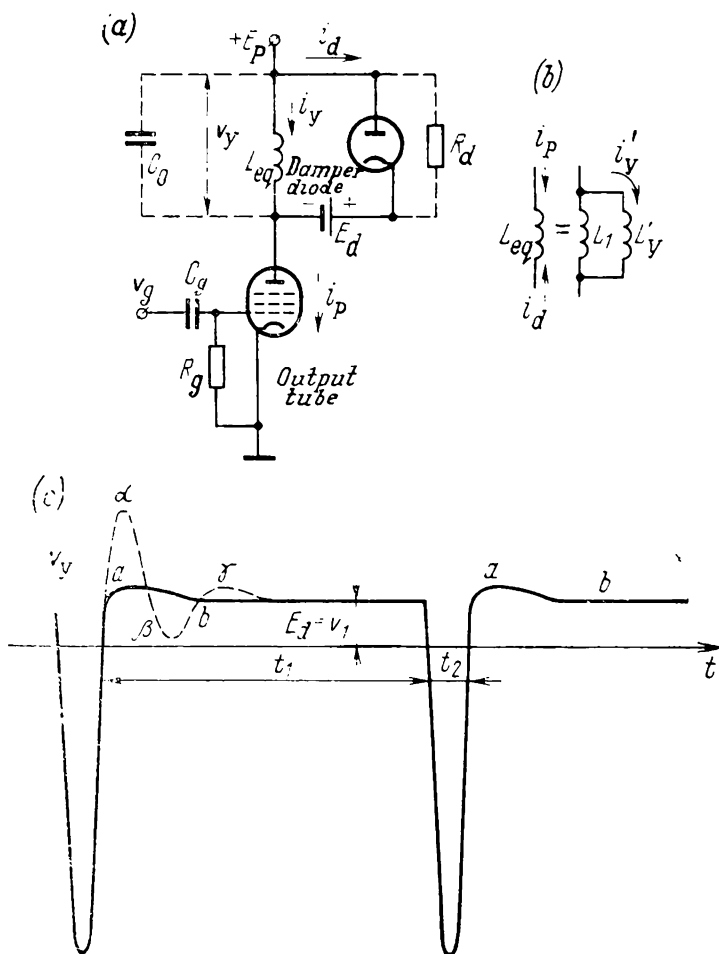


Fig. 3.8. Simplified circuit of the horizontal output stage using a damper diode (a) damper diode in the plate circuit; (b) equivalent inductance; (c) suppression of sine wave component in scan voltage by damper diode

the advent of large-screen, wide-angle picture tubes it became obvious that this form of damping was wasteful. If we draw a somewhat arbitrary analogy between the horizontal scanning circuit using two tubes, output and damper, and a push-pull power amplifier also

using two tubes, then the horizontal output stage just discussed may be said to operate Class *A*. By extending this analogy, we could cause the output tube and the damper diode of the horizontal output stage to operate Class *B* as we usually do with an amplifier. In Class *B* operation, the two tubes would operate in turn, and the current drawn from the supply source would be halved in comparison with

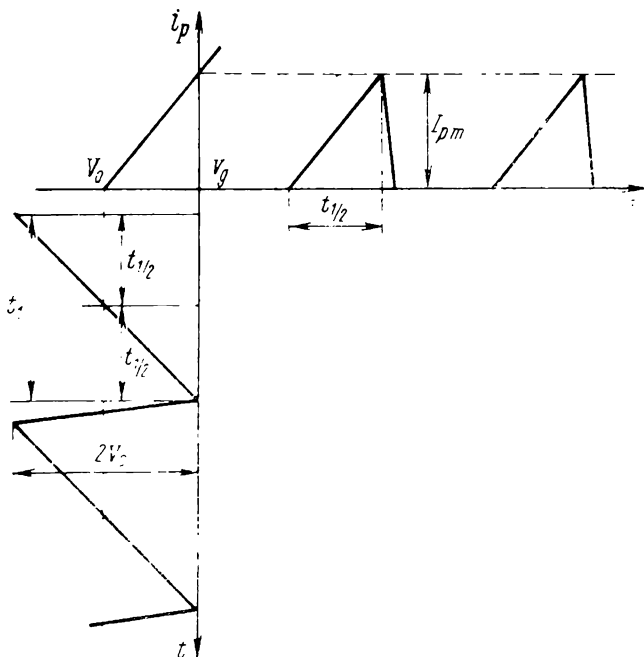


Fig. 3.9. Illustrating class *B* operation

Class *A* operation for the same swing of sawtooth current. Present-day horizontal scanning circuits operate in an economy class, very close to Class *B* (or midway between Classes *A* and *B*).

In an ideal case (the plate current-grid voltage characteristic of the output tube is a straight line), Class *B* operation can be obtained by doubling (in comparison with Class *A*) the amplitude of sawtooth grid voltage (Fig. 3.9). In other words, if the voltage span on the plate current-grid voltage curve from zero to cut-off is V_0 , the amplitude of the grid voltage should be $V_g = 2V_0$, provided the plate current-grid voltage characteristic is linear and so is the sawtooth grid voltage. The waveforms of currents in and voltages across the equivalent inductance of the circuit of Fig. 3.8*a*, operating Class *B* are shown in Fig. 3.10*a* and *b*. Within the region *ab* (the first half of the scan) the output valve is driven to cut-off by the negative

voltage applied to the control grid, and the damper diode alone is conducting and shunts parasitic harmonic oscillations (Fig. 3.10b).

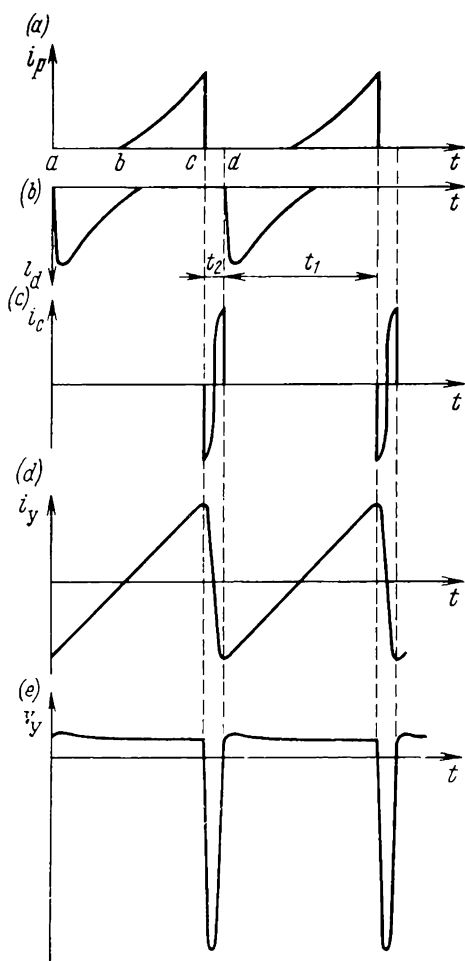


Fig. 3.10. Waveforms of currents and voltages in the circuit of Fig. 3.9a

(a) output-tube plate-current pulses; (b) damper-diode current pulses; (c) retrace current pulses; (d) sawtooth yoke current; (e) yoke voltage

At point *b*, the damper diode ceases conducting (the voltage across L_y falls below bias voltage E_d , and this bias voltage drives the damper diode to cut-off). At instant *b*, the voltage applied to the control grid renders the output tube conducting, and the plate current it draws, i_p , has the waveform shown in Fig. 3.10a. The algebraic sum of the currents

$$i_{Ly} = i_p + i_d$$

shown in the plot of Fig. 3.10d is the yoke current. Because the output tube is conducting only during half each scan (region *bc*), the direct component of the current supplied by the source is half as great as it is in class A operation. In other words, the power dissipated by this source is halved, too.

As is seen from Fig. 3.8a, none of the sides of the damper diode bias voltage source, E_d , is returned to earth. Because of this, the necessary bias voltage cannot be taken from the usual supply sources used in the receiver. In the older circuits this voltage is derived by a self-bias network from the average compo-

nent of the current through the damper diode itself (Fig. 3.11a). The circuit of the damper diode includes a parallel combination of a resistor and a capacitor, and the desired potential difference is produced automatically. As always in such cases, the bias capa-

citor C_b serves to smoothen the ripple due to the a.c. component; the desired self-bias voltage is set by adjusting the value of R_b . Because the pulse repetition frequency is relatively high (15,625 Hz), the capacitance C_b may be not very high (anywhere between 0.1 and 0.2 μF).

The above horizontal output stage operating Class B was used in many TV receivers at one time. However, it suffered from a major drawback, namely that much power was dissipated across R_b in

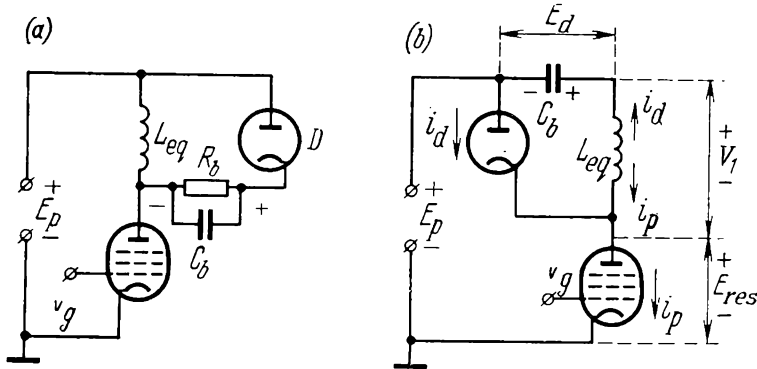


Fig. 3.11. Operation of the damper diode

(a) self-bias in the damper circuit; (b) simplified circuit of horizontal output stage using voltage boost (power feedback)

the self-bias network of the damper diode. For example, assuming an average damper diode current of $i_0 = 30$ mA and a bias voltage of $E_d = 400$ V, the power dissipated by R_b would be 12 W.

The next significant step in the development of horizontal-scanning circuits has been one in which the energy stored by L_{eq} is not dissipated wastefully in R_b , but is recovered and fed back to the plate of the output tube to boost the d.c. power supply. Known as the voltage-boost or power-feedback scanning circuit, it has now become universal. It is indispensable in tube TV receivers with large-screen picture tubes. For better insight into operation of this horizontal scanning circuit, it is important to stress the following. Referring to Fig. 3.11a, it may be concluded that in a properly aligned circuit the average currents of the output tube and damper diode (often called the booster diode) are equal. Because of this, the bias resistor R_b in the damper bias circuit may be replaced by the output tube. During the first half of scan, when only the damper diode is conducting and the output (drive) valve is driven to cut-off, the diode charges the bias (or, rather, boost) capacitor C_b . During the second half of scan, when the damper diode is no longer conducting, but the output tube is, the boost capacitor C_b discharges through the

tube. Because the average charge and discharge currents are the same, the average voltage across the capacitor remains unchanged. The circuit operating by this principle is illustrated in Fig. 3.11*b*. Here, too, the operation is Class *B*. During the second half of scan, when the diode turns off, the output tube is rendered conducting, and its plate voltage is now made up of plate supply voltage E_p and capacitor voltage E_d , connected in series aiding. This recovered voltage, E_d , is the boost voltage in this circuit. In practice, the

amount of voltage boost may sometimes exceed the plate supply voltage.

The advantage of boosting the plate supply voltage of the output tube is as follows. Magnetic energy A_L is defined as

$$A_L = L_{eq} I_m^2 / 2 \quad (3.20)$$

where L_{eq} is the inductance in the plate circuit of the output tube (and in the damper diode), and I_m is the current pulse passing through this inductance.

In existing 110-degree picture tubes the magnetic energy needed for beam deflection must be more than doubled in comparison with the older 70-degree tubes.

However, little would be gained by achieving this through

an increase in I_m , because power losses would rise and tubes of higher power ratings capable of passing a fairly heavy plate current would have to be employed. The remaining alternative is to do this by increasing the equivalent inductance. In existing tube TV sets, L_{eq} is 800 to 1000 mH, and the voltage drop across it during the active scan is $V_1 = 600$ to 800 V.

The distribution of voltage in the plate circuit of the output tube utilizing power feedback is shown in Fig. 3.12. So that during active scan the plate voltage would not fall below a minimum (residual) voltage $E_{res} = 80$ to 100 V, that is, so that the pronounced nonlinearity of the plate current-plate voltage characteristics to the left of E_{res} would not result in a pronounced nonlinearity of the deflection current, the following inequality must be satisfied:

$$E_{total} = E_p + E_d \geq E_{res} + V_1 \quad (3.21)$$

For example, at $E_{res} = 100$ V, $V_1 = 600$ V, $E_p = 250$ V (these are all practical figures), the total plate supply voltage of the out-

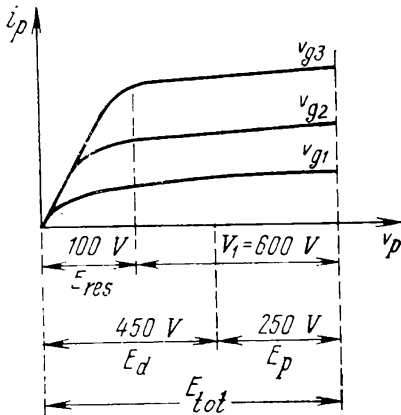


Fig. 3.12. Plate current-plate voltage characteristic of the tube in a volta-boost (power-feedback) scanning circuit

put tube must be $E_{total} = E_{res} + V_1 = 700$ V, and the voltage across the boost capacitor, $E_d = E_{total} - E_p = 450$ V.

The advantages offered by voltage boost (or power feedback) may be summed up as follows. Firstly, energy dissipation in the bias resistor R_b is avoided. Secondly, the required plate current pulse I_m may be reduced through an increase in the equivalent inductance L_{eq} . Thirdly, the increase in the equivalent inductance reduces nonlinearity in the sawtooth voltage during scan [see Eq. (3.17)]. Fourthly, the increase in L_{eq} brings about an increase in scan voltage V_1 [see Eq. (3.5)], and this in turn raises retrace voltage V_{2m} [see Eq. (3.8)]. In this way, the problem of deriving high-voltage supply for the second anode of the picture tube is simplified.

To simplify the deflection system and to make it more reliable in operation, it appears advantageous to reduce the number of turns in the yoke coils. The coils will then be smaller in size and easier to make. However, a decrease in the number of coil turns for the same specified deflecting ampere-turns necessitates an increase in the amplitude of deflecting current. Rather than to use an output tube of greater power rating, resort is made to a matching transformer. Thus, the matching transformer in the horizontal output circuit serves to match the yoke and the output tube in terms of current. Also, this transformer can appropriately be tapped down to provide connection for the diode. Many other circuits — the H. V. rectifier, the width control, the AGC circuit, etc., are likewise connected to the horizontal output circuit via suitable taps on this horizontal output transformer.

The horizontal output transformer is a pulse transformer. It is expected to satisfy the following principal requirements:

1. It should be capable of operating over a sufficiently wide frequency range. Recalling that the fundamental frequency of current and voltage in the line-scan transformer is 15,625 Hz, its operating frequency range should be about 300 kHz, out to the 20th harmonic.

2. Iron losses which increase rapidly with frequency must be within specified limits.

3. Insulation between windings, between windings and core should be capable of standing up to retrace voltage pulses.

4. Turn-to-turn capacitance and winding-to-core capacitance should be kept to a minimum so as to ensure the desired broad frequency range.

5. Leakage inductance should be as small as practicable for better transfer of pulses from the primary into the secondary.

These requirements are closely interrelated and, unfortunately, conflicting. For example, improvement in insulation may lead to an increased stray capacitance; a decrease in stray capacitance by use of sectionalized coils would result in an increased leakage inductance.

For the most part, line-scan circuits employ autotransformers rather than transformers. An autotransformer provides better coupling between the windings, is smaller in size, and is simpler to make. To reduce eddy-current losses, the core material is ferrite which has a high reluctivity and a relatively high permeability.

As already noted, the yoke is tapped down on the autotransformer so that the voltage is markedly stepped down (and the current is stepped up in proportion). Therefore, it is important to select an

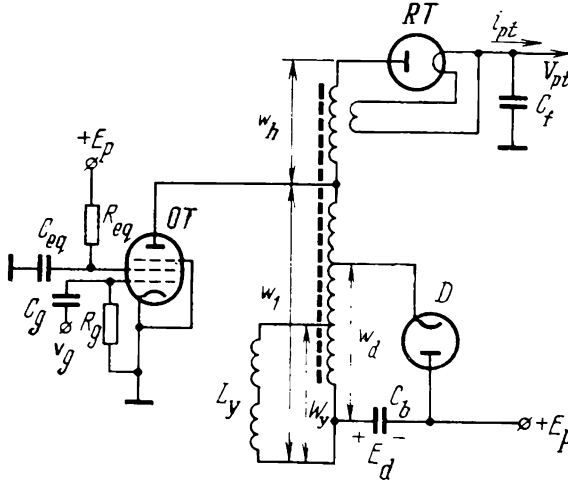


Fig. 3.13. Circuit of horizontal output stage

appropriate tap on the transformer for the yoke. Departure from an optimal matching ratio (tap position) may result in an excessive power for the output (drive) tube to handle, an undesirable decrease in horizontal amplitude (width), an increase in retrace time, and a decrease in second-anode (ultor) supply voltage.

An optimum matching ratio (tap position) should be chosen so as to give the specified deflecting (yoke) ampere-turns $I_m w_y$, number of yoke coil turns w_y , yoke inductance L_y , the maximum safe plate voltage surge V_{2m} during retrace, and retrace time t_2 . Using Eqs. (3.5) and (3.8), we may write

$$V_{1y} = L_y \frac{2I_{ym}}{t_1} = L_y \frac{2(I_m w_y)}{w_y t_1}$$

$$V_{2m} = 1.57 V_{1y} t_1 / t_2$$

whence, the yoke-to-output matching ratio is

$$n_y = V_1 / V_{1y} = \frac{V_{2m} w_y t_2}{\pi I_m w_y L_y} \quad (3.22)$$

The rectifier feeding the anode circuit of the picture tube utilizes the retrace voltage pulses coming from the line-scan output stage. The circuit of this rectifier is shown in Fig. 3.13. The H.V. pulses arising during retrace are stepped up by a suitable winding, w_h , to an appropriate magnitude and applied to a high-voltage rectifier tube, RT , which contains a filter capacitor, C_f , in its cathode lead. Operation of this rectifier will be clear from reference to Fig. 3.14. The power drawn by the anode circuit of a picture tube can be found from its anode voltage and current:

$$P_0 = V_{pt} i_{pt}$$

Since the efficiency of a practical high-voltage rectifier, η_r , is 70 to 80%, the power delivered to the picture tube by the line-scan circuit is

$$P_r = P_0 / \eta_r = V_{pt} i_{pt} / \eta_r \quad (3.23)$$

If the H.V. supply, V_{pt} , of the picture tube and the retrace voltage V_{2m} at the plate of the sweep tube are specified in advance, the

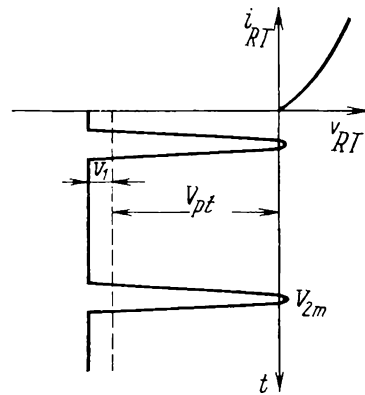


Fig. 3.14. Explaining operation of the H.V. rectifier

$i_{RT} = f(v_{RT})$ is the volt-ampere characteristic of the high-voltage rectifier tube; V_{pt} —rectified voltage across filter capacitor C_f in the circuit of Fig. 3.13

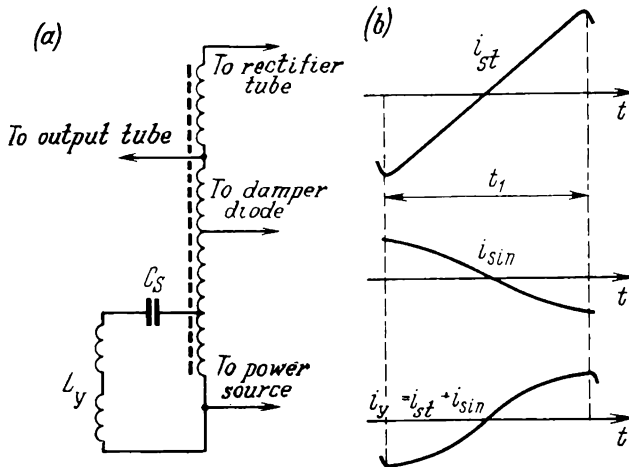


Fig. 3.15. Correction of symmetric distortion

(a) by additional capacitor C_s to give yoke current an S shape; (b) generation of S-shaped current

number of turns that the winding w_h should have may be found by the equation

$$w_h = (V_{pt} - V_{2m}) w_p / V_{2m} \quad (3.24)$$

In Sec. 2.10 we have shown the causes of symmetric picture distortions. To correct them, the deflecting current during trace should be given an S -curvature opposite to that shown in Fig. 2.23a. A sufficiently simple method to produce a current of this shape in the line-sweep circuit is to place a capacitor, C_S , of an appropriate value, in series with the yoke (Fig. 3.15a).

The sinusoidal current, i_{sin} , produced by the resonant circuit $L_y C_S$ is superimposed on the sawtooth current, i_{st} , caused in the yoke L_y by the pulse voltage supplied by the autotransformer.

As is seen from Fig. 3.15b, when the amplitude, phase and frequency of the sinusoidal current are properly selected, the total yoke current acquires the desired S -curvature during trace.

According to calculations carried out for the Soviet-made 59JK2B picture tube, the resonant frequency of the $L_y C_S$ circuit is $f_r = 4.35$ kHz. This implies that the circuit should be tuned to a frequency which is by a factor of 3.6 lower than the line scan frequency, $f_h = 15,625$ Hz.

3.4. Line Sweep Driver Circuit (Sawtooth Generator)

The perfectly linear voltage waveform at the grid of the output tube during trace (see Figs. 3.5 and 3.10) is an idealization resorted to in order to simplify the explanation of the processes taking place in the circuit. In practical circuits the grid voltage must have a far more complicated waveform so as to ensure the correct operation of the output stage.

Figure 3.16 compares the idealized and the practical grid voltage waveforms (the dashed line $ABCD$ and the waveform $\alpha\beta\gamma\delta$, respectively). The basic qualitative distinction of the practical waveform from the idealized one is that it is heavily inflected during trace (a large amount of nonlinearity). This inflection of grid voltage during trace is intended to compensate for the reverse inflection of the plate current-grid voltage characteristic, $i_p = f(v_g)$, of the output tube. As a result, the plate current pulse MN during trace rises in a more linear fashion.

All varieties of the generators that drive the line-scan output stage (sawtooth generators) always incorporate an assembly, usually called a discharge-tube circuit or stage, which generates sawtooth voltage. One type of the discharge-tube circuit is shown in Fig. 3.17a. The control grid of the discharge tube accepts narrow positive pulses which drive the tube into conduction during retrace. During scan, the tube is cut off, and the capacitor C_1 charges via resistor R_1 from

plate source E_p exponentially. During retrace, when the tube is conducting, the capacitor C_1 discharges through the tube. For nor-

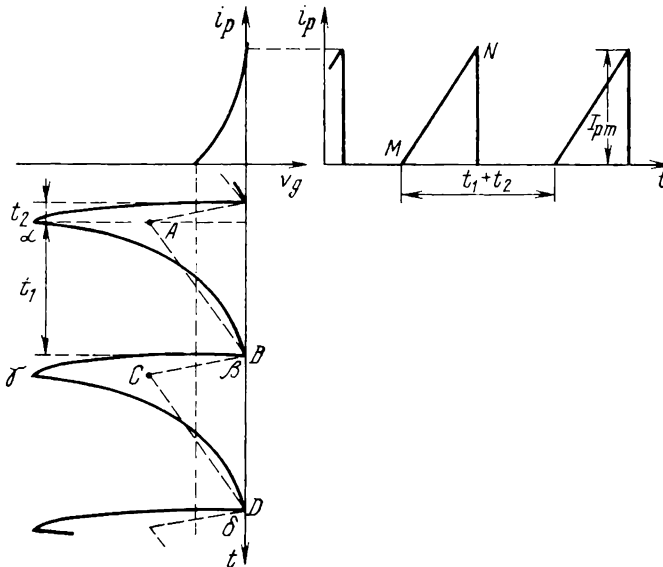


Fig. 3.16. Idealized waveform (dotted line ABC) and practical waveform ($\alpha\beta\gamma$) of horizontal output tube grid voltage

mal operation it is important that the resistance of the conducting valve, R_0 , be negligible, $R_0 \ll R_1$.

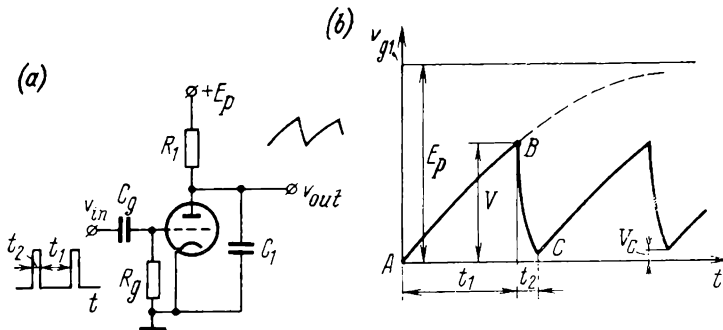


Fig. 3.17. Operation of the discharge tube
(a) discharge-tube circuit; (b) waveform of discharge-tube plate voltage

The plate voltage waveform of the tube (across the capacitor C_1) is shown in Fig. 3.17b. Its exponential rise (curve AB) during trace,

t_1 , may be described by the following expression:

$$v_{C_1} = E_p [1 - \exp(-t/R_1 C_1)] \quad (3.25)$$

At point B , $t = t_1$, whence the amplitude of sawtooth voltage is

$$V = E_p [1 - \exp(-t_1/R_1 C_1)] \quad (3.26)$$

The nonlinearity factor of sawtooth voltage is determined by differentiating Eq. (3.25):

$$\beta = \frac{|dv_{C_1}/dt|_{t=0} - |dv_{C_1}/dt|_{t=t_1}}{|dv_{C_1}/dt|_{t=0}} = 1 - \exp(-t_1/R_1 C_1) \quad (3.27)$$

whence

$$R_1 C_1 = -t_1 / \ln(1 - \beta) \quad (3.28)$$

Referring to Eq. (3.26), the amplitude of sawtooth voltage can be connected to the nonlinearity factor by the following relation:

$$V = \beta E_p \quad (3.29)$$

Thus, an increase in the amplitude of V , with the supply voltage E_p held constant, would inevitably lead to an increase in nonlinearity.

During retrace, the capacitor C_1 discharges through the resistance R_0 of the conducting tube. In practical circuits, the discharge time constant is chosen to be small—one-half to one-third of retrace time. Therefore, a negligible proportion of voltage exists at point C . Also, because $R_1 \gg R_0$, the amount by which C_1 re-charges through R_1 during retrace may be neglected.

During retrace, the voltage across the capacitor C_1 decays exponentially:

$$v_{C_1} = V \exp(-t/R_0 C_1) \quad (3.30)$$

Setting the residual voltage at point C equal to $V_C = 0.05$ V, the retrace time constant may be defined as

$$R_0 C_1 = t_2 / 3 \quad (3.31)$$

where R_0 is the resistance of the conducting tube.

The narrow positive pulses applied to the discharge tube during retrace are supplied by a master oscillator. The more recent trend has been towards using an astable cathode-coupled multivibrator as the master oscillator. Being an unsymmetrical oscillator, this type of multivibrator operates satisfactorily when there is a marked difference in duration between trace and retrace.

The multivibrator circuit is shown in Fig. 3.18a. The capacitor C_g couples the plate of the first tube to the grid of the second. Cathode coupling is provided by a common resistor, R_k , in the cathode circuits of both tubes. Sawtooth voltage is generated owing to the

inclusion of a resistor, R_1 , and a capacitor, C_1 , in the plate circuit of tube T_2 . As a result, this tube doubles as the second arm of the multivibrator and the discharge tube of the sweep output circuit.

During trace, when T_2 is cut off, the capacitor C_1 is being charged at a relatively slow rate from the plate supply source, E_p , via the

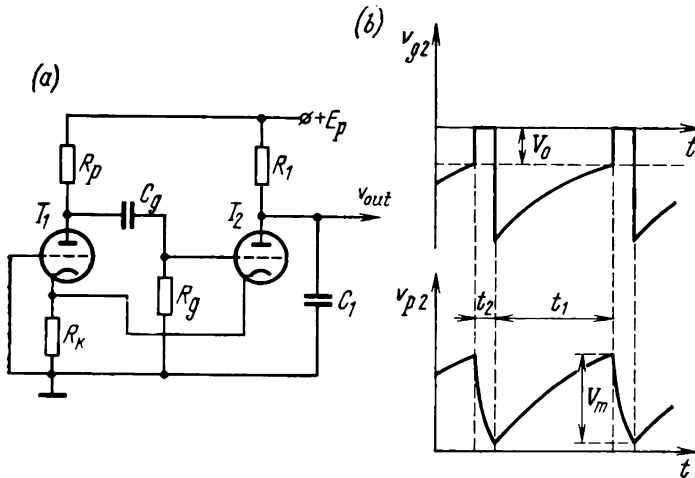


Fig. 3.18. Multivibrator combined with a discharge tube
(a) circuit; (b) waveforms of grid and plate voltages of tube T_2 .

resistor R_1 . During retrace, T_2 is conducting, and C_1 discharges rapidly through the tube resistance and the cathode resistor R_k . The waveforms of plate and grid voltages of tube T_2 are shown in Fig. 3.18b.

3.5. Features of the Vertical Scanning Generator

In broadcast television, the vertical scan frequency is 50 Hz.

Because of the low vertical frequency, there is a good deal of difference in operation between the vertical and horizontal scanning circuits. This difference may basically be summed up as follows:

1. The shunt capacitances, so decisive in the horizontal scanning circuit, have practically no effect on the waveform of the low-frequency pulses generated by the vertical scanning circuit.

2. The vertical output transformer operating at low frequencies has low iron losses, and the core material need not have a high reluctance (which is the case with the ferrite materials used in horizontal output transformers). Instead, use may be made of ordinary electrical-sheet steel.

3. The low operating frequency, the relatively slow rate of change of currents and voltages make unnecessary the use of a damper

diode. For the same reason, the retrace pulses are only a small fraction of those arising in the horizontal sweep circuit. As a result, the vertical sweep circuit may use ordinary output tubes.

4. Because the deflecting current during trace changes at a relatively low rate, the emf of self-induction across the deflection yoke is negligible in comparison with the voltage drop across the yoke resistance, and the effect of this emf may be neglected. That is, the deflection yoke may be considered to be purely resistive during trace.

3.6. Tube Vertical Output Stage

In the older makes of TV receivers, the vertical output stage incorporates a choke to couple the deflection yoke to the plate of the output tube. The choke-coupled circuit is relatively simple (Fig. 3.19a),

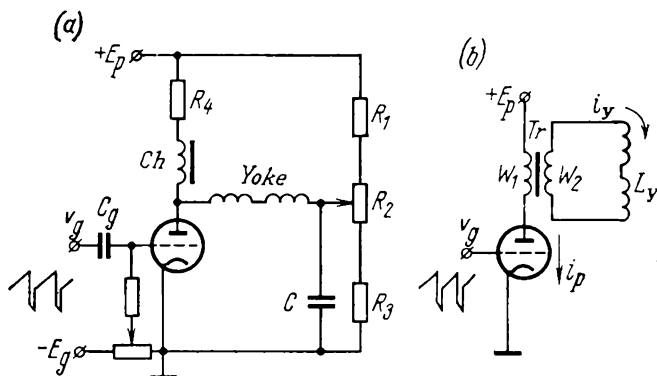


Fig. 3.19. Vertical output stage
(a) choke-coupled; (b) transformer-coupled

but it requires that the yoke coils should have a great number of turns (10 to 16 thousand per pair). Present-day TV receivers employ a transformer-coupled output stage, in which the coils have a markedly smaller number of turns (300 to 500 turns per pair). As a result, the deflection system is simpler in design and shows better performance.

Because choke coupling is mainly used in transistor sweep circuits, it will be taken up in an appropriate section. This section will be concerned with the transformer-coupled output stage.

As already noted, the vertical deflection coils in present-day TV receivers have as few as several hundred turns each. Because of the drastic reduction in the number of turns in comparison with the choke-coupled circuit, the need arises to increase the amplitude of deflecting current in proportion, so as to maintain the required deflecting ampere-turns. When the limit for the plate current pulse

of the output tube is set in advance, the desired increase in deflecting current can be obtained by use of a transformer with a high step-down (voltage) ratio (Fig. 3.19b).

Transformer-coupled output stages were not used in the older TV receivers because a moderately sized transformer would excessively distort the linearity of deflecting current during trace. It took some time to find a remedy for this nonlinearity.

To make the study of the output stage more convenient, we shall replace the transformer with its equivalent circuit (Fig. 3.20a).

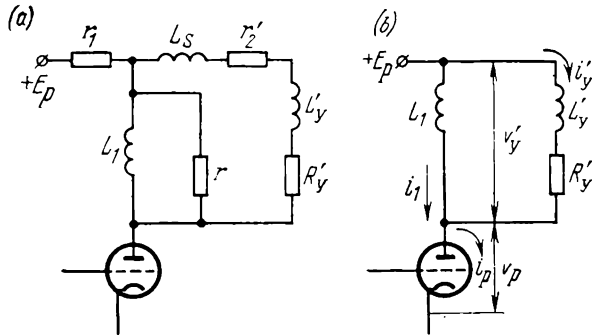


Fig. 3.20. Equivalent circuits of vertical transformer-coupled output stage
(a) complete circuit; (b) simplified circuit

Here, L'_y and R'_y are the yoke inductance and resistance scaled up to appear in (referred to) the transformer primary (plate circuit):

$$\begin{aligned} L'_y &= L_y n^2 \\ R'_y &= R_y n^2 \end{aligned} \quad (3.32)$$

where $n = w_1/w_2$ is the turns ratio.

The remaining notation in the equivalent circuit is as follows.

$r'_2 = r_2 n^2$ = resistance of the secondary (output) winding referred to the primary (input) winding

L_s = leakage inductance

L_1 = inductance of the primary winding

r_1 = resistance of the primary winding

r = equivalent eddy-current and magnetization loss resistance of the transformer

As already noted, the vertical scan circuit operates at relatively low frequencies (from 50 to 1000 Hz). Because of this, the circuit may be simplified. Since iron loss at such frequencies is small, r may be set equal to infinity. The leakage inductance L_s at low frequencies has a negligible effect, and it may be omitted from the equivalent circuit. The resistance r'_2 of the secondary can be lumped with the

yoke resistance R'_y . The resistance of the primary winding, r_1 , may be lumped with the internal resistance of the tube. After all of these simplifications, the equivalent circuit takes the form shown in Fig. 3.20b.

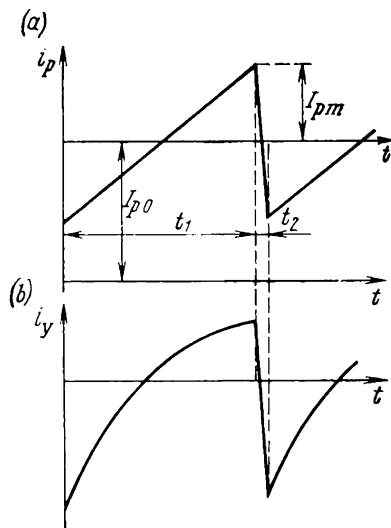


Fig. 3.21. Waveforms of currents in the circuit of Fig. 3.20a and b
(a) plate current linearly varying during scan; (b) yoke current with a large amount of nonlinearity

The deflection-yoke resistance R_y is ordinarily low, anywhere between 5 and 10 ohms. However, when scaled up to appear in the plate circuit (referred to the primary), it becomes appreciable. Assuming a turns ratio of $n = 30$ (which is a practical figure), we can see that this resistance is scaled up about 1000 times:

$$R'_y = R_y n^2 = (5 \text{ to } 10) \times 30^2 = 4500 \text{ to } 9000 \text{ ohms}$$

The yoke inductance (referred to the primary) is scaled up in the same proportion. The high value of R'_y has a marked effect on the operation of the vertical output stage. Above all, it affects the linearity of the current in the yoke.

Suppose that the current through

the tube during trace is ideally linear (Fig. 3.21a):

$$i_p = I_{pm} (2t/t_1 - 1) + I_{po} \quad (3.33)$$

Then the yoke current i'_y will vary exponentially, which is an indication of a pronounced nonlinearity. The nonlinearity of this current is defined as

$$\beta = \frac{|di'_y/dt|_{t=0} - |di'_y/dt|_{t=t_1}}{|di'_y/dt|_{t=0}} = 1 - \exp(-m) \quad (3.34)$$

where

$$m = R'_y t_1 / (L_1 + L'_y) \quad (3.35)$$

For example, for $n = 31.6$, $L_1 = 25$ H (the Soviet-made TBK-70 vertical output transformer), $R_y = 8$ ohms, $L_y = 25$ H (a type OC-70 unified deflection yoke assembly), and $t_1 = 19$ ms, the nonlinearity is prohibitively excessive: $\beta = 0.99$.

As follows from Eqs. (3.34) and (3.35), nonlinearity can be reduced either by decreasing the yoke resistance R'_y referred to the primary or by increasing the inductance L_1 of the primary winding. With a tolerable amount of nonlinearity such that $L_1 \gg L'_y$, the requisite

inductance of the transformer primary may be determined from Eq. (3.35). Setting $\beta = 5\%$, we get

$$L_1 = R'_y t_1 / \beta - L'_y = 3000 \text{ H}$$

Obviously, such a high value of inductance can hardly be adopted for mass-produced TV receivers (in them L_1 is usually 30 to 40 H).

In existing vertical output stages with a moderate transformer primary inductance the nonlinearity of the deflecting current can be controlled by the choice of plate current waveform. It has been found that apart from a linear component the plate current should contain a quadratic component.

To determine the required anode current waveform, we assume that during trace the deflecting current i_y varies in an ideally linear manner (Fig. 3.22a):

$$i'_y = I'_{ym} (2t/t_1 - 1) \quad (3.36)$$

The voltage across the yoke impedance (referred to the transformer primary) is defined (see Fig. 3.20b) as:

$$v'_y = L'_y (di'_y/dt) + R'_y i'_y \quad (3.37)$$

Substituting (3.36) in (3.37) gives

$$v'_y = L'_y (2I'_{ym}/t_1) + R'_y I'_{ym} (2t/t_1 - 1) \quad (3.38)$$

The current in the transformer primary is

$$i_1 = \frac{1}{L_1} \int v'_y dt \quad (3.39)$$

Noting Eq. (3.38), we may write

$$i_1 = (L'_y/L_1) 2I'_{ym} (t/t_1) - (R'_y t_1/L_1) I'_{ym} (t/t_1) + (R'_y t_1/L_1) (t/t_1)^2 + I_{01} \quad (3.40)$$

where I_{01} (the constant of integration) corresponds to the primary current at the start of scan ($t = 0$).

The plate current of the tube is the sum of the primary current and the yoke current referred to the primary:

$$i_p = i'_y + i_1 \quad (3.41)$$

or

$$i_p = a_0 + a_1 (t/t_1) + a_2 (t/t_1)^2 \quad (3.42)$$

where

$$\begin{aligned} a_0 &= I_{01} \\ a_1 &= I'_{ym} [2(1 + L'_y/L_1) - (R'_y t_1/L_1)] \\ a_2 &= (R'_y t_1/L_1) I'_{ym} \end{aligned} \quad (3.43)$$

From Eq. (3.42) we may draw an important conclusion, namely that in order to obtain a linear yoke current the current supplied

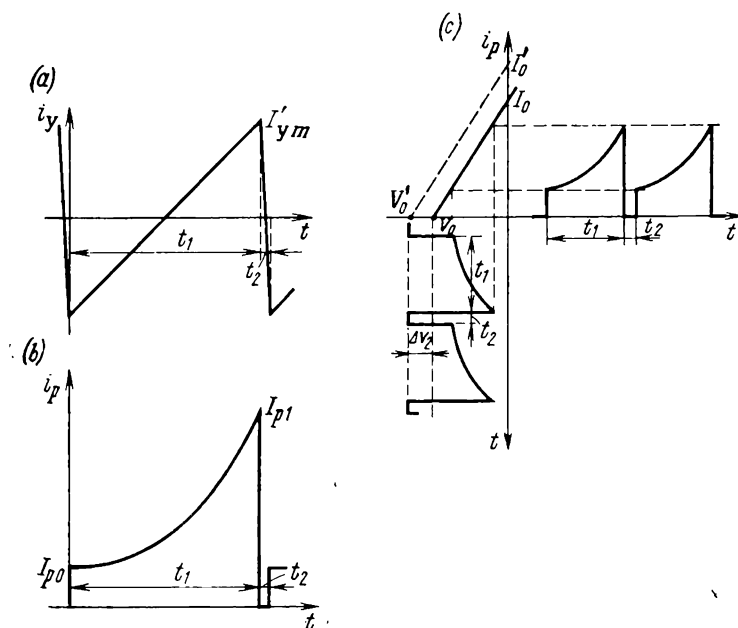


Fig. 3.22. Waveforms of currents in vertical output stage (a) yoke current; (b) output-tube plate current; (c) plate-current and grid-voltage waveforms in the case of an idealized plate-grid characteristic of the output tube

by the output tube should obey the quadratic parabola law. The waveform of plate current needed to produce a linear yoke current is shown in Fig. 3.22b.

3.7. Vertical Output Stage Driver

To determine the waveform that the grid voltage of the output tube should have in order to cause the current to obey the quadratic law, we shall assume that the plate current-grid voltage characteristic, $i_p = f(v_g)$, is ideally linear (Fig. 3.22c). Then the grid voltage should be identical in waveform with the current, that is, be a quadratic parabola:

$$v_g = a_0 + a_1(t/t_1) + a_2(t/t_1)^2 \quad (3.44)$$

The plate current and grid voltage waveforms are shown in Fig. 3.22c.

Because the plate load of the output valve has an inductive component (L_1 and L'_y in the diagram of Fig. 3.20), a positive plate pulse running into several hundred volts arises during retrace when the currents in the circuit are varying at a relatively high rate. As a result, the plate current-grid voltage characteristic during retrace is shifted somewhat to the left (the dashed line $V'_o I'_o$ in Fig. 3.22c). To compensate for this shift, that is, to cut off the tube reliably during retrace, an additional negative pulse (Δv_2 in the figure) should be added to the grid voltage.

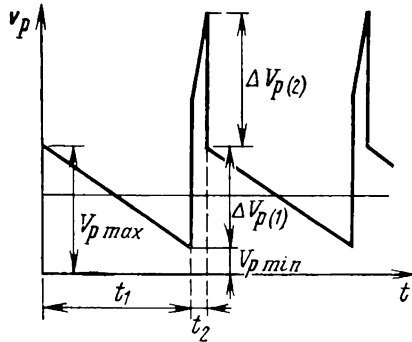


Fig. 3.23. Waveform of output-tube plate voltage

As a rule, the drive voltage having the waveform determined by Eq. (3.46) is shaped by a feedback circuit placed between the plate circuit and the control grid of the output tube and consisting of integrating or differentiating elements. For better insight into the operation of the feedback circuit, we shall first determine the waveform of the output tube plate voltage utilized as input to the feedback circuit. Referring to Fig. 3.20b and using Eq. (3.40), we obtain the following expression for the plate voltage of the valve:

$$v_p = E_p - v_y = \left(E_p + R'_y I'_{ym} L'_y \frac{2I'_{ym}}{t_1} \right) - 2R'_y I'_{ym} (t/t_1) = V_{p \max} - \Delta V_{p(1)} (t/t_1) \quad (3.45)$$

The plate voltage waveform fitting Eq. (3.45) is shown in Fig. 3.23. The positive retrace plate pulse, ΔV_{p2} , is mainly determined by the emf of self-induction of the yoke:

$$\Delta V_{p2} = L'_y 2I'_{ym} / t_1 \quad (3.46)$$

As an example, we shall examine a widely used vertical scanning generator with feedback applied over a differentiating network (Fig. 3.24). The plate voltage is taken from the primary w_1 of the output transformer Tr_1 to the input of a differentiating network, $R_1 C_1$. The differentiated voltage is fed via R_3 to the control grid of the output tube, which also accepts the sawtooth voltage via R_4 from the plate of the discharge tube operating in the conventional manner. The network $C_3 R_5$ eliminates the d.c. component. The manner in which the grid voltage is given the desired waveform will be clear from Fig. 3.25. The plate voltage of the output tube has the waveform represented by the curve v_p (compare it with Fig. 3.23).

At the output of the differentiating network, R_1C_1 , this voltage comes by a characteristic concave inflection v_b during trace. This inflection is due to the exponential component with a time constant R_1C_1 in the output voltage. During trace, the voltage v_b may be visualized

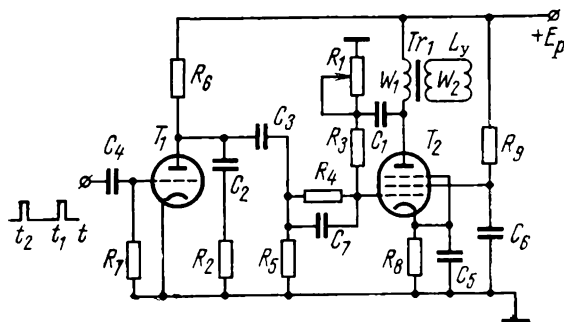


Fig. 3.24. Circuit of a vertical scan generator with feedback via a differentiating network

as made up of two components, v_c and v_d , the former being a non-linear and the latter a linear (decreasing) function of time. The component v_c may be approximated by a quadratic parabola

$$v_c \approx a_2 t^2 \quad (3.47)$$

and the component v_d as

$$v_d = -a'_1 t \quad (3.48)$$

The voltage supplied by the discharge tube during trace may be assumed to be an approximately linear (rising) function of time

$$v_e = a''_1 t \quad (3.49)$$

The amplitude of the voltage supplied by the discharge tube should be chosen sufficiently large so that, when combined with the component v_b in the grid circuit of the output tube, it can not only make up for the falling linear component v_d , but also give the requisite surplus:

$$v_e + v_d = (a''_1 - a'_1) t = a_1 t; \quad (a_1 = a''_1 - a'_1; \quad a''_1 > a'_1) \quad (3.50)$$

Thus, the grid voltage of the output tube during trace is defined as

$$v_f = v_b + v_e = v_c + v_d + v_e = a_2 t^2 - a'_1 t + a''_1 t = a_1 t + a_2 t^2 \quad (3.51)$$

and has the required waveform (compare with Fig. 3.22c). The voltage v_g is produced at the grid of the output tube during the complete sweep cycle (including trace and retrace). During retrace, narrow positive pulses Δv_{p2} appear at the plate (Fig. 3.23). Applied via the differentiating network to the control grid of the output tube,

these pulses might interfere with driving this tube to cut-off during retrace. To avoid this, the circuit of Fig. 3.24 has been extended

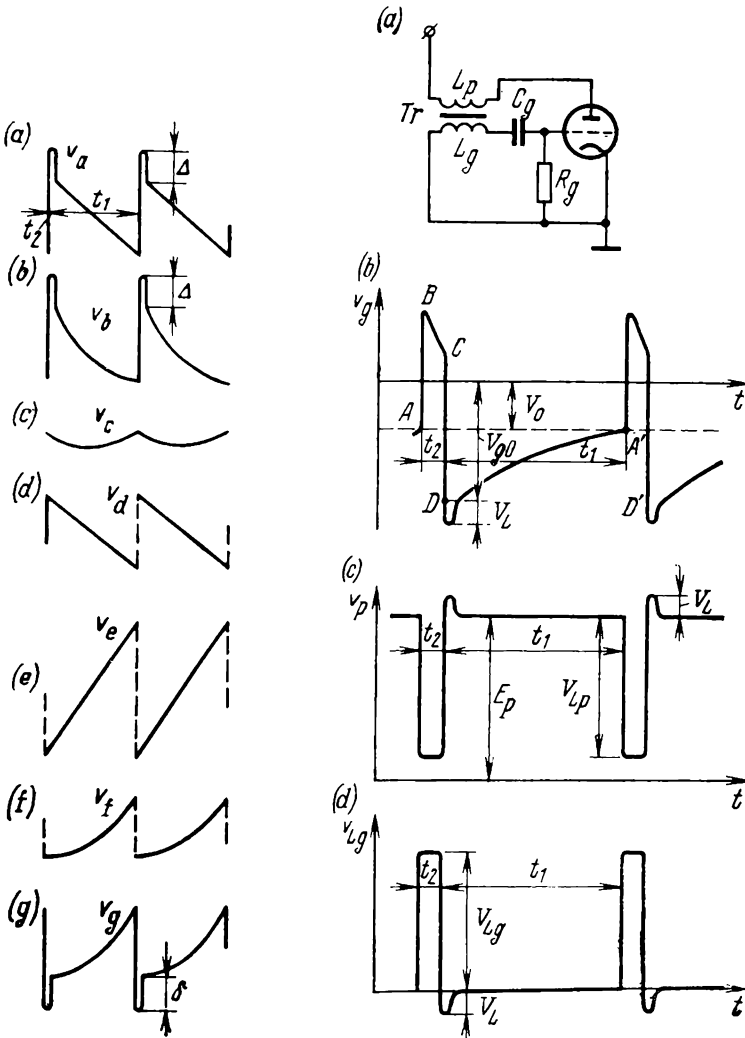


Fig. 3.25. Waveforms of output-tube plate and grid voltages in the circuit of Fig. 3.24

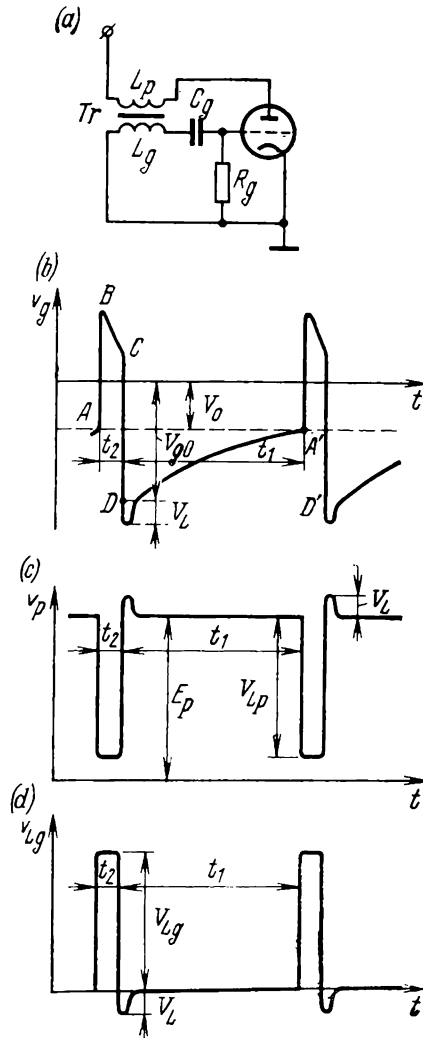


Fig. 3.26. Blocking oscillator
(a) circuit; (b) waveform of grid voltage; (c) waveform of plate voltage; (d) waveform of voltage across transformer grid winding

to include two more elements, a capacitor, C_7 , and a resistor, R_2 . The capacitor C_7 together with C_2 and C_3 connected in series with

it provides a bypass to ground for these pulses. R_2 is provided to produce a negative cut-off pulse Δv_{g2} (Fig. 3.22c). During retrace, when the discharge tube T_1 is conducting, the discharge current of capacitor C_2 flows through R_2 and produces a narrow negative voltage pulse which reaches the grid of the output tube together with the sawtooth voltage (Fig. 3.22c). This mixture of narrow negative retrace pulses and sawtooth voltage is called sawtooth pulse voltage.

During retrace, the grid of the discharge tube should be fed narrow positive pulses in order to render that tube conducting for the discharge current of the capacitor C_2 (Fig. 3.24). This purpose is served

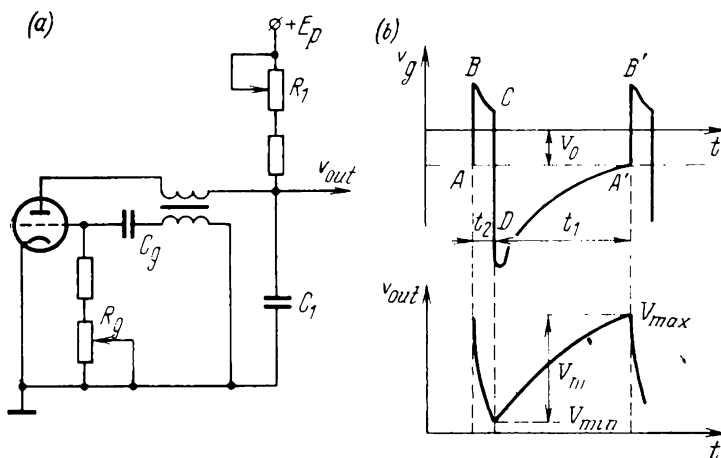


Fig. 3.27. Blocking oscillator combined with a discharge tube
(a) circuit; (b) grid voltage waveform; (c) output voltage waveform

by the vertical oscillator which is held in synchronism with the vertical sweep circuit by sync pulses.

The traditional vertical oscillator is a blocking oscillator. In comparison with a multivibrator, the blocking oscillator offers the advantages of simple circuit, simple and reliable self-excitation, and ability to generate pulses with a high pulse period to pulse duration ratio. It is also important that the blocking oscillator uses only one tube, a triode. Among its disadvantages are reduced frequency stability (in comparison with the multivibrator) and the need for a fairly complicated transformer used to provide positive feedback.

The most commonly used circuit of the blocking oscillator is shown in Fig. 3.26a. Since the grid and plate voltages are in anti-phase, in order to obtain positive feedback, another phase reversal is needed. This is done by a transformer connected between plate and grid. The

elements R_g and C_g mainly determine the period of oscillation. The greater the time constant $R_g C_g$, the longer the period.

Typical pulse voltage waveforms of a blocking oscillator are shown in Fig. 3.26*b*, *c* and *d*.

In most TV receivers, as a way of reducing the count of circuit components and tubes, the blocking oscillator and the discharge-tube circuit utilize a common tube (Fig. 3.27*a*). The waveforms of the voltages existing at the tube grid and across the output capacitor C_1 are shown in Fig. 3.27*b* and *c*. The grid voltage v_g has mainly the same waveform as that existing in a conventional blocking oscillator. During retrace, t_2 , when the tube is conducting, the capacitor C_1 discharges through the relatively low resistance of the plate-cathode space. Within the portion DA' , when the tube is cut off (trace interval, t_1) the capacitor C_1 charges exponentially from the plate supply E_p via the resistor R_1 . The period of oscillation can be adjusted with the resistor R_g , and the amplitude of sawtooth voltage with the resistor R_1 .

3.8. Transistor Horizontal Scanning Generator

Transistorized TV receivers offer a number of advantages over their tube counterparts. The most important advantages are:

1. Portability. A transistor TV set is small in size, practically equal to that of the picture tube, and light in weight. Among other things, these qualities have been utilized in TV sets for cars, hikes, etc.

2. Substantial saving in power consumption (from mains or any other source). This economy is especially important for the line sweep circuit where the output transistor operates as a switch. In the ON state this transistor has a very low saturation resistance (a few ohms). Therefore, the power dissipated on this resistance is negligible in comparison with that dissipated in a tube circuit. Besides, a few more tens of watts are saved because transistorized sweep circuits have no filament or heater circuits.

3. Improved reliability. Since transistors have a long service life, the need for repair occurs more seldom.

The power taken by a tube and a transistorized horizontal scanning generator for the Soviet-made 59JK2B picture tube is compared in Table 3.1. The respective block diagrams are shown in Fig. 3.28. The total power consumption of a tube sweep circuit is $P_{tube} = 54.2$ W, and that of a transistorized circuit is $P_t = 16$ W. In other words, a tube circuit draws 3.4 times more power than its transistorized counterpart. On the average, a TV set draws a total of $P_{tv} = 170$ W, and a tube-based line scan circuit accounts for 32% of this total. It is to be stressed that the filament (heater) power, $P_f = 28.7$ W, accounts for more than half the total power dissipated by a tube-based line-scan circuit.

Table 3.1

Stage	Tube generator				Transistor generator	
	tube type	Power, W			transistor type	power, W
		plate	screen grid	filament		
Output stage	6П36С	15.0	2	12.6	KT802A	10.0
Damper	6Д20П	5.0	—	11.34	Д302	2.4
Buffer	—	—	—	—	KT801A	0.5
HV rectifier	1П21П	3.0	—	0.97	5ГЕ600А	3.0
Drive_oscillator	6Н1П	0.5	—	3.8	МП42А	0.1

However, the use of transistors in scanning generators still runs into difficulties and suffers from specific drawbacks. Among them are:

1. The horizontal output transistor has a peak power rating half or even a third as great as that of the horizontal output tube.

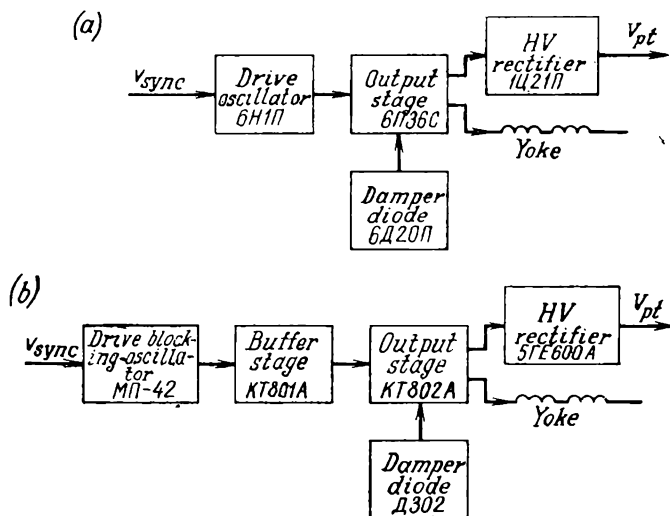


Fig. 3.28. Block diagrams of (a) tube horizontal scanning generator and (b) transistor horizontal scanning generator

2. A higher driver power (in the base circuit) is needed for transistors than for tubes. This is not only because the base circuit acts as an additional load. The low input resistance of the transistor and pronounced nonlinearity of the input characteristic, $i_C = f(v_{BE})$, necessitate a complication in the circuit matching the output of a preceding stage to the input of the next.

3. Marked spread in parameters between transistors even of the same type necessitates individual alignment of the circuit following the replacement of a faulty transistor.

4. The parameters and operating conditions of transistor circuits are heavily dependent on temperature. This is especially true of the vertical scanning generator where the typical output stage

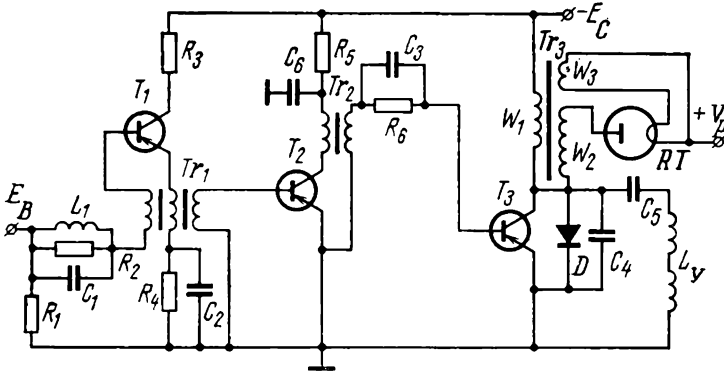


Fig. 3.29. Circuit of a transistor horizontal scanning generator

operates Class A, and where the temperature-induced changes in this class of operation result in marked distortions in the vertical deflecting current.

5. There is an appreciable time lag as the horizontal output transistor switches from trace to retrace. This time lag entails an increase in power consumption and impairs the waveform of the deflecting current.

However, advances in transistor technology hold out promise that these shortcomings will be overcome before long.

An example of the transistorized horizontal scanning generator is shown in Fig. 3.29. The output stage (transistor T_3) uses both a choke and a transformer. The winding w_1 of transformer Tr_3 acts as a choke for the deflection yoke, L_y , coupled to this winding via an interstage capacitor, C_5 (which can also supply S-compensation of the sawtooth current). During retrace, high-voltage pulses arise across the step-up winding w_2 . These pulses are rectified by a high-voltage rectifying tube, RT . The rectified voltage, V_p , is applied to the main anode of the picture tube. The tertiary winding, w_3 , supplies filament voltage for the high-voltage rectifier tube. Connected in parallel with the collector circuit of the output transistor T_3 are damper diode D and retrace capacitor C_4 . The buffer stage (transistor T_2) matches the low-impedance base of the output transistor to the high-impedance blocking oscillator (transistor T_1).

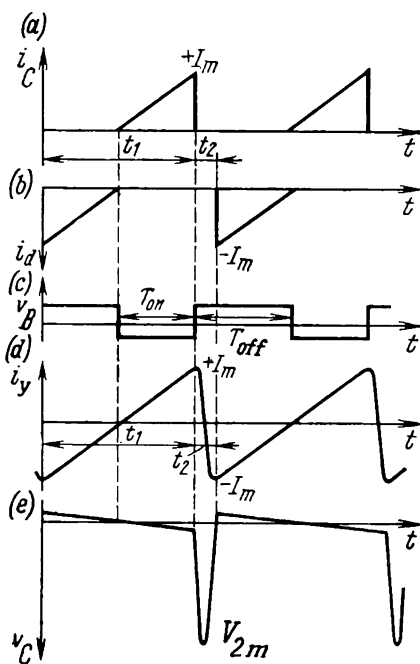


Fig. 3.30. Waveforms of currents and voltages in the circuit of Fig. 3.29

(a) output-transistor collector current; (b) damper-diode current; (c) output-transistor base voltage; (d) yoke current; (e) output-transistor collector voltage

output stage are shown in Fig. 3.32. The output stage (transistor T_5) is a choke-coupled circuit. The deflection yoke L_y is coupled to the winding w_1 of the choke Ch by an interstage

The speed-up network C_3R_6 permits a faster turn-off for the output transistor at the start of scan. R_4 and C_2 are time defining elements: the time constant R_4C_2 determines the period of oscillations taking place in the blocking oscillator. The tuned circuit $L_1R_2C_1$ stabilizes the frequency of oscillations. The base (terminal E_B) of the transistor used as the blocking oscillator accepts a control voltage from an automatic phase control circuit. This voltage synchronizes the blocking oscillator.

Somewhat idealized, the waveforms of currents and voltages existing in the output stage are shown in Fig. 3.30.

3.9. Transistorized Vertical Scanning Generator

One of the likely arrangements for the transistorized vertical scan circuit appears in Fig. 3.31, and the relevant current and voltage waveforms existing in the

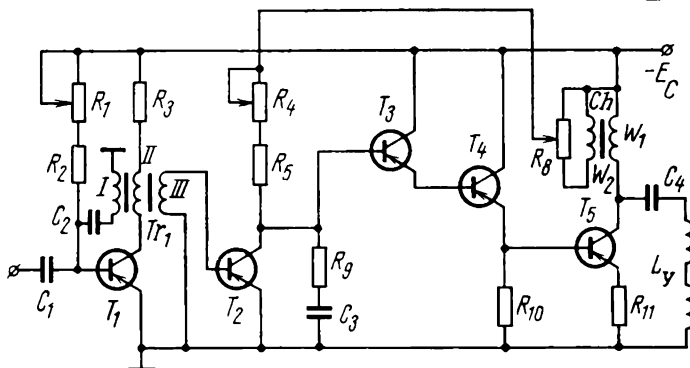


Fig. 3.31. Circuit of a transistor vertical scanning generator

capacitor C_4 . The secondary winding w_2 brings about a phase reversal in the collector voltage and feeds this voltage to the feedback circuit. The variable resistor R_8 is used to adjust the feedback voltage (the vertical linearity control). The feedback voltage and the supply voltage, E_C , are fed together to the collector of the discharge transistor T_2 . During trace, capacitor C_3 accumulates charge due to a parabolic voltage. The narrow retrace voltage pulses appearing across resistor R_9 are utilized to cut off the output transistor reliably during retrace. The variable resistor R_4 is used to adjust the drive voltage for the output transistor (the height control). The emitter follower built around a compound-connected transistor (transistors T_3 and T_4) matches the high-impedance collector circuit of the discharge transistor T_2 to the low-impedance base circuit of the output transistor T_5 . The transistor T_1 is utilized in the blocking oscillator. The variable resistor R_1 is used to adjust the period of free-running oscillations. Sync pulses are injected into the base circuit of the blocking oscillator.

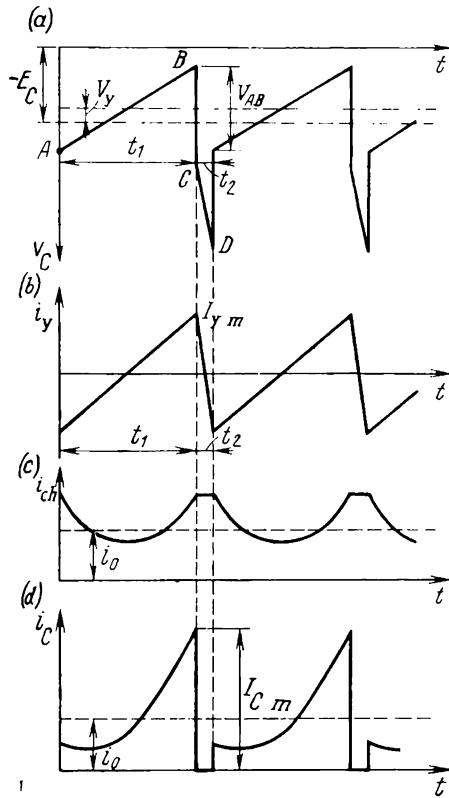


Fig. 3.32. Waveform of currents and voltages in the vertical output stage

(a) output-transistor collector voltage; (b) yoke current; (c) choke current; (d) collector current

CHAPTER FOUR

THE FREQUENCY SPECTRUM OF THE TELEVISION SIGNAL

4.1. Upper and Lower Boundaries of the Television Spectrum

The television signal occupies a frequency spectrum many times that used in, say, radio broadcasting. If, on the basis of practical experience, we assume that the radio signal of a sufficiently good quality needs a bandwidth of about 12 kHz and that the bandwidth needed by the television signal is 6 MHz, the ratio will be

$$(6 \times 10^6) \div (12 \times 10^3) = 500$$

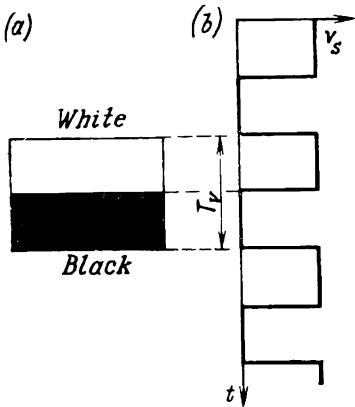


Fig. 4.1. Determining the minimum frequency of the television spectrum

(a) simple example of a static image on a TV screen; (b) corresponding signal

This bandwidth makes it unfeasible to transmit high-quality TV programs at medium and short frequencies. The only choice left is to use the VHF and UHF bands. A major limitation of these bands is that messages can be transmitted and received only within the so-called line-of-sight distance (60 to 80 km). In other words televiewers can only receive programs from a local TV centre; domestic receivers have no facilities that would enable them to pick up remote centres directly.

Consider the factors determining the maximum and minimum frequencies of the television signal. For a stationary image, the minimum

frequency is determined by the number of frames per second (or the number of fields per second in the case of interlaced scan).

A simple example of a static image is shown in Fig. 4.1a; it consists of two bars, one white and the other black. As is seen from Fig. 4.1b, the respective signal is a train of pulses following at a period equal to the time necessary to transmit one frame or one vertical scan interval, T_v .

The frequency of these pulses (the fundamental term in the Fourier series representing these pulses) is equal to the frame or vertical scanning frequency. For a specified vertical frequency, it is impos-

sible to think up a static picture for which the fundamental frequency would be lower than the frame frequency.

Thus, the minimum frequency of the television signal may be defined by a simple relation of the form

$$f_{\min} = 1/T_v = n \text{ frames/s} \quad (4.1)$$

With interlaced scan, the image shown in Fig. 4.1a will be practically the same in both the even and the odd fields (the difference

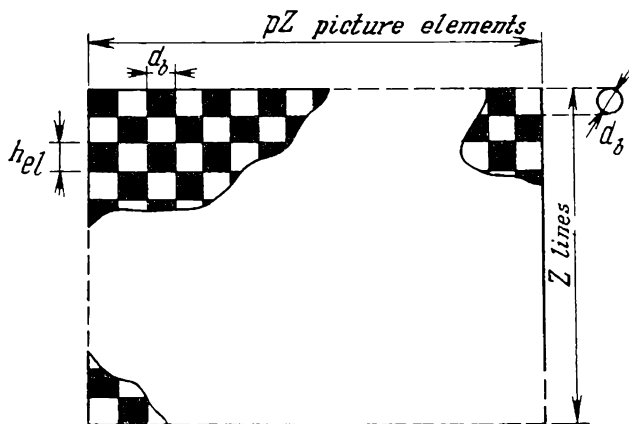


Fig. 4.2. Determining the maximum frequency of the television spectrum

in signal pulse shape and duration between adjacent fields can only be equal to one period of line or horizontal scan, or in per unit terms, $T_h/T_{field} = 64 \mu s / (20 \times 10^3 \mu s) = 3.2 \times 10^{-5}$). Because of this, the minimum frequency for interlaced scanning may be taken equal to the number of fields transmitted per second:

$$f_{\min} = 2n = 50 \text{ Hz} \quad (4.2)$$

where n is the number of frames per second.

The maximum frequency of the television spectrum depends on the fine detail in the image that can be reproduced on the TV screen. The picture tube should incorporate facilities to focus the beam so that at the point where it strikes the phosphor its diameter d_b be equal to the line width:

$$d_b = h/Z$$

where h is the frame height and Z is the number of lines per frame.

In other words, given the same horizontal and vertical resolution, the minimum size of alternating black and white elements along and across the lines must be equal to the beam diameter (Fig. 4.2).

In determining the maximum frequency of the television signal spectrum, we assume that the picture elements are arranged as alternate black and white squares along the scanning line (the checkerboard pattern in Fig. 4.2), each square having the height and width equal to the diameter of the scanning beam. The number of pairs of such squares scanned every second will define the maximum frequency of the television signal spectrum.

Number of pairs per line is $pZ/2$ (where $p = 4/3$ is the aspect ratio).

Number of pairs per frame is $(pZ/2) Z$.

Number of pairs of elements scanned every second is $(pZ/2) Zn$ (n is the number of frames per second).

This expression defines the maximum frequency, f_{\max} , of the television signal spectrum:

$$f_{\max} = (npZ^2)/2 \quad (4.3)$$

Now we shall compute the maximum frequency for a practical television system in which: the number of lines per frame is $Z = 625$, the aspect ratio is $p = 4/3$, and the number of frames per second (sufficiently high to exceed the flicker frequency) is $n = 50$. Substituting these figures in Eq. (4.3) gives:

$$f_{\max} = npZ^2/2 = 50 \times 4 \times (625)^2 \div (3 \times 2) \approx 13 \text{ MHz}$$

Thus, a fairly broad bandwidth would be needed. A signal requiring such a wide bandwidth would be difficult to amplify and transmit by radio without distortion. It is likewise important that a very small number of television channels could then be accommodated in the allocated frequency band.

One way to reduce the bandwidth requirements is to employ interlaced scan in broadcast television (briefly described in Sec. 1.5). This technique enables the frame frequency to be halved without causing an unpleasant sensation due to flicker. In other words, the maximum frequency of the signal spectrum can be halved without practically any detriment to picture quality.

In interlacing, the image is scanned in two groups of lines, each group comprising a field. One field includes odd lines 1, 3, 5,, $(2q + 1)$ and the other, even lines 2, 4, 6, . . . , $2q$ (see Fig. 1.17). As a result, two images are reproduced on the screen each frame period, differing but little from each other, especially in coarse detail. Since during each field the beam scans half as many lines, each field contains half as much information about the scene in comparison with a full frame. However, the viewer combines the two fields in his mind's eye into a single image reproducing a complete scene.

Fields are scanned at the rate of 50 per second, which is more than enough to exceed the flicker frequency; at the same time the maxim-

um frequency of the television signal is halved:

$$f_{\max} = n_f (Z/2) pZ/2 = n_f pZ^2/4 = 50 \times 4 \times (625)^2 \div (3 \times 4) = 6.5 \text{ MHz}$$

In view of the effect that aperture distortion has on the reproduction of fine detail (see Sec. 1.11) and also of the impairment in vertical resolution due to the line structure of the television picture (see Sec. 1.10), the maximum frequency f_{\max} may be reduced still more without detriment to picture quality. Thus, the practical equation defining the maximum frequency of the television signal takes the form

$$f_{\max} = k (npZ^2)/2 \quad (4.4)$$

where k is a practical factor to be chosen in the range 0.8-0.9. Then,

$$f_{\max} = 5 \text{ to } 6 \text{ MHz}$$

4.2. Line Structure of the Television Spectrum

What sets the television spectrum apart from that of, say, a sound signal is that it has a line structure. In other words, instead of a continuum of frequencies, the above defined frequency range, $f_{\min} = 50 \text{ Hz}$ to $f_{\max} = 6 \text{ MHz}$, contains discrete frequencies which are multiples of the frame and line frequencies. The rather large gaps between them are left unoccupied. In colour television, these gaps are successfully utilized for the insertion of colouring information.

The line structure of the television spectrum will be demonstrated with the following example. Let there be two images on a TV screen, one being a horizontal bar in which the luminance decays towards the top and bottom edges of the raster (Fig. 4.3a), and the other being a similar, but vertical bar, with the luminance falling off towards the left- and right-hand edges of the raster (Fig. 4.3c). The waveforms of the respective signals fed to the control electrode of the picture tube are shown in Fig. 4.3b and 4.3d (the origin of coordinates is placed at the centre of the image). To simplify the further reasoning, the functions of Fig. 4.3b and d may be written in the following simple form:

$$\begin{aligned} v_v &= V_v [\exp(-vt^2)] \\ v_h &= V_h [\exp(-ht^2)] \end{aligned} \quad (4.5)$$

In the case of a continuous periodic scan, the signal waveforms for the images shown in Fig. 4.3a and c will be periodic functions (Fig. 4.4) with a period $T = T_v$ for the case illustrated in Fig. 4.3b and $T = T_h$ for the case of Fig. 4.3d:

$$\begin{aligned} v_v &= V_v \exp[-v(t - \alpha T_v)^2] \\ v_h &= V_h \exp[-h(t - \beta T_h)^2] \end{aligned} \quad (4.6)$$

where α and β are the numbers of periods (0, 1, 2, . . .).

These functions may also be expanded into a Fourier series:

$$v_v = \sum_{q=0}^{\infty} V_{m_v} \cos m\omega_v t \quad (4.7)$$

$$v_h = \sum_{q=0}^{\infty} V_{q_h} \cos q\omega_h t \quad (4.8)$$

Their spectra are shown in Fig. 4.5a and b. Since one frame can accommodate a maximum number of $Z/2$ pairs of black and white

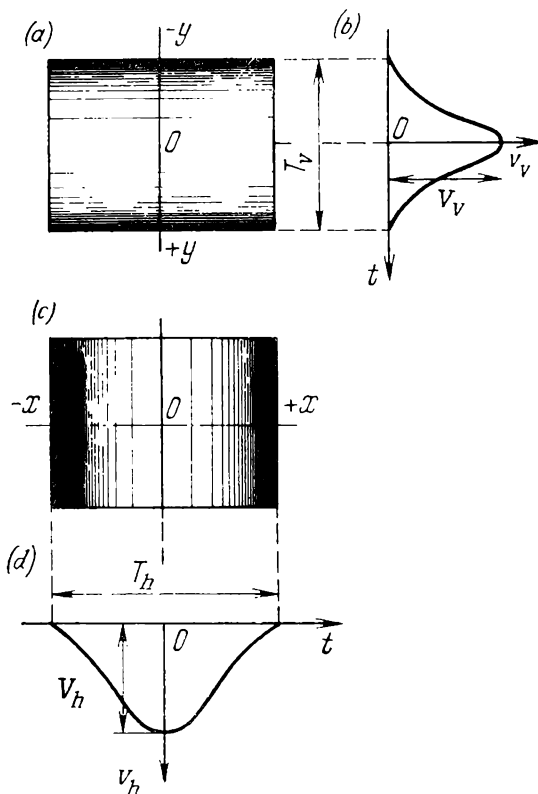


Fig. 4.3. Demonstration of the line structure of the television signal spectrum, using simple test charts

(a) horizontal bars; (b) corresponding signal; (c) vertical bars; (d) corresponding signal

lines (any further increase in the number of pairs is limited by the number of lines per frame adopted), the maximum frequency of the spectrum for the case of Fig. 4.5a (and Fig. 4.3a, b) is given by

$$f_{\max, v} = (Z/2) f_v = f_h/2 \quad (4.9)$$

The maximum frequency for the case of Fig. 4.5b is given by Eq. (4.5). Replacing the product nZ in that equation by the line

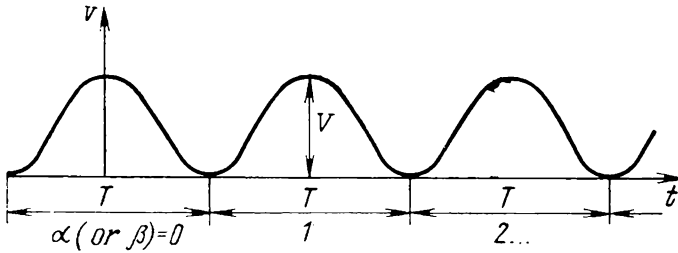


Fig. 4.4. Example of a periodic television signal

frequency $f_h = nZ$ gives

$$f_{\max, h} = (kpZ/2) f_h \quad (4.10)$$

Now we consider a more elaborate case where the signal applied to the control electrode of the picture tube is the product of two

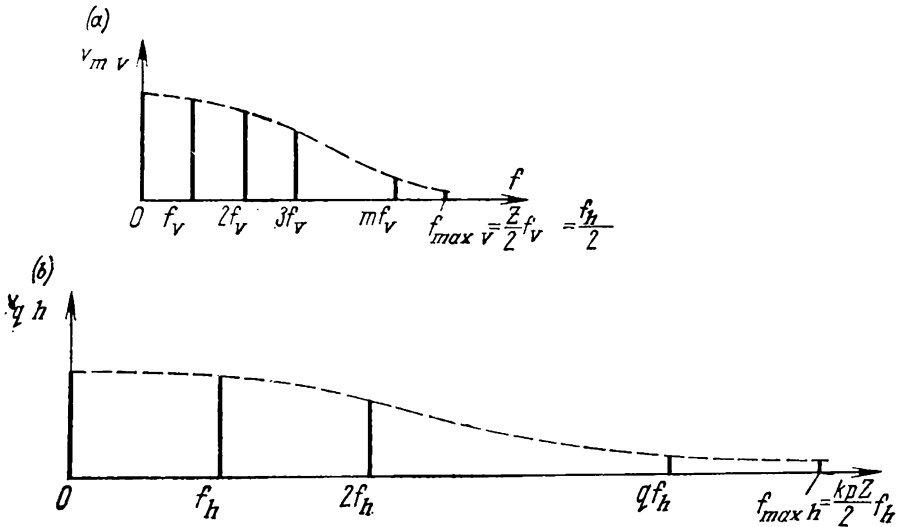


Fig. 4.5. Signal spectrum

(a) corresponding to the image of Fig. 4.3a; (b) corresponding to the image of Fig. 4.3c

signals:

$$\begin{aligned} v_v &= V_v \exp[-v(t - \alpha T_v)^2] \quad \text{and} \quad v_h = V_h \exp[-h(t - \beta T_h)^2]; \\ v_{v, h} &= V_{v, h} \exp[-v(t - \alpha T_v)^2] \exp[-h(t - \beta T_h)^2] \end{aligned} \quad (4.11)$$

The associated image will appear on the screen as a luminous spot with the luminance decaying towards the periphery in all directions from the centre (Fig. 4.6a). In three dimensions the distribution

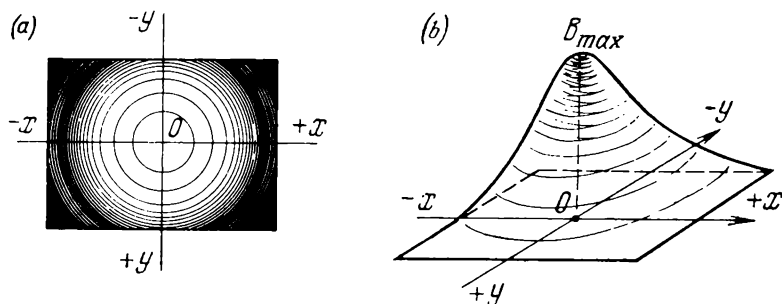


Fig. 4.6. Product of signals shown in Fig. 4.3b and d
(a) resultant image; (b) luminance distribution

of luminance in this case is shown in Fig. 4.6b. An oscillogram showing variations in the signal with time is given in Fig. 4.7. As is

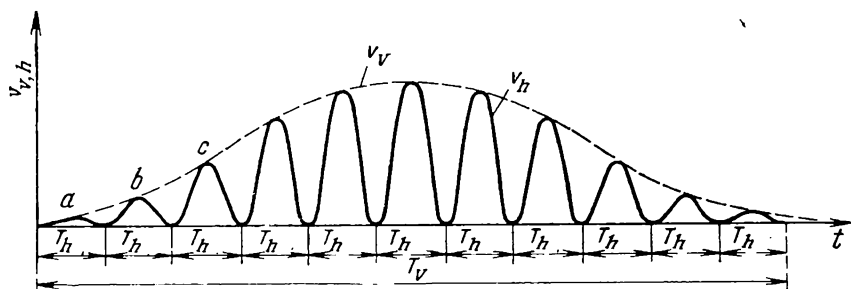


Fig. 4.7. Television signal corresponding to the image shown in Fig. 4.6a

seen, the complete signal is a periodic sequence of waveforms a , b and c produced by the line frequency and amplitude-modulated by frame frequency.

Multiplying together two time functions means multiplying together their spectral components. Thus, the spectrum of the product $v_v v_h$ is the sum of all likely products of the harmonics of frame and line frequencies:

$$v_{v,h} = \sum_{m=0}^{\infty} \sum_{q=0}^{\infty} V_{m,q} \cos m\omega_v t \cos q\omega_h t \quad (4.12)$$

where q is the order of the harmonics of the line-scanning frequency and m is the order of the harmonics of the frame-scanning frequency.

Using an elementary equation from trigonometry

$$\cos \alpha \cos \beta = \frac{1}{2} \cos (\alpha - \beta) + \frac{1}{2} \cos (\alpha + \beta)$$

any component of the spectrum $v_{m v}, q_h$ can be expressed as the sum of two side frequencies:

$$v_{m v, q h} = \frac{1}{2} V_{m q} \cos (m \omega_v - q \omega_h) t_h + \frac{1}{2} V_{m q} \cos (m \omega_v + q \omega_h) t \quad (4.13)$$

The spectrum fitting Eq. (4.13) is shown in Fig. 4.8. As is seen, grouped around the line frequency harmonics, $q f_h$ ($q = 0, 1, 2, \dots$),

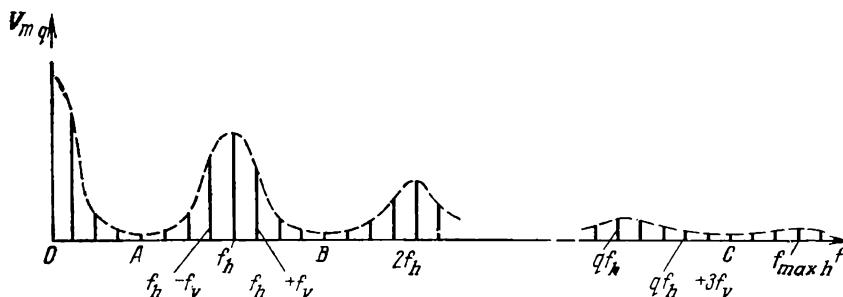


Fig. 4.8. Line spectrum of the television signal

acting as carriers, are the lower and upper side frequencies, $q f_h - m f_v$ and $q f_h + m f_v$ ($m = 0, 1, 2, \dots$), and there are no other frequencies in the gaps between them. It is also to be noted that the energy midway between the line-frequency harmonics (segments A, B, C, ...) is negligible. This property of the television spectrum has been utilized in existing colour television systems. As a result, the spectral composition of the colour television signal has been made equal to that of the black-and-white signal by a technique known as frequency interleaving (or frequency interlace).

4.3. Spectrum of the D.C. Component

Apart from the main television spectrum extending from 50 Hz to about 6 MHz, there is also a small region from zero to two or three hertz. This region is associated with the so-called *d.c.* component, B_{dc} (Fig. 4.9a).

The part the *d.c.* component plays will be clear from Fig. 4.9b,

which shows the distribution of luminance, B_{sign} , along a line (where x is the coordinate or path of the scanning beam and u is the velocity of the beam). Apart from the alternating luminance component, B_{ac} , the signal also contains an average luminance, B_{dc} , which shows how bright the image is on the whole. In some cases (for example, when a test chart is transmitted for several hours in succession) the average luminance will not change, and the frequency of the d.c. component is zero. Very often, however (especially

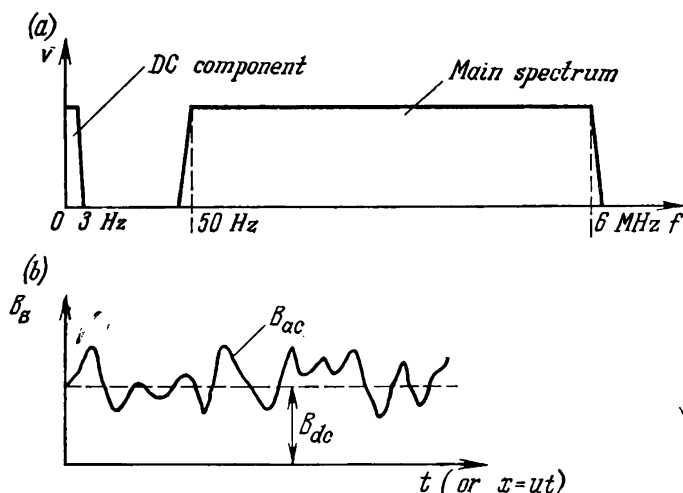


Fig. 4.9. D.C. component
(a) location of its spectrum; (b) in a television signal

when a film is transmitted) the average luminance varies. If the variations occur more than two or three times per second, the viewer will sense them as an unpleasant flicker. This sets the limit to the spectrum of the d.c. component.

Ordinary multistage video amplifiers are unable to amplify the d.c. component because the interstage capacitors will block any signals at frequencies close to zero. This is why the d.c. component is amplified in an indirect way: to begin with, the blanking pulses which are part of the composite television signal (see Sec. 5.1) are amplitude-modulated by the d.c. component so as to translate the latter into the main signal spectrum, after which the d.c. component is amplified along with that signal.

At the receiving end, the blanking pulses are detected, and this restores the d.c. component which is then reinserted in the signal spectrum. The circuit performing this function is called the black level restorer.

4.4. R.F. Spectrum for the Television Signal

Television signals are transmitted in the VHF band, by amplitude modulation of the carrier.

In the Soviet Union, the carrier frequencies allocated to television broadcasts (black-and-white and colour) extend from 48 to 230 MHz and are divided among 12 channels, or programs. Work is under way to utilize the higher frequencies.

Each channel, apart from the video signal, also accommodates the respective sound signal. To improve quality and enhance noise immunity, sound is transmitted by frequency modulation.

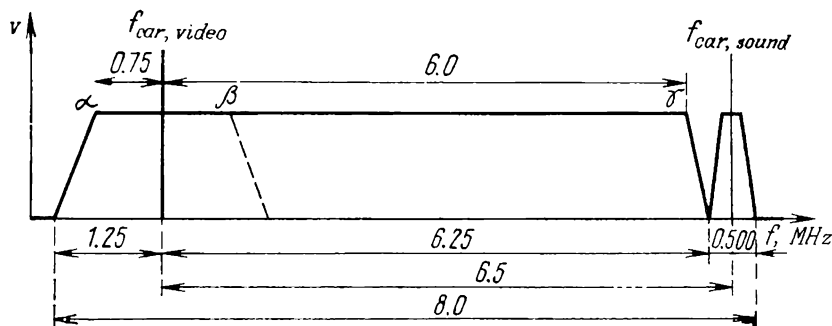


Fig. 4.10. Positions of video and sound signals within a TV broadcast channel

As will be recalled, the modulation of the video carrier produces two side bands, lower and upper. In other words, the video spectrum about 6 MHz wide is nearly doubled to 12 MHz after modulation. To enable the standard communication channel (with a bandwidth of 8 MHz) to handle the modulated video signal, the lower sideband is substantially suppressed (Fig. 4.10). This sideband cannot be completely suppressed for technical reasons. The remainder of the lower sideband (vestigial sideband) is 1.25 MHz.

The manner in which a television channel is utilized is shown in Fig. 4.10. The l.f. components of the video signal (labelled α and β) are transmitted by both the lower and the upper sideband. Therefore, their transmission is not accompanied by distortion. The transmission of the h.f. components of the video signals (portion $\beta\gamma$) is accompanied by specific (quadrature) distortion, but this distortion is passed almost unnoticed in fine detail.

GENERATION OF THE TELEVISION SIGNAL

5.1. Standard Video Signal Waveform

The video signal, fully complete for transmission (or the composite video signal), contains the following four components:

1. The camera signal consisting of pulses which correspond to the luminances of the scanned picture elements.
2. The line (horizontal) and frame (vertical) sync pulses to synchronize the respective sweep circuits in the receiver.

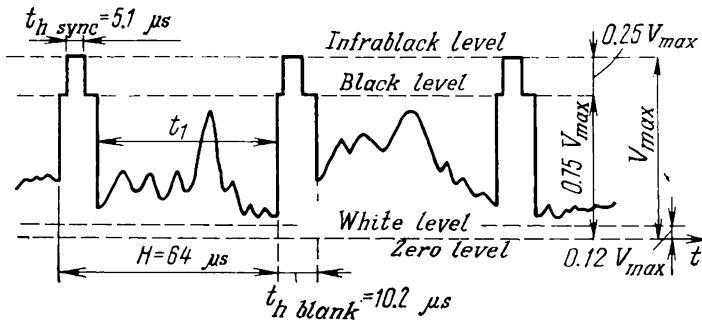


Fig. 5.1. Waveform of the video signal in the absence of frame pulses

3. The line (horizontal) and frame (vertical) blanking pulses to blank the beam in the receiver during the retrace motion.
4. The d.c. component used as reference.

It appears more instructive to examine the structure of the composite television signal over a time interval separately in the absence and in the presence of frame pulses.

In the former case, the video signal has the waveform shown in Fig. 5.1. During the time interval t_1 (that is, during the trace motion) the camera signal is transmitted, corresponding to the luminances of the various elements along the line. The instantaneous values of the camera signal voltage occupy the interval between the white level and the black level. During retrace, a horizontal blanking pulse with a duration of $t_{h, blank} = 10.2 \mu s$ is transmitted. The horizontal sync pulse with a duration of $t_{h, sync} = 5.1 \mu s$ is superimposed on the blanking pulse.

tant indicator of picture quality defined by Eq. (1.31): $\beta = B_{\max}/B_{\min}$.

In the absence of retrace blanking, we would have to add the retrace luminance to the denominator of Eq. (1.31): $\beta_1 = B_{\max}/(B_{\min} + B_r)$, and the contrast would be decreased several-fold.

A second function of blanking pulses is to convey the d.c. component. For this purpose, the amplitude of the blanking pulses is varied in accordance with the voltage of the d.c. component (amplitude modulation). Figure 5.3 shows two cases: I—the average horizontal luminance B_{av} (d.c. component) is small (although there

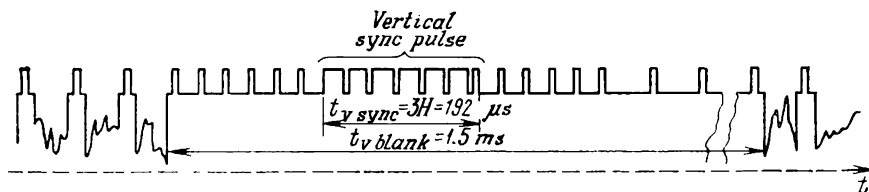


Fig. 5.4. Waveform of the video signal in the presence of frame pulses

may be highlights A, B, \dots); II—the average horizontal luminance B_{av} is high (although there may be lowlights A, B, \dots). As is seen from Fig. 5.3, the blanking pulses have different amplitudes in these two cases. The lighter lines (on the average) are associated with blanking pulses having greater amplitudes. When the video signal applied to the control electrode of the picture tube is properly adjusted, the tops of the blanking pulses α, β must always be at the level V_0 corresponding to the complete blanking of the beam during retrace. When the blanking pulses are clamped this way, the luminance B_{av} of dark lines will be low and that of light lines will be high.

The structure of the video signal during the transmission of frame pulses is shown in Fig. 5.4. The vertical blanking pulse which blanks the beam during the retrace motion of the vertical scan has a duration of $t_{v \text{ blank}} = 1.5 \text{ ms}$. The total vertical scan period is $V = 20 \text{ ms}$ (50 fields per second are transmitted). The vertical retrace ratio is

$$t_{v \text{ blank}}/V = 1.5 \div 20 \times 100\% = 7.5\%$$

The need to blank the beam during vertical retrace is not connected to the loss of contrast. Failure to blank the beam during vertical retrace would manifest itself as widely separated, fine light lines which appear to cross-hatch the picture (Fig. 5.5). This distortion can be explained as follows. During vertical retrace, the beam moves upwards from the lower to the upper part of the picture. In the meantime, the line scan generator keeps running and causes the

beam to scan horizontally, and this horizontal scanning leaves the light "cross-hatching" lines. Their number, m_r , can be found from the relation

$$m_r = t_{v \text{ blank}}/H = 1500 \mu\text{s}/64 \mu\text{s} = 23.5$$

A complete frame made up of two fields would have twice as many "cross-hatching" lines: $2m_r = 47$. With interlaced scanning, the "cross-hatching" lines of one field appear between the "cross-hatching" lines of the second field. No such lines appear when the beam is blanked during vertical retrace.

Like the horizontal blanking pulse, the vertical one carries a relatively narrower vertical sync pulse. Under the USSR standard, it occupies three line periods:

$$t_{\text{sync } v} = 3H = 3 \times 64 = 192 \mu\text{s}$$

The difference in duration between the vertical and horizontal sync pulses is considerable:

$$t_{\text{sync } v}/t_{\text{sync } h} = 192 \div 5.1 = 37.5$$

Owing to this difference, relatively simple means can be used to separate the horizontal from the vertical pulses in the TV receiver.



Fig. 5.5. Image distortion in the absence of vertical blanking pulses

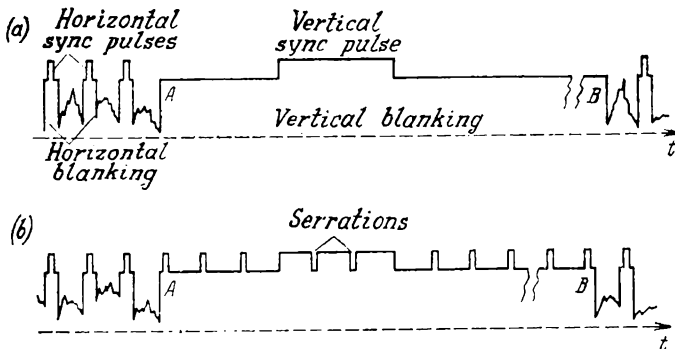


Fig. 5.6. (a) Simplified signal waveform; (b) serrations in vertical sync pulse

Since during vertical retrace the beam is blanked and no camera signal is reproduced, it would appear unnecessary to transmit horizontal sync pulses in the meantime. That is, it would seem sufficient to use the simpler signal waveform shown in Fig. 5.6a. Unfortunate-

ly, this would produce prohibitive distortion in several tens of lines at the top of the picture. This would happen because the line scan generator would lose its synchronization in the region AB where horizontal sync pulses are absent, and its free-running frequency might drift appreciably away from the repetition frequency of horizontal sync pulses. After the instant B , it would then take several tens of sync pulses to pull the line scan generator back into synchronism. Lack of synchronization during the first lines of the frame would cause instability in the position of details in the top

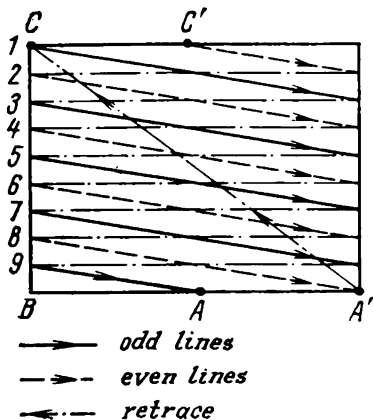


Fig. 5.7. Interlaced raster

part of the frame. In other words, horizontal sync pulses must be transmitted along with vertical blanking and sync pulses (see Fig. 5.6b). To avoid an increase in the maximum amplitude of the video signal, the horizontal sync pulses transmitted during the existence of a vertical sync pulse are inserted as so-called serrations. An appropriate circuit in the TV receiver will then derive normal horizontal sync pulses from these serrations.

Comparison of the plots in Figs. 5.6b and 5.4 brings out a marked difference between them. The point is that the repetition frequency of horizontal sync pulses in the standard television signal is doubled before, during and after the existence of vertical sync pulses. This is an outcome of using interlaced scan in order to reduce the bandwidth needed for the television signal (see Sec. 4.1). In interlaced scanning, each field accommodates a whole number of lines plus a half-line ($625 \div 2 = 312.5$). Then, if the first (odd) field starts at the beginning of a line (point C in Fig. 5.7), the second (even) field will start at the remaining half-line (point C') and terminate at the end of a complete line (point A'). In this way, odd and even lines are interlaced in the proper manner.

It is seen from the plot of Fig. 5.7 that for an odd field the instant at which the vertical scan switches from trace to retrace (point A) lags behind the instant where the nearest line B starts by the duration of a half-line, $H/2$; for an even field, the segment BA' corresponds to the period of a complete line, H . Because of this, the time interval between adjacent horizontal and vertical sync pulses changes, too (Fig. 5.8). Also, there is a change in the number of serrations (there are three serrations for an odd field and two for an even field).

These two factors—change of phase between adjacent horizontal and vertical sync pulses and change in the number of serrations—firstly, complicate the circuit of the synchronizing signal generator and, secondly and more important, bring about a marked difference in the pulse structure of the signal between odd and even fields (see

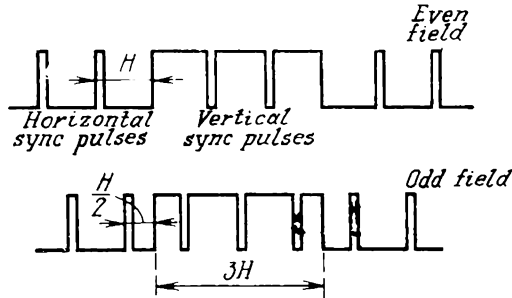


Fig. 5.8. Difference between alternate fields in the absence of equalizing pulses

Fig. 5.8). Unless appropriate measures are taken, vertical synchronization might be upset and interlaced scanning would be lost fully or at least in part. This matter will be discussed in greater detail in Chapter 6.

An identical pulse structure in the odd and even fields can be obtained by doubling the repetition frequency of horizontal sync

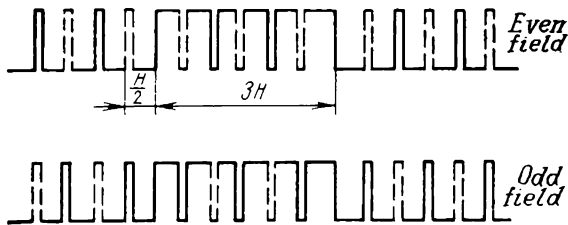


Fig. 5.9. Insertion of equalizing pulses between vertical sync pulses

pulses before, during and some time after the existence of the vertical sync pulse. The pulse structure of a signal in which additional horizontal sync pulses (shown by the dashed lines) are used is shown in Fig. 5.9. Now the relative position of adjacent horizontal and vertical sync pulses and the number of serrations within the vertical sync pulse are the same ("equalized") for both odd and even fields. Hence, the sync pulses following at twice the line frequency are called

equalizing sync pulses. The duration of equalizing sync pulses is halved:

$$t_{eq} = t_{sync} h/2 = 5.1 \div 2 = 2.55 \mu s$$

in order that the average equalizing-pulse component should not exceed the average component of the line sync pulses occurring away

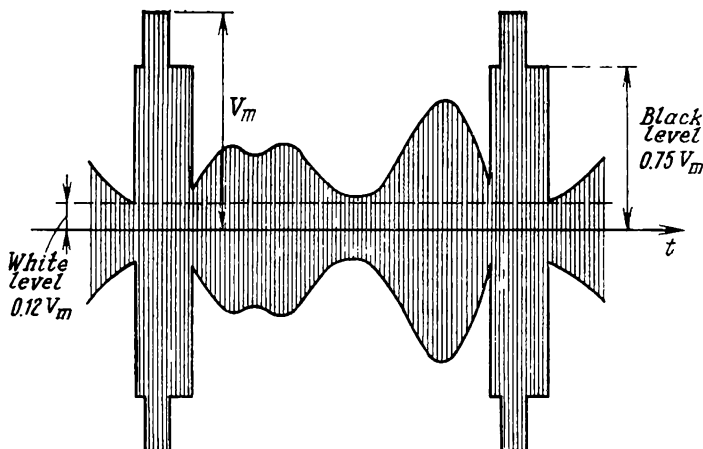


Fig. 5.10. Waveform of the television signal radiated by a transmitting antenna

from the serrated vertical sync pulse; otherwise, synchronization might be erratic.

The structure of the composite television signal radiated by the antenna of a TV centre is shown in Fig. 5.10.

5.2. Synchronizing Signal Generator

All pulses that make up the composite television signal, namely, sync pulses, blanking pulses, equalizing pulses and serrations, are produced and shaped by a suitable device called the synchronizing signal generator which is part of the equipment of a TV centre.

Apart from the pulses needed for the normal operation of a TV receiver, that is, its scan and blank-pulse generators, the sync signal generator also produces the pulses needed for the transmitting equipment, namely, to synchronize the scan generators of the camera tubes, to blank their beams during retrace, etc. Accordingly, a typical sync signal generator comprises three basic elements:

- (1) a timing system;
- (2) a pulse shaper;
- (3) an amplifier-distributor unit.

Consider each of these units in turn.

To obtain proper interlace in which the lines of a field occupy precisely the spacings between the lines of the next field, a complete frame is arranged to have an odd number of scan lines (under the Soviet standard, $Z = 625$ lines). Then, each field will contain a whole number of lines plus a half-line: $Z/2 = 312.5$. This is the reason why the field frequency, $f_{field} = 2f_r = 50$ fields/s, must be rigidly locked to the line frequency, $f_h = f_{field}(Z/2) = 50 \times 625 \div 2 = 15,625$ lines/s. Because of this, we cannot use two independently operating timing systems, one for vertical and the other for horizontal scan. With independent timing systems, it might well happen that one field would have 312 lines and the next, 313. Although the complete frame would still have 625 lines, the odd-field lines would be superimposed on the even-field lines, there would be no interlace, and the vertical resolution would be halved.

The line and field frequencies are rigidly locked together by the pulse frequency divider. However, if we chose the line frequency as reference and attempted to derive the field frequency from it by division, the division factor k of such a circuit would be a fractional number:

$$k = f_h / f_{field} = 15,625 \div 50 = 312.5$$

An electronic circuit having a fractional division factor is very difficult to construct. This is why the sync signal generator utilizes frequency dividers with an integer division factor, and the reference frequency, f_{ref} , is chosen to be twice the line frequency:

$$f_{ref} = 2f_h$$

and the divisions factor is

$$k = f_{ref} / f_{field} = 31,250 \div 50 = 625$$

A simplified block diagram of the timing system is shown in Fig. 5.11. The free-running master oscillator, MO (usually a Hartley oscillator) operates at twice the horizontal scanning frequency: $f_{MO} = 2f_h = 31,250$ Hz. The oscillator output is divided by $k = 625$, so that voltage pulses appear at the output of the frequency divider, following at the field scanning frequency, $f_{field} = f_{MO}/625 = 31,250 \div 625 = 50$ Hz.

It should be noted that a reliable single-stage circuit operating at a division factor of 625 is difficult to construct. Destabilizing factors (small variations in supply voltages, ambient temperature and the like) may readily lead to spontaneous changes in the division (or count-down) factor. Thus, instead of $k = 625/1$, it may readily take on any next value, such as $624/1$ or $626/1$, etc. This is why resort is usually made to a multi-stage circuit, each stage being assigned a small division factor, ordinarily less than 10. This has been one of the

reasons for the choice of 625 lines per scanning frame. For interlaced scan, there should be an odd number of lines per frame. However, $Z = 623$ or $Z = 627$ cannot qualify as the requisite number of lines

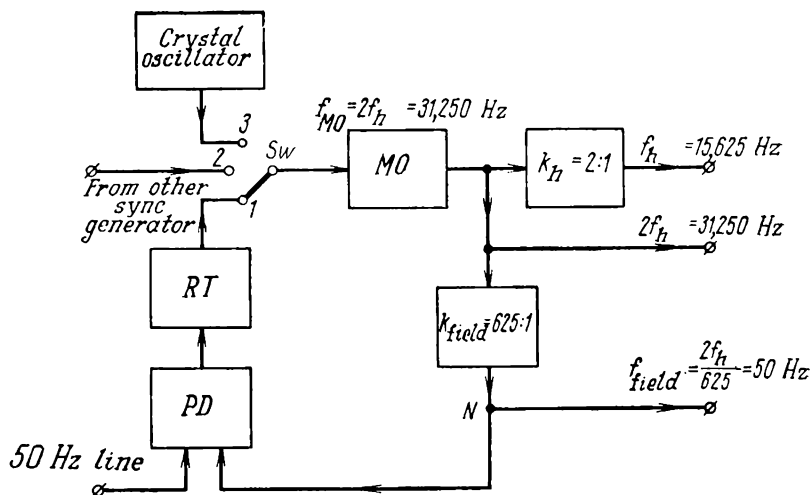


Fig. 5.11. Simplified block diagram of the timing unit of a synchronizing generator

per scan, because they are simple numbers which cannot be factored. In contrast, $Z = 625 = 5 \times 5 \times 5 \times 5 = 5^4$, and so we can use a four-stage divider such that

$$k = k_1 k_2 k_3 k_4 = 5 \times 5 \times 5 \times 5 \div 1 = 625 \div 1$$

In the course of evolution, various circuit configurations have been tried as frequency dividers for the sync signal generator, every next being a considerable improvement on its predecessor, as regards reliability, alignment, tuning and size.

Referring to Fig. 5.11, the timing unit of the sync signal generator has three outputs:

- (1) pulses at the line scanning frequency (obtained as twice the line frequency is divided by two), utilized to form horizontal sync and blanking pulses;
- (2) pulses at twice the line scanning frequency utilized to form equalizing and serrated pulses;
- (3) pulses at the field scanning frequency, utilized to form vertical sync and blanking pulses*.

* In Soviet usage, the terms frame and field (e.g., pulse, frequency, etc.) are used interchangeably. To avoid confusion, they will be qualified in the text where necessary.

The master oscillator of the timing system is capable of operating in any one of three modes (selected with the switch Sw in Fig. 5.11). In mode 1, the vertical pulses are rigidly locked to the supply mains in both frequency and phase. This locking renders supply-mains interference stationary and therefore unnoticeable on the TV screen (see Sec. 1.4). To effect locking, the vertical pulses and the mains voltage are applied to the two inputs of a phase discriminator, PD . The discriminator output delivers a constant (or slowly varying) voltage which drives a reactance control element (which may be a reactance tube or a reactance transistor, RT). The magnitude and polarity of this correction voltage correspond to the magnitude and sign of the phase difference between the voltages being compared. The reactance tube connected across the tuned circuit of the master oscillator is forced to vary its dynamic capacitance according to the magnitude of the voltage at its input. In this way, the frequency and phase of the master oscillator are automatically controlled to remain at their assigned values; via the k -count-down frequency divider this action is extended to cover both the frequency and phase of the frame (rather field) pulses. In mode 2 (which may be called external lock control), the master oscillator is locked in with an external control source over a radio link or a cable line. This mode is used where TV programs are exchanged between cities or internationally and the local sync signal generator must be precisely locked to the remote one. In mode 3 (crystal lock control), the master oscillator is stabilized by a crystal-controlled oscillator. In this case, an extremely high frequency stability is ensured for the sync pulses.

Consider the operating principle of the sync generator timing system. Present-day sync generators use transistors almost exclusively. The frequency-divider section utilizes predominantly trigger flip-flops, or binary counters. The circuit of a trigger flip-flop is shown in Fig. 5.12a.

In this circuit, delayed positive feedback is effected by application of the collector voltage of one transistor to the base of the other (via resistors R_1 and R_2). When the circuit is properly aligned, one of the transistors is initially in the OFF state and the other in the ON (conducting) state. Arrival of a positive input pulse at the capacitor C_3 causes the flip-flop to change state so that the cut-off transistor is switched to the ON state and the conducting transistor to the OFF state.

One of these two stable states may continue for any time, however long, until a positive input pulse again causes the flip-flop to change state.

Operation of the flip-flop as a scale-of-two circuit is illustrated in Fig. 5.12b. On passing through diode D_2 and resistor R_1 , the input pulse, I , turns off transistor T_1 (while positive feedback causes

the other transistor T_2 to turn on at the same time). The output voltage v_{out} is picked off terminal D in the divider rather than point B , the collector. This is done in order that the low saturation resistance of the conducting transistor T_2 cannot shunt the input circuit of the succeeding divider stage.

The next input pulse, 2, causes the flip-flop to change state in the reverse direction so that transistor T_1 is rendered conducting and transistor T_2 non-conducting. As is seen from the figure, the output pulses v_{out} follow at twice the period of the input pulses.

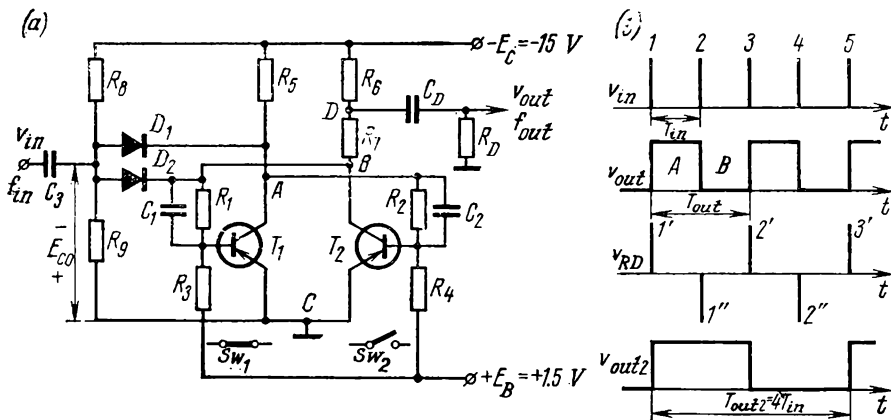


Fig. 5.12. Operation of a trigger flip-flop
(a) circuit; (b) timing diagrams of a trigger flip-flop as a frequency divider

If the output pulses of the circuit shown in Fig. 5.12a be applied to the input of a similar flip-flop, this second flip-flop will count them down by two again. In this way, a two-stage divider (using four transistors) gives a count-down ratio $k_2 = 2 \times 2 : 1 = 4 : 1$ (v_{out2} in Fig. 5.12b).

The output pulses of one divider stage should be fed to the next via a differentiating network (C_3R_9 in Fig. 5.12a). The narrow pulses appearing at its output are preferable in the control of the next stage, because they are short and cannot therefore affect the waveform and duration of the output pulses of the next divider stage. Thus, these output pulses will solely depend on the circuit parameters of the divider.

Apart from positive pulses $1', 2', \dots$, the differentiating network forms negative pulses $1'', 2'', \dots$. However, they do not affect the operation of the flip-flop because they cannot pass through the diodes D_1 and D_2 .

A chain of n flip-flops will have an overall count-down ratio of $k_n = 2^n$. Thus, flip-flops, or binary scalars, can only count down

in some even ratio which is the n th power of two. For example, a five-stage divider of this type gives a count-down of $k_5 = 2^5 = 32 : 1$. On the other hand, the Soviet television standard requires that the count-down ratio be $k_5 = 25 : 1$ (then two such dividers would give the desired overall count-down ratio of $k_{overall} = k_5 k_5 = 25 \times (25 : 1) = 625 : 1$).

A $32 : 1$ divider can be turned into a $25 : 1$ counter by use of a special form of interstage feedback in the divider. The idea of this feedback will be clear from reference to Fig. 5.13a. From the output (network $C_2 R_2$) of the two-stage divider, the differentiated pulses v_{out} are applied by a feedback element, FB (which is usually a single-stage amplifier or an emitter follower), to the input of the first flip-flop. The pulse waveforms and timing that exist in a circuit with feedback are shown in Fig. 5.13b. The input of the first flip-flop accepts the sum of input pulses $1, 2, 3$, and of feedback pulses $1', 4', 7', \dots$. Pulse 1 causes the first flip-flop to change state while feedback pulse $1'$ throws it over back, etc. As a result, two pulses, A and B , and a space, C , are formed during interval $1-3$. Without feedback (Fig. 5.13b), there would be only one pulse, A , and one space, B , within the same interval.

The differentiating network $R_1 C_1$ delivers pulses v_{out1} which control the second flip-flop (negative pulses are omitted because they do not contribute to circuit operation). As is seen from Fig. 5.13b, the pulses appearing at the output of the second flip-flop have a period T_{out} which is three times that of the input pulses. Thus, the overall count-down ratio is $k_{overall} = 3T_{out}/T_{out} = 3 : 1$.

Pulses 1 and $1'$ do not coincide in time in Fig. 5.13b, because the feedback path, FB, delays pulses $1', 4', 7', \dots$. The delay, τ_d (Fig. 5.13b), is responsible for the appearance of additional (feedback) pulses at the circuit input.

A $25 : 1$ divider can be a five-stage flip-flop circuit with feedback applied from the output of the last (fifth) flip-flop to the inputs of the first three flip-flops. A block-diagram of such a divider is shown in Fig. 5.14a. Without feedback, this divider would give a count down $k_5 = 2^5 = 32 : 1$ instead of $25 : 1$. Feedback from the output of the fifth flip-flop adds one more pulse to the first three flip-flops. For example, one more, 26th, pulse, $1'$, is applied to the first flip-flop after 25 pulses (Fig. 5.14b). Because all flip-flops divide in the ratio $2 : 1$, the first flip-flop halves the number of input pulses: $26 \div 2 = 13$. To these thirteen pulses arriving at the input of the second flip-flop, feedback adds one more, 14th, pulse. The second flip-flop halves them, too, so that seven pulses are applied to the third flip-flop, to which one more, 8th, pulse is added by feedback. Because no feedback is applied to the succeeding stages, the number 8 is divided by two three times in the third, fourth and

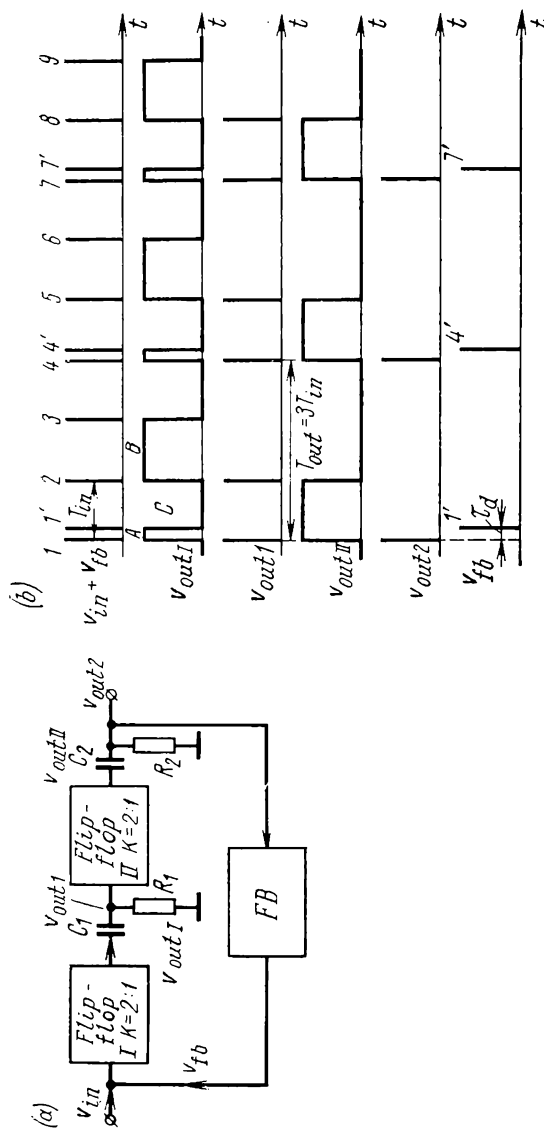


Fig. 5.13. Reduction in count-down ratio by use of interstage feedback
(a) block diagram; (b) timing diagram for odd count-down ratio

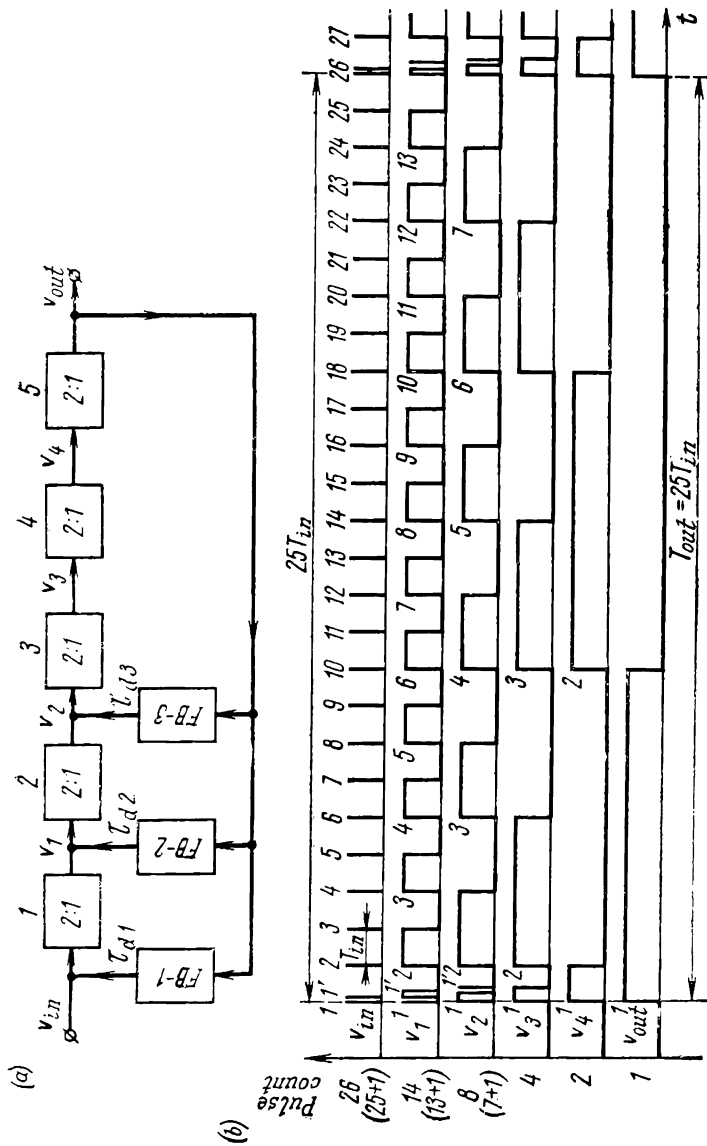


Fig. 5.14. (a) Circuit of a 25:1 divider using interstage feedback and (b) its timing diagram

fifth flip-flops, $8 \div (2 \times 2 \times 2) = 1$. Thus, only one pulse appears at the output of the divider for every twenty-five applied to its input, and the overall count-down ratio is thus $k_5 = 25 : 1$.

It is important to note that if the feedback pulses applied to the first, second and third flip-flops are not to coincide in time, the time delays provided by the feedback elements, FB-1, FB-2 and FB-3, should satisfy the following inequalities: $\tau_{d1} < \tau_{d2} < \tau_{d3}$.

Two five-stage dividers with feedback, such as examined above, give the requisite overall count-down ratio:

$$k_{\text{overall}} = k_5 \times k_5 = (25 : 1) \times (25 : 1) = 625 : 1$$

5.3. Pulse Shaper

The pulse shaper incorporates multivibrators, delay lines, limiters and adders, intended to produce the composite sync signal from the three kinds of pulses appearing at the output of the timing unit (see Fig. 5.11), namely f_h , $2f_h$, and f_{field} .

The circuit of a single-shot multivibrator commonly used in the sync signal generator to shape and phase in pulses widely varying

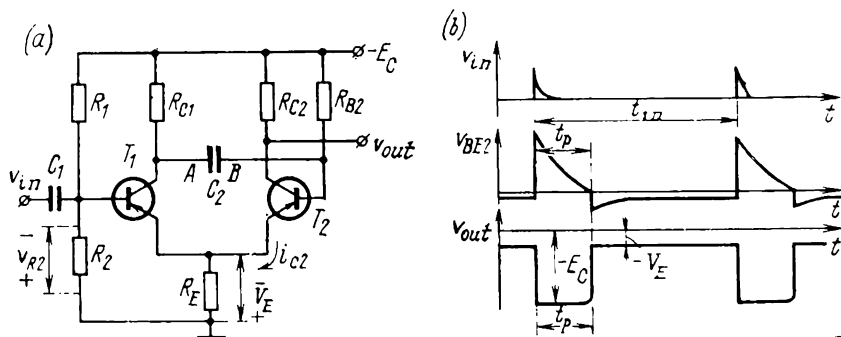


Fig. 5.15. Single-shot multivibrator
(a) circuit; (b) basic voltage waveforms

in duration is shown in Fig. 5.15a. In this circuit, positive feedback is provided by coupling the collector of the first transistor T_1 to the base of the second, T_2 , via a capacitor, C_2 , and also by placing a resistor, R_E , in the emitter circuit of both transistors. The voltage divider made up of R_1 and R_2 stabilizes the potential at the base of T_1 when it is in the ON condition. Initially, the transistor T_1 is OFF and T_2 is ON. In this condition, the multivibrator can be maintained for any time, however long, by the voltage V_E appearing across R_E due to the flow of current i_{C2} of the conducting transistor

T_2 . In this condition, the following relation should be satisfied:

$$V_{R_2} + V_{E_1} > 0 \quad (5.1)$$

In this state, the saturation resistance of T_2 is negligible in comparison with the other resistances in the circuit. Therefore, it may be assumed that C_2 charges to the voltage

$$V_{C_2} = V_{AB} = V_0 = -E_C + V_{E_1} \quad (5.2)$$

When a narrow negative pulse is applied to the input, the inequality (5.1) is no longer satisfied, transistor T_1 is rendered conducting, and the positive change of voltage arising at its collector is conveyed via C_2 to the base of T_2 and drives it to cut-off. The

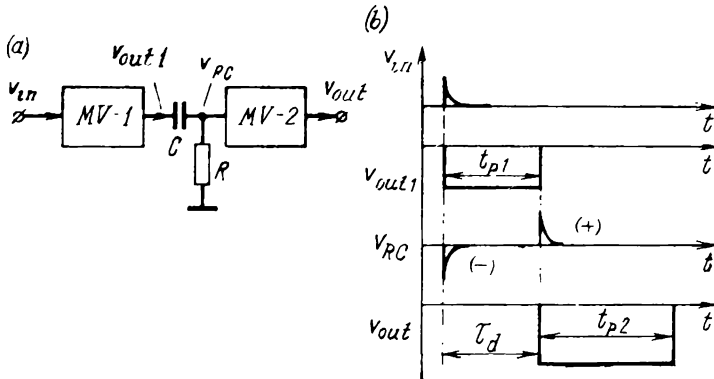


Fig. 5.16. Operation of single-shot multivibrators as pulse delay circuits
(a) block diagram; (b) waveforms

emitter voltage, V_E , drops as suddenly, and transistor T_1 is driven to conduction. The duration of the new state in which T_1 is conducting and T_2 is off is determined by the time required for the capacitor C_2 to re-charge. The waveforms of voltages existing at the main points of the single-shot multivibrator are shown in Fig. 5.15b. The pulse duration can conveniently be adjusted by varying the capacitance of C_2 or the resistance of R_{B_2} .

It is often necessary to produce pulses delayed from the input pulse by a considerable time interval. Ordinary delay lines assembled from L and C elements would be too bulky and would be wasteful because of the losses in and reflections from the many circuit elements. A convenient way-out is to use several single-shot multivibrators connected in series. The operation of such an arrangement will be clear from reference to Fig. 5.16a. Two multivibrators are coupled together by a differentiating RC -network. The function of this network is to derive narrow pulses needed to trigger the second multivibrator from broad rectangular pulses. The pulse waveforms existing in the circuit of Fig. 5.16a are shown in Fig. 5.16b.

The trigger pulses v_{in} are applied to the first multivibrator whose output furnishes pulses v_{out1} of duration t_{p1} determined by its

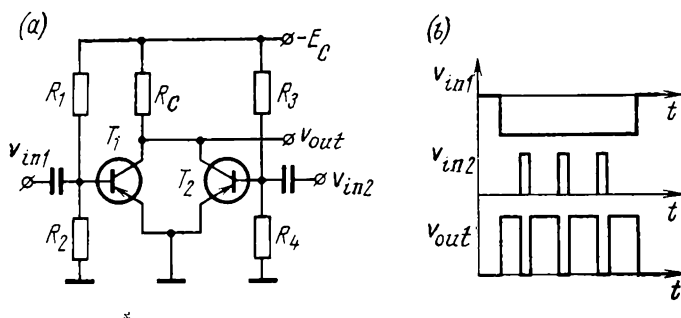


Fig. 5.17. Transistorized adder
(a) circuit; (b) waveforms

time-defining elements. The differentiating RC -network delivers narrow pulses v_{RC} corresponding to the leading and trailing edges

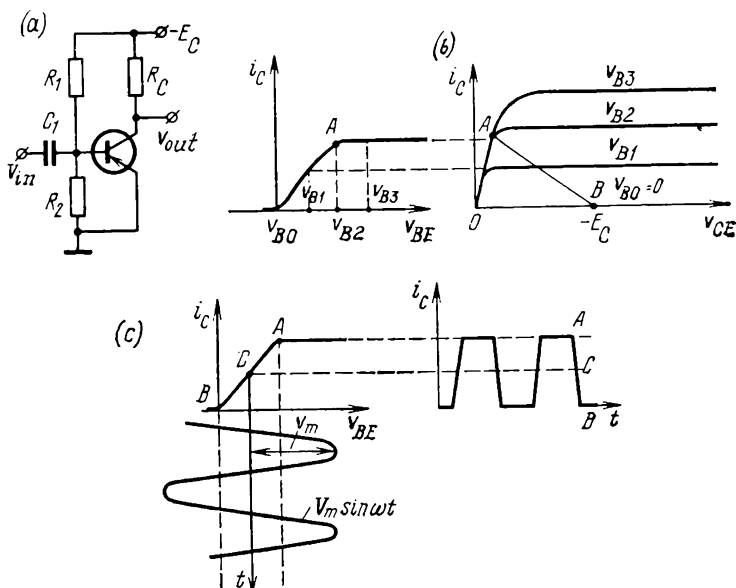


Fig. 5.18. Amplifier-limiter

(a) circuit; (b) Q -point selection; (c) conversion of sinewave into square pulses by slicing

of the pulse v_{out1} . The positive (+) pulses trigger the second multivibrator which generates pulses of duration t_{p2} . The second multivibrator is said to be triggered by the trailing edges of pulses from

the first multivibrator. The time delay τ_d between the input pulse v_{in} and the output pulse v_{out} is determined by the time interval t_{p1} .

An adder for two pulse voltages may be the circuit of Fig. 5.17a which contains two transistors with a common resistor, R_C , in their collector circuits. The input voltages v_{in1} and v_{in2} are amplified by the transistor stages T_1 and T_2 and combined in the common load R_C . This circuit performs algebraic summation in the sense that if one of the input signals is applied in anti-phase, the two signals will be subtracted in the common load, as shown in Fig. 5.17b.

To give pulses a waveform close to rectangular, use is often made of transistor circuits operating as limiters. In appearance, the circuit of such a limiter may be not unlike that of an amplifier (Fig. 5.18a). The difference between the two lies in how the circuit resistances and supply voltages are chosen. As a rule, limiting action is obtained by increasing the value of R_C and reducing the supply collector voltage, $-E_C$. As a result, the considerable slope, $1/R_C$, of the load line AB and the reduced supply voltage $-E_C$ (Fig. 5.18b) cause the output pulses to be limited by collector current cut-off at negative peaks (point B) and by collector current saturation at positive peaks (point A). The voltage injected into the base (which may well be a sinusoidal one, as in Fig. 5.18c) is clipped in the collector circuit into nearly rectangular pulses.

The flip-flops, multivibrators, limiters and delay circuits serve all to produce the composite television signal specified by an appropriate standard (see Fig. 5.4).

More recently, sync signal generators have come to be built around state-of-the-art micromodules and integrated circuits, especially in the form of frequency dividers, logic gates, pulse shapers, etc. These elements have appreciably improved the reliability and stability of the sync signal generator along with a reduction in its mass and size.

SYNCHRONIZATION OF SCANNING GENERATORS

6.1. Impulsive Synchronization

Apart from picture information, the television signal should also convey additional information about the instantaneous position (coordinates) of the beam in the camera tube so that the beam in the picture tube can follow it in precise synchronism. This additional information in the form of sync pulses is transmitted over the same channel with the main video signal. In broadcast television, two

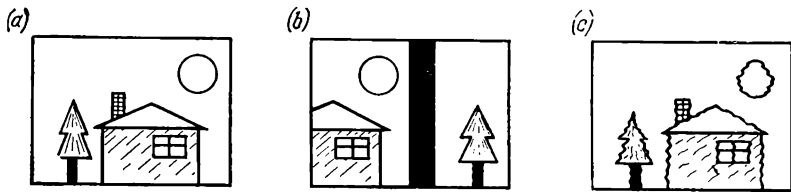


Fig. 6.1. Effect of synchronization on picture quality
(a) proper synchronization; (b) lack of horizontal synchronization; (c) lack of horizontal synchronization

techniques are used for the transmission of sync pulses, either between the black level and the infrablack (or blacker-than-black) level where no picture signals ever appear (amplitude interleaving), or during retrace when no picture signals exist either (time interleaving).

Figure 6.1a shows a television picture obtained with a properly operating sync channel. Lack of synchronism (difference in scanning frequencies between the camera and picture tubes) results in a complete distortion of the reproduced image and the formation of erratic patterns on the screen. Out-of-phase condition (with normal synchronism) manifests itself in several forms. Firstly, a consistent phase difference causes the image to shift so that it appears poorly framed (Fig. 6.1b). Secondly, relatively small phase fluctuations in vertical scan upset proper interlace so that the even lines of one field are superimposed on the odd lines of the other and vertical resolution is impaired. Considerable phase fluctuations in vertical scan cause the image to jitter vertically. Thirdly, phase fluctuations in hori-

zontal scan impair horizontal resolution. Closely spaced fine details merge together and cannot be resolved any longer. Fourthly, in the case of phase fluctuations in horizontal scan, vertical and oblique lines in the image are scalloped, and this distorts the picture unpleasantly (Fig. 6.1c).

The sync pulses appropriately interspersed in the composite television signal are separated from the picture signals and blanking

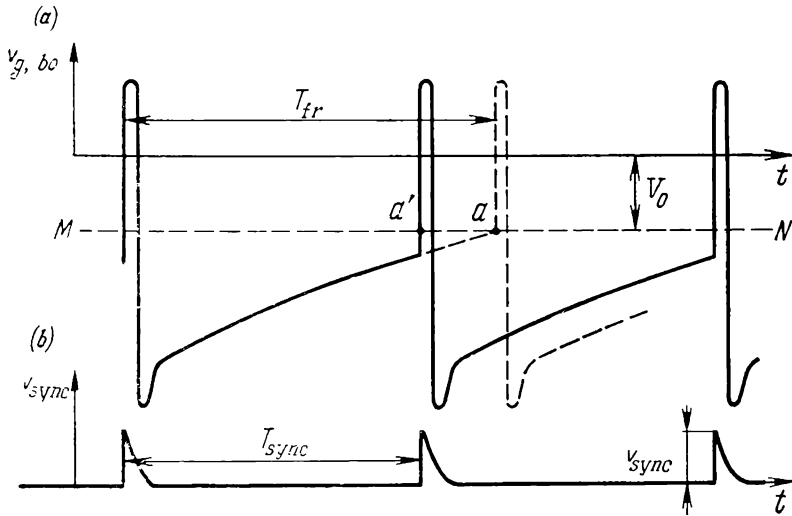


Fig. 6.2. Impulsive synchronization of the blocking oscillator
(a) grid voltage waveform; (b) sync pulses

pulses in the receiver. Then the composite sync pulses are separated into vertical and horizontal sync pulses and utilized to synchronize the oscillators of the respective scanning generators.

Using a blocking oscillator as an example, synchronization is illustrated in Fig. 6.2. The sync pulses are injected into the grid circuit of the blocking oscillator tube. For proper synchronization it is important that the repetition period of sync pulses be somewhat shorter than the free-running period of the blocking oscillator, that is, $T_{sync} < T_{fr}$.

The sync pulses applied to the grid of the blocking oscillator tube should be in positive polarity. From Fig. 6.2 it is seen that the sync pulses shorten the period of free oscillations and force the tube to conduct earlier than it would do so in the absence of sync pulses. The positive sync pulses cause the grid voltage v_g to shift beyond the cut-off voltage V_0 at point a' which appears to the left of point a in Fig. 6.2a.

Consider how sync pulses can be injected into the blocking oscillator. Positive pulses are applied to the grid. One of the likely arrangements for this purpose is shown in Fig. 6.3a. The circuit of Fig. 6.3b

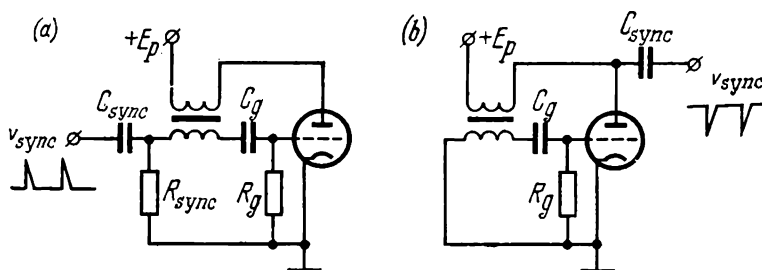


Fig. 6.3. Insertion of sync pulses into the blocking oscillator
(a) into grid lead; (b) into plate lead

serves to apply negative sync pulses to the plate of the blocking oscillator tube (or rather, to the plate winding of the blocking-oscillator transformer). Across the grid winding of the transformer

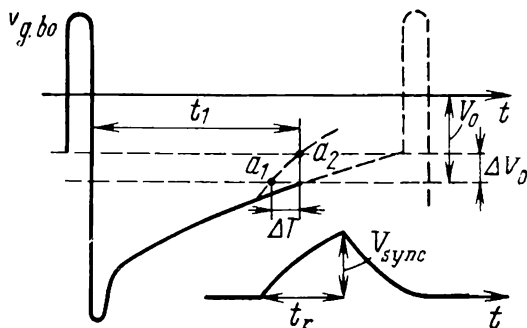


Fig. 6.4. Effect of sync pulse rise time on accuracy of the blocking oscillator

these pulses are in positive polarity. In this way, the circuit of Fig. 6.3b likewise applies positive sync pulses to the grid of the blocking oscillator tube.

Because supply voltages are always unstable, the cut-off voltage varies in a random manner. The maximum change in this voltage is designated ΔV_0 in Fig. 6.4. Since the rise time, t_r , of a sync pulse is nonzero, the instants of transition across the cut-off line, a_1 and a_2 , are shifted along the time axis. It follows from the figure that fluctuations, ΔT , in the period are related to fluctuations in cut-off voltage, ΔV_0 , and to the rise time, t_r , of the sync pulse. When the

sync pulse has an ideally steep leading edge (the rise time is zero, $t_r = 0$), fluctuations in the period of the blocking oscillator are zero ($\Delta T = 0$).

The finite rise time, t_r , of sync pulses brings about an instability in the period of the oscillator also because there is a noise voltage in the sync pulse (Fig. 6.5a). The noise voltage with a peak-to-peak

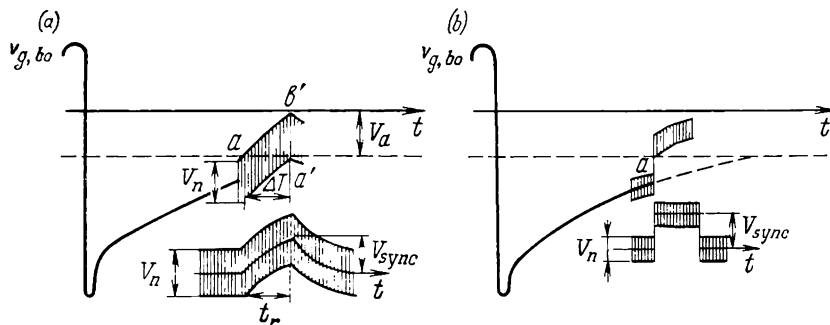


Fig. 6.5. Effect of noise on synchronization
(a) finite rise time; (b) rise time of zero (idealized case)

amplitude V_n is superimposed on the sync pulses of amplitude V_{sync} and rise time t_r ; as shown in the figure the presence of noise makes uncertain the instant a at which the tube is rendered conductive. Figure 6.5b shows an idealized case where $t_r = 0$. In such a case, noise voltage does not affect the instant when the oscillator tube is rendered conductive.

6.2. Block Diagram of the Impulsive Synchronization System

In block-diagram form, the impulsive synchronization system of a TV receiver is shown in Fig. 6.6. This system synchronizes the oscillators of the line and frame sweep circuits. The composite television signal emerging from the video amplifier is then applied to two points in the receiver circuit. Firstly, this signal is applied to the control electrode of the picture tube in order to control the beam current. Secondly, it is applied to the input of an amplitude separator which separates the sync pulses from the composite video signal. In connecting the video amplifier to the amplitude separator it is important to remember that the input capacitance of the separator might shunt the video amplifier output and bring about a sizeable fall in its frequency response which would in turn impair the horizontal resolution of the picture. The effect of this shunt capacitance is usually mitigated by the insertion of a coupling resistor, R_c .

The amplitude separator, as its name implies, effects amplitude separation of the synchronizing signals from the composite video signal by utilizing the fact that sync pulses occupy the region between the black level (blanking level or pedestal) and the infrablack

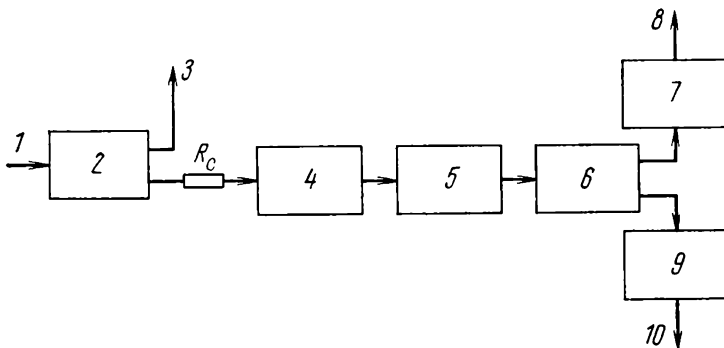


Fig. 6.6. Block diagram of an impulsive synchronization system

1—from video detector; 2—video amplifier; 3—to picture-tube control electrode; 4—amplitude separator; 5—amplifier-limiter; 6—sync pulse separation circuits; 7—vertical oscillator; 8—to vertical output stage; 9—horizontal oscillator; 10—to horizontal output stage

(or blacker-than-black) level (see Fig. 5.1) where no other components of the composite video signal can ever occur.

In many TV receivers, using tubes and transistors alike, the amplitude separator is followed by an amplifier-limiter. This stage makes the synchronization system still more noise-immune by limiting noise by a predetermined amount.

Then the composite sync signal containing horizontal and vertical sync pulses is applied to circuits which develop the horizontal sync pulses independently of the vertical sync pulses. This separation is possible owing to a considerable difference in duration between the two sync pulses.

The ratio of their durations is

$$t_{sync, v}/t_{sync, h} = 192:5.1 = 37.5$$

A few remarks about the need for sync pulse separation is in order. If the sync pulses were not separated, the horizontal sync pulses would break through as far as the vertical oscillator and would upset interlace, thereby producing an unpleasant vertical jitter of the picture. On their part, the vertical sync pulses would break through as far as the horizontal oscillator and would cause part of the picture to jitter horizontally.

Almost universally, the job of separating horizontal and vertical sync pulses is done by differentiating and integrating RC -networks. A differentiating network rejects vertical sync pulses and develops

the horizontal sync pulses, while an integrating network does the job the other way around. The sync pulses thus developed are then fed to the grid (base) circuit of the tube (transistor) used in the respective sweep oscillator. The polarity of these pulses must be such that they will render the oscillator tube (transistor) conducting.

6.3. Separation of the Composite Synchronizing Signal from the Video Signal

As already noted, the sync pulses occupy the space between the black level and the infrablack (blacker-than-black) level. No other components of the composite video signal—blanking pulses or picture signals—can ever occur there. The sync pulses are maintained at 25% of the maximum amplitude of the video signal irrespective of the luminance or content of the scene.

The swing, V_0 , of the beam current-*vs*-grid voltage characteristic, that is, the voltage range from zero potential at the control electrode to cut-off voltage, is usually 100 to 120 V (Fig. 6.7). It should be stressed that in practice the television signal never has a swing that large. In the region near $v_g \approx 0$ (the shaded area in Fig. 6.7) the image is heavily defocused due to an excessive beam current. Therefore, in our further calculations we shall use the effective portion of the beam current-*vs*-grid voltage characteristic such that $\Delta V_g = 60$ V. Then the maximum amplitude of the sync pulse will be

$$V_{sync, max} = 0.25 \Delta V_g = 0.25 \times 60 = 15 \text{ V}$$

If receivers are at a great distance from a TV centre, the signal at the output of the video amplifier may be considerably weaker. Therefore, for approximate calculations it will be reasonable to use a value half as great, $V_{sync} = 7$ V.

The most commonly used and simplest amplitude separator is the clipper-limiter built around a triode (Fig. 6.8). This circuit is not unlike an *RC*-coupled amplifier with the only difference that there is no self-bias elements in the cathode circuit of the tube. Nor is there any external bias in the control-grid circuit. In the circuit of Fig. 6.8 the triode provides limiting action, that is, it clips the portions of the video signal reaching into the areas where the grid draws current and the plate current is cut off. The polarity of the video signal applied to the grid should be such that the sync pulse is positive. The operation of the clipper circuit is illustrated by Fig. 6.9. As long as the plate supply voltage, E_{p1} , is low, the swing of the plate current-grid voltage characteristic of the tube will remain small, and the tube will clip both the blanking pulses and the camera signal, so that only sync pulses are developed across the plate load, R_3 . When the plate supply voltage rises to a high

value (E_{p2}), the cut-off voltage V_{02} might be excessively high and other components of the composite video signal might break through

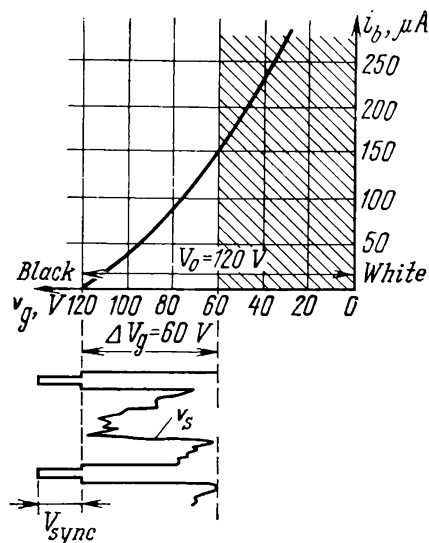


Fig. 6.7. Modulation characteristic of a picture tube

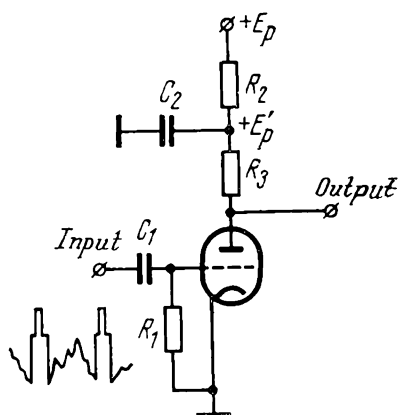


Fig. 6.8. Triode amplitude separator

into the plate circuit apart from the sync pulses. This would upset the synchronization of the scanning generators, and the image on

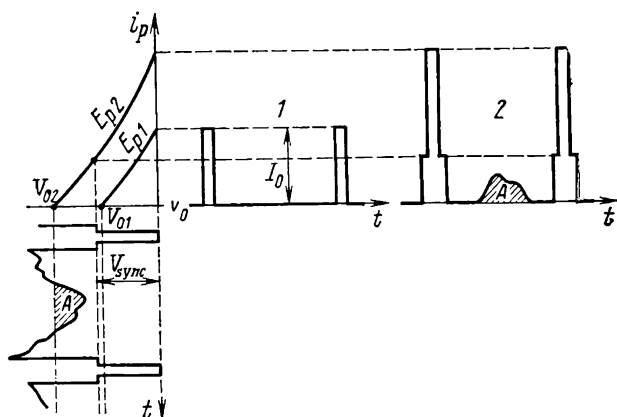


Fig. 6.9. Effect of plate voltage on operation of the amplitude separator
1—correct plate voltage; 2—excessive plate voltage

the screen might be distorted. This implies that the cut-off voltage on the plate current-grid voltage characteristic must be equal to or

somewhat smaller than the amplitude of the sync pulses, that is, $V_{01} \leq V_{sync}$. For example, if $V_{sync} = 7$ V, then V_0 must be about 5 V.

The plate supply voltage of a TV receiver is usually 250 to 300 V. This voltage is excessive for the sync amplitude separator. The excess voltage is dropped across a resistor, R_2 . C_2 is a filter capacitor. As a result, the actual plate supply voltage for the sync amplitude separator is $E_p' < E_p$. The plate load resistor, R_3 , from which the separated sync pulses are picked off is chosen from the same considerations as in a.f. amplifiers. Because the amplitude-separator tube is a triode, the ratio of the plate load resistor to the dynamic a.c. resistance of the tube, $\alpha = R_3/R_d$, must be chosen to be about 3.

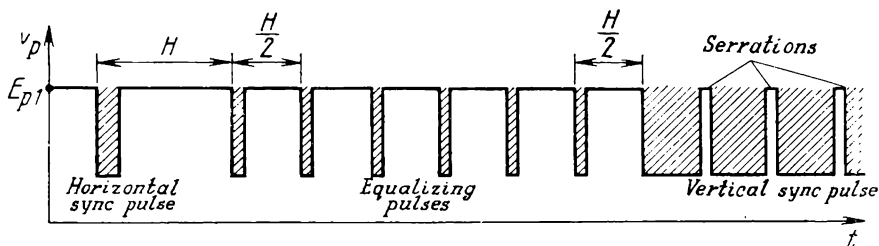


Fig. 6.10. Sync pulses in the plate circuit of the amplitude separator

Greater values of α will not increase the amplification, but bring down the amplitude of the h.f. components in the output signal of the amplitude separator. This would extend the rise time of the horizontal sync pulses and impair the accuracy of line-scan synchronization.

An approximate waveform of sync pulses in the plate circuit of the sync amplitude separator is shown in Fig. 6.10. In selecting a circuit to feed sync pulses to the respective scanning generator, it is important to remember that these pulses must be in negative polarity.

In the sync amplitude separator, the fixed bias voltage at the tube grid is generated automatically by the flow of grid current. In this way, the sync pulses are clamped to a fixed-voltage reference level. Without this clamping action the operation of the sync amplitude separator would be impossible. For better insight into the action of the clamp circuit, we shall refer to Fig. 6.11a. Suppose that initially the capacitor C_1 (see Fig. 6.8) is uncharged, and the sync pulses reach into the area where the grid draws current (portion A in the plot of Fig. 6.11a). The grid current due to these pulses will charge the capacitor C_1 , and it will acquire an additional voltage negative with respect to the grid. This voltage will keep rising until the sync pulses enter the grid-current area any longer (portion B in the plot of Fig. 6.11a). The mode of operation in which the sync

tips are held at $v_g = 0$ is maintained automatically. As a proof, suppose that the sync tips fall to the left of the point $v_g = 0$

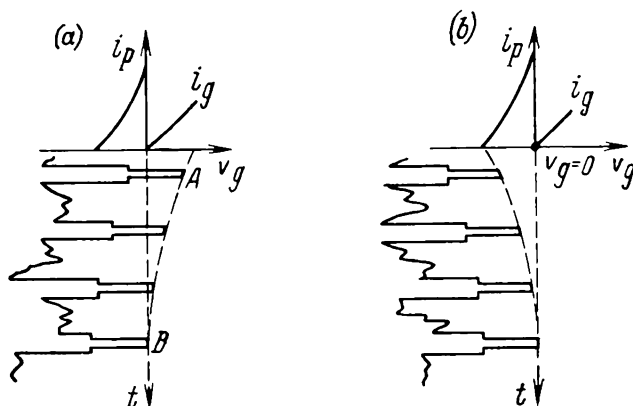


Fig. 6.11. Clamping of sync pulse tips to zero level
(a) in the presence of grid current; (b) in the absence of grid current

(Fig. 6.11b). In such a case, the grid would draw no current, and the capacitor C_1 would gradually discharge through the resistor R_1

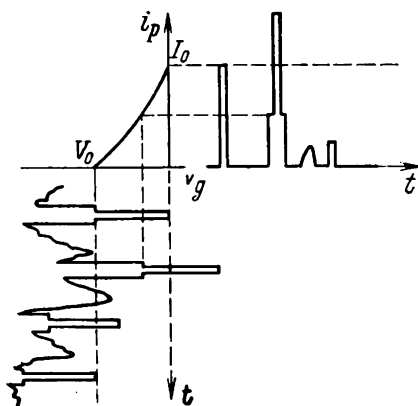


Fig. 6.12. Erratic operation of the amplitude separator in the absence of clamping

with the result that the Q -point of the tube would be shifted to the right. In the opposite case, if the sync tips occurred to the right of the point $v_g = 0$ (Fig. 6.11a), the grid would draw current, thereby causing the capacitor C_1 to acquire an additional charge and shifting the Q -point to the left. This dynamic equilibrium in which the sync tips are automatically maintained at a fixed-voltage reference level is called clamping. If no clamping action were provided in the grid circuit of the sync amplitude separator, then changes in the picture content and in the amplitude of blanking pulses would enable un-

wanted components of the video signal to break through into the plate circuit of the separator. As a result, the sync pulses might be markedly decreased or suppressed altogether (Fig. 6.12).

6.4. Transistor Amplitude Separator

The amplitude separator using a *PNP* transistor needs a video signal with negative sync pulses in order to drive its base circuit. However, when applied to the cathode of the picture tube, this signal must contain positive sync pulses. To reconcile these conflicting requirements, it is advantageous to feed the video signal to the separator from an emitter follower placed ahead of the output stage of the video amplifier as shown in Fig. 6.13. This arrangement has

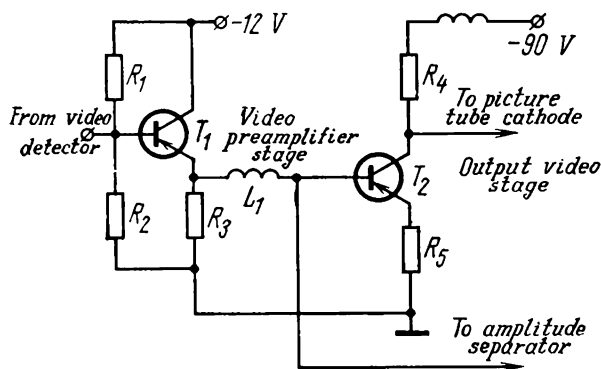


Fig. 6.13. Injection of a video signal from an emitter follower to an amplitude separator

an added advantage because the base circuit of the separator does not load the collector circuit of the output transistor and cannot therefore affect the frequency response and gain of the output video stage.

The circuit of a transistorized single-stage sync amplitude separator is shown in Fig. 6.14a. Its operation is illustrated by the plot of Fig. 6.14b. The negative sync pulses arriving at the base of the transistor as part of composite video via the capacitor C_1 should drive the transistor to saturation for the duration of their existence. Between sync pulses (when the camera signal and blanking pulses are transmitted), the positive bias voltage V_{bias} forming across C_1 due to the base current must reliably cut off the separator transistor. In this way, the sync pulses are clipped in the collector circuit from two sides: the negative peaks are flattened by the collector current cut-off and the positive peaks by saturation (Fig. 6.14b). This limiting action substantially improves the immunity of the amplitude separator towards fluctuation noise.

A substantially better performance is shown by a two-stage sync amplitude separator (Fig. 6.15a). Among other things, it offers a better immunity to noise and shows stable operation even at low input signals. Also, the succeeding stages, such as the horizontal automatic phase control (APC) circuit and the vertical sync pulse integrator circuits, only slightly affect the operation of the two-stage separator. It is important to note that the circuit of Fig. 6.15a does not require its circuit components to be carefully matched.

The collector of the transistor T_1 is directly coupled to the base of the second transistor T_2 , in such a way that T_2 is OFF and T_1

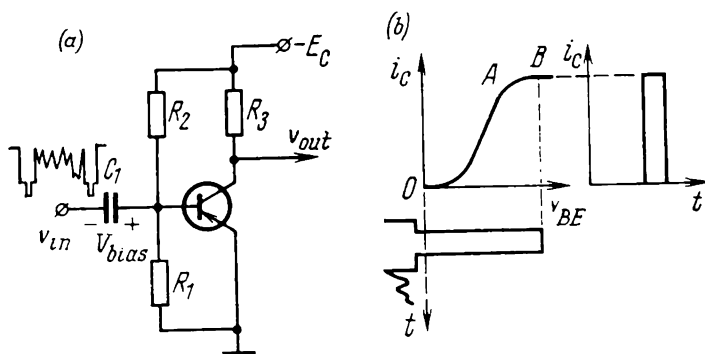


Fig. 6.14. Single-stage transistor amplitude separator
(a) circuit; (b) waveforms

is ON as long as the sync tips are passing through. Any noise that might arise at the sync tips cannot pass on to output because T_2 is held OFF by the self-bias voltage E_{bias} produced across R_4 and C_2 and applied to the base of T_2 via the conducting transistor T_1 . When the current through T_1 drops to zero during the sync interval, its collector voltage might rise to the value of collector supply voltage, $-E_C$. However, this rise is limited by the equivalent base-emitter diode of transistor T_2 .

The collector and emitter circuits of T_2 contain resistors R_7 and R_5 , respectively. Their function is to ensure that bipolar horizontal sync pulses can be applied to the balanced detector of the automatic phase control circuit*. The vertical sync pulses are developed across R_6 . The capacitor C_3 which shunts R_6 is chosen such that the network R_6C_3 presents a practical short-circuit to the relatively short horizontal sync pulses and the only load for them is R_7 . The pulse waveforms at the characteristic points of the circuit of Fig. 6.15a are shown in Fig. 6.15b.

* See Sec. 6.6.

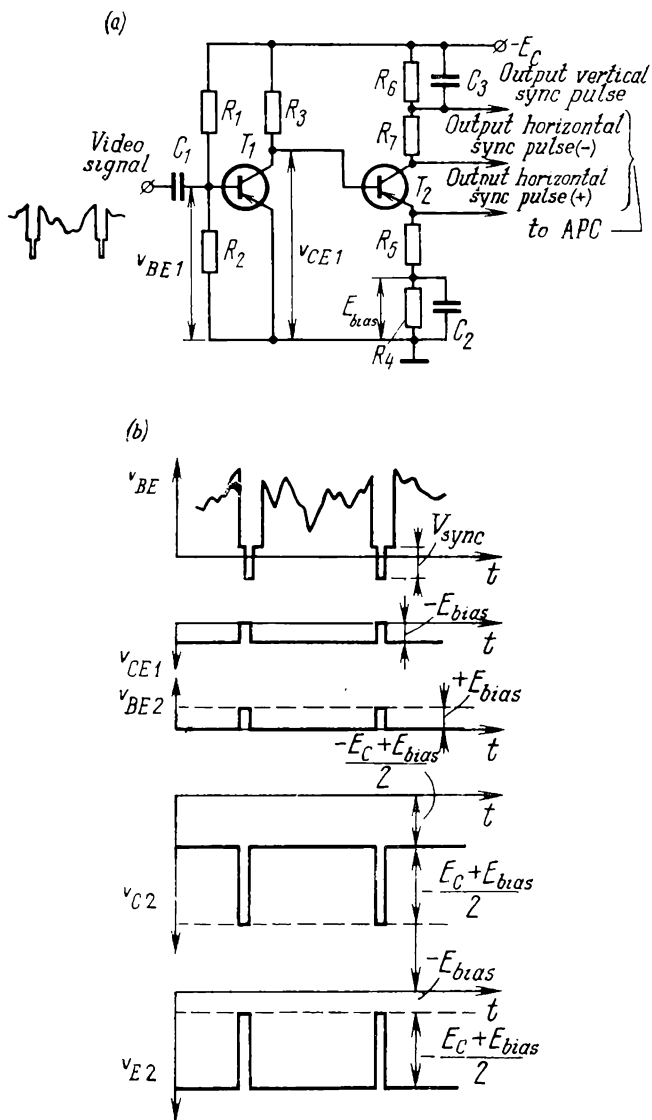


Fig. 6.15. Two-stage transistor amplitude separator
(a) circuit; (b) waveforms

6.5. Separation of Horizontal from Vertical Sync Pulses

Differentiator circuit for horizontal sync pulses. The horizontal sync pulses are developed from the composite sync signal by a differentiator circuit such as shown in Fig. 6.16a. For normal operation

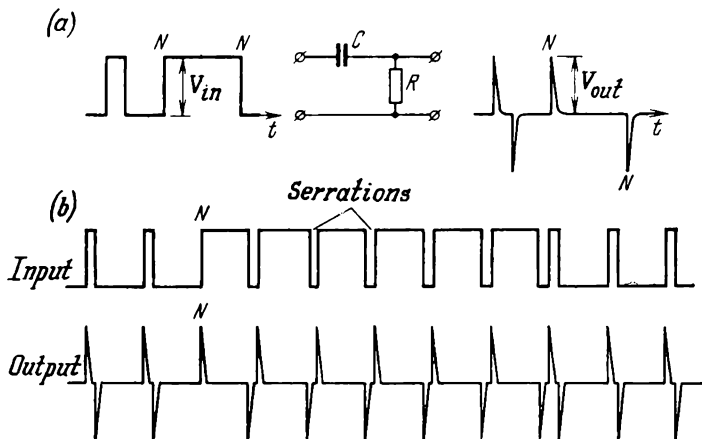


Fig. 6.16. Differentiator circuit for horizontal sync pulses
(a) waveforms; (b) suppression of vertical sync pulses

of the differentiator circuit, its time constant is chosen to be one-half to one-third of the duration of the horizontal sync pulse:

$$RC = t_{sync, h} \div (2 \text{ to } 3) = 1.7 \text{ to } 2.5 \mu\text{s}$$

As a result, the capacitor C can charge quickly when the composite sync signal is applied to the input and discharge as quickly when the applied signal ceases. The input and output waveforms of the differentiator circuit are shown in Fig. 6.16b. As is seen, the output waveform contains no vertical sync pulses, and the voltage peaks, or sharp pulses, left (N) are utilized as horizontal sync pulses. The serrations in the input vertical sync pulse are converted by the differentiator into pulses in no way differing from the output horizontal sync pulses.

If we ignore the stray parameters of the differentiator circuit, such as the internal impedance of the input pulse source (which, in our case, may be the output impedance of the amplitude separator or amplifier-limiter) and the stray capacitance, the amplitude of the input signal must be equal to that of the output pulses. In practice, the stray parameters considerably impair the performance of

the differentiator by reducing the amplitude and extending the rise time of the output pulses.

Integrator circuit for vertical sync pulses. The vertical sync pulses are developed from the composite sync signal by an integrator circuit such as shown in Fig. 6.17. In this circuit the output voltage is picked off the capacitor C . For its operation the integrator circuit

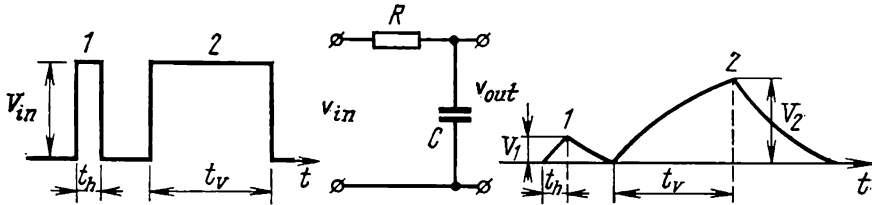


Fig. 6.17. Integrator circuit for vertical sync pulses

depends on the substantial difference in duration between the vertical and horizontal sync pulses:

$$t_v/t_h = 192 \mu\text{s} \div 5.1 \mu\text{s} = 37.5$$

Suppose that the integrator circuit accepts two kinds of rectangular pulses: the narrow horizontal sync pulse, 1, and the wide (simplified) vertical sync pulse, 2. Because these pulses charge the capacitor C through the resistor R gradually, the amplitude of the output pulses will depend on their duration and it will be decreasing with decreasing pulse duration. In this way, the difference in pulse duration is transformed into the difference in amplitude between output pulses.

If the integrator circuit accepts a rectangular pulse of amplitude V_{in} (shown by the dashed line in Fig. 6.18a), the output voltage will obey the exponential law:

$$v_{out} = V_{in} [1 - \exp(-t/RC)] \quad (6.1)$$

In the plot of Fig. 6.18a, t_h and t_v stand respectively for the duration of the horizontal and vertical sync pulses. The degree of horizontal rejection by the integrator circuit may be expressed as the ratio of the vertical sync pulse amplitude, $V_{v, out}$, to that of the horizontal sync pulses, $V_{h, out}$, existing at the output of the integrator circuit:

$$k_1 = V_{v, out}/V_{h, out} \quad (6.2)$$

The degree of rejection depends on the time constant RC and the pulse durations, t_v and t_h . Recalling that $t_v/t_h = 37.5$ and using

Eq. (6.1), we get

$$k_1 = V_{v, out}/V_{h, out} = \frac{1 - \exp(-t_v/RC)}{1 - \exp(-t_h/RC)} = \frac{1 - \exp(-37.5t_h/RC)}{1 - \exp(-t_h/RC)} \quad (6.3)$$

A plot of $k_1 = f(RC/t_h)$ based on Eq. (6.3) is shown in Fig. 6.18*b*. As is seen, for better horizontal sync rejection, the time constant should be made long. However, a long time constant would extend

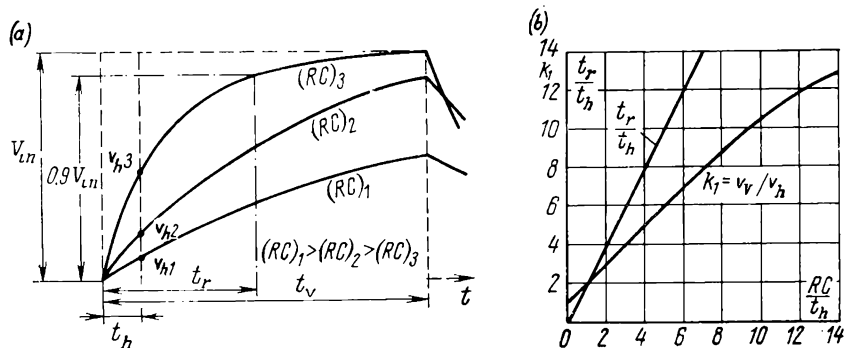


Fig. 6.18. Effect of time constant on operation of the integrator circuit

(a) horizontal-pulse output amplitude v_h as a function of time constant; (b) output-pulse rise time and degree of rejection as functions of time constant

the rise time of the vertical sync pulse, and this would make synchronization erratic and upset the interlace (see Fig. 6.4). In rough terms, the rise time of the vertical sync pulse may be estimated as

$$t_r \approx 2RC \quad (6.4)$$

For reference, the relation $t_r/t_h = 2RC/t_h$ is shown in Fig. 6.18*b*.

A single-section integrator circuit provides a degree of rejection ranging between 7 and 9, which is not sufficient. If it were used in a practical receiver, the output signal could still contain a considerable amount of horizontal sync pulses, and these would upset the synchronization of the vertical scanning generator.

Thus, the choice of the time constant for the integrator circuit involves conflicting requirements. On the one hand, the time constant should be made as long as practicable so as to remove all traces of the horizontal sync pulses. On the other, a long time constant would lead to a prohibitive extension in the rise time and, as a consequence, to a decrease in the slope of the vertical sync pulse. This conflict is unsurmountable for a single-section integrator circuit, but it is easily resolvable by a two- or three-section circuit.

The circuit of a two-section integrator is shown in Fig. 6.19*a*. The parameters R_2 and C_2 of each section are usually made the same. With properly matched circuit parameters, this form of integrator

considerably improves the degree of separation and increases the slope of the output vertical sync pulses in comparison with a single-section circuit.

For better insight into the operation of a two-section integrator circuit, it is convenient to divide it into two single-section RC -networks (Fig. 6.19b). The input of the first accepts a rectangular pulse, and the output delivers an intermediate pulse the initial portion of which is not so sharply rising, that is, it has no steep

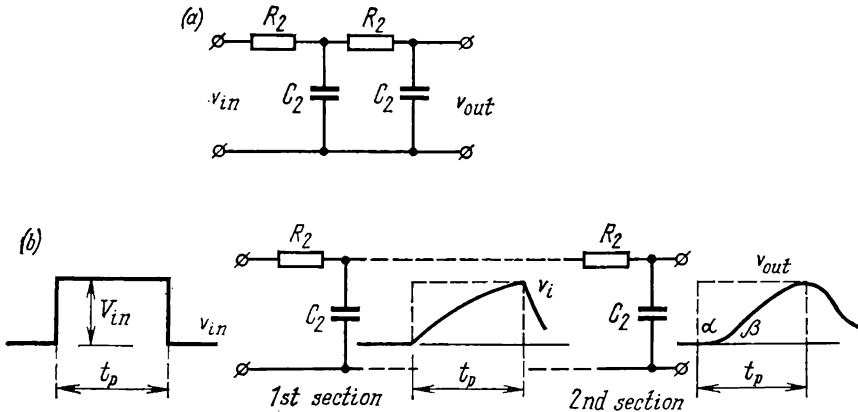


Fig. 6.19. Two-section integrator circuit
(a) circuit; (b) waveforms

leading edge. Thus, the second RC -network is driven by a gradually rising voltage rather than by a sudden change of voltage. Accordingly the voltage across the capacitor in the second network rises initially at a markedly slower rate than that across the first capacitor (portion α , β). It is not until after the voltage across the first capacitor reaches a substantial value that the voltage across the second capacitor begins to rise at a faster rate.

For ease of comparison, Fig. 6.20 shows the output pulses from the single-section network, 1, and from the two-section network, 2, cascaded together. With the circuit parameters of the two-section network properly matched (such that $R_2C_2 < RC$), the output vertical sync pulse has a faster rise time and the horizontal sync pulse is removed more completely. Mathematically, the dependence of the output voltage on time for a two-section integrating network in response to a rectangular pulse excitation may be described as

$$v_{out} = V_{in} (1 - 1.17e^{-0.38t/RC} + 0.17e^{-2.69t/RC}) \quad (6.5)$$

This expression contains two exponential terms; the first decays slowly and the second faster with time.

A plot relating v_{out}/v_{in} to t/R_2C_2 for a two-section integrator and based on Eq. (6.5) is shown in Fig. 6.21. On its basis we may write the following approximate expression for the rise time of the output pulse

$$t_r \approx 4R_2C_2 \quad (6.6)$$

from which we can determine the improvement in the removal of the horizontal sync pulse from the composite sync signal, assuming, for example, that the rise time is the same in a single-section and a two-section integrator. Let the limiting rise time of the output

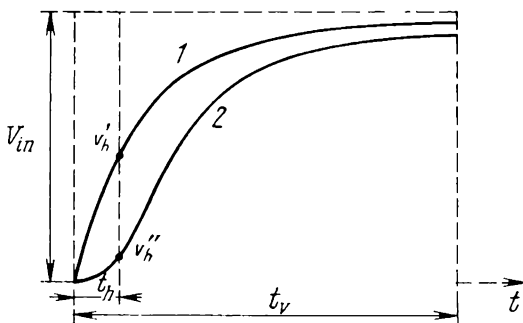


Fig. 6.20. Comparison of output pulses from (1) a single-section and (2) a two-section integrator circuit

vertical sync pulse be $t_r = 80 \mu s$ for both a single-section and a two-section integrator. The respective degrees of horizontal sync rejection are $k_1 = 8.5$ and $k_2 = 40$. Thus, in comparison with the single-section network, the two-section integrator shows a performance $k_2/k_1 = 40 \div 8.5 = 4.7$ times better.

It is to be stressed that the improvement in the removal of horizontal sync pulses (or in the rise time of the output pulse) that a two-section integrator gives over a single-section network can be obtained only when the network sections have different time constants, $R_2C_2 < RC$, where R_2C_2 is the time constant of a section in a two-section integrator. In our example, $R_2C_2/RC = 0.5$.

Now that we have looked into the operation of an integrating network, we are in a position to explain the function of equalizing pulses in the standard television signal in greater detail (see Sec. 5.1). To begin with, imagine that the composite sync signal (a mixture of vertical and horizontal sync pulses) applied to the input of the integrator network contains no equalizing pulses at twice the line scanning frequency (Fig. 6.22a, b). To obtain proper interlace, it is essential that the horizontal sync pulses of even fields lie midway between those of odd fields. As is seen from Fig. 6.22a and b, this is achieved

by causing the leading edges of vertical sync pulses in even and odd fields, LE_e and LE_o , to coincide precisely. However, the vertical sync pulses appearing at the output of the integrator circuit will differ in waveform because of the difference in the pulse structure (Fig. 6 22c). This difference in output wave form is due to two factors.

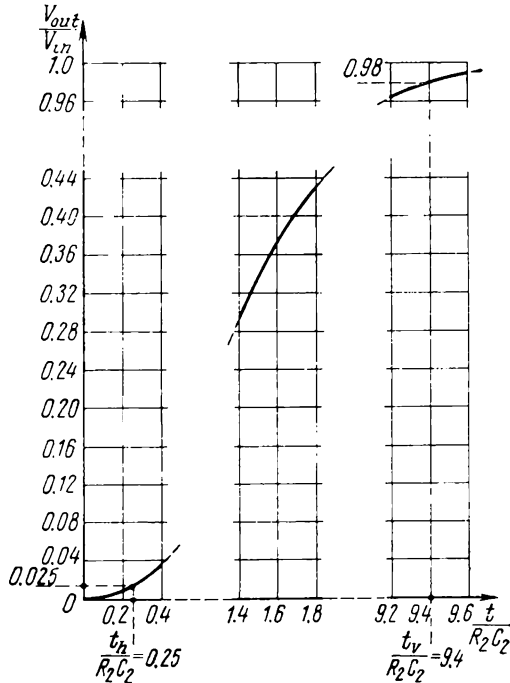


Fig. 6.21. Output voltage of a two-section integrator circuit as a function of time

Firstly, the time interval between the leading edge of a vertical sync pulse and that of the adjacent horizontal sync pulse is equal to the line scan interval, H , for even fields, and to half that interval, $H/2$, for odd fields, and this difference causes the output voltage to take on a different value at the beginning of the vertical sync pulse (point a in Fig. 6.22c). Secondly, adjacent fields have a different number of serrations (two in even fields and three in odd fields), and this fact accentuates the difference in waveform between the pulses still more. As a result, for a given synchronization level, V_{av} (the line MN in Fig. 6.22c), the instants b and c at which the oscillator is synchronized would be shifted by ΔT , thereby causing the even lines of the picture to be superimposed on the odd ones. At

$\Delta T = H/2$, this superimposition would be complete, there would be no interlace scanning, and the vertical resolution would be halved. The injection of equalizing pulses at twice the line scan frequency

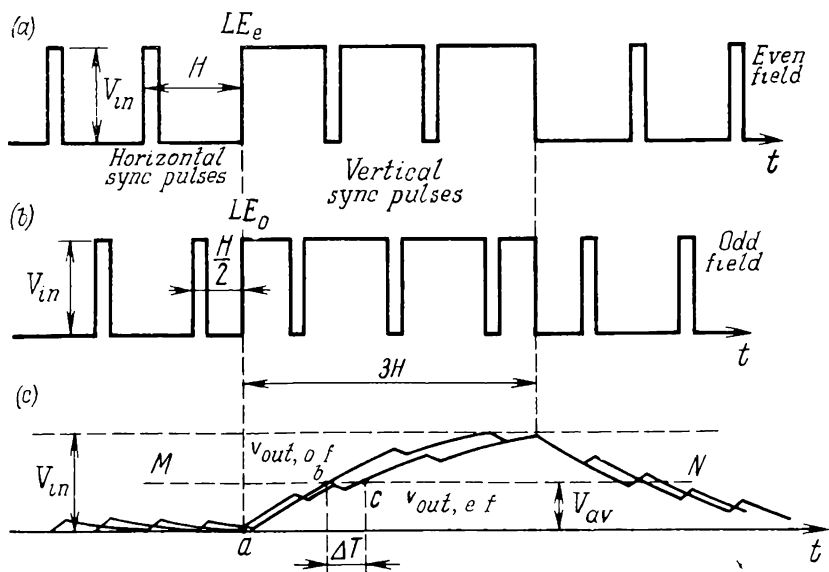


Fig. 6.22. Explaining the function of equalizing pulses at twice horizontal frequency

(a) even-field sync pulse; (b) odd-field sync pulse; (c) corresponding voltage waveform at integrator output

before, during and after the vertical sync pulse (see Fig. 5.4) eliminates both factors responsible for differences in waveform between the vertical sync pulses of adjacent fields at the output of the integrator circuit, thereby securing the requisite quality of interlace.

6.6. Inertia-Type Horizontal Synchronization

In impulsive synchronization, each input pulse can trigger the horizontal oscillator. Should this pulse be due to noise or interference, a line (or even several lines) would be distorted in the reproduced image. Amplitude separation of sync pulses from interfering pulses does not give an appreciable improvement in noise immunity.

A more characteristic difference between sync and interfering pulses is utilized for their separation in the synchronization system based on automatic phase lock control (APC). This difference consists in that sync pulses follow at a fixed period while interfering pulses occur randomly and at no fixed repetition period. The APC circuit

compares the frequency and phase of the line-scan generator with those of horizontal sync pulses. Should they differ, the APC circuit will act upon the line scan generator to change its frequency and phase as may be necessary. Since they have no definite frequency, interfering pulses are separated by this circuit from any other voltages and have almost no effect on the performance of the synchronization system.

Another distinction of this form of synchronization is that it possesses what is differently called as the flywheel effect, memory, or inertia: frequency comparison is extended over a relatively long time

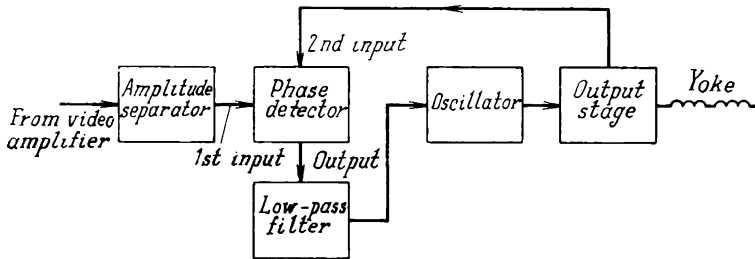


Fig. 6.23. Block diagram of a phase-lock (APC) horizontal synchronization system

interval (determined by the time constant of the APC circuit). As a result, the distortion or disappearance of some sync pulses due to the action of noise or interference has no marked effect.

It should be stressed that this form of synchronization is utilized only for horizontal oscillators; vertical oscillators do not need it because the sync pulses applied to the vertical oscillator are passed through an integrator circuit which, in addition to horizontal sync pulses, also effectively removes any noise.

A block diagram of a synchronization system utilizing APC appears in Fig. 6.23. The video signal generated by the video amplifier of the TV receiver is applied to a sync amplitude separator. From the separator, the sync pulses are fed to the first input of a phase detector, the second input of which accepts pulses from the horizontal output stage. The d.c. voltage appearing at the output of the phase detector, having magnitude and polarity corresponding to the difference in phase between the applied voltages, contains interfering and sync pulses. The unwanted components are removed by a low-pass filter which only leaves d.c. (or rather, a slowly varying) voltage. This voltage is injected into the base (or grid) circuit of the controlled oscillator and corrects its frequency as may be necessary.

The circuit of a typical horizontal APC system is shown in Fig. 6.24. Consider operation of this circuit. The second (output) transistor,

T_2 , of the two-stage sync amplitude separator (see Fig. 6.15a) has two outputs, O_1 (in the collector circuit) and O_2 (in the emitter circuit). The sync pulses appearing at these outputs are routed via

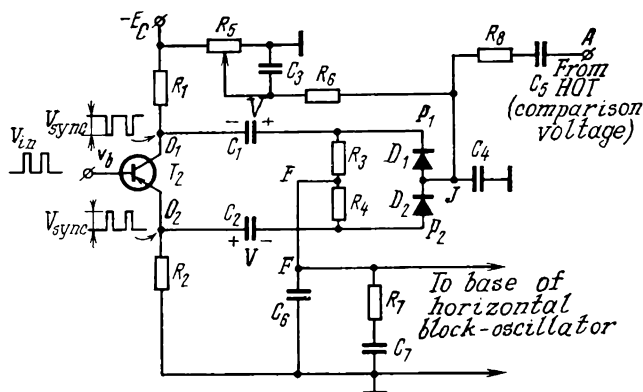


Fig. 6.24. Circuit of a typical horizontal phase-lock (APC) synchronization system

capacitors C_1 and C_2 to the diodes D_1 and D_2 . As a result, the capacitors C_1 and C_2 are charged by the sync pulses to a d.c. voltage, V .

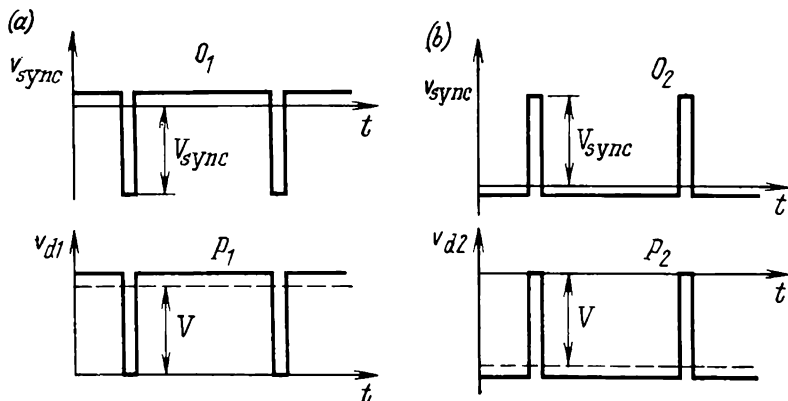


Fig. 6.25. Voltage waveforms at (a) points O_1 and P_1 and (b) at points O_2 and P_2 of the circuit in Fig. 6.24

equal to the amplitude of sync pulses, V_{sync} . To simplify the analysis, assume that no reference pulses are applied to the input A from the horizontal output transformer. Then a voltage appears across the diodes D_1 and D_2 (points P_1 and P_2), consisting of a d.c. component, V , and an a.c. (pulse) component, v_{sync} (Fig. 6.25). The a.c. compo-

nent, v_{sync} , is suppressed by elementary low-pass filters, R_3C_6 and R_4C_6 (which may be called integrator circuits). As a result, the outputs of the low-pass filters (point F in the diagram of Fig. 6.24) deliver only the d.c. components. Since, however, these d.c. components, arriving at point F from points P_1 and P_2 , are equal in magnitude and opposite in polarity, they cancel out, that is, the d.c. component vanishes at point F , too. This is how the bridge circuit comprising the diodes D_1 and D_2 and the resistors R_1 and R_4 balances out the d.c. component initially (in the quiescent state).

In actual operation, when the horizontal output transformer, HOT , feeds reference pulses to the input A and the sync pulses come

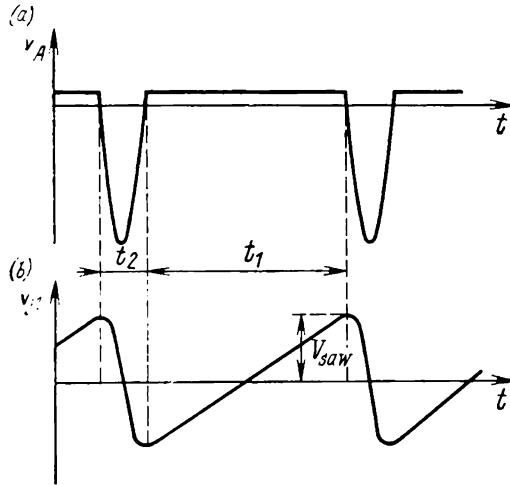


Fig. 6.26. (a) Retrace voltage pulses from the horizontal output stage; (b) generation of a sawtooth comparison voltage

along, mixed with noise, the filters R_3C_6 and R_4C_6 suppress all a.c. voltages: noise pulses, sync pulses, and reference pulses. A d.c. voltage of an appropriate polarity appears at point F only when the sync and reference pulses differ in phase.

The reference pulses, which are retrace pulses, are usually taken from a special winding on the horizontal output transformer. They are applied to the common junction, J , of the diodes via a suitable integrating network made up of the capacitor C_4 and a series-shunt combination of the resistors R_8 and R_6 . The capacitor C_5 prevents the bias voltage (developed across R_5) from reaching the horizontal output transformer.

The function of the integrating network R_8C_4 is to convert the pulse voltage v_A coming from the horizontal output transformer into a sawtooth voltage, v_J (Fig. 6.26). In this way, the rectangular pul-

ses are compared with the integrated (sawtooth) retrace pulses for frequency and phase.

The operation of the phase detector will be clear from reference to Fig. 6.27. For the balanced diode phase detector to operate correctly,

it is important that the amplitude of the sync pulses, V_{sync} , be greater than twice that of the sawtooth retrace voltage: $V_{sync} \geq 2V_{saw}$.

Comparison for phase takes place during retrace, t_2 . If the centre of a sync pulse (Fig. 6.27a) coincides with the centre of a reference pulse, there is no phase difference, and no additional voltage appears at the output of the low-pass filter (point F in Fig. 6.24). If, on the other hand, the sawtooth retrace voltage leads the sync pulse in phase (Fig. 6.27b), the sync pulses rise somewhat, so that C_1 acquires an additional charge and C_2 loses some charge. As a result, a positive error voltage appears at the point F , equal to $V'_{er} = |V'_1 - V'_2|$.

Should the sawtooth voltage lag behind the sync pulse in phase (Fig. 6.27c), a negative error voltage will appear at the point F (Fig. 6.24), equal to $V''_{er} = -|V'_1 - V'_2|$.

In this way, a departure from phase centre upsets the balance of the bridge circuit formed by the two diodes D_1 and D_2 and the two resistors R_3 and R_4 .

As already noted, the filters R_3C_6 and R_4C_6 (see Fig. 6.24) serve to suppress the a.c. components in the voltage coming from the phase detector. This voltage is made up of sync pulses, the sawtooth reference

voltage, and noise voltage. The capacitor C_6 provides a low-impedance path for these voltages to ground, so that only d.c. (or, rather, a slowly varying) voltage remains at the point F , which is used as the control voltage for the controlled horizontal oscillator. The longer the time constant of the filter, the better it suppresses

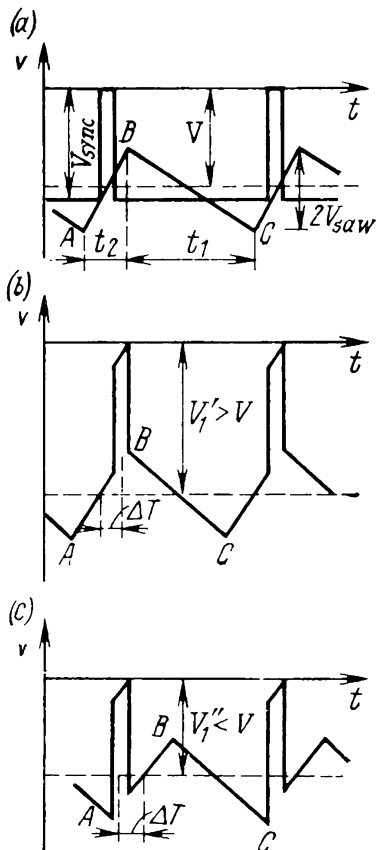


Fig. 6.27. Phase detector

(a) zero phase difference between sync pulses and comparison voltage; (b) sync pulses lag behind comparison voltage in phase; (c) sync pulses lead comparison voltage in phase

impulsive noise. However, if this time constant were made too long, the circuit would be excessively sluggish. Then the control voltage, V_{er} , appearing at the output of the filter, corresponding to the phase difference between the voltages being compared, would not be able to charge C_6 for a long time, and the output voltage across C_6 , fed to the base circuit of the oscillator transistor would take a much longer time in bringing the oscillator frequency up to the repetition frequency of the sync pulses. Because of this, any departure from proper synchronization would be removed only gradually, and the image would show a curved top part noticeable to the eye. If, on the other hand, the time constant of the filter were chosen too short, the a.c.

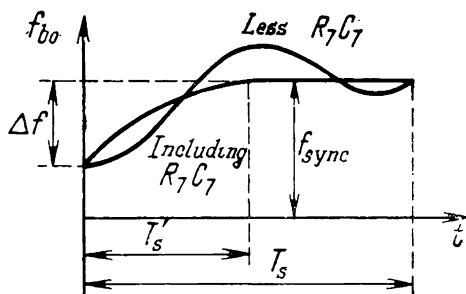


Fig. 6.28. Operation of R_7C_7 network in the circuit of Fig. 6.24

component would not be suppressed at point F and, on passing into the base circuit of the oscillator transistor, would upset horizontal synchronization.

The time lag of the horizontal APC circuit can be reduced while securing good a.c. suppression in the control voltage by inclusion of a damping network, R_7C_7 . It may sometimes happen that the horizontal oscillator jumps out of synchronism (such as when the video signal is suddenly decreased in amplitude due to manual contrast adjustment, sustained action of a series of noise pulses, or a sudden change in supply voltage). It takes some time for the unsynchronized oscillator to pull into synchronism again, mainly because the filter R_3C_6 (R_4C_6) has a relatively long time constant or, which is the same, shows a considerable time lag. In other words, the control voltage taken from C_6 changes at a slower rate than the frequency of the controlled oscillator.

Both calculations and experience show that the restoration of frequency in the horizontal oscillator may follow the law of damped oscillations (Fig. 6.28). The settling time, T_s , may be considerable. Under certain conditions, frequency variations might be undamped; that is, the oscillator might continually hunt about the sync pulse

frequency. All this is avoided as the settling time is drastically cut down by the damping network R_7C_7 . As follows from Fig. 6.28, with this network, synchronization is restored faster and without hunting.

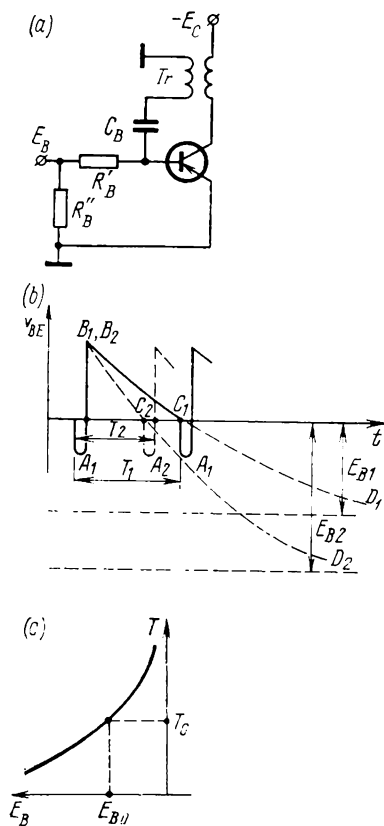


Fig. 6.29. Control of blocking-oscillator period by varying its base bias

(a) circuit; (b) base voltage pulse waveform; (c) control characteristic

The frequency and, as a consequence, phase of the oscillator can be held within the requisite range by applying the control (error) voltage to the grid (base) of the oscillator tube (transistor) from the APC circuit (point *F* in Fig. 6.24). Consider this holding action, using the transistor blocking oscillator (shown in Fig. 6.29a) as an example. The waveform of the voltage applied to its base is shown in Fig. 6.29b. Owing to the positive feedback supplied by the transformer T_r , the capacitor C_B rapidly charges by the base current (pulse A_1). Within the portion $B_1C_1D_1$ the capacitor re-charges exponentially [the time constant is $(R'_B + R''_B)C_B$]. If the transistor were not rendered conductive at time C_1 , the capacitor would keep charging to the voltage E_{B1} applied from the APC low-pass filter (made up of R_3, R_4, R_7, C_6 and C_7 in Fig. 6.24). However, at time C_1 the transistor is driven to conduction, and a pulse (A_1) is produced again owing to the positive feedback thereby applied.

Figure 6.29b also shows the voltage waveform, $B_2C_2A_2$, for another (higher) APC voltage, ($|E_{B2}| > E_{B1}|$). As is seen, the period T

depends on the magnitude of E_B (in our example, $T_2 < T_1$). The control characteristic, $T = f(E_B)$ is shown in Fig. 6.29c. The quiescent point, E_{B0} , is positioned by applying fixed bias from R_5 (see Fig. 6.24). The value of bias voltage, E_{B0} , sets the initial period T_0 for the blocking oscillator. Thus, the variable resistor R_5 is in fact an element of manual horizontal hold control.

CHAPTER SEVEN

CAMERA TUBES

7.1. Basic Characteristics of Camera Tubes

This chapter will examine the design and operating principle of camera, or pick-up, tubes which are important elements of the camera chain, intended to provide an electrical signal by forming an electron current or charge-density image from an optical image. Attention will be focused on the tube types most commonly used in broadcast and closed-circuit television, but some space will also be devoted to the iconoscope. Although no longer in use, the iconoscope deserves a detailed mention in view of the part it has played in the progress of television and also because its principle of operation remains the basis of present-day camera tubes of more advanced designs.

It is customary to class camera tubes on the basis of several factors. The most important among them are: signal-to-noise ratio, sensitivity, resolving power, and spectral response.

Conversion of an optical image into an electrical signal is accompanied by current fluctuations, or noise. This form of noise is assessed in terms of the signal-to-noise ratio specified for each tube. This ratio does not take account of all noise that may appear on the TV screen, because there are other sources of noise in the camera chain. Yet, it defines the share contributed by the camera tube.

The sensitivity of a camera tube defines the illumination that the scene being televised must be given in order that the tube can operate normally. The higher the sensitivity, the lower the illumination needed. When comparing camera tubes for sensitivity, the signal-to-noise ratio must be held fixed. Numerically, the sensitivity of a camera tube may be defined as the reciprocal of the illumination needed at the input to (or on the photocathode of) the camera tube in order to obtain the desired signal-to-noise ratio.

The resolving power of a camera tube is a measure of its ability to generate an electrical signal representing picture detail.

The spectral characteristic of a camera tube defines the dependence of the camera signal on the wavelength of incident light for the same power at all wavelengths. The above characteristics depend on the design, principle of operation and photo-sensitive materials of camera tubes. It is convenient therefore to take up the matter of photo-emission.

7.2. Photoemission and Basic Laws

Conversion of an optical image into an electrical signal in camera tubes may be based on photoemission (outer photoelectric effect) or photoconduction (inner photoelectric effect). In the former case, a camera tube has a photocathode which utilizes a material capable of photoemission. When light strikes the photocathode, electrons are continually emitted from its surface. If an electric field is set up between the photocathode and anode (collector) in order to accelerate the emitted electrons the latter will form a photocurrent. If the accelerating field is of sufficient intensity, all electrons leaving the photocathode will reach the collector, and the photocurrent will reach saturation.

The basic laws that govern photoelectric emission were established by A. G. Stoletov and A. Einstein.

1. *Stoletov's law.* During his investigations of photoelectric emission in 1888-1890, Stoletov discovered that the saturation photocurrent is proportional to the luminous flux causing it (on the condition that the incident light remains constant in spectrum), that is:

$$i_{ph} = \varepsilon F \quad (7.1)$$

where ε is a proportionality factor describing the light sensitivity of the photocathode; it is equal to i_{ph} when the luminous flux is 1 lumen, and is given in microamperes per lumen.

2. *Einstein's law.* The maximum kinetic energy of photoelectrons is a linear function of the frequency of incident light and is independent of its intensity:

$$(mv_{\max}^2)/2 = h\nu - P_e \quad (7.2)$$

where P_e = electronic work function

h = Planck's constant

ν = frequency

m = mass of an electron

v_{\max} = maximum velocity

From the above equation deduced by Einstein in 1905 it follows that if the product $h\nu$ defining the energy of a photon exceeds the electronic work function, P_e , the excess energy will be converted to the kinetic energy of the liberated electron. The product $h\nu = P_e$ defines the threshold below which no photoelectric emission is possible. Since the energy of a quantum is proportional to ν , the minimum radiation frequency at which the photoemissive effect is possible is defined as $\nu_{\min} = P_e/h$. This frequency and the corresponding maximum wavelength of light $\lambda_{\max} = c/\nu_{\min} = ch/P_e$ is called the red boundary or threshold of the photoemissive effect.

The best photoemissive surfaces are so-called composite photocathodes. A composite photocathode is a film several hundred or thou-

sand atomic layers thick, applied to a metal or an insulating substrate. By making this film from an alkaline metal (say, caesium), it is possible to reduce the electronic work function. The red boundary of some composite photocathodes occurs at $\lambda_{max} = 1.5$ to $1.7 \mu\text{m}$, that is, lies in the infra-red region.

7.3. Spectral Reponse Characteristics of Photocathodes

As already defined, the spectral response characteristic of a photocathode is the dependence of its photocurrent on the wavelength of incident monochromatic light of constant power. The spectral response of a photocathode can be measured by allowing a monochromatic radiation of wavelength λ to strike its surface. Then, dividing the saturation photocurrent, i_{ph} , into the incident luminous flux or radiant energy will give the spectral sensitivity of the photocathode at wavelength λ . If we vary the wavelength of incident monochromatic radiation over the wavelength range of interest, we shall obtain the spectral response of the photocathode within that range. In practice, the spectral response characteristic is usually plotted in relative units. Let, for example, there be the spectral response, $i_{ph} = f(\lambda)$, of a photocathode, measured at a radiant power of 1 W. Let also the characteristic have a peak, $i_{ph,0} = f(\lambda_0)$, at some wavelength λ_0 . Then the relative sensitivity will be defined as

$$e(\lambda) = [i_{ph}(\lambda)]/i_{ph,0} \quad (7.3)$$

The spectral response characteristics of some composite photocathodes are shown in Fig. 7.1. Curve 1 applies to a silver-caesium-oxygen photocathode. This type of photocathode has the following structure. A thin layer of silver acting as substrate is applied to a glass plate. The external surface of the substrate is oxidized. Then a thin layer of caesium is evaporated onto the substrate. The silver substrate is connected to the external terminal of the photocathode. As is seen from Fig. 7.1, the peak response of the silver-caesium-oxygen photocathode, 1, occurs in the infra-red region ($\lambda \approx 750 \text{ nm}$). There are also several response peaks in the ultra-violet region at $\lambda < 400 \text{ nm}$ (not shown in the figure).

Curve 2 of Fig. 7.1 applies to an antimony-caesium photocathode. This type of photocathode may or may not have a metal backing (say, nickel), and be deposited directly on the glass bulb; its peak response occurs in the range of 420 to 440 nm. By activating a finished antimony-caesium photocathode with oxygen, the peak of spectral sensitivity can be shifted towards the longer wavelengths. Antimony-caesium photocathodes have a high quantum efficiency, which may reach about 1/3 electron per photon at $\lambda = 400$ to 440 nm.

Recently, multicomponent (multi-alkaline) photocathodes have been developed, in which use is made of antimony, sodium, potassium and caesium. The spectral response of a multi-alkaline photocathode

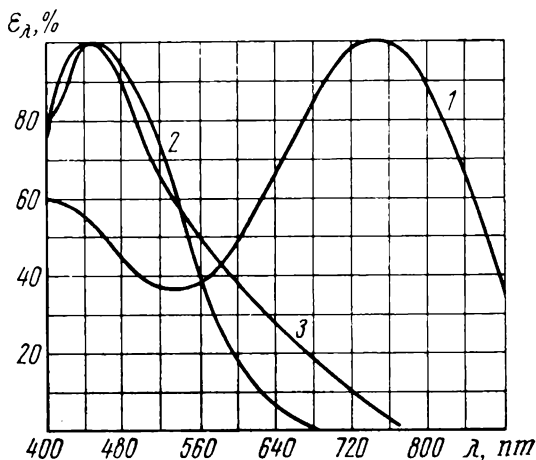


Fig. 7.1. Spectral response characteristic of photocathodes
1 — silver-caesium-oxygen; 2 — antimony-caesium; 3 — multi-alkaline

(curve 3 in Fig. 7.1) is expanded within the longer wavelength portion of the spectrum in comparison with that of the antimony-caesium photocathode. The quantum efficiency of a multi-alkaline photocathode is 1.5 to 2 times that of an antimony-caesium variety.

7.4. Integral Sensitivity of Photocathodes

In order to measure the spectral response of a photocathode, one needs a monochromatic light source of varying wavelength, which causes certain difficulties in practice. Also, a practical photocathode is most often exposed to white light. This is the reason why resort is made to the integral sensitivity of a photocathode, that is, its sensitivity to light not decomposed into spectrum components. The integral sensitivity of a photocathode is a function of the saturation photocurrent produced when the photocathode is illuminated by white light of unit power from a standard source. If the power distribution in the spectrum of the light source is specified by the function $\rho(\lambda, T)$, where T is the temperature of the luminous body, then the saturation current of the photocathode having a spectral response $\varepsilon(\lambda)$ may be defined as

$$i = i_{ph, 0} \int_{\lambda_1}^{\lambda_2} \varepsilon(\lambda) \rho(\lambda, T) d\lambda \quad (7.4)$$

The integral is taken over the interval between λ_1 and λ_2 where both $\varepsilon(\lambda)$ and $\rho(\lambda, T)$ are non-zero.

The total power emitted by the source, in watts, is

$$P = \int_{\lambda_1}^{\lambda_2} \rho(\lambda, T) d\lambda \quad (7.5)$$

By definition, the spectral sensitivity in $\mu\text{A/W}$ is

$$\varepsilon = \frac{i_{ph, 0} \int_{\lambda_1}^{\lambda_2} \varepsilon(\lambda) \rho(\lambda, T) d\lambda}{\int_{\lambda_1}^{\lambda_2} \rho(\lambda, T) d\lambda} \quad (7.6)$$

Another common definition of integral sensitivity is as the ratio of saturation photocurrent to incident luminous flux. In such a case (see Sec. 12):

$$\varepsilon' = \frac{i_{ph, 0} \int_{\lambda_1}^{\lambda_2} \varepsilon(\lambda) \rho(\lambda, T) d\lambda}{683 \int_{\lambda_{ph}}^{\lambda_{cr}} v(\lambda) \rho(\lambda, T) d\lambda} \quad (7.7)$$

It is seen from Eq. (7.7) that the integral sensitivity of a photocathode is decided not only by the spectral response, $\varepsilon(\lambda)$, but also by the spectral power distribution of the light source. To remove uncertainty in measuring sensitivity, it is common practice to employ a standard light source which is a 100-W gas-filled tungsten-filament lamp at a temperature of 2840 to 2870 K. The integral sensitivity of the most commonly used photocathodes is summarized in Table 7.1.

Table 7.1

Photocathode	Integral sensitivity at colour temperature of 2840-2870 K, $\mu\text{A/lumen}$
Silver-caesium-oxygen	15-30
Antimony-caesium	30-70
Antimony-cadmium-sodium	50
Antimony-cadmium-sodium-caesium	180

7.5. Nonstorage Camera Tubes

The mechanical image analyzers used in the early television systems were all of the nonstorage type. The magnitude of the signal generated by the photocell in a mechanical television system using,

say, a Nipkow disc (see Sec. 1.3) is decided by the amount of luminous energy incident on its photocathode during the time interval required to scan one picture element. If the time required to scan a complete frame, that is, to complete one vertical scan, is T_v and the picture is analyzed into N elements, the time required to transmit each element, t_{el} , is T_v/N . The number of elements, N , in present-day television systems is very great. Under the USSR standard, the picture is analyzed into more than 400,000 elements. The scan time per element, $t_{el} \approx 0.07 \mu\text{s}$, is a negligible fraction of the vertical scan time, $T_v = 1/25 \text{ s} = 40,000 \mu\text{s}$. Nonstorage tubes utilize only the luminous flux reflected from a picture element during this brief interval (equal to t_{el}). In this sense, the systems operating on this principle may be called instantaneous.

The image dissector and the flying-spot camera tube are likewise nonstorage types. In sketch form, the construction of the Soviet-made ЛН-604 image dissector is shown in Fig. 7.2. It has a translucent antimony-caesium photocathode, 2, applied to the faceplate, 1, of the tube envelope. The photocathode is made translucent because it emits photoelectrons from its vacuum side, and incident light must be free to pass through the body of the material. The photoelectrons leaving the photocathode are accelerated by a potential difference of about 2 kV between the photocathode and the accelerating electrode, 3. The greater proportion of electrons is then captured by an aperture plate, 4, and only those escaping this capture and passing through the aperture, 5, contribute to the electrical signal. The aperture size is equal to that of a raster element.

In the aperture plane, the electrons are focused by a focusing coil, 6. Two sets of scanning coils which produce mutually perpendicular magnetic fields sweep the electron beam over the aperture. One set of coils (at 7 in Fig. 7.2a) sweeps the whole beam, 8, horizontally (line scan), and the other set of coils (not shown in the sketch) do so vertically (frame scan). As the beam scans the aperture, the electrons corresponding to each element and to each line scanned pass in turn through the aperture, and reach a secondary-emission multiplier which amplifies the signal.

The secondary-emission multiplier in the ЛН-604 image dissector has 14 stages. The secondary emitters (dynodes) of the multiplier are made in the form of discs (schematically shown by the dashed lines, 9, in Fig. 7.2a). In greater detail, their design is shown in Fig. 7.2b. Each dynode is a metal mesh connected to inclined metal plates suitably treated to enhance secondary emission, σ . This multiplier structure is known as a Venetian blind. The dynodes are connected to the "+" side of an H. V. source so that the potential at every next dynode (which are numbered, starting from the aperture plate, 4) is higher than that at the previous one. On passing 13 multiplication stages, the electron beam reaches the last dynode num-

bered 10 in Fig. 7.2a. The secondary electrons leaving the last dynode, 10, are collected by a collector shield, 11. The collector is held at a positive potential chosen to be above that on the last dynode, 10,

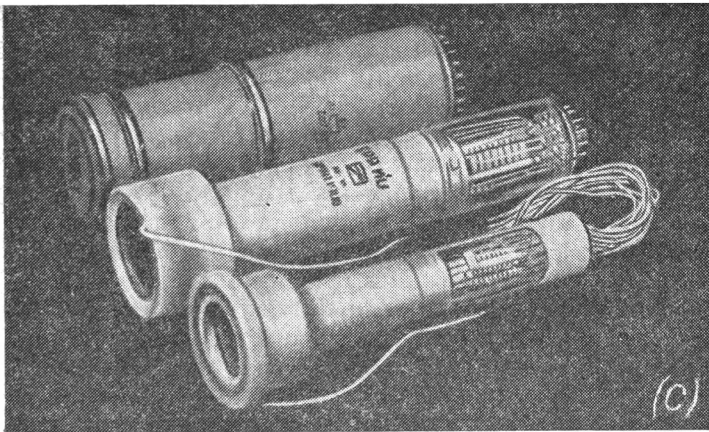
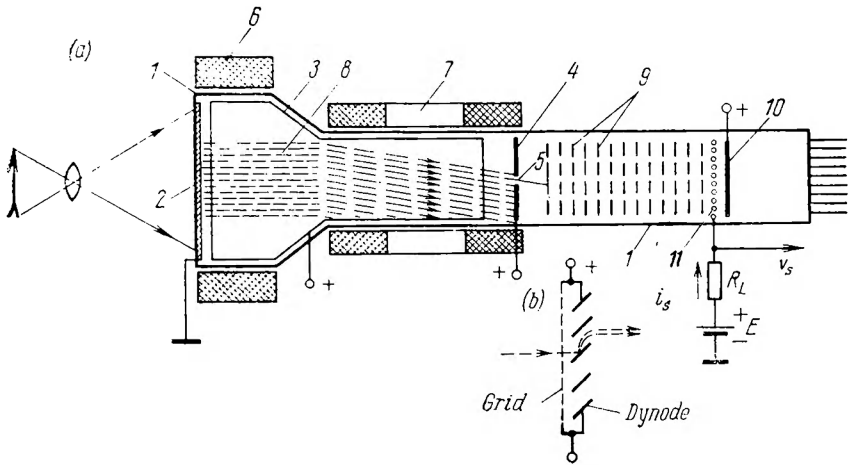


Fig. 7.2. Image dissector

(a) internal arrangement; (b) secondary emission multiplier stage; (c) commercial image dissectors

so as to improve the collection of secondary electrons. These electrons form the signal current which is allowed to pass through the load resistor, R_L . The direction of current flow is shown by the arrow in Fig. 7.2a. The secondary-emission multiplier builds up the signal

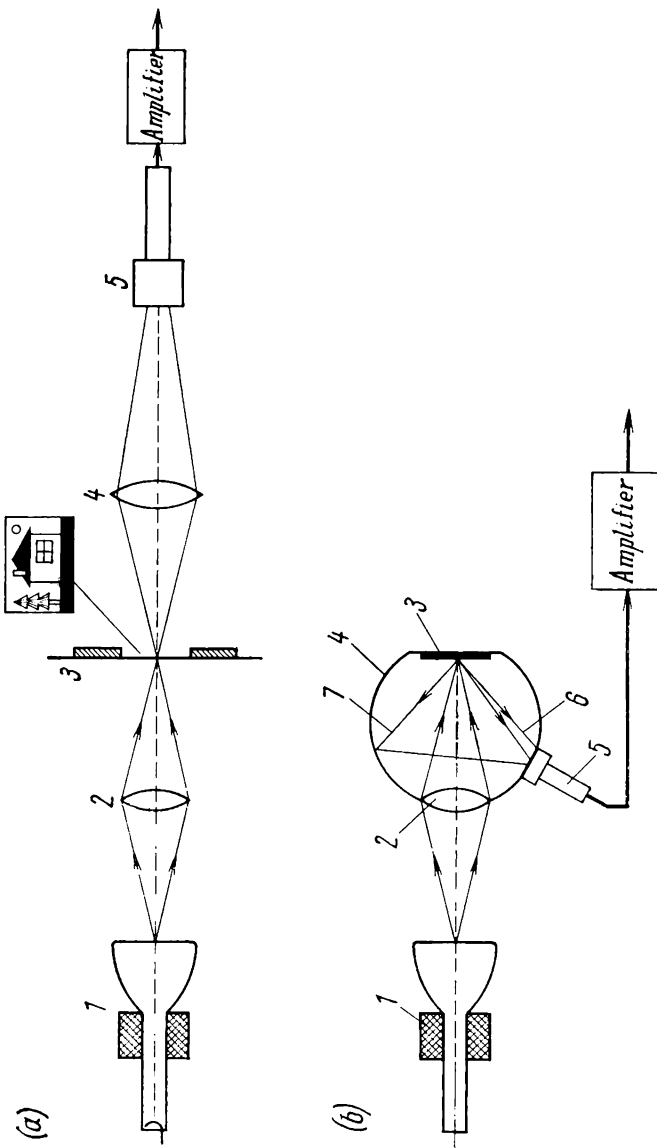


Fig. 7.3. Flying-spot system
 (a) optical train of a flying-spot system for transparencies; 1—raster-forming kinescope; 2—objective lens; 3—slide transparency; 4—multiplier phototube; (b) optical train of a flying-spot system for photographs; 1—raster-forming kinescope; 2—objective lens; 3—photograph; 4—light-collecting sphere; 5—multiplier phototube; 6 and 7—light reflected from photograph

current flowing through the load resistor R_L to a considerable magnitude of about $i_s \approx 100 \mu A$.

Several types of image dissectors are made in the USSR (Fig. 7.2c). In one of them (the JИИ-602) intended for closed-circuit television the beam is focused and deflected electrostatically. A very important quality of the image dissector is that the signal current is a linear function of the target illumination which is essential in closed-circuit systems.

A major limitation of the image dissector is low sensitivity which is typical of any nonstorage camera tube.

Calculations show that with an integral photocathode sensitivity of $\varepsilon = 70 \mu A/\text{lumen}$, a photocathode surface area of $S_{ph} = 10^{-3} \text{ m}^2$, and a satisfactory signal-to-noise ratio of $\psi = 50$ (these are all practical figures), the illumination of the photocathode must be $E_{ph} = 10,000 \text{ lux}$. Because of the camera lenses used in TV studios, the illumination of the scene must be at least 100 times that of the photocathode: $E_{sc} \approx 100 E_{ph} = 1 \text{ million lux}$. In other words, the image dissector is unsuitable for studio transmissions (see Table 1.2, Sec. 1.2). However, it can be employed in closed-circuit television where the scenes being televised are brightly illuminated or luminous themselves.

The optical train of the flying-spot system, also classed among nonstorage types, is shown in Fig. 7.3a. It is mainly intended for transmission from slides and transparencies. The primary source of light for the production of a picture in the flying-spot system is the raster-forming kinescope, 1. This kinescope is scanned with a sharply focused electron beam. The beam is deflected vertically and horizontally by coils in the usual manner. The light produced by the scanning spot is focused on a transparency or film, 3, by an objective lens, 2. The light passing through the film is collected by a condenser lens, 4, onto the photocathode of a photomultiplier tube, 5. The current at the output from the multiplier is proportional to the film density at the point scanned by the spot. In this way, the spot scans the entire area of each frame, and the multiplier phototube delivers the picture signal. The flying-spot tube can also be employed for transmission of optical images from an opaque material. In such a case, the multiplier phototube collects light reflected from the subject copy (Fig. 7.3b). Among the merits of the flying-spot tube are high signal-to-noise ratio and high resolving power.

7.6. Storage-Type Camera Tubes

Every instant, a nonstorage camera tube, such as the image dissector or the flying-spot tube, utilizes only the photoelectrons emitted by one surface element of the photocathode scanned by the beam during that brief interval. In other words, at any instant the signal utilizes

only $1/N$ part of the photocathode surface although the remaining parts are emitting electrons continually.

Schematically, the generation of a signal from a picture element in a nonstorage system is illustrated in Fig. 7.4a. As light moves from one target element to another, the switch Sw closes, and the photocurrent from that element is allowed to flow through the load

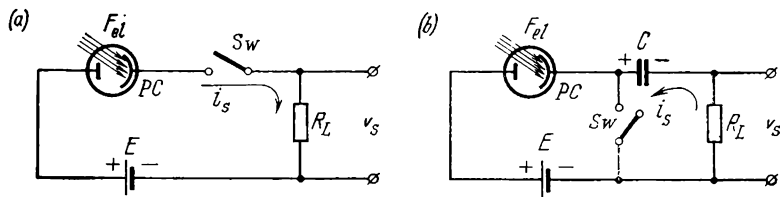


Fig. 7.4. Connection of photocells in circuit
(a) in a nonstorage system; (b) in a storage system

resistor R_L . The signal current, i_s , is decided by the luminous flux, F_{el} , and the integral sensitivity, ε , of the phototube, expressed in amperes per lumen. The video voltage across the load resistor is

$$v_s = i_{ph} R_L = i_s R_L = \varepsilon F_{el} R_L \quad (7.8)$$

Let us determine the light energy utilized to produce the signal in a nonstorage system. The light energy, L_{el} , is defined as the product of the luminous flux by the time of illumination and is expressed in lumens-second. In our case, it is

$$L_{el} = F_{el} t_{el} \quad (7.9)$$

where t_{el} is the scan time per target element (that is, the time during which the switch Sw is closed). The same target element will be scanned again after the frame interval, T_v ; between scans the light energy incident on this element will not be utilized. This energy is given by

$$L_{el, v} = F_{el} T_v \quad (7.10)$$

Using Eqs. (7.9) and (7.10), we can determine the part of light energy utilized to produce the picture signal:

$$L_{el}/L_{el, v} = t_{el}/T_v = 1/N \quad (7.11)$$

where N is the number of elements per frame.

As already noted, the number of picture elements in existing television systems is very great ($N \approx 5 \times 10^5$). Therefore, the ratio of utilized energy to incident energy in nonstorage systems does not exceed one-five hundred thousandth, which fact impairs the signal-to-noise ratio.

The sensitivity of the transmission system can be enhanced by building up the electric charge liberated by light energy between scans, or during the vertical scan interval. For the first time, the idea of storing the electric energy produced by a phototube on a capacitor was advanced by B. L. Rosing. The utilization of the storage effect in camera tubes was first formulated by Ch. F. Jenkins in 1928. In diagrammatic form, this is illustrated in Fig. 7.4b. As is seen, the added element is a storage capacitor, C . The photocurrent, i_{ph} , flows through and builds up charge across the capacitor throughout the complete vertical (or frame) scan interval, T_v . This charging current is constant:

$$i_c = i_{ph} = eF_{el} \approx \text{const} \quad (7.12)$$

The constancy of the charging current is explained by the properties of a vacuum photocell. Its volt-ampere characteristics, that is, the dependence of photocurrent on applied voltage, are shown in Fig. 7.5. The parameter is the incident luminous flux, F . It is seen from Fig. 7.5 that as the applied voltage is varied from v_{ph1} to v_{ph2} , the photocurrent i_{ph} remains unchanged (the photocell is in the saturated condition), and

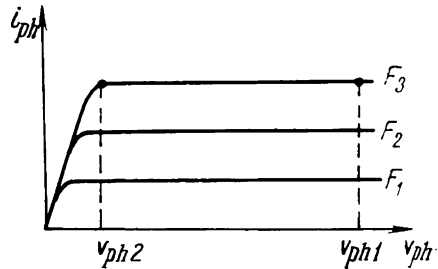


Fig. 7.5. Volt-ampere characteristics of a vacuum photocell

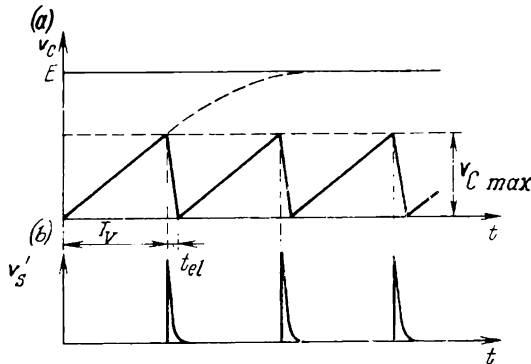


Fig. 7.6. Generation of a signal in a storage system
(a) voltage across storage capacitor; (b) signal across load resistor

the photocell may be likened to a current generator. If we increase the luminous flux, the saturation current will increase, too. In Fig. 7.5, $F_1 < F_2 < F_3$.

As the capacitor builds up charge, the voltage across it rises linearly (Fig. 7.6a) because the voltage across a capacitor is related to

the current flowing through that capacitor by the relation

$$v_C = \frac{1}{C} \int_0 i_{ph} dt$$

and at $i_C = \epsilon F_{el} = \text{constant}$, it is

$$v_C = (\epsilon F_{el}/C) t$$

that is, the voltage across the capacitor is a linear function of time. As is seen from Fig. 7.4*b*, an increase in the voltage across the capacitor, v_C , brings about a decrease in the voltage applied to the photocell, v_{ph} , because $v_{ph} = E - v_C$. As long as v_{ph} exceeds v_{ph2} in the course of charge (Fig. 7.5), the photocurrent remains constant, $i_{ph} = \text{constant}$, and the voltage across the storage capacitor rises linearly. If, in the course of charge, v_{ph} falls below v_{ph2} , any further increase in v_C will be nonlinear, as is shown by the dashed line in Fig. 7.6*a*. Upon closure of the switch Sw at time $t = T_v$ (see Fig. 7.4*b*), the capacitor will rapidly discharge through the load resistor, R_L (because its resistance is substantially smaller than that of the photocell), and a voltage pulse will develop across it, which is the signal voltage, v_s (Fig. 7.6*b*). As the switch opens and closes periodically, a sequence of short pulses develops across the load resistor R_L .

Let us determine the increase in the signal due to the use of the storage effect. The voltage that builds up across the capacitor C over time T_v is given by

$$V_{C_0} = \frac{\epsilon F_{el}}{C} \int_0^{T_v} dt = (\epsilon F_{el}/C) T_v \quad (7.13)$$

The capacitor discharges through the load resistor R_L exponentially,

$$v_C = V_{C_0} \exp(-t/R_L C)$$

(Fig. 7.6*b*), and when the switch Sw is closed this voltage is applied to the resistor R_L . The average signal voltage across the load resistor is

$$V_{av} = \frac{V_{C_0}}{t_{el}} \int_0^{t_{el}} \exp(-t/R_L C) dt \approx (V_{C_0}/t_{el}) R_L C \quad (7.14)$$

In evaluating the integral, Eq. (7.14), it has been assumed that the capacitor C will discharge completely in time t_{el} . Substituting for V_{C_0} in Eq. (7.14) yields

$$V_{av} = \epsilon F_{el} R_L (T_v/t_{el}) \quad (7.15)$$

In a nonstorage system, the signal voltage across the load resistor R_L , according to Eq. (7.8), is

$$V_s = i_{ph} R_L = \epsilon F_{el} R_L \quad (7.16)$$

Dividing V_{av} by V_s , that is, Eq. (7.15) by Eq. (7.16) gives the gain in the signal voltage:

$$V_{av}/V_s = T_v/t_{el} = N \quad (7.17)$$

Thus, the storage effect builds up the signal voltage $N \approx 500,000$ times.

If the storage effect is to be fully utilized, it is necessary to build the photoemissive surface so that it contains N elementary cells, 1, 2,

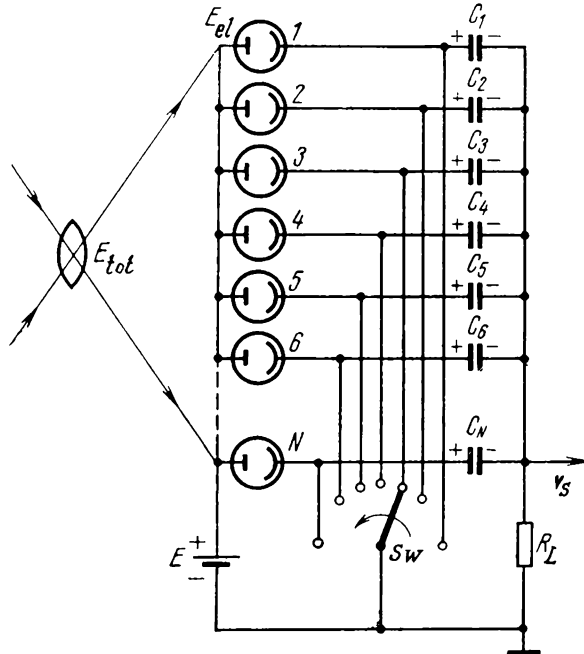


Fig. 7.7. Equivalent circuit of a storage camera tube

3, . . . , N , isolated from one another but combined on a common panel (see Fig. 0.2). An equivalent circuit of such a surface is shown in Fig. 7.7. Each cell is represented by a combination of a separate storage capacitor and a separate photocell. The supply source E and the load resistor R_L are common to all. The charging current flowing through the capacitors $C_1, C_2, C_3, \dots, C_N$ as shown in the figure is determined by the elementary luminous fluxes incident on the respective photocells, $F_{el1}, F_{el2}, F_{el3}, \dots, F_{eln}$. The greater the luminous flux, F_{el} , the faster the capacitors will accumulate charge. During the time T_v the capacitors will accumulate different charges. The storage capacitors will discharge through the load resistor R_L

in turn, according to the sequence in which the commutator switch Sw makes its N contacts. The signal voltage across the load resistor R_L will be a sequence of peaked pulses (Fig. 7.8). In practice, the

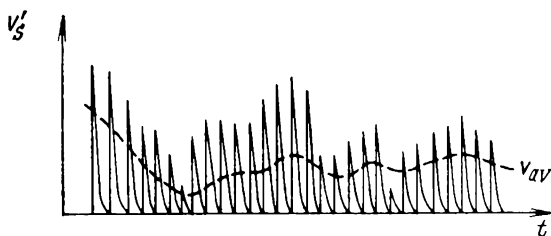


Fig. 7.8. Generation of a video signal in a storage system

signal is smoothed because the amplifier circuit has a limited bandwidth, and the signal takes the form shown by the dashed line in Fig. 7.8. In real camera tubes, the function of a commutator switch is performed by the electron beam.

7.7. Potential of an Insulated Target

In storage camera tubes, an optical image is converted into an electrical signal by means of an electron beam which scans an insulated electrode, the target. The target is a thin plate made from a dielectric or semiconductor material backed by a thin layer of metal from one side. It acts as a storage element in the camera tube.

Studies conducted by S.I. Katayev in 1932 and later by M. Knoll and B. Keisan have shown that the equilibrium potential of an electrode in a vacuum is maintained by secondary electron emission. Secondary electrons can be emitted by both conductors and dielectrics. Basically, secondary electron emission may be summed up as follows:

1. The number of secondary electrons leaving the target is proportional to the number of incident (primary) electrons.
2. The ratio of secondary to primary electrons depends on the velocity of primary electrons and the target material.
3. For the velocities of primary electrons observed in camera tubes, the energy of the bulk of secondary electrons does not exceed a few electron-volts.

For an insight into how the target potential is affected by an incident electron beam, we shall use the set-up shown in Fig. 7.9. The source of primary electrons is a heated cathode which together with the collector (anode) in the form of a cylinder and a metal target is placed in a vacuum. The voltage, V_a , between collector and cathode can be adjusted by a potentiometer, R_1 . The target voltage with

respect to cathode, V_T , can be measured with a voltmeter. Since the voltmeter has a very high internal resistance, the target may be taken as being insulated from any other electrodes and ground. The capacitor, C_T , shown connected across the voltmeter represents the shunt stray capacitance of the target with respect to ground. The set-up shown in the figure has provision for setting the initial potential on

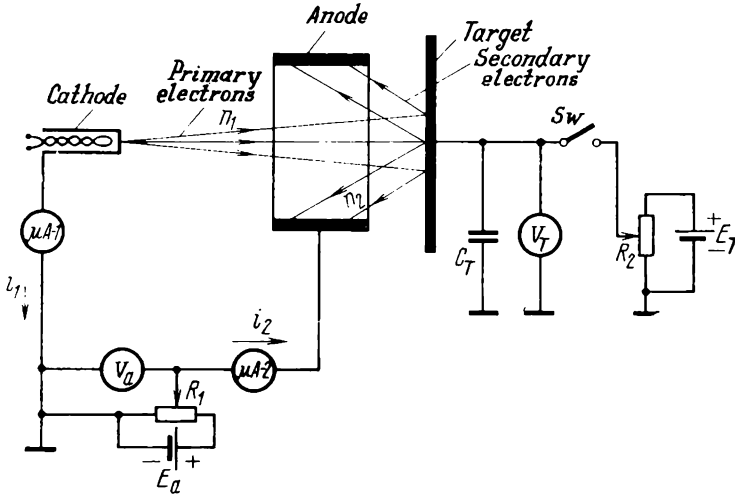


Fig. 7.9. Set-up for investigation of secondary emission

the target. When the switch Sw is closed, the target is set to a potential equal to that at the contact arm of the potentiometer R_2 . After the switch is opened, this potential will be maintained until C_T discharges gradually through the internal resistance of the voltmeter.

The electrons liberated by the thermionic cathode are driven by an accelerating field towards the target and impinge upon it. As will be recalled, the velocity with which the electrons approach the target (neglecting that at which they leave the cathode) is determined by the potential difference between cathode and target. Under primary electron bombardment, the target releases secondary electrons. If the collector is at a higher potential than the target, all of the secondary electrons will be collected. Let n_1 designate the number of primary electrons liberated by the thermionic cathode during unit of time, and n_2 the number of secondary electrons leaving the target in the same time interval. The ratio of the two numbers

$$\sigma = n_2/n_1 \quad (7.18)$$

is called the secondary emission ratio.

The currents, i_1 and i_2 , in the cathode and collector circuits, as measured by the microammeters $\mu A1$ and $\mu A2$ (Fig. 7.9), are proportional to n_1 and n_2 , respectively. Obviously, the secondary emission ratio can be determined experimentally as the ratio

$$\sigma = i_2/i_1 \quad (7.18a)$$

The experimental set-up of Fig. 7.9 can also be used to determine the dependence of the secondary emission ratio on the energy of primary electrons. This can be done by closing the switch Sw , varying the voltage V_T with the potentiometer R_2 , and measuring

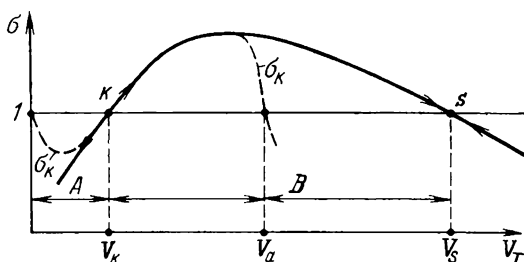


Fig. 7.10. Secondary emission ratio as a function of target voltage

the currents in the cathode and collector circuits, i_1 and i_2 . So that the anode can collect all of the secondaries, an accelerating field must be set up between collector and target. To this end, the collector potential V_C is adjusted to a value above the maximum likely target potential, V_T . The experimental dependence of the secondary emission ratio σ , on cathode-to-target voltage, V_T , is shown in the plot of Fig. 7.10. As is seen, when the accelerating voltage is low, $\sigma < 1$. This is because the energy of the primary electrons is too low to bring about secondary emission. If V_T is close to zero, the primaries are intercepted by the collector, while at $V_T = 0$ the cathode current has its path completely through the collector which is at a high positive potential. In this case, although there is no secondary emission, the microammeters will give the same reading, that is, $i_1 = i_2$, and we might conclude that the secondary emission factor is unity. Let the secondary emission ratio measured under these conditions be called the apparent ratio and designated as σ_k . In Fig. 7.10 the relation $\sigma_k = f(V_T)$ is shown by the dashed line.

As the accelerating voltage is raised, the primary electrons gain kinetic energy, so that all of them reach the target and the secondary emission ratio exceeds unity. Point K corresponds to $\sigma = 1$. On passing through the peak, the curve rolls off quietly until σ is again equal to unity at point S . The points K and S and the respective voltages, V_K and V_S , are called critical.

Now we shall see how an isolated target assumes its potential. This condition can be simulated in the set-up of Fig. 7.9 by opening the switch Sw . We shall conduct several experiments as follows.

1. Close the switch Sw for some time and set the wiper on the potentiometer R_2 so that the voltmeter reads $V_{T, init} < V_K$. The entire surface of the target will assume the same potential, $V_{T, init}$. Now open the switch. Owing to the charge on the capacitor C_T the target will maintain the initial potential for some time. Because the accelerating voltage, $V_{T, init}$, is lower than V_K , then, according to Fig. 7.10, $\sigma < 1$. In other words, the number of primaries, n_1 , reaching the target per unit time exceeds the number of secondaries, n_2 , leaving the target. Since the charge on an electron is negative, the target potential decreases. This decrease in the target potential, registered by the instrument, will continue until the accelerating voltage, V_T , falls to zero, and $\sigma_k = 1$. At $\sigma_k = 1$, all primary electrons are intercepted by the collector, so that $i_1 = i_2$, and the target potential remains unchanged and equal to the cathode potential.

In the foregoing, we have assumed that the electrons leaving the cathode have zero initial velocity. Actually, some electrons have an energy sufficient to reach the target surface. As a rule these electrons bring down the steady-state (equilibrium) potential on the target relative to the cathode by 1 to 3 V. This condition in which the target potential falls to that of the cathode is called the low-velocity beam operation. In the plot of Fig. 7.10 the region corresponding to this form of operation is labelled A.

2. Now assume that the initial target potential, $V_{T, init}$, is greater than V_K but lower than V_S . Then $\sigma > 1$, that is, the number of secondary electrons released by the target will exceed the number of primaries. The direction in which the target potential will change under the bombardment by primary electrons in the circumstances depends on the collector potential, V_C . Two cases are of interest: $V_C > V_{T, init}$ and $V_C < V_{T, init}$. When $V_C > V_{T, init}$, an accelerating field exists between the target and the collector, and secondary electrons are driven towards the collector. Since $V_C > V_{T, init}$, the target potential gradually rises until it becomes equal to the collector potential. When $V_T = V_C$, the accelerating electric field ceases, and a negative space charge forms near the target which forces most secondaries to travel back to the target. Only a fraction of secondaries having a sufficient energy are able to reach the collector. Upon reaching the value equal to V_C , the target potential will not change any longer. This is an indication that $i_1 = i_2$ and $\sigma_k = 1$. Gradual decrease in σ_k as $V_T \rightarrow V_C$ is shown by the dashed line in Fig. 7.10. When $V_C < V_{T, init}$, that is when the target is at a positive potential with respect to the collector, a decelerating electric field exists between the target and collector, and

all secondaries are returned to the target. The continual arrival of primaries brings down the target potential until it equals the collector potential, that is, until $V_T = V_C$.

This condition is called the high-velocity beam operation. The region corresponding to this condition is labelled *B* in Fig. 7.10. Within the high-velocity-beam region, the initial target potential, $V_{T, init}$, adjusted arbitrarily in the range $V_K < V_{T, init} < V_S$, is forced by the electron beam towards V_C . Here, as in region *A*, the initial velocity of secondary electrons is important, and because of this the equilibrium target potential exceeds the collector potential by 1 to 3 V.

3. In the last experiment, we choose V_C to be higher than V_S , and the initial target potential is adjusted with the aid of the switch Sw and the potentiometer R_p to be higher than V_K . In the circumstances, the electron beam will force the target potential to rise. However, an equilibrium will be reached only when the equality $V_T = V_S$ is satisfied. As a proof, assume that the cathode-to-target voltage has exceeded V_S . Then, as follows from Fig. 7.10, $\sigma < 1$, and the target potential begins to decrease. Thus, the point *S* represents a stable equilibrium. When $V_C > V_S$, any departure of the target potential from V_S is automatically made up for by secondary electron emission. This is shown in Fig. 7.10 by the arrows converging towards the point *S* from two sides. Conversely, the point *K* represents an unsteady equilibrium. Should the target potential exceed V_K , it will keep rising until it reaches the collector potential. In Fig. 7.10 this condition is illustrated by the arrows going away from point *K* in opposite directions.

In the above experiment, we had to pre-set the initial potential on the target with a switch, Sw . In practical camera tubes, the target bombarded by primary electrons is fabricated from a dielectric, and no switch can be provided to set an initial potential on this surface. Nor is this necessary. The manner in which the target comes up to its initial potential can be traced by reference to the above mentioned picture tube in which the phosphor screen is in fact an insulated target (if it has no aluminium backing). When H.V. is applied to the anode, the screen becomes luminous, and this is an indication that the potential on its surface has exceeded the critical value, V_K . How does the potential of the insulated target (screen) in a camera tube exceed this critical value? The point is that when H.V. is applied to the anode, all of the surface of the glass envelope, except some regions adjacent to the anode may be at zero potential. Due to surface leakage (because glass is no perfect dielectric), these areas assume a positive potential. As the electric field causes the electron beam to bend towards the anode, electrons strike these areas, and where the potential is above V_K , the secondary emission ratio exceeds unity, that is, $\sigma > 1$. As the surface charge builds up

due to the secondary electrons leaving for the anode, the surface potential rises, and so does the potential on adjacent areas. In this way, a charge wave is formed, travelling over the surface of the glass envelope. Some time later, the potential on the inner surface of the glass envelope and on the screen becomes equal to V_C . About the same events take place in camera tubes utilizing the high-velocity beam operation.

7.8. Iconoscope

The first camera tube utilizing the storage principle was that proposed by S.I. Katayev of the Soviet Union in 1931. Somewhat later, a similar tube was developed by V.K. Zworykin of the United States. Named the iconoscope by the inventor, it was first made in 1933. The advent of image-storage tubes gave big impetus to the further progress of television.

The construction and general appearance of the iconoscope are shown in Fig. 7.11. An image of the scene is formed by a lens, 1, on a photosensitive storage element or target consisting of a thin mica sheet, 2, on which discrete particles (globules) of photoemissive silver, 3, are deposited to form a mosaic on the left-hand side (in the diagram), and there is a continuous metal deposit, called the signal plate, 4, on the right-hand side. The mosaic target is mounted inside a glass bulb, 5, to the inner surface of which is deposited a metal layer, 6, acting as collector or anode. It collects secondary electrons and photoelectrons liberated by the mosaic. The electron beam that scans the mosaic is produced by an electron gun consisting of a thermionic cathode, 7, a modulator, 8, and a focusing electrode, 9, all built into the narrow neck of the tube at an angle of about 60° to the mosaic surface. The beam is deflected by the magnetic field of a deflection system, or yoke, 10.

In examining the principle of image storage, we noted that its application requires isolated photocells, storage capacitors and a switch. In the iconoscope the function of the switch is performed by the scanning beam incident on the mosaic at an angle, and that of storage capacitors by the capacitance between each photoemissive globule and the signal plate. In the equivalent circuit of Fig. 7.12, the mosaic target is shown greatly enlarged. The plates of the storage capacitors C are the electrically insulated mosaic globules, 1, and the metal signal plate, 2.

In Fig. 7.7, the right-hand plates of the storage capacitors are connected by a common wire; in Fig. 7.12 they are replaced by the continuous signal plate, applied to a thin mica plate, 3. At the same time, as already noted, the mosaic globules act as elementary photocells insulated from one another.

To simplify the examination of the physical processes taking place in the iconoscope, we assume that initially the lens is closed (see

Fig. 7.11(a) and that the beam scans the non-illuminated mosaic. Because no light strikes the mosaic surface, no photoelectrons are

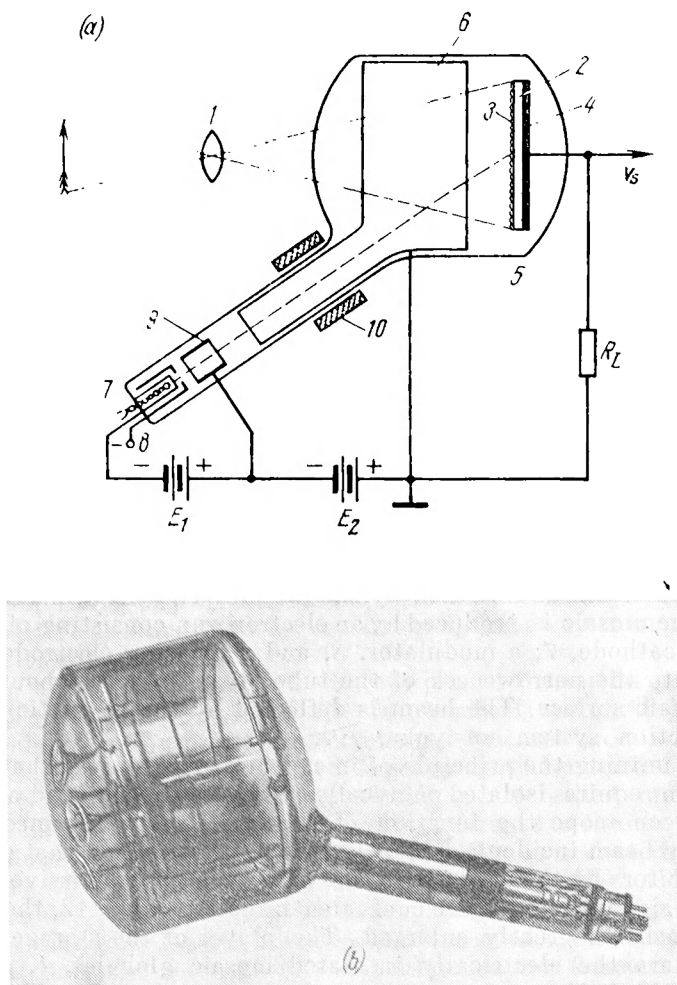


Fig. 7.11. Iconoscope
(a) internal arrangement; (b) external appearance

liberated, and everything that occurs can only be attributed to secondary electron emission. As the electron beam giving rise to a current i_1 scans the mosaic elements, it causes secondary electrons to be liberated in amounts such that the secondary emission ratio is

$\sigma \approx 5$. We have already learned that the scanning beam can be operated in two modes: low-velocity and high-velocity. The iconoscope uses a high-velocity beam, because the voltage acting between cathode and anode, equal to $E_1 + E_2$ (see Fig. 7.11) is about 1000 V. In the high-velocity beam operation, the target potential is equal to the anode potential. In the circumstances, not all secondary electrons

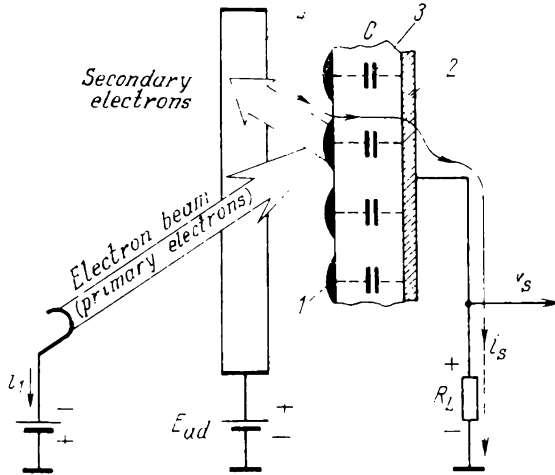


Fig. 7.12. Generation of a signal in an iconoscope

leave the mosaic. Depending on the initial velocity, some of the ejected electrons return to the scanned mosaic element and some fall on adjacent elements. The greater proportion of secondary electrons having a sufficient initial velocity are capable, however, of reaching the collector. These electrons give rise to a current, i_s . Owing to this current, the mosaic potential may be a few volts above that of the collector. Measurements have shown that in the iconoscope the potential at the scanned mosaic element is 3 V above the collector potential. Because the collector is grounded, the mosaic target is at a potential of +3 V. This potential is known as the upper equilibrium potential.

After the scanning beam leaves a mosaic element, the potential of that element rapidly decreases because its surface collects the secondary electrons which are liberated as adjacent mosaic elements are scanned and which do not have a sufficient energy to overcome the retarding field existing between the anode and the mosaic. The stream of scattered electrons is considerably weaker than the stream of electrons leaving the mosaic element being scanned, but it exists for a time interval (equal to the frame scanning interval) markedly

longer than that during which a mosaic element is scanned. This is why the potential on a mosaic element between two scans drops to a negative value. This value is known as the lower equilibrium potential.

Measurements have shown the lower equilibrium potential to be -1 to -1.5 V.

Thus, as the electron beam scans the mosaic, the charge on the mosaic surface is re-distributed, and the mosaic potential rises from the lower equilibrium value of -1.5 V to the upper equilibrium value of $+3$ V.

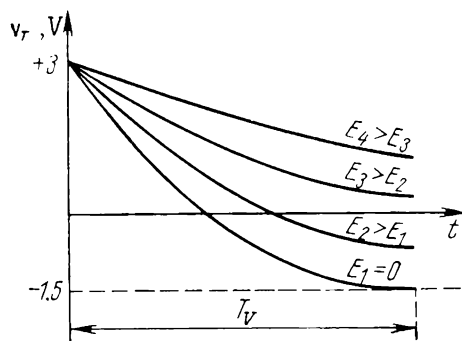


Fig. 7.13. Variations in mosaic-element voltage between scans

When the lens is open, an optical image is thrown onto the mosaic, and photoelectrons are now liberated. Like secondary electrons, these photoelectrons have a low velocity. In the absence of an accelerating field, only some of them can reach the anode, while the others fall back on the mosaic. The continuous emission of photoelectrons from the mosaic changes the lower equilibrium potential. The

manner in which the mosaic elements assume the lower equilibrium potential after the beam moves on for different values of illumination, E , is illustrated in the plot of Fig. 7.13. When no light falls on the mosaic, $E_1 = 0$, and during the vertical (frame) scanning interval T_v the mosaic potential, V_T , falls from $+3$ V to -1.5 V. When $E_2 > E_1$, photoelectrons cause the mosaic potential to vary at a slower rate, so that it fails to reach the lower equilibrium value during the interval T_v . At sufficiently high values of illumination, the potential on the mosaic elements will fall by the next scan, but it will remain positive. Thus, between consecutive scans the individual mosaic elements assume different potentials which are proportional to the luminance of the elements of the scene. The higher the luminance of a scene element, the higher the potential on the respective mosaic element. In this way, a charge image is produced on the mosaic, corresponding to the picture being televised.

The manner in which the mosaic potential is distributed along a line is shown in Fig. 7.14. The scanning beam is at point x_1 . At this point, the potential is equal to the upper equilibrium value. As the beam moves along the line, the charge image is evened out (neutralized). The potentials on the mosaic elements to the left of

point x_1 gradually fall after the beam leaves them, due to the capture of scattered electrons. It is seen from Fig. 7.14 that the change in potential occurring as the beam scans an illuminated mosaic element, ΔV_1 , is smaller than when the beam scans an unilluminated element, ΔV_2 . Now let us see how a video signal is formed in the iconoscope. For this purpose, we shall refer to Fig. 7.12. The electron beam gives rise to secondary electron emission from the surface of the mosaic element being scanned. The secondary electrons reach the collector and complete the path containing a series combination of storage capacitors C and load resistor R_L . The signal current, i_s , traversing the load resistor, R_L , flows in the direction shown by the arrow in Fig. 7.12. As follows from Fig. 7.14, when the beam scans highly

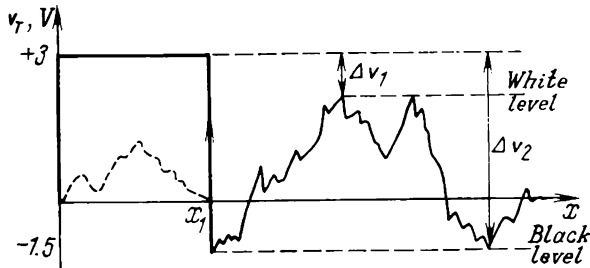


Fig. 7.14. Potential distribution along a line during scan

illuminated mosaic elements the change of potential, ΔV_1 , is relatively small, but this change is considerable, ΔV_2 , when the beam scans unilluminated elements. The rise in potential on the left-hand plates of the elementary capacitors due to current i_2 , that is, the build-up of charge on the elementary capacitors, occurs during the time interval required to scan one mosaic element. During the same time interval, the capacitors having the same capacitance receive a different charge and, as a consequence, they give rise to different signal currents. As a result, black areas in the picture being televised give rise to a greater current, and white areas to a smaller current.

The signal current flowing through R_L produces a voltage drop such that the top terminal of the resistor is positive relative to ground (see Fig. 7.12). Yet, the video signal at the tube output is in negative polarity. This is because in television practice a signal is taken to be positive if white picture areas produce a higher potential and black areas a lower potential. In the iconoscope white elements produce a lower current than black areas do; therefore, a lower potential corresponds to white and a higher potential to black.

The light transfer (signal current-versus-mosaic illumination) characteristic of the iconoscope is shown in Fig. 7.15a as an i_s -vs-

E curve. At low levels of illumination this characteristic is a straight line. As the illumination increases, the signal current rises insignificantly. On the average, with an accuracy sufficient for practical purposes, the i_s -vs- E characteristic of the iconoscope may be approximated with a parabola, $i_s = kE^\gamma$, where k is a proportionality factor, and $\gamma = 0.5$ is the exponent describing the nonlinearity of the characteristic.

The mosaic illumination required to produce a sufficiently strong signal is about 40 luxes. The illumination of the scene being televised must be much higher. Even with an $f/3.5$ lens the illumination

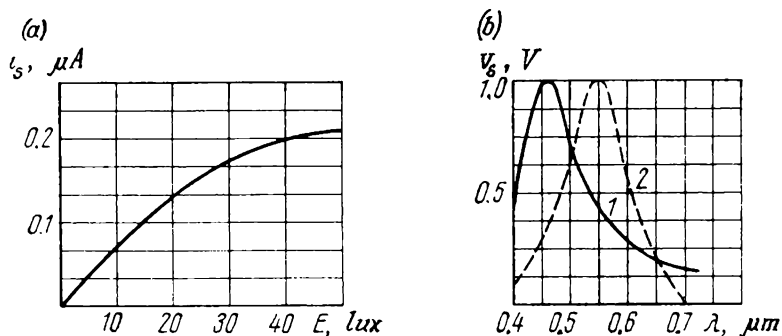


Fig. 7.15. (a) Light-transfer characteristic and (b) spectral response characteristic

1—signal voltage; 2—relative visibility curve

of the scene must be about 5000 luxes. Since, however, in practice the lens has to be "stopped down" in order to secure a sufficient depth of focus, the illumination of the scene must be up to 10,000 luxes.

The low sensitivity of the iconoscope camera may be attributed to several factors. Firstly, for constructional reasons, a considerable distance has to be left between the bulb faceplate and the mosaic target, and the lens cannot be placed close enough to the latter. As a result, lenses of short focal length, which have a large numerical aperture, cannot be used. Secondly, the mosaic in the iconoscope is fairly large in size, and this requires that the optical image be of a comparable size. It is a well-established fact that in order to reproduce a large image with sufficient sharpness of focus, the lens must be heavily "stopped down", and this cuts down the amount of light admitted. Thirdly, the iconoscope itself has a very low sensitivity. The storage principle is utilized in the iconoscope to the extent of only 5%. This is because there is an insufficient supply of photoelectrons from the mosaic surface in the absence of an accelerating field between the mosaic and collector. The efficiency of storage is

therefore low, and the charge image is shallow. This is a fundamental limitation traceable to the use of a high-velocity beam in the iconoscope. As was noted in the previous section, in the high-velocity beam operation the target potential "follows" the collector potential, and no electric field can be set up to collect electrons from the mosaic surface. If an additional source were placed in the collector circuit, as shown by the dashed line in Fig. 7.12, the mosaic potential would automatically increase by E , and the accelerating field thus produced would disappear soon.

The spectral response curve of the iconoscope is shown in Fig. 7.15*b*. For comparison, this figure also shows the relative luminosity curve, $v(\lambda)$, of the human eye. As is seen, the peak spectral response of the iconoscope occurs in the short-wavelength region; that is, in comparison with the human eye the iconoscope is more sensitive to blue light. Because of this, there is a degree of distortion in tone rendition. It is also to be noted that because of redistribution of photoelectrons on the mosaic surface the form of the spectral response varies with the content of the scene being televised.

An outstanding achievement in its time, the iconoscope has largely dropped out of use today because of unsurmountable limitations. We have already mentioned its low sensitivity. A few remarks are in order about its other disadvantages.

To begin with, there is the shading effect caused by the random distribution of secondary electrons over the mosaic surface. Partly, this happens because the distance from the central area of the mosaic to the collector is considerably longer than it is from the periphery. It should also be noted that the electric field near the mosaic is anything but uniform due to variations in the space charge. The space charge density is a maximum in the central part of the mosaic and also in the areas corresponding to the start of the raster. As a result, the video signal at the tube output is distorted, and the image reproduced on the viewing screen appears as if the original scene is illuminated unevenly. The shading effect is so strong that the need arises to compensate for it.

The shading effect is compensated in the amplifier circuit of the TV centre by injecting a suitable correction signal from a shading signal generator into the video signal. This generator produces sawtooth, parabolic and sinusoidal signals at line and frame scanning frequency. By combining them in an appropriate proportion, a compensating signal of the desired pattern is obtained. Unfortunately, this method does not do away with the shading effect completely, because the correction patterns have to be varied as the scene content varies, which the shading-control operator cannot always do in time.

A further limitation of the iconoscope is the keystone distortion of the raster, arising because the electron beam strikes the mosaic

at an angle. As is seen from Fig. 7.16a, the distance l_1 from the top of the mosaic to the deflection centre O is longer than the distance l_2 from the deflection centre to the bottom of the mosaic. Since the horizontal deflection angle is the same, the top line in the raster appears much longer than the bottom line. Keystone distortion is usually corrected by varying the deflection angle in the horizontal

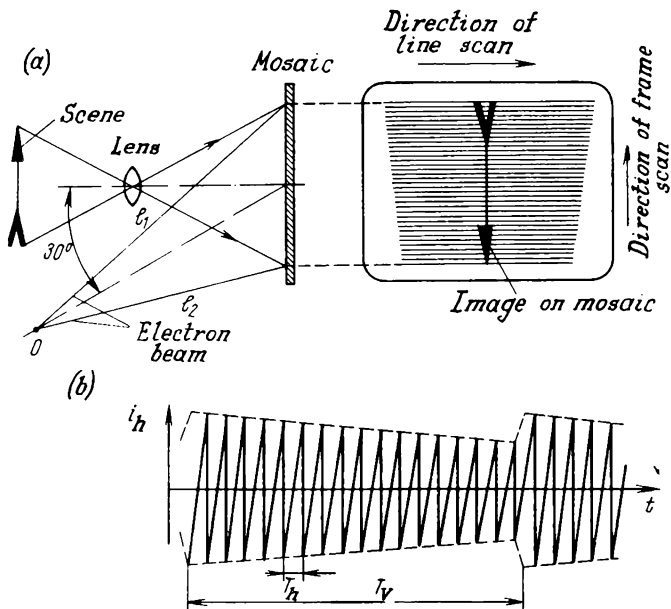


Fig. 7.16. Keystone distortion in the iconoscope
(a) origin of distortion; (b) distortion compensation

direction. The horizontal deflection angle is a minimum when the beam scans the top lines of the raster. As the beam moves downwards, the deflection angle is increased. The deflection angle is varied by modulating the current in the horizontal yoke, as is shown in Fig. 7.16b. The envelope of the modulated signal has the shape of a sawtooth and a frequency equal to the frame scan frequency. It should be stressed that the swing of the sawtooth current decreases with time, as follows from Fig. 7.16b, rather than increases, as might be concluded from Fig. 7.16a. The point is that in camera tubes frame scan proceeds from bottom upwards and not the other way around as in picture tubes, because the lens forms an inverted optical image on the mosaic (see Fig. 7.16a).

7.9. Image Iconoscope

The image iconoscope, also a camera pick-up tube,[†] was proposed by P.V. Shmakov and P.V. Timofeyev of the Soviet Union in 1933.

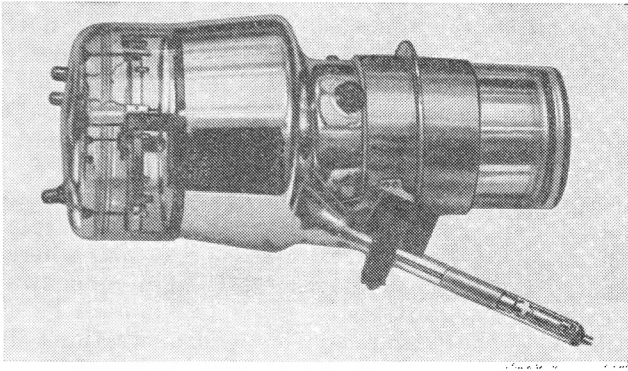


Fig. 7.17. Image iconoscope

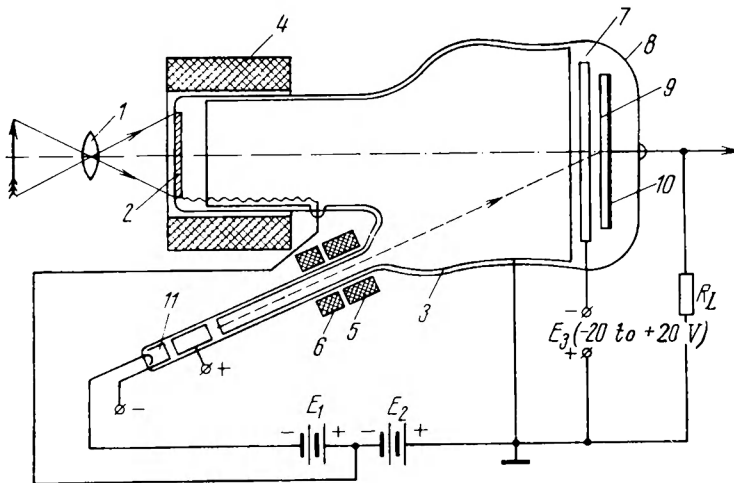


Fig. 7.18. Internal arrangement of the image iconoscope
1—lens; 2—photocathode; 3—collector; 4—image coil; 5—deflection yoke; 6—focuser; 7—intermediate electrode; 8—envelope; 9—target; 10—signal plate; 11—electron gun

It differs from the iconoscope in having a separate image section. The general appearance and construction of the tube are illustrated in Figs. 7.17 and 7.18.

An image of the scene being televised is formed by a lens, 1, on a transparent continuous photocathode, 2. In the Sovite-made ЛИ-7 image iconoscope, most commonly used of all types, an antimony-caesium photocathode is used. The translucent backing of the photocathode is held at a negative potential, $-E_2$, relative to the collector, 3. The accelerating potential difference between photocathode and collector causes the liberated photoelectrons to move towards the target, and the current due to photoelectrons reaches saturation, owing to which incident light is utilized more efficiently. The image section has an image focusing coil, 4, which produces a magnetic field. The magnetic field and the accelerating electric field focus the photoelectrons in the plane of the target.

The image focusing coil is considerably shorter than the tube. However, it operates on an entirely different principle than the short focusing coil in the picture tube (see Sec. 2.4) where the electron beam is focused by both the magnetic field concentrated inside the coil and by the edge fields. A short coil cannot be used in the image section as it would cause considerable aberrations. The picture tube has to do with the transfer of an image of the crossover to the viewing screen (see Sec. 2.3). The crossover diameter is by a factor of several hundred smaller than the neck diameter, and the beam is mainly focused by the magnetic field concentrated near the tube axis. In the image iconoscope, the electron emission pattern is transferred from the photocathode whose diameter is more than one-third of the bulb diameter, and aberrations are therefore more pronounced.

The image focusing coil of the image iconoscope introduces no distortion in the electron emission pattern and is in effect an immersion magnetic lens. As is seen from Fig. 7.19, the photocathode, 1, is immersed in the magnetic field of the coil where the field intensity is a maximum. The lines of force in the magnetic field due to coil 2 are practically orthogonal to the photocathode. An electron emitted from, say, point *a* on the photocathode at right angles to its surface is acted upon by the electric field in which the lines of force are parallel with the *z*-axis, while the magnetic field inside the coil has no effect on its trajectory. As the electron approaches the edge of the coil, however, the effect of the magnetic field increases. Consider the motion of an electron in the edge area. If the magnetic lines of force are directed as shown in the figure, the interaction of an electron travelling at velocity \bar{u}_z with the radial component of field intensity, \bar{H}_r , will give rise to a force directed beyond and at right angles to the plane of the drawing. In turn, this force will give rise to an angular (rotational) velocity \bar{u}_θ . On its part, the vector product of the rotational velocity \bar{u}_θ by the longitudinal component of field intensity, \bar{H}_z , will give rise to a force, \bar{F}_r , tending to pull the electron away from the *z*-axis. As a result, the tra-

jectory of an electron in the edge area is bent away from the axis. The electron emitted from point a on the photocathode will arrive at point a' on the target, 4, lying farther away from the z -axis than the point a . The line $a'b'$ and the whole electron image 5, will be turned through an angle α relative to the original optical image, 6, on the photocathode.

The trajectories aa' and bb' , that is, the trajectories of electrons emitted parallel with the z -axis, are the principal trajectories. Electrons emitted from the photocathode at various angles to the z -axis

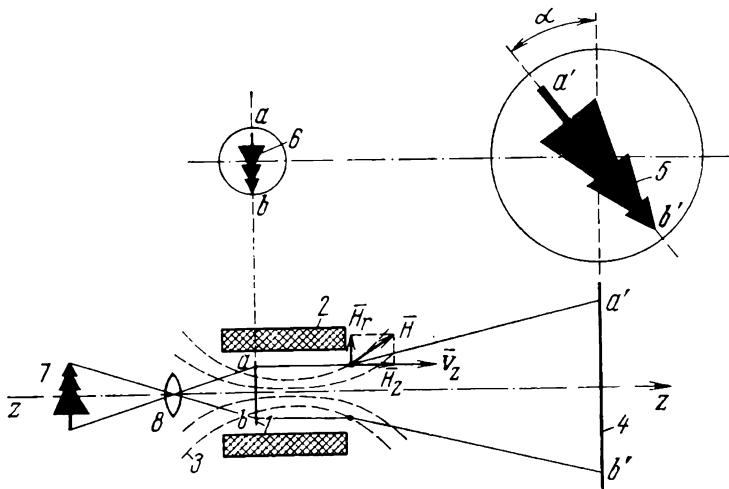


Fig. 7.19. Operating principle of the image focusing coil

1—photocathode; 2—coil; 3—magnetic lines of force; 4—target; 5—electron image on the target; 6—optical image on the photocathode; 7—scene being televised; 8—objective lens

are caused to travel in a spiral around the principal trajectories. If the magnetic field is sufficiently strong, these electrons will again be collected at one point on the principal trajectory in the target plane. In this way, the immersion magnetic lens in the image section spreads the trajectories of electrons emitted from different points on the photocathode but focuses the elementary beams originating at each point on the photocathode.

The photoelectrons approaching the target have a high kinetic energy because the accelerating voltage, E_2 , acting between photocathode and anode, is usually 800 V.

In contrast to the mosaic target of the iconoscope, the target (or storage plate) of the image iconoscope (at 9 in Fig. 7.18) is insensitive to light. It is made from a thin mica sheet onto the right-hand side (in the diagram) of which a metal layer (the signal plate) is deposited. The signal plate is connected to an external terminal and the

load resistor R_L . The left-hand side of the storage plate is suitably treated (for example, it may be given a deposit of AgCs film) to be a good secondary emitter under electron bombardment. The electron image pattern, as it is focused on the target, causes secondary electrons to be emitted from the surface and produces a positive charge image corresponding to the illumination of the photocathode. Because photoelectrons have a high energy and the secondary emission ratio is $\sigma \approx 5$, image transfer is accompanied by signal amplification. Since there is no accelerating field, not all secondary electrons are able to leave the target. Like the iconoscope, the image iconoscope suffers from a random re-distribution of electrons over the target surface, which produces spurious shading signals. The incomplete collection of secondary electrons does not make it possible to fully utilize the signal amplification provided by secondary emission.

The integral light sensitivity of a continuous photocathode is two or three times as great as that of a mosaic. This is why the image iconoscope can produce a sufficiently strong video signal with a photocathode illumination of as low as 25 or 30 luxes, which is about half as great as is necessary for the iconoscope mosaic. The image iconoscope camera can use high-speed short-focus lenses because the photocathode is applied to the bulb faceplate. As a result, the TV camera sensitivity is greatly enhanced and a good depth of field can be obtained with a scene illumination of 2500 to 3500 luxes.

The charge image stored on the target is scanned by the scanning electron beam and video information is obtained from the signal plate by capacitive coupling, in the same manner as in the iconoscope. The scanning beam strikes the target surface at an angle of 30° , which fact causes keystone distortion. The scanning beam is focused and deflected by a magnetic field. The cathode potential relative to the collector is $E_1 + E_2 = -1200$ V. A correcting frame, 10° , is placed next to the target, which serves to improve the collection of electrons from the target surface and to minimize the spurious shading. The optimum voltage, E_3 , for this frame is usually found by trial and error and ranges between $+20$ and -20 V.

7.10. Camera Tubes Using a Low-Velocity Beam

Basically, the limitations of the iconoscope and image iconoscope are due to the use of a high-velocity beam striking the target surface at an angle. The beam incident at an angle produces keystone distortion, while the high-velocity beam (in the absence of an accelerating field between target and collector) causes unwanted shading effects. The absence of an accelerating field also stands in the way of fully utilizing the charge storage efficiently. In explaining the charge storage principle by reference to a model (see Fig. 7.7) we

assumed that the source E enabled all electrons to be collected from the photocathodes of the elementary photocells (the condition of saturation), and that the switch connecting the load resistor in turn to each of the elementary storage capacitors was an ideal switch.

However, the exploring beam in the iconoscope and image iconoscope is not an ideal switch. Because of the high velocity of electrons, the scanning process is accompanied by the emission of a great number of secondary electrons; as a consequence, the target potential becomes equal to that of the collector, the accelerating field disappears, and the electrons are randomly re-distributed over the target surface, thereby producing the undesirable shading.

These disadvantages could be avoided by use of a low-velocity beam, that is, by use of low-velocity scanning (labelled A in the model diagram). Then, as follows from Sec. 7.7, the target would assume a potential equal to that of the cathode. Since cathode potential is below anode potential, an accelerating electric field would be set up between anode and target in low-velocity scanning, and the collection of secondary electrons by the collector would be more effective. Unfortunately, low-velocity scanning cannot be used in the iconoscope and the image iconoscope for several reasons. Firstly, the scanning efficiency of a low-velocity beam materially depends on the angle of incidence — variations in the angle of incidence in the course of scan would cause the output signal to change considerably. Secondly, in travelling from the centre of the focusing coil to the target (which takes a markedly longer time due to the low velocity of electrons) the beam would be defocused — since all electrons are negatively charged, they would repel one another, thereby causing the beam to spread. Yet, low-velocity scanning is utilized in camera tubes specifically designed for this purpose. These tubes use two-sided targets on which a charge pattern is stored on one side and scanned on the other side. Owing to a two-sided target, the camera tube is a symmetrical cylinder in which the electron gun is arranged along the tube axis. Another feature of this type of camera tube is the use of a special deflecting and focusing system efficiently focusing the scanning beam and causing electrons to fall on the target surface at right angles at all points. The basis of this system is a long focusing coil producing a uniform magnetic field between cathode and target. In camera tubes, the long focusing coil does two jobs: it transfers the electron emission pattern and focuses the low-velocity beam. Consider how the image focusing coil operates in transferring the electron emission pattern by reference to Fig. 7.20*a*, which shows a glass cylinder, 1 , with a translucent photocathode, 2 , deposited on one end, and a phosphor, 3 , on the opposite end. The inner surface of the phosphor is given a thin coat of metal, 4 , through which the photoelectrons liberated by the photocathode can readily pass under the action of an accelerating voltage.

The cylinder is placed inside a long focusing coil, 5, which sets up a magnetic field, H , within the envelope, so that the magnetic lines of force are arranged parallel to the zz' axis of the tube. An optical

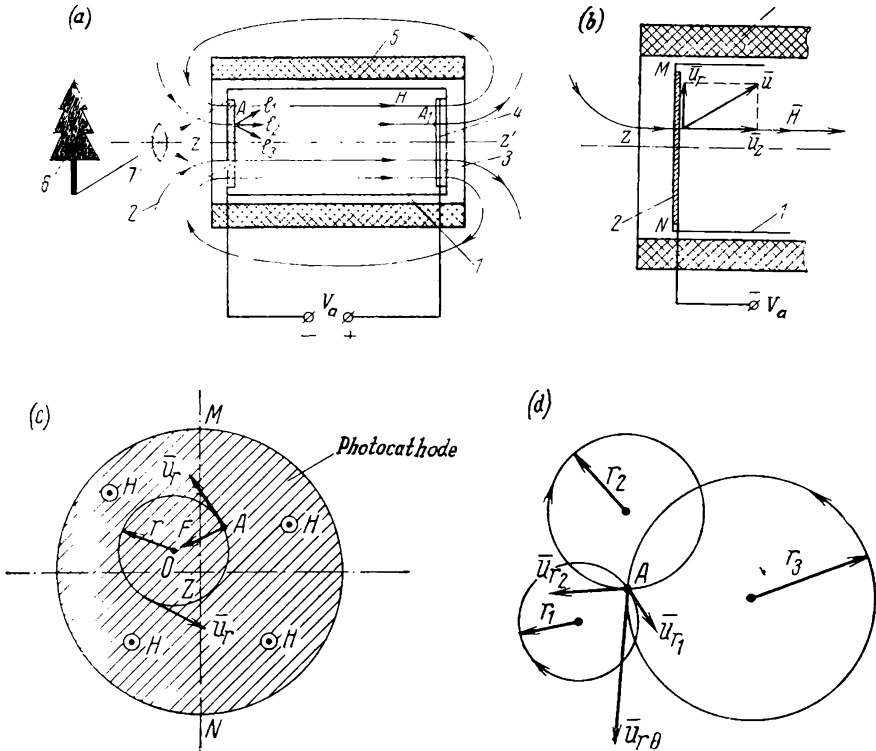


Fig. 7.20. Long focusing coil

- a) construction; (b) resolution of velocity vector \vec{u} into longitudinal component \vec{u}_z and transverse component \vec{u}_r ; (c) electron paths in a plane parallel to the plane of the photocathode; (d) effect of initial velocity \vec{u} on the radii of circles described by electrons

image of the scene, 6, is formed by a lens, 7, on the photocathode.

In image-transfer camera tubes, the phosphor screen is replaced by a storage plate, or target. A layer of phosphor is often applied instead of a target in experimental tubes in order to evaluate visually the quality of focusing and to align the scanning systems. Also, the device in question is not unlike an electron-optical image intensifier which converts a faint, sometimes invisible image to a bright visible one. If the photocathode be made of a material sensitive to the invisible infra-red or ultra-violet light, the device can convert an invisible to visible image.

The photoelectrons liberated at different points on the photocathode in amounts proportional to the illumination at each point are driven by an accelerator potential V_a to a velocity sufficient for them to pass through the metal plate, 4, and excite the phosphor 3. As a result, the phosphor screen presents an image having greater contrast and brightness than that on the photocathode.

The purpose of the focusing coil, 5, is to cause all electrons emitted from any point, A , on the photocathode to converge to a single point, A_1 , on the phosphor. In the absence of such focusing, the electrons, e_1, e_2, e_3, \dots , emitted from point A at different angles would reach the phosphor at different points.

To simplify the explanation, we resolve the initial velocity vector \bar{u} of a photoelectron into two components, longitudinal, \bar{u}_z , and transverse, \bar{u}_r (Fig. 7.20b).

The velocity component \bar{u}_z does not interact with the field intensity \bar{H} because the angle between the two vectors is zero. On the other hand, the angle between \bar{u}_r and \bar{H} is 90° , and Lorentz' force is given by

$$F = eu_r H \quad (7.19)$$

Applying the left-hand rule, we can readily prove that the vector \bar{F} lies in the plane passing through the photocathode (that is, in the plane of the left-hand faceplate of the bulb). For further examination we turn the bulb so that the plane of the photocathode is in the plane of the drawing (Fig. 7.20c). From the elementary theory of electromagnetism it is known that an electron residing in a uniform magnetic field H and having an initial velocity u_r the vector of which is contained in a plane perpendicular to the vector \bar{H} will be caused by Lorentz' force \bar{F} to describe a circle of constant radius r , while the vector \bar{u}_r will remain unchanged in magnitude and will only change in direction so that at any point on this circle \bar{u}_r will be tangent to the circle. The radius of the circle is

$$r = mu_r / eH \quad (7.20)$$

and the time of one revolution is

$$T = 2\pi m / eH \quad (7.21)$$

where m and e are the mass and charge of an electron.

The electrons e_1, e_2, e_3, \dots , emitted from any point A on the photocathode surface (Fig. 7.20d) have in the photocathode plane the radial velocity vectors $\bar{u}_{r1}, \bar{u}_{r2}, \bar{u}_{r3}, \dots$, which differ in both magnitude and direction. The radii r_1, r_2, r_3, \dots , of the circular paths described by these electrons are likewise different and, according to Eq. (7.20) proportional to the velocity u_r . On the other hand, according to Eq. (7.21), the time per revolution, T , is independent

of u_r ; that is, electrons simultaneously emitted from point A will converge to point A_1 along their respective circular paths also all *at the same time*.

Apart from the circular motion described above, the photoelectrons are caused by the velocity u_z to be in a longitudinal motion.

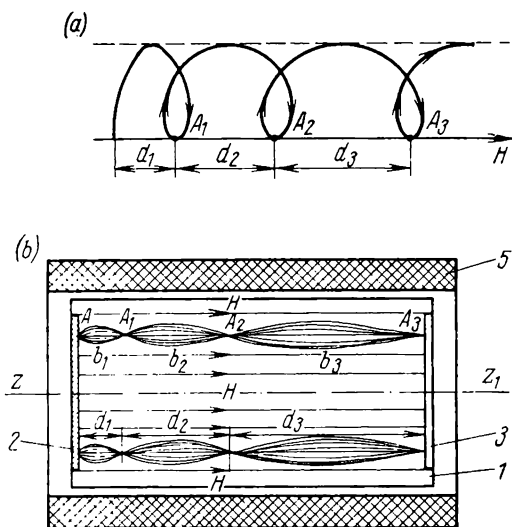


Fig. 7.21. Path of an electron in the field of the long focusing coil
(a) an electron moving in a spiral: around the circle due to u_r , and translationally due to u_z ;
(b) formation of nodes and loops

In the absence of an accelerating voltage, V_a , the magnitude of u_z is solely decided by the initial velocity u_{zi} . In the presence of V_a , the longitudinal velocity at the right-hand end of the bulb (at the phosphor) rises to

$$u_{z\text{ tot}} = u_{zi} + u_z V_a = u_{zi} + \sqrt{(2e)/mV_a}$$

In practice, $u_z V_a \gg u_{zi}$, and so,

$$u_{z\text{ tot}} \approx \sqrt{(2e)/mV_a} \quad (7.22)$$

Thus, each electron emitted from the photocathode travels along a spiral: round a circle due to \bar{u}_r and longitudinally due to \bar{u}_z . A projection of the electron path on the plane of the drawing is shown in Fig. 7.21a. After one revolution (one turn of a spiral) in time T , the electron will again cross the line of force H at point A_1 . Since all electrons emitted at the same time from point A complete one revolution in the same time T , they will converge to points $A_1, A_2,$

A_3, \dots , all at the same time. The electron beam leaving point A has the shape of a spindle (Fig. 7.21*b*) with nodes A_1, A_2, A_3, \dots , where the electrons converge to a single point on the line of force, and loops, or anti-nodes, b_1, b_2, b_3, \dots , where the beam diameter is a maximum*. Obviously, this diameter is determined by the maximum radial velocity, $u_{r \max}$, in the beam.

For good focusing it is essential that the nodes of the electron beams occur on the phosphor surface. This is achieved by varying the current in (and, as a consequence, the field intensity, H , due to) the focusing coil.

As is seen from Fig. 7.21, the distance d between adjacent nodes (the pitch of the spiral) increases from left to right. This is because the voltage V_a accelerates the electrons in their travel along the envelope so that they cover a progressively longer distance in the same time interval, T . The value of d_n is given by

$$d_n = d_1(2n - 1) \quad (7.23)$$

where n is the pitch number of the spiral path. As a result, the electrons emitted by the photocathode complete one or more revolutions about the lines of force of the magnetic field and land each at a particular point on the phosphor.

As already noted, another function of a long-focus coil is to focus the electron beam emitted by the thermionic cathode of a low-velocity-beam camera tube. In sketch form, the respective arrangement is shown in Fig. 7.22*a*. The thermionic cathode, 1, the control electrode, 2, and the accelerating electrode, 3, form between them an immersion lens which contracts the electron beam to a crossover (see Sec. 2.3). Within the region AD the beam slows down because the potential at the target, 4, is zero very nearly.

The bulb, 5, of the device is enclosed in a long focus coil, 6. The beam is deflected by a yoke, 7. The electrons travel along a spiral which follows the line of force $ABCD$. The separation between nodes is reduced because the electrons travel at a reduced velocity.

Within the space MN where the deflecting field, H_d , is at work, the resultant field intensity, H_r , is a vector sum of two fields, \bar{H}_d and \bar{H}_f , and the line of force assumes a kink, BC . Here the beam is deflected through a distance h . If there were no focusing field, H_f , the electrons slowed down near the target, 4, would spread at random over its surface.

Figure 7.22*b* shows the distribution of the potential (relative to cathode) along the tube axis. The negative potential at the modulator, 2, controls the beam current. Owing to a sudden rise in the

* In Figs. 7.21 and 7.22, the beam diameter at anti-nodes is strongly exaggerated. In some tubes, this diameter does not exceed a few tenths of a millimetre.

potential at the accelerating electrode, 3, a very efficient immersion lens is produced. Closer to the target, the potential is brought down to zero, and the electrons are gradually slowed down.

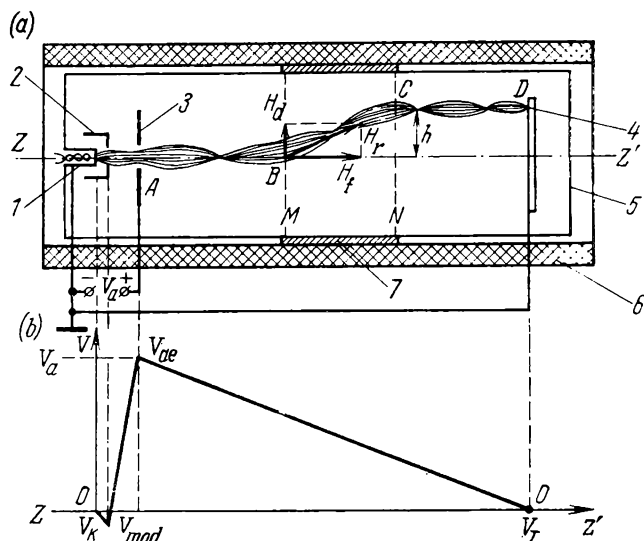


Fig. 7.22. Deflection of the electron beam in low-velocity-beam camera tubes (a) internal arrangement of the tube; (b) distribution of potential (relative to cathode) along the tube axis

7.11. Image Orthicon

The image orthicon was developed in the United States in 1946. However, its key element, a two-sided target, had been proposed much earlier, in 1938, by G.V. Braude of the Soviet Union.

The image orthicon consists essentially of three separate sections termed the image section, the scanning section, and the multiplier section (Fig. 7.23a). The image to be televised is focused on the transparent photocathode, 1, by a lens, 2. The photocathode is usually of the bismuth-silver-caesium type and is held at a negative voltage about 450 V relative to the cathode. The electrons emitted by the photocathode under the action of incident light are accelerated by an image-accelerator electrode of tubular construction, placed next to the photocathode, towards the target-mesh assembly. The photoelectrons are brought to sharp focus at a corresponding position on the target by the axial magnetic field produced by an external focus coil, 3. The target-mesh, 4, assembly consists of a thin glass membrane (about $5 \mu\text{m}$ thick) stretched tightly over the end of a ring electrode, 5, and acting as target, and an extremely fine

mesh, 6, maintained at a slightly positive potential (1 or 2 V) with respect to the glass target. The target mesh is fabricated by an electrolytic process and has about 200 meshes per square millimetre.

The scanning electron beam is produced by an electron gun made up of a thermionic cathode, 7, a modulator (or control grid), 8, and

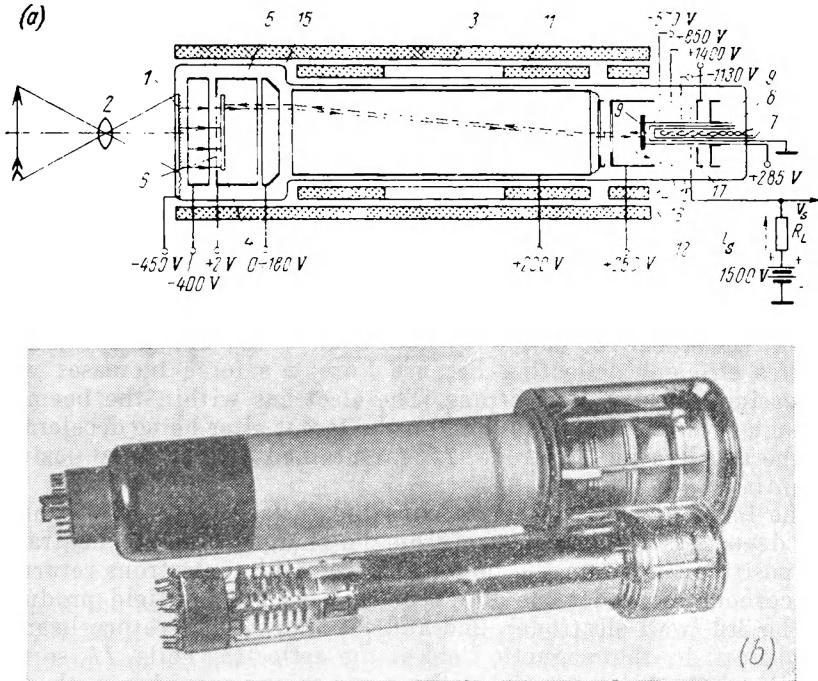


Fig. 7.23. Image orthicon

(a) internal arrangement; (b) external appearance of image orthicons with bulb diameters of 75 mm and 115 mm

an anode (or accelerating and masking grid), 9. Apart from electric focusing provided by the immersion lens of the photocathode assembly, the beam is further focused by the axial magnetic field produced by the long focus coil, 3.

The scanning electron beam is deflected by the radial magnetic field produced by deflecting coils, 11. The joint action of the focusing and deflecting fields causes the electrons to travel as shown in the figure. Emerging from the opening in the first anode, 9, the electron beam travels along the axis of the tube. The minute departures from the axis due to inaccuracies in the assembly of the cathode unit are corrected by alignment coils, 12. The electron beam is cau-

sed to deflect within the area of the radial magnetic field produced by the deflecting coils, *11*. In the space adjacent to the target, the beam is acted upon by the axial focusing field alone and again moves parallel to the tube axis so that the electrons strike the target, *4*, at right angles. It should be recalled (see Sec. 7.10) that in low-velocity-beam scanning the beam must be made to strike the target at right angles for any angle of deflection. Failure to satisfy this requirement produces variations in the signal. Most often this trouble occurs as the beam moves away from the centre to the edge of the target. Because of this, the signal is strongest at the centre and somewhat weaker at the edges of the target.

The velocity of the electrons is changed more than once as they travel from cathode to target. As will be recalled, the velocity of electrons inside the tube is decided by the potentials at the electrodes by which the electrons pass. The first anode, *9*, of the Soviet-made JII-201 image orthicon is maintained at +285 V, the second anode at +250 V, and the third anode (the wall electrode) at +200 V. Thus, the electrons travel at a sufficiently high velocity within the range of action of deflection coils, *11*, and this fact ensures efficient deflection because Lorentz's force increases with increasing velocity of electrons. The electrons within the beam go through several spirals and land on the target after being decelerated by the decelerating electrode, *15*, maintained at a slightly positive potential.

The incident electron beam scans the surface of the glass target and deposits sufficient electrons on the charged areas to neutralize the positive charge on the target. The remaining electrons return to the cathode, *8*, under the action of the accelerating field produced by the 3rd (wall electrode), 2nd and 1st anodes. The return beam is acted upon by the magnetic field of the deflecting coils, *11*, so that the return path is essentially the same as the scanning path. The return electrons land on the collector disc, *8*, which also acts as the first dynode of the electron multiplier assembled around the cathode. The remaining dynodes, *14*, *15* and *16*, are rings arranged in the fashion of a Venetian blind. The operation of a secondary-electron multiplier was examined in Sec. 7.5 in connection with the image dissector tube.

Soviet-made image orthicons usually have five stages of multiplication, including the dynodes *14*, *15* and *16*, the first anode *9*, and the collector *17*. The dynodes *14*, *15*, *16* and *17* are maintained at positive potentials which increase in the order given. The highest potential (+1.5 kV) is applied to the collector *16* made in the form of a mesh; it collects the secondary electrons leaving the dynode *17*. The collector circuit contains a load resistor, R_L , from which a video signal voltage, V_s , is taken. The signal current, i_s , traverses the load resistor in the direction labelled in Fig. 7.23a.

Before we take up the generation of the video signal in the image orthicon, it is worth while to examine the operation of a two-sided target. Its equivalent circuit appears in Fig. 7.24a. In this circuit, the capacitor C_2 represents the target element whose size is decided by the diameter of the scanning beam. The boundaries of the target elements are marked by the dashed lines aa' and bb' . The capacitors C_1 and C_3 represent the capacitances of the left- and right-hand

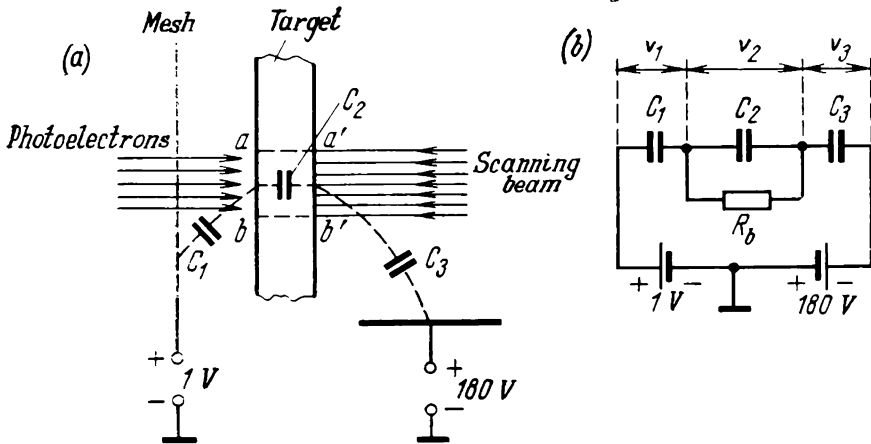


Fig. 7.24. Equivalent circuit of a double-sided target
(a) equivalent circuit of the target capacitance; (b) voltage distribution

sides of the target element with respect to the mesh and electrode 15 (Fig. 7.23a). Photoelectrons passing through the mesh reach the left-hand side of the target. The secondary electrons emitted by the target are collected by the mesh which is maintained at a slightly positive potential (about +1 V). The image section of the image orthicon utilizes a high-velocity electron beam. The secondary emission ratio of the target is $\sigma > 1$, and this produces an amplification of charge. The emission of secondary electrons produces a charge image on the left-hand side of the target. Secondary electrons are collected from the surface of the target at a sufficiently high rate because the mesh is closely spaced from its surface (at a distance of 40 to 50 μm). When enough light strikes the surface of the photocathode, the positive potential on some areas of the target may reach that of the mesh. In the absence of an accelerating field, this is accompanied by the spread of secondary electrons over the target surface, which fact limits the attainable depth of the charge image.

Now consider how the charge image stored on the left-hand side is scanned from the right-hand side of the target. The capacitance, C_2 , of the target element is considerably greater than C_1 because the

target is extremely thin (down to 5 μm) and has a considerable dielectric constant. The ratio C_2/C_1 may be of the order of 100 to 1. C_3 is likewise considerably smaller than C_2 because the distance to the ring electrode, 15, is large. According to Fig. 7.24b, the voltage generated across C_1 by secondary emission is shared between C_2 and C_3 . Since $C_2 \gg C_3$, then $V_2 \ll V_3$ and $V_2 \approx 0$. This implies that the left- and right-hand sides of the target are at practically the same potential, and the charge image may well be scanned from the right-hand side. This is done by an electron beam having a very

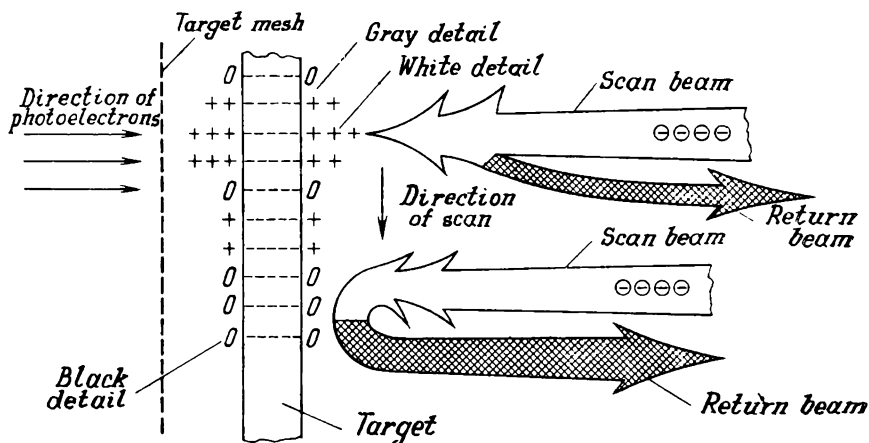


Fig. 7.25. Scanning the charge image on the target of an image orthicon

low velocity near the target surface. In schematic form, the charge image stored by the target is shown in Fig. 7.25 where the “+” sign applies to the positive potential. The target elements receiving photoelectrons from the illuminated areas of the photocathode and having the highest positive potential are labelled “+++”; “gray” elements are marked “++”, and black ones, “0”. The electron beam scans the surface of the target and deposits enough electrons on the charged areas to neutralize the charge and drive it down to the potential of the cathode in the electron gun, that is, to zero. The number of electrons required to neutralize the charge stored by a particular target element depends on its potential which in turn depends on the illumination of the image element televised. The higher the potential, the greater the number of electrons deposited on the target and the smaller their number returning towards the cathode. In this way, the current of the return beam is amplitude-modulated by the loss of electrons to the charges on the target, which fact is illustrated in Fig. 7.25 by changes in the width of the return beam.

During scan, the capacitance C_3 (Fig. 7.24) is shorted out by the scanning beam (because the tube cathode is grounded), and the capacitance C_1 discharges through the target capacitance C_2 . During the frame scanning interval, until the beam scans the same element again, the capacitance C_1 re-accumulates the charge, and the target capacitance gradually discharges through the bleeder resistor, R_b . To facilitate the discharge of C_2 , the target is fabricated from a special grade of glass having a sufficiently high conductivity.

The manner in which the beam current is amplified and the signal voltage is produced across the load resistor, R_L , is shown in

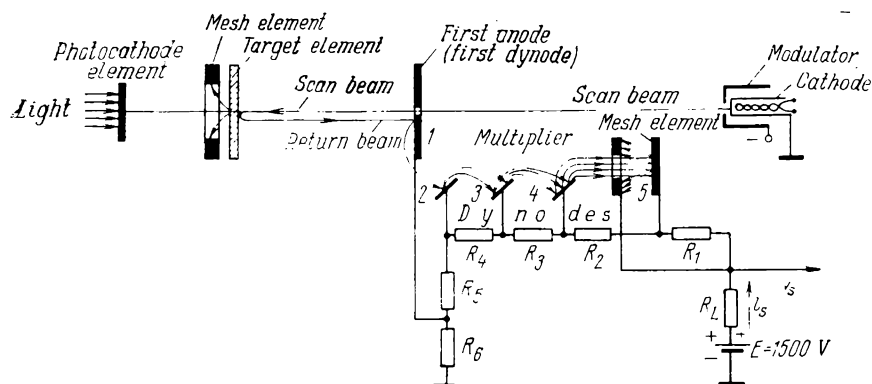


Fig. 7.26. Generation of a signal in an image orthicon

Fig. 7.26. The electrons reflected from the target surface are driven by the accelerating electric field towards the first anode (at 9 in Fig. 7.23a) from which they knock out secondary electrons. The first anode 1 also acts as the first dynode of the electron multiplier. As the electrons are reflected from the target, the beam is de-focused, and the return beam has a greater cross-sectional area than the scan beam. The first anode intercepts some of the electrons in the return beam, and the secondary electrons knocked out of it are driven by the accelerating electric field towards the 2nd, 3rd, 4th and 5th dynodes of the multiplier. On being reflected from the last, 5th, dynode, the electrons are collected by the grid (collector) whose circuit contains the load resistor, R_L , and the supply source, E .

The potentials at the dynodes are set by a voltage divider using resistors R_1 through R_6 . In most Soviet-made image orthicons, the first dynode is maintained at +285 V, and the last at +1.4 kV. The potential at the collector is practically equal to that of the supply source, that is +1.5 kV. A five-stage multiplier provides an amplification of about 1000.

The collected electrons give rise to the signal current, i_s , in the load resistor. In present-day image orthicons, the signal current is up to 100 μA , which is 400 to 500 times the current in the iconoscope. The signal at the tube output is in positive polarity. This is because when the beam scans the target element corresponding to a black picture element, practically all of the electron beam is turned back (see Fig. 7.25) and the signal current has a maximum value. When the beam scans white elements, the signal current is a minimum. As a result, for the direction of current flow shown in Fig. 7.26 the potential at the top terminal of the load resistor, R_L , from which

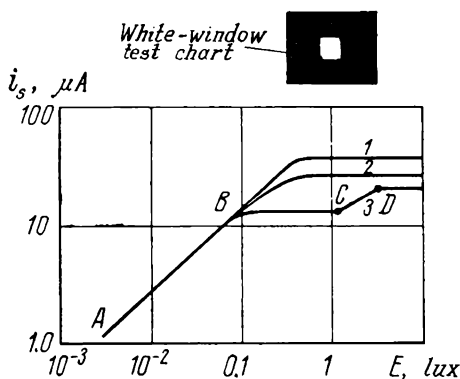


Fig. 7.27. Light-transfer characteristic of Soviet-made image orthicons
1—JII-201; 2—JII-213; 3—JII-17

the signal voltage, V_s , is taken, decreases with decreasing illumination of the picture element scanned. The whitest picture elements produce the highest potential at the top terminal of the load resistor, R_L , and, as a consequence, the strongest signal.

The light transfer characteristics of image orthicons are shown in Fig. 7.27. Curves 1, 2 and 3 relate the signal to the illumination of the photocathode in the Soviet-made JII-201, JII-213 and JII-17 image orthicons when the image being televised is a white square against a

black background (a test chart). Referring to Fig. 7.27, there is a linear relation between the signal current and illumination within the initial portion of the light transfer characteristic. At the knee, the saturation condition is attained (curves 1 and 2) where the signal current is no longer dependent on illumination. This form of the light transfer characteristics may be explained as follows. As long as the illumination of the scene remains low (not over 0.1 lux), the target potential lies below that of the target mesh (at 6 in Fig. 7.23a), which is essential for the effective collection of secondary electrons from the target surface. As the scene illumination increases, the charge image grows deeper and the signal gains in magnitude. The point of inflection (knee) on the curve corresponds to the condition when the target areas representing the white picture elements reach the mesh potential, and no secondary electrons are collected any longer. Referring to Fig. 7.27, the signal current of the JII-201 image orthicon in the saturation mode exceeds the signal current of the JII-213 tube. This is because the spacing between mesh and

target in the former is closer than it is in the latter. As a consequence, the capacitance C_1 (see Fig. 7.24) and the charge that it can store are greater.

The light transfer characteristic of the JII-17 image orthicon has two points of inflection, B and C (curve 3). This form of the light transfer characteristic is typical of wide-spaced tubes (those with a greater spacing between mesh and target). It is to be noted that of the three tubes under consideration this spacing is widest in the JII-17 tube. According to some investigators, in the case of wide mesh-to-target spacing the generation of the output signal is affected by the capacitance between adjacent target areas. When the beam scans one area it also brings down the potential of adjacent areas, which fact results in an increase of the signal within the portion CD of the light transfer characteristic.

As long as the tube operates within the linear portion of its light transfer characteristic, the response to luminance gradations is independent of the scene content. Also, it is to be noted that the signal generated during retrace is the same as the signal associated with black areas in the scene being televised. This is because during retrace the scanning beam of the image orthicon is blanked by a negative blanking pulse applied to the target mesh. As long as the blanking pulse exists, all electrons in the scanning beam turn back. A similar situation exists when the beam scans black picture elements (see Fig. 7.25). This property of the image orthicon enables the d.c. component to be restored at any point of the TV circuit by clamping the black level.

An idea about the resolving power of the image orthicon can be gleaned from the amplitude response curves shown in Fig. 7.28. Curve 1 applies to tubes with a bulb diameter of 75 mm (the JII-17) and curve 2 to tubes of an improved resolving power such as the Soviet-made JII-221 and JII-222 which have a bulb diameter of 115 mm. In the latter tubes, the surface area of the photocathode is the same as in the tube with a diameter of 75 mm, but the electron image is transferred onto the target with a magnification of about 1.5 times. On a large-sized target, scanning is accompanied by less pronounced aperture distortions. As a result, the signal at

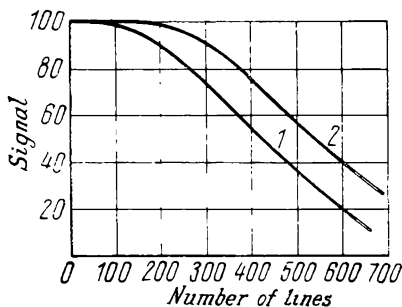


Fig. 7.28. Amplitude response (aperture) characteristics of image orthicons (signal is in percent)

1—75-mm diameter bulb; 2—112-mm diameter bulb

600 lines per frame is approximately twice as great as that of an ordinary image orthicon.

To-day the image orthicon has found a wide field of application. It is used in TV cameras for the transmission of white-and-black and colour scenes and also in closed-circuit systems. The wide use of the image orthicon has been promoted by its high resolution and sensitivity. However, the early image orthicons had a relatively low signal-to-noise ratio. In the image orthicon the signal-to-noise ratio is mainly determined by shot noise in the scanning beam. For this reason, the tube had often to be operated at a minimum beam current. Another way of improving the signal-to-noise ratio is to increase the storage capacitance of the target. To this end, the mesh is closely spaced to the target and both are made large in size. Present-day image orthicons have a signal-to-noise ratio of over 60 to 1.

Among the demerits of image orthicons are variations in the signal because the electrons scanning the central and peripheral areas of the target differ in velocity, and halation. Halation occurs when bright or highly reflecting objects fall within the field of view of the camera. In such cases, secondary electrons are re-distributed over the target surface and bring down the potential of adjacent areas. On the viewing screen, highlights appear surrounded by a dark halo.

7.12. Vidicon

The vidicon is a camera tube utilizing the inner photoelectric, or photoconductive, effect. The idea to use this type of camera tube was first advanced by A. A. Chernyshev of the Soviet Union in 1925. The first commercial vidicons, however, appeared in 1950. In sketch form, the arrangement of the vidicon is shown in Fig. 7.29a. The photoconductive target, *1*, is deposited on the vacuum (rear) side of the faceplate of a cylindrical tube bulb. The electron beam is produced by an electron gun composed of a thermionic cathode, *2*, a control grid (or modulator), *3*, intended to control the beam current, and the first anode, *4*. It is followed by a second anode *5*, which extends into a cylindrical electrode, *6*, closed by a fine metal mesh intended to produce a uniform electric field near the target. In some types, the second anode and the equalizing mesh form a single element. In such a case, the equalizing metal mesh is attached directly to the end of the second anode. The first anode is fitted with an aperture stop to limit the diameter of the electron beam. As a rule, the aperture is not more than 50 to 60 μm in diameter. The second anode produces an equipotential region within which the electron beam is deflected, and also operates as the collector of secondary electrons liberated by the target. In most Soviet-made vidicons, the first and second anodes are maintained at nearly the

same potential ranging between 300 and 500 V. The equalizing mesh is held at a higher potential of about +1 kV.

A detail view of the target is shown in Fig. 7.29b. It consists of a light-transparent video output or signal plate, 1, which is a thin film of metal deposited by vacuum evaporation on a transparent optical flat, 2, and topped by a photoconductive film 2 or 3 μm

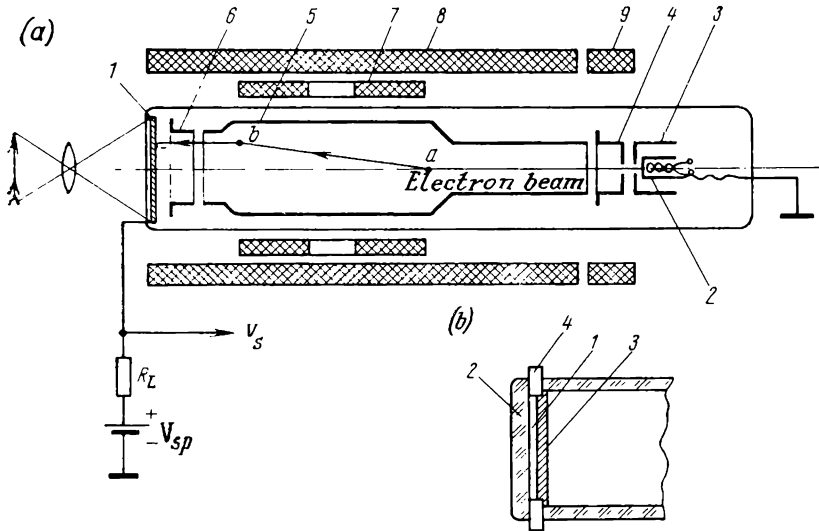


Fig. 7.29. Vidicon

(a) internal arrangement: 1—target; 2—cathode; 3—modulator; 4—first anode; 5—second anode; 6—equalizing mesh; 7—deflection yoke; 8—focusing coil; 9—correcting coils; (b) detail of design: 1—signal plate; 2—optical flat; 3—photoconductor; 4—signal-electrode connection

thick. The signal plate, 1, is in contact with a metal disc, 4, serving as an output terminal. The signal plate circuit contains a load resistor, R_L .

As already stated, the vidicon utilizes the inner photoelectric or photoconductive effect. In this effect, the electric conductivity of a material changes as a result of absorption of incident electromagnetic radiation which may be visible light, infra-red or ultra-violet rays. Photon absorption frees the electron from its tight bond to a lattice site in a filled band and causes it to move into a conduction band, thereby increasing the conductivity of the material.

The physical processes taking place in this photoconductive films are extremely complex and have not yet been investigated completely. In brief, the photoconductive layer is an insulator in the dark. When the target is illuminated, the photoconductive layer absorbs photons, and these produce an increase in the number of charge

carriers within the photoconductive layer. When the image to be televised is focused onto the target, its individual areas (elements) acquire a different resistance, thereby producing a resistance image.

The generation of a video signal in the vidicon can best be studied by reference to its equivalent circuit shown in Fig. 7.30. The scanning beam has a finite cross-sectional area in the target plane. The

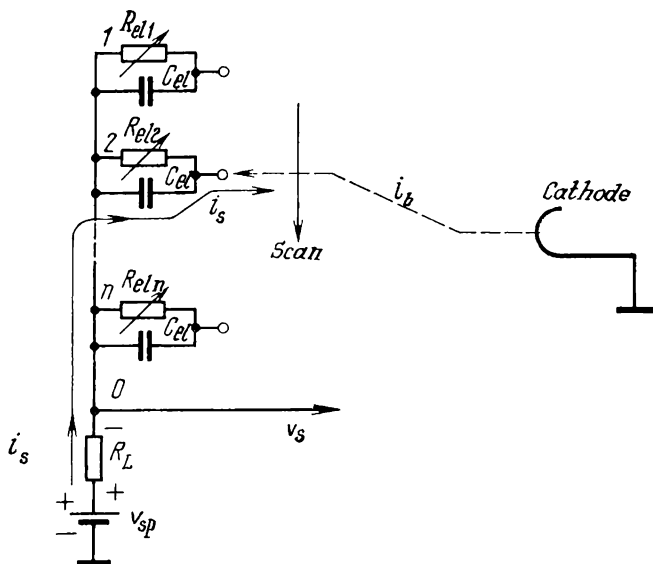


Fig. 7.30. Equivalent circuit of the vidicon

capacitance of the capacitor formed by the vacuum side of the target element and the signal plate is labelled C_{el} and the resistance of the target element is labelled R_{el} . When the image to be televised is focused onto the target the elementary resistances, R_{el} , are different. The highest (dark) resistance is displayed by the non-illuminated target elements. When a beam of low-velocity electrons scans the target surface, the potential on the vacuum side of the target is driven to cathode potential, that is, to zero (in Fig. 7.29a the cathode is grounded). The potential on the signal plate, V_{sp} , is usually chosen to range between +10 and +100 V with respect to cathode. During scan, the elementary capacitors of the target are charged to the signal-plate voltage, V_{sp} . In the interval between scans, the elementary capacitors, C_{el} , of the target discharge into the elementary resistors, R_{el} , so that the potentials on the right-hand (vacuum-side) plates of these capacitors rise towards the signal-

plate potential. Since $R_{el} = f(E)$, the discharge time constant $\tau_d = R_{el}C_{el}$ is determined by the illumination of the respective target element. The greater the illumination, the smaller the value of R_{el} , and the more the capacitor C_{el} will discharge. During the frame scan interval a charge image forms on the vacuum side of the target. The potential of non-illuminated (black) target elements remains practically zero, while the illuminated target elements acquire a positive potential which increases with illumination. The output signal is generated in relation to the charging of the elementary capacitors by the electron beam. When the beam scans an illuminated (highlight) target element having a positive potential, a considerable proportion of electrons in the beam are deposited on the target; when the beam scans an unilluminated target element having a nearly zero potential, the electron beam is reflected from the target surface and turns back towards the cathode. The charging of the elementary capacitors is accompanied by the generation of the signal current, i_s , which flows as shown by the arrow in Fig. 7.30, that is, opposite to the flow of electrons, and is returned via the electron beam and cathode to ground. The greater the illumination, the greater the current traversing the load resistor, R_L , and the lower the potential at point a from which the video signal is picked off. Highlights (white picture elements) correspond to a lower potential; in other words, the output signal of the vidicon is white negative.

The deflection system of the vidicon must ensure that the beam lands on the target at right angles, irrespective of the deflection angle. As in the image orthicon, the effectiveness of scanning the charge image depends on the angle at which the scanning beam lands on the target surface. The normal incidence of the beam on the target is ensured by the fact that the deflection-focusing system produces a suitably shaped magnetic field inside the tube. The operation of this type of deflection-focusing system has been examined in Sec. 7.10. The deflection coils (at 7 in Fig. 7.29a) produce the transverse component of the magnetic field, and the focusing coil, 8, produces the axial component. The electrons emitted by the cathode assembly travel first along the tube axis because the trajectory of the electrons as far as point a is only affected by the magnetic field of the focusing coil. The beam is deflected within the region ab under the action of the transverse magnetic field produced by coils 7 and the field due to the focusing coil, 8. Past point b , the electrons are again under the action of only the focusing field and land on the target surface at right angles.

In comparison with the image orthicon, the vidicon is simpler in construction and contains considerably fewer parts. However, some of its assemblies are fairly difficult to make. In part, this is because the device is small in size. In the Soviet Union, the vidicons available commercially have bulbs with a diameter of 38, 27 and 13 mm,

The size of the image area in the most commonly used 27-mm vidicon is 1.2 cm², which is one-fifth to one-sixth of that in the 78-mm image orthicon and 1/90 of that of the mosaic target in the iconoscope. For good resolution it is essential that the beam be carefully focused to a diameter of a few tens of micrometres. This imposes exacting requirements on the accuracy of fabrication of the cathode assembly and the deflection-focusing system. To correct the distortions caused by inaccuracies in the fabrication of the cathode assembly, the deflection-focusing system includes two pairs of alignment coils (at 9 in Fig. 7.29a). Another difficulty in reducing the beam to a small

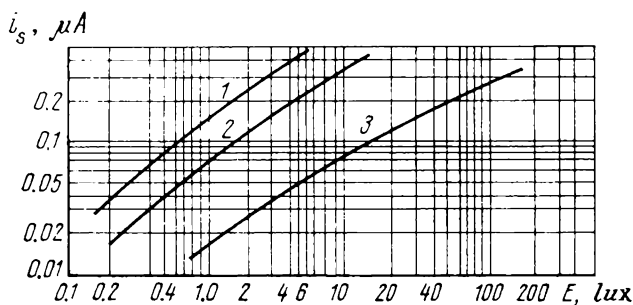


Fig. 7.31. Light-transfer characteristics of the ЛИ-415 vidicon for different values of V_{sp}

1— V_{sp1} ; 2— V_{sp2} ; 3— V_{sp3}

diameter is due to the fact that electrons repel one another because they carry charge of the same sign. This is especially strongly felt in low-velocity-beam operation.

In recent years the vidicon has found many uses as a movie pickup in television, in industrial closed-circuit systems, space television circuits, and in colour TV cameras. The vidicon has won this popularity owing to its small size and weight, high reliability, and simple maintenance. Through a proper choice of target material, it is possible to build vidicons sensitive to X-rays, ultra-violet and infra-red light. For use in the visible region of the spectrum, the target material may be selenium and compounds of sulphur, selenium, antimony and arsenic. For operation in the infra-red, the target is made of lead sulphide (PbS), and for the ultra-violet from selenium which has a broad spectral sensitivity characteristic.

Typical light transfer characteristics of the Soviet-made ЛИ-415 vidicon for different signal-plate voltages, V_{sp} ($V_{sp1} > V_{sp2} > V_{sp3}$), are shown in Fig. 7.31, and the spectral sensitivity characteristics of the ЛИ-415 and ЛИ-418 vidicons in Fig. 7.32. For comparison, the plot includes a relative sensitivity curve (the dashed line). As is seen from Fig. 7.32, the peak of the spectral response of

the vidicon is shifted into the short-wavelength region of the spectrum, a fact responsible for incorrect tone rendition. The blue and violet details of the image being televised will appear excessively light on the screen of a black-and-white picture tube.

Another limitation of the vidicon, nonexistent in other types of tubes, is time lag. It is especially troublesome when the scene involves fast motion, as it results in defocusing and even the complete loss of fast-moving details. It is customary to class time lag according

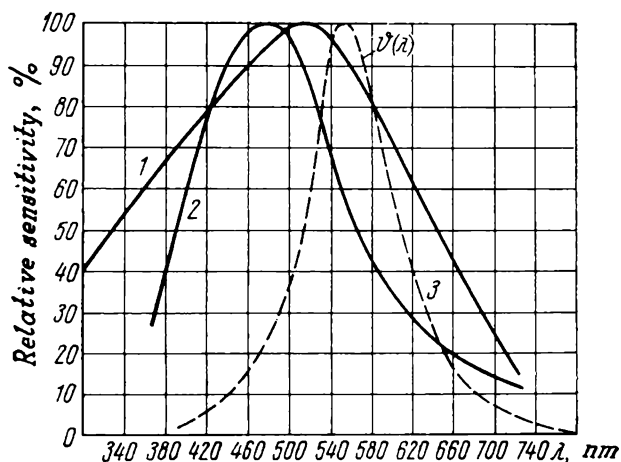


Fig 7.32. Spectral sensitivity characteristics of Soviet-made vidicons
1—ЛИ-415; 2—ЛИ-418; 3—relative visibility curve

to the factor causing it, namely as photoelectric lag and scanning lag. The photoelectric component of lag is related to the physical processes taking place in the photoconductive target. In contrast to photoemission, the photoconductive effect, that is an increase in conductivity, occurs some time after changes in photoexcitation; similarly a decrease in conductivity upon removal of photoexcitation takes place within a finite span of time. The photoelectric lag depends on the type of photoconductor used, the amount of impurities it contains, manufacturing techniques, and illumination level.

Scanning lag arises from the fact that the beam current is too small. Because of this, it takes several scan cycles to completely neutralize the charge image stored by the target. The residual signal left over from several previous frames causes moving objects to appear out of focus on the screen of a conventional TV receiver. The scanning component of time lag can be reduced by increasing the beam current. Unfortunately, this is not easy to do because an increase in beam current has to be achieved without causing the beam

to spread in the target plane. Otherwise, the result would be a poorly focused image.

The total time lag of the vidicon is strongly dependent on the illumination of the photoconductive target. The greater the illumination, the smaller the photoelectric component of time lag. Also, with a high illumination (as follows from Fig. 7.31), the tube can be operated at a low value of V_{sp} , and this in turn brings down the scanning component of lag. This form of operation is used in TV movie-pickup cameras. In this application the low sensitivity of the vidicon is of minor importance, because a high level of illumination can be obtained within the small surface area of the movie

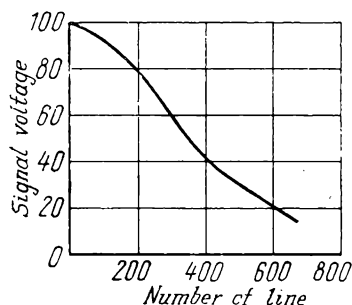


Fig. 7.33. Amplitude response (aperture) characteristic of the JII-421 vidicon (signal is in per cent)

frame without particular difficulty. In industrial closed-circuit systems televizing static or slowly moving scenes, time lag is unimportant, and maximum sensitivity can be achieved by raising V_{sp} . However, operation at maximum sensitivity due to an increase in V_{sp} produces a marked increase in the dark current of the target, and the resistance of the unilluminated target elements is drastically reduced. Because the dark current is different for different target areas, the signal suffers a considerable nonuniformity which impairs picture quality.

The aperture characteristic of the JII-421 vidicon with a bulb diameter of 26 mm is shown in Fig. 7.33. As is seen, at 600 lines the depth of modulation is 20% which is comparable with the performance of a 75-mm image orthicon (see Fig. 7.28). Given the same condition, the Soviet-made 38-mm vidicons produce 40% modulation.

The vidicon is a promising camera tube. Owing to the use of a photoconductor as target, the vidicon can successfully operate at an illumination of as low as 0.1 lux, which is comparable with the performance of camera tubes utilizing the outer or photoemissive effect. The photoconductive effect avoids the undesirable re-distribution of photoelectrons. Since the charge image is scanned by a low-velocity beam, the secondary electrons liberated as the target is scanned are effectively collected, and there is no shading. A very important advantage of the vidicon is that the signal contains accurate black-level information. When the beam scans an unilluminated target element (the capacitor C_{el} is charged), the scanning beam is completely turned back from the target. The signal is generated under similar conditions during retrace when blanking pulses are applied to the control grid (modulator) of the cathode assembly,

and the beam is cut off before it can reach the target surface. As a result, the signal generated by the tube during retrace corresponds to the black level or differs from it (owing to the dark current) by a fixed amount. This property of the vidicon may be utilized (where necessary) in order to restore the d.c. component by clamping the signal level during retrace.

7.13. Plumbicon

The plumbicon is a recent addition to the family of camera tubes. In fact, it is not unlike the vidicon, but it differs from the latter in the target material used and the physical processes that take place in it.

Before taking up the plumbicon as such, it will be worth while to look into the factors that stand in the way of reducing time lag in the vidicon without detriment to high sensitivity. As is noted in the previous section, scanning lag arises from the fact that a single scan cycle cannot completely neutralize the charge stored by the elementary capacitors, C_{el} . In principle, scanning lag can be reduced in two ways, namely (1) by raising the beam current and (2) by bringing down the value of C_{el} . Since an increase in beam current impairs beam focusing, it would seem natural to use the second approach, that is, to reduce the value of C_{el} . To this end, it would suffice to increase the thickness of the target. Unfortunately, this would do no good, either. As C_{el} is decreased, the time constant of the target, $R_{el}C_{el}$, is decreased, too. In the vidicon, C_{el} charges during scan and discharges into R_{el} (see Sec. 7.10) in the interval between frame scans. For complete utilization of the storage effect, it is important that the discharge continue throughout the complete frame scan interval. If C_{el} were reduced, the highlight target areas (where R_{el} is low) would discharge well before the end of the frame scan period, and the storage effect would not be fully utilized. In other words, a decrease in C_{el} should be accompanied by an increase in R_{el} so that the time constant $R_{el}C_{el}$ can be held constant. An increase in R_{el} , however, poses some additional requirements. Firstly, in order to retain the signal level the resistance of both highlight and lowlight target areas must be increased. It is only then that the depth of the resistance image (the ratio of maximum to minimum resistance of a target element) can be kept unchanged. Secondly, an increase in the resistance of lowlight target elements (that is, in the dark resistance of the target) ought not to be accompanied by an impairment in other properties of the target, such as an increased photoelectric lag or decreased sensitivity.

The above requirements can be met if the photoconductive target be replaced by one of a photodiode type. A reverse-biased P.V. photodiode would ensure low photoelectric lag and a high dark resistance.

Unfortunately, an ordinary PN photodiode cannot be used as target because both the P and N regions have a low surface resistance, and no charge image can be formed as the charge carriers would spread all over the target surface. This is why a more elaborate target is employed in the plumbicon. It is deposited on the vacuum side of the bulb faceplate and has three layers possessing P , I and N conduction, respectively. In sketch form, the construction of the target is shown in Fig. 7.34. A thin, light-transparent signal plate is deposited on an optical flat; the signal plate is a conductor and is

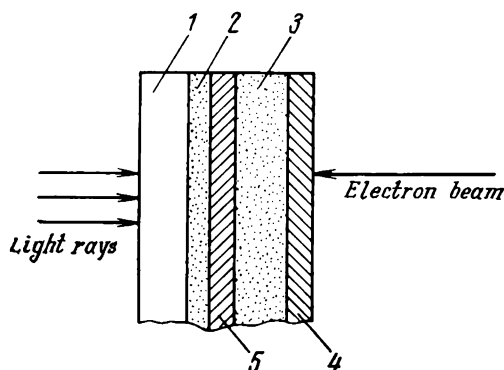


Fig. 7.34. Target of a plumbicon

1—optical flat; 2—signal plate; 3— I -layer; 4— P -layer; 5— N -layer

used to couple out the output signal. The N -conduction layer is likewise thin and light-transparent. Light is free to pass through the signal plate and the N -layer. The I -conduction layer (that is, one possessing intrinsic conduction) is 10 to 15 μm thick (which is greater than the thickness of the remaining two layers and two or three times that of the target in the conventional vidicon) and absorbs the bulk of incident light. The last, P -conduction, layer is made extremely thin to avoid the spreading of charge between target areas at different potential (the material of the P -layer has a higher conductivity than the I -layer). The I -layer is made from lead oxide (PbO) with an ordered lattice. Lead-oxide crystals are the shape of needles measuring 0.1 μm by 0.1 μm by 1 μm and arranged at right angles to the target surface. When use is made of a chemically pure material, the layer has a lower trap concentration than in the usual photoconductors. The I -layer has a very high dark resistance because the resistivity of the source material exceeds 10^8 ohms m .

In the target, an electric field is produced by a voltage, V_{sp} , applied in positive polarity to the signal plate. Because the low-velocity scanning beam drives the opposite side (the P -layer) of

the target to the cathode potential, the $P-N$ junction is reverse-biased, and this adds to the dark resistance of the target.

When light strikes the target, all charge carriers produced in the I -layer pass through the entire I -region without recombination owing to the low trap concentration and high electric field intensity in that region. Owing to the ability of carriers to travel a long distance, the plumbicon target can be made thicker without raising its photoelectric lag and retaining high sensitivity. The increase in target thickness reduces C_{el} responsible for scanning lag.

The plumbicon shows a fairly high performance. Its resolution is close to that of a 115-mm image orthicon. The sensitivity is 400 $\mu\text{A/lumen}$, so that the tube can be operated at a photocathode illumination of 1 or 2 luxes. Time lag is negligible. Image retention is as low as 5% as against 25 to 30% in the vidicon. The plumbicon has a linear light transfer characteristic, which is a major advantage for colour television.

Because of its high performance, the plumbicon has found a wide field of application in television.

7.14. Monoscope

The monoscope is a camera tube that generates a video signal from a fixed pattern (most often, a test chart) inside the tube.

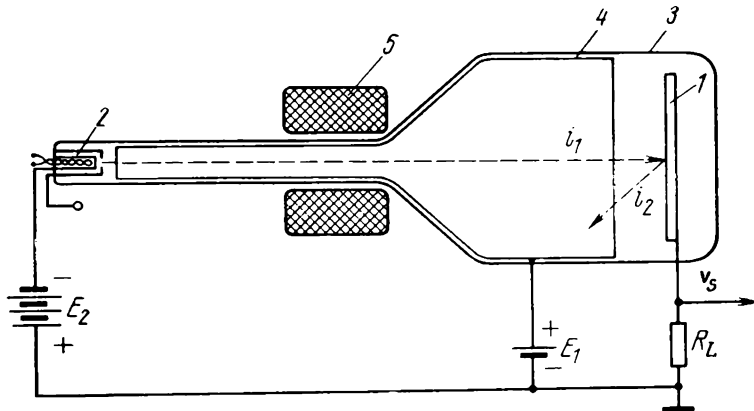


Fig. 7.35. Monoscope camera tube

1—target; 2—cathode; 3—glass bulb; 4—collector electrode; 5—deflection yoke

The signal plate (at 1 in Fig. 7.35) is generally made of aluminium foil that has been oxidized to provide a surface having a high secondary-emission ratio. The pattern to be reproduced is printed on the oxidized surface with a special carbon-containing ink having a rela-

tively low secondary-emission ratio. The electrons liberated by the cathode, 2, enter a strong accelerating field produced by sources E_1 and E_2 . The potential difference between the cathode and the collector electrode, 4, is ordinarily 1.1 to 1.2 kV. The collector electrode is maintained at a positive potential between +100 and +250 V with respect to the target and effectively collects all secondary electrons emitted by the signal plate. The signal current is determined by the difference $i_2 - i_1$. Since $i_2 = \sigma i_1$, the signal current can be found from the relation

$$i_s = i_2 - i_1 = i_1 (\sigma - 1)$$

that is, the signal current is decided by the range of the secondary-emission ratio.

The monoscope has a high signal-to-noise ratio, high picture definition, and good contrast. Owing to these qualities, the monoscope is employed as a source of test signals for checking the performance of television equipment. The Soviet-made ЛИ-22 monoscope transmits test chart 0249.

CHAPTER EIGHT

TELEVISION BROADCASTING

8.1. Expansion of TV Broadcasting

The engineering facilities used for TV broadcasting form a large and elaborate complex comprising program TV centres, high- and low-power relay stations. The equipment of a TV program centre turns out programs, and relay stations pass them on to receivers in outlying regions. The production of a TV program involves the efforts of script writers, directors, their associates, actors, composers, and musicians. A program TV centre must have an ample supply of scenery, shops to make stage properties, and other auxiliary services. This list, far from being complete, shows that a TV centre is an expensive thing to run.

In the early years of television, emphasis was mainly placed on program TV centres. With the advent of long-haul radio-relay, cable and satellite links, it has become possible to exchange TV programs between distant towns, to build relay stations, and to cut down investment in expensive TV program centres. TV program centres and high-power relay stations are now supplemented by a great number of low-power relay transmitters.

Further effort in the Soviet Union is planned to be put in colour television. Colour telecasts, started in the Soviet Union on November 7, 1967, the 50th anniversary of the October 1917 Revolution, will gradually oust black-and-white television. To-day Soviet makers turn out several makes of colour TV receivers and the necessary transmitting equipment.

A very important task in this field is to improve the reliability of TV receivers and to transistorize TV equipment so as to save electricity. This task is being handled by a large team of scientists and engineers.

8.2. Equipment of a Program TV Centre

A block diagram of a program TV centre is shown in Fig. 8.1. As is seen, it comprises a studio-control section, a VHF-UHF radio transmitter, a field camera unit (or units), a power supply department, and a number of auxiliary services. The studio-control section converts the optical image to be televised and program sound into

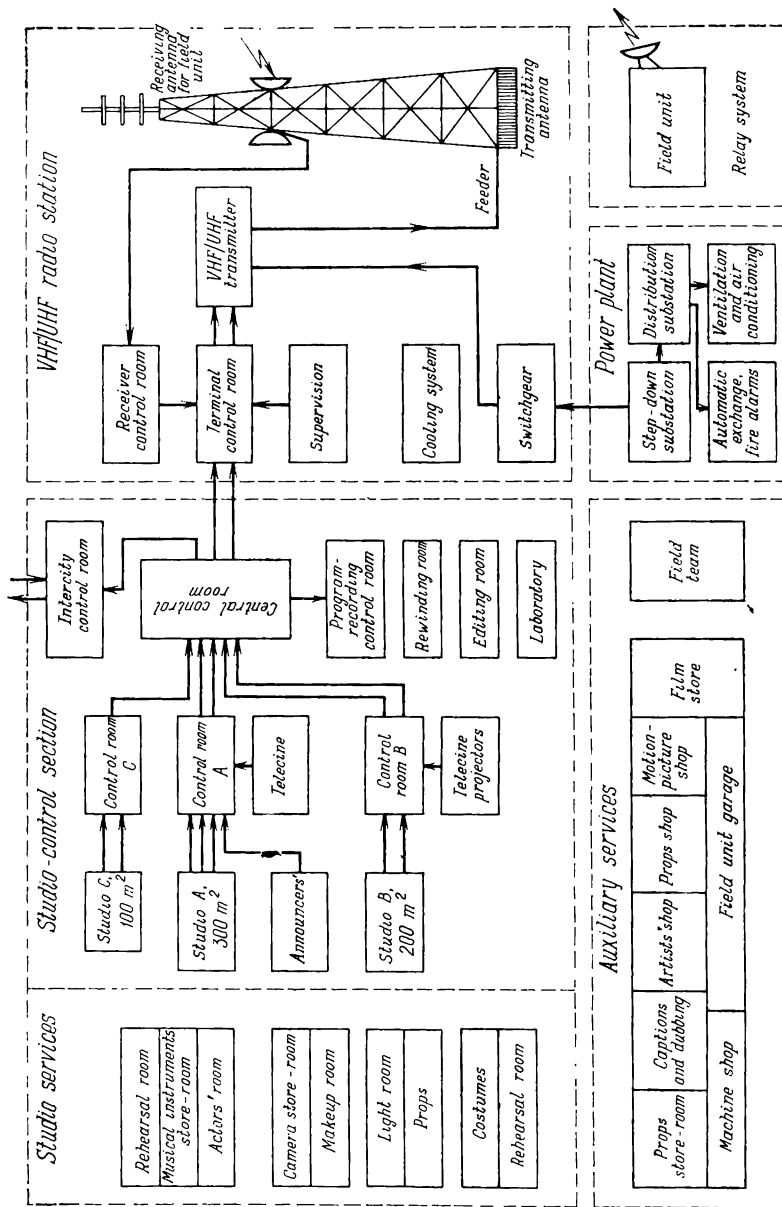


Fig. 8.1. Block diagram of a programming TV centre

electric signals. The studio-control section consists of studios and control rooms. The latter may be intended for studio work, film transmission, intercity exchange, central control, and program-recording on cine film and magnetic tape. A TV studio is a suitably equipped room (Fig. 8.2). Live pickups from a studio have many advantages over those from, say, a theater, because a studio has everything to show the actors and the scenes acted out in the best

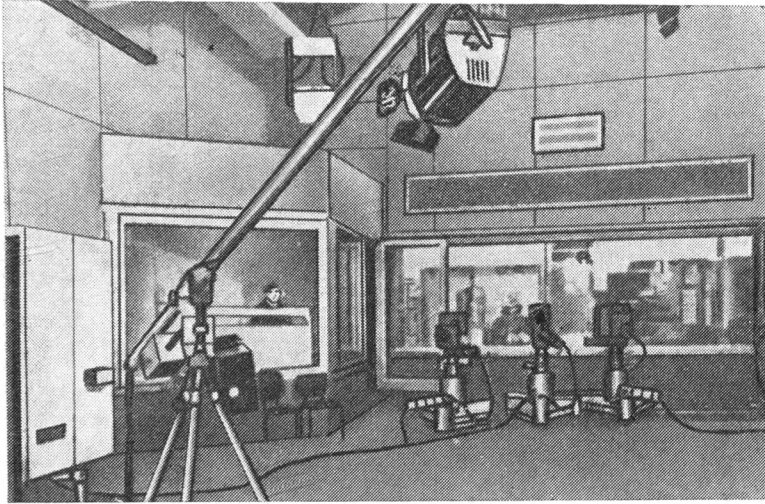


Fig. 8.2. A TV studio

way. This, above all, calls for proper lighting of the stage. The lights can be installed on balconies or suspended from the ceiling and operated (that is, switched on and off, lifted, lowered, or turned around) remotely. This is convenient and avoids interference with the image and sound at the instants when the lights are manipulated. Since the lights give up much heat, the studios are fitted with air conditioners.

TV cameras are mounted on tripods, studio pedestals, or cranelike dollies and connected by a multiconductor flexible cable to the equipment in the control room. The control room (Fig. 8.3) is separated from the studio by a sound-proof window. The control console installed at the window gives support to picture monitors which reproduce the images picked up by the cameras. Sitting at the control console, the production supervisor or program director can see everything taking place in the studio, watch operation of the cameras on his monitor, and switch the necessary one in circuit.

The manner in which the signal generated by a camera is processed will be clear from reference to the block diagram of Fig. 8.4. The video signal appearing at the output of the pickup tube is applied to a picture preamplifier. This signal is 10 to 20 mV from a vidicon camera and 100 to 150 mV from an image orthicon camera. The preamplifier built into the camera case boosts the signal to 0.2-0.3 V. With this signal from the preamplifier, it is an easy matter to avoid

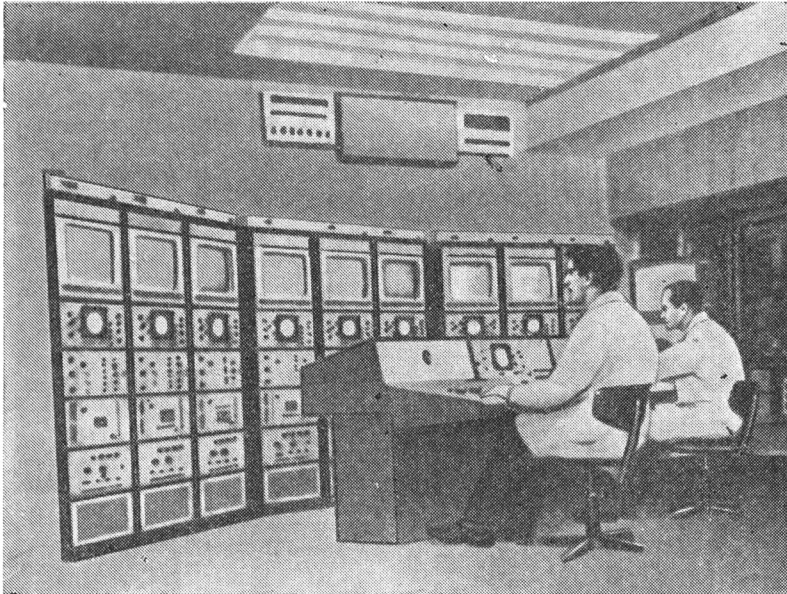


Fig. 8.3. Control room

any inductive pickup in the camera cable (from supply circuits, intercom system, etc.). Signal amplification above that figure has no sense because this would require a more complex camera and, as a corollary, an increase in weight and size.

The camera cable feeds the video signal to the intermediate picture amplifier installed in the control room. The intermediate amplifier raises the signal to 1 V, corrects it for frequency distortion caused by the cable, aperture distortion, and nonlinear distortion, and also inserts blanking pulses. The camera including the built-in preamplifier, the camera cable and the intermediate picture amplifier make up between them the camera chain. From the camera chain, the video signal is fed to a mixer-switcher. With its aid, the production supervisor can select or mix signals from one or several cameras.

From the mixer-switcher, the video signal goes to a line amplifier which boosts the signal and inserts the composite sync signal. As a rule, this amplifier incorporates an automatic gain control (AGC) circuit. The need for AGC arises from the fact that the input of the line amplifier can accept signals from different cameras, and these signals may differ in strength. The AGC circuit removes these variations caused by switching the camera chains and produces a stable

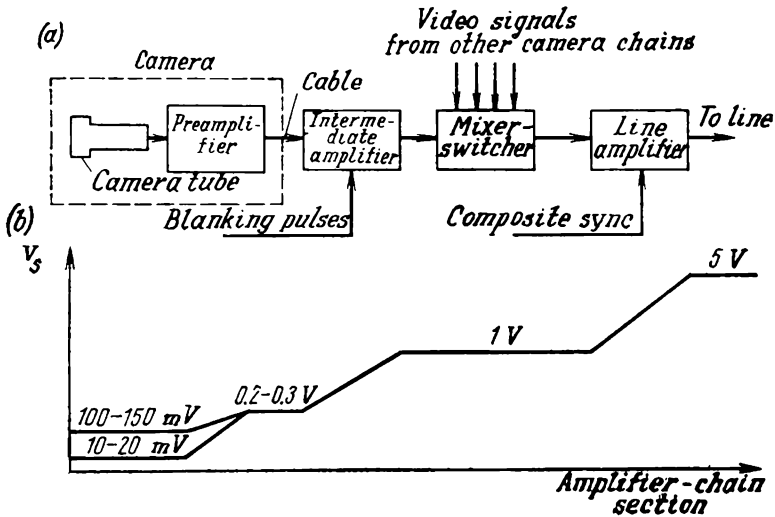


Fig. 8.4. Amplifier chain of a TV centre
(a) block diagram; (b) level diagram

video signal of 5 V. From the line amplifier, the video signal is channelled by a cable line to a VHF/UHF transmitter station which has separate transmitters for video and sound, suitable antennas, transmission lines and auxiliary facilities.

Power for the studio, control rooms, lighting systems, ventilation, etc. comes from an associated power plant which also incorporates step-down and stabilizing devices. The auxiliary services make scenery and stage props, do the film dubbing, etc.

Local TV centres are usually organized along the same lines but on a more modest scale and have therefore limited programming capabilities.

A field camera unit is usually arranged in a van. A block diagram of a field camera unit is shown in Fig. 8.5. The field cameras are usually installed in, say, a theater, a stadium, and the like. Signals are relayed over cables to the equipment installed in the van. The camera chain of a field camera unit incorporates an intermediate

picture amplifier, 2, a mixer-switcher, 4, and a line amplifier (main and reserve), 5. There is also a picture monitor, 3, to observe the picture quality. All these units are built into a control console at which the production supervisor is sitting. From the line amplifier, the video signal is fed to the transmitter control units, 6, and also, over cables, to radio transmitters, 7. Field-camera units usually employ UHF or SHF transmitters which are installed together with their parabolic antennas either on the TV van or the roof of a nearby building. One transmitter is held in reserve and the other is operating.

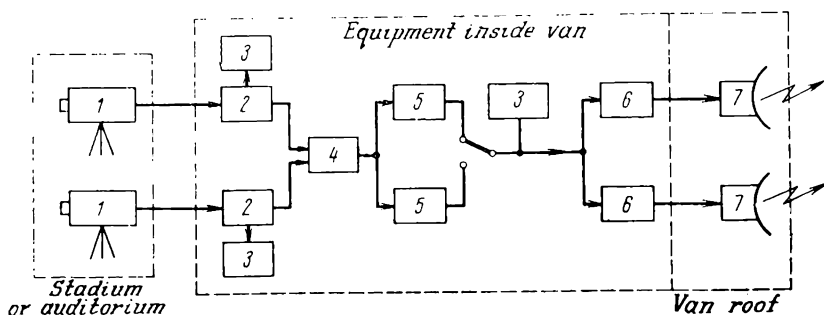


Fig. 8.5. Block diagram of a field camera unit

1—camera; 2—intermediate picture amplifier; 3—picture monitor; 4—mixer-switcher; 5—line amplifier; 6—transmitter control unit; 7—transmitters and parabolic antennas

Their antennas are oriented to point precisely at the TV centre tower. The receiving antennas of the TV centre are mounted at the top of the microwave tower so as to be on the line-of-sight to the field camera unit. The signals they pick up are then amplified and fed to the modulator of the TV centre transmitter.

The Ostankino TV engineering centre in Moscow, which is Europe's largest, occupies a huge building with a space of 1,100,000 cubic metres. The TV transmitter mounted on a tower standing 533 m high (including its antennas) enables TV programs to be received on a regular basis within a radius of 160 to 170 km. The Centre turns out six TV programs (including one colour) which total between them up to 50 hours a day, and produces feature films totalling 200 hours and documentary films totalling over 1000 hours a year. The Centre also includes eleven field camera units, the former Shabolovka TV centre in Moscow, a TV theatre, and stationary TV relay stations.

The core of the Ostankino complex is 21 TV studios with a total floor area of about 10,000 m², including ten production studios (one occupying 1000 m², four 600 m² each, and five 150 m² each), seven programming studios of 60 m² each, and four motion-picture studios (one 1000 m² in floor area and three 600 m² each). The studios are equipped with air conditioners, three studios have mechanisms to

position the stage at any height. The lighting systems in the studios are remotely controlled to a predetermined program so that the illumination found to be the best during rehearsals can be reproduced exactly. All production studios have systems to supply water and compressed air to simulate the wind, rain, and the like. With each studio are associated an actors' room, a make-up room, etc.

Each studio-control section includes an engineering control room, a video engineer room, an audio engineer room, a lighting control room, a film camera control room, a video recording control room, etc. The total floor area occupied by the studio-control section including a 600-sq.m studio is 2500 to 8000 m². Each studio-control section at the Ostankino Centre has capabilities comparable with those of a fairly large TV centre.

In its organization and set-up, the Ostankino Centre markedly differs from the ordinary TV centre shown in block-diagram form in Fig. 8.1. It has been designed as a nation-wide facility with a large amount of production. Since wide use is made of external programming sources and video recording, many programs are produced by a separate program-control section which has equipment similar to that of the studio-control unit, but with wider switching capabilities.

In producing a program, a program director at the Ostankino Centre may use up to 50 signal sources, including 40 external sources and ten local sources. The external sources include the studio-control units of the Centre and the remaining program-control units, the video recording unit, field-camera units, and relay transmitters. The local sources are the announcer's cameras, the studio cameras, the video tape recorders, etc. The program director's room houses the video and sound engineers' consoles, a rack carrying picture monitors, sound tape recorders, a console for remote control of the announcer's cameras, and a program control unit.

The engineering control room is situated next to the director's room and separated from it by a window. Standing next to the window is the video engineer's console in front of which are arranged the camera-chain, signal-regeneration and monitoring and testing cabinets. The remaining equipment is built into cabinets arranged along the walls of the room. The video engineer's console carries all the operation controls of the cameras and camera chains (f-setting, gain, correction signal level, etc.), adjustments of the video signal regeneration units. This arrangement of the console and controls enables the video engineer to keep watch on all signals at a time and carry out whatever adjustments may be necessary.

The central control room at the Ostankino Centre is a complex of switching and channelling equipment. It accepts signals from all sources utilized by the directors to produce their programs, namely from the ten studio-control sections, the seven program-control

sections, the video recording section, the Shabolovka studio, city and intercity relay lines. From the central control room, the programs are relayed to the TV transmitters, the intercity program exchange room, and to some auxiliary services.

8.3. TV Cameras

A television camera converts the optical image to be televised into electric signals. In the Soviet Union, television centres use image orthicon studio cameras and vidicon announcer cameras.

For a number of years, the Soviet TV centres used KT-5A image iconoscope cameras first made in 1952 and KT-6 image orthicon

cameras dating back to 1954. They were followed by the KT-87 cameras (Fig. 8.6) designed specifically for the Ostankino Centre and using 114-mm image orthicons (the ЛН-221 for studio work and the ЛН-222 for field work) and KT-91 announcer cameras using the ЛН-421 vidicon.

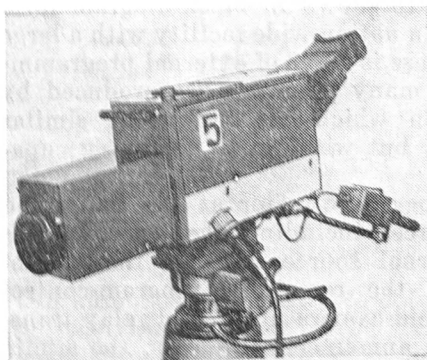


Fig. 8.6. External appearance of a KT-87 television camera

A simplified block diagram of a TV camera is shown in Fig. 8.7. An image of the scene being televised is thrown by a light optical system, 1, onto the photocathode of the camera tube, 2. The light optical system may be a comp-

lement of light lenses mounted on a turret at the front of the camera, or a zoom lens (a lens whose focal length or angle of view can be adjusted continuously without losing the focus). In the former case, the focal length is changed in steps by turning the handle of the lens turret. In the latter, this is done continuously by changing the relative position of the lens elements.

The camera tube is enclosed in a deflection-focusing system, or yoke, which focuses the scanning beam (coil 3) and deflects it (coil 4). From the camera tube, the signal voltage, V_s , is fed to a picture preamplifier, 5, whence (output *b*) it is channelled over the camera cable to the camera-control unit.

During retrace, the beam of the camera tube is cut off by blanking pulses coming in the camera over the camera cable. As a rule, the camera cable has three coaxial conductors for the video signal and the sync pulses intended for the scanning generators, and 21 to 28 con-

ductors varying in cross-sectional area to energize and control the camera. The sawtooth currents required for line and frame scans come from the line and frame scan generator units, 6. The sync pulses supplied by the sync generator amplifier-distributor are applied to inputs *d* and *e* of the camera. The camera-tube blanking pulses applied to input *c* are first amplified by an amplifier, 7.

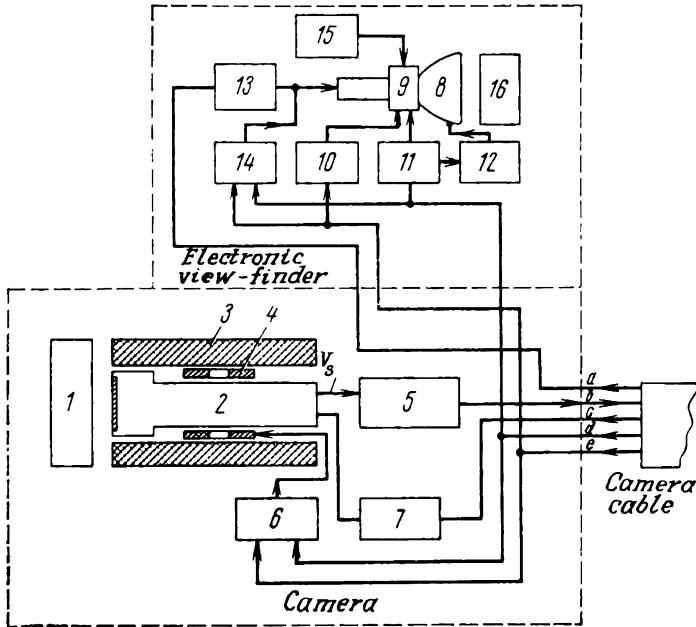


Fig. 8.7. Block diagram of a television camera

1—optical system; 2—camera tube; 3—focusing coil; 4—deflection yoke; 5—preamplifier; 6—sweep unit; 7—blanking pulse amplifier; 8—picture tube; 9—picture-tube deflection yoke; 10—vertical scanning generator; 11—horizontal scanning generator; 12—HV rectifier; 13—video amplifier; 14—picture-tube blanking-pulse mixer; 15—current stabilizer; 16—magnifier

Television cameras are usually fitted with an electronic viewfinder which is a small picture monitor using a miniature picture tube, 8. The viewfinder has a frame scan generator, 10, and a line scan generator, 11, to scan its electron beam. Anode voltage for the viewfinder picture tube is supplied by an HV rectifier, 12. Viewfinders ordinarily use magnetically focused picture tubes. The current traversing the focusing coil of the picture-tube deflection yoke 9 is stabilized by a current stabilizer, 15. The video signal fed to the viewfinder comes over the camera cable from the control room where it is processed as required. The video amplifier, 13, gives it an additional amplification. Blanking pulses for the picture tube are supplied by the

mixer, 14. In front of the viewfinder screen there is a magnifier, 16, which magnifies the image 1.5 to 2 times for convenient observation.

An electronic viewfinder adds to the complexity of the camera, and increases its weight and size. Yet, its advantages over the optical variety (such as used on photographic cameras) are such that it is now universally employed. Electronic viewfinders are free from variations in picture brightness with scene illumination, parallax error and the need to adjust the optical section each time the lens is changed; the quality of focus can be checked by the image viewed.

From reference to a complete block diagram of a television camera it will be seen that it includes a number of auxiliary circuits and elements which make unnecessary camera adjustment during operation and facilitate the alignment and adjustment of the camera units prior to air time.

One of the mounting arrangements for studio and field cameras is a studio pedestal. When mounted on a studio pedestal the camera can be moved freely about the studio, lifted and lowered above the floor, panned and tilted as required.

Television cameras use lenses differing in viewing angle so as to produce images to different scales. According to the viewing angle there may be (1) narrow-angle (15 to 20°) or telephoto lenses; (2) universal lenses (with a viewing angle of 20 to 60°) and (3) wide-angle lenses (with a viewing angle of more than 60°). Most often, use is made of universal lenses because they suit the scenes most often televised and have a sufficiently high speed. The Soviet-made universal lenses include the HELIOS-40T (with a viewing angle of 28°) and the ERA-1TV (with a viewing angle of 34°). The letters "T" and "TV" stand for "television". Narrow-angle or telephoto lenses are used for close-ups, and they are usually employed in mobile field cameras. When a close-up lens is swung in instead of a universal one, the televiewer feels as if he is moving towards the object or scene being televised. Typical close-up lenses of Soviet manufacture are the TAIR-11TV (with a viewing angle of 8°) and the OT-500 (with a viewing angle of 4.7°). Wide-angle lenses are used in cases where wide-angle location shots are to be made. Among them are the Soviet-made ORION-15 (with a viewing angle of 75°), and the MIR-1 (with a viewing angle of 60°). The lens complement of a camera is mounted on a lens turret screwed into the front of the camera case. Positioning of each lens in front of the pick-up tube is accomplished by means of a handle and a mechanical detent.

Wider capabilities are offered by zoom lenses. As already noted, the focal length or viewing angle of a zoom lens can be adjusted continuously without the loss of focus, and this appears to the viewer as if he is approaching or receding from the scene. For example, a zoom lens can track a football player across the entire width or length of the football field while keeping in the correct proportion the

size of the player and ball. Present-day zoom lenses are elaborate optical systems. In order to adjust the focal length without affecting the focus of the image on the photocathode, the individual lens elements are moved relative to one another. As will be recalled, motion of a lens element relative to another along the optical axis changes

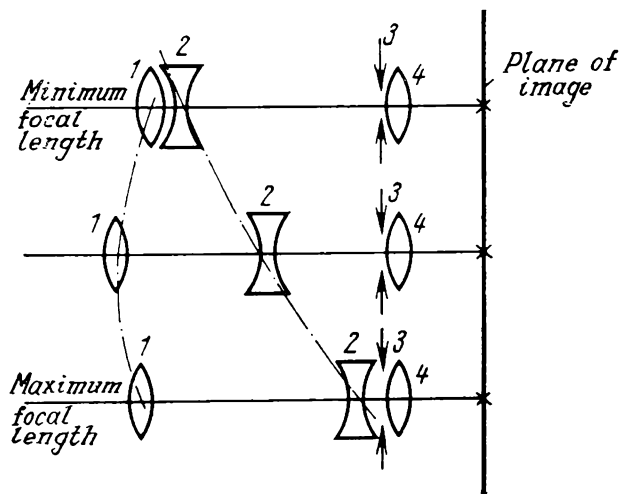


Fig. 8.8. Optical train of a zoom lens

1—positive lens; 2—negative lens; 3—aperture stop; 4—fixed lens

the total focal length of the entire system. For example, if we change the spacing d between two lens elements with focal lengths f_1 and f_2 , the total focal length of this two-element system defined as

$$f_{tot} = \frac{f_1 f_2}{f_1 + f_2 - d}$$

will change too. However, the change in the focal length in this case would cause the plane of the image to move relative to the plane of the tube photocathode as well. To keep the image plane in a fixed position, one more lens element has to be moved in addition to the elements that change its focal length.

The optical arrangement of a zoom lens is illustrated in Fig. 8.8. The focal length is varied by moving a negative lens, 2 (shown by the dash-dot line). The change in the position of the image plane is compensated for by moving the front positive lens element, 1. The opening of the diaphragm, 3, placed in front of the stationary lens element, 4, is adjusted as the focal length is varied so as to maintain a constant f -number of the lens and, as a consequence, a constant illumination of the photocathode.

8.4. Television Film Equipment

Motion-picture films account for a considerable share of the TV broadcasting time total. Three film widths are generally used in the motion-picture industry: 35-mm, 16-mm and 8-mm. The first is mostly used for feature films, while 16-mm and 8-mm sizes are used

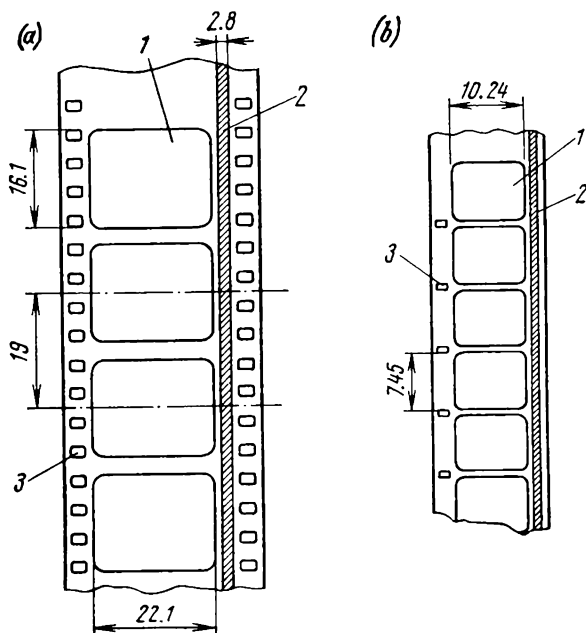


Fig. 8.9. Utilization of (a) 35-mm film; (b) 16-mm film
1—frame; 2—sound track; 3—perforations

for TV documentaries and also for home movies. The arrangement of frames and sound tracks on 35-mm and 16-mm film is shown in Fig. 8.9. As is seen, each frame occupies only a part of the film width, the remainder being taken up by the sound track and perforations. The perforations are provided in order that the film can be intermittently pulled through the film gate both at shooting and projection. The frame rate of motion-picture film is 24 frames per second, each frame being actually at rest in the film gate during its exposure onto the screen. As the film is pulled down, a shutter interrupts the light flux passing through the film so as to avoid smearing the image on the screen. The shutter opens only when the next frame takes up a stationary position in the film gate.

Operation of a television motion-picture projector is illustrated in Fig. 8.10. Light from a light source, 1, is thrown by a mirror, 2, and lenses, 3 and 5, onto the surface of the film, 6. The size of the image being formed is limited by an opaque film gate, 7. Another lens, 8, forms an image of each frame on the target of a film pickup tube, 9. The light flux is interrupted by a shutter, 4, which rotates at 3000 rpm. The film is pulled down intermittently by a claw, 12, as it enters the perforations in the film.

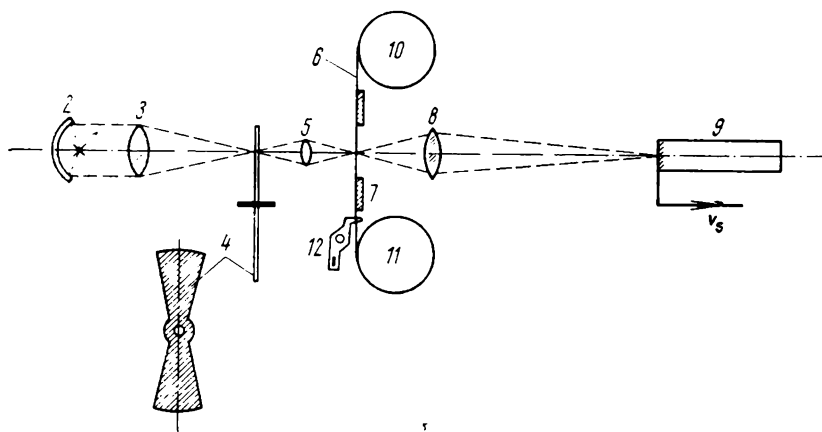


Fig. 8.10. Optical train of a television motion-picture projector
 1—light source; 2—reflecting mirror; 3—objective lens; 4—shutter; 5—lens; 6—film; 7—film gate; 8—lens; 9—camera tube; 10—supply reel; 11—take-up reel; 12—claw

tube, 9. The light flux is interrupted by a shutter, 4, which rotates at 3000 rpm. The film is pulled down intermittently by a claw, 12, as it enters the perforations in the film.

Motion pictures are usually taken at 24 frames per second. If a motion-picture film were shown at the same frame rate, the spectator would notice the flicker. To avoid this, the light flux must be additionally interrupted between frames. In the plot of Fig. 8.11, the black squares correspond to the time intervals when no light is supplied to the film and the film is being pulled down; the shaded squares correspond to the time intervals when the light flux is additionally interrupted by the shutter while the film is at rest. As is seen from Fig. 8.11a, each frame is exposed twice, and the total number of flashes per second is doubled, that is, the film is exposed at 48 flashes per second which is above the flicker rate. For comparison, the plot of Fig. 8.11b shows the frame scanning rate used in television. The black stripes (1.6 ms) correspond to the frame retrace intervals. If a film frame image were formed on the target of a camera pickup tube (usually, the vidicon), the target would be illuminated by short light pulses or flashes (represented by the unshaded squares in the plot of Fig. 8.11b). However, the motion-picture projector and the camera would be operating out of synchronism. As follows from

Fig. 8.11a and b, the time taken to pull down the motion-picture film is considerably longer than the frame retrace time. The pull-down time is 10.6 ms, which is 25% of the motion-picture frame time; the retrace time in television does not exceed 8% of the frame scan period. As a result, one part of each television field would be scanned when the target is illuminated and another part when the target is dark. Scanning while the target is dark ("memory" operation)

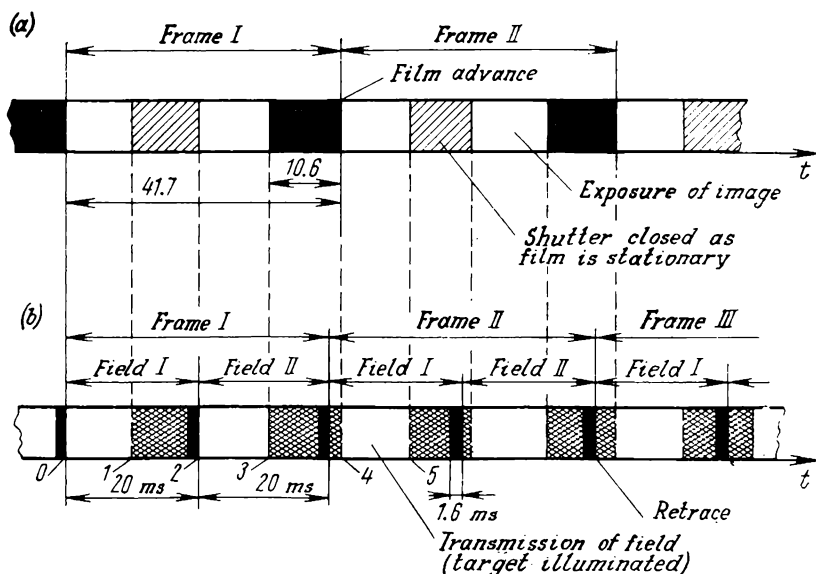


Fig. 8.11. Frame sequencing in (a) motion pictures and (b) television

somewhat reduces the output signal of the tube and the contrast of that part of the image which is scanned dark. In Fig. 8.11b these time intervals are represented by doubly shaded squares. Lack of synchronism between film pull-down and frame scanning would shift the point where the interruption of light begins (points 1, 3, and 5 in Fig. 8.11b) relative to the point where the scanning of the field starts (points 0, 2, and 4), and move vertically the area reproduced at reduced contrast. These distortions can be avoided by pulling down the film at 25 frames per second as in television and by reducing the pull-down time to 1.6 ms, that is, making it equal to the frame retrace time. Increasing the motion-picture frame rate to 25 per second poses no technical difficulties, nor does it entail any marked distortion in the image. The increase in the motion-picture pull-down rate is a mere 4% of the rate adopted in motion-picture projection. The distortions caused in moving objects are passed

unnoticed to the eye. There is no excessive change of pitch in the sound either.

The second problem of reducing the film pull-down time to 1.6 ms (that is, by a factor of six) runs into serious difficulties because the mechanical load on the film would increase 35 to 40 times. Ordinary 35-mm film cannot stand load of this magnitude and breaks down. This is why television film projectors use the ordinary pull-down mechanisms but the frame rate of film is stepped up to 25 per second. With this arrangement it is possible to bring the film motion into coincidence with the television frame rate. As before, part of the image is scanned while the target is dark. However, with the vidicon film camera the attendant distortion remains unnoticeable. The photoelectric component of time lag in the vidicon (see Sec. 7.10) is responsible for the fact that the signal generated when the target is illuminated differs but little from that generated when the target is dark ("memory scanning"). It is likewise important that when a motion-picture projector and the associated television film camera run in synchronism, the image will always be distorted within the same portion of the raster, the distortion will be stationary and therefore hardly noticeable. The vidicon target is illuminated 30 to 50% of the field time.

8.5. Amplification of the Video Signal in TV Cameras (Noise Compensation)

In the image iconoscope and vidicon, the signal current usually is 0.1 to 0.3 μA . Amplification of a weak signal like that runs into certain technical difficulties, primarily because of the presence of noise in the amplifier. This noise arises basically from two sources: the random thermal motion of electrons in conductors and random emission of electrons from thermionic and photoelectric cathodes. The former is known as thermal or Johnson noise and the latter shot noise.

In a television camera, noise mainly originates in the camera tube, the tube load resistor from which the video signal is taken, and the preamplifier tube (or transistor). The succeeding stages contribute progressively less noise, and their share may in a first approximation be neglected.

Thermal, or Johnson, noise is proportional to the absolute temperature and the bandwidth according to the following formula:

$$\bar{v}_t^2 = 4kTR\Delta f \quad (8.1)$$

where \bar{v}_t^2 = mean square of thermal noise voltage
 k = Boltzmann's constant, $k = 1.38 \times 10^{-23}$ J deg $^{-1}$
 T = absolute temperature, Kelvin

R = resistance, ohms

Δf = bandwidth over which thermal noise is determined, Hz

The maximum frequency of the television signal, $f_{\max} = 6.5$ MHz, is many times the minimum frequency, $f_{\min} = 50$ Hz. Therefore, without impairing accuracy, we may put in Eq. (8.1) that

$$\Delta f = f_{\max} - f_{\min} \approx f_{\max}$$

If the resistance of the load resistor is sufficiently high, at frequencies close to f_{\max} account must be taken of the shunting effect produced by stray capacitances in the circuit. Then Eq. (8.1) need only take account of the resistive component of impedance.

The mean square of shot noise current is defined as

$$\bar{i}_{sh}^2 = 2i_0 e \Delta f \quad (8.2)$$

where \bar{i}_0 = average of full emission current

e = electron charge, 1.6×10^{-9} C

Δf = bandwidth assumed equal to f_{\max}

Equation (8.2) applies where the device (say, a tube) is operating in the saturation region. If there is a space charge near the cathode, the equation should be modified to include a correction factor covering the attenuation of the shot current (usually 0.5 or 0.6).

It is customary to assess noise in amplifying tubes and field-effect transistors in terms of the equivalent noise resistance, R_n . By definition, R_n is a noisy (fictitious) resistor such that when the thermal fluctuations arising across it are applied to the control grid of an idealized (shot-free) tube, the plate current will suffer fluctuations equal to those in a real tube. The noise resistance of amplifying tubes is usually stated in their data sheets. Also, it may be computed by the following equations:

for a triode

$$R_n = (2.5 \text{ to } 3.5)/g_m \quad (8.3)$$

where g_m is the transconductance of the tube;

for a pentode

$$R_n = (2.5/g_m) \frac{i_p}{i_p + i_{sc}} (1 + 8i_{sc}/g_m) \quad (8.4)$$

where i_p is the plate current and i_{sc} is the screen-grid current;

for a field-effect transistor

$$R_n = 0.7/g_m \quad (8.5)$$

The noise contributed by various elements of the television camera can be expressed as follows. The rms shot noise current in the scanning beam of the pickup tube is

$$\sqrt{\bar{i}_n^2} = \sqrt{2e i_b f_{\max}} \quad (8.6)$$

For $i_b = 5 \times 10^{-7}$ A (the vidicon tube), $f_{\max} = 6.5$ MHz, and $\sqrt{i_n^2} \approx 1 \times 10^{-9}$ A.

Assuming (from practice) that the vidicon signal current is $i_s = 0.2 \mu\text{A}$, the signal-to-rms noise ratio of the tube will be

$$\psi_t = i_s / \sqrt{i_n^2} = (0.2 \times 10^{-6}) / (1 \times 10^{-9}) = 200$$

The actual signal-to-noise ratio for the vidicon is somewhat lower because in the above calculations we have omitted the fluctuations due to the equivalent resistance of the target.

Let us determine the signal-to-noise ratio at the amplifier output, neglecting the fluctuations due to the camera tube and assuming that all noise comes from the load resistor of the tube and the first amplifier stage. We shall also assume that the gain K_0 of the amplifier is flat over the frequency range of interest. Then the mean square value of voltage due to thermal fluctuations at the output of this amplifier will be

$$\bar{v}_{i, \text{out}}^2 = 4kTR_L K_0^2 f_{\max} \quad (8.7)$$

The shot noise due to the first stage is

$$\bar{v}_{sh, \text{out}}^2 = 4kTR_n K_0^2 f_{\max} \quad (8.8)$$

The total mean square value of noise at the amplifier output is

$$\bar{v}_{n, \text{out}}^2 = \bar{v}_{i, \text{out}}^2 + \bar{v}_{sh, \text{out}}^2 = 4kTK_0^2 f_{\max} (R_L + R_n) \quad (8.9)$$

Since a camera pickup tube is a current generator, the signal voltage at the amplifier output may be defined as

$$v_{s, \text{out}} = i_s R_L K_0 \quad (8.10)$$

On the basis of Eqs. (8.9) and (8.10) the following expression may be written for the signal-to-noise ratio

$$\psi_{\text{out}} = v_s / \sqrt{\bar{v}_{n, \text{out}}^2} = i_s R_L / \sqrt{4kTf_{\max} (R_L + R_n)} \quad (8.11)$$

For $R_n = 500$, $i_s = 0.2 \mu\text{A}$, and $R_L = 1$ kilohm, $\psi_{\text{out}} \approx 15.5$.

From comparison of the above result with the signal-to-noise ratio deduced earlier it is seen that the ratio has been reduced to less than one-tenth of its former value. In other words, the signal-to-noise ratio at the output of a television camera is wholly decided by the quality of the preamplifier. This finding holds for the vidicon and image iconoscope. In the case of the image orthicon, the share of fluctuation noise contributed by the preamplifier is negligible, because the output signal current is 80 to 100 μA , or 800 to 1000 times as great as the vidicon signal. The signal-to-noise ratio for a camera using the image orthicon is completely controlled by the quality of the pickup tube used.

In determining ψ_{out} , we have assumed that the gain is flat over the bandwidth of the amplifier. To meet this condition, the load resistor has been chosen to be sufficiently small ($R_L = 1$ kilohm), so that the input circuit made up of the parallel connection of R_L and shunt capacitance C_L (Fig. 8.12a) will not introduce frequency distortion.

It is possible to raise the signal-to-noise ratio by using a higher value for R_L and by compensating the ensuing frequency distortion

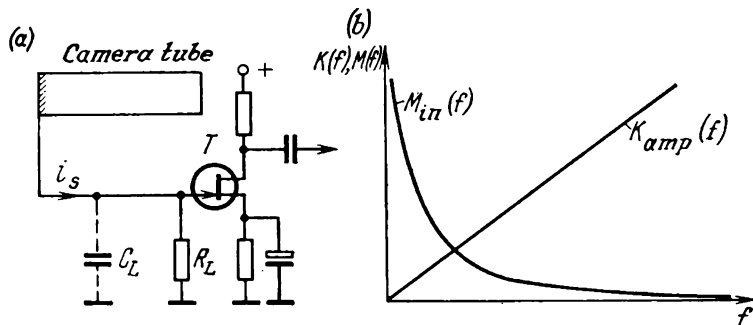


Fig. 8.12. Shunt resistive noise compensation
(a) input circuit; (b) frequency response of the input circuit and amplifier

in the amplifier. This method, shunt resistive noise compensation, was proposed by G.V. Braude of the Soviet Union in 1933. It boils down to the following.

A pickup tube may be looked upon as a current generator with a high internal resistance, R_i , running into 10^6 to 10^7 ohms. For $R_L \leq 0.1R_i$, it is safe to assume that the signal current, i_s , is independent of the load resistance, R_L , and, as a consequence, the voltage at the amplifier input is proportional to the load resistance. The idea underlying the resistive noise compensation is to reduce the effect of the internal noise in the amplifier by increasing the amplitude of the output signal. This is achieved by selecting high values for the load resistor (of the order of 10^4 to 10^6 ohms). In considering what happens in the amplifier input circuit at a high value of R_L (see Fig. 8.12a), it is important to take account of the shunt capacitance, C_L . It is a combination of the input capacitance of the transistor (or tube), the output capacitance of the pickup tube, and the wiring capacitance, and usually is 35 to 50 pF. In the high-frequency end of the range, the impedance of the $R_L C_L$ network falls, and this brings about a reduction in the output signal.

The dependence of the magnitude of frequency distortion on frequency may be expressed as

$$|M_{in}(f)| = 1/\sqrt{1 + 4\pi^2 f^2 R_L^2 C_L^2} \quad (8.12)$$

A plot of the function $|M_{in}(f)|$ appears in Fig. 8.12*b*. This distortion is equivalent to the action that an integrating network with a time constant $R_L C_L$ can produce on the signal. At high values of R_L the distortion of the video signal in the input circuit becomes prohibitively heavy, and it must be compensated for in a succeeding stage of the amplifier. For complete compensation it is important that the gain of the amplifier be

$$|K_{amp}(f)| = K_0 \sqrt{1 + 4\pi^2 f^2 R_L^2 C_L^2} \quad (8.13)$$

where K_0 is the low-frequency gain. A plot of Eq. (8.13) appears in Fig. 8.12*b*. The resultant gain of the preamplifier, with account taken of the input circuit, is

$$|M_{in}(f)| \cdot |K_{amp}(f)| = K_0 = \text{constant} \quad (8.14)$$

This improvement in the signal-to-noise ratio may be explained as follows. The output signal of the amplifier is proportional to the load resistance, R_L . The rms value of thermal noise, $\sqrt{\bar{v}_{t,out}^2}$, as follows from Eq. (8.7), is proportional to $\sqrt{\bar{R}}$. Hence, an increase in R_L causes the signal-to-noise ratio to increase in proportion to $\sqrt{\bar{R}_L}$. This conclusion applies to relatively low values of R_L where the shunting effect of stray capacitances is nonexistent. At higher values of R_L , the improvement in the signal-to-noise ratio is proportional to $\sqrt{\bar{R}_L}$ at low frequencies only. The limit for the increase in R_L is set by the possibility of h.f. compensation in the amplifier. There is another factor responsible for the increase in the signal-to-noise ratio: resistive noise compensation causes the signal to increase at low and medium frequencies, and the effect of noise existing in the first amplifier stage is reduced.

The signal-to-noise ratio in the case of resistive noise compensation may be computed as follows. The mean square value of the thermal noise due to R_L at the amplifier output, subject to Eq. (8.14), is given by

$$\bar{v}_{t,out}^2 = 4kTR_L K_0^2 f_{\max} \quad (8.15)$$

The mean square value of the shot noise due to the first stage as measured at the amplifier output is

$$\bar{v}_{sh,out}^2 = 4kTR_n \int_{f_{\min}}^{f_{\max}} |K_{amp}(f)|^2 df \quad (8.16)$$

Substituting for $|K_{amp}(f)|$ from Eq. (8.13), setting $f_{\min} = 0$ and integrating, we get

$$\bar{v}_{sh,out}^2 = 4kTR_n K_0^2 f_{\max} \left(1 + \frac{4\pi^2 C_L^2 R_L^2 f_{\max}^2}{3} \right) \quad (8.17)$$

The mean square value of the total noise voltage at the amplifier output is

$$\begin{aligned}\bar{v}_{n, out}^2 &= \bar{v}_{i, out}^2 + \bar{v}_{sh, out}^2 \\ &= 4kTK_0^2 f_{\max}^2 \left[R_L + R_n \left(1 + \frac{4\pi^2 C_L^2 R_L^2 f_{\max}^2}{3} \right) \right]\end{aligned}\quad (8.18)$$

and the signal-to-noise ratio is

$$\psi'_{out} = \frac{i_s R_L}{2 \sqrt{kT f_{\max} \left[R_L + R_n \left(1 + \frac{4\pi^2 C_L^2 R_L^2 f_{\max}^2}{3} \right) \right]}} \quad (8.19)$$

For $C_L = 20$ pF, $i_s = 0.2$ μ A, $R_L = 100$ kilohms and $R_n = 500$ ohms, $\psi'_{out} = 55$.

From comparison of ψ'_{out} with ψ_{out} , Eq. (8.11), found for the case where no noise compensation is employed ($R_L = 1$ kilohm), it is seen that the improvement in the signal-to-noise ratio is by

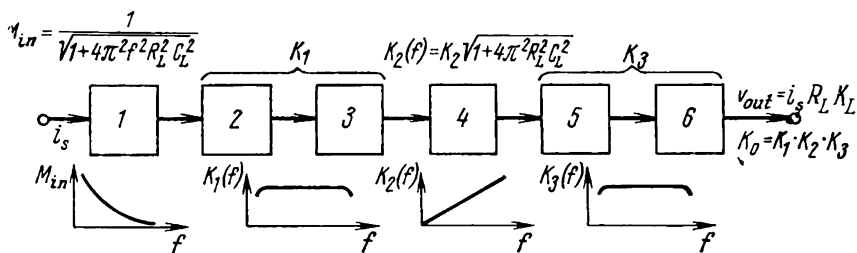


Fig. 8.13. Block diagram of a preamplifier using shunt resistive noise compensation

1—input circuit; 2—first stage; 3 and 5—wide-band amplifier stages; 4—input-circuit compensation stage (differentiating stage); 6—matching stage

a factor of 3.5. Thus, an increase in load resistance combined with the subsequent frequency compensation substantially improves the signal-to-noise ratio at the amplifier output.

In block-diagram form, a preamplifier employing resistive noise compensation is shown in Fig. 8.13, where at 2, 3 and 5 are broad-band amplifier stages, at 4 is the frequency compensation stage for the input circuit, and at 6 is a stage (usually, a cathode- or an emitter-follower) to match the output impedance of the amplifier to the characteristic impedance of the camera cable. The overall low-frequency gain is $K_0 = K_1 K_2 K_3$. The camera preamplifier may be built around transistors or tubes. The crucial factor is the choice of the amplifying element for the first stage. It should have a low intrinsic noise and a high input resistance. The latter requirement is important because the input impedance of the stage is connected across the load resistor,

R_L . With a low input impedance, the total load resistance may turn out to be insufficient for noise compensation. Vacuum tubes possess a higher input resistance than bipolar transistors. Therefore the input stage of the camera preamplifier is often built around tubes (or nuvistors), and the remaining stages around transistors. Field-effect transistors having high input resistance (such as the Soviet-made КП303) enable the noise-compensated camera preamplifier to be based wholly on transistors.

A frequency compensation stage for the input circuit of the camera preamplifier is shown in Fig. 8.14. To obtain the desired frequency response, the circuit utilizes resistive-capacitive current feedback. To this end, the resistor (R_4 and part of R_5) in the emitter lead is bypassed by a low-value capacitor, C_2 . At low frequencies, the shunting effect of C_2 may be ignored. As a result, a large amount of negative feedback is applied, and the stage gain is greatly reduced.

With increasing frequency, the shunting effect of C_2 increases, thereby bringing down the amount of negative feedback and raising the stage gain. By appropriately adjusting the amount of negative feedback with the potentiometer R_5 and the variable capacitor C_2 , it is possible to compensate for frequency distortion in the input circuit completely.

In 1941, Braude proposed an improved series-inductive circuit for noise compensation based on the inclusion of an inductance in the load impedance. More specifically, the pickup tube is loaded into a filter (Fig. 8.15a) made up of the output capacitance C_1 of the pickup tube, the input capacitance C_2 of the amplifier and the inductance L of a series coil. As with shunt resistive compensation, the value of R_L is chosen sufficiently high. By adjustment of its circuit parameters, the L -section filter is tuned to resonate at one of the mid-frequencies of the television signal spectrum. The resonant frequency is defined as

$$f_r = 1 / \left(2\pi \sqrt{L \frac{C_1 C_2}{C_1 + C_2}} \right) \quad (8.20)$$

As a rule, $f_r = 1/\sqrt{2} f_{\max}$. As is shown in Fig. 8.15b [curve $M'_{in}(f)$], the signal markedly rises in magnitude at the resonant frequency. To compensate for the frequency distortion introduced by the input circuit the frequency response of the amplifier must be more elaborate (curve $K'_{amp}(f)$ in Fig. 8.15b).

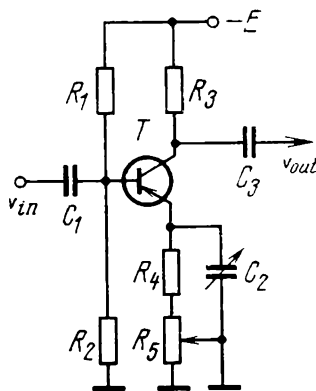


Fig. 8.14. Frequency compensation in the case of shunt resistive noise compensation

The additional improvement (by a factor of 2 to 2.5) in the signal-to-noise ratio provided by the series inductive compensation scheme is due to the fact that the signal is boosted at the input to the

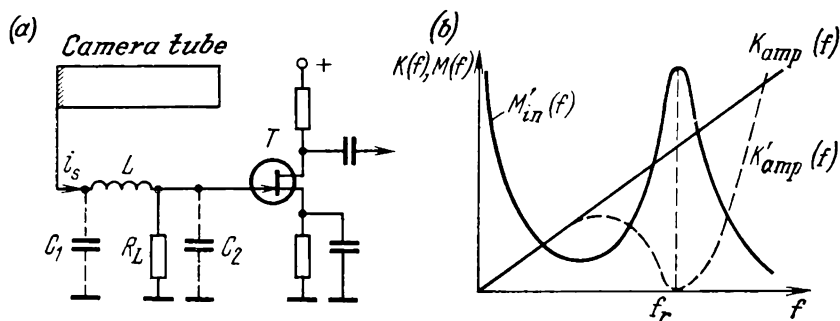


Fig. 8.15. Series inductive noise compensation
(a) input circuit; (b) frequency responses of the input circuit and amplifier

first amplifier stage at frequencies close to f_r and that the effect of thermal noise originating in R_L is reduced. This is also true of the effect produced by the noise originating in the transistor, T (see Fig. 8.15a). The noise power due to the first amplifier stage, as is seen from Eq. (8.16), is proportional to the square of the amplifier gain, $|K^2_{amp}(f)|$ (omitting the input circuit), which is smaller in the case of series inductive compensation (curve $K'_{amp}(f)$ in Fig. 8.15b) than it is with shunt resistive compensation [curve $K_{amp}(f)$].

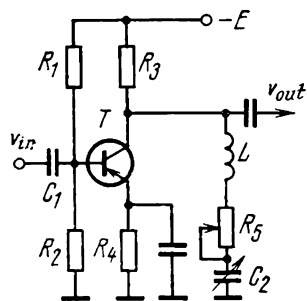


Fig. 8.16. Input-circuit frequency compensation stage near f_r in the case of series inductive noise compensation

To secure the desired frequency response, the amplifier using series inductive noise compensation and a stage which provides continuous high-frequency compensation (see Fig. 8.14) includes a notch network. This form of amplifier stage is shown in Fig. 8.16. At high frequencies, the network LR_5C_2 is placed across the collector load resistor of the

transistor, T . At the resonant frequency, the notch network has a minimum impedance. The frequency response of the amplifier stage incorporating a notch network is shown as the curve $M_{notch}(f)$ in Fig. 8.17. At the resonant frequency, the stage brings down the signal drastically, thereby compensating for the distortion introduced by the input circuit. The notch network can be tuned to

the resonant frequency, f_r , by adjusting the capacitance of the capacitor C_2 . The variable resistor R_5 provides a means for adjusting the network Q -factor and, as a consequence, its frequency response and

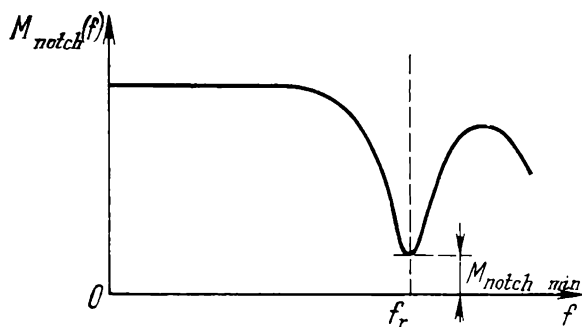


Fig. 8.17. Frequency response of a stage using a notch filter

$M_{notch, \min}(f)$. By appropriately aligning the compensating stages of Figs. 8.14 and 8.16, it is possible to cancel all frequency distortion introduced by the input circuit and to make the amplifier response flat over the entire frequency range.

8.6. D.C. Restoration

As is shown in Chapter 4, the television signal carrying accurate information about variations in the scene luminance contains a direct-current (d.c.) component. As the scene content changes, the d.c. varies slowly, doing so at the rate of 0 to 3 Hz. In view of this frequency, it would appear advantageous to amplify the television signal by d.c. amplifiers. It has proved practicable, however, to transmit the d.c. component in an indirect way, by restoring it at the correct point in the transmission circuit by means of so-called clippers.

Figure 8.18a and b shows the video signals associated with a single line formed in televising an image of two vertical white stripes against a black background, 1, and two black stripes against a white background, 2. The d.c. components, v'_0 and v''_0 , are measured from the horizontal axis to the dashed lines $M'N'$ and $M''N''$, respectively. The dashed lines are drawn at the signal values, v'_s and v''_s , averaged over a line scan period, T_h .

The d.c. component is usually lost during the amplification of the video signal, because the stages of the video amplifier are coupled by d.c. blocking capacitors. Oscillograms of video signals which have lost their d.c. components are shown in Fig. 8.20c and d ($v'_s - v'_0$ and $v''_s - v''_0$). The signal values averaged over a line scan

period, T_h , are equal to zero because the areas under the oscillograms representing the positive and negative values of the same signal voltage (having double and single cross-hatching, respectively) are

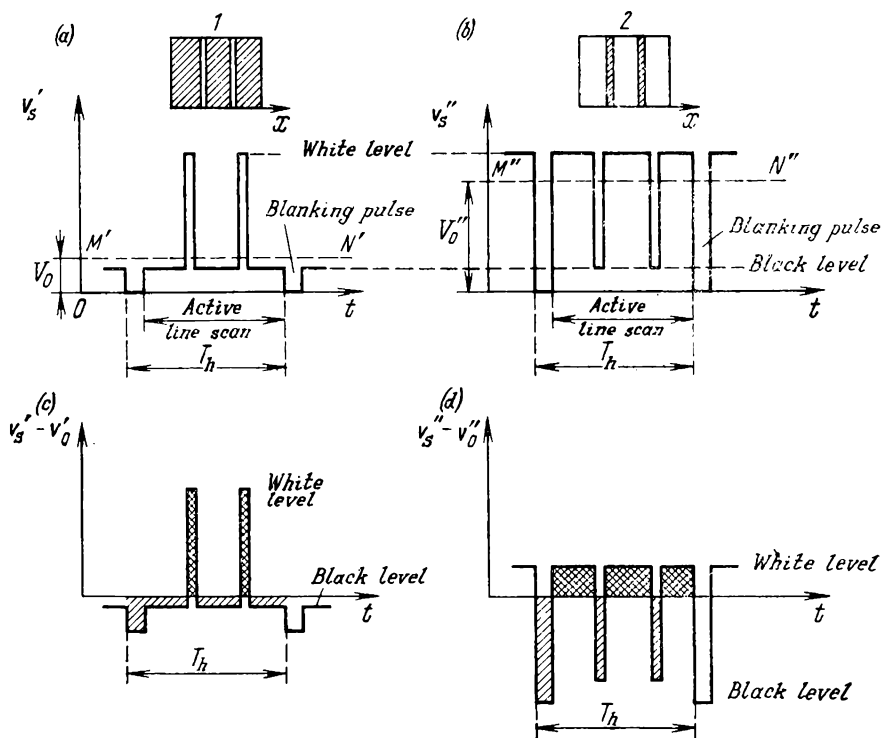


Fig. 8.18. Television signals

(a) and (b) containing d.c. component; (c) and (d) without d.c. component

equal. It can be noted from Fig. 8.18c and d that when the d.c. component is lost the white and black levels have varying voltage.

No accurately scaled reproduction of the luminance values seen by the camera is possible, if an image were reproduced on the picture tube by means of a video signal having no d.c. component. Figure 8.19 shows the light transfer characteristic of a picture tube, that is the screen luminance as a function of the voltage applied to the control grid (modulator), v_M .

Suppose that the video signal applied to the modulator corresponds to case 1 (two white stripes against a black background). Using the BRIGHTNESS and CONTRAST controls on the TV

tude of the d.c. component. Unfortunately, it is not always possible to use the black or white level as reference, because some lines of the image scanned may contain no white or black elements. This purpose can best be served by blanking pulses because they are present in the video signal always. Fixing the tips of blanking pulses at

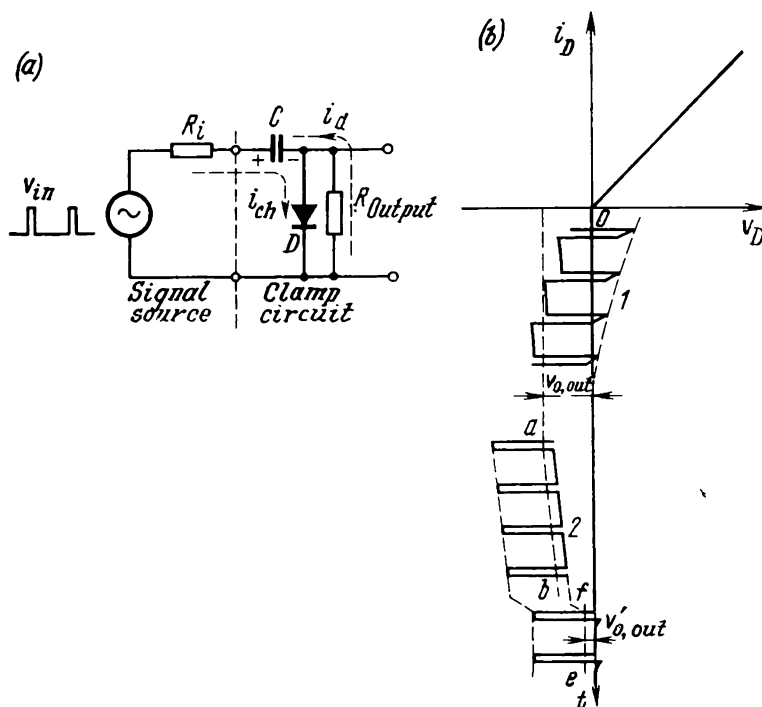


Fig. 8.20. Simple d.c. restorer
(a) circuit; (b) level clamping

a certain d.c. level will automatically restore the d.c. component, provided their position with respect to the white or black level within the video signal does not change in the course of transmission.

Both storage and nonstorage types of television systems (the vidicon, plumbicon and image orthicon tubes in the former case, and the flying-spot and image dissector types, in the latter), when they operate within the linear portion of their light transfer characteristics, generate a video signal where the black level is fixed at the tips of blanking pulses or separated from them by a small amount (set up) which remains unchanged in the course of transmission. This property of the television signal is utilized in order to restore the d.c. component by means of a simple d.c. restorer circuit shown in Fig. 8.20a.

A simple d.c. restorer consists of a diode, D , a resistor, R , and a capacitor, C . The television signal is applied from the source represented in the circuit of Fig. 8.20a by an equivalent generator with an internal impedance R_i . The manner in which the level is fixed will be clear from reference to Fig. 8.20b. When the first pulse is applied to the input of the circuit, a current, i_{ch} , flows through the capacitor C and the diode D , and the capacitor accumulates some charge. Between two pulses, the diode is turned off, and the capacitor C discharges through R , R_i and the signal source. The discharge time constant, $\tau_d = (R + R_i) C$, usually exceeds the charge time constant, $\tau_{ch} = (R_d + R_i) C$ considerably, because the forward resistance R_d of the diode does not exceed a few tens of ohms, while the resistance of resistor R (including that of the nonconducting diode connected in parallel) runs into hundreds of kilohms. Because of this, the discharge between pulses proceeds slowly and the capacitor C loses only an insignificant part of its charge. Each new pulse adds a further portion of energy to the capacitor C and the voltage across it rises continually, which fact causes the output voltage waveform to shift gradually to the left. After several cycles, the pulse tips will be fixed at the zero level (ground potential). The magnitude of the d.c. component appearing at the output of the d.c. restorer in response to signal 1 is $v_{0, out}$. If now signal 2 be applied to the d.c. restorer, the capacitor C will discharge for several cycles until the sync pulse tips are again fixed at zero level. In the steady state, a d.c. component, $v'_{0, out}$, will appear at the restorer output. A disadvantage of this circuit is the difference in the speed of response to a decreasing and an increasing d.c. component. When the d.c. component is increasing (signal 1), the capacitor charges; when the d.c. component is decreasing (signal 2), the capacitor discharges. Since $\tau_d \gg \tau_{ch}$, the fall of the d.c. component at the circuit output to $v'_{0, out}$ takes more time to complete than its rise; this is shown in Fig. 8.20b (regions *ab* and *fe*). Another disadvantage of a simple d.c. restorer is the distortion of the signal waveform (the tilt of the pulse top, Fig. 8.20b).

Better performance is shown by keyed or gated d.c. restorers. The circuit of one such restorer or clamp circuit is shown in Fig. 8.21. The video signal is applied to the input, T_1 . The clamp circuit is placed between T_1 and T_2 . It is made up of diodes, D_1 and D_2 , and resistors, R_3 and R_4 , forming between them a bridge circuit. The potential at point *a* can be set with the variable resistor R_5 . Keying or gating pulses are applied to one pair of opposite junctions, *c* and *d*, via capacitors C_1 and C_2 . The keying pulses follow at line scan frequency, in time with blanking pulses of the video signal, and are taken from terminals 1 and 2 of a transformer. The transistor T_3 amplifies the keying pulses, and the transformer acts as a phase inverter. Terminal 1 furnishes positive pulses, and terminal 2,

internal resistance as practicable. To this end, the transistor T_1 is connected in an emitter-follower circuit. An important advantage of a keyed clamp circuit is a sizeable reduction in the waveform of the signal being clamped, because between pulses both diodes are OFF, and C can only discharge into the high-value reverse resistances of D_1 and D_2 and the input resistance of T_2 . In order to obtain a high input resistance, T_2 is arranged in a common-collector circuit. The diodes D_1 and D_2 are chosen to offer the highest possible reverse resistance and the lowest possible forward resistance.

Gated or keyed restorers have found wide use in TV centre equipment. They are included in the intermediate and line video amplifiers, in the amplifiers of picture monitors, and at the input to the radio transmitter.

8.7. Aperture Compensation

It has been shown in Chapter 1 that aperture distortion is essentially the loss in sharpness of detail and gradations of luminance. In a way, it is not unlike the signal waveform distortion caused by

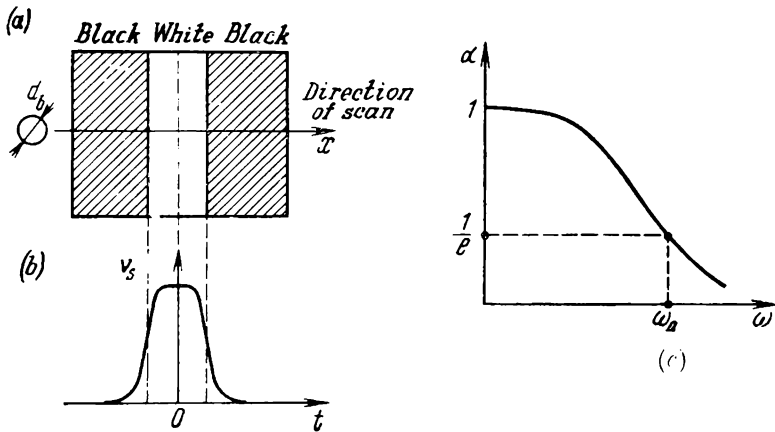


Fig. 8.22. Signal waveform in the case of a symmetrical scanning beam
(a) image transmitted; (b) video signal; (c) approximating function

the drooping high-frequency response of the video circuit. There is, however, a very important difference between them, which necessitates the use of special schemes for the reduction of aperture distortion. In video amplifiers, frequency distortion is usually accompanied by phase distortion. In contrast, aperture distortion, if it has been caused by an electron beam symmetrical in cross-section, will not be accompanied by any phase shift of the individual spectral components. This aspect of aperture distortion is illustrated in Fig. 8.22a and b. When an image of a vertical white stripe against a black

background is scanned by a symmetrical beam with a diameter d_b , the video signal is likewise symmetrical about the vertical axis. In other words, it is an even function, and the train of such pulses may be expressed as a Fourier series containing several cosine terms. Correspondingly, the aperture characteristic must be approximated by an even function.

Aperture correctors may be of any one of two commonly used types. One is based on the use of differentiating networks. Differential aperture compensation reduces to the following. The aperture characteristic is approximated by an even function of the form

$$\alpha = \exp - (\omega/\omega_0)^2 \quad (8.21)$$

where ω_0 is the frequency at which the signal amplitude reduces to $1/e$ of its original value (where e is the base of natural logarithms). Graphically, the function $\exp - (\omega/\omega_0)^2$ is shown in Fig. 8.22c. Equation (8.21) may be expanded into a power series

$$\alpha = \frac{1}{1 + a_1 (\omega/\omega_0)^2 + a_2 (\omega/\omega_0)^4 + a_3 (\omega/\omega_0)^6 + \dots} \quad (8.22)$$

where $a_1 = 1/1!$, $a_2 = 1/2!$, $a_3 = 1/3!$, etc.

An aperture corrector should give a high-frequency boost, that is, have a frequency response (which is opposite in its effect to that above) of the form

$$\alpha_1 = 1 + a_1 (\omega/\omega_0)^2 + a_2 (\omega/\omega_0)^4 + \dots \quad (8.23)$$

Differential aperture compensation reduces to the synthesis of the frequency response described by Eq. (8.23). As follows from Eq. (8.23), the overall frequency response $\alpha_1 = f(\omega)$ may be represented as the sum of frequency response $a_1 (\omega/\omega_0)^2$, $a_2 (\omega/\omega_0)^4$, etc. This type of response can be instrumented with ordinary differentiating networks. The frequency response of a single-section differentiating network (Fig. 8.23a) is defined as

$$A_1(\omega) = (\omega RC) / \sqrt{1 + (\omega RC)^2} \quad (8.24)$$

When the time constant RC is appropriately chosen, the inequality $\omega RC \ll 1$ is satisfied and

$$A_1(\omega) \approx \omega RC \quad (8.25)$$

The phase response then is

$$\varphi_1(\omega) = \pi/2 - \arctan \omega RC \quad (8.26)$$

On satisfying the inequality $\omega RC \ll 1$, we get

$$\varphi_1(\omega) = \pi/2$$

The frequency and phase response of a single-section differentiating network are shown in Fig. 8.23b and c.

It can be shown that a series combination of two differentiating networks will have a frequency response of the form

$$A_2(\omega) = R_1^2 C_1^2 \omega^2$$

and that of four networks

$$A_4(\omega) = R_2^4 C_2^4 \omega^4$$

The phase shift equal to $\pi/2$ for a single-section network rises to π for two networks in series, and to 2π for four networks in series.

In practice, use is made of more elaborate differentiating networks which secure a greater gain and a linear phase response owing to the

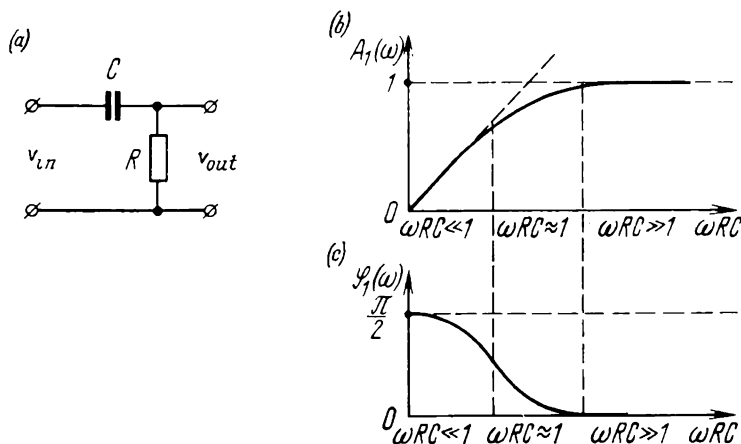


Fig. 8.23. Differentiating network
(a) circuit; (b) frequency response; (c) phase response

use of a greater count of circuit elements. There are also double-differentiation networks which generate a second-derivative signal directly.

In block-diagram form, a differentiating aperture corrector is shown in Fig. 8.24. Here, the drooping high-frequency response is compensated by adding second- and fourth-derivative signals to the main signal. This is done in summators, Σ_1 and Σ_2 . The circuit generating the second-derivative signal contains a phase inverter because a two-section differentiator inverts the phase of the input signal (changes it by π). The delay lines DL_1 and DL_2 provide time match between the main and compensating signals if, instead of simple differentiators, more elaborate networks introducing a time delay are used.

In practice it is common to limit the generation of compensating signals to the second derivative for simplicity.

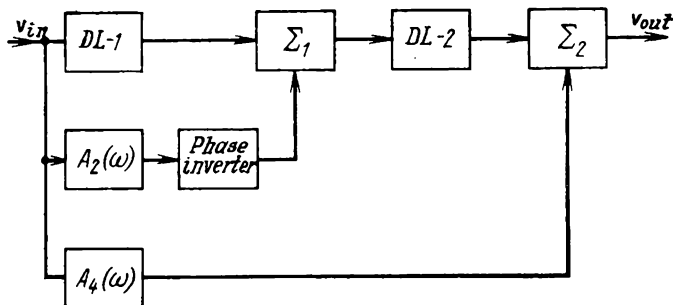


Fig. 8.24. Block diagram of a differentiating aperture corrector

It is interesting to examine differentiating aperture compensation in the time domain. Suppose that the signal being transmitted

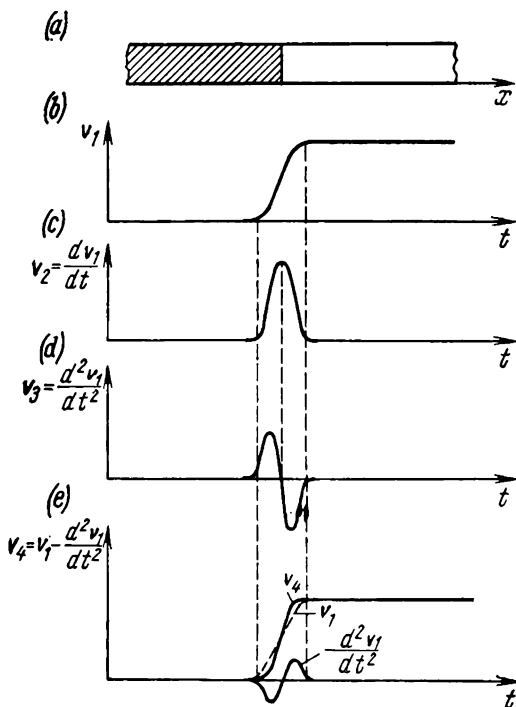


Fig. 8.25. Operation of a differentiating aperture corrector

(a) image transmitted; (b) video signal; (c) first-derivative signal; (d) second-derivative signal; (e) corrected signal

(Fig. 8.25a) represents a sudden change in luminance sharply delineated by a boundary between black and white. Because of aperture

distortion the signal V_1 at the output of the pickup tube takes the form shown in Fig. 8.25*b*. The first- and second-derivative signals are shown in Fig. 8.25*c* and *d*. Adding together the main signal V_1 and the second-derivative signal taken in opposite polarity (Fig. 8.25*e*) produces a signal, V_4 , with a steeper leading edge, which is equivalent to boosting the frequency response. It is to be noted that adding together the original signal and the compensating signal without polarity reversal of the latter would impair the frequency response.

Figure 8.26 shows a simple differentiating aperture corrector employing a second-derivative compensating signal. The original

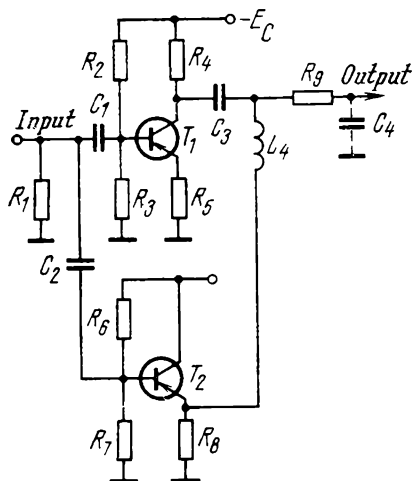


Fig. 8.26. Circuit of a differentiating aperture corrector

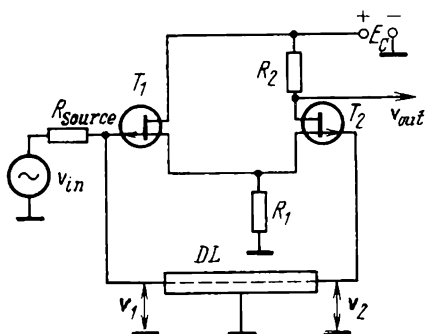


Fig. 8.27. Delay-line aperture corrector

signal is applied to two transistors, T_1 and T_2 , via d.c. blocking capacitors, C_1 and C_2 . The collector circuit of T_1 contains a network, C_3L_4 , tuned to resonate at the maximum frequency of the signal and acting as a double differentiator. This is so because when the resonant circuit is tuned to the maximum signal frequency, its frequency response (at frequencies just below the limiting one) is close in shape to a quadratic parabola, and this enables the second derivative of the original signal to be obtained. The main signal is passed on to the output from the load of the emitter follower via a coil, L_4 . The compensating signal is given the right polarity by the transistor T_1 operating as a phase inverter. Resistor R_9 prevents the boost in frequency response due to the resonant circuit formed by the inductance L_1 and the input capacitance of the succeeding stage.

The frequency response of the aperture corrector examined above is defined by Eq. (8.23). Since, however, compensation utilizes the second derivative, only the first terms are retained

$$\alpha_1 = 1 + a_1 (\omega/\omega_{\max})^2 \quad (8.27)$$

where $a_1 = K_1/K_2$

K_1 = gain of the stage using transistor T_1

K_2 = gain of the emitter follower, T_2

The other most commonly used method of aperture compensation uses a delay line. The circuit of such an aperture corrector is shown in Fig. 8.27. The signal to be corrected, V_{in} , is taken from the preceding stage to the gate of a field-effect transistor, T_1 , connected in a source-follower circuit. The signal V_{in} is at the same time applied to a delay line, DL . From the delay line the signal goes to the gate of T_2 which has a common resistor R_1 with T_1 in the source circuit. The output impedance of the signal source is chosen to be equal to the characteristic impedance of the transmission line. Since the input resistance of a field-effect transistor is sufficiently high, it may be assumed that the delay line is open at its output (receiving end). When an open-circuited delay line is connected to a source of harmonic oscillation having an internal impedance equal to the characteristic impedance of the line, standing waves arise in the line, and the voltage at a distance x from the line end is

$$v_x = V_{in} \cos \omega x/u \quad (8.28)$$

where u is the signal velocity along the line and ω is the angular frequency of the drive generator.

If the line is of length l , the voltage at its input can be found by substituting l in Eq. (8.28)

$$v_1 = V_{in} \cos \omega (l/u) = V_{in} \cos \omega \tau_d \quad (8.29)$$

because $l/u = \tau_d$ is equal to the delay introduced by the delay line.

The voltage at the opened end of the line can be obtained from Eq. (8.28), with x set equal to zero:

$$v_2 = v_{in} \quad (8.30)$$

that is, the voltage at the open-circuited receiving end of the line is equal to that of the signal source, is in phase with it, and is independent of frequency. In contrast, v_1 depends on both the line parameters and frequency. Plots of v_1 and v_2 as functions of frequency are shown in Fig. 8.28.

The output voltage taken from the drain of T_2 is proportional to the difference between v_1 and v_2 . To prove this, let v_1 at some instant be positive. Because T_1 is connected in a source-follower circuit, its source voltage is positive, too. The same voltage exists at the source of T_2 . Application of a positive voltage to the source

of T_2 is equivalent to applying a negative voltage to its gate. In addition to the voltage proportional to v_1 , the gate of T_2 accepts v_2

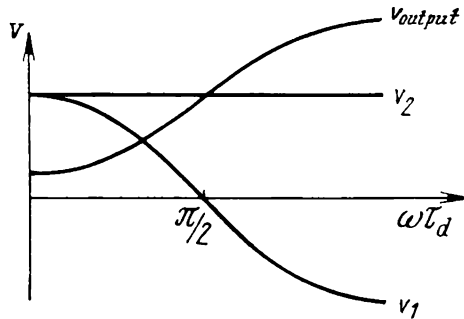


Fig. 8.28. Voltages at different points in the circuit of Fig. 8.27 as functions of signal frequency

which is in phase with the signal voltage and, as a consequence, is in positive polarity. Thus, we may write

$$v_{out} = v_1 K_1 - v_2 K_2 \quad (8.31)$$

where K_1 = gain of the circuit between the gate of T_1 and the drain of T_2

K_2 = amplification factor of T_2

On the basis of Eqs. (8.29) and (8.30), we get

$$v_{out} = -v_{in} K_2 (1 - K_1/K_2 \cos \omega \tau_d) \quad (8.32)$$

The overall gain of the circuit is

$$K = v_{out}/v_{in} = K_2 (1 - K_1/K_2 \cos \omega \tau_d) \quad (8.33)$$

As is seen, the device gives the high-frequency amplitude boost. The plot of output voltage as a function of frequency (see Fig. 8.28) has the shape of a truncated cosinusoid. Although it is an even function, it differs markedly from the optimal one described by Eq. (8.23). Better compensation could be secured by use of several delay lines differing in τ_d . In practice, however, it is usual to employ only one delay line. The type of delay line most commonly used in aperture correctors is a section of a special delay cable, such as the Soviet-made PK3-401. This cable has a characteristic impedance of 401 ohms and a delay of 0.6 μ s per linear metre.

As already noted, an aperture corrector ought not to produce phase shifts. Equation (8.33) for the gain of an aperture corrector is a real function, which implies that the corrector will not introduce any phase distortion.

As follows from Eq. (8.33), the gain is a maximum when $\omega\tau_d = \pi$. The frequency response peak of a corrector should occur at the maximum frequency, ω_{\max} , of the television signal where aperture distortion is a maximum. That is,

$$\tau_d = \pi/\omega_{\max} = 1/(2f_{\max})$$

Assuming that $f_{\max} = 6.5$ MHz, we have

$$\tau_d = 0.07 \text{ } \mu\text{s}$$

Noting that type PK3-401 cable has a delay of $0.6 \text{ } \mu\text{s}$ per metre, the necessary value of τ_d is obtained with a cable length

$$l = 0.07/0.6 = 0.128 \text{ m}$$

8.8. Gamma Correction

The quality of the picture reproduced on a picture tube can be greatly affected by the amplitude (or light) transfer characteristics of the television circuit. The latter contains a great number of elements which may show a nonlinear amplitude response. These are the pickup tube, the video amplifier at the TV centre, the modulator and r.f. stages of the TV transmitter, the r.f. and i.f. amplifiers of the receiver, the detector, video amplifier and, finally, the picture tube. Most of the elements listed above, such as the video amplifiers, transmitter modulator, detector and i.f. amplifier of the receiver, will not introduce appreciable nonlinearity. This is secured through proper design. Thus, the nonlinearity in a television system is mainly attributable to the pickup and picture tubes.

The amplitude (light) transfer characteristic of a pickup tube relates the signal current to the illumination of its photocathode, $i_s = f(E)$. Since the illumination of the photocathode is proportional to the luminance of the scene, B_s , and the voltage across the load resistor of the pickup tube is proportional to the signal current, we may write

$$V_s = \varphi(B_s)$$

In practice, it is convenient to approximate the light transfer characteristic as

$$v_s = k B_s^{\gamma_1} \quad (8.34)$$

where γ_1 is the so-called gamma exponent defining the shape of the light transfer characteristic. Different pickup tubes widely differ in the gamma exponent, but usually $\gamma_1 \leq 1$. For the image iconoscope it is usually assumed that $\gamma_1 = 0.5$; for the vidicon, $\gamma_1 = 0.6$ to 0.7 ; for the image orthicon and plumbicon $\gamma_1 = 0.8$ to 1 . These values of γ_1 are approximate. In practice the light transfer characteristics

of pickup tubes can vary within certain limits with the operating conditions of the tube and the scene content.

The light transfer characteristic of a picture tube relates the screen brightness to the voltage applied to its modulating electrode, $B_p = F(V_s)$. With accuracy sufficient for most practical cases, this relation may be approximated by a function of the form

$$B_p = k_2 V_s^{\gamma_2} \quad (8.35)$$

As a rule, picture tubes have the gamma exponent γ_2 ranging from 2 or 3 to unity. Assuming that the remaining elements of the television system are linear, the overall amplitude transfer characteristic "from light to light" may be determined analytically by substituting the expression for v_s from Eq. (8.34) into Eq. (8.35):

$$B_p = k_2 (k_1 B_s^{\gamma_1})^{\gamma_2} = k B_s^{\gamma^*} \quad (8.36)$$

where $k = k_1^{\gamma_2} k_2$ and $\gamma = \gamma_1 \gamma_2$.

It is seen from Eq. (8.36) that the gamma exponent of the overall amplitude transfer characteristic of a television system is determined by the product of γ_1 and γ_2 . In Eq. (8.36) the factor k has complex dimensions dependent on γ_1 and γ_2 , that is, on the types of tubes used. In practice, so as to drop this factor from computations, it is convenient to express B_p and B_s in relative units. When the luminance of the picture and scene is a maximum, it follows from Eq. (8.36) that

$$B_{p, \max} = k B_{s, \max}^{\gamma} \quad (8.37)$$

Dividing Eq. (8.36) into Eq. (8.37) gives

$$B_p/B_{p, \max} = (B_s/B_{s, \max})^{\gamma} \quad (8.38)$$

It is convenient to express the overall amplitude transfer characteristic in relative units because the terms entering Eq. (8.38) take values ranging from 0 to 1, and $k = 1$. The amplitude transfer characteristics of a complete television system shown in Fig. 8.29 apply to three cases as follows: straight line 0-1 to $\gamma = 1$, curve 0-2 to $\gamma = 2$, and curve 0-1/2 to $\gamma = 0.5$.

Whether there is nonlinear distortion or not can be ascertained by applying an image of the step wedge to the input of the television system. Faithful reproduction is only possible at $\gamma = 1$. When $\gamma \neq 1$, the correct reproduction of luminance gradations is no longer possible. As is seen from the figure, change in luminance between the individual gradations becomes unequal (gradations 1 through 4). Visually, change of luminance between gradations 1, 2

* For simplicity, the amplifier chain has been assumed to have a gain of unity; this will not affect the final result, however.

and 3 become undistinguishable at the output (m_{out}). The number of luminance gradations distinguishable at the receiving end reduces to four. Thus, nonlinear distortion in black-and-white television appears as luminance distortion.

It is not always that luminance distortion due to the nonlinearity of the amplitude (or light) transfer characteristic should impair the

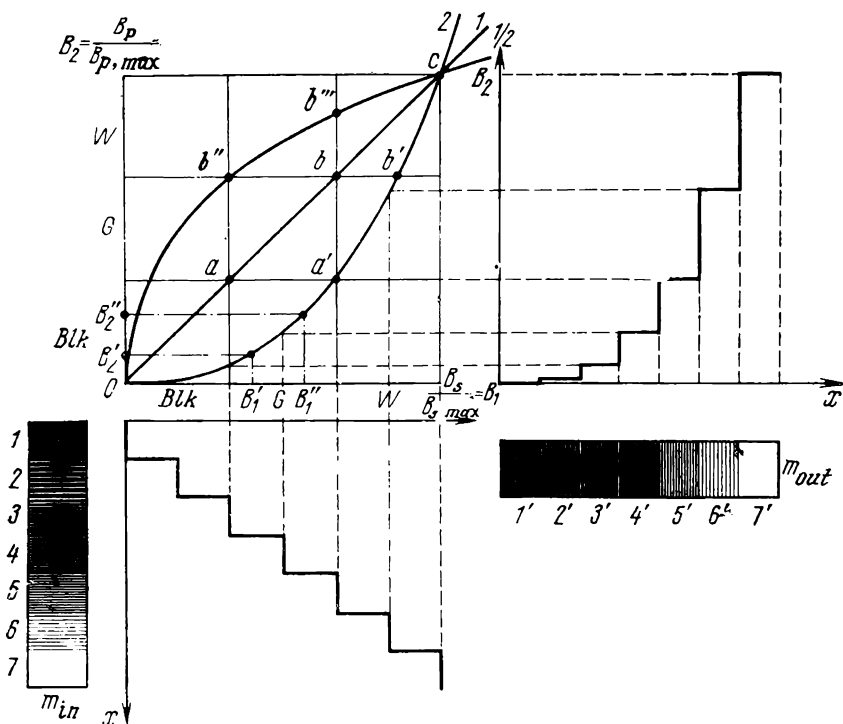


Fig. 8.29. Origin of nonlinear distortion

quality of the visual image. The point is that the contrast of the picture reproduced on the picture tube is usually markedly lower than that of the scene being televised. In the circumstances, the picture visible on the picture tube will always differ from the original scene, even though the transmission system may be linear. If the light transfer characteristic is moderately concave (that is, if $\gamma > 1$), the picture seen on the picture tube will subjectively be improved by this distortion. For better understanding, we shall divide the range from 0 to 1 into three equal parts along both the B_1 and B_2 axis (see Fig. 8.29), and call them black (*Blk*), gray (*G*) and white (*W*), respectively. When the characteristic *0-1* is ideally linear,

the black, gray and white areas on the photocathode of the pickup tube will be represented by the black, gray and white areas on the picture tube in the same relative amounts (points a , b and c). If the characteristic is nonlinear, 0-2, black and gray areas will be rendered as only black areas (point a'). Thus, nonlinear characteristic 0-2 causes the shadows and the gray tones to appear blacker. This is not unlike making prints from an underexposed negative on a contrast photographic paper, when areas of low contrast become darker. It may be said that nonlinear characteristic 0-2 "touches up" the television picture and makes it appear crisper and more contrast. However this sort of electronic touch-up may add too much of black to the picture, and this would appear as if drawn in carbon. This is why, in choosing the degree of knee in the light transfer characteristic 0-2, it is important to avoid excess contrast.

Conversely, the luminous distortion due to characteristic 0-1/2 considerably impairs the picture quality. It is seen from Fig. 8.29 black becomes gray to a considerable degree (point b'') and gray changes to white (points b'' and b''').

Practically, it has been found that the gamma exponent in black-and-white television should be 1.5 to 2.

In colour television, the entire system between the camera scene and the reproduced picture must be free from nonlinearity in the amplitude transfer characteristic, as this would distort colour rendition.

A nonlinear amplitude transfer characteristic may be made reasonably linear through the use of a gamma corrector. As a rule, a gamma corrector is included in the studio and control room equipment. For its effect a gamma corrector depends on the use of nonlinear elements whose nonlinearity can be adjusted in such a way that the gamma exponent of the television system can be changed as may be necessary. As an example, Fig. 8.30 shows the circuit of a popular gamma corrector. In this circuit, the amount of negative feedback is varied in a nonlinear fashion according to the instantaneous value of the television signal applied to the gate of a field-effect transistor, T . In the no-signal condition, the diodes D_1 and D_2 in the source circuit are driven to cut-off by voltages V_1 and V_2 . When the signal attains a certain positive value, V_{s1} , at the gate, the diode D_1 is rendered conducting, and the resistance of the source circuit falls from the initial value, $R_{s1} = R_1$, to a new value, $R_{s2} = R_1 R_2 / (R_1 + R_2)$. When the signal rises still more to V_{s2} , the diode D_2 becomes conducting, and the resistance of the source circuit falls farther to $R_{s3} = R_{s2} R_3 / (R_{s2} + R_3)$, because R_3 is now connected in parallel with R_{s2} . The gain of a stage using a field-effect transistor, with the source-circuit resistor not bypassed by a capacitor, is given by

$$K = v_{out}/v_{in} = S_d R_d$$

where $S_d = S/(1 + SR_s)$ is the dynamic slope (see the plot of Fig. 8.31a); R_d is the resistor in the drain circuit; R_s is the resistor in the source circuit; S is the static slope.

Thus, insertion of a resistor in the source circuit, R_s , reduces the stage gain. If we recall that R_s in the circuit of Fig. 8.30 decreases

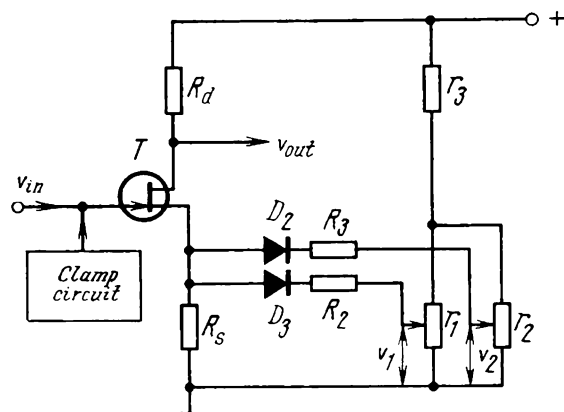


Fig. 8.30. Circuit of the gamma corrector

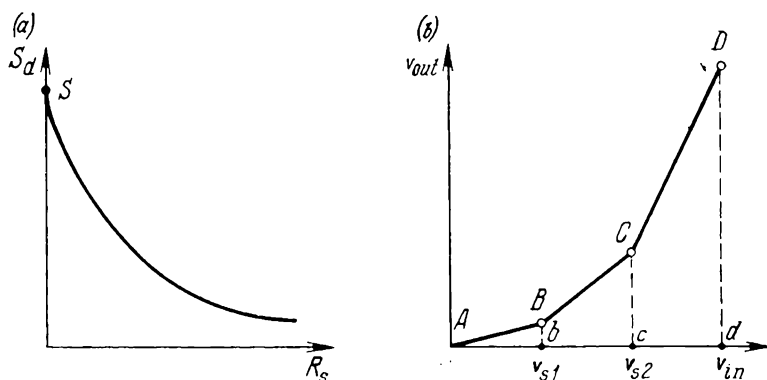


Fig. 8.31. Response of a gamma corrector with a nonlinear load in the drain circuit

(a) dynamic slope as a function of source-circuit resistance; (b) amplitude response

with increasing signal at the gate, we find that the gain rises with a rise in this signal (Fig. 8.31b). The broken line $ABCD$ representing the dependence of v_{out} on v_{in} may be approximated by a parabola of the form $V_{out} = kV_{in}^\gamma$.

As the number of diodes placed in the source circuit is increased, the approximation becomes more precise. The value of the gamma exponent, γ , can be adjusted with potentiometer r_1 and r_2 which set the delay voltages, V_1 and V_2 .

CHAPTER NINE

TELEVISION RECORDING

9.1. Role of Television Recording

Television programs are recorded in order to save them for repeated reproduction. Also, a considerable proportion of programs is pre-recorded in advance. The advantages of pre-recorded programs may be summed up as follows:

1. The burden on people involved in program production is reduced and there is an improvement in the quality and esthetic aspect of programs, because any defects in performance can be removed by subsequent editing.

2. Program production is simplified. A program can be produced and pre-recorded in parts at the time convenient to the performers. With video recording, the load on the studio equipment may be distributed more evenly.

3. Pre-recorded programs can readily be exchanged between cities and between countries without unduly overloading the communication channels.

4. Pre-recorded programs can be shown to viewers in different time zones when it is convenient to them.

In the Soviet Union, two methods of television recording are in use: (a) optical and (b) magnetic or signal-waveform. Of the two methods, magnetic or signal-waveform recording is used most. Magnetic recording has an important advantage over optical recording in that recorded tapes can be played back immediately after recording, without the chemical processing involved in optical recording. Yet, optical recording remains in use because the cost of film is only a small fraction of that of magnetic tape. Table 9.1 compares the quantity of film and tape needed for one hour of display along with the respective cost data.

Table 9.1

Recording medium	35-mm film	16-mm film	50.8-mm tape
Length, m	1800	750	1140
Relative cost	1.0	0.42	8.5

It is seen from the table that the cost of a tape record is 8.5 times that of a record on 35-mm film and 20 times that of a record on 16-mm film. The high cost of magnetic tape is the main obstacle to a wider use of magnetic recording. Thus, there is ground for believing that optical recording will retain its importance for many years to come.

9.2. Optical Recording

Basically, optical recording (also known as kinerecording, telerecording or film recording) is the production of a motion-picture record of the television image displayed on a high-quality (high luminance, high-contrast, high-resolution) picture monitor.

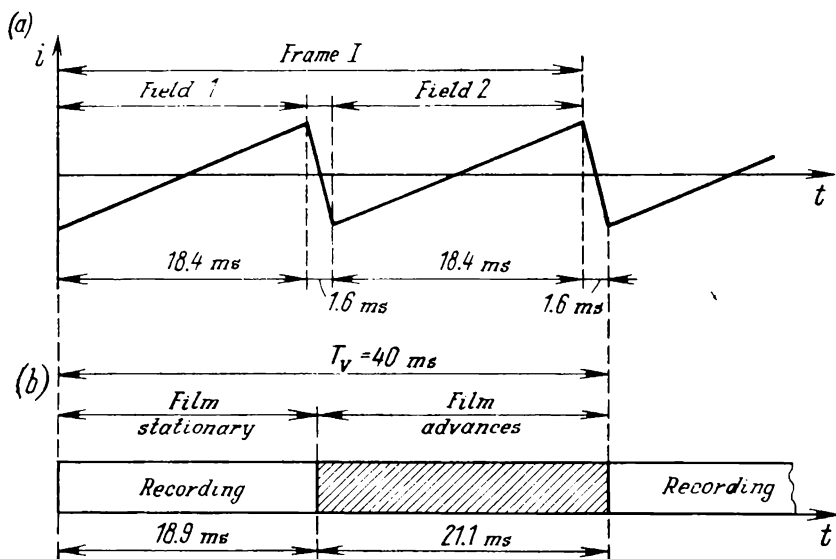


Fig. 9.1. Frame sequencing in (a) television and (b) motion pictures

The production of a high-quality motion-picture record of the television image runs into appreciable difficulties arising from the differences between the motion-picture and television standards (see Sec. 8.5), namely the difference in vertical retrace time (for a motion-picture projector, this may be arbitrarily assumed equal to the pull-down time). As will be recalled, in television two fields are scanned during one frame scan interval equal to $T_v = 40 \text{ ms}$ (Fig. 9.1a). Of this time, 18.4 ms is taken up to scan each field, and 1.6 ms by retrace. In cine cameras operating at 25 frames/s, 21.1 ms is taken up to pull down the film, and 18.9 ms to take a shot of the scene (Fig. 9.1b).

A simplified sketch of a cine camera is shown in Fig. 9.2a. The television image displayed by a picture monitor, 10, is thrown by a lens, 1, onto film, 5. The light beam passing through the film gate, 3, is periodically interrupted by a rotating shutter 2 which is a metal disc with a cut-out as shown in Fig. 9.2b. During the time interval when the light beam is interrupted, the claw, 4, enters perforations in the

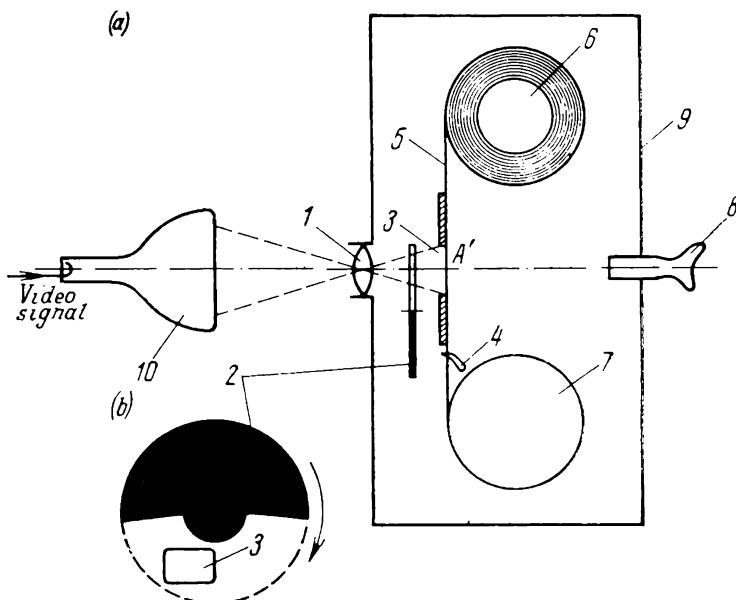


Fig. 9.2. Simplified sketch of a cine camera

1—lens; 2—shutter; 3—film gate; 4—claw; 5—film; 6—payout spool; 7—takeup spool; 8—view-finder; 9—light-tight case; 10—picture tube

film and pulls it down for a distance equal to the frame height. Then the shutter allows light from the monitor screen to pass through the next film frame, and this is exposed. In this way, the film is transported from the payout to the takeup spool (at 6 and 7 in Fig. 9.2, respectively).

The film pull-down (transportation) time is 21.1 ms, which is greatly in excess of the vertical retrace time in television ($T_r = 1.6$ ms). Because of this, an ordinary cine camera cannot record both fields of a television image from the picture monitor. As is seen from Fig. 9.1b, only one field has time to be recorded while the film remains stationary. The other field cannot be recorded because the film is being pulled down in the cine camera while the field is being scanned on the monitor. Omission of even or odd fields during optical recording results in the loss of half the raster lines and reduction in vertical

resolution. Despite this, this method was used at one time because the apparatus it required was simple and reliable.

It has proved difficult to design a cine camera with a pull-down time not exceeding the vertical retrace time (4 ms), which would be able to record both fields of each television frame. For one thing, reduction in pull-down time entails an increase in the force applied to the film. In the case of 35-mm film, this increase is about 35 to 40 times, and this would cause damage to the film.

There is a recording technique by which the vertical resolution of the image is retained at a pull-down time of 21.1 ms. It uses a picture monitor with a long-persistence phosphor. When the picture monitor displays the first field, the shutter in the cine camera is closed, the film is being pulled down, and no recording takes place. In this way, the pull-down is performed within the time interval occupied by an odd television field and vertical retrace. When the picture monitor displays the second field, the film is stationary, the shutter allows light to pass through, and the actual exposure is made of the second field and also of the previous (odd) field stored by the monitor phosphor owing to its long persistence. Unfortunately, this technique is accompanied by distortion. For one thing, the various areas of the image differ in brightness and contrast on film because of decay in phosphor luminescence. This form of distortion can be compensated for by applying correcting signals to the picture monitor. However, the generation and application of compensating signals and the associated adjustment of the equipment complicate the operation. For another, fast motion is reproduced with distortion because the phosphor has a long persistence; this distortion cannot be corrected at all. For all limitations, however, this technique has been the only one for a number of years.

Distortion in the recorded image can be markedly reduced through the use of a cine camera with a fast pull-down. The difficulty of film pull-down within the vertical blanking time (1.6 ms) has already been noted. Yet, there is optical-recording equipment, such as the Soviet-made MIG telecine camera, in which 35-mm film is pulled down in 3.3 ms (which, unfortunately, is still twice as long as the vertical blanking time). In this camera, film pull-down performed by a specially designed claw begins 0.85 ms before the start of a vertical blanking pulse and terminates 0.85 ms after the blanking pulse ceases. This results in the loss of 10 to 15 lines at the bottom and 10 to 15 lines at the top of the picture, and is usually passed unnoticed by viewers.

It should be noted that the wear of film in fast pull-down recording equipment is less critical than it is in reproducers, because recording is done once, while films are reproduced repeatedly. Fast pull-down recording equipment produces high-quality records, which fact makes this technique promising.

The optical recording techniques examined above still fail to meet the requirements of broadcast television. For one thing, they cannot be used to make film records of colour television images. The experimental equipment developed to date cannot produce records of satisfactory quality. For another, the loss of definition in recording black-and-white images is prohibitively heavy. Above all, this happens because optical recording adds to the aperture distortion ordinarily occurring in the television system. The additional aperture distortion is due to the picture monitor from which the television image is recorded, the cine camera lens, and the film. Currently, work is under way on optical recording equipment utilizing the electron beam or laser light and avoiding many of the intermediate operations. There is every reason to believe that before long there will be equipment capable of making high-quality records and meeting service requirements.

9.3. Magnetic Recording

Magnetic recording of electric signals utilizes the property of ferromagnetic materials to be magnetized and to retain their magnetized condition for a long time. The magnetic recording medium is usually fabricated in the form of tape consisting of a thin ferromagnetic coating applied to a nonmagnetic base. Tape for television recorders uses a plastic (polyester) base which has a high strength and other valuable mechanical properties. The ferromagnetic coating is usually iron oxide. The individual grains of the coating measure a few fractions of a micrometre. The iron oxide is deposited on the plastic base in the form of a suspension. The binder is a special varnish.

An electric signal is recorded on magnetic tape by a magnetic head. The magnetic head (Fig. 9.3a) consists essentially of a magnetic circuit, 1, with an air gap, Δ , and a winding, 2, traversed by the signal current being recorded. Magnetic lines of force, 3, issue from the head gap and complete their path through the ferromagnetic coating on tape, 4, because the coating has a lower reluctance than the nonmagnetic material which fills the head gap. The shape of the magnetic field in the head gap is shown in Fig. 9.3b. The magnetic field threading the tape has two components, \bar{H}_x and \bar{H}_y . In the head gap, Δ , the component \bar{H}_x is directed along the tape axis (the longitudinal component), the field component \bar{H}_y at the pole pieces is directed across the tape (transverse component). The component \bar{H}_y threads the tape at the *N* and *S* poles in opposite directions.

As the tape is moved relative to the head, the latter magnetizes its ferromagnetic coating, and the magnetic field is distributed as shown in Fig. 9.3c. The tape is magnetized only longitudinally, because the vertical component H_y threads each portion of tape

twice: first at the N pole and second at the S pole (see Fig. 9.3*b*). Since, however, H_y reverses sign as the tape moves in the x -direction (Fig. 9.3*c*), the resultant residual magnetization due to H_y is about zero, and H_y has practically no effect on recording.

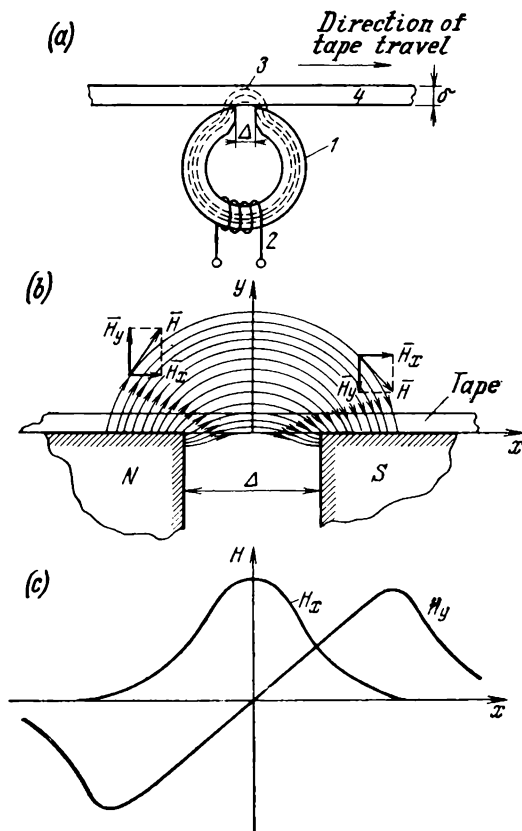


Fig. 9.3. Magnetic tape recording

(a) magnetic head position relative to tape: 1—magnetic core; 2—coil; 3—magnetic lines of force; 4—tape; (b) magnetic lines of force in the head; (c) H_x and H_y as functions of coordinate x

If the field intensity in the head gap varies sinusoidally in time (Fig. 9.4*a*), and if the tape moves at a uniform speed past the head, the spatial distribution of residual magnetization in the tape will likewise be sinusoidal. This distribution fits the same plot of Fig. 9.4*a*, except that the distance x along tape is plotted as abscissae. The direction of residual magnetic lines of force in tape of thickness δ is shown in Fig. 9.4*b*. In Fig. 9.4*c*, the record is repre-

sented by a chain of elementary magnets whose fields oppose one another. The length of each magnet is half the wavelength, λ , of the signal being recorded. The wavelength of the record, defined as the

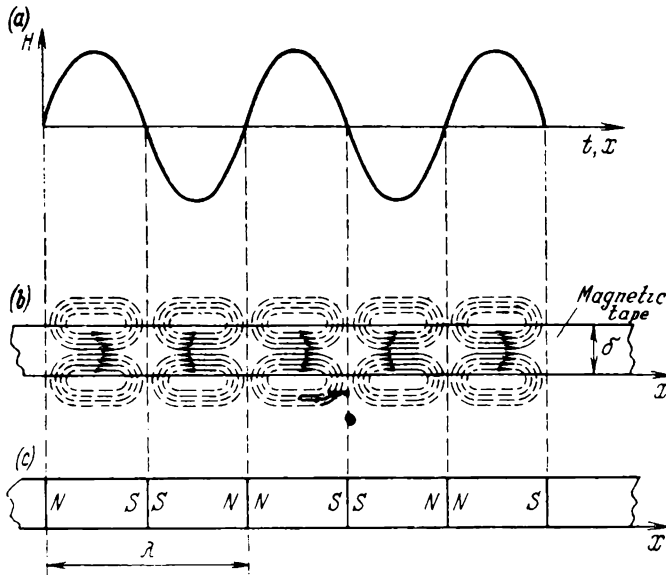


Fig. 9.4. Residual magnetization

(a) change of magnetic induction with time; (b) magnetic lines of force due to residual magnetic field; (c) arrangement of elementary magnets

distance between two points at zero residual magnetization (see Fig. 9.4c) depends on both the signal frequency, f , and the head-to-tape speed, u :

$$\lambda = u/f \quad (9.1)$$

The least wavelength that can be recorded and reproduced by the tape-head system defines the resolution of the recorder. Records are reproduced by a playback head built along essentially the same lines as the recording head. During playback, the tape is moved past the head, the magnetic lines of force complete their path through the head core which has a lower reluctance (in comparison with the head gap, Δ). Figure 9.5 shows the distribution of the magnetic field for two characteristic positions of the head gap with respect to the poles of elementary magnets.

In the first case (Fig. 9.5a and d), the magnetic lines of force complete their path through the magnetic circuit and induce an emf in the head winding. In the second case (Fig. 9.5b, c), the magnetic lines of force complete their path through the top of the core, outside

the winding, and the emf is zero. If a sinusoidal signal of angular frequency ω has been recorded on tape, the distribution of magnetic flux Φ along the x -axis of tape in the case of an ideal (distortion-free) magnetic system will be described as

$$\Phi = \Phi_0 \sin(\omega/u_r) x \quad (9.2)$$

where u_r is the head-to-tape speed in recording and Φ_0 is the amplitude of magnetic flux.

The emf induced in the head winding during playback may be defined as a derivative, $w (d\Phi/dt)$. To differentiate Eq. (9.2) with

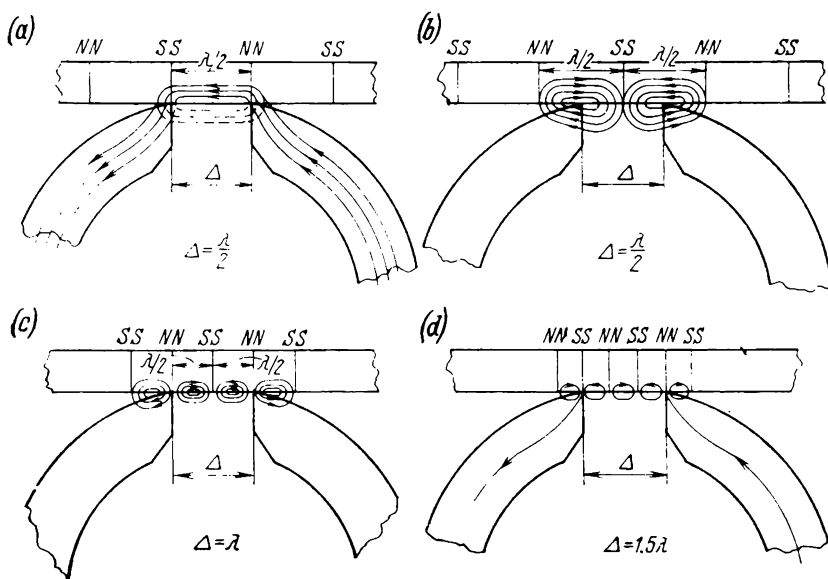


Fig. 9.5. Playback of tape records at different wavelengths

(a) $\Delta = \lambda/2$; (b) $\Delta = \lambda/2$; (c) $\Delta = \lambda$; (d) $\Delta = 1.5 \lambda$

respect to time, we replace x by $u_p t$, where u_p is the head-to-tape speed during playback

$$E = -w (d\Phi/dt) = \Phi_0 \omega w (u_p/u_r) \cos \omega t \quad (9.3)$$

If the head-to-tape speed is the same in recording and playback, that is, if $u_r = u_p$, Eq. (9.3) may be re-written as

$$E = \Phi_0 \omega w \cos \omega t \quad (9.4)$$

It is seen from Eq. (9.4) that the emf induced in the head winding during playback is proportional to the signal frequency. An idealized transfer characteristic of the tape-head system is shown by the

full line in Fig. 9.6. As is seen, frequency response 1 in accordance with Eq. (9.4) is a slant straight line. Its slope is 6 dB per octave.* The slope of the frequency response results in frequency distortion in the video signal. This distortion can be corrected by suitably adjusting the frequency response of the television tape recorder.

Equation (9.4) holds in cases where the wavelength, λ , being reproduced exceeds the head gap. If the wavelength is equal to the head gap, $\lambda = \Delta$ (Fig. 9.5c), the magnetic lines of force will complete

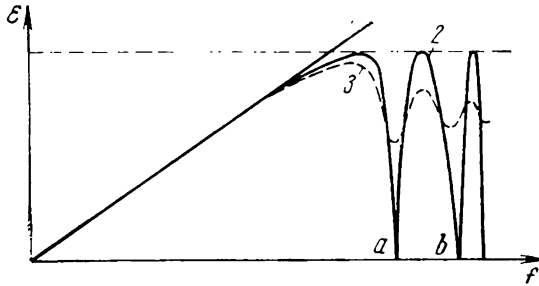


Fig. 9.6. Frequency response of the head-tape system
1—idealized; 2—adjusted for air gap; 3—experimental

their path through the top of the magnetic circuit without inducing an emf in the winding. When $\Delta = 1.5\lambda$ (Fig. 9.5d) the magnetic lines of force will thread the winding, and the emf will be a maximum. The magnetic field is set up by three elementary magnets of which two are connected in opposition and their magnetic fields cancel out, while the third magnetizes the core. It can be shown that as the wavelength λ is gradually decreased, the amplitude of the playback signal falls to zero at

$$\Delta = n\lambda \quad (9.5)$$

and is a maximum at

$$\Delta = (2n + 1)/2\lambda \quad (9.6)$$

where $n = 1, 2, 3, \dots$

Let us determine the frequencies at which the frequency response during recording and playback has maxima and minima. On the basis of Eq. (9.1),

$$f = u/\lambda \quad (9.7)$$

* An octave is the interval encompassing eight tones of the musical scale. The eighth tone has twice the frequency of the first. According to Eq. (9.4), doubling ω (increase by an octave) causes E to double, too. Thus, $20 \log 2 = 6$ dB.

By solving Eq. (9.5) for λ and substituting the result in Eq. (9.7), we get

$$f(v_s=0) = (u/\Delta) n \quad (9.8)$$

Similarly, using Eqs. (9.6) and (9.7), for a maximum we get

$$f_{v_s, \max} = \frac{2n+1}{2} (u/\Delta) \quad (9.9)$$

In view of Eqs. (9.8) and (9.9), the high-frequency response becomes oscillatory (curve 2 in the plot of Fig. 9.6). However, the experimental frequency response (curve 3 in Fig. 9.6) has no pronounced maxima or minima, which may be due to some factors that have been left out of consideration.

The head gap is chosen such that the effective frequency range lies to the left of the first minimum (at a in Fig. 9.6) on the frequency response curve. In television tape recorders, the head gap does not exceed 3 or 4 μm . In laboratory equipment, it is possible to make the head gap as small as 1 μm . However, the extent of the magnetic field exceeds the head gap, and the effective head gap turns out to be greater than the geometric one.

Magnetic tape for r.f. signals must have a thin magnetic coating with a smooth surface for good contact with the head. The contact face of the head should be machined to a high surface finish. To reduce eddy-current losses, the head core is assembled from magnetic-alloy laminations 0.25 to 0.3 mm thick bonded together or from ferrite. Good performance is shown by heads with the pole-pieces made from a magnetic alloy and the core from ferrite. Apart from a good frequency response, such heads have a high wear resistance which is an important asset because magnetic tape is highly abrasive.

A distinction of television recording is that the signal spans a wide bandwidth, and this calls for magnetic heads with an extremely narrow head gap, Δ . However, there is a limit to the head gap, set mainly by existing manufacturing methods. In turn, the minimum attainable head gap, Δ , sets the limit to the minimum wavelength that can be recorded. As follows from Eq. (9.1), the wavelength that can be recorded is decided not only by the signal frequency, f , but also by the head-to-tape speed. Let us find the speed required to record a television signal with $f_{\max} = 6.5 \text{ MHz}$ on a tape recorder with a head gap of $\Delta = 5 \mu\text{m}$. Suppose that the signal will be reproduced faithfully (Fig. 9.5c) when $\lambda = \Delta$. Then, on the basis of Eq. (9.1),

$$u = \lambda f = 5 \times 10^{-6} \times 6.5 \times 10^6 = 3250 \text{ cm/s}$$

It should be noted that the head-to-tape speed for the magnetic recording of a sound signal with $f_{\max} = 10 \text{ kHz}$ is as low as 38.1 cm/s. The high writing speed required in television recording results in the consumption of a large quantity of tape.

To assess the capabilities of longitudinal recording, we shall consider the performance of the television tape recorder developed by the Radio Corporation of America (RCA). This machine uses magnetic tape 6.35 mm wide and 19 μm thick. The effective head gap is 1 μm . At a head-to-tape speed of 6.1 m/s, a reel of tape 50 cm in diameter will provide a record/playback time of as short as 15 min.

The limitations of longitudinal recording have spurred the search for novel approaches. Of the great many improvements proposed to date, mention should be made of transverse recording (in the Soviet Union, it is employed in the KADR and ELEKTRON machines).

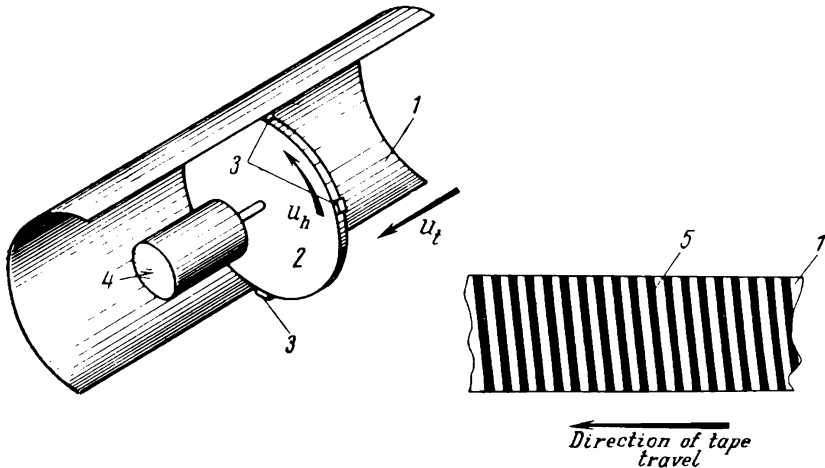


Fig. 9.7. Transverse recording

1—tape; 2—disc; 3—magnetic heads; 4—electric motor; 5—track

The principle of transverse recording will be clear from reference to Fig. 9.7. A wide magnetic tape, 1, is advanced in the direction indicated by the arrow. There are four magnetic heads, 3, mounted on a disc, 2. The head-mounting disc is carried by the shaft of an electric motor, 4. In order to maintain the desired contour, the flat magnetic tape is cupped around the head disc by a hollow concave guide from which air is exhausted (not shown in the figure). As the disc is rotated (see Fig. 9.7) and the tape is advanced, the tracks, 5, are laid down across the tape. If the circumferential speed, u_h , of the heads is considerably higher than the tape speed, u_t , the tracks make an angle of close to 90° with the edge of the tape.

In transverse recording, the tape speed may considerably be reduced. For example, for a disc 50 mm in diameter, mounting four heads rotating at 250 rps, the television signal can be recorded at a tape speed of $u_t = 40 \text{ cm/s}$ which is practically equal to that used in sound recording (38.1 cm/s).

It is to be noted that in transverse recording the reduction is achieved in the speed of longitudinal tape motion, while the head-to-tape speed remains high as before (40 m/s) owing to the rotation of the disc. In this way the tape length required to record a program of a given duration is reduced by transverse recording owing to an increase in tape width. However transverse recording utilizes the tape area far better than longitudinal recording where the track occupies a negligible width of tape. Reduction of tape width to that of the track is out of the question as this would make the tape mechanically weak. This is why in longitudinal recording on 6.25-mm tape one frame requires a tape area of 75 cm². This is eleven times as great as the frame area on, say, 35-mm film, where it is as little as 6.65 cm². In transverse recording the tracks are arranged more sparingly, and one television frame requires only 8 cm² of tape area. In other words, the density of magnetic recording approaches that of optical recording.

Passage from one track to the next is accomplished by change of heads. This necessitates that the signal being recorded be transferred from the previous to the next head, too, which is usually done by an electronic switch. A video signal cannot be switched instantaneously, and the signal transfer is ordinarily accompanied by a characteristic spurious signal which gives rise to well-defined dots on the television image. To avoid this interference, the signal is usually switched during line retrace, within the horizontal blanking pulse.

Since, in accordance with Eq. (9.4), the emf in the head is proportional to the signal frequency, it is negligible when low-frequency signals are recorded. As a way out, it is usual in television recording to translate the signal to a higher frequency by frequency modulation because FM signals are more immune to noise.

During both recording and playback, variations in contact between the tape and head and flaws on the tape surface (erosion of the ferromagnetic coating, foreign inclusions, discontinuities, and the like) give rise to parasitic amplitude modulation. In transverse recording, parasitic amplitude modulation may also arise from longitudinal vibrations of the tape which cause the head to shift relative to the track, and also from differences in performance between the heads. The noise due to these causes may reach an appreciable level. With frequency modulation, the signal is limited in amplitude after reproduction, and this minimizes the effect of interference.

9.4. Design Features of a Television Tape Recorder

A television tape recorder is a fairly complex piece of electronic equipment. We have already listed the stringent requirements that a good magnetic head is expected to meet. The requirements are as stringent for the other elements of a tape recorder.

A television tape recorder may be visualized as made up of four essential units:

- (1) A tape transport and magnetic-head assembly.
- (2) Automatic control for tape and head speed.
- (3) A recording channel.
- (4) A reproduction (or playback) channel.

The magnetic heads used in television tape recorders are usually made with a composite magnetic circuit in which the core is of ferrite and the pole-pieces coming in contact with the tape are from

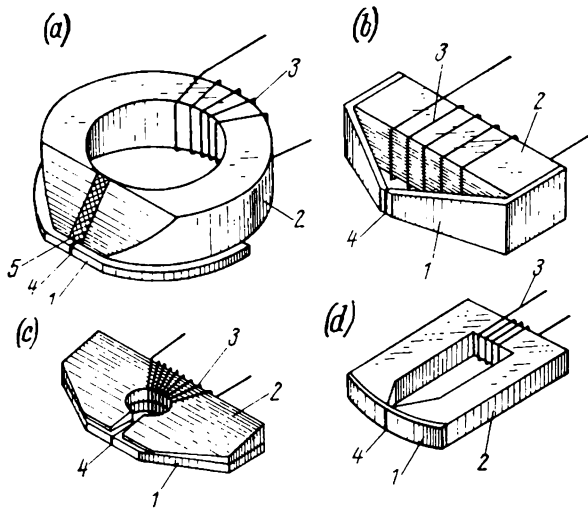


Fig. 9.8. Magnetic heads using composite cores
1—pole pieces; 2—ferrite core; 3—coil; 4—air gap; 5—copper spacer

a magnetic alloy. Figure 9.8 shows several designs of magnetic heads used in television tape recorders. In the head shown in Fig. 9.8a, the pole-pieces, 1, are in contact with the side surface of a ferrite core, 2. The gap between the pole-pieces at their point of contact with the tape is closed by a copper shim, 5. The non-magnetic properties of the copper shim make the magnetic lines of force spread out slightly into the space above the surface of the gap and enable them to penetrate better into the magnetic material of the recording medium. The core is chamfered so that its cross-section reduces towards the gap, 4. This is done in order to concentrate the magnetic field within a limited area. The magnetic field is produced by the current traversing the coil, 3.

The pole-pieces of the head shown in Fig. 9.8b are in contact with the side surface of the ferrite core, 2, those of the head shown in Fig. 9.8c are in contact with the ends of a rectangular ferrite core,

and those of the head shown in Fig. 9.8*d* are made in the form of cover-straps.

Since the tape moves at a high speed relative to the head, the surface of the latter may reach a temperature of several hundred degrees. This is why the material selected for the pole-pieces should have an appropriate Curie point*. One such alloy is Al-Si-Fe which has a Curie point of 500°C and possesses the necessary mechanical and electric properties.

In transverse recording, the magnetic heads are equiangularly mounted on the periphery of a rotating disc (Fig. 9.9). The signal is applied in recording and picked off during playback by a pickoff device which may be contact or contactless. A contact pickoff has a rotor attached to the head disc and a stator section mounted on the baseboard. The rotor (see Fig. 9.9) has five rings of which four are connected to the head coils, and the fifth which is common to all heads is connected to the disc housing. Each ring is in contact with two brushes, one brush on either side. The contact type of pickoff calls for regular servicing to clean the rings and to change brushes. Also, the rubbing contacts are sources of noise. More recent makes of television tape recorders use contactless pickoffs of the transformer type, each consisting of four transformers wound on ferrite cores.

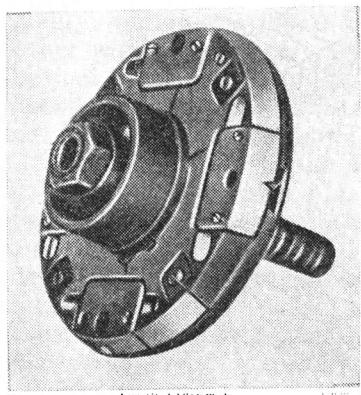


Fig. 9.9. Magnetic heads on a rotating disc

In sketch form, the construction of such a transformer is shown in Fig. 9.10. The stator, 1, attached to the base-plate of the head assembly has a slot which receives a coil, 2. The rotor, 3, likewise has a slot receiving another coil, 4, arranged on the outside. The rotor is mounted on a shaft 5 which also carries the head assembly. The outside diameter of the rotor is somewhat smaller than the inside diameter of the stator, so that an air gap, 6, of length Δl is formed between them after assembly. The magnetic lines of force, 7, thread both coils and complete their path through the air gap. During operation, the rotor assembly rotates together with the shaft and head assembly. One end of the rotor coil is connected to the coil of one of the four heads, and the opposite end is returned to ground. The signal is transferred by the magnetic field which

* The Curie point of a ferromagnetic material is the critical temperature at which the material loses its permanent or spontaneous magnetization.

links the air gap. In recording, the signal is applied to the stator coil, induced into the rotor coil and applied to the magnetic head. During playback, the events occur in reverse order.

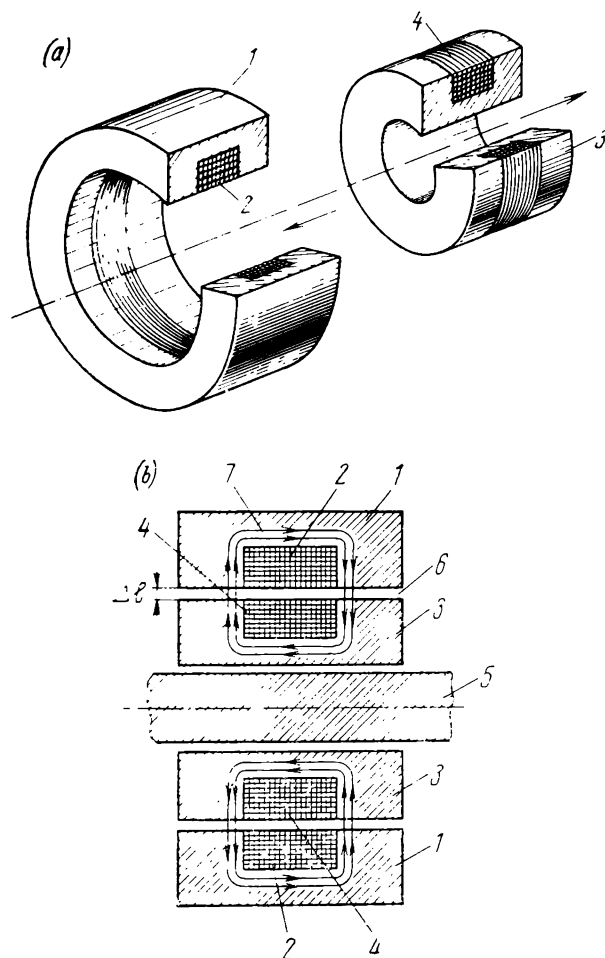


Fig. 9.10. Pickoff transformer

(a) general appearance; (b) section along axis: 1—stator; 2—coil wire; 3—rotor; 4—rotor coil; 5—shaft; 6—air gap; 7—magnetic lines of force

The head disc (or drum) is driven by a three-phase, 15-20 W, 15,000-rpm high-precision hysteresis motor. The level of precision is such that shaft wobbling will not exceed 2 μm .

The tape 3 is maintained in close contact with the moving heads by a hollow concave guide, 1, positioned relative to the head disc

as shown in Fig. 9.11a and b, and by a vacuum which is applied at the guide side of the tape. Vacuum suction slots, 4, communicate with a vacuum pump. The top of the concave guide is bevelled, 6, so that the heads, 9, come in contact with the tape tangentially. The tape is prevented against transverse displacement by a limit stop, 7. The bottom edge of the tape is held against the limit stop

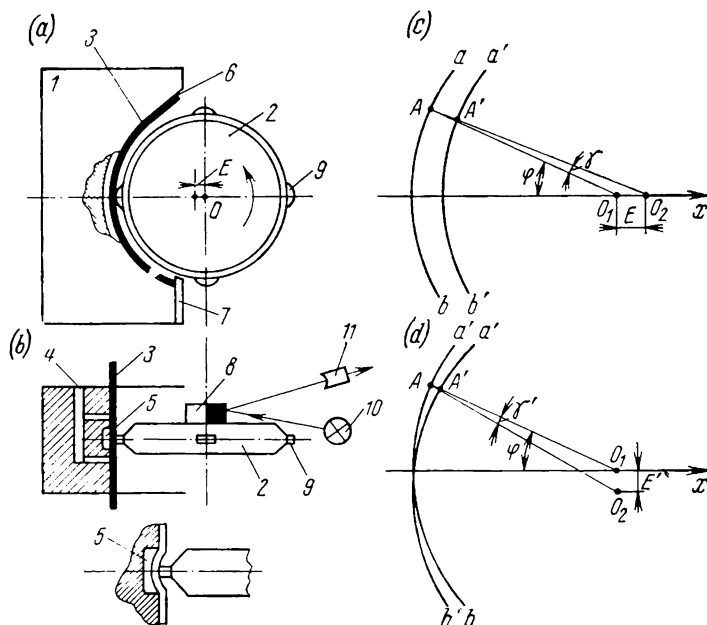


Fig. 9.11. Concave guide and its position relative to head assembly
(a) side view; (b) top view; (c) longitudinal eccentricity; (d) transverse eccentricity; 1—concave guide; 2—head assembly; 3—tape; 4—suction slot; 5—guide groove; 6—guide bevel; 7—limit stop; 8—photocell shutter; 9—magnetic heads; 10—light source; 11—photocell

by the force applied by rotation of the disc, 2. At the point of contact between the heads and tape the concave guide has a groove, 5. The pole-pieces of the heads projecting beyond the disc press the tape into the groove and stretch it a little, thereby securing close contact essential for recording h.f. signals. Special care is taken to build the concave guide to a high degree of precision. Above all, it is necessary so that records made at different TV centres can be exchanged. By international agreement, the concave guide should be curved to a radius of 26.248 mm accurate to within ± 0.013 mm.

The concave guide must be held in a precise position relative to the head assembly. For the purpose of adjustment, the guide is set up on a carriage which can be moved vertically and horizon-

tally as may be necessary. The need for adjustment may arise during playback because the dimensions of tape can change due to variations in the ambient conditions (temperature and humidity) at the time of recording and reproduction and also due to the difference in pull applied by different tape transport systems. The guide is adjusted for position by a servo operated remotely from a control room or automatically.

The difference in relative position between the head drum and the concave guide during recording and playback gives rise to time errors. Fig. 9.11*c* and *d* illustrates the time errors arising as a result of longitudinal and transverse eccentricity. Suppose that at the time of recording the centre of the head assembly and the centre of guide curvature occur both at point O_1 . As the disc rotates, the point of contact between head and tape, A , will then move along the arc ab .

Now suppose that during playback the centre of the head assembly moves to point O_2 , resulting in an eccentricity, E . Because of this, the tape will be pressed into the groove of the concave guide for a shorter depth, and the point of contact A' will move along the arc $a'b'$. It is seen from Fig. 9.11*c* that the record element which would normally be reproduced as the head turns through an angle φ relative to the horizontal axis will now be played back as the head rotates through an angle $\varphi + \gamma$. This additional angle γ is responsible for the time error:

$$\Delta t = \gamma / \omega \quad (9.12)$$

where ω is the angular velocity of the disc.

The time error arising from longitudinal eccentricity depends on the angle of rotation. When $\varphi = 0$, the head picks the signal off the middle of the tape, the lines AO_1 and $A'O_2$ are coincident, and the time error is zero. As the head moves towards the edge of the tape, the error increases. Because the head disc is rotating continuously, time distortion recurs at a frequency which is a multiple of the vertical scan frequency, and this results in the geometric distortion of the image on the monitor screen, as is shown in Fig. 9.12*a*. Transverse eccentricity E' (see Fig. 9.11*d*) also causes time error and image distortion as shown in Fig. 9.12*b*.

Apart from the distortion related to mechanical misalignment of the head assembly and the guide, television tape recorders are subject to distortion arising from imperfections in the tape transport system. A typical arrangement of the tape transport system is shown in Fig. 9.13. All components of the tape transport mechanism (also known as the motor board) are mounted on a baseboard, 1. On the left is the supply-reel assembly, 2, and on the right the take-up reel assembly, 3. Each assembly comprises a drive motor, a reel clamp, and a brake. The supply-reel and take-up reel motors rotate

in the direction of arrows in Fig. 9.13. The brakes are designed to stop both reels simultaneously and almost instantaneously without

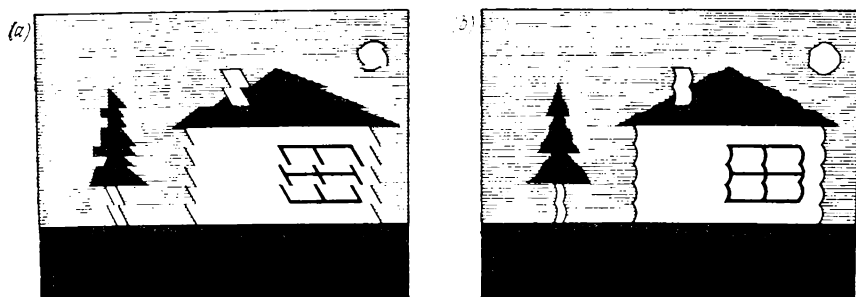


Fig. 9.12. Distortion in tape-recorded pictures

(a) effect of longitudinal eccentricity; (b) effect of transverse eccentricity

any risk of throwing slack tape off the supply reel or stretching or snapping the tape going onto the take-up reel. In operation, the

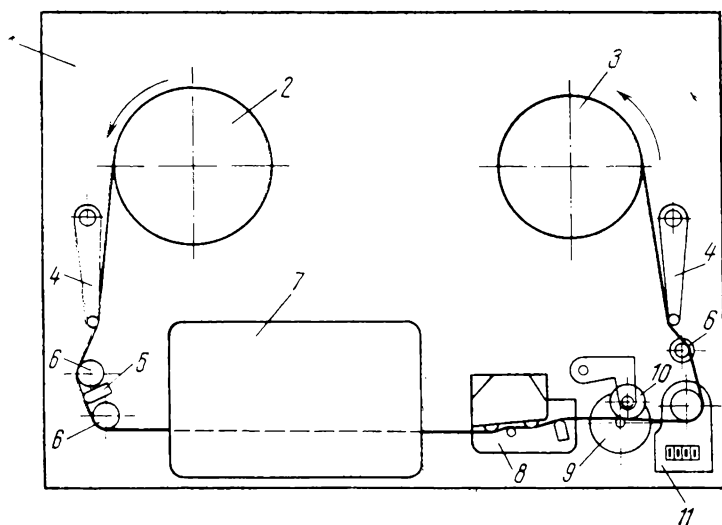


Fig. 9.13. Tape transport system of a video tape recorder

1—baseboard; 2—supply-reel assembly; 3—takeup-reel assembly; 4—tension arms; 5—erase head; 6—guide rollers; 7—rotating head assembly; 8—sound recording head; 9—drive motor; 10—pinch roller; 11—playing time indicator

tape is stretched taut by tension arms, 4. In some makes of tape recorders, tape tension is controlled automatically, irrespective of the radius of the supply or take-up reels. The tape unwound from

the supply reel is directed by guide rollers, 6, to the erase head, 5, and then to the rotating head assembly, 7, where the video signal is recorded. The sound signal is recorded on a separate track by a magnetic head, 8. The tape is advanced at a constant speed by a drive motor 9, whose shaft is used as the capstan against which the tape is pressed by a pinch roller, 10. To prevent tape from slipping over the capstan, its surface is treated to make it slightly rough. Since it is necessary to maintain the speed constant to within

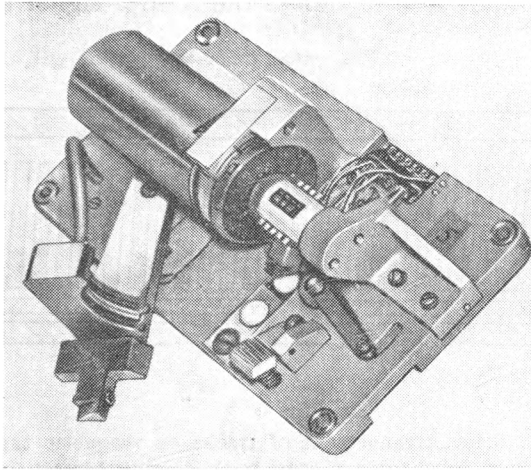


Fig. 9.14. External appearance of a head assembly and concave guide

0.1%, accurate manufacture of the capstan and pinch roller is essential. To assist the user, it is general practice to provide a playing time indicator, 11, with a dial calibrated in seconds or minutes. General appearance of the head assembly and the concave guide is shown in Fig. 9.14.

As a precaution against momentary variations in tape speed (which may be caused by, say, variations in the rotational speed of the capstan), and the attendant wow and flutter, the tape transport usually includes idle rollers which act as mechanical low-pass filters.

Accurate manufacture of the tape transport mechanism does not do away with the need to maintain constant head-to-tape speed at recording and playback. In transverse recording, each rotating head should follow a particular track on tape. However, it may be prevented from doing so by factors other than those involved in manufacture, such as variations in tape length in service or storage, variations in supply voltage, and the like. This is why television tape

recorders usually incorporate two automatic control systems, one to control tape speed and the other to control the rotational speed of the head disc. The tape speed control system is usually operative during playback and enables the heads to follow their respective tracks. In brief, this system operates as follows.

During recording, a separate magnetic head records a control signal of 250 Hz along the lower edge of the tape. During playback, the control track is read by the same head, and the signal is fed to a phase discriminator where it is compared with a reference signal. Variations in tape speed modulate the control signal in phase, and

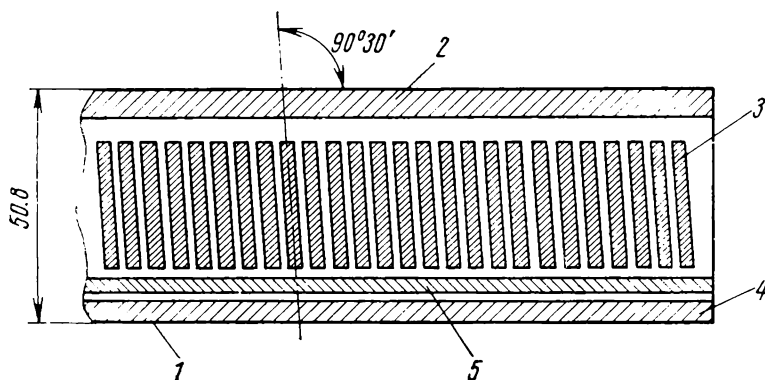


Fig. 9.15. Arrangement of tracks on magnetic tape

1—support edge; 2—sound track; 3—video track; 4—control track; 5—cueing track

this gives rise to what is called an error signal. The error signal produced by the phase discriminator is fed to a controlled-frequency generator which energizes the drive motor in accordance with the magnitude and sign of the error signal. The reference signal utilized in the phase discriminator is supplied by a photoelectric detector mounted on the shaft of the head-disc drive motor. The photoelectric detector is made up of a light source, 10 (see Fig. 9.11) throwing a beam of light onto a shutter, 8, which reflects light onto a photocell, 11. In rotating, the shutter chops up (modulates) the light beam, and this produces current pulses at the output of the photocell. After amplification and shaping, the reference signal is applied to the phase discriminator. The error signal lasts until the reference and control signal are again equal in frequency, that is, until the tape and the heads have come up to the same speeds as they were during recording.

The arrangement of the various tracks on tape in the case of transverse recording is shown in Fig. 9.15. The central part of the tape is occupied by video signals. The track recorded along the top edge is used for the accompanying sound (at 2 in Fig. 9.15). The tracks

recorded along the bottom edge are the control track, 4, and the cueing track, 5.

Apart from television tape recorders using four magnetic heads, there are machines with one and two rotating heads. An advantage of these machines is a very simple tape transport system, but their performance is considerably lower and they are usually intended for use under field conditions or in the homes. In such applications, the reduced resolution (not over 300 lines) is not an objection.

In recording colour television programs, it is essential that all circuits in the tape recorder be kept in proper alignment. It may be added that the signals in the SECAM system are simpler to record than those in the NTSC system.

CHAPTER TEN

TELEVISION RELAY SYSTEMS

10.1. Ways and Means of Extending the Coverage of Television Service

A typical television broadcast station usually covers an area within a radius of 60 to 80 km. This is because the radio waves within the VHF and UHF bands allocated to television service cannot bend around the Earth's curvature and are only propagated within the line-of-sight distance from the transmitter antenna.

In the circumstances, the height of transmitting and receiving antennas becomes a critical factor. Since receiving antennas cannot be taller than a few tens of metres and any further increase in their height is not economical, the transmission distance is solely determined by the height of the transmitting antenna at the television broadcast station. For example, in order to extend the coverage of the Ostankino Centre in Moscow to 120 km, a huge tower standing more than 500 m tall has been built. However, such towers are very expensive to build and cannot possibly provide a means for extending the coverage of television service. The alternatives ordinarily used are radio, cable and satellite television relay systems. Each type has merits and demerits of its own, and this defines the field of application for them.

10.2. Radio Relay Systems

Radio relay (or microwave) lines and systems constitute a subject in its own right. Therefore, in a book on television it is appropriate to dwell only on the job that this form of communication does within the television broadcast service.

Radio relay systems usually operate in the microwave region (UHF and SHF bands) for which reason they are often referred to as microwave systems or links. Microwave relay stations are spaced 40 to 50 km apart, and their antenna systems are set up on towers 50 to 70 m tall. Most microwave relay stations are designed to operate unattended. Watch on their performance is maintained by means of telemetry information relayed to attended stations.

The advantages offered by microwave links over other forms of relay systems may be summed up as follows.

1. Capital and maintenance costs are low.
2. Television signals can be dropped at any point on a link for use by adjacent areas.

3. Short time is needed for construction.

In some localities, however, it is difficult, if at all possible, to space relay stations 40 to 50 km apart. This above all applies to the taiga, mountains, deserts, and large bodies of water. In these conditions, it is more advantageous to build tropospheric-scatter relay links.

For its operation, a tropospheric-scatter link depends on the fact that microwaves, in propagating through the atmosphere, are forward-scattered from discontinuities in the troposphere. Troposcatter repeaters may be spaced 300 to 400 km apart. For reliable service, however, their transmitters must have a power output of several tens of kilowatts which is at least 100 times the power output of an ordinary radio-relay transmitter. The transmitting and receiving antennas used in troposcatter systems have a surface area of 600 m² which is 100 to 150 times the surface area of an antenna in conventional radio-relay systems. However, the cost of a troposcatter system in inaccessible localities is only a fraction of that of a conventional radio relay system because the number of repeaters needed is reduced to one-fifth or one-sixth.

10.3. Cable Relay Systems

In some cases, it is more advantageous to relay television programs for long distances over special trunk-line cables. The construction of such a cable is shown in Fig. 10.1. It has four coaxial pairs, 1, between which are placed conductors used for telephony, engineering (service) purposes and instrumentation. The design of equipment for cable relay systems is governed by the electric characteristics of the cable used. The attenuation introduced at a frequency f by a Soviet-made cable pair one kilometre long is

$$\alpha \approx 2.45 \sqrt{f}$$

where α is the attenuation in dB and f is the signal frequency in MHz. In other words, the attenuation in a coaxial pair is proportional to \sqrt{f} . At a frequency

of 1 MHz the per-unit attenuation of the cable is 2.45 dB/km.

Coaxial pairs also introduce appreciable phase distortion which is especially pronounced at frequencies below 1 MHz. Television

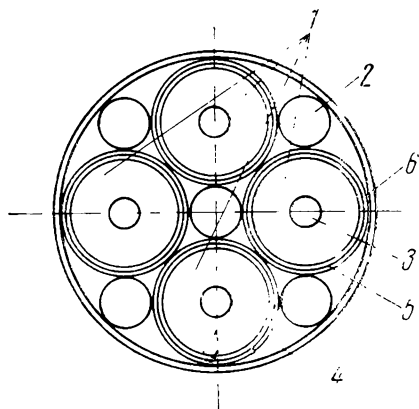


Fig. 10.1. Type KM-4 trunk-line cable

1—coaxial pair; 2—signal quad; 3—central conductor; 4—insulating cover; 5—metal braiding; 6—sheath

signals in the frequency range 50 Hz-6 MHz can be transmitted over coaxial cables for short distances (10 to 20 km). Further increase in the transmission distance results in the accumulation of phase distortion which is difficult to make up for. Also, at frequencies

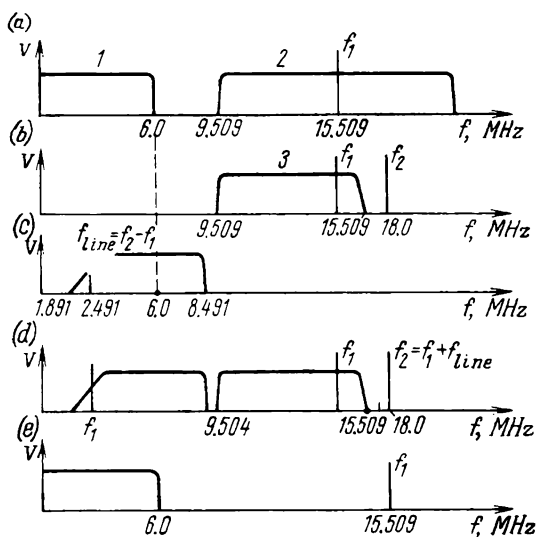


Fig. 10.2. Signal frequency translations for transmission over a coaxial cable line (in accordance with Fig. 10.3)

(a) at modulator 1; (b) at filter 1; (c) at filter 2; (d) at demodulator 1; (e) at filter 2

below a few tens of kilohertz coaxial pairs are subject to hum pickup at commercial frequency. To avoid these undesirable effects, the television signals transmitted over cables are amplitude-modulated.

To reduce the bandwidth requirements, only one sideband of the modulated signal should preferably be transmitted. However, its separation from the remainder of the signal poses considerable engineering difficulties because the minimum frequency of the modulated television signal differs from the carrier by only 50 Hz. For this reason, in transmission over coaxial cable the lower sideband is reduced only partly, with the remainder usually not exceeding 10% of its original width.

The frequency translations that the signal spectrum undergoes at the sending and receiving terminals of a coaxial cable relay line are shown in Fig. 10.2. The frequencies used in Fig. 10.2 are those employed in the Soviet-made K-1920 multichannel coaxial cable

system*. The television signal is modulated on an r.f. carrier, f_1 , so that the signal spectrum is translated into the high-frequency region as shown in Fig. 10.2a (where at 1 is the baseband, and at 2 is the modulated signal spectrum). In the K-1920 system the carrier f_1 is 15.509 MHz. With this choice of the carrier frequency, filters can readily separate the modulated signal spectrum in the range from 9.509 to 15.509 MHz. The signal spectrum, 3, at the filter output is shown in Fig. 10.2b. After the desired part of the modulated signal spectrum has been separated, it is moved downward so that it will fall within the line frequency range by modulating it onto a second carrier frequency, $f_2 = 18$ MHz. After translation into the low-frequency region, the signal is finally shaped by filters (Fig. 10.2c). The carrier in the middle of the linear slope is called the line frequency, and the spectrum shown in Fig. 10.2c is the line spectrum.

Signal frequency translation by two steps of modulation described above is used in order that the signal can be shifted into the high-frequency region by a small amount and that the line carrier frequency, $f_{line} = 2.491$ MHz, can be placed well below the maximum frequency of the television signal (which is 6 MHz). In conventional amplitude modulation, the requirement is that the carrier be at least twice as high as the modulating signal.

In block-diagram form, the arrangement of the transmitting terminal is shown in Fig. 10.3a. It includes amplifiers, two modulators, and filters. At the input to the first modulator, a clamp circuit inserts the d.c. component in the television signal. The two carrier frequencies, f_1 and f_2 , are derived as follows. There are two oscillators. One is thermostatted and crystal-controlled; it generates f_{line} . The requirements for the frequency stability of the other are less stringent; it generates f_1 . The second carrier frequency, f_2 , is obtained by heterodyning f_1 and f_{line} and retaining their sum by means of a filter:

$$f_2 = f_{line} + f_1 \quad (10.1)$$

With f_1 and f_2 derived as explained above, the overall stability of f_2 is solely decided by that of f_{line} . As a proof, assume that f_{line} is held constant and f_1 changes by Δf . Then

$$f'_1 = f_1 + \Delta f \quad (10.2)$$

The frequency at the output of the frequency converter will likewise change:

$$f'_2 = f_{line} + f'_1 = f_{line} + f_1 + \Delta f = f_2 + \Delta f \quad (10.3)$$

* The K-1920 multichannel system using KM-4 coaxial cable has a capacity of 1920 two-way telephone circuits, or 300 two-way telephone circuits and one two-way television channel.

As is seen from Fig. 10.2*b*, the line carrier frequency is independent of Δf :

$$f_{line} = f'_2 - f'_1 = f_2 - f_1$$

At the receiving terminal, the signal is frequency-translated in reverse order. To begin with, demodulator 1 (Fig. 10.3*b*) trans-

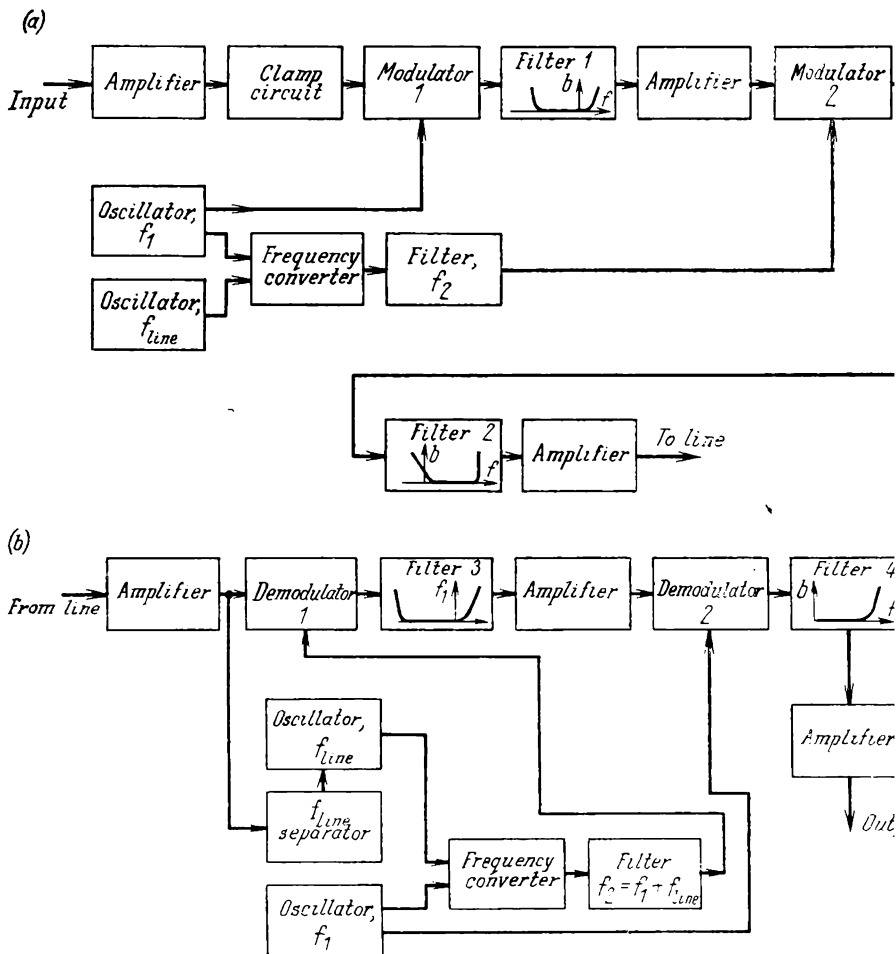


Fig. 10.3. Block diagram of coaxial cable system

(a) transmitting terminal; (b) receiving terminal

slates the line spectrum (Fig. 10.2*d*) into the high-frequency region. For this purpose, the receiving terminal supplies a carrier frequency. $f_2 = f_1 + f_{line} = 18$ MHz. After filter 3 (Fig. 10.2*d*) has separated

the spectrum region in the range 9.504-15.509 MHz, the signal is detected by a synchronous detector, 2. Synchronous detection enhances the noise immunity of the system and reduces distortion due to the partial reduction of the sideband. For synchronous detection at the receiving terminal it is important to have information about the frequency and phase of the line-carrier oscillator at the transmitting terminal, because this oscillator decides changes in the frequency and phase of the received carrier. For this purpose, the signal appearing at the amplifier output is fed to a circuit which separates f_{line} . The signal thus isolated controls the local oscillator f_{line} . The second carrier, f_2 , is derived by heterodyning, as is done at the transmitting terminal.

The frequency band below 1.891 MHz, not occupied by the television signal, is utilized for the transmission of the accompanying sound and 300 telephone conversations. It should be noted that the values of f_1 , f_2 and f_{line} stated in Fig. 10.2 have been chosen so as to minimize cross-talk between the telephone and television channels.

10.4. Satellite Relay Systems

In the early years, the TV networks in the USSR were mainly concentrated in densely-populated areas. If the remaining areas were to receive TV programs by the then existing techniques, it would be necessary to build hundreds of television broadcast and relay stations and to set up thousands of kilometres of radio relay links. The utilization of this equipment would be low because it would be set up in the remote and sparsely populated regions of Siberia, the Soviet Far East and Far North. A much better solution to the problem was offered by satellite communication links. The first super-long television relay system through the MOLNIYA-1 satellite was open to traffic in April, 1965. It relayed programs between Moscow and Vladivostok, between Moscow and Paris, and other cities.

In less than two years a network of ground-based stations, known as the ORBITA system, was built in the Soviet Union and put in operation on November, 2, 1967, to handle television and other information relayed via the MOLNIYA-1 satellite. These stations were built in Magadan, Yakutsk, Ashkhabad, Khabarovsk, Chita, Bratsk and other outlying communities of the USSR. This system has made the programs originating in Moscow available to 20 million viewers.

Signals can be relayed via a satellite to the Earth in two ways:

- (1) Using an artificial earth satellite as a passive reflector for radio waves.
- (2) Using an artificial earth satellite as an active repeater.

A passive communications satellite is usually a large sphere made from a thin metallized plastic film. A major advantage of a passive satellite is that it carries no electronic gear. Its major disadvantage is that it reflects incident radio waves in all directions so that the receiving antenna can pick up only a small fraction of the transmitted signal. Systems based on active repeater satellites have wider capabilities. An active repeater satellite carries equipment necessary to boost the signal to be relayed.

A very important consideration in the design of a satellite relay system is the choice of orbits (the angle an orbit makes with the plane of the equator, its height and shape). The orbit will in the final analysis decide the duration of contact between the satellite and ground-based stations, both transmitting and receiving, the transmitter power output required, and other equipment characteristics. Of special interest are orbits in the equatorial plane. When placed in an equatorial orbit about 36,000 km high, a satellite would appear stationary with respect to the Earth (if it is orbiting in the same direction as the Earth is spinning) because its period would be 24 hours, and the duration of contact would be unlimited. Unfortunately, a 24-hour satellite (as it is sometimes called) would not be visible to polar regions of the globe. Also, placing a satellite in a 24-hour orbit poses considerable engineering difficulties. Because of the large quantity of propellant needed for its carrier rocket, the 24-hour satellite would carry a smaller payload than a satellite injected in an elliptical orbit.

On April 23, 1965, the Soviet Union launched its MOLNIYA-1 communication satellite into an elliptical orbit with an apogee of 39,957 km and a perigee of 548 km and inclined at an angle of 65° to the equator (Fig. 10.4)*. The orbit's apogee is above the Northern Hemisphere, its perigee is above the Southern Hemisphere, and the sidereal period** of the satellite is 12 hours exactly. This orbit is very convenient because the satellite circles the Earth twice every day, travelling over the Soviet Union during the first circle and over North America during the second.

A satellite placed in an elliptical orbit travels at a varying speed which is a maximum at perigee and a minimum at apogee. In other words, the satellite traverses the region around perigee faster than the region around apogee. Because of this, each contact between the satellite and ground-based stations is maintained for about 9 hours.

* (Of satellites, both natural and artificial), apogee is the point in the orbit farthest from the Earth, and perigee is the point in the same orbit closest to the Earth.

** Sidereal period is defined as the time required for a satellite to move from a particular position among the stars back to the same longitude again, as seen from the Earth.

The MOLNIYA-1 satellite has an air-tight cylindrical hull enclosing electronic gear. On the outside it carries six solar-battery panels and two parabolic antennas. One head of the cylindrical

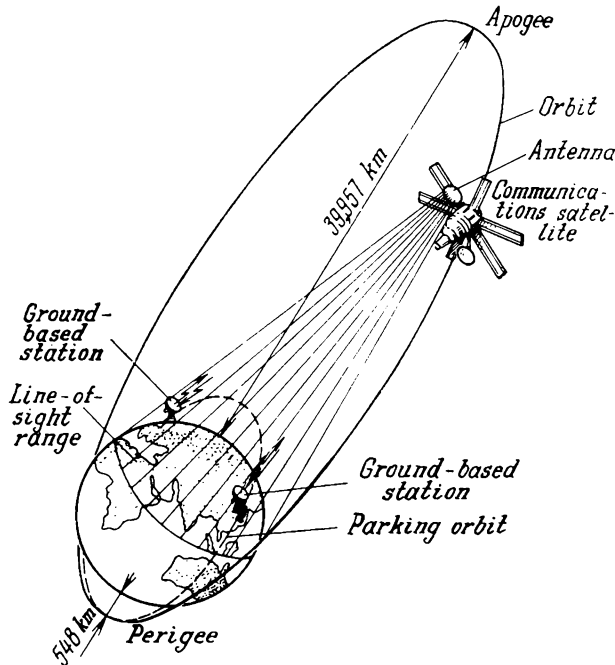


Fig. 10.4. Long-distance communication link using MOLNIYA-1 satellite

hull mounts a propulsion unit and a system of vernier rockets to adjust the orbit. At the opposite end there is an astrotracker to orient the satellite in space.

The repeater equipment carried by the satellite includes a high-sensitivity radio receiver, two antennas (main and standby) capable of picking up weak signals from ground-based stations and relaying them back to the Earth at a higher power level, a transmitter operating in the range 800-1000 MHz and emitting 40 W, and a travelling-wave-tube (TWT) amplifier.

The arrangement of a satellite relay between two points on the Earth by means of a single MOLNIYA-1 satellite is shown in Fig. 10.4. In fact, there may be any number of receiving stations on the Earth. The ORBIT system has 40 such stations.

The ORBIT system operates as follows (Fig. 10.5). The television signal originating at a programming TV centre is relayed by

a television broadcast station to the MOLNIYA-1 satellite. The satellite receives, amplifies and relays the signal to the receiving stations of the ORBIT system. The signal picked up by an ORBIT

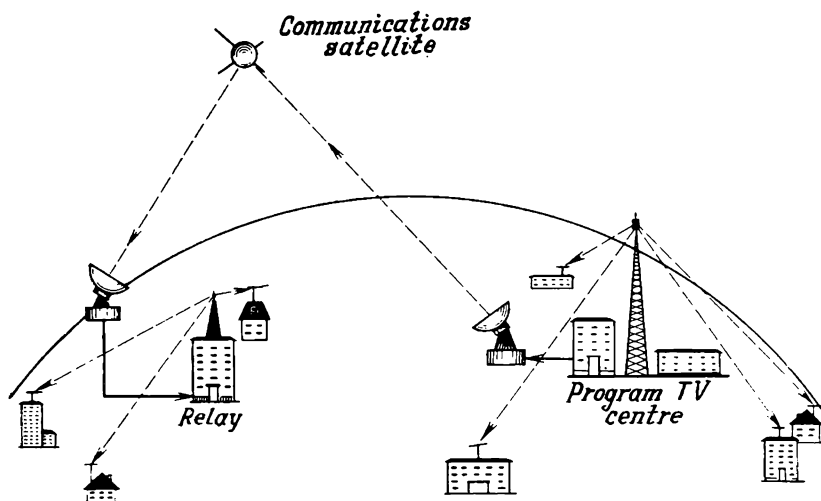


Fig. 10.5. Operation of the ORBIT system

receiving station is channelled over a junction link to a repeater or a local television broadcast station which relays it further to its subscribers who can see the program on their receivers.

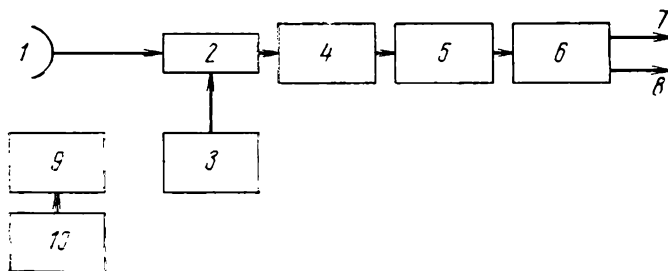


Fig. 10.6. Simplified block diagram of an ORBIT receiving terminal

1 — antenna; 2 — directional coupler; 3 — monitor; 4 — parametric amplifier; 5 — receiving equipment; 6 — video and sound separator; 7 — video signal; 8 — sound signal; 9 — antenna drive; 10 — antenna tracking system

An ORBIT station is housed in a circular reinforced-concrete building which also doubles as the base for an antenna system with a parabolic reflector 12 m in diameter. The antenna is made to

track the satellite by drives controlled by program-tracking apparatus. The reflector is fabricated from an aluminium alloy and weighs about 5.5 metric tons. The central control room of the station houses receiving, tracking and control equipment. In simplified block-diagram form, the arrangement of an ORBIT station is shown in Fig. 10.6. The signal picked up by the antenna is fed via a directional coupler to a parametric amplifier. For better sensitivity, the first amplifier stage is held at liquid-nitrogen temperature where the noise temperature does not exceed 80 K. The amplified signal is then heterodyned to produce an intermediate frequency. The parametric amplifier and the i.f. preamplifier are located close to the antenna. There are also an i.f. main amplifier, a limiter, and a frequency detector. Past the detector, the composite signal is applied to circuits which separate the visual and aural signals.

CHAPTER ELEVEN

COLOUR TELEVISION

11.1. Colour Television Systems

To-day, three basic colour television systems are in use: the NTSC (National Television System Committee) system, the SECAM (Séquence de Couleurs Avec Mémoire) system, and the PAL (Phase Alternation Line) system.

Soviet scientists and engineers have made sizeable contributions to the theory and practice of television. For a number of years, regular colour programs were transmitted in Moscow, using sequential and simultaneous colour addition. Several modifications of colour television were developed, among them the NIIR system later called the SECAM-IV system. This work, both theoretical and experimental, was conducted in cooperation with French specialists. On October 1, 1967, the SECAM system was put in operation in the USSR and France at the same time. In addition to France and the Soviet Union, this system has now been adopted by the German Democratic Republic, Czechoslovakia, Bulgaria, Hungary, and the North-African countries.

The NTSC system and its outgrowth, the PAL system are in use in the United States, Japan, Canada, the Federal Republic of Germany, and Great Britain.

Many pieces of equipment used at the transmitting and receiving terminals are identical in the three systems. The methods and techniques used to convert light images into electrical signals and output circuits in the colour TV set are the same in the three systems. They only differ in the methods by which information is relayed from camera to receiver.

11.2. Basic Facts from Colorimetry

Colour television is far more complex than black-and-white television. Yet, the advantages of the colour picture more than offset this increase in complexity. Among other things, the colour image is more expressive, natural, well-defined and crisp. Colour is a key feature in many productions, say, about painters, journeys, festivities, athletic events, etc. In many closed-circuit television systems such as used in medicine, metallurgy and transport, colour is as essential.

.

Nature around us displays a wide gamut of colours and hues. It has been found that the normal human eye can discern up to 180 colour hues. This does not mean to say that in order to transmit this wealth of colour information the communication channel must have a capacity 180 times as great as that of the usual black-and-white channel. Owing to the remarkable property of the human eye, three-colour vision, a colour channel needs only three times the capacity of a black-and-white channel. In fact, this requirement can be reduced still more by special technical measures (to be discussed later).

For the first time, a three-colour theory of vision was proposed by M.V. Lomonosov of Russia back in 1756. A hundred and fifty

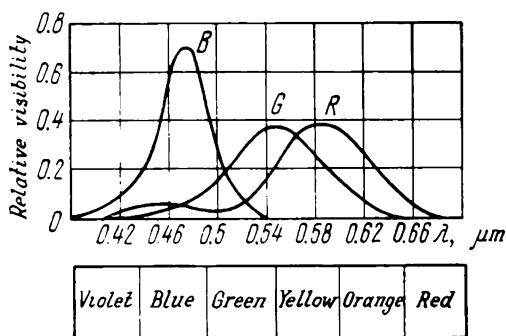


Fig. 11.1. Sensitivity of the eye as a function of light wavelength for the three kinds of cones

years later. Helmholtz formulated this theory in the manner we know it today. By this theory, apart from rods highly sensitive to light and completely insensitive to colour, the retina has three kinds of cones, which are differently responsive to visible radiation. The action of light on one kind of cones produces the sensation of red colour, on a second kind the sensation of green colour, and on a third the sensation of blue. These three colours, red (*R*), green (*G*) and blue (*B*), are called primary colours. Any other colour can be matched by a combination of these three primaries taken in appropriate amounts.

The plot of Fig. 11.1 relates the sensitivity of the eye to the wavelength of light for the three types of cones, as obtained experimentally by N.T. Fedorov of the Soviet Union. The areas under the curves *R*, *G*, and *B* are equal. This checks with the assumption that if the three kinds of cones are given the same amount of excitation, the sensation will be that of white colour. The primary colours *R*, *G* and *B* are independent of one another; that is, none can be obtained by mixing together the remaining two.

Experiments with colour matching can conveniently be done with a prism, P , which has two dull-white faces A and B (Fig. 11.2a). The light flux, Φ , to be compared, is allowed to fall on one face, while the other face receives the amounts of R , G and B required to match the unknown colour. These amounts can be adjusted until the two faces of the prism match exactly in both brightness and hue. The match is expressed by the basic colour equation

$$\Phi = f'F = r'R + g'G + b'B \quad (11.1)$$

which is satisfied in both qualitative and quantitative terms.

In the above equation, R , G and B are the unit amounts of electromagnetic power (say, 1 W) of the primary red, green and blue

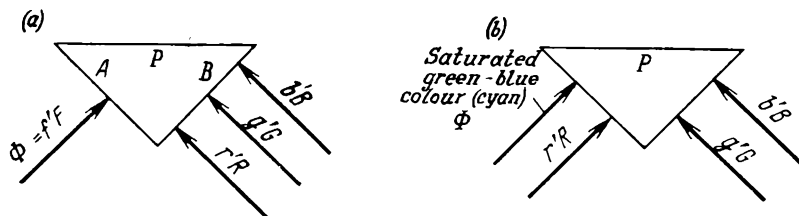


Fig. 11.2. Colour matching by means of a prism

(a) all three tristimulus values are positive; (b) red primary R is negative

light. The coefficients r' , g' and b' show how many units of R , G and B must be taken to match the unknown light, Φ , and are called its *tristimulus values*. The flux Φ may alternatively be expressed as the product of the unit power, F (say, 1 W) by the factor f' representing the number of these units in the flux Φ .

To make the matter more definite, the following monochromatic radiations have been assumed as primaries for colorimetric purposes:

$$\left. \begin{array}{l} R: \lambda_R = 700 \text{ nm} \\ G: \lambda_G = 546.1 \text{ nm} \\ B: \lambda_B = 435.8 \text{ nm} \end{array} \right\} \text{ spectral lines of mercury vapours}$$

This group of primaries defines the generally accepted colorimetric system, RGB . However, this RGB system fails to achieve a match for some colours qualitatively or quantitatively with any relative amounts of the primaries unless one primary is transferred to the unknown. Figure 11.2b illustrates a case where a saturated green-blue (cyan) flux cannot be matched by any combination of primaries. However, by transferring the red primary from the right-hand to the left-hand face of the prism, it is possible to adjust r' , g' and b' until the two faces of the prism match exactly in appearance without changing the quantity and quality of the flux $\Phi = f'F$. Hence, one of the primaries (in our case, this is red) will

enter Eq. (11.1) with a minus sign:

$$f'F + r'R = g'G + b'B$$

or

$$f'F = g'G + b'B - r'R \quad (11.2)$$

In colorimetry, it is customary to represent the matching and mixing of colours by a method known as the colour triangle. In this representation, the three primaries appear one at each of the three vertices of an equilateral triangle, RGB (Fig. 11.3a), as light sources of equal power. If we turn on any one of these sources, the intensity of the light that it gives up will naturally decrease as we

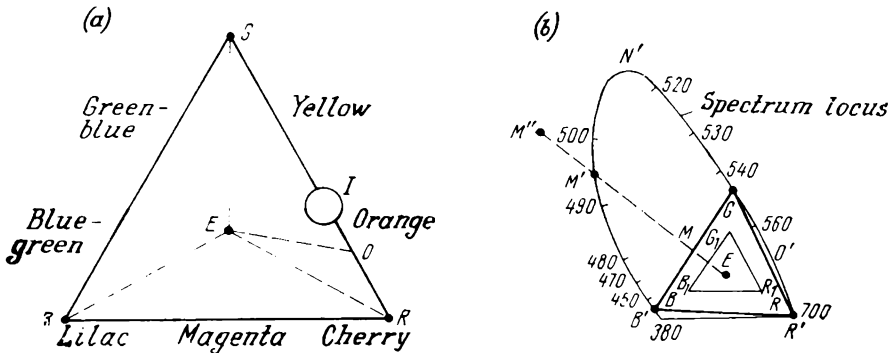


Fig. 11.3. (a) Equilateral colour triangle; (b) location of the colour triangle inside the spectrum locus

move away from it. For simplicity, we assume that the intensity of light coming from the source R drops to zero at the vertices G and B (for this to happen, the triangle RGB must be sufficiently large). This condition must also apply to the sources G and B .

To illustrate the laws by which colours are mixed and matched, imagine a hollow, frosted glass sphere. This sphere will serve as a kind of indicator, I .

Experiment one. Turn on one source, say R . The sphere placed next to the source will be filled with red light. As it is moved from R along the line RG or RB , the sphere will remain red, but it will grow progressively darker, until it turns to black at point G (or B).

Experiment two. Turn on two light sources, R and G . Near these sources, the sphere will be either red or green. In intermediate positions on the line RG the sphere will change in colour. From this experiment we may conclude that on moving from the source R to the source G , the colour of the sphere gradually changes from red to orange, from orange to yellow, and from yellow to green. In other words, orange and yellow can be obtained by combining (mix-

ing) two colours, red and green. In effect, orange differs from, say, yellow, in the greater proportion of red.

Experiment three. Turn on two sources, B and G . On moving from B to G , the colour of the sphere will gradually change from blue to blue-green, from blue-green to green-blue, and from green-blue to green.

Experiment four. Move the sphere along the line BR and note it change consecutively in colour to blue, violet, lilac, purple, cherry-red, and red.

Experiment five. Turn on the three sources. By manipulating the sphere, we are able to locate a point within the triangle RGB where the sphere appears white. Thus, white colour (or light) can be obtained by mixing together suitable amounts of the three primaries. If the primaries thus combined are equal in energy, the *equal-energy-white light*, E , will be obtained at the intersection of the medians of the triangle, that is, at its centroid, or centre of gravity.

Experiment six. Move the sphere along the line RE . The red colour of the sphere will not change, but its saturation will. Red will appear diluted with white. At the point R the sphere will be saturated in red. As it approaches the white point E , its red fades by passing through all hues of pink. At the point E the saturation falls to zero, and the sphere takes on white colour.

In a similar way, as the sphere is moved along, say, the line BE , its colour will not change (it will remain blue), but its saturation will gradually diminish. Along this line, the sphere will pass from saturated blue through hues of blue to take on perfect white at the point E . This sequence of events generally holds for all other straight-line segments connecting the white-colour (light) point, E , with all points on the sides of the colour triangle, RGB . For example, on moving from the saturated orange point along the line OE the sphere will not change its orange hue, but its saturation will change. Artists and painters obtain the saturation they want by adding white to their paints. Obviously, this will not change the colour of a paint, but its saturation will be different. It is important to note that real sources of light cannot have 100% saturation. Whatever source of red (green or blue) we may take, a lantern with a light filter, a picture-tube phosphor, etc., its saturation will always be less than 100%. It has been found that theoretically 100%-saturation can only occur in cases where the source emits energy at precisely one wavelength (or frequency). Such a source is called *monochromatic*. Experiments have shown that all hues discernible by the human eye are located on the sides RG , GB and BR of the colour triangle RGB . The colours found along the line RG are called "warm", and those along the side BG , "cold". These names arise from the fact that the "warm" gamut of colours—red,

orange, yellow and emerald—best suit bright, sun-filled and gay scenes, while the “cold” colours are more appropriate to twilight, a cold winter scene, or a sea storm.

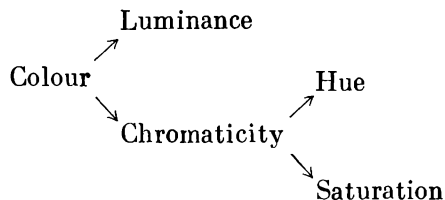
The colour phosphors used in Soviet-made colour picture tubes do not have 100% saturation, either. This is why in Fig. 11.3*b* the colour triangle $R_1G_1B_1$ whose vertices correspond to the colour of these phosphors lies inside the colorimetric triangle RGB (the primaries of this system have 100% saturation because they are produced by monochromatic sources with wavelengths $\lambda_R = 700$ nm, $\lambda_G = 546.1$ nm and $\lambda_B = 435.8$ nm).

Points lying inside the colour triangle $R_1G_1B_1$ represent all colours that can be obtained by mixing the primaries of the phosphors involved. The points outside the triangle represent the colours that cannot be matched by available colour picture tubes. In this case, the saturation (let it be symbolized as p) increases on moving along the straight line from point E ($p = 0$) towards any point M on the sides of the triangle (Fig. 11.3*b*), but it never reaches a 100-% value; the latter is attained at point M' lying on the same line farther away from E than M . The point M' ($p = 100\%$) represents a monochromatic light source. The curve connecting all monochromatic points, B' , M' , N' , O' and R' , is called a spectrum locus or curve of spectral colours, and all points on this locus represent colours with 100-% saturation (see Fig. 11.3*b*). It is customary to label points on the spectrum locus with figures stating the respective wavelength of monochromatic radiation. Since the relative visibility curve of the human eye (see the colour plate, Fig. 1.3), ranges from $\lambda_1 = 380$ nm to $\lambda_2 = 700$ nm, the horseshoe spectrum locus is an open figure. The line connecting the extreme points of the horseshoe curve (380 nm and 700 nm) is called the line of purples, $B'R'$. This line contains the points of saturated colours obtained by adding together the colours B' and R' in various amounts.

The curve of spectral colours and the line of purples cover between them all colours visible to the human eye. The points lying outside the locus (for example, M'' in Fig. 11.3*b*) represent no real colours and have therefore no physical significance. Thus, any colour visible to the human eye is characterized by a set of three colour attributes, namely luminance Y^* , hue λ , and purity or saturation p . While luminance is a quantitative attribute of colour, defining its effect on the eye, hue and purity (or saturation) are qualitative attributes responsible for difference in visual sensations. For convenience in calculations these qualitative attributes are customarily expressed in quantitative terms, too, hue as the wavelength λ of the respective monochromatic light, and purity or saturation as the percentage of white it contains.

* In colorimetry, it is customary to replace brightness B by luminance Y .

The two attributes, hue and saturation, together give chromaticity. Thus,



Where only knowledge of chromaticity is required, it is convenient to work in terms of the relative amounts of the three primaries (usually referred to as trichromatic coefficients). Expressions for the trichromatic coefficients r , g , and b can be derived from the basic colour match equation, Eq. (11.1). It is known from experiments that the luminance of a colour mixture is equal to the sum of the luminances of the constituent colours. Therefore, leaving out qualitative attributes, we may write

$$f' = r' + g' + b' = m$$

where m is the sum of the luminances of the three primaries, called the colour modulus. Dividing both sides of Eq. (11.1) by the colour modulus gives

$$(f'/m) F = (r'/m) R + (g'/m) G + (b'/m) B$$

The trichromatic coefficients

$$\begin{aligned} r &= r'/m = r'/(r' + g' + b'); & g &= g'/(r' + g' + b') \\ b &= b'/(r' + g' + b') \end{aligned} \quad (11.3)$$

define the relative amounts of the primaries R , G and B needed to match a given colour of unit flux, F :

$$F = rR + gG + bB \quad (11.4)$$

Equation (11.4) makes it possible to represent the chromaticity of any light by a point inside the equilateral colour triangle RGB (Fig. 11.4a) of unit height. When the position of the point F inside the triangle is specified (or known) in advance, the perpendicular distances from the colour point to the sides of the triangle will give the relative amounts (trichromatic coefficients) of the three primaries R , G and B in the light flux F . In the example of Fig. 11.4a,

$$F = 0.52R + 0.3G + 0.18B$$

and

$$r + g + b = 0.52 + 0.3 + 0.18 = 1$$

Conversely, when the trichromatic coefficients are specified in advance, the point inside the colour triangle can be located by the rules of mechanics for the centre of gravity, or centroid. For example, let the trichromatic coefficient specified in advance be $r = 0.15$, $g = 0.25$ and $b = 0.6$. We seek to locate the point F representing the chromaticity of the total flux. We place the vectors $r = 0.15$, $g = 0.25$ and $b = 0.6$ as masses at the respective vertices of the colour triangle (Fig. 11.4*b*). To begin with, we find the centroid, F_1 , for two masses (say, r and g) by the equation:

$$l_g/(l_g + l_r) = r/(r + g) = 0.15/(0.15 + 0.25) = 0.375$$

If the height is $h = 1$, the length of the side is

$$l_g + l_r = 1.16$$

Hence,

$$l_g = 0.375 \times 1.16 = 0.435$$

$$l_r = (l_g + l_r) - l_g = 1.16 - 0.435 = 0.725$$

The total mass at the point F_1 is

$$r + g = 0.15 + 0.25 = 0.4$$

The sought point F lies on the straight line connecting the points B and F_1 . Its position can be defined as

$$l_b/(l_b + l_{F_1}) = (r + g)/(r + g + b) = 0.4/1 = 0.4$$

For $l_b = l_{F_1} = 1.02$

$$l_b = 0.4 \times 1.02 = 0.408$$

The chromaticities represented by points on the chromaticity diagram, Fig. 11.4*a*, lying outside the colour triangle (say, N) cannot be matched by any combination of the primaries R , G and B . As is shown in Fig. 11.2*b*, a proper match in this case can only be secured by adding one of the primaries to the colour to be matched, Φ .

Naturally, this would change the chromaticity seen on the left-hand field (face of the prism). In other words, for the colour represented by the point N one of the primaries will enter the basic colour match equation, Eq. (11.2), with a minus sign.

By drawing a straight line to join the point N to the white-colour point E , we find that the chosen amounts of primaries can match the given hue, λ_N , but at a lower saturation, $p_N < p_N$. To sum up, mixing together the three primaries, R , G and B , can match any hue, but not any saturation.

If the three primaries of the colorimetric system, R ($\lambda_R = 700$ nm), G ($\lambda_G = 546.1$ nm) and B ($\lambda_B = 435.8$ nm),[†] are expressed in energy

units (say, $R = G = B = 1$ W of radiant energy), the *equal-energy* white point E will lie at the centroid of the triangle RGB . Its trichromatic coefficients will then be equal, that is, $r_E = g_E = b_E$ (Fig. 11.4a). In practice, however, it is more convenient to express the primaries in the accepted light units (the light watt,

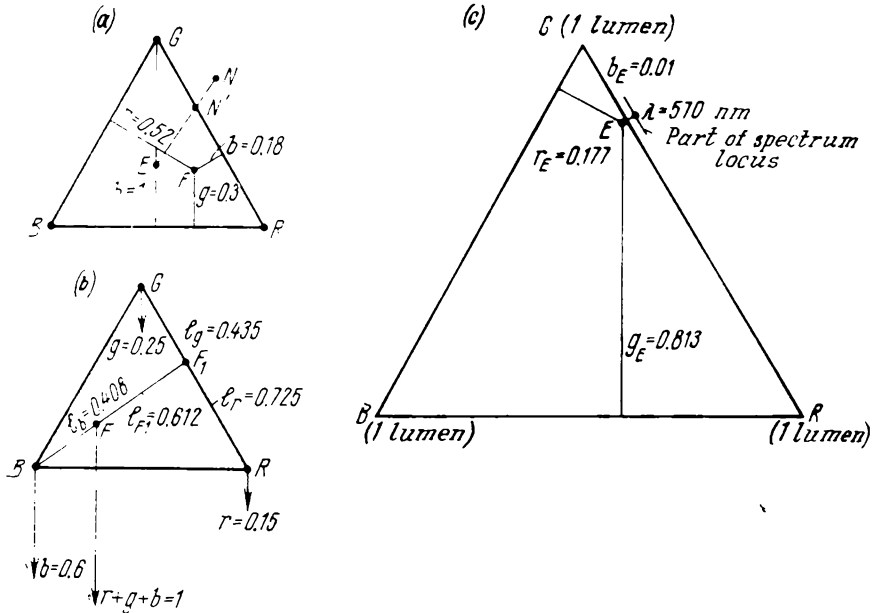


Fig. 11.4. Use of the colour triangle in the calculation of (a) trichromatic coefficients r , g and b ; (b) colour mixture from known r , g and b ; (c) position of equal-energy colour point E

the lumen, the candela per square metre, or the lux). Since the human eye is not uniformly sensitive to different wavelengths (see the relative visibility diagram in the colour plate, Fig. 1.3), being most sensitive to green, moderately sensitive to red, and least sensitive to blue, one watt of radiant energy associated with each of the three primaries corresponds to a different number of units of a particular light quantity (say, of luminous flux). Experiments have shown that if 1 W of red be equal to a lumens, then 1 W of $G = 4.5907 \times a_{\text{lumen}}$ and 1 W of $B = 0.0601 \times a_{\text{lumen}}$. That is, if the ratio of the energies associated with the three primaries be equal to unity

$$R_W : G_W : B_W = 1 : 1 : 1 \quad (11.5)$$

then their fluxes (in lumens) will be in the following ratio:

$$F_{R(\text{lumen})} : F_{G(\text{lumen})} : F_{B(\text{lumen})} = 1 : 4.5907 : 0.0601 \quad (11.6)$$

As already noted, equal-energy white, E , is matched by combining equal amounts of the three primaries:

$$E_W = r_E R_W + g_E G_W + b_E B_W$$

where

$$r_E = g_E = b_E = 1/3$$

that is

$$E_W = R_W/3 + G_W/3 + B_W/3 \quad (11.7)$$

If the primaries be expressed in lumens, then from Eqs. (11.6) and (11.7) we get

$$E_{\text{lumen}} = R_{\text{lumen}}/3 + 4.5907 G_{\text{lumen}}/3 + 0.0601 B_{\text{lumen}}/3$$

In this case, the trichromatic coefficients of E are defined as

$$r_E = \frac{1}{1 + 4.5907 + 0.0601} = 0.177$$

$$g_E = \frac{4.5907}{1 + 4.5907 + 0.0601} = 0.813$$

$$b_E = \frac{0.0601}{1 + 4.5907 + 0.0601} = 0.01$$

The colour triangle, RGB (lumens), in which the equi-point E has the above tristimulus values ($r_E = 0.177$, $g_E = 0.813$ and $b_E = 0.01$) is shown in Fig. 11.4c. In this triangle, the equi-point E is shifted towards the side RG and practically coincides with the point $\lambda = 570$ nm on the spectrum locus. No room is left for intermediate colours between white, E , and $\lambda = 570$ nm on the chromaticity diagram. To make it more convenient for practical use, the points representing colours should be arranged in a different way inside the triangle.

On the basis of the foregoing, the following limitations of the RGB (lumen) colorimetric system may be stated:

(1) for many colours to be matched, the basic match equation, Eq. (11.1), contains one of the primaries with a minus sign;

(2) the equi-point E is shifted towards the side RG of the colour triangle;

(3) in order to specify the radiant flux (or luminance) of a colour combined from the three primaries, it is necessary to know the tristimulus values r' , g' , and b' of all the three primaries, R , G and B .

In 1931, the Commission Internationale de l'Eclairage (International Commission on Illumination), the CIE (ICI) for short, adopted a new international standard method of specifying colour, the XYZ system of colour representation. It is based on an equilateral right-angled colour triangle (Fig. 11.5a) in which the vertices represent a new set of "nonphysical" primaries referred to as X , Y and Z . A mixture of these three primaries can match any physical colour having *any saturation and any hue*.

The spectrum locus and the line of purples, which define between them an area of all physical colours, lie inside the triangle XYZ . This implies that the basic colour match equation

$$F = x'X + y'Y + z'Z \quad (11.8)$$

contains the components $x'X$, $y'Y$ and $z'Z$ with only a plus sign for any real colour always.

The points at which the CIE primaries X , Y and Z are located lie outside the spectrum locus and the line of purples. This is an indication that the saturation at these points exceeds 100%, which fact has no physical meaning. This is why the primaries X , Y and Z are nonphysical or non-real. However, they may well be used for a variety of colorimetric calculations.

In Fig. 11.5a, the colour triangle of the RGB system, $\lambda_R = 700$ nm, $\lambda_G = 546.1$ nm and $\lambda_B = 435.8$ nm, is shown lying inside the XYZ colour triangle of the CIE system. If R , G and B be expressed in units of radiant flux, the two sets of primaries, RGB and XYZ , may be connected by the following equations:

$$\left. \begin{aligned} X &= 0.4184R - 0.4185G + 0.0001B \\ Y &= -0.1587R + 1.1589G - 0.0002B \\ Z &= -0.0828R + 0.0721G + 0.0107B \end{aligned} \right\} \quad (11.9)$$

Substituting $R = G = B = 1$ W in Eq. (11.9) gives:

$$\begin{aligned} X &= 0.4184 \times 1 - 0.4185 \times 1 + 0.0001 \times 1 = 0 \\ Y &= -0.1587 \times 1 + 1.1589 \times 1 - 0.0002 \times 1 = 1 \text{ W} \\ Z &= -0.0828 \times 1 + 0.0721 \times 1 + 0.0107 \times 1 = 0 \end{aligned}$$

From the above relations it is seen that the radiant flux of unit amounts of X and Z is zero, that due to Y is equal to 1 W. In other words, in Eq. (11.8), the radiant flux is solely decided by $y'Y$.

Like Eqs. (11.3), the CIE trichromatic coefficients defining the chromaticity of the colour to be matched are defined as

$$\left. \begin{aligned} x &= \frac{x'}{x' + y' + z'} = x'/m \\ y &= \frac{y'}{x' + y' + z'} = y'/m \\ z &= \frac{z'}{x' + y' + z'} = z'/m \end{aligned} \right\} \quad (11.10)$$

where $m = x' + y' + z'$ is the colour modulus.

It follows from Eq. (11.10) that

$$x + y + z = 1 \quad (11.11)$$

so that only two trichromatic coefficients are necessary to specify the colour. These usually are x and y ; the third z can be found from

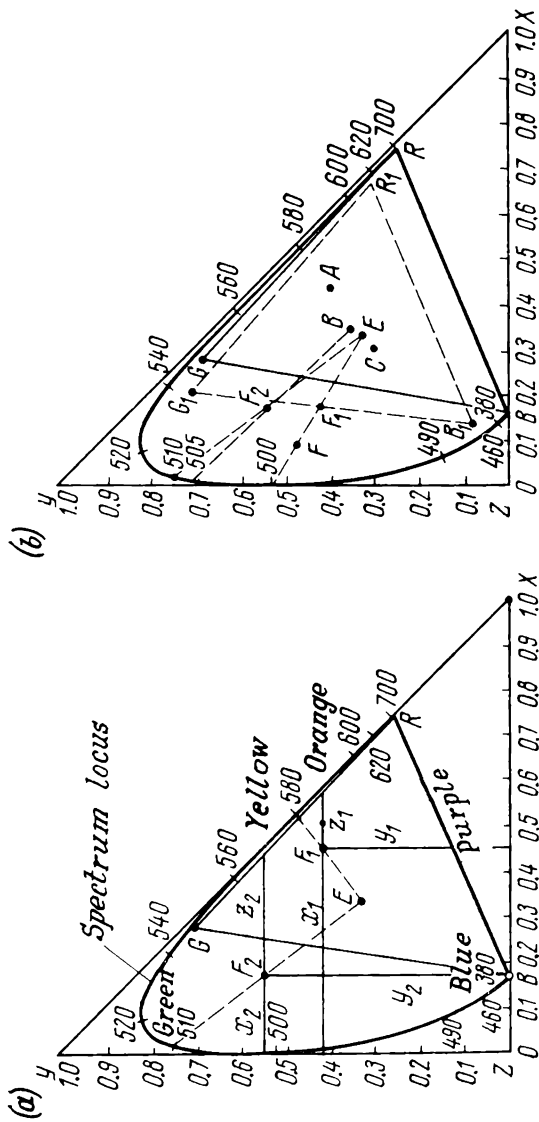


Fig. 11.5. XYZ colour triangle and spectrum locus
(a) calculations in the XYZ system; (b) coordinates of Standard Illuminants and colour triangle for phosphors of colour picture tubes

Eq. (11.11). It is important to note that in the CIE system the tri-chromatic coefficients of equal-energy white, E , are equal:

$$x_E = y_E = z_E = 1/3 \quad (11.12)$$

As an example of using the CIE chromaticity diagram, let us determine the chromaticity of two colours, F_1 and F_2 (Fig. 11.5a).

For F_1 : $x_1 = 0.450$, $y_1 = 0.425$, $z_1 = 1 - (x_1 + y_1) = 0.125$

For F_2 : $x_2 = 0.175$, $y_2 = 0.550$, $z_2 = 0.275$

Two coordinates, x and y , completely specify the chromaticity. However, it is often desired to have separate information about the hue and saturation of the colour. The hue is defined by the intersection of the straight line EF and the spectrum locus. Thus, for the colour point F_1 , $\lambda_{F_1} = 580$ nm, and for the colour point F_2 , $\lambda_{F_2} = 510$ nm.

The saturation p is defined as

$$p = \frac{y_\lambda}{y_F} \cdot \frac{y_F - y_E}{y_\lambda - y_E} \times 100\% \quad (11.13)$$

where y_λ = locus point defining the hue

y_F = point representing the colour to be matched, F
 $y_E = 1/3$ = equal-energy white, E

Applying Eq. (11.13) yields:

for F_1 :

$$y_{\lambda_1} = 0.475$$

$$y_{F_1} = 0.425$$

$$p_1 = \frac{0.475}{0.425} \cdot \frac{0.425 - 0.333}{0.475 - 0.333} \times 100\% = 8.6\%$$

for F_2 :

$$y_{\lambda_2} = 0.750$$

$$y_{F_2} = 0.550$$

$$p_2 = \frac{0.750}{0.550} \cdot \frac{0.550 - 0.333}{0.750 - 0.333} \times 100\% = 7.8\%$$

In accordance with Eq. (11.3), the saturation of white, E , is zero, and that of a monochromatic colour is 100%. As a proof, for the equal-energy white point E :

$$y_F = y_E = 1/3$$

and

$$p_E = \frac{y_\lambda}{y_E} \cdot \frac{y_E - y_E}{y_\lambda - y_E} \times 100\% = 0$$

For a monochromatic colour,

$$y_\lambda = y_F$$

and

$$p_\lambda = \frac{y_\lambda}{y_\lambda} \cdot \frac{y_\lambda - y_E}{y_\lambda - y_E} \times 100\% = 100\%$$

A source of equal-energy white E is a hypothetical entity non-existent in reality. In television practice, three standard illuminants known as A , B and C are employed instead. Illuminant A simulates night-time artificial illumination; Illuminants B and C , natural daylight illumination. Their colours are very close to the radiation emitted by the filament of an incandescent lamp at the temperatures listed in Table 11.1 which also gives some other characteristics of the Illuminants A , B and C .

Table 11.1

Illuminant	Colour temperature, K	Natural analog	x	y	Hue, nm	Saturation, %
A	2854	Ordinary incandescent lamp	0.448	0.407	583	65
B	4800	Cloudy day	0.348	0.352	574	15
C	6500	Sunny day, blue sky	0.310	0.316	482	5

The points representing the Illuminants A , B , C and E are shown in Fig. 11.5*b*. As is seen, if a real illuminant (say, B) be taken as reference instead of equal-energy white E , the hue and saturation will change. For example, at point F_2 , $\lambda_{(B)} = 505$ nm instead of $\lambda_{(E)} = 510$ nm, and

$$p_{(B)} = \frac{y_{\lambda_{(B)}}}{y_{F_2}} \cdot \frac{y_{F_2} - y_{(B)}}{y_{\lambda_{(B)}} - y_{(B)}} = \frac{0.710}{0.550} \cdot \frac{0.550 - 0.352}{0.710 - 0.352} \times 100\% = 71\%$$

instead of $p_{(E)} = 78\%$.

On the basis of many experiments, the spectrum locus may arbitrarily be divided into the various colour regions as shown on the colour plate of Fig. 11.6. It should be recalled, however, that the boundaries between the actual colour regions are not so well defined as they are in the figure.

Experience shows that the chromaticity of objects (for example, textiles) visible to the eye depends on the nature of the light source used. In order to define chromaticity by the position of a point on the chromaticity diagram, it is essential to know the energy distribution of the light source with wavelength (in the form of a chart or table). Then the chromaticity can be calculated by use of the photometric quantities known as distribution coefficients, \bar{r} , \bar{g} and \bar{b} . The significance of these coefficients may be explained as follows. Suppose there is a device which can be arranged to emit any monochromatic colour the representing point of which is located on the spectrum locus. The source is set to emit 1 W of power. With the power of the illuminant held constant, the luminance observed by the eye depends on the wavelength of light (see the

colour plate in Fig. 1.3). The distribution coefficients \bar{r} , \bar{g} and \bar{b} define the luminous flux $\bar{f}(\lambda)$ of monochromatic radiation of 1 W both quantitatively and qualitatively:

$$\bar{f}(\lambda) = \bar{r}(\lambda) + \bar{g}(\lambda) + \bar{b}(\lambda) \quad (11.14)$$

Since the *RGB* triangle lies wholly inside the spectrum locus (see Fig. 11.3*b*), one of the coefficients on the right-hand side of Eq. (11.14) is bound to be negative, and this would complicate calculations. The experimental tristimulus values \bar{r} , \bar{g} and \bar{b} can be converted to the CIE distribution coefficients. Table 11.2 summarizes them for a series of wavelengths. As is seen, the CIE distribution coefficient

Table 11.2

λ , nm	Distribution coefficients			$\rho(\lambda)$	$\bar{x}\rho$	$\bar{y}\rho$	$\bar{z}\rho$
	\bar{x}	\bar{y}	\bar{z}				
400	0.014	0.000	0.068	0.00	0.000	0.000	0.000
420	0.134	0.004	0.646	0.00	0.000	0.000	0.000
440	0.348	0.023	1.747	0.00	0.000	0.000	0.000
460	0.291	0.060	1.669	0.00	0.000	0.000	0.000
470	0.195	0.091	1.288	0.02	0.004	0.002	0.026
480	0.096	0.139	0.813	0.07	0.007	0.010	0.057
490	0.032	0.208	0.465	0.14	0.004	0.029	0.065
500	0.005	0.323	0.272	0.25	0.001	0.081	0.068
510	0.009	0.503	0.158	0.60	0.005	0.300	0.095
520	0.063	0.710	0.078	0.96	0.060	0.681	0.075
530	0.165	0.862	0.042	0.96	0.158	0.825	0.040
540	0.290	0.954	0.020	0.72	0.202	0.686	0.014
550	0.433	0.995	0.009	0.40	0.174	0.398	0.004
560	0.595	0.995	0.004	0.25	0.149	0.248	0.001
570	0.762	0.952	0.002	0.17	0.129	0.162	0.000
580	0.916	0.870	0.002	0.12	0.110	0.104	0.000
590	1.026	0.757	0.001	0.08	0.082	0.060	0.000
600	1.062	0.631	0.001	0.05	0.053	0.031	0.000
610	1.003	0.503	0.000	0.02	0.020	0.001	0.000
620	0.854	0.381	0.000	0.00	0.000	0.000	0.000
640	0.448	0.175	0.000	0.00	0.000	0.000	0.000
660	0.165	0.061	0.000	0.00	0.000	0.000	0.000
680	0.047	0.017	0.000	0.00	0.000	0.000	0.000
700	0.011	0.004	0.000	0.00	0.000	0.000	0.000

ents \bar{x} , \bar{y} and \bar{z} remain positive over the entire visible spectrum.

The manner in which the chromaticity of a source (that is, its chromaticity coordinates x and y on the CIE diagram) is found will be clear from the following example. Figure 11.7 shows the spectral

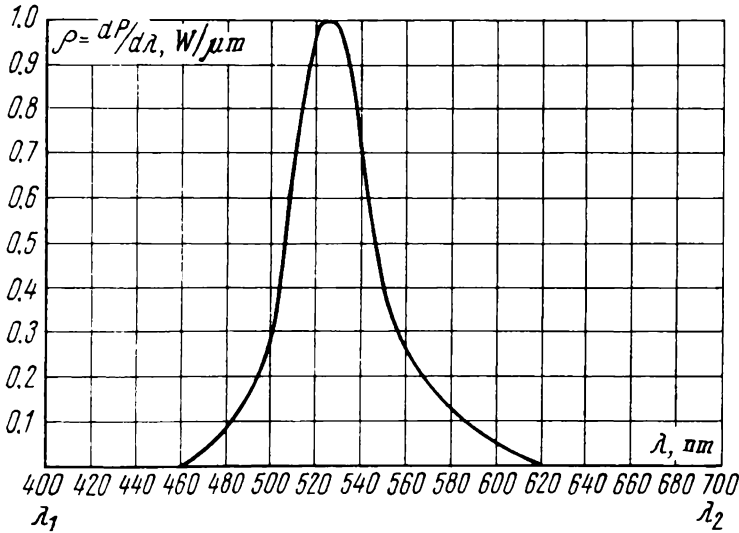


Fig. 11.7. Spectral response of a green-emitting phosphor for a typical colour picture tube

response of a green phosphor answering the chemical formula $\text{Zn}_2\text{SiO}_4\text{Mn}$; this is one of the three phosphors used in a colour picture tube. The power distribution of the radiation is laid off as ordinate. The differential of this power (in watts) is defined as

$$dP = \rho d\lambda$$

Accordingly, the differential of the luminous flux (in watts) is

$$dF = \bar{x}\rho d\lambda + \bar{y}\rho d\lambda + \bar{z}\rho d\lambda \quad (11.15)$$

The total luminous flux F emitted by green phosphor is found by integrating Eq. (11.15)

$$F = \int_{\lambda_1}^{\lambda_2} \bar{x}\rho d\lambda + \int_{\lambda_1}^{\lambda_2} \bar{y}\rho d\lambda + \int_{\lambda_1}^{\lambda_2} \bar{z}\rho d\lambda = x'X + y'Y + z'Z \quad (11.16)$$

The tristimulus values x' , y' and z' are found by the equations

$$\begin{aligned} x' &= \int_{\lambda_1=400 \text{ nm}}^{\lambda_2=700 \text{ nm}} \bar{x}\rho \, d\lambda; & y' &= \int_{\lambda_1}^{\lambda_2} \bar{y}\rho \, d\lambda; \\ z' &= \int_{\lambda_1}^{\lambda_2} \bar{z}\rho \, d\lambda \end{aligned} \quad (11.17)$$

where $\rho = dp/d\lambda$ is the spectral distribution of the colour power.

In practice, integration is replaced by summation:

$$x' \approx \sum_1^n \rho_n \bar{x}_n; \quad y' \approx \sum_1^n \rho_n \bar{y}_n; \quad z' \approx \sum_1^n \rho_n \bar{z}_n \quad (11.18)$$

In such cases, the accuracy of the result improves as the quantizing interval along the axis of abscissae, $\Delta\lambda = (\lambda_2 - \lambda_1)/n$, is reduced (that is, as the number of samples, n , is increased). In Fig. 11.7, $n = 35$. The ordinates of the spectral response are tabulated in Table 11.2.

According to this Table and Eq. (11.18), we get:

$$x' = \sum_1^n \rho_n \bar{x} = 1.158, \quad y' = \sum_1^n \rho_n \bar{y} = 3.618, \quad z' = \sum_1^n \rho_n \bar{z} = 0.345$$

Once x' , y' and z' are known, it is an easy matter to find the trichromatic coefficients:

$$\begin{aligned} x &= \frac{x'}{x' + y' + z'} = \frac{1.158}{1.158 + 3.618 + 0.345} = 0.215 \\ y &= \frac{y'}{x' + y' + z'} = \frac{3.618}{1.158 + 3.618 + 0.345} = 0.706 \\ z &= 1 - (x + y) = 1 - (0.215 + 0.706) = 0.079 \end{aligned}$$

In the Soviet Union, the phosphors used for colour picture tubes answer the following chemical formulae: blue, ZnSAg ; green, $\text{Zn}_2\text{SiO}_4\text{Mn}$; and red, $\text{Zn}_3(\text{PO}_4)_2$. These phosphors have a sufficiently narrow spectral response and a high light output. The trichromatic coefficients of these phosphors in the CIE chromaticity diagram are

$$\begin{aligned} x_R &= 0.67; & y_R &= 0.33 \\ x_G &= 0.21; & y_G &= 0.71 \\ x_B &= 0.14; & y_B &= 0.08 \end{aligned}$$

The respective colour triangle, $R_1G_1B_1$, is enclosed inside the chromaticity diagram of Fig. 11.5*b*. The area of the triangle represents the maximum attainable saturation of the colours on the co-

lour picture tube. For example, the colour represented by point F will not be reproduced by the colour picture tube at its nominal saturation, $p_F = 76\%$; the actual saturation will fall to $p_{F_1} = 57.5\%$. The hue, however, will remain unaffected: $\lambda_{F_1} = \lambda_F = 500 \text{ nm}$.

11.3. Sequential Colour Television System

In colour television, the picture can be produced in any one of two ways, namely by adding the colours sequentially or simultaneously. The sequential method is illustrated on the colour plate of Fig. 11.8a. In front of a projector, P , emitting a cone of white light, there is a rotating disc carrying light filters which are made from a thin film painted a particular colour. If the disc be rotating at a sufficiently high speed, the individual colours thrown onto the viewing screen, S , in turn will add to produce a mixed colour. For example, if the disc carries a red and a green filter, the resultant spot on the screen will be orange; if there are three filters: red, green and blue, they will produce a white light spot.

The principle of simultaneous colour display is illustrated in the colour plate of Fig. 11.8b. Three primary colours, red, green and blue are supplied by three lights and are superimposed on the screen, S , into a composite light spot possessing the full colour gamut of the sources.

For an insight into the operation of so-called compatible colour systems, it will be worth while to take a closer view at a system effecting sequential colour representation. A simplified block diagram of this system is shown in Fig. 11.9a.

In front of a conventional (black-and-white) camera is a rotating disc carrying three light filters painted red (R), green (G), and blue (B). The speed of the disc is adjusted so that all of the scene thrown onto the photocathode of the camera tube can be scanned during the interval needed for one colour to move past the camera lens. After amplification, the signal is fed to a transmitter which emits it into the air.

At the receiving terminal, the signal is picked up by an antenna which feeds it into a receiver where it is processed by a detector and a video amplifier and applied to the control electrode of a black-and-white picture tube. In front of the picture tube is another rotating disc carrying light filters similar to those in front of the camera tube. The viewer watches the image through this rotating disc.

Obviously, for correct colour reproduction it is important that the drive motors and filter discs be properly synchronized mechanically in addition to the electronic synchronization of scanning in the camera and picture tubes. In the block diagram of Fig. 11.9b the need for this mechanical synchronization is shown by arrows pointing from the motor to the video amplifier (at the transmitting

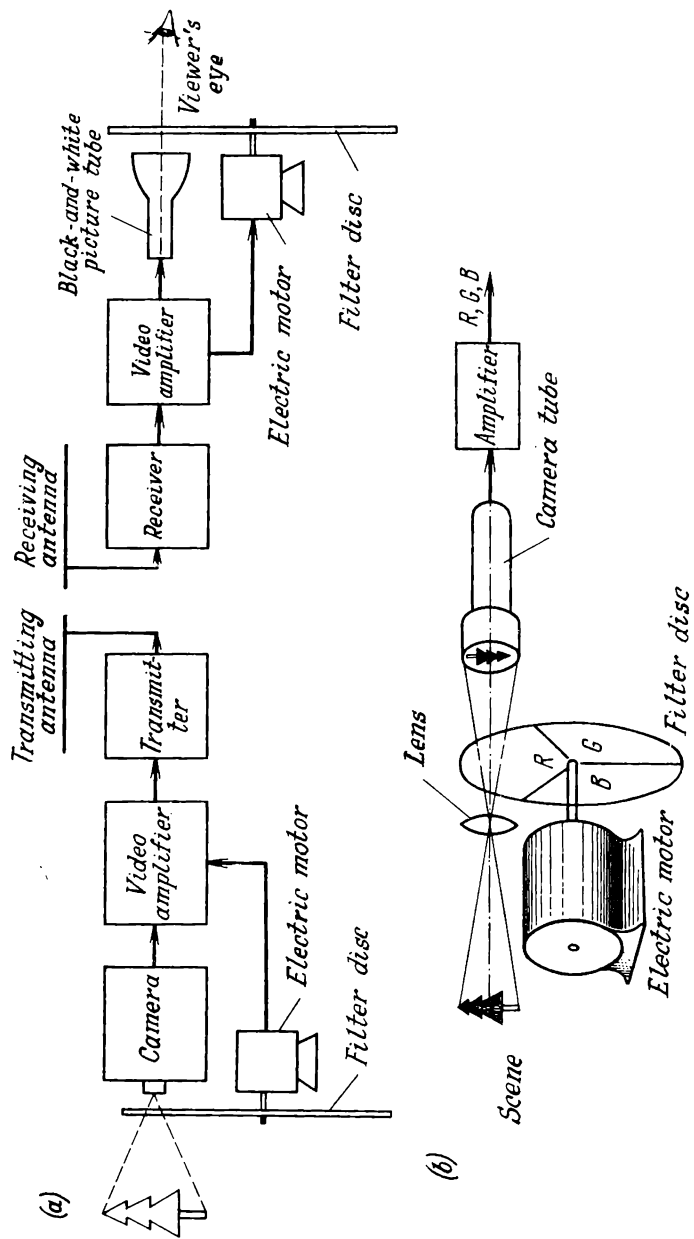


Fig. 11.9. Sequential colour television system
(a) block diagram; (b) arrangement of analyzer

terminal) and from the video amplifier to the motor (at the receiving terminal).

The transmitting disc analyzes the image being televised into colours. The image, *O* (see the colour plate, Fig. 11.10a), formed by superimposition of colours, is separated into three sequential single-colour frames, *R*, *G* and *B*.

By the laws of colour mixing and matching, the yellow wall of the house or the yellow sun in this figure is transmitted by a combination of two frames, red and green, and the white window by three frames. If the disc is rotating fast enough, the individual single-colour frames will merge into a multi-colour picture which is a faithful reproduction of the original scene.

Among the advantages of sequential television systems are the simplicity of the idea, use of only one camera tube and only one conventional (black-and-white) picture tube, and simplicity of colour synchronization. It might appear that by simply adding a drive motor and a filter disc at the transmitting and receiving terminals of a black-and-white system one could readily convert it to colour television.

In fact, a sequential colour system can successfully be used in some special cases, but it has proved unsuitable for broadcast television. This is because it needs a prohibitively large bandwidth for the television signal, large-size picture tubes are difficult to use, colour gaps appear in the transmission of fast-moving objects, and compatibility is out of the question.

Let us examine the above limitations, starting with the last one — lack of compatibility. The black-and-white TV sets now in use in both the Soviet Union and abroad run into tens of millions. Obviously, any colour system must be based on principles which would agree with the standards adopted for black-and-white television.

The most important indicators of this standard are the bandwidth occupied by the television signal, line and frame scan rates or frequencies. If a colour system fails to meet the requirements for at least these two indicators, the owner of a black-and-white TV receiver would have to buy a colour set. Or, if a person has got a colour TV receiver, he would not be able to receive black-and-white programs.

The principle of compatibility as applied to colour television defines the property of a colour television system which permits substantially normal monochrome reception of the transmission by typical unaltered black-and-white receivers. Conversely, this implies that a typical unaltered colour receiver can normally receive monochrome transmissions. Compatibility is the coexistence of colour and monochrome television; it is a vital condition for a gradual transition to all-colour television.

As already noted, sequential colour television systems fail to satisfy the requirement for compatibility. The principal road-block is so-called colour flicker.

Consider the problem of colour flicker with reference to the sequential colour system shown in block-diagram form in Fig. 11.9. If, to preserve compatibility, we retain the same line and frame rates as are used in monochrome television, unpleasant and irritating colour flicker would be visible on the screen. The manner in which this colour flicker develops can be seen from the following simple example. Suppose that the object being televised is a red flag against a blue background (see the colour plate of Fig. 11.10*b*). The field rate in television is 50 fields per second, that is, $T_{field} = 1/f_{field} = 1/50$ s. In the circumstances, each colour would appear with a period of $T_{colour} = 3T_{field} = 3/50$ s. In other words, the primaries would be displayed at a rate which is one-third of the field frequency, $f_{colour} = f_{field}/3 = 50/3 = 16.7$ Hz, which is much below the fusion frequency, and this is perceived as flicker.

To avoid colour flicker, a sequential colour system would have to use a frame frequency three times as high. Then the line and frame scan rates would have to be increased in proportion, and the line and frame scan generators of a conventional monochrome receiver would not be able to operate normally unless modified considerably, which runs counter to the definition of compatibility.

As the frame rate is increased threefold, the bandwidth required for the television signal must likewise be increased threefold, and a sequential colour system fails to meet the requirement for this indicator too.

11.4. Simultaneous Colour Television Systems

A simplified block diagram of a simultaneous colour television system (the transmitting terminal) is shown in Fig. 11.11*a*. Light reflected from the object being televised falls on dichroic mirrors. A dichroic mirror (to be examined in detail later) has the property of reflecting rays of one colour and transmitting rays of the remaining colours. For example, mirror 1 will reflect rays 1-2 of blue colour and transmit rays 1-4 of green and red colour.

Mirror 4 will reflect red rays 4-6 and transmit green rays 4-5. As a result, only one of the three primaries, *R*, *G* or *B*, is allowed to reach the photocathode of each of the three pickup tubes.

So that the three signals can be emitted by a single transmitter, they must be modulated onto different subcarriers. For this purpose, the video signals *G* and *B*, after they have been amplified, are fed to modulators which also accept subcarrier frequencies f_B and f_G . From the modulators, the signals *B* and *G* spaced apart on the frequency axis are conveyed along with the video signal *R* to a mi-

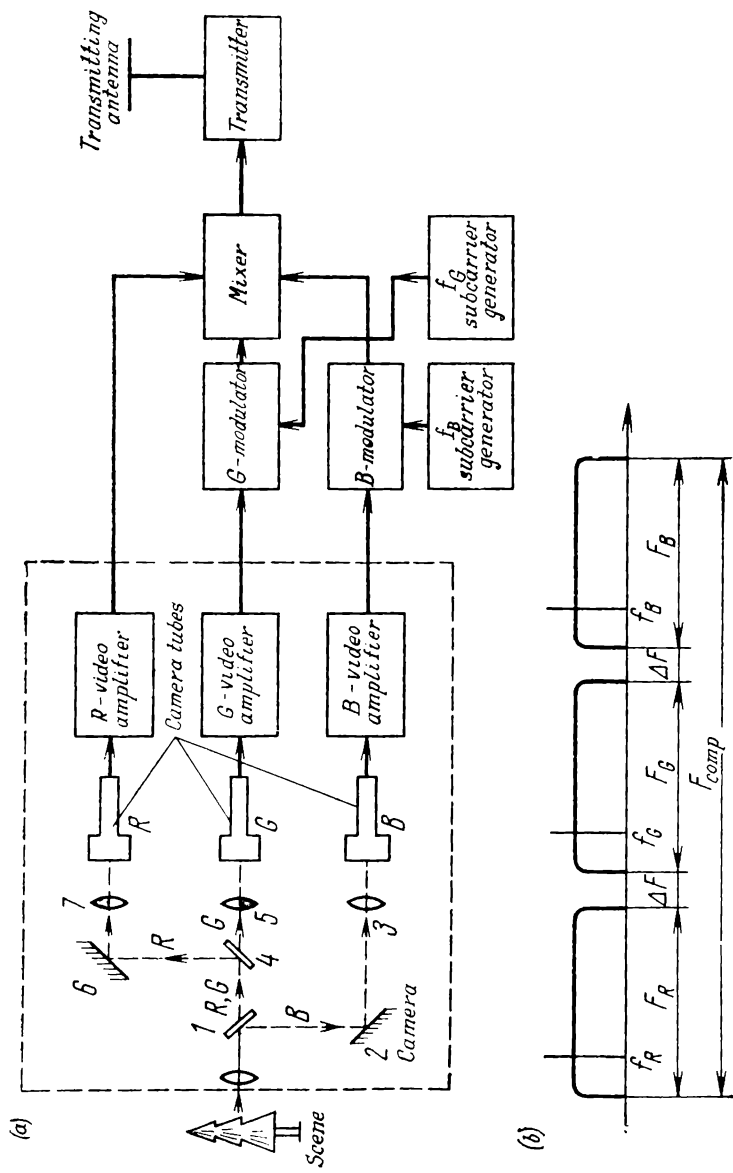


Fig. 11.11. Simultaneous colour television system
 (a) simplified block diagram of the transmitting terminal; (b) frequency spectrum; 1, 4—dichroic mirrors; 2, 6—ordinary mirrors; 3, 5, 7—lenses

xer. The composite signal is then fed from the mixer to the transmitter where the composite signal made up of the video signal R , the modulated signals B and G is modulated onto a carrier. As a result, the three video signals are spaced apart on the frequency axis as shown in Fig. 11.11*b*.

Assuming that the three colour signals occupy the same bandwidths, that is, $F = F_R = F_G = F_B = 6$ MHz, the bandwidth taken up by the total colour signal of a simultaneous system would be

$$F_{total} = 3F + 2\Delta F = 3 \times 6 + 2 \times 0.5 = 19 \text{ MHz}$$

The guard bands, ΔF , are necessary in order that the band-pass filters at the receiving terminal can reliably separate the individual colour signals. Thus, the signal emitted by the transmitter would occupy a bandwidth of about 20 MHz.

The line and frame scan rates of any of the three pickup tubes in a simultaneous system are the same as used in monochrome equipment. Thus, in this respect, the simultaneous system is also a compatible system. However, it is incompatible because of the bandwidth needed for the television signal. Fortunately, there are techniques by which the bandwidth requirement can be reduced to the standard one (about 6 MHz) without any detriment to the quality of the received picture, thereby making the system a compatible one in this respect, too. The techniques used for the purpose will be taken up later.

Important optical elements of the camera in a simultaneous colour system are dichroic mirrors (at 1 and 4 in Fig. 11.11*a*). They serve a double purpose. Firstly, they split the light coming from the scene being televised into three beams in accordance with the number of pickup tubes used. Secondly, they analyze the light into the constituent colours.

A dichroic mirror is illustrated in Fig. 11.12*a*. A plate of highly polished glass is given a coat of thin translucent dielectric film. As it falls on the mirror, a beam of white light, I_1 , is partly reflected (rays I_2 and I_3), and partly transmitted (ray I_4). Depending on the film thickness, the refractive indexes of the glass, n_1 , and film, n_2 , and the wavelength (that is, colour) of light, the beams reflected from the interface between glass and film (I_2) and from the interface between film and air (I_3) may happen to be in phase, in anti-phase, or somewhere in between. In other words, the energies they carry may be added together or cancel out either partly or completely. Thus, the intensity of reflected light is decided by the wavelength. Typical plots of reflectance

$$\rho = (I_2 + I_3)/I_1 \quad (11.19)$$

and transmittance

$$\tau = I_4/I_1 \quad (11.20)$$

are shown in Fig. 11.12b. As is seen, the sum of transmitted and reflected light (accurate to loss) is equal to incident light

$$\rho + \tau = 1$$

To improve the colour selectivity of dichroic mirrors, they are given a film coating of several layers (Fig. 11.12c). By suitably matching the individual films for refractive index, thickness and sequence, it is possible to improve the dependence of reflectance, ρ , and transmittance, τ , on wavelength, that is, to make portion 2-3 (Fig. 11.12b) more steep and the transmission and reflection regions, 1-2 and 3-4, more flat.

A block-diagram of the receiver used in a simultaneous colour display system is shown in Fig. 11.13. On passing through the antenna, radio receiver, and amplifier, the signal goes to three band-pass filters which separate the signal R and the subcarriers f_G and f_B modulated by the signals G and B . After detection and amplification, each of the signals G and B is applied to the control grid of the respective projection picture tube. It would be possible to use monochrome picture tubes in combination with suitable colour filters placed in front of the screen. It is more effective to employ picture tubes in which the cathode phosphor emits one of the three primaries, that is, red (zinc phosphate, $\text{Zn}_3(\text{PO}_4)_2$), green (willemite, $\text{Zn}_2\text{SiO}_4\text{Mn}$), or blue (zinc sulphide, $\text{ZnS}\cdot\text{Ag}$). If the object being televised has the shape shown in Fig. 11.9, one of three images, R , G or B , will be visible on the three colour picture tubes. It should be stressed that in a sequential system these images will appear in

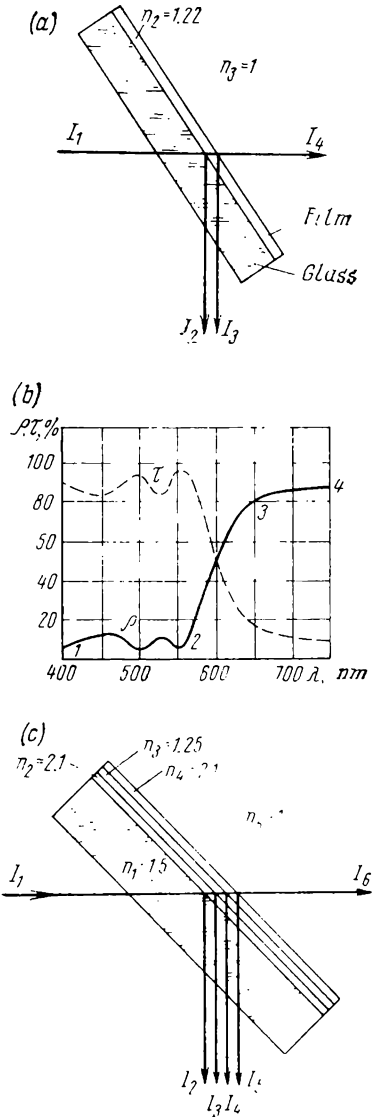


Fig. 11.12. Dichroic mirrors
(a) single-film mirror; (b) reflectance ρ and transmittance τ as functions of light wavelength; (c) multilayer mirror

turn on the same picture tube. In a simultaneous system, the three colour images appear on the three picture tubes at the same time.

Projection lenses throw these colour images from the individual picture tubes onto a large screen where the various colours are mixed.

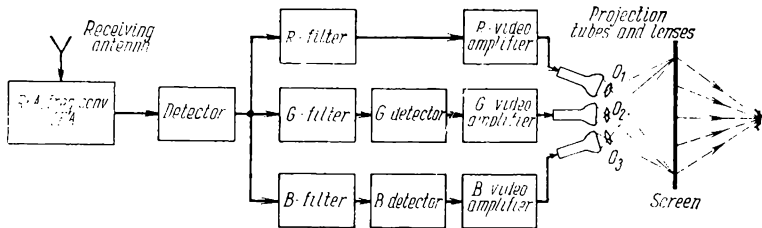


Fig. 11.13. Block diagram of the receiver in a simultaneous colour display system

Sometimes it may be convenient to make this viewing screen from frosted glass and to watch the colour image from the side opposite to the picture tube.

11.5. Colour Picture Tube

Of the several types of colour picture tube, widest use is made of the shadow-mask tube. This is a directly viewed display device capable of reproducing either full-colour or black-and-white pictures. The tri-colour viewing screen is composed of an orderly array of phosphor dots arranged in a triangular fashion (dot trios). The manufacture of the shadow-mask tube is a well-developed process. Unfortunately, this type of tube suffers from a number of limitations notable among which are elaborate design, the need for beam-convergence magnets, colour-purity magnets, etc. Because of these additional elements, difficulties sometimes arise in the use of the shadow-mask tube. This is why work has been under way for some time to develop a picture tube based on a different principle. Although a variety of novel-type tubes have been developed, they are inferior in performance to the shadow-mask tube.

Consider the operation of the shadow-mask three-gun tube in greater detail (Fig. 11.14). The viewing screen is an orderly array or mosaic of several hundred thousand phosphor dot trios, each trio consisting of a red-emitting, a green-emitting and a blue-emitting dot. These trios of *R*, *G* and *B* dots are arranged in a pattern regularly repeated along the line (Fig. 11.14a). For its operation, the picture tube depends on the fact that at some distance from the screen the observer cannot discern the individual dots any longer and perceives them as a single picture element. In Soviet television, the image is composed of about 500,000 elements. Thus, the phosphor dots on a colour picture tube total about 1.5 million.

The shadow-mask tube has three electron guns (at 1 in Fig. 11.14*b*), each producing an electron beam, 2, for one of the colour phosphors. For convenience, these beams may be referred to as red, green and blue. The intensity of the beams is controlled by voltages E_R , E_G and E_B applied independently of one another to the control electrodes of the respective guns. However, the three beams are simultaneously deflected both vertically and horizontally by a common deflection system, or yoke, 3.

So that each electron beam can only strike the phosphor dot of its particular colour, a so-called shadow mask, 5, is placed in front

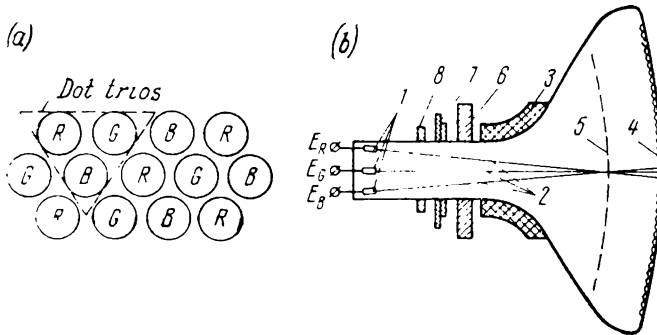


Fig. 11.14. Shadow-mask three-gun colour picture tube

(a) phosphor mosaic; (b) internal arrangement of the tube: 1—electron guns; 2—electron beam; 3—deflection yoke; 4—phosphor; 5—shadow mask; 6—beam convergence magnets; 7—colour purity control magnets; 8—blue-beam convergence magnet

of the phosphor screen, 4. The shadow mask is a curved metal plate 0.15 mm thick with an array of round holes, each hole being aligned with a particular phosphor dot triangle.

The electron optics of the tube is arranged so that the three beams are made to converge onto a common hole on the mask. Owing to this arrangement, the electron beams, in scanning vertically and horizontally, approach the mask from such a direction that each strikes only the phosphor dot of its particular colour immediately beyond the hole in the mask (Fig. 11.15*a*). If there were no mask, each beam, in scanning the lines and frames, would excite dots of the other two colours in addition to that of its particular colour. The selective action of the mask is illustrated in Fig. 11.15*b* where, for simplicity, only one green beam is shown in five positions labelled *a*, *b*, *c*, *d* and *e*. When the deflection yoke causes the beam to leave dot *G*, the area *AB* masks the dots *B* and *R* from the "green" beam. In a similar way, the remaining two beams are directed by holes in the mask so that they can only strike dots of their particular colours.

With its three electron guns and dot screen, the shadow-mask colour picture tube is more elaborate in design and construction than

a monochrome kinescope. Also, as already noted, the colour picture tube has additional elements mounted on the tube neck (see Fig. 11.14*b*). These are electromagnets 6 to facilitate convergence of the three beams over the mask surface, colour purity control magnets 7, and horizontal control magnet 8 of the blue beam. The need for these refinements in design can be explained as follows.

No matter what effort is put into picture-tube assembly, there will always be some inaccuracy in the relative alignment of the guns and

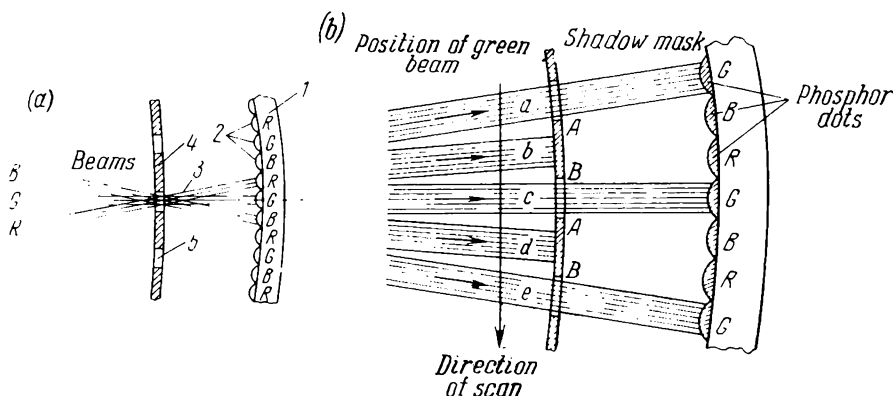


Fig. 11.15. Shadow-mask tube

(a) paths of beams through mask apertures: 1—tube faceplate; 2—phosphors; 3—electron beams; 4—shadow mask; 5—mask apertures; (b) beam shadowing

the mask, and the beams passing through mask holes might strike the dots they ought not to. For example, the red beam might strike blue and green dots somewhere on the screen. To avoid this, colour purity control magnets 7 are provided. One design of the colour purity control magnet is shown in Fig. 11.16. It is made up of two rings, 1 and 2, magnetized across the diameter, nested into each other and mounted on the neck of the picture tube, 3. Each ring can be rotated around the tube axis by lugs 4 and 5. In Fig. 11.16*a* the relative position of the rings is such that their magnetic fields add together and the field intensity H is a maximum. The electron beams R , G and B inside the rings are shifted through a maximum distance shown by the arrow in the figure. Moving the rings apart (through the angle α in Fig. 11.16*b*) reduces the field intensity and, as a consequence, the distance through which the beams are shifted. Obviously, at $\alpha = 90^\circ$, the field intensity falls to zero. At $\alpha > 90^\circ$, the field intensity changes sign, and the beams are shifted in the opposite direction.

If rings 1 and 2 be rotated in the same direction (the angle β in Fig. 11.16), the beams inside the rings will be tilted through an appropriate amount.

During alignment of a TV set, the angles α and β are matched by trial and error until any inaccuracy of electron-gun assembly and installation is compensated for.

For the shadow-mask tube to operate correctly, the three beams must pass through the same hole at any point on the mask surface

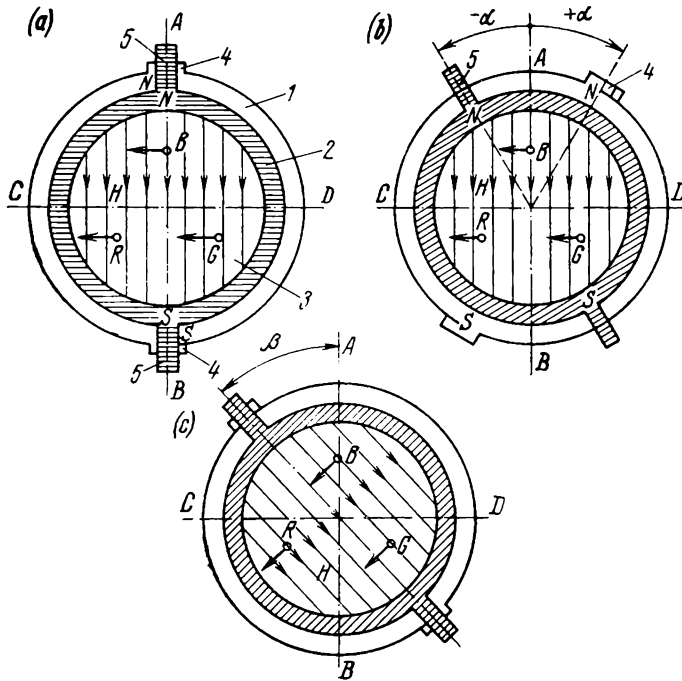


Fig. 11.16. Colour purity control

(a) at maximum field intensity; (b) reduction in field intensity by separation of rings; (c) rotation of field; 1, 2—rings magnetized on diameter; 3—tube neck; 4, 5—lugs to rotate rings

at the same time. Colour purity is not sufficient to satisfy this requirement. As is seen in Fig. 11.17, it may so happen that, although they strike phosphor dots of their respective colours the three beams pass through different holes in the mask and fail therefore to converge onto the same colour dot triangle. This results in what is known as colour-dot break-up which adds stray colour fringes to the image contour, especially at the screen periphery (in the case of large beam deflection). This defect is corrected by an arrangement which causes the three beam to converge onto the same hole at any point on the mask surface. This device is put on the tube neck, close to the deflection yoke. In sketch form, this device is shown in Fig. 11.18a. It consists of three static-convergence permanent magnets 1 and

three dynamic-convergence electromagnets 2. There are also radial-convergence magnetic poles inside and outside the tube neck, 3 and 4, respectively.

The static convergence magnets are steel cylinders magnetized across their diameters. The outer end of each magnet has a slot for screwdriver adjustment. The action of the static convergence magnets is illustrated in Fig. 11.18*b* where the green beam is selected

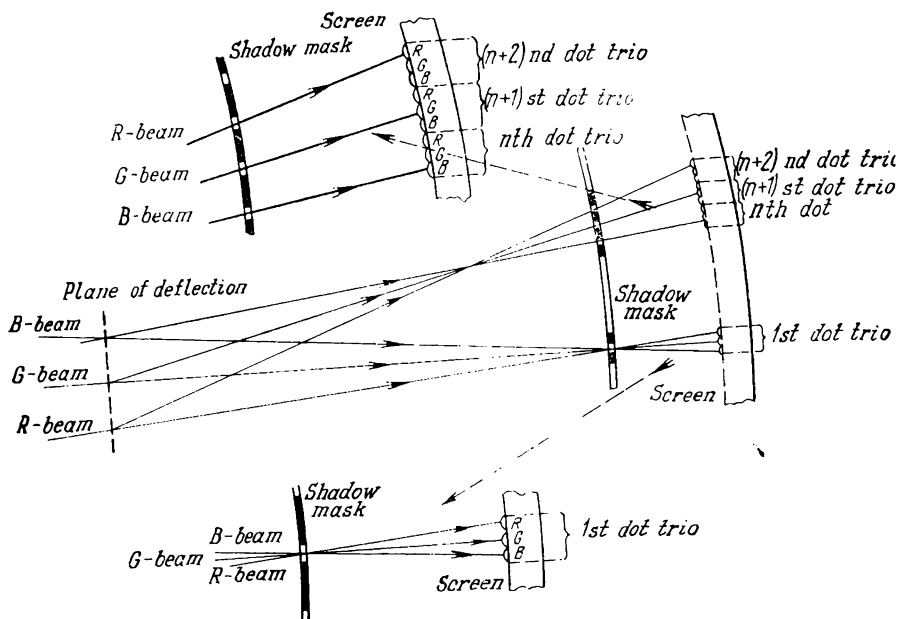


Fig. 11.17. Colour-dot break-up

as an example. Rotation of magnet 1 adjusts the magnitude and reverses the polarity of the magnetic field in the air gap between pole pieces 4 where the electron beam passes. In this way, the beam is additionally shifted along the radius of the tube neck.

By rotating the static convergence magnets (together with the horizontal-shift magnet of the blue beam, which is described later), it is possible to cause the three beams to pass through the same mask hole at the centre of the screen. However, the beams will no longer converge at the screen periphery as they are deflected by the fields of the yoke (see Fig. 11.17).

This failure to converge is handled by dynamic convergence electromagnets 2. Their coils *L* are energized with a current at the line scan frequency, and their coils *F* with a current at the frame scan frequency. These currents are generated to have a sawtooth-parabolic

waveform (shown in Fig. 11.19) by a suitable circuit in the receiver. The convergence currents can be adjusted for the relative content

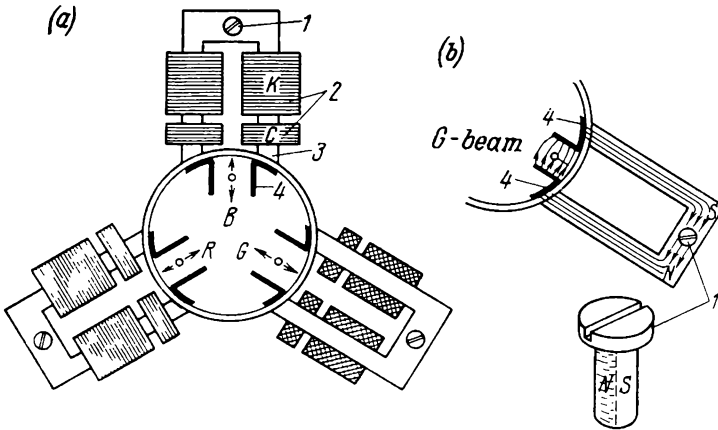


Fig. 11.18. Beam convergence control

(a) overall arrangement; (b) convergence magnets; 1—static-convergence magnet; 2—dynamic convergence magnets; 3, 4—pole pieces outside and inside the tube neck

of the sawtooth and parabolic components with controls located on the receiver chassis. As is seen from Fig. 11.19, at points *A*, that is, when the beams converge to the centre of the screen, the dynamic convergence currents are zero, and only the static convergence magnets are at work. As the beams are deflected from the centre to the edges of the screen, the dynamic convergence currents rise and correct the beam trajectory as appropriate.

Again, because of inaccuracies in electron-gun assembly, the above arrangement can secure the convergence of only two beams, as shown in Fig. 11.20*a*. While rotation of the convergence magnets for the red and green beams will converge these two beams at point *O* in the central hole of the mask, the blue beam may well miss this point *O*, as is seen from the figure. This deficiency is made up for by the blue-beam positioning magnets. These magnets are put around the

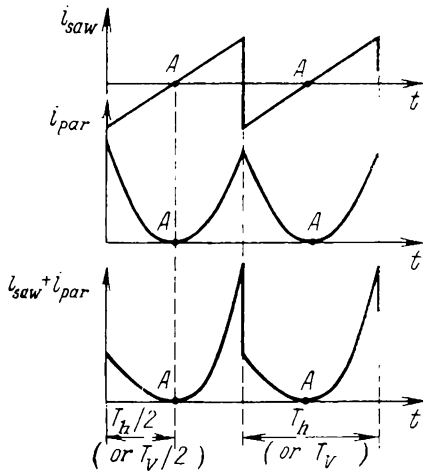


Fig. 11.19. Waveform of currents in dynamic convergence magnet coils

neck of the tube and can be adjusted so as to shift the blue beam additionally relative to the remaining two beams. In sketch form one possible arrangement is shown in Fig. 11.20*b*. Rotation of a magnetic screw NS , varies the width of the air gap, Δ , and as a consequence the intensity of the field affecting the amount by which the blue beam can be shifted within the region AB .

The deflection yoke of a colour picture tube is far more elaborate in design than its counterpart in a monochrome tube. For one thing,

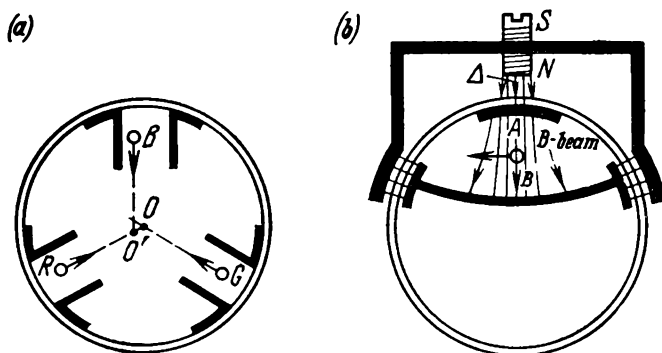


Fig. 11.20. Blue-beam shift control

(a) illustrating the need for shift control; (b) an arrangement of control

the colour picture tube has a wider neck than the monochrome one and needs a higher anode voltage. For another, the yoke must be manufactured to far closer tolerances and accurately positioned on the tube neck, as even minute variations in the magnitude and symmetry of the field would impair colour purity. The yoke has an additional adjustment by which the deflection coils can be moved within 15 mm along the tube axis. This enhances colour purity and beam convergence.

An important disadvantage of the shadow-mask tube is that each beam must have a considerably greater power than the beam of a monochrome tube. The point is that the mask intercepts a sizeable proportion of electrons and, if the beam power were not increased severalfold, there would be insufficient excitation for the phosphor beyond the mask. For example, the beam current and the main anode voltage for a monochrome tube are 100 μA and 16 kV, respectively. For a colour picture tube these figures are 600 μA and 25 kV.

11.6. Luminance Signal

An unmodified black-and-white TV receiver cannot reproduce the image (in monochrome, of course) produced by a simultaneous colour system also because the video signal in this system does not

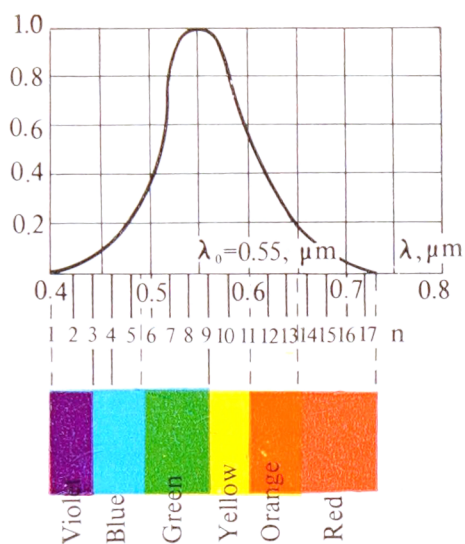


Fig. 11.3. Spectral characteristic of the average human eye

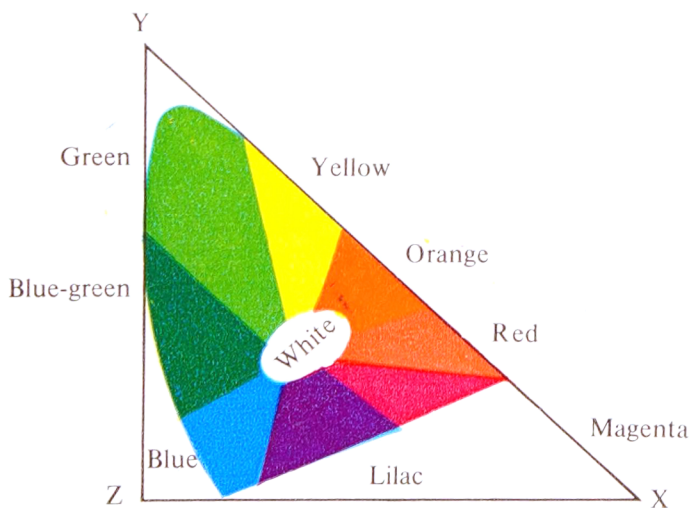


Fig. 11.6. Position of colours within the spectrum locus

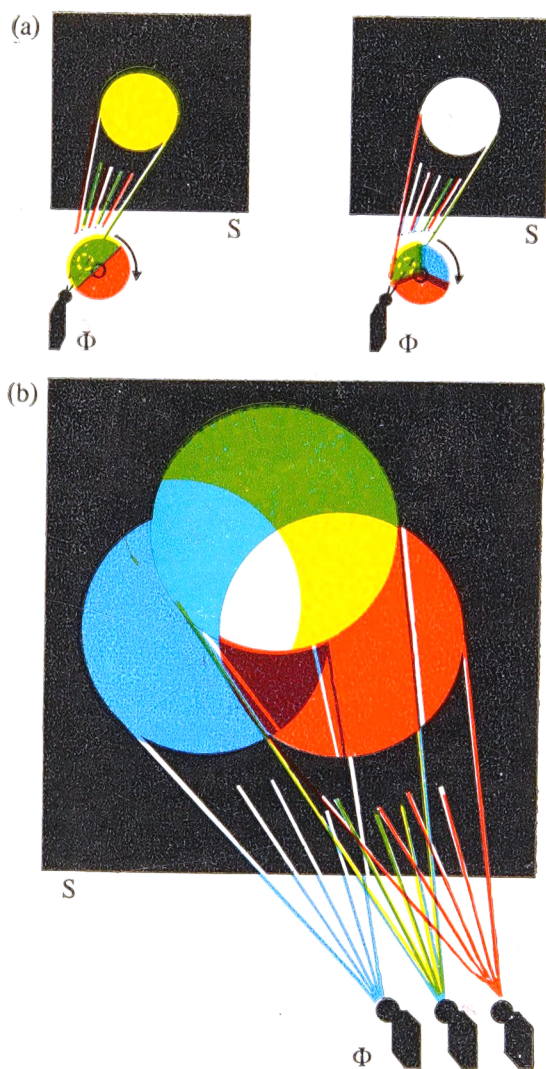


Fig. 11.8. Colour mixing
a) sequential; *(b)* simultaneous

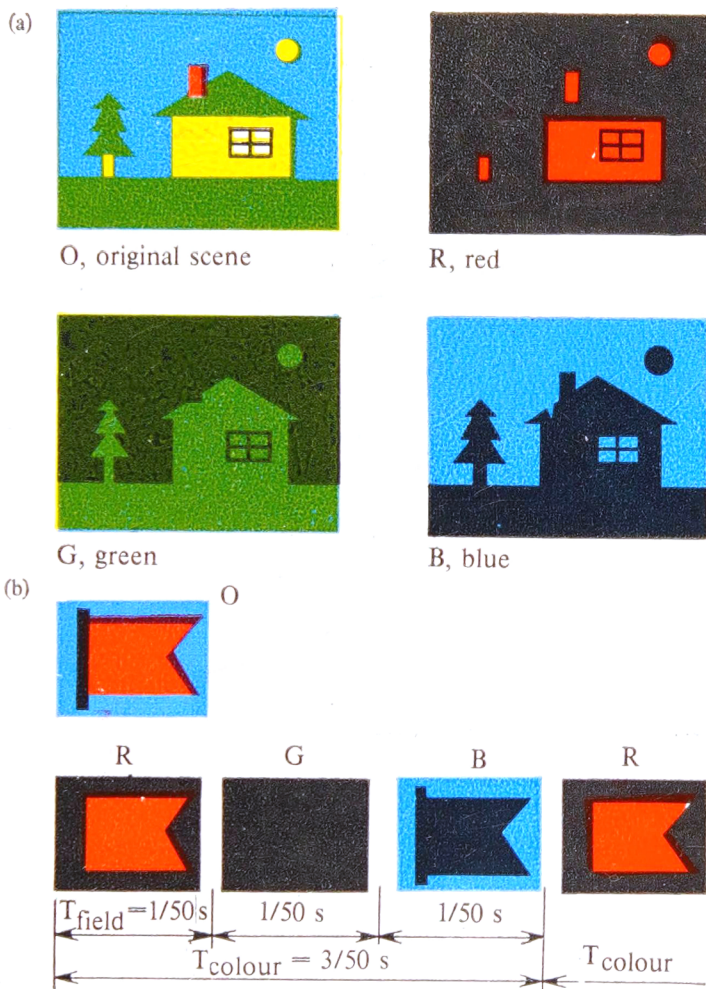


Fig. 11.10. Reproduction of a colour image
(a) the primary colours R, G and B; (b) colour flicker

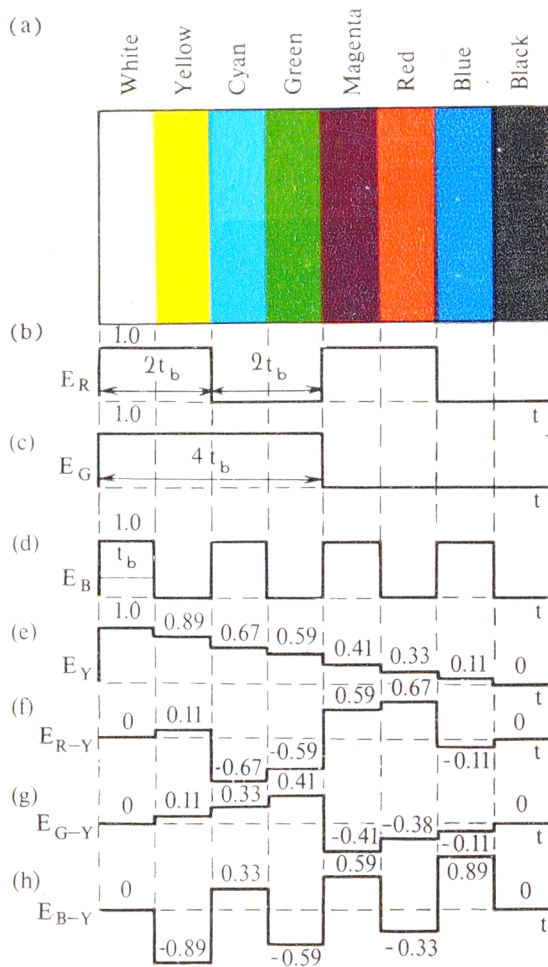


Fig. 12.13. Colour-bar-chart signals

a) colour bars displayed by colour TV receiver; (b) E_R signal; (c) E_G signal; (d) E_B signal;
 (e) E_Y signal; (f) E_{R-Y} signal; (g) E_{G-Y} signal; (h) E_{B-Y} signal

carry the component corresponding to a black-and-white picture. It is possible, by suitably adjusting a monochrome receiver, to reproduce in black-and-white one of the colour images, R , G or B . However, none can replace a black-and-white picture (see Fig. 11.9).

For compatibility, it is therefore necessary that in addition to information about colour, the transmitter of a colour television system should send a signal corresponding to a black-and-white picture. This is usually called the luminance signal because the various areas of a black-and-white picture only differ in luminance. The luminance signal can be obtained by adding together the signals representing the three primaries, R , G and B . However, the three voltages contributing to the luminance signal must be taken in different amounts because the human eye responds to the primaries differently. Also, in deciding on the amounts in which the primaries should be mixed in order to obtain the luminance signal, it is important to take into account the coordinates of the selected primaries (the vertices of the triangles on the chromaticity diagram of Fig. 11.6a). Calculations show that if the primaries be selected in accordance with Fig. 11.6a, the relative amounts of R , G and B in the luminance (that is, black-and-white) signal will be

$$E_Y = 0.30E_R + 0.59E_G + 0.11E_B \quad (11.21)$$

Or, in words, the luminance signal associated with whites of the picture should contain 30% red, 59% green, and 11% blue.

This equation, pivotal to colour television, needs some explanation. Suppose that a simple pattern made up of a white stripe against a black background is projected onto the photocathodes of the three pickup tubes. The dichroic mirrors will split light from the white stripe into three colour components, R , G and B . The gain of the three video amplifiers can be adjusted so that their output voltages will be the same, that is:

$$E_R = E_G = E_B$$

This is preliminary adjustment of the relative sensitivity of a three-tube camera.

The luminance signal (essential to operation of a black-and-white TV receiver) is produced by means of a so-called matrix. The circuit of a simple matrix composed of four resistors (three voltage dividers) is shown in Fig. 11.21. If the values of R_1 , R_2 and R_3 are chosen to be sufficiently high in comparison with R_{out} , the voltage dividers are mutually isolated, so that the following voltages are developed across the resistor R_{out} : $E_{R\ out} = E_R (R_{out}/R_1)$, $E_{G\ out} = E_G (R_{out}/R_2)$ and $E_{B\ out} = E_B (R_{out}/R_3)$. By setting the scale factors equal to $R_{out}/R_1 = 0.30$, $R_{out}/R_2 = 0.59$ and $R_{out}/R_3 = 0.11$, the following luminance signal will be secured at the matrix

output:

$$E_Y = E_{R_{out}} + E_{G_{out}} + E_{B_{out}} = 0.30E_R + 0.59E_G + 0.11E_B$$

The example that follows provides a better insight into the significance of the above equation to colour television. Let the objects to be televised be two areas of the same intensity of radiation, blue and white. To an observer watching the two areas on a colour reproducer the two areas will appear differing in luminance. In accordance with the above equation the luminance of the blue area will be equal to 11% of that of the white area. On a black-and-white reproducer, the areas will no longer appear coloured. However, because of matrixing, the luminance of the blue area will again be equal to 11%

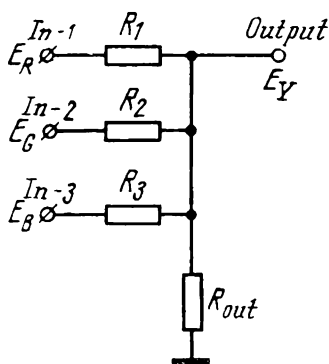


Fig. 11.21. Matrix circuit

of that of the white area (obviously, for the blue area the voltages E_R and E_G entering the equation for E_Y and coming from the red and blue pickup tubes disappear, and $E_Y = 0.11 E_B$).

To keep the bandwidth needed for the television signal unchanged upon insertion of the luminance signal, one of the "colouring" signals, E_R , E_G or E_B , should be dropped from the transmission. This may be done on the basis of the same equation for E_Y . If the receiving terminal picks up two colour signals, say E_R and E_B , in addition to the luminance signal, the third colouring signal, E_G , can

be derived by matrixing. It follows from the equation for E_Y that

$$E_G = (1/0.59) (E_B - 0.11E_R - 0.30E_R) \quad (11.22)$$

In other words, the three inputs to the matrix (similar to that shown in Fig. 11.21) at the receiving terminal should be the signals E_Y , E_B and E_R , respectively, and the scale factors R_{out}/R_1 , R_{out}/R_2 and R_{out}/R_3 , should be adjusted as appropriate. The "-" signs in front of E_B and E_R indicate that the polarity of these signals should be inverted by a phase-inverting stage before they are applied to the matrix. The gain of the succeeding stages should be adjusted so as to introduce a correction factor of $1/0.59$. In this way, by use of matrixing in the receiver it is possible to derive four signals, E_Y , E_R , E_B and E_G , from three input signals, E_Y , E_R and E_B .

A block diagram of the transmitting terminal of a colour television system using the signals E_Y , E_R and E_B appears in Fig. 11.22, and the spectrum of the composite video signal fed to the transmitter is shown in Fig. 11.23. The width of this composite video signal

does not differ from that of the system spectrum in Fig. 11.11a, but a black-and-white receiver tuned to the spectrum portion E_Y and therefore receiving the luminance signal can reproduce a colour

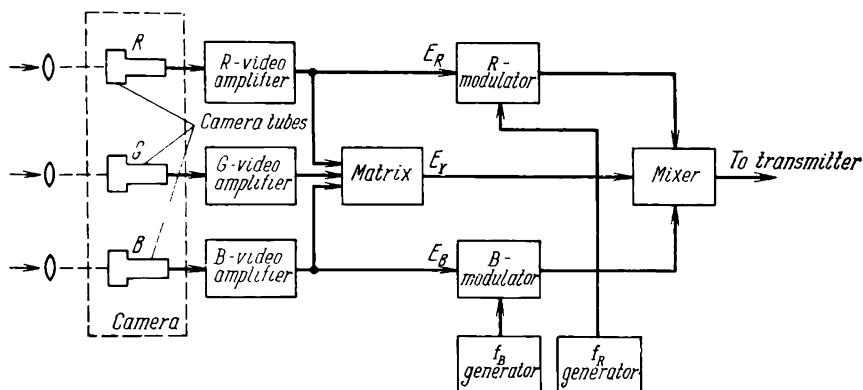


Fig. 11.22. Block diagram of the transmitting terminal of a simultaneous colour television system with derivation of the luminance signal

program in black and white. On the other hand, a colour receiver accepting the luminance signal E_Y of black-and-white television can reproduce it in black and white on its colour picture tube. For

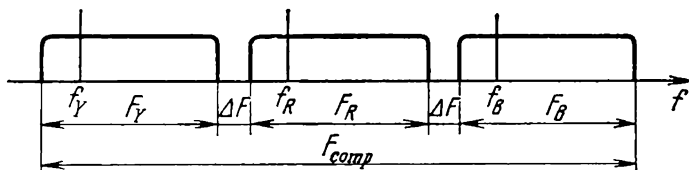


Fig. 11.23. Spectrum of the composite video signal fed to the transmitter

this to be possible, it is only necessary that the luminance signal arrive in synchronism at the three control electrodes of the tri-colour picture tube. White will then be produced as a sum of the three colours emitted by the respective dot phosphors.

11.7. Bandwidth of Fine Detail

The human eye discerns the colours of fine detail poorly. This property of the eye has been utilized to reduce the frequency spectrum required for the colour television signal. For a better understanding of the matter, it will be necessary first to establish the relationship between the size of picture detail and the maximum frequency needed for its transmission. Figure 11.24a shows, in simpli-

fied form, a picture line on which black and white detail alternate regularly. Because of aperture distortion, the signal voltage V_s representing this line (Fig. 11.24*b*) no longer has the shape of a square wave. For simplicity, we will assume that it is a sinusoid of a frequency $f_d = 1/2T_d$.

On the basis of the obvious relations (see Fig. 11.24*a* and *b*), $T_h/2T_d = l/2d$, we get $f_d = 1/2T_d = l/2dT_h$ where T_h is the line scan time. With the line length, l , and the line scan time, T_h , fixed

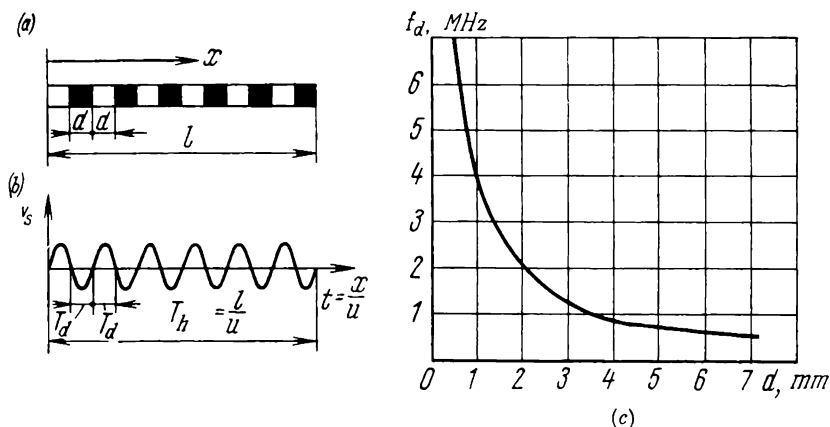


Fig. 11.24. Relation between the size of details and bandwidth
(*a*) position of details on a line; (*b*) signal corresponding to fine detail; (*c*) bandwidth as a function of the size of fine detail (l —line length; d —detail size; u —beam velocity; T_d —interval needed to transmit one detail; T_h —line scanning interval)

in advance, the product $f_d d$ is a constant. That is, a progressively higher frequency, f_d , is required to transmit a progressively diminishing detail, d .

Figure 11.24*c* shows a plot of this maximum frequency, f_d , as a function of the detail size, d , for $l = 480$ mm (the Soviet-made 59JK3U colour picture tube) and $T_h = 51$ μ s (these are all data taken from practice). Using the above equation and the plot of Fig. 11.24*c*, the detail size can be expressed (as this is often done in television) in megahertz rather than in millimetres. For example, very fine detail occupy a range from 3 to 6 MHz, fine detail from 1 to 3 MHz, and medium detail from 0.5 to 1 MHz.

To go back to the property of the eye mentioned above, experiments have shown that the colour saturation of detail progressively decreases as detail size decreases. This is illustrated in the plot of Fig. 11.25 which relates the visible saturation of detail to its equivalent size and colour. As is seen, the decrease in the size of saturated blue detail (with black spaces) is accompanied by a rapid fall in the visible saturation which becomes equal to practically zero at $f_d = 0.5$

to 0.6 MHz. In other words, fine blue detail will appear light-gray against a dark background at these frequencies. Red detail retains its chromaticity for a longer time and does not appear discoloured until the size corresponding to $f_d = 1.4$ to 1.6 MHz. Fine green detail retains its visible chromaticity up to practically the maximum frequency of the television spectrum. This loss of colour vision on fine detail is related to difference in the spectral sensitivity of the eye (see the colour plate, Fig. 1.3), which is a maximum to green,

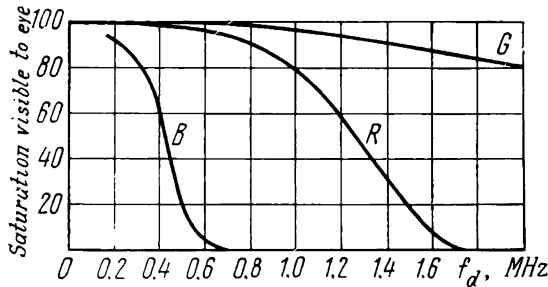


Fig. 11.25. Apparent saturation (%) as a function of the size and colour of detail

medium to red, and low to blue. It is to be noted also that, apart from the loss of visible saturation, fine colour detail becomes progressively less resolvable. For example, blue details with an equivalent size of over 0.6 to 0.8 MHz merge to form a continuous gray background. Red details are no longer resolvable (without colour) at over 1.6 to 1.8 MHz. The eye retains a maximum resolving power for green detail only.

This property of the eye makes it possible markedly to reduce the total bandwidth for the colour television signal. That is, the full frequency spectrum, $F_R = F_G = F_B = F = 6$ MHz, need not be transmitted in each of the three chromaticity channels (see Fig. 11.23). Referring to the plot of Fig. 11.25 and inserting appropriate filters in the block diagram of Fig. 11.22, we may assume that $F_B = 0.5$ MHz, $F_R = 1.5$ MHz, and $F_G = 6$ MHz. Taking into account the two guard bands, $2\Delta F = 1$ MHz (see Fig. 11.11b), the total bandwidth needed will be

$$F'_{tot} = F_B + F_R + F_G + 2\Delta F = 0.5 + 1.5 + 6 + 1 = 9 \text{ MHz}$$

In other words, the total bandwidth can be reduced by a factor of

$$F_{tot}/F'_{tot} = 19 \div 9 = 2.1$$

11.8. Colour-Signal Band-Sharing

Although the reduction in the frequency spectrum for red and blue enables the total spectrum to be more than halved! ($F'_{tot} = 9$ MHz), it still exceeds the standard channel allocated to black-and-white television (see Fig. 4.10), and fails to satisfy the requirement for compatibility. A further decrease in the bandwidth is based on the fact

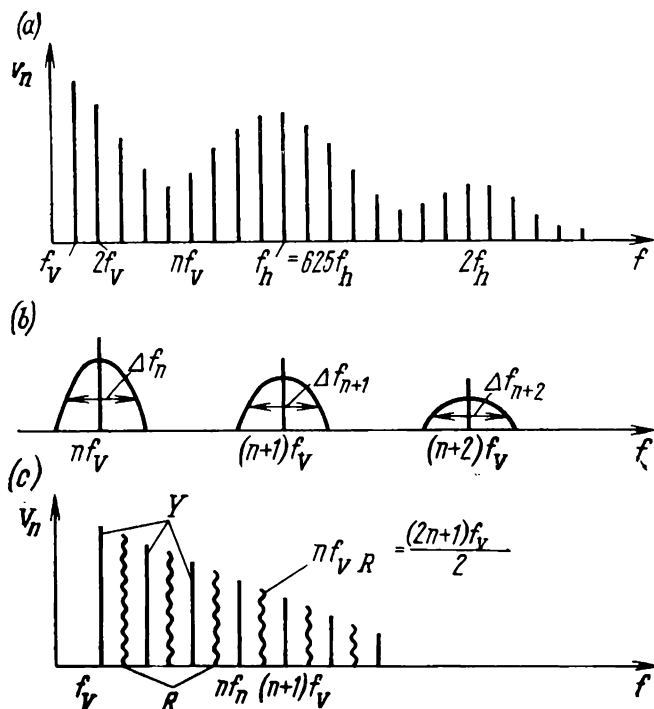


Fig. 11.26. (a) Line spectrum of the television signal; (b) same, with motion in the scene; (c) band-sharing

that the television signal has a line spectrum. As is shown in Chapter 4, the spectrum components occur only at frequencies which are integral multiples (harmonics) of line and frame frequencies, rather than fill the frequency axis continuously (Fig. 11.26a). The spaces between the line components nf_v , $(n+1)f_v$, ... of the luminance signal, E_Y , may obviously be utilized for the insertion of the colouring signals, E_B and E_R , thereby making the total spectrum of the colour television signal more compact.

When the picture contains motion, the spectrum will not be a purely line one; in this case each line broadens in a lower and an up-

per sideband which are not harmonics of the line or frame frequencies (Fig. 11.26*b*). The width, Δf_n , of these sidebands increases progressively with increasing velocity of motion. Yet, the gaps between the line components are large enough for the insertion of colouring information.

The colouring signals, E_B and E_R , appearing at the output of the respective video amplifiers (see Fig. 11.11*a*) have likewise a line spectrum, because these signals are generated by the same pickup tubes and the scan generators as the luminance signal, E_Y . On this basis, the compact packaging of information can be achieved by interleaving the spectra of the luminance and colouring signals. To explain how this can be done, we shall examine one colouring signal, say, E_R . In simplified form, the relative positions of the harmonics of the luminance signal (straight-line segments) and of the colouring signal (wave lines) are shown in Fig. 11.26*c*. For the components of the colouring signal to fall in between the luminance harmonics, it is essential that their frequencies be arithmetic means:

$$nf_{vR} = \frac{(n+1)f_v + nf_v}{2} = \frac{(2n+1)f_v}{2}$$

where $(2n+1)f_v$ is an odd harmonic of the frame (or vertical scan) frequency of the luminance signal.

Thus, the frequency nf_{vR} filling the gap is an odd harmonic of half the frame frequency, $(2n+1)(f_v/2)$.

Figure 11.27*a* explains how colour-signal band-sharing was achieved in an early television system. The spectral components of the colouring signals are inserted between the components of the luminance signals by means of two subcarriers, f_R and f_B . For correct interleaving, it is important that the subcarriers f_R and f_B be odd harmonics of one-half frame (or, which is the same, one-half line) frequency. It is to be noted that

$$f_h/f_v = 15,625/25 = 625$$

and so an odd harmonic of one-half frame frequency at a sufficiently high value of n is at the same time an odd harmonic of one-half line frequency.

As is shown in Fig. 11.27*a*, the spectra of the colouring signals R and B are transmitted on a single sideband as a way of saving bandwidth.

The signal of a compatible colour television system having the spectrum similar to that shown in the figure can be received by an unmodified black-and-white receiver and reproduced in black-and-white. In principle, the colouring signals, R and B , lying within the spectrum of the luminance signal, should not be seen on the picture tube. The example that follows will explain the matter.

Suppose that the colouring signal consists of only a sinewave, $f_R = [(2n + 1) f_v]/2$

Calculate how many cycles of this sinewave can be accommodated in a frame, that is, in two fields in the case of interlaced scanning. The period of the sinewave is

$$T_R = 1/f_R = 2/[(2n + 1) f_v]$$

The frame period is

$$T_v = 1/f_v$$

whence

$$T_v/T_R = (2n + 1)/2 = n + 1/2$$

That is, the image can accommodate a whole number, n , of cycles plus a half-cycle. Because of this half-cycle, the sinewave f_R will

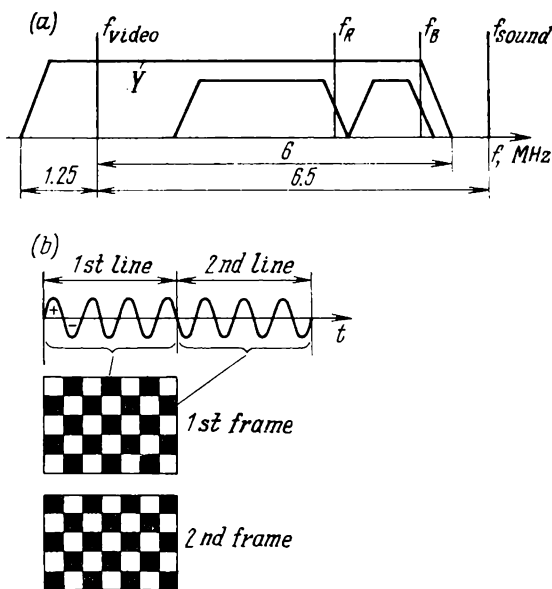


Fig. 11.27. Band-sharing of colour signals

(a) shared spectrum; (b) compensation of colour-signal harmonics in the viewer's eye

undergo a phase reversal between successive frames (Fig. 11.27b), and its positive half-cycles representing white will be replaced every next frame by negative half-cycles representing black. In this way, the interference will be compensated in the observer's eye. With more complex colouring signals containing a multitude of harmonics of one-half frame (or, which is the same, one-half line) frequency, the screen of a black-and-white picture tube will display a

false image alternating between positive and negative on alternate field scans; that is, it will cancel out in the observer's memory between frames.

It should be noted that such a false image will flicker at a frequency, f_{fi} , lying well below the fusion frequency, F_f , which is about 50 Hz for large detail:

$$f_{fi} = f_o/2 = 25 \div 2 = 12.5 \text{ Hz} < F_f$$

Flicker becomes less noticeable as the object being televised decreases in size. Therefore, in order to minimize the flicker, the spectra of the R and B signals (see Fig. 11.27a) are located as closely to the maximum frequency of the spectrum of the Y signal as practicable. Then the flickering false images of R and B will be made up of only fine detail, and the flicker will be drastically reduced. But even then the screen will display interference in the form of fine scintillating dots constituting a nuisance to the viewer. This fine-dot form of interference is especially noticeable when it is produced by the subcarrier because its amplitude is substantially greater than that of any other component of the colouring signal. This is why special measures are taken to suppress it.

11.9. Colour-Difference Signals

It has been explained in the preceding section that the colouring signals E_R and E_B transmitted inside the spectrum of the luminance signal, E_Y , will not be visible on a black-and-white receiver because they have opposite phase in successive frames and cancel out in the observer's eye. However, the flicker frequency of these false images is very low (12.5 Hz) and, unless suitable measures are taken, the observer would see an interfering signal as a fine-dot pattern. This interfering pattern also exists during the transmission of black-and-white scenes, because pickup tubes decompose such scenes into three colour images, with the result that the signals E_R and E_B (and of course E_G) are generated. Thus, even during the transmission of black-and-white images the complete signal will contain the colouring signals E_R and E_B in addition to the luminance signal, E_Y . It should be noted that most colour images contain numerous black-and-white areas. Also, there is a great number of areas with low saturation, that is, areas which are predominantly pink, light-blue, greenish, etc. Elements of detail with high saturation are fairly rare. Therefore, removal of interference due to the fine-dot pattern arising from colouring signals E_R and E_B within black-and-white and unsaturated areas would markedly improve the quality of television transmission as a whole.

In all present-day compatible colour television systems the interference due to the fine-dot structure is removed by replacing the

colouring signals E_R and E_B in the complete colour television signal by colour-difference (or chrominance) signals, $E_R - E_Y$ and $E_B - E_Y$. These signals are generated by suitable matrix circuits in the transmitting equipment by subtracting the luminance signal from the respective colouring signal (Fig. 11.28a).

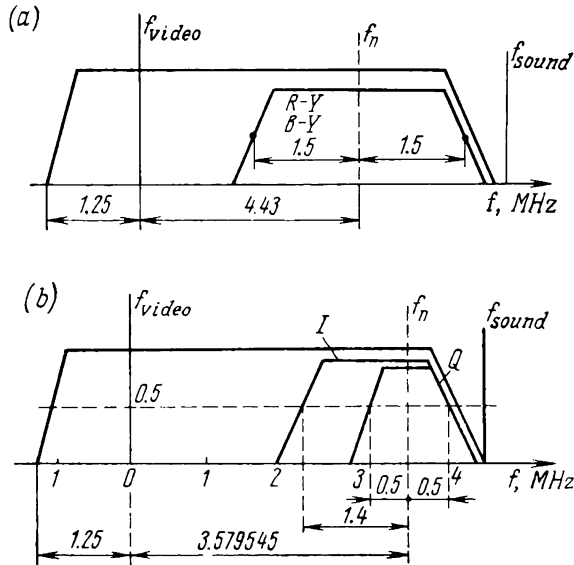


Fig. 11.28. Signal spectrum of a compatible television system
(a) band-sharing in the case of synchronous quadratic modulation; (b) NTSC signal spectrum

A major distinction of colour-difference signals is that they are equal to zero within the white and gray areas of the image. As a proof, subtracting E_Y , Eq. (11.21), from E_R and E_B gives the following equations for colour-difference signals:

$$E_{R-Y} = E_R - E_Y = 0.70E_R - 0.59E_G - 0.11E_B \quad (11.23)$$

$$E_{B-Y} = E_B - E_Y = 0.89E_B - 0.59E_G - 0.30E_R \quad (11.24)$$

On the basis of the above equations, the colour-difference signals are produced by matrix circuits. Since, for black-and-white images, $E_R = E_B = E_G = E_Y$, then $E_{R-Y} = 0$ and $E_{B-Y} = 0$. Thus, within the white and gray areas of an image, colour-difference signals are equal to zero. However, they are not equal to zero within elements of detail with a low saturation; yet they are small and do not produce an appreciable interference.

A colour TV receiver incorporates appropriate matrix circuits which derive the three primary colour signals, E_R , E_G and E_B , from the three signals E_Y , E_{R-Y} and E_{B-Y} . As will be shown shortly, a colour picture tube may well act as such a matrix.

11.10. NTSC Compatible Colour Television System

The spectrum of the colour television signal shown in Fig. 11.27a suffers from a number of major limitations. Firstly, the left-hand (lower) components of the colour signal lie too close to the l.f. components of the luminance signal, and the interference they produce would be objectionable. Secondly, the presence of two subcarriers, f_R and f_B , would produce on the image a multitude of interference patterns arising from the fact that f_R, f_B, f_Y, f_{sound} and their harmonics would beat together. The number and intensity of such interference patterns can markedly be reduced if the same subcarrier be used for both colouring signals.

This is done in the NTSC compatible colour television system (Fig. 11.28b). So that the receiving terminal can separate the colour-difference (chrominance) signals modulated onto the same subcarrier, the transmitting terminal of the NTSC system uses synchronous quadratic modulation. Synchronous quadratic modulation boils down to the following. Both chrominance signals, E_{R-Y} , and E_{B-Y} , are modulated onto the same subcarrier, f_{sc} (Fig. 11.29a) supplied by a crystal-controlled oscillator. This subcarrier is applied to the $R-Y$ and $B-Y$ modulators in phase quadrature (that is, displaced 90 electrical degrees from each other).

The $R-Y$ and $B-Y$ modulators are balanced circuits. This means that their output voltages are proportional to the products of input voltages and there is no subcarrier (it is suppressed). In this way, the interfering action of the colour subcarrier is done away with. Modulated onto the subcarrier, the two chrominance signals are added together linearly in the combiner unit, to form a composite colour signal:

$$V_{colour} = V_{R-Y} + V_{B-Y} = kE_{R-Y} \cos \omega_{sc}t + kE_{B-Y} \sin \omega_{sc}t$$

where k is a proportionality coefficient.

In phasor-diagram form, the composite colour signal is shown in Fig. 11.29b. The chrominance signals vary in amplitude according to the colour of the image area being scanned, but they remain in phase quadrature. Accordingly their sum phasor, \bar{V}_{colour} , varies in both magnitude, V_{colour} , and phase, ϕ . For clarity, let us determine chrominance signals for some characteristic colours: red, yellow, green, cyan and magenta. For red,

$$E_R = 1 \text{ V}; \quad E_B = 0$$

$$E_G = 0$$

$$E_{Y_r} = 0.11E_B + 0.59E_G + 0.30E_R = 0.30E_R = 0.3 \text{ V}$$

$$E_{B-Y} = E_B - E_Y = 0 - 0.3 = -0.3 \text{ V}$$

$$E_{R-Y} = E_R - E_Y = 1 - 0.3 = 0.7 \text{ V}$$

The phasor diagram for red appears in Fig. 11.29c. The primary signals E_R , E_G and E_B , the luminance signal and the respective

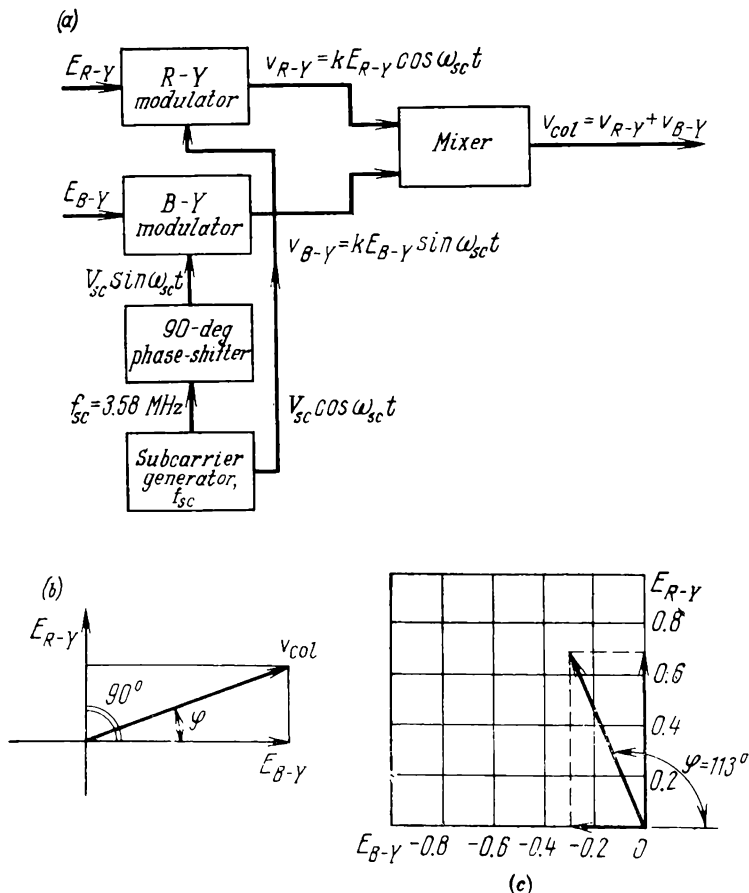


Fig. 11.29. Synchronous quadratic modulation

(a) block diagram; (b) chrominance signal phasor; (c) length and phase of saturated red phasor

chrominance signals for the colours listed above and computed as explained in the example are given in Table 11.3 which also lists the phase shift ϕ of the phasor \bar{V}_{colour} relative to the phasor E_{B-Y} taken as reference.

The positions and relative magnitudes of the total colouring signal, V_{colour} , for all cases tabulated in Table 11.3 are shown in Fig. 11.30. For white, both chrominance signals are equal to zero; that is the point representing white on the phasor diagram lies at the origin of coordinates 0.

Table 11.3

Colour	E_R	E_B	E_G	E_Y	E_{R-Y}	E_{B-Y}	ϕ , deg
Red	1	0	0	0.3	0.7	-0.3	113
Yellow	1	0	1	0.89	0.11	-0.89	173
Green	0	0	1	0.59	-0.59	-0.59	225
Cyan	0	1	1	0.7	-0.7	-0.3	293
Blue	0	1	0	0.11	-0.11	0.89	353
Magenta	1	1	0	0.41	0.59	0.59	45

The length of the phasor V_{colour} defines saturation, and its position (or the phase shift ϕ) its hue. In other words, a complete colour-

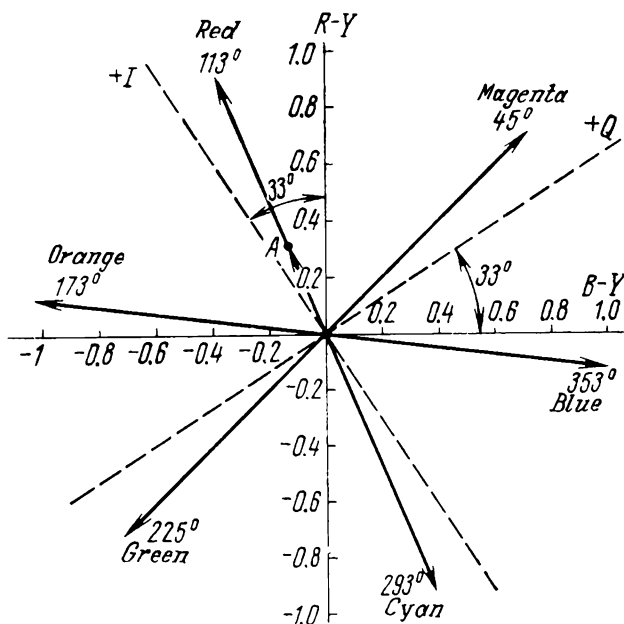


Fig. 11.30. Positions of chrominance signal phasors for different hues

ring signal is both amplitude-modulated (for saturation) and phase-modulated (for hue).

The television receivers operating by the NTSC standard incorporate a circuit to analyze the total colouring signal into two chrominance signals. Operation of the circuit, called a synchronous detector, is illustrated by the block diagram of Fig. 11.31. The $R-Y$ and $B-Y$ synchronous detectors are similar in operating prin-

ciple to the balanced modulators used in the transmitting terminal (see Fig. 11.29a). Their output voltages should be proportional to the product of two input voltages.

The first inputs of the synchronous detectors accept the complete colouring signal at the same time; the second inputs are fed a sine-wave voltage from a local oscillator. This sinewave voltage is applied

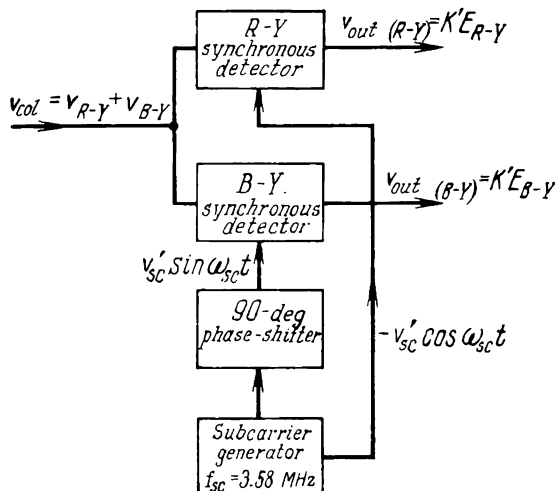


Fig. 11.31. Block diagram of synchronous detection

to the detectors likewise in phase quadrature. The output voltage of the synchronous detector is the product of the two input voltages and has the form

$$V_{out(R-Y)} = V_{colour} V'_{sc} \cos \omega_{sc} t = kV'_{sc} (E_{R-Y}) \cos \omega_{sc} t \cos \omega_{sc} t + kV'_{sc} (E_{B-Y}) \sin \omega_{sc} t \cos \omega_{sc} t$$

Using the elementary trigonometric equations

$$\cos \alpha \cos \alpha = 1/2 (1 + \cos 2\alpha)$$

and

$$\sin \alpha \cos \alpha = 1/2 \sin 2\alpha$$

and designating $k' = kV'_{sc}/2$, we get

$$V_{out(R-Y)} = k'E_{R-Y} + k'E_{R-Y} \cos 2\omega_{sc} t + k'E_{B-Y} \sin 2\omega_{sc} t$$

The first term on the right-hand side of the above expression is a chrominance signal. The remaining two terms are r.f. signals (their subcarrier is $2\omega_{sc}$) and can readily be suppressed by low-pass filters.

Similarly, the output of the $B-Y$ chrominance detector is

$$V_{out(B-Y)} = k' E_{B-Y} - k' E_{B-Y} \cos 2\omega_{sc}t + k' E_{(R-Y)} \sin 2\omega_{sc}t$$

In simplified form, a block diagram of the transmitting terminal of a compatible television system using chrominance signals and synchronous quadratic modulation is shown in Fig. 11.32a. The

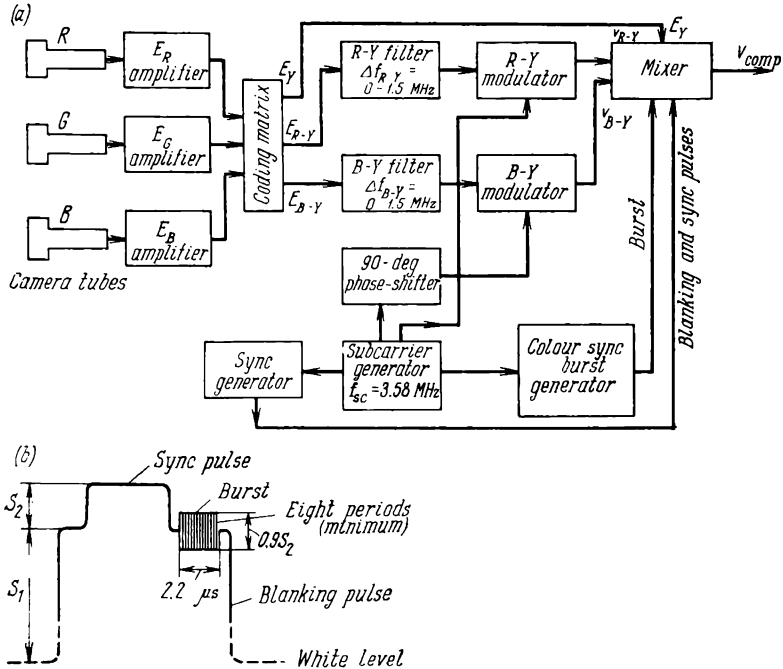


Fig. 11.32. NTSC system

(a) block diagram of the transmitting terminal; (b) horizontal blanking pulse, sync pulse, and colour burst

three primary signals generated by the three pickup tubes are amplified and applied to a coding matrix where they are combined algebraically to produce a luminance signal, E_Y , and two chrominance signals, E_{B-Y} and E_{R-Y} . The primaries E_R , E_G , and E_B are combined by the matrix in accordance with Eqs. (11.21), (11.24) and (11.23).

Then the chrominance spectra are clipped by filters with a pass-band of 0 to 1.5 MHz. It should be noted that an actual system would include independent gamma correctors* for each of the three

* In the literature on colour television, it is customary to prime the signals subjected to gamma correction. For example, E'_{R-Y} . For simplicity, the primes have been dropped in this book.

channels, and delay lines to secure precise time coincidence between the signals E_Y , E_{R-Y} and E_{B-Y} in the combiner.

In synchronous quadratic modulators, the chrominance signals are modulated onto the sinewave and cosinewave components of the subcarrier (see Fig. 11.29a). The combiner accepts all the signals

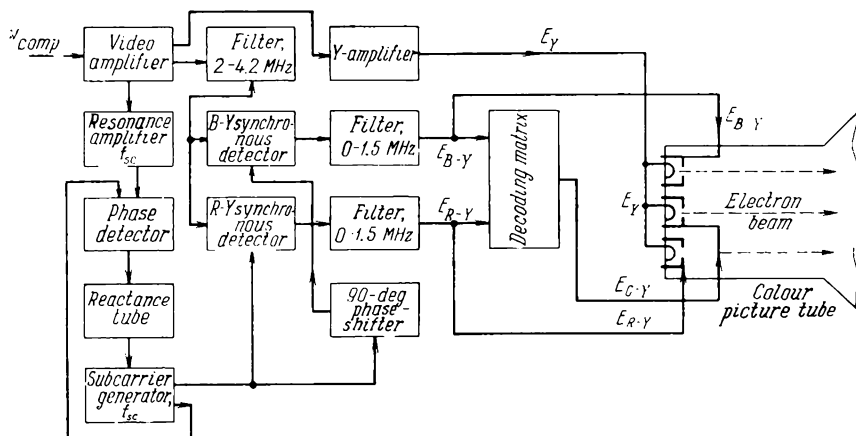


Fig. 11.33. Block diagram of the receiving terminal

that make up a composite colour television signal, that is the luminance signal E_Y , the chrominance signals E_{R-Y} and E_{B-Y} in quadrature on the same subcarrier, blanking, scan sync and colour sync pulses.

In order that the subcarrier, f_{sc} , be an odd harmonic of half the frame (line) scanning frequency, the subcarrier generator and the sync generator must be linked in a suitable manner by a frequency divider, as shown in the block diagram.

In all synchronous detectors of a colour TV receiver, the subcarrier must be in the same phase (accurate to within 5°) with the subcarrier at the transmitting end, or else the received image would display wrong hues. For this purpose, a colour subcarrier burst (8 to 10 cycles) is inserted into the composite television signal during the line blanking interval, to establish a reference for demodulating the chrominance signal. The waveform of this colour burst is shown in Fig. 11.32b. The frequency and phase of the colour burst are precisely equal to those of the chrominance subcarrier at the transmitting end.

Consider the block diagram of the receiving terminal shown in Fig. 11.33. After amplification at r.f. and i.f. and detection (the respective circuits are not shown in the diagram of Fig. 11.33 as they are analogous to those in a black-and-white receiver), the com-

posite colour television signal is amplified and applied to three units at the same time:

1. A resonant amplifier tuned to the subcarrier f_{sc} and extracting the colour burst. From the resonant amplifier, the colour burst goes to a phase detector which compares it in phase with the output of a local oscillator. The resultant error voltage is fed from the phase detector to a reactance-tube circuit which controls the local oscillator to obtain the desired phase.

2. A filter with a passband of 2 to 4.2 MHz. From the filter, the signal goes to the synchronous detectors. The filter blocks the passage of all frequencies lying outside the spectrum of the chrominance signals. In this way, it minimizes the effect of a considerable proportion of the luminance signal, E_Y , on operation of the chrominance channel.

3. The three parallel-connected cathodes of the colour picture tube.

After separation, the three chrominance signals are applied to the respective control electrodes. In this case, the picture tube operates as a matrix. That is, the three primary signals $E_1 = E_{R-Y} + E_Y = E_R$, $E_2 = E_{G-Y} + E_Y = E_G$, $E_3 = E_{B-Y} + E_Y = E_B$ are generated between its cathodes and control electrodes.

As is seen, the use of colour-difference, or chrominance, signals does not add to the complexity of the colour TV receiver. In fact, in the absence of colouring signals, the luminance signal E_Y is applied simultaneously to the three cathodes of the colour picture tube, and the colour receiver reproduces the black and white image without any need for switching.

The synchronous detectors whose operation has already been explained are contained in the chrominance channel. Past the filters with a passband of 0 to 1.5 MHz, the chrominance signals, E_{R-Y} and E_{B-Y} , are applied to a decoding matrix. The matrix adds together these two signals algebraically and derives the third chrominance signal.

The expression defining this signal in terms of the other two has the form

$$E_{G-Y} = -0.51E_{R-Y} - 0.19E_{B-Y} \quad (11.25)$$

11.11. *I*- and *Q*-Signals

As a way of reducing the bandwidth required for the chrominance signals, the NTSC compatible colour television system uses two chrominance signals designated E_I and E_Q which differ in composition from the E_{R-Y} and E_{B-Y} signals examined earlier, and are defined as

$$\begin{aligned} E_I &= 0.74E_{R-Y} - 0.27E_{B-Y} \\ E_Q &= 0.48E_{R-Y} + 0.41E_{B-Y} \end{aligned}$$

Experiments have shown that a reduction in the size of colour details is accompanied not only by a decrease in their saturation, but also by changes in the subjectively visible hue. For example, red and yellow fine details appear as orange, while blue and green as cyan. The I (in-phase) and Q (quadrature) signals employed in the NTSC system have been chosen in order to utilize this acuity of vision for colour. The I phasor in the diagram (the dashed lines in Fig. 11.30) extends from orange to cyan. The Q -phasor extends from yellow-green to magenta. When the I -signal is active alone (in the absence of the Q -signal), this produces orange-cyan reproduction of fine details. When both the I -signal and the Q -signal are active, this produces full-colour reproduction of larger areas.

As an illustration, let us refer to Fig. 11.28*b* which shows the spectrum of the signal used in the NTSC system. As is seen, the colour of large details is transmitted by two sidebands of both chrominance signals, extending from 0 to 0.5 MHz on either side of the subcarrier, $f_{sc} = 3.58$ MHz. In the case of fine details (down to 1.4 MHz), only the lower sideband of the I signal is retained; the upper sideband from 0.5 MHz upwards is suppressed. As has already been noted, the I signal alone can only produce orange-cyan reproduction. To sum up, large details up to 0.5 MHz are reproduced in full colour, finer details up to 1.4 MHz in only two colours, and still finer detail uncoloured.

Referring to the phasor diagram of Fig. 11.30, the I and Q signals should be shifted in phase through 33° relative to the R - Y and B - Y signals. This is done by an additional phase-inverter in the synchronous quadrature modulator.

Owing to the use of I and Q signals, the coding and decoding devices (used in the transmitting and receiving terminals, respectively) are markedly more elaborate, and this tells on both the cost and reliability of colour TV receivers. It is to be noted that the use of I and Q signals instead of R - Y and B - Y signals improves picture quality insignificantly.

11.12. SECAM Colour Television System

In 1954, Henri de France, a French engineer, published a description of a new colour television system called the "Henri de France System". In his system, the luminance signal was replaced by the colouring signals, E_R and E_G , transmitted on alternate line scans (sequential chrominance). The third colouring signal, E_B , was carried by a subcarrier within a narrow bandwidth. Because of a number of limitations, this system did not find practical application. In 1956-1957 it gave way to a new design from which a whole family of systems has grown under the common name of SECAM.

In 1960-1961, the SECAM system was modified to enable the colour-difference signals to be frequency-modulated onto a subcarrier, which considerably improved the performance of the system. The use of frequency modulation and the sequential transmission of chrominance signals are the major distinctions of SECAM from the NTSC system. In a SECAM receiver the chrominance signals are recovered on a time rather than on a phase basis, and this has rendered unnecessary any synchronous detectors. Frequency modulation has made the SECAM system insensitive to amplitude-frequency and phase distortion in the transmission circuit.

The sequential transmission of chrominance signals is based on the following consideration. As already noted, the inability of the human eye to see the colour of fine details makes it possible to limit the bandwidth for the chrominance signals to 1.5 MHz. Since the bandwidth occupied by the composite television signal is 6 MHz and is adequate for the reproduction of the finest details transmitted in black-and-white form by the luminance signal, E_Y , coloured details would have a size along lines at least $6 \text{ MHz} \div 1.5 \text{ MHz} = 4$ times as great as that of the finest details. In a similar way, it is possible to increase three or four times the size of coloured details across the lines.

Precisely this fact is utilized in the optimized SECAM system. The chrominance signals are transmitted on alternate line scans, say, the E_{R-Y} signal during one line scan interval and the E_{B-Y} signal during the next, and so on. In this way, colour information for both the E_{R-Y} and the E_{B-Y} signal is derived from only half the total number of lines. It is assumed that on the missing lines colour information is practically identical to that on the adjacent ones. Thus, for colouring signals each frame scan will contain half as many lines, and this leads to a proportionate increase in the vertical size of coloured details. This does not entail any impairment in vertical resolution, because the finer details are reproduced by virtue of the luminance signal, E_Y , from the frame scan containing the full complement of lines.

For normal operation, a SECAM receiver should have all three chrominance signals E_{R-Y} , E_{B-Y} and E_{G-Y} available at the same time. For this purpose it is necessary for the receiver to store the transmitted chrominance signal long enough to use it twice—once as it is being transmitted, and a second time on the next line, when it is not being transmitted. The storage capacity is provided by a delay line with a delay time of exactly one line-scan interval, $\tau_d = T_h = 64 \mu\text{s}$. For the first time, the signal is taken at the input to the delay line, and for the second, from its output, as shown in Fig. 11.34. Since the chrominance signals are transmitted on alternate lines and the line delay is likewise equal to one line interval, different chrominance signals exist at the input to and output from

the line at the same instant. For example, if the signal at the input to the line is E_{R-Y} , that at its output will be E_{B-Y} . In this way, the

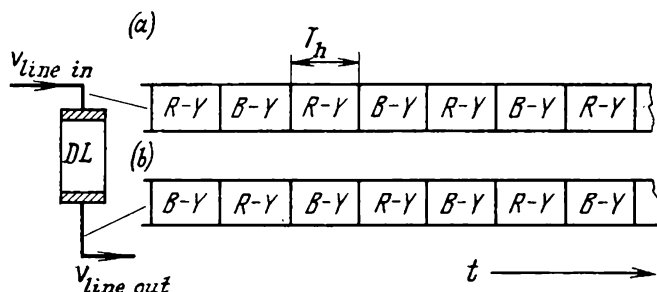


Fig. 11.34. Sequence of chrominance signals
(a) at input to delay line; (b) at output from delay line

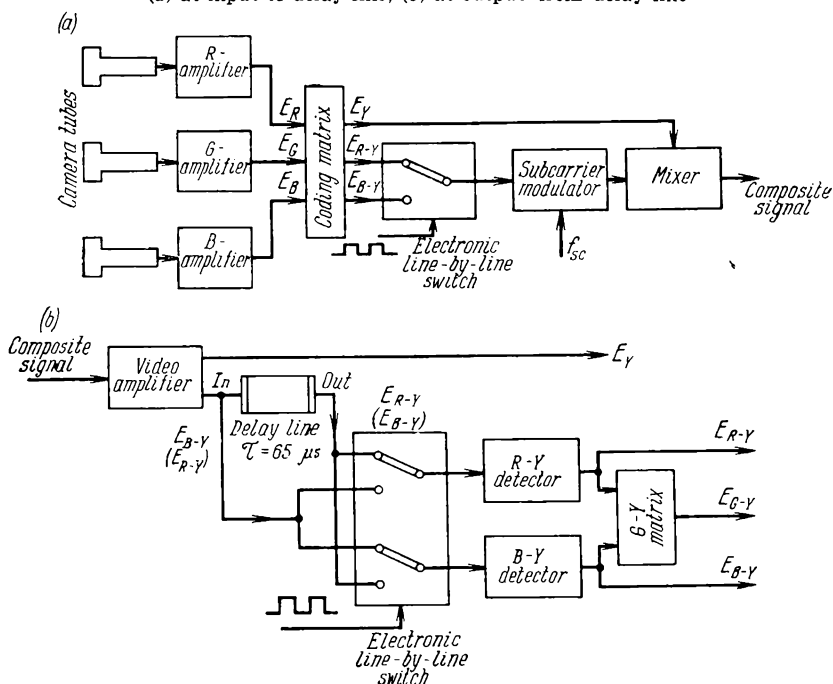


Fig. 11.35. SECAM system

(a) generation of chrominance signal at the transmitting terminal; (b) extraction of chrominance signal at the receiving terminal

delay line enables both chrominance signals to be available at the same instant. The third chrominance signal E_{G-Y} can readily then be derived by a suitable matrix.

Referring to Fig. 11.34, the E_{R-Y} and E_{B-Y} signals alternate at the input to and output from the delay line periodically. Hence arises the need for switching the two inputs of the matrix in such a way that the first input will always accept only, say, the E_{R-Y} signal and the second, only the E_{B-Y} signal. This purpose in the receiver is served by an electronic line-by-line switch.

In a very simplified manner, the operation of the SECAM system is illustrated in Fig. 11.35. As in any other system, the coding matrix of the transmitting terminal (Fig. 11.35a) produces three signals, namely the luminance signal E_Y and two chrominance signals, E_{R-Y} and E_{B-Y} . The electronic line-by-line switch operating at the line scanning frequency routes the colour-difference signals in turn to the subcarrier modulator. The mixer produces a composite colour television signal. In the receiver (Fig. 11.35b) the colour-difference signals existing at the input to and output from the delay line are routed by an electronic line-by-line switch and frequency detectors to the two inputs of a decoding matrix which derives the third colour-difference signal, E_{G-Y} . As is seen, with the chrominance signals transmitted sequentially (on alternate line scans), the delay line enables the three chrominance signals to be generated in the receiver at the same time. This is why the SECAM system is sometimes classed as sequential-simultaneous.

11.13. Basic Parameters of the SECAM System

As already noted, the SECAM system has undergone a number of changes in the course of its evolution. Today, this system has six modifications using frequency modulation. Since the preceding modifications are only of an historical interest, we shall refer to them only where it may be necessary for a better understanding of the manner in which the latest modification, the SECAM-IIIB (or SECAM-OPT) also adopted in the Soviet Union, is operated.

In the SECAM system, the chrominance signals are frequency-modulated onto a subcarrier. To reduce the visibility of interfering signals, the colour subcarrier and its sidebands are located in the h.f. part of the luminance signal spectrum. A reduced bandwidth is utilized for E_{R-Y} and E_{B-Y} so that colour information can fully be accommodated within the frequency band allocated to it. The SECAM system is compatible with black-and-white television because its basic parameters correspond to the black-and-white television standards (adopted in the Soviet Union and France). The horizontal resolution is 625 lines, the field rate is 50 Hz, the sound and video carrier separation is 6.5 MHz. The primary colour signals are generated and, the primary-colour coordinates and the reference white are selected in the same manner as in the NTSC system. That is, the luminance signal is determined by Eq. (11.21), and the chro-

minance signals by Eqs. (11.23) and (11.24). To avoid colour errors, the R , G and B signals fed to the coding matrix are first subjected to gamma correction. The amplitude characteristic of the gamma corrector is chosen such that the overall transfer characteristic of the television system be linear from camera to picture tube, and there is a linear relation between the light entering the camera and the light emitted by the picture tube. The transfer gradient (gamma exponent) of the colour picture tube is assumed to be $\gamma_{pt} = 2.8$.

To improve compatibility and noise immunity, the frequency modulator is fed modified, or weighted, chrominance signals which are symbolized D_R and D_B . These signals are derived from E_{R-Y} and E_{B-Y} as follows:

$$D_R = k_R E_{R-Y} = -1.9 E_{R-Y} \quad (11.26)$$

$$D_B = k_B E_{B-Y} = 1.5 E_{B-Y} \quad (11.27)$$

The weighting factors $k_R = -1.9$ and $k_B = 1.5$ have been introduced in order to enhance compatibility and noise immunity. From the values of E_{R-Y} and E_{B-Y} given in Table 11.3 it is seen that the extremal values of E_{R-Y} are obtained during the transmission of red (+0.7) and cyan (-0.7). The extremal values of E_{B-Y} are obtained during the transmission of yellow (-0.89) and blue (+0.89). If E_{R-Y} and E_{B-Y} were applied to the frequency modulator, the frequency deviation during the transmission of E_{B-Y} would be greater than during that of E_{R-Y} . The situation is rectified by the introduction of the weighting factors k_R and k_B . Now the two signals attain the same extremal values:

$$D_R = k_R E_{R-Y} = 1.9 \times 0.7 = 1.33$$

$$D_B = k_B E_{B-Y} = 1.5 \times 0.89 = 1.33$$

The fact that k_R takes a minus sign indicates that the polarity of E_{R-Y} is reversed. Negative polarity has been chosen for E_{R-Y} from the following considerations. From statistical data on the colour signals existing in various scenes it has been found that E_{R-Y} is predominantly positive and E_{B-Y} is predominantly negative. By reversing the polarity of E_{R-Y} it is arranged that negative frequency deviation is predominant during the transmission of both signals, D_R and D_B , thereby enhancing system stability towards limiting the upper sideband of the chrominance signals by communication links. When D_R and D_B are added to E_Y , the swing of the colour subcarrier is chosen to be about 25% of that of the luminance signal from black to white.

In the SECAM-IIIB system, the signals D_R and D_B are subjected to low- and high-frequency preemphasis or predistortion as a way of improving the protection of the colouring signal against noise and interference, and compatibility still more. Low-frequency pre-

distortion or preemphasis consists in that the high-frequency component of the chrominance signal spectrum is boosted by a network whose frequency response is defined as

$$A_{lf}(f) = \frac{1 + j(f/f_1)}{1 + j(f/af_1)} \quad (11.28)$$

where $a = 3$ and $f_1 = 85$ kHz.

In graphical form, the frequency response of the low-frequency preemphasizer is shown in Fig. 11.36. At the receiving terminal, the normal distribution of energy is re-established by a restorer network

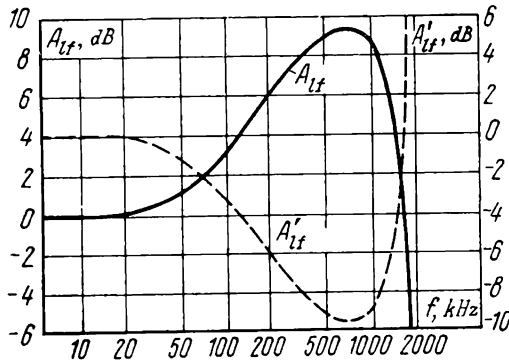


Fig. 11.36. Low-frequency preemphasis of colour-difference signals

$A_{lf}(f)$ —frequency response of the circuit at the transmitting end; $A'_{lf}(f)$ —frequency response of the correcting network in the receiver

which has a frequency response (shown by the dashed line in Fig. 11.36) just opposite to that of the preemphasizer and attenuates the high frequencies of the detected signals.

High-frequency preemphasis is applied to the FM chrominance signals. A suitable high-frequency preemphasizer boosts the amplitude of the subcarrier, should it depart from its nominal value, f_0 . The frequency response of the high-frequency preemphasizer is defined as

$$A_{hf}(f) = \frac{1 + j16F}{1 + j1.26F} \quad (11.29)$$

where $F = f/f_0 - f_0/f$ and $f_0 = 4.286$ MHz.

A plot of Eq. (11.29) appears in Fig. 11.37. As is seen, the high-frequency preemphasizer increases the amplitude of the modulated signal, should the subcarrier depart from its centre value, f_0 . At the receiving terminal (in the receiver) the normal distribution of energy is re-established by a high-frequency restorer network which has a frequency response (shown by the dashed line in Fig. 11.37) just opposite to that of the preemphasizer.

The rationale of frequency preemphasis is as follows. As will be recalled, the effect of interference and noise on an *FM* signal decreases with increasing index of modulation (defined as the ratio of the frequency deviation to the highest frequency of the modulating signal). In the SECAM system, the use of a large deviation is out of the question, as this would broaden the spectrum of chrominance signals too much, thereby impairing compatibility. Therefore, it is important to improve noise immunity without having to raise the modulation index.

Consider a case where the detector accepts a signal of voltage V_s and frequency f_s , and also an interference of voltage V_{int} and fre-

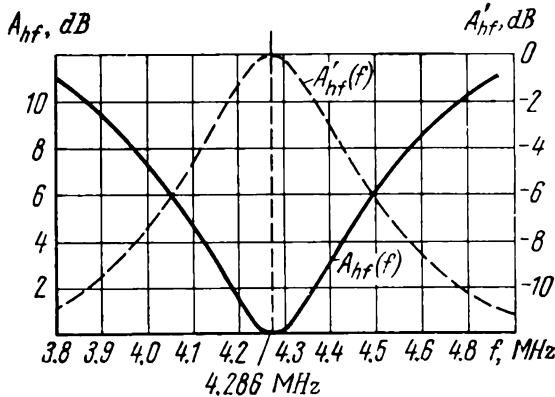


Fig. 11.37. H.f. preemphasis of colour-difference signals

$A_{hf}(f)$ — frequency response of the circuit at the transmitting end; $A'_{hf}(f)$ — frequency response of the compensating network in the receiver

quency f_{int} . The manner in which the relative value of the interfering signal (V_{int}/V_s) at the detector output in an *AM* receiver and an *FM* receiver depends on the difference between the signal and interference frequency, f_s and f_{int} , is shown in Fig. 11.38. As is seen, in *AM* reception the relative magnitude of the interference signal is independent of $F = f_s - f_{int}$. In *FM* reception, the interference at the output of the frequency detector rises with rising F . If the noise frequency is exactly equal to the subcarrier, the noise at the output of the frequency detector will be equal to zero. As the subcarrier deviates more and more from its centre value under the action of the modulating signals D_R and D_B , the noise increases in magnitude. To improve noise immunity, it is customary to boost the high modulating frequencies at the transmitting terminal and to attenuate them at the receiving terminal.

High-frequency preemphasis also serves to improve compatibility because it reduces the visibility of the subcarrier during the trans-

mission of black and white details in the picture and also of details having low saturation. In such cases, the signals D_R and D_B are zero very nearly, the frequency deviation is a minimum, all energy of the modulated chrominance signals occurs at the minimum, and on the frequency response curve of the high-frequency preemphasizer (see Fig. 11.37).

A third form of preemphasis is additional amplitude modulation applied to the *FM* subcarrier. The additional amplitude modula-

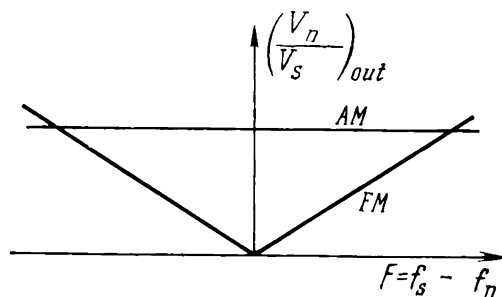


Fig. 11.38. Signal-to-noise ratio in the case of *AM* and *FM* signals

tion is used for the following reason. In a colour TV receiver the luminance signal is a noise from the stand-point of the chrominance signal. The energy that the luminance signal carries within the frequency band allotted to the chrominance signals and, as a consequence, the magnitude of the resultant noise depends on the scene content. Here, preemphasis consists in that if the swing of the luminance signal occurring within the frequency band of the chrominance signal exceeds 70% of the nominal amplitude of the subcarrier, the chrominance signal is boosted temporarily. As a consequence, noise in the chrominance signal of the receiver due to the action of the luminance signal is reduced. If the luminance signal is such that its energy within the frequency band of the chrominance signals is low, no additional amplitude modulation is applied. This considerably improves the signal to noise ratio in the receiver.

The SECAM-IIIB system differs markedly from its predecessors in that it uses two subcarriers which are harmonics of the line scanning frequency:

$$f_{0R} = 282f_h = 4406.25 \text{ kHz} \pm 2 \text{ kHz}$$

$$f_{0B} = 272f_h = 4250.00 \text{ kHz} \pm 2 \text{ kHz}$$

where $f_h = 15,625 \text{ Hz}$ is the line scan frequency. The frequency deviation is different for D_R and D_B , being $\Delta f_R = 280 \pm 9 \text{ kHz}$ (on D_R lines) and $\Delta f_B = 230 \text{ kHz}$ (on D_B lines). The SECAM-IIIB signal spectrum is shown in Fig. 11.39.

The reason for using two subcarriers is this. In the early modifications of the SECAM system a single centre frequency was used for both colour-difference signals, equal to $f_c = 4.43$ MHz. The frequency response of the high-frequency preemphasizer was arranged to have the lowest value at this centre frequency (see Fig. 11.37). However, it was disclosed that for most scenes the red colour gave rise to a good deal of noise. Noise suppression by high-frequency preemphasis depends on the signal frequency. Since in the SECAM system information about the colour being transmitted is conveyed by the subcarrier, noise suppression was different for different colours.

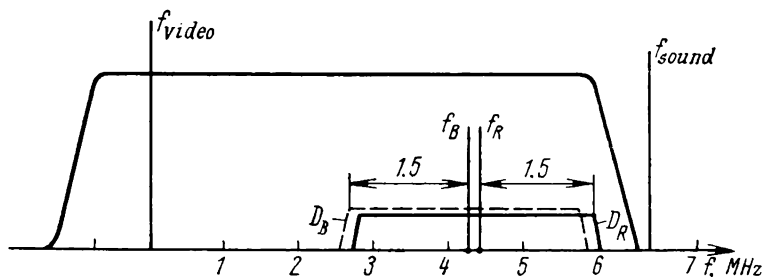


Fig. 11.39. Signal spectrum of SECAM-IIIB

As calculations and experiments showed, noise suppression was a maximum at the frequency for which the bell-shaped curve has a minimum, and decreased as the subcarrier was shifted either way. The subcarrier had its assigned value when the colour-difference signals were equal to zero. As has already been shown, this happens during the transmission of black and white areas of the picture. In other words, the conditions of transmission were optimal for black and white areas and not for red details (on which noise was most visible). As a compromise, it was decided that the frequencies by which red colour is transmitted should be located in both the D_R and D_B signal in the same region close to the minimum on the frequency response of the high-frequency preemphasizer. To achieve this, the centre frequencies of the D_R and D_B signals has been shifted by about 150 kHz. The precise values of the subcarriers have been chosen to be multiples of line scan frequency. The frequency deviation for D_R has likewise been taken somewhat greater in order to reduce fluctuation noise on red-coloured areas of the picture.

11.14. Block Diagrams of the SECAM Coder and Decoder

A block diagram of the SECAM coder is shown in Fig. 11.40. The primary colour signals E_R , E_G and E_B are applied to a coding matrix which derives the signals E_Y , D_R and D_B . Then the signals

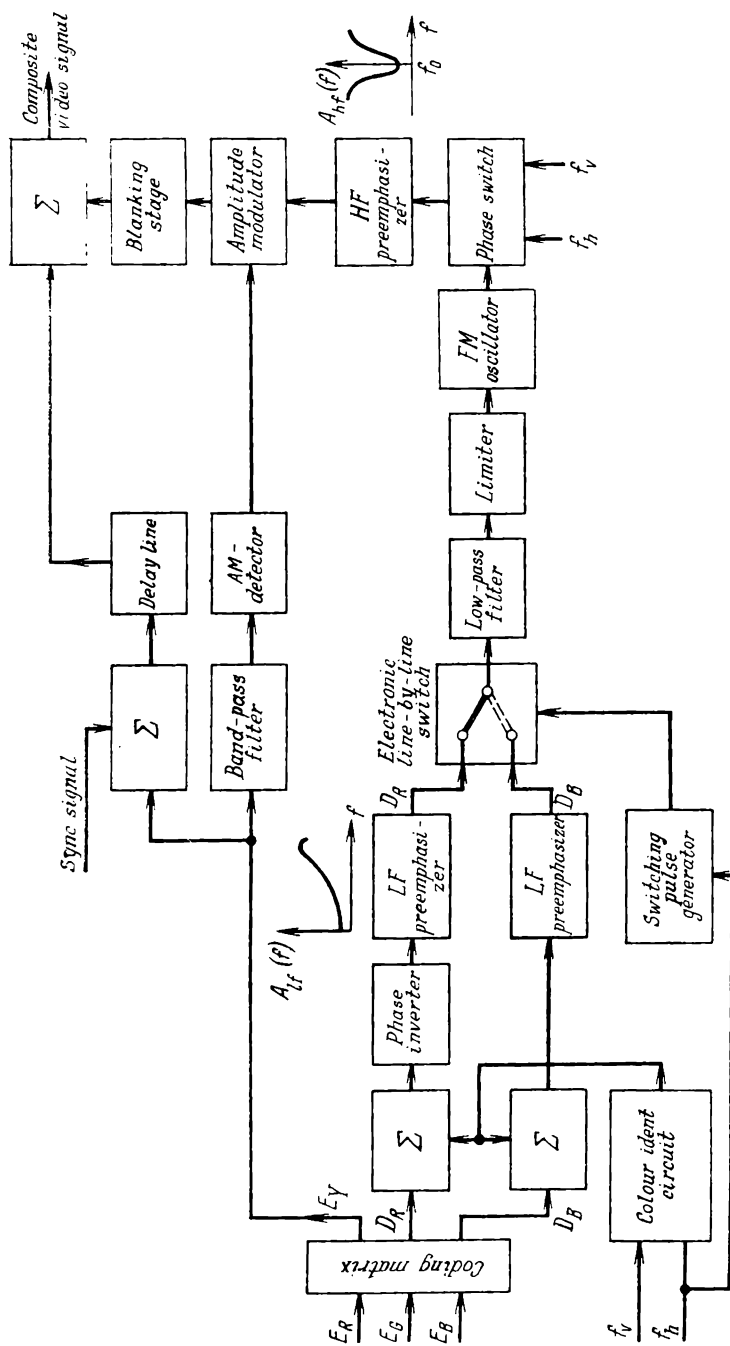


Fig. 11.40. Block diagram of the SECAM coder

D_R and D_B are fed to mixers which also accept colour identification (ident) signals. The colour identification signals essential to the correct operation of the electronic line-by-line switch of the receiver are generated by a colour ident generator. The signal D_R goes to a low-frequency preemphasizer via a phase inverter which changes its sign, and the signal D_B is taken directly from the mixer. Then follows an electronic switch which feeds the signals D_R and D_B to the same modulator in proper sequence and a low-pass filter, LPF , followed by a limiter to clip the spikes on the video signal after passage through the low-frequency preemphasizer.

The FM oscillator is a fairly complex part of the coder. In order to accomplish the frequency modulation of two subcarriers while keeping them at precisely their assigned frequencies, use has to be made of three oscillators, one FM oscillator and two shock-excited crystal-controlled oscillators. The frequency is stabilized by automatically locking the FM oscillator in phase to the crystal-controlled oscillators operating at f_{0R} and f_{0B} . Phase-lock action takes place during the line blanking interval.

The FM signal is applied to a phase switch which reverses the phase of the subcarrier periodically. The need for the phase reversal of the subcarrier can be explained as follows. In connection with the NTSC system it has been noted that the chrominance signals are cancelled on a black-and-white reproducer owing to the fact that the subcarrier is equal to an odd harmonic of half the line frequency. In the SECAM system, both subcarriers are harmonics of the line frequency. Therefore, unless suitable measures are taken, no noise cancellation would take place. For this purpose, the phase (polarity) of the subcarrier is forced to change at the transmitting end. For the first time the phase is reversed on a third line, and additionally during a third field. Practice has shown that this technique can considerably reduce the visibility of the subcarrier. The electronic switch is controlled by pulses following at the line and frame frequencies, f_h and f_v .

The next element of the coder is the h.f. preemphasizer from which the signal goes to an amplitude modulator. The latter is controlled by a signal coming from the amplitude detector which detects the luminance signal, E_Y , extracted by the band-pass filter with a passband of 2.5 to 6 MHz. The blanking stage which follows the amplitude modulator blanks (cuts off) the chrominance signals for the duration of the frame and line sync pulses so that the chrominance signals would not interfere with the synchronization of the scan circuits.

The luminance signal, E_Y , and the chrominance signals are added together in the mixer. Prior to that, a sync signal is inserted into E_Y . The delay line is provided in the luminance channel in order to match the luminance and chrominance signals in time. The chrominance

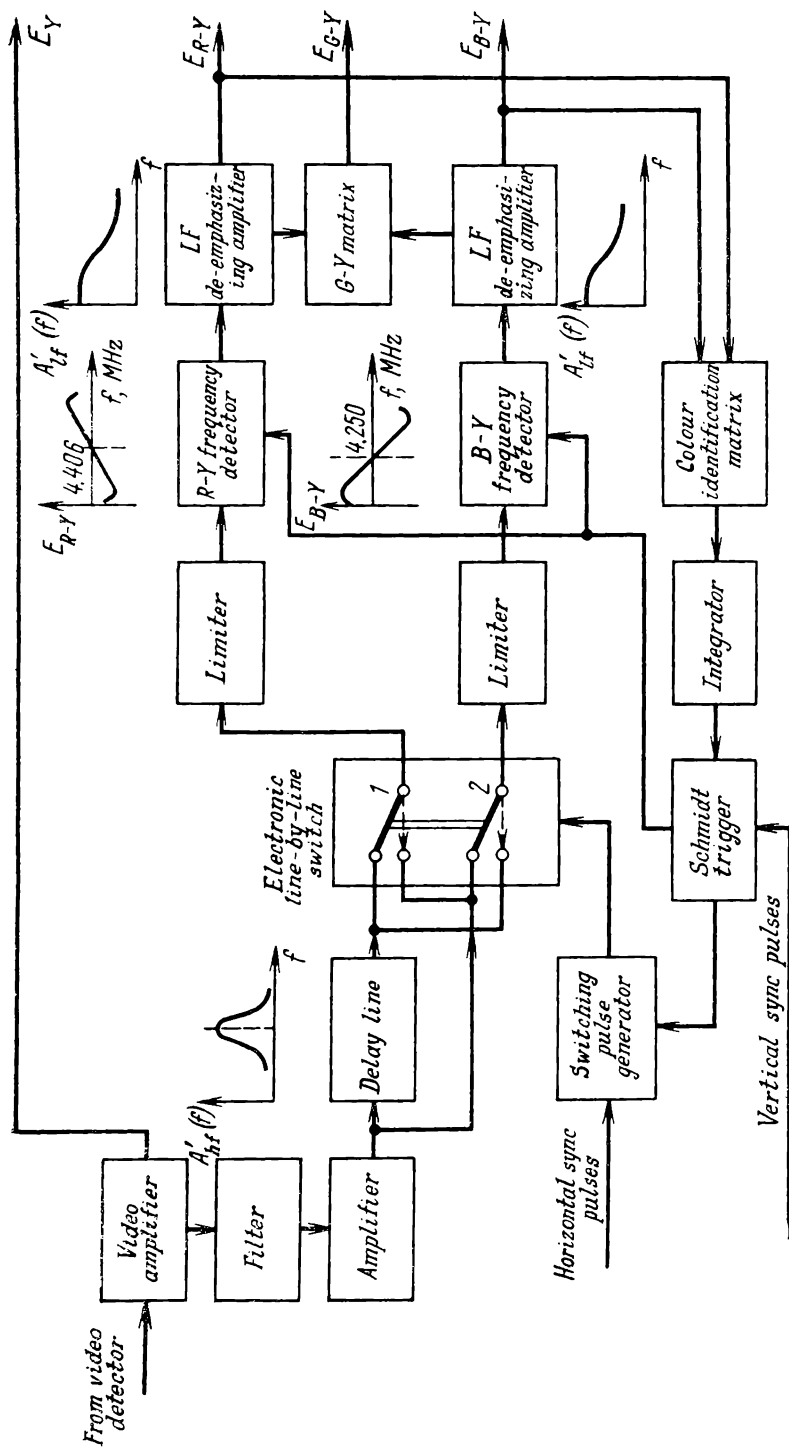


Fig. 11.41. Block diagram of the SECAM decoder

signals usually suffer a spurious time delay relative to the luminance signal E_Y in the low-pass filter and other narrow-band circuits of the coder.

The decoder of a colour TV receiver recovers the chrominance signals. A simplified block diagram of the decoder is shown in Fig. 11.41. The video amplifier of the luminance signal, E_Y , feeds its output to a bandpass amplifier with a bell-shaped frequency response (see Fig. 11.37). The bandpass amplifier separates the *FM* chrominance signals from the luminance signal and restores the normal distribution of energy shifted previously by the high-frequency pre-emphasizer. After amplification, the signal goes to a delay line with a delay time of $\tau_d = 64 \mu\text{s}$. From the electronic line-by-line switch, the *FM* chrominance signals are fed to frequency detectors. The frequency detectors in the *R-Y* and *B-Y* channels have amplitude characteristics with opposite slopes. Therefore, when the signal frequency goes down, the detector of the *R-Y* channel delivers a negative voltage and that of the *B-Y* channel, a positive voltage. For this reason, the chrominance signals (the D_R and D_B signals), arriving at the receiver in opposite polarities, come out of the detectors in the same polarity. From the frequency detectors, the E_{R-Y} and E_{B-Y} signals derived by the detection of the D_R and D_B signals are applied to video amplifiers where the normal distribution of energy shifted by the previous low-frequency preemphasis is restored.

The E_{G-Y} signal is derived by a matrix whose inputs accept the E_{R-Y} and E_{B-Y} signals. As a result, three colour-difference signals, E_{R-Y} , E_{B-Y} and E_{G-Y} , exist at the output of the decoder. For the E_{R-Y} and E_{B-Y} signals to reach their respective channels, it is important that the line-by-line switch be operating in the right sequence. This sequence is maintained by pulses generated by a switching pulse generator. Immediate control of the switching pulse generator is accomplished by a colour-identification circuit made up of a colour ident matrix, an integrating network, and a Schmitt trigger.

11.15. Operation of the Line-by-Line Switch and the Colour Identification Circuit

As already noted, the electronic line-by-line switch in the receiver should operate in such a way that the E_{R-Y} and E_{B-Y} signals can always be directed to the right demodulator. This calls for a proper colour identification which in turns needs an appropriate information. This comes in the form of a colour identification (synchronizing) signal. It is convenient to transmit a colour identification signal either during the line blanking interval, immediately after the scan sync pulse, or during the frame blanking interval. Theoretically, a colour identification signal need not be transmitted all the time, as it would suffice to set the correct phase for the line-by-line switch

once at the start of a program. Actually, however, the correct phase of the switch may be, and usually is, upset by noise finding its way into the chrominance channel of the receiver. Accordingly, a colour synchronizing signal has to be transmitted at regular intervals, to enable the receiver to check its switching sequence.

In the SECAM system, the colour identification signal is transmitted at the field rate, following the completion of the equalizing pulses which in turn follow the vertical sync pulse. The colour identification signals are produced by the coder as a train of nine trapezoidal negative-going pulses. These pulses with a duration of one line scan interval are inserted by the coder into the two colour-difference signals. Since E_{R-Y} is usually transmitted in negative polarity, it is passed through a phase inverter in the coder. The colour identification pulses reverse their polarity together with the E_{R-Y} signal, and they become positive (Fig. 11.42a). Switching between line scans, the switch routes the E_{R-Y} and E_{B-Y} signals on to output in turn. Since the switch keeps operating during the transmission of vertical blanking pulses, the colour identification pulses pass on to output in alternate polarity. The colour identification signals are applied to the frequency modulator which frequency-modulates them onto the subcarrier. The subcarrier frequency-modulated by colour ident signals is shown in Fig. 11.42b.

On passing through the h.f. preemphasizer whose frequency response is anything but flat, the colour ident signal is additionally amplitude-modulated.

The deflection and colour identification signals are shown in Fig. 11.42c. The colour ident signal occupies from the 7th to the 15th line in odd fields and from the 320th to the 328th line in even fields. In the receiver, after h.f. preemphasis has been removed, the amplitude modulation of the chrominance signals is eliminated. Together with the E_{R-Y} and E_{B-Y} signals, the colour ident signal is fed to the frequency detector. As long as the electronic line-by-line switch is operating in the correct phase, the colour ident pulses appearing at the output of the $R-Y$ channel are negative. Those appearing at the output of the $B-Y$ channel will likewise be negative because the amplitude characteristics of the $R-Y$ and $B-Y$ frequency detectors have opposite slopes (see Fig. 11.41).

If line-by-line switching happens to be in a wrong phase, the colour ident signals will be positive at the output of both channels. From the outputs of the $R-Y$ and $B-Y$ channels, the signals go to the colour identification matrix which adds them together. The sum signal is integrated and applied to a Schmitt trigger which also accepts negative vertical sync pulses. A simplified circuit of the Schmitt trigger is shown in Fig. 11.43a. It operates as follows. When the negative potential at the base of transistor T_1 rises to v_{on} (Fig. 11.43b), the transistor is rendered conducting and will remain in this state

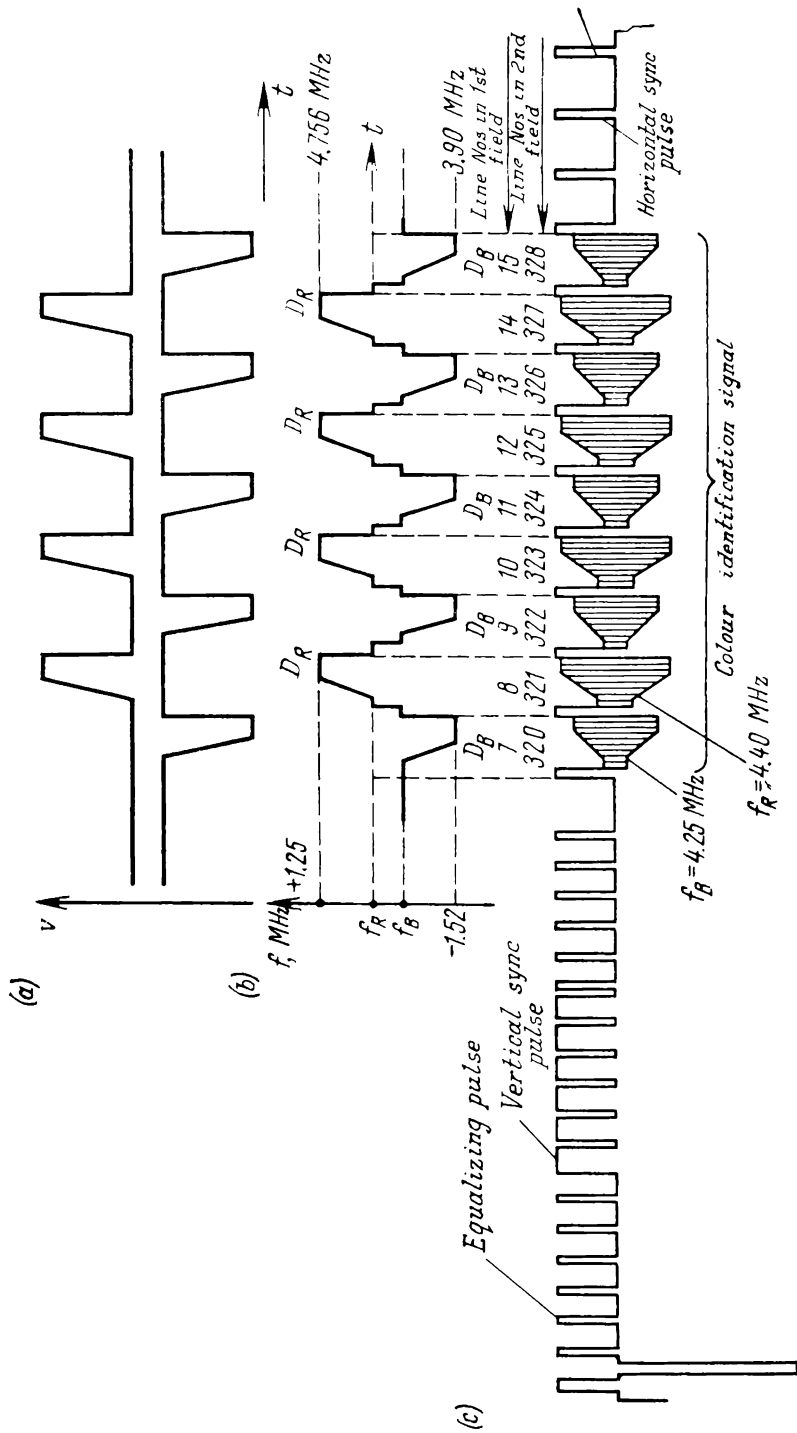


Fig. 11.42. Colour identification (ident) signals

(a) ident signals for D_R and D_B ; (b) variations in subcarrier during transmission of colour ident signals; (c) colour ident signals at coder output

as long as the potential becomes more negative. If, now, the potential at the base of T_1 be brought down, the stage will turn off at a potential, v_{off} , lower than v_{on} . In the chrominance unit, the bias voltage of the Schmitt trigger is set between v_{off} and v_{on} (Fig. 11.43b) by means of R_2 . The base of T_1 is fed differentiated vertical sync pulses as shown in Fig. 11.43c. The leading edge of a vertical sync

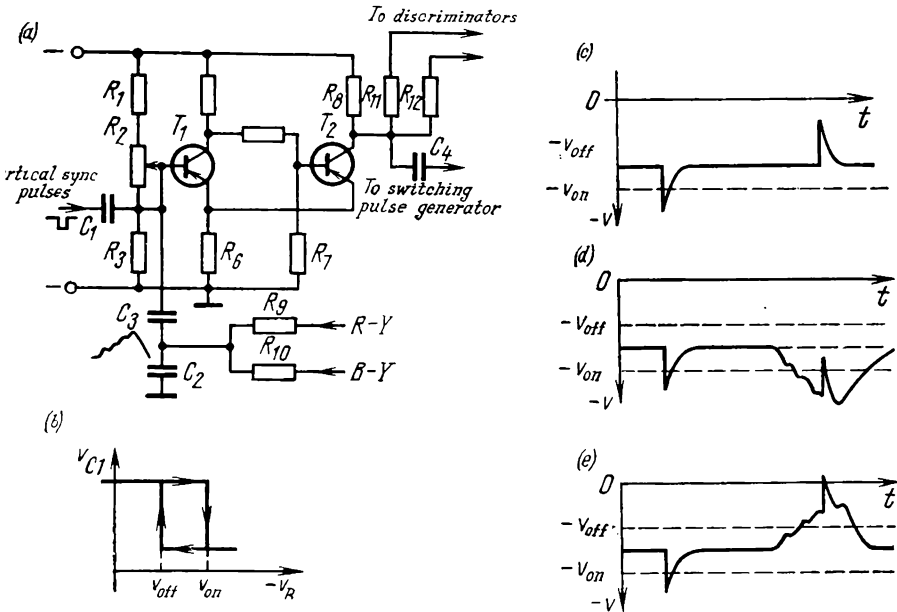


Fig. 11.43. Operation of the colour identification circuit in the receiver
 (a) circuit of Schmitt trigger; (b) operation of the Schmitt trigger; (c) control signal from Schmitt trigger during reception of black-and-white programs; (d) control signal in the case of correct switching phase; (e) control signal in the case of wrong switching phase

pulse drives T_1 into conduction (and T_2 to cut-off) while the trailing edge has an opposite effect. As a result, square pulses are formed at the collector of T_2 , which are utilized as bias voltage for the frequency detectors in the $R-Y$ and $B-Y$ channels. As a result, the channels of the chrominance unit are turned on for the duration of the vertical blanking pulses and are turned off for the rest of time. Via capacitor C_4 , the pulses are fed to the switching pulse generator which is a T -flip-flop built around transistors T_1 and T_2 (Fig. 11.43a). The flip-flop causes the switching phase to reverse every field. The above sequence of events applies to the reception of a black-and-white program.

When the receiver is switched to a colour program, the colour identification pulses are routed from the outputs of the $R-Y$ and

B - Y channels, via resistors R_9 and R_{10} to capacitor C_2 which together with R_9 and R_{10} makes up an integrating network. From C_2 , the signal is applied to the base of T_1 , which also accepts the differentiated vertical sync pulse. If the switch is operating at the correct phase, the colour identification signals will be in negative polarity. Since they match in time the trailing edge of the vertical blanking pulse, the signal at the base of T_1 has the form shown in Fig. 11.43d, and both chrominance channels are turned on. If the switch is operating in the wrong phase (Fig. 11.43e), the colour identification pulses will be positive, the Schmitt trigger will change

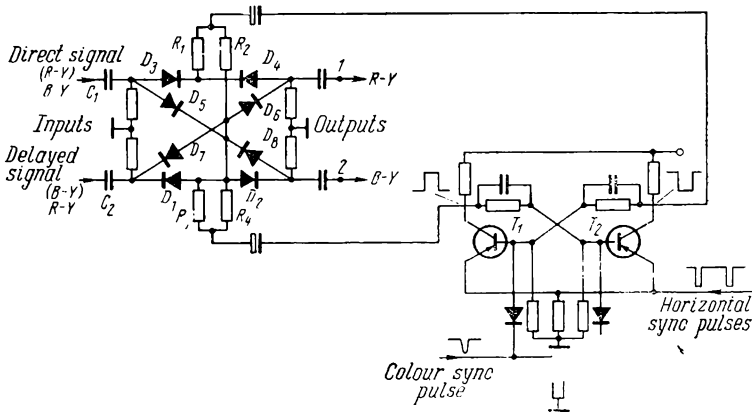


Fig. 11.44. Circuit of the electronic line-by-line switch

state, the pulse appearing at the collector of T_2 will turn off the chrominance channel, and the T -flip-flop will receive a corrective pulse, causing it to adjust the switching phase.

The circuit of the electronic line-by-line switch is shown in Fig. 11.44. It is built around crystal diodes D_1 through D_8 . Switching pulses are applied to the diodes via resistors R_1/R_2 and R_3/R_4 . The chrominance signal taken from the delay line input (the direct signal) is applied to the switch via capacitor C_1 , and that taken from the delay line output, via capacitor C_2 . If the pulse at the collector of T_1 is in positive polarity, diodes D_1 and D_2 are turned on and diodes D_5 and D_8 are off. The conducting diodes D_1 and D_2 pass the E_{B-Y} signal on to the switch output. When the pulse at the collector of T_2 is in negative polarity, diodes D_3 and D_4 turn on and diodes D_5 and D_8 are off, and the $R-Y$ signal is passed on to the switch output. In this way, the $R-Y$ signal exists at output 1 and the $B-Y$ signal at output 2. When the T -flip-flop changes state a negative pulse appears at the collector of T_1 and turns on diodes D_5 and D_8 ;

and these pass the direct $B-Y$ signal on to the switch output 2. At the same time, the pulse existing at the collector of T_2 turns on diodes D_6 and D_7 and turns off diodes D_3 and D_4 , thereby enabling the $R-Y$ signal from the delay line output to pass on to output 1. The horizontal sync pulses which cause the T -flip-flop to change state are applied to the emitters of T_1 and T_2 , and the colour ident pulse is applied to their bases.

11.16. Delay Line

As already noted, in order to recover the chrominance signals a SECAM receiver should include a delay line. This delay line should delay the chrominance signals with a bandwidth of about 3 MHz for $\tau_d = T_h = 64 \mu\text{s}$. Lumped-parameter delay lines composed of coils and capacitors and capable of handling signals with a bandwidth like that stated above can provide a delay of not more than a few microseconds. Special delay cables are no good, either. For

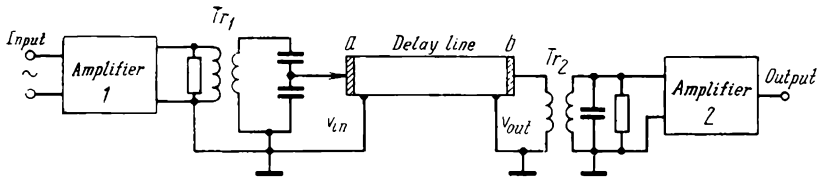


Fig. 11.45. Connection of an ultrasonic delay line

example, Soviet-made type PK3-401 cable introduces a delay of $0.7 \mu\text{s}$ per metre. Therefore, in order to obtain a delay of $\tau_d = 64 \mu\text{s}$, one has to use 80 m of this cable and to pack all of it inside the receiver. This is why SECAM receivers use specially designed miniature ultrasonic delay lines which can provide the desired delay time.

An ultrasonic delay line operates on the principle that electric signals are transformed into ultrasound at the input end of the device and back to electric signals at its output. The transducers at the input and output ends are connected by an acoustical waveguide which may be fabricated from steel, quartz, glass, water, or mercury. Where the signal is to be delayed for $\tau_d = 64 \mu\text{s}$, it is preferable to use ultrasonic delay lines with a solid waveguide.

In diagrammatic form, connection of an ultrasonic delay line in a circuit is shown in Fig. 11.45. The input signal is applied to an amplifier, 1. From the amplifier, the signal is then routed via a matching transformer to excite a piezoelectric transducer, a . For its operation this transducer depends on the well-known piezo-electric effect. The transducer converts electric signals into ultrasound which is then propagated in a sound-conducting medium. Another

transducer, b , at the receiving end converts the ultrasonic waves back into electric signals. The delayed signal is then fed via a matching circuit to an amplifier 2.

If the delayed signal is to be free from distortion, it is important that the piezoelectric transducers have a flat frequency response, that is, produce about the same signal at any frequency of the spectrum. Unfortunately, piezoelectric transducers show good performance at the high-frequency end and a poor performance at the low-frequency end of the range. Because of this, the signal spectrum is

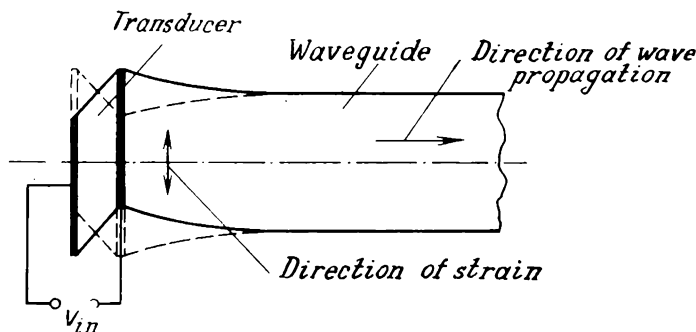


Fig. 11.46. Excitation of transverse mode in a delay line

usually modulated into the higher-frequency end of the range. In the SECAM system the chrominance signals to be delayed are already modulated onto the subcarrier, that is, translated into the high-frequency end. The chrominance signals are detected after they have passed through the delay line.

The delay lines used in SECAM receivers may have their waveguides fabricated from steel, glass or quartz. The waveguide is a bar with piezoelectric ceramic transducers attached to each end. Each transducer is 0.24 to 0.25 mm thick. For this thickness, the resonant frequency of the transducers is 4.4. MHz, which corresponds to the chrominance subcarrier frequency.

The delay line of a colour TV receiver is usually excited in a transverse acoustical mode. As is seen from Fig. 11.46, the applied electric field causes the transducer to deform in the transverse direction (at right angles to the direction of propagation of waves).

A typical delay line has a passband of 1.8 to 2 MHz (with the frequency response flat within 3 dB), an attenuation of 19 to 22 dB over the band, an input impedance of 80 ohms shunted by 100 pF at the subcarrier frequency. The low input impedance of the delay line necessitates the use of matching transformers (Tr_1 and Tr_2 in Fig. 11.45). The attenuation introduced by the line is made up for by an amplifier, 2.

11.17. Basic Features of the PAL System

Like in the NTSC system, the PAL (Phase Alternation Line) system uses synchronous quadrature modulation of the subcarrier with chrominance signals. Its basic difference is that the subcarrier of one of the colouring signals is reversed in phase on alternate lines in order to avoid phase distortion. As in the SECAM system, the chrominance signals in a PAL receiver are separated by a delay line. This is why the PAL system may be said to stand midway between the NTSC and SECAM systems.

Basically, the PAL system differs in the following. The E_{R-Y} and E_{B-Y} signals are transmitted by quadrature-modulating th

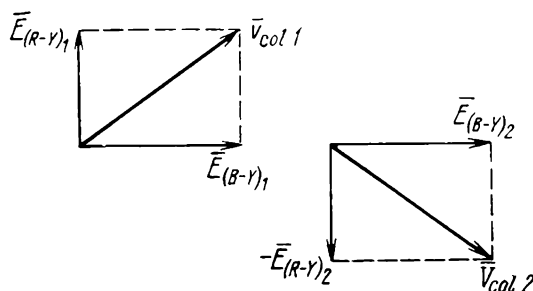


Fig. 11.47. Phasor diagrams of colouring signals in adjacent lines

colour subcarriers. However, the phase of the subcarrier intended for the transmission of the E_{R-Y} signal reverses from one line to the next. Phasor diagrams of chrominance signals on two successive lines are shown in Fig. 11.47. In the receiver, a delay line with a delay time of $\tau_d = 64 \mu s$ stores the chrominance signals for one line interval, after which the signals transmitted during the two successive line intervals are combined. It is assumed that the signals on two successive lines do not practically differ from each other. The manner in which the signals are combined is illustrated in Fig. 11.48a. The phasors representing the $E_{(R-Y)_1}$ and $E_{(R-Y)_2}$ signals are equal in magnitude and opposite in direction. On being combined, they cancel out.

The phasors representing the $E_{(B-Y)_1}$ and $E_{(B-Y)_2}$ signals are equal in magnitude and have the same direction. On combining, they form a signal twice as great, $2E_{(B-Y)}$. Subtracting $E_{(R-Y)_2}$ and $E_{(B-Y)_2}$ from $E_{(R-Y)_1}$ and $E_{(B-Y)_1}$, respectively gives a signal, $2E_{(R-Y)}$. This is shown in Fig. 11.48b. For clarity, the figure illustrates how the $E_{(R-Y)_1}$ and $E_{(B-Y)_1}$ are added to, rather than subtracted from, the $E_{(R-Y)_2}$ and $E_{(B-Y)_2}$ signals, taken in opposite polarity. After the signals shown in Fig. 11.48b are reversed in polarity, the phasor $E_{(B-Y)_2}$ becomes opposite in direction to the phasor $E_{(B-Y)_1}$, and,

on combining, they cancel out, while the $E_{(R-Y)_1}$ and $E_{(R-Y)_2}$ add together to form the $2E_{(R-Y)}$ signal.

Thus, a PAL receiver can separate the $E_{(R-Y)}$ and $E_{(B-Y)}$ signals without resort to synchronous detection. As was noted in connection with the NTSC compatible colour television system, it is sensitive to phase distortion due to the use of synchronous quadrature modulation. The phase errors arising in the signal transmission circuit

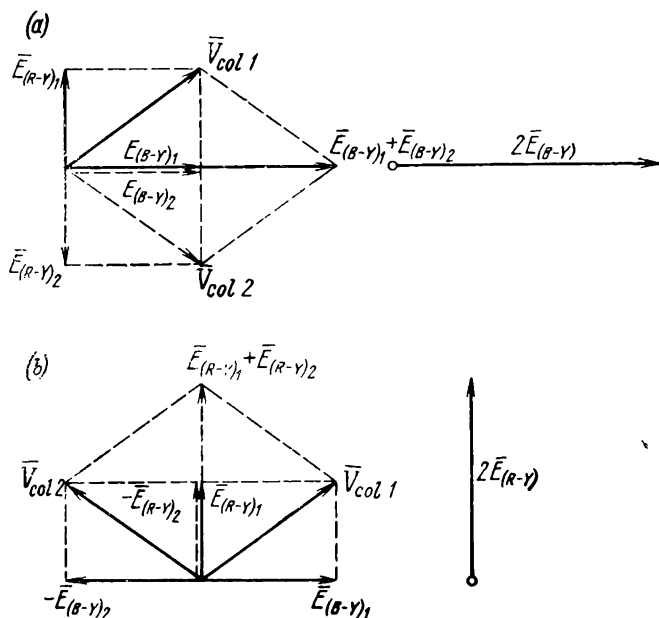


Fig. 11.48. (a) Addition and (b) subtraction of colour-difference signals on adjacent lines

give rise to "cross-colour". In the PAL system, the receiver might use ordinary detectors, but they would have to be supplied a locally restored subcarrier, and their cost would be comparable to that of a synchronous detector. This is why PAL receivers use the same synchronous detectors as are employed in the NTSC system. However, cross-colour due to phase errors is less pronounced.

The cancellation of cross-colour in the PAL system is explained in Fig. 11.49. Suppose that phase distortion in the transmission circuit has caused the quadrature-modulated signal, v_c , to shift through an angle $\Delta\phi$ from the correct position. In Fig. 11.49a, the colour subcarrier phasor, $\bar{v}'_{col 1}$, is shown shifted in phase through the angle $\Delta\phi$ from the reference phasor $\bar{v}_{col 1}$, counter-clockwise.

In Fig. 11.49b, the signal from the next line, \vec{v}_{col2} , is shifted in phase through the same angle in the same direction. Chrominance signals are added together by the rules of vector addition. As is seen from Fig. 11.49c, on combining, \vec{v}_{col1} and \vec{v}_{col2} produce a resultant phasor, \vec{v}_s , approximately equal in magnitude to twice the original terms of the phasor sum, and in the same direction as the original phasor.

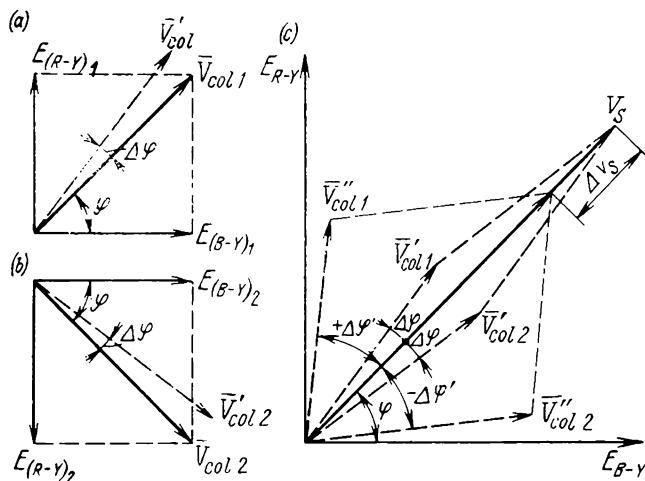


Fig. 11.49. Cancellation of cross-colour in the PAL system

Phase shift is cancelled irrespective of the magnitude of $\Delta\varphi$: the resultant phasor will always be in the same direction as the original one. However, its magnitude will change with changes in the phase error, as can be seen from Fig. 11.49c which illustrates the manner in which the phasors \vec{v}_{col1} and \vec{v}_{col2} are combined in the case of a phase error, $\Delta\varphi$, considerably greater than $\Delta\varphi$. As is seen, the resultant phasor is in the same direction as before, but its magnitude has diminished by $\Delta\varphi_s$. Thus, in the case of large phase errors, cancellation is incomplete. Because the magnitude of \vec{v}_s determines the saturation of the colour transmitted, the error $\Delta\varphi_s$ determines the magnitude of the saturation error.

A simplified block diagram of a PAL coder is shown in Fig. 11.50. It comprises an oscillator to generate a colour subcarrier of 4.43 MHz, a matrix to derive the colour difference (chrominance) signals, E_{R-Y} and E_{B-Y} , and the luminance signal E_Y from the primary-colour signals E_R , E_G and E_B , two modulators, and a mixer. The colour subcarrier is applied to the $R-Y$ modulator via a phase inverter. The phase of the colour subcarrier is switched by an electronic

switch keyed by suitable pulses at line scanning frequency. The switching is done at zero phase during the transmission of one line, and at 180° phase during the next line. The E_{R-Y} and E_{B-Y} signals are modulated onto the colour subcarrier in the same manner as in the NTSC system. The modulated E_{R-Y} and E_{B-Y} signals are combined with the E_Y signal in the mixer.

A simplified block diagram of a PAL decoder is shown in Fig. 11.51. The signal arriving from the video amplifier is applied to a band-pass filter which separates the colouring signals from the composite

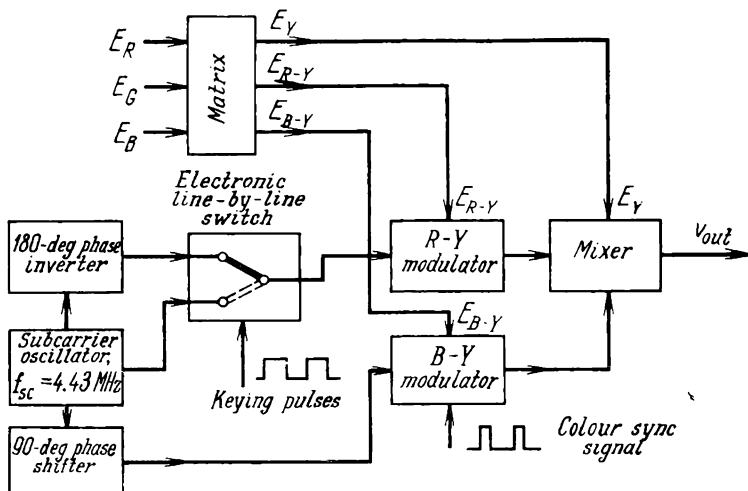


Fig. 11.50. PAL coder

signal. Then the colouring signals are applied to a summing and a subtracting network and to the E_{R-Y} and E_{B-Y} synchronous detectors. The detectors also accept from the subcarrier oscillator the colour subcarrier of 4.43 MHz restored by a circuit similar to that used in NTSC receivers. The phase of the reference subcarrier applied to the E_{B-Y} synchronous detector differs from that of the oscillator by 90° . The phase of the reference subcarrier applied to the E_{R-Y} synchronous detector is periodically reversed between successive lines by an electronic switch.

The phase reversal of the reference subcarrier in the $R-Y$ channel should occur at the same time as that of the subcarrier at the $R-Y$ modulator in the coder. To maintain time coincidence, the switch is keyed by colour sync pulses. Phase reversal of the subcarrier in the receiver is necessary for the correct detection of the E_{R-Y} signal whose polarity is periodically reversed in the coder at the transmitting terminal.

In connection with the NTSC system, it was noted that in order to make chrominance signals invisible on a black-and-white receiver, the colour subcarrier is chosen to be an odd harmonic (multiple) of half the line scan frequency, that is, $f_{sc} = (2n + 1)f_h/2$. The dot-pattern interference caused by the colour subcarrier cancels out

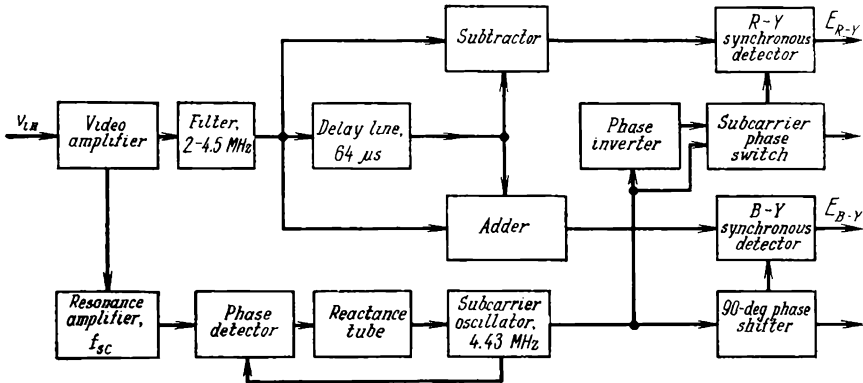


Fig. 11.51. PAL decoder

in the viewer's eye over two frames. In the PAL system, this method would not work because the deliberate phase reversal of the E_{R-Y} signal between successive lines and frames in the coder along with phase reversal of the subcarrier (due to the choice of the subcarrier frequency) would change the phase by 360° . That is, the phase would remain unchanged, and there would be no cancellation of the interference caused by the subcarrier.

Experiments have shown that the subcarrier in the PAL system is least visible if it is shifted through $f_h/4 + 25$ Hz from the even (284th) harmonic of line frequency.

CHAPTER TWELVE

TELEVISION TEST AND ALIGNMENT PROCEDURES

12.1. Objectives of Test and Alignment Procedures in Television

Tests and alignment form a very important and broad field of activities in television service. The capability of any television standards can be utilized completely only if all elements of the television system from the camera to the receiver are adjusted and aligned correctly.

An all-embracing criterion of picture quality is still lacking, and one has to measure its fundamental parameters separately. Among them are luminance, contrast, number of luminance gradations transmitted, resolution, sharpness, halation, streaking, fold-overs, fluctuation noise, periodic noise, nonlinear and geometric raster distortion, beam convergence, quality of colour synchronization, colour purity, etc. This list, far from complete, applies only to the quantitative indicators of the picture displayed on a picture monitor or a TV receiver.

Both in manufacture and operation of television apparatus, the need exists to measure the characteristics of the various elements of equipment. For example, in order to assess the quality of a pickup tube, one has to measure its light transfer characteristic, aperture characteristic, spectral response, stray signal levels, etc.

A huge number of techniques, procedures and instruments are used in television for the purpose of testing and alignment. Many techniques and procedures may further be modified to suit specific conditions. For example, the techniques and procedures used under laboratory conditions may markedly differ from those used at a factory or on an assembly line where a high rate of measurements is important. A retailer should be able to make measurements by simple means. In service, measurements should be carried out and the results recorded automatically in the course of transmission.

This Chapter will outline only the basic tests and measurements specific to television service.

12.2. Testing the Performance of a Receiver with a Test Pattern

The performance of television equipment and, especially, TV receivers can be tested by means of a test pattern usually televised prior to and also during breaks in a program. In the Soviet Union, use is made of the type TIT-0249 test chart shown in Fig. 12.1. This is a geometric pattern containing a group of lines and circles which

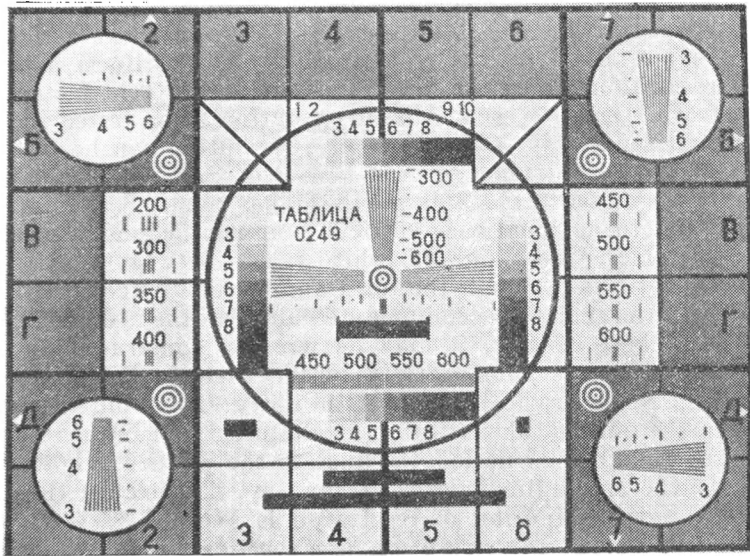


Fig. 12.1. TIT-0249 test chart (No. 2, 1949)

make it possible to reveal all the qualitative aspects of the television picture. The test chart is divided into squares which are numbered from 1 to 8 horizontally and labelled with letters from A to E (Russian alphabet) vertically. This is how, in brief, the test pattern can be used.

1. **Picture size and aspect.** To obtain an optimum picture size on a picture tube, adjust the horizontal and vertical size controls so that the white triangles in squares B-1, A-2, A-7, B-8, Д-8, E-7, E-2 and Д-1 are close to the outer frame of the receiver. At the same time, it is important to adjust the correct aspect ratio (4-to-3). Should the aspect be adjusted incorrectly, the squares would appear as unequal-sided rectangles, and the large circle in the middle of the screen and the smaller circles at the corners would turn to ellipses. For 110-degree picture tubes the aspect ratio is 5-to-4, and it

is permissible to let the leftmost and rightmost squares move (for about half their width) beyond the frame in order to correct the respective distortion.

2. **Scan nonlinearity.** Should the squares be compressed on one side and stretched on the other, this is an indication that the sawtooth current energizing the deflection yoke during scan is nonlinear. This nonlinearity is especially noticeable on the middle and outer circles which take on an egg-shaped form.

3. **Picture resolution.** Resolution is a very important quality of the television picture. This is why any test chart includes a number of elements which enable resolution to be tested at various points of the frame. Vertical resolution (across the lines) and horizontal resolution (along the lines) depends on different factors, and the test chart enables each form of resolution to be tested independently and separately. Quantitatively, resolution can be tested by means of horizontal and vertical lines (see Sec. 1.9). The television picture under the USSR standard has about 600 lines. This implies that in an ideal case vertical resolution cannot exceed 600 lines (300 black traces and 300 white spaces between them). Since the aspect ratio is $p = 4:3$, the total number of vertical lines of the same width that can be accommodated along a line is $600 \times 4 \div 3 = 800$. Because of this, it may be wrongly construed that horizontal resolution is substantially better than vertical resolution because the aspect ratio is more than unity. To avoid this misconception, the number of vertical lines defining horizontal resolution is counted within the line length equal to the picture height, rather than over the entire line length. In this way, the effect of the aspect ratio on the determination of resolution is avoided.

A test for horizontal resolution uses vertical wedges on the test chart. Each of these wedges is made up of nine fanlike lines and eight spaces between them. These wedges are located at three points on the test chart: in the bottom-left and top-right circles and above the centre of the middle large circle. The numbers standing next to the wedges (300, 400, etc.) give the number of lines (black and white together) that can be accommodated within the line length equal to the frame height at the pitch and width corresponding to the markings on the wedges (zeroes in the numbers of the corner wedges are omitted to save space). Additionally, horizontal resolution can be tested by means of vertical lines in squares B-2, Г-2, B-7, Г-7, Д-4 and Д-5; the numbers above these lines give their pitch which is equal to that marked on the wedges.

A test for vertical resolution is carried out, using the horizontal wedges located inside the top-left and bottom-right circles, and also on the left and right of the centre of the large middle circle.

To determine resolution, watch the respective wedge from a close distance and note the marking at which the individual black lines

can still be resolved. When a TV receiver is well aligned, the individual lines should be resolvable at the 500 to 550 markings.

4. **Interlace scan.** Partial or complete loss of interlace (most often because of poor synchronization of the frame scan generator) will above all lead to poor vertical resolution. The poor quality of interlace will manifest itself as a decrease in the number of resolvable lines on the horizontal wedges. Also, these lines will run fanlike towards the narrow part of the wedge. This defect is called moire (Fig. 12.2).

How accurately the lines of adjacent fields interlace can be determined from the appearance of the fine diagonal lines in squares

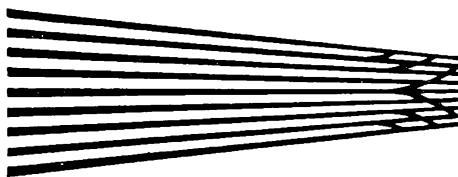


Fig. 12.2. Moire in the narrow part of a horizontal wedge due to poor interlace scanning

B-3 and B-6. With normal interlacing, these lines have no serrations. The appearance of serrations is an indication that the lines of adjacent fields partly overlap (known as line pairing).

5. **Luminance gradations.** A test for the luminance gradations of the television picture is run, using the graded stripes inside the middle circle (squares Б-4, Б-5, Д-4, Д-5, Б-3, Г-3, Б-6 and Г-6). Each stripe is divided into ten rectangles in descending order of luminance, that is, from the whitest white to the blackest black. The performance is satisfactory if the picture tube reproduces seven to eight such gradations.

6. **Low-frequency response.** As has been shown earlier (see Sec. 4.5), phase and amplitude distortion at low frequencies can conveniently be observed as the tilting of the top of square pulses. For this purpose the test chart includes black rectangles varying in length along the lines (squares Д-3, Д-6, Е-3, Е-4, Е-5 and Е-6). In the absence of distortion, signals corresponding to these rectangles will have the shape of square pulses of different length. Low-frequency distortion (see Fig. 4.19) brings about a re-distribution of luminance within the rectangles so that in the direction of the horizontal scan the black top of a rectangle becomes progressively lighter and a still lighter "tail" forms immediately beyond the right-hand side of the rectangle (see Fig. 12.3). This form of distortion grows more noticeable with the length of the rectangle.

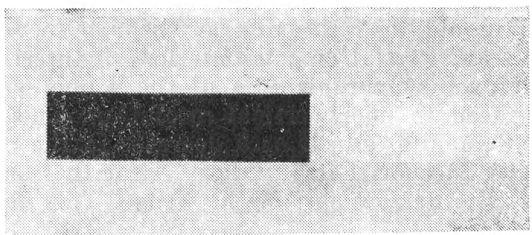


Fig. 12.3. Irregular frequency response at low frequencies, as revealed by a lighter tail at the end of a test rectangle

12.3. Amplitude and Frequency Response Tests

The frequency responses of the various elements of a television system may be measured by an ordinary frequency response analyzer. However, this instrument is useful only where the circuits under test contain no d.c. restorers. Otherwise, a d.c. restorer needs for its operation a composite television signal, that is, one containing line and frame blanking pulses. To facilitate the measurement of amplitude-frequency responses at high frequencies, a number of test-signal generators have been developed. An example of the test signals they generate is shown in Fig. 12.4*a*. It consists of six bursts of sinewave oscillations at different frequencies usually ranging between 0.5 and 6 MHz. The duration of the test signal is chosen such that it will not exceed the effective line length. After passage through the device under test, the signal takes on the shape shown in Fig. 12.4*b*. The amount of distortion is estimated from the amplitudes of the six component frequencies.

An advantage of the multiburst test signal is that it can be used for testing any television circuits and communication channels during program transmission.

It has been noted in Sec. 5.1 that the duration of a vertical blanking pulse is $25H$, of which the interval equal to $3H$ is utilized for the transmission of leading equalizing pulses and an equal interval is taken up by the vertical sync pulse. Following the trailing equalizing pulses on the vertical blanking pulse are a group of horizontal sync pulses. The gaps between the horizontal sync pulses within this time interval can be utilized for the insertion of test signals. In Fig. 12.5, the gaps between the 19th and 22nd horizontal sync pulses recommended by the CCIR (the International Radio Consultative Committee) for the transmission of test signals over national lines (inside a country) are shaded. The test signals adopted for international lines are transmitted during the 17th and 18th lines. During an even field, test signals occupy the

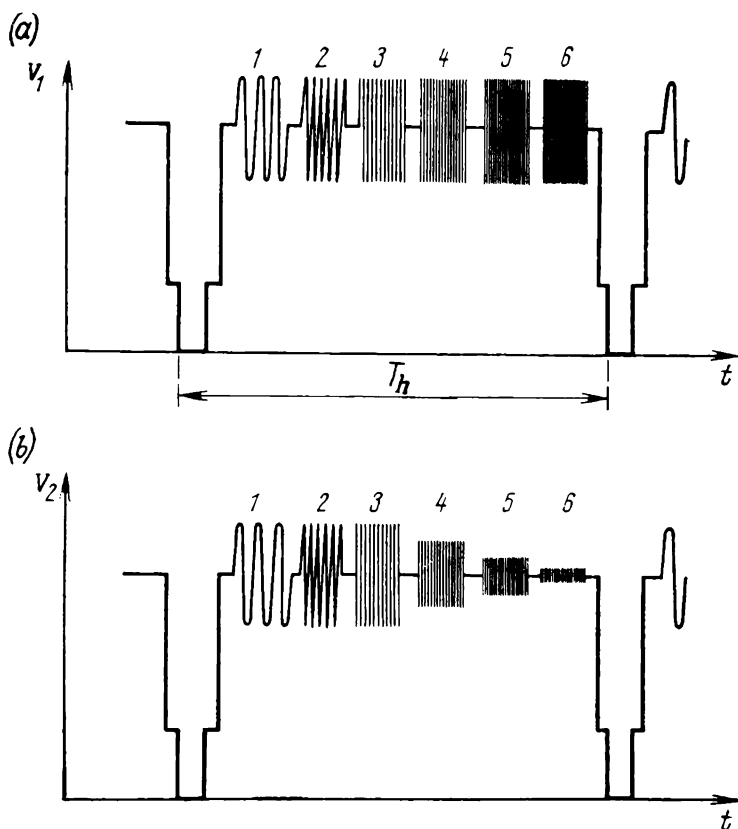


Fig. 12.4. Multiburst test signal for amplitude-frequency response measurements
(a) at input to circuit under test; (b) at output from the same circuit

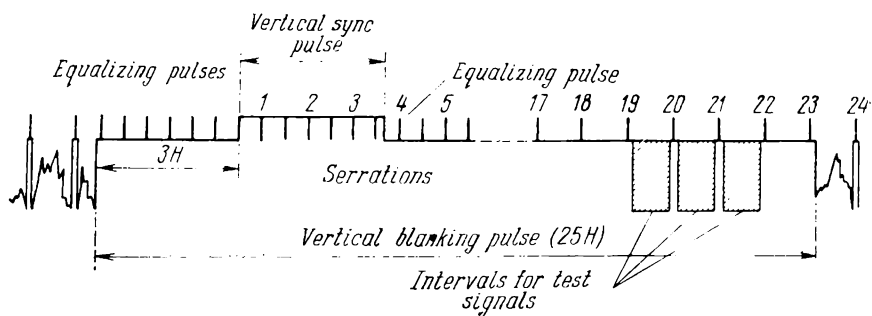


Fig. 12.5. Position of test signals inside the vertical blanking interval

330th through 334th lines of the raster. During a test signal the picture tube is blanked (by a vertical blanking pulse), and there is no interference with the reception of the test signal. Nor do test signals have any effect on the quality of synchronization because they are inserted between the white and black levels.

12.4. Transient Response Tests

Transient response is tested by a transient response analyzer which generates a square test pulse. The pulse rise time is measured by means of a time mark generator incorporated in the transient response analyzer. The time mark generator is a highly stable

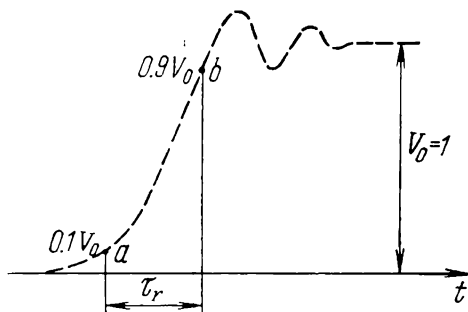


Fig. 12.6. Transient-response test signal

harmonic oscillator. Its output voltage is fed to the modulating electrode of an oscilloscope. The positive half-cycles of the sinewave signal brighten up the phosphor, while the negative half-cycles decrease its luminance. With a sufficiently high calibration voltage, the oscillogram appears as a chain of dashes (Fig. 12.6) on the oscilloscope. The rise time, τ_r , is found by counting the number

of black and white dashes between points *a* and *b* on the oscillogram and multiplying the count by the period of the calibration voltage. The rise time of the pulse is the time during which the voltage rises from 0.1 to 0.9 of its maximum value.

If the circuit under test includes a clamper, the test signal must contain blanking pulses as in the case of frequency response tests.

Square pulses are not always satisfactory in testing the transmission of the h.f. part of the signal spectrum. The point is that the equipment intended for the transmission of television signals has a limited bandwidth, and its frequency response is limited to that of the low-pass filter. Square test pulses encompass a range of frequencies which extend beyond the maximum frequency of the transmission channel. An oscilloscope would display a distorted waveform because the test signal spectrum would be limited, though the television signal which has a narrower bandwidth would pass through undistorted. Another disadvantage of square test pulses is that distortion, if any is present, would make it difficult to fix the 0.1 V_0 and 0.9 V_0 levels between which the rise time is measured. Errors are likely to creep in also in determining the total swing of the

signal because of overshoots and tilt of the pulse top. As a way out, the characteristics of a television channel are ordinarily tested by

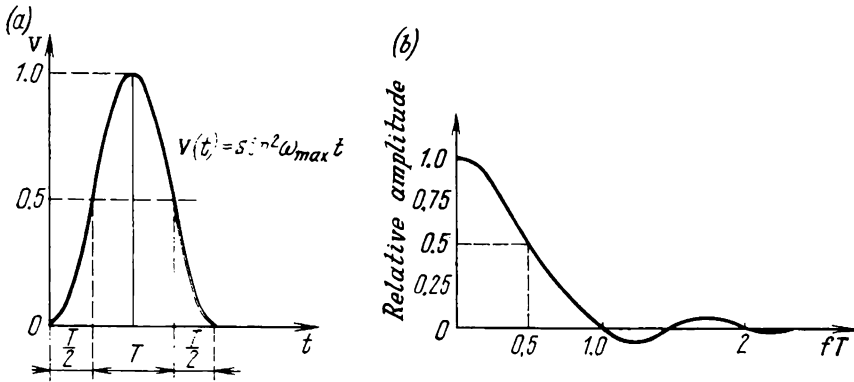


Fig. 12.7. Measurements in a television channel by means of sine-squared pulses
(a) test signal waveform; (b) test signal spectrum

means of a so-called sine-squared test signal, $V(t) = \sin^2 \omega_{\max} t$. A plot of this signal for $V = 1$ is shown in Fig. 12.7a and its frequency spectrum in Fig. 12.7b. The two are closely related.

As is seen from Fig. 12.7b, the relative amplitude of spectral components is zero at $fT = 1$, and the bulk of the spectrum energy occurs between 0 and fT . This property of the spectrum of a sine-squared pulse makes it convenient for use in tests. This is so because the duration, T , of the test pulse can always be adjusted so that its spectral components do not fall beyond f_{\max} (see Fig. 12.7a). Let, for example, there be a device with a bandwidth of $f_{\max} = 6.5$ MHz. Then $T = 1/f_{\max} = 1 \div 6.5 \times 10^{-6} = 0.154 \mu\text{s}$. A pulse of this duration will pass through the device undistorted because

the latter's frequency response is flat up to 6.5 MHz. Should the device have a bandwidth of less than 6.5 MHz, the h.f. components

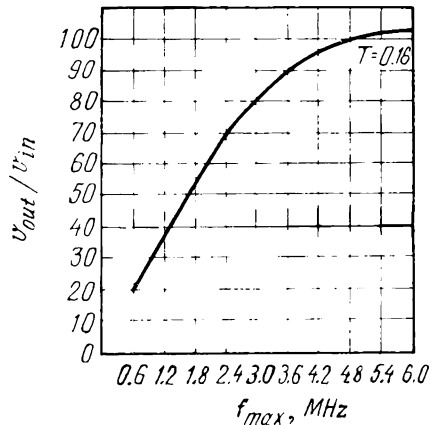


Fig. 12.8. Relative output voltage of sine-squared pulse as a function of the maximum frequency of the television channel

will be lost and the pulse voltage at the output of the device will be reduced.

The plot of Fig. 12.8 relates the decrease in the voltage of the sine-squared pulse of $0.154 \mu\text{s}$ duration at the output of a device to the maximum frequency, f_{max} , of its frequency response. The input to output pulse amplitude ratio is laid off as ordinate. As is seen from the plot, the increase in the maximum frequency from 0.6 to

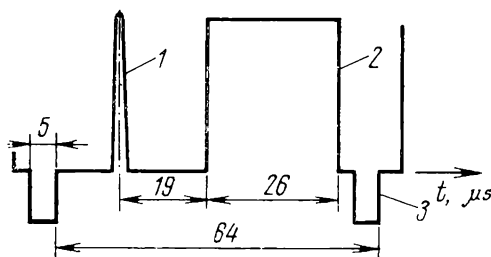


Fig. 12.9. CRO display of the test signal
1—sine-squared pulse; 2—reference pulse; 3—horizontal sync pulse

3.5 MHz entails a practically proportional rise in the amplitude of output voltage. Thus, variations in the magnitude of the sine-squared test signal give an idea about the frequency response of the device under test. In practice, use is ordinarily made of test pulses with durations of 0.16 to 0.17 or 0.08 to 0.1 μs , because they enable frequency distortion to be assessed in the 3-6 MHz range.

To measure the extent of decrease in the amplitude of the sine-squared test signals on passage through an amplifier or a communication link, it is advisable to accompany it with a longer reference signal whose magnitude would be independent of the frequency distortion introduced. A CRO display of the test signal often used in television service is shown in Fig. 12.9. It has a duration of 64 μs and contains a sine-squared pulse, 1, a reference signal (a square pulse of 26 μs duration), a blanking pulse, 2, and a sync pulse, 3.

12.5. Testing the Video Channel for Amplitude Linearity

The amplitude linearity of the video channel can be tested by means of sawtooth voltage such as shown in Fig. 12.10a. The test signal is repeated at the line scan frequency and contains blanking pulses essential to the normal operation of the clamper circuit. The signal voltage applied to the input of the device under test should be equal to the nominal input voltage for which the device is designed. If the device has a nonlinear amplitude response, the waveform of the test signal at the output terminal will be distorted

(Fig. 12.10*b*). Sawtooth voltage pulses are convenient to use because they make it possible to evaluate amplitude linearity within each portion of the amplitude range. However, a numerical evaluation of amplitude nonlinearity is difficult. Because of this, the

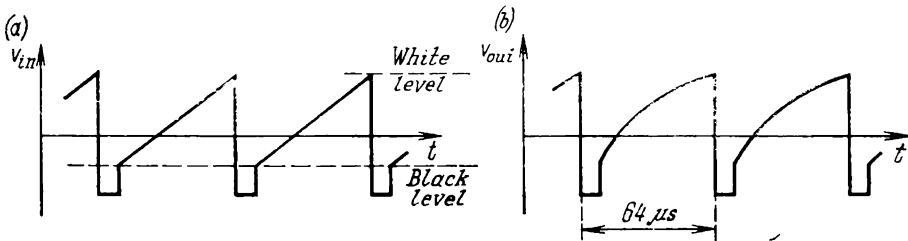


Fig. 12.10. Test signal to measure nonlinear distortion
(a) at input to the circuit under test; (b) at output of the same circuit

usefulness of sawtooth voltage pulses is limited to approximate tests of the amplitude response and adjustment of the gamma corrector. For ease of adjustment, the desired amplitude response may

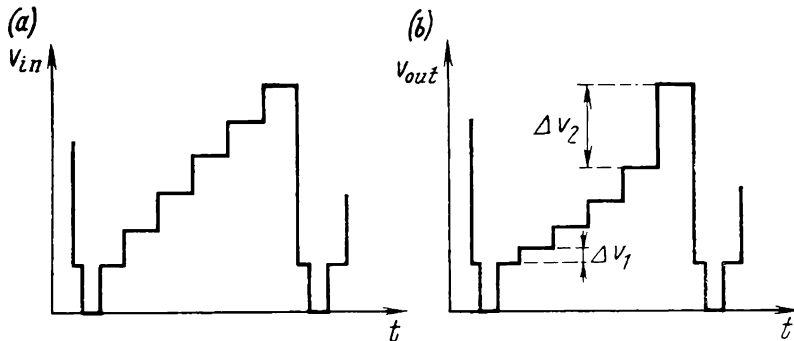


Fig. 12.11. Stair-step test signal
(a) at input to the circuit under test; (b) at output from the same circuit

be drawn on a thin plate of acrylic plastic or a photographic film, and this plate or film may then be used as an overlay on the screen of an oscilloscope.

The procedure is simplified when use is made of a stair-step test signal (Fig. 12.11*a*). Such a signal contains a number of equal steps. On passing through a device having some nonlinearity in amplitude response, the steps change in size (Fig. 12.11*b*). The amount of nonlinearity is evaluated from the ratio of the minimum swing, ΔV_1 , to the maximum swing, ΔV_2 . In practice, the stair-step test signal will contain from eight to ten equal steps because

a greater number of steps would make the measurements more difficult. The stair-step signal reveals a nonlinear amplitude response within individual portions of the amplitude range, while a sawtooth signal does so for the whole of the range. The accuracy of amplitude response tests using a stair-step signal is 5 to 10%.

Better results can be obtained by superimposing an h.f. sine-wave signal upon the sawtooth or stair-step signal. Figure 12.12a

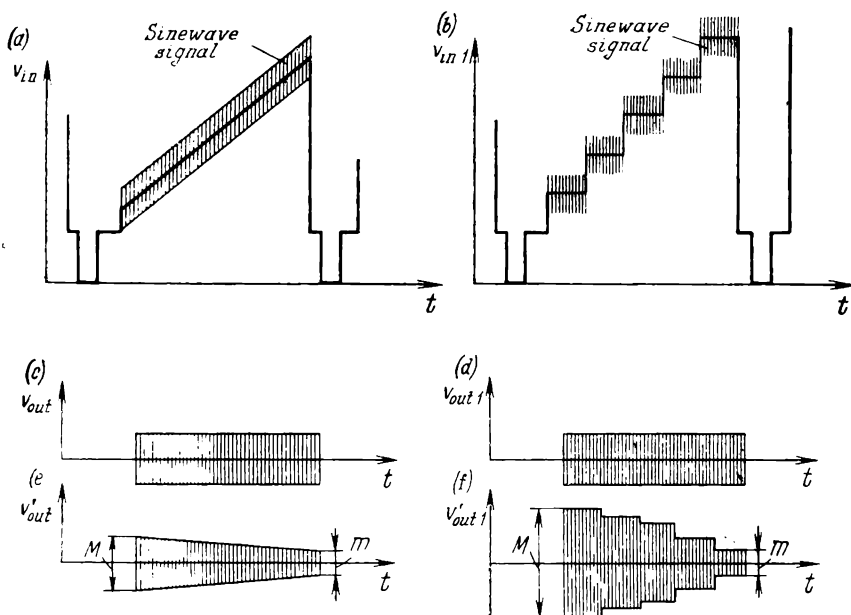


Fig. 12.12. Superimposition of sinewave voltage on test signals
(a) ramp and sinewave signals; (b) staircase and sinewave signals; (c) and (d) at filter output;
(e) and (f) at filter output in the case of nonlinear distortion

and *b* shows an h.f. sinewave voltage superimposed on a ramp and a stair-step signal. At the output of the device under test this composite signal is passed through a narrow-band filter tuned to the frequency of the sinewave signal. If the device under test has a linear amplitude response, the output signal will have the shape shown in Fig. 12.12c and d. Nonlinear amplitude response manifests itself as variations in the amplitude of the sinewave signal (Fig. 12.12e and f).

The amplitude response nonlinearity can be found by the equation:

$$n = (1 + m/M) \times 100\%$$

where *m* is the minimum amplitude and *M* is the maximum amplitude of the sinewave signal.

12.6. Colour Bar Chart Signal for Colour Television

The test signal widely used in colour television is one forming vertical or horizontal colour bars on a colour picture tube (Fig. 12.13a on the colour plate). As a rule, these are the primary colours (red, green and blue), their complements (cyan, magenta and yellow), and also white and black.

During the testing, alignment and repair of colour TV receivers this colour-bar test signal can be used for the following purposes:

1. To equalize the levels of the direct and delayed colouring signals in the chrominance unit.
2. To test the waveform of colour-difference signals (on an oscilloscope).
3. To test the h.f. and l.f. deemphasizers (restorers).
4. To test and align the luminance and chrominance matrices.
5. To test and align the colour synchronizing circuits.
6. To test the reproduction of the primary and complementary colours.
7. To test the frequency detectors in the chrominance unit.

The colour-bar test signal is produced by an electronic colour bar generator. Consider in brief how this is done.

The composite colour television signal contains the luminance signal E_Y and the colour-difference or chrominance signals E_{R-Y} and E_{B-Y} . Let us determine the magnitudes of the signals E_Y , E_{R-Y} and E_{B-Y} corresponding to the colour-bar-chart picture (see Fig. 12.13a on the colour plate). The magnitude of E_Y can be found by the equation (see Sec. 11.6):

$$E_Y = 0.3E_R + 0.59E_G + 0.11E_B$$

If a separate line of the picture is scanned, there will be its own value of E_Y for each colour being transmitted. For example, for the white bar,

$$E_R = E_B = E_G = 1$$

Then,

$$E_Y = 0.3 + 0.59 + 0.11 = 1$$

When, say, the yellow bar is transmitted,

$$E_R = E_G = 1$$

and

$$E_B = 0$$

Then,

$$E_Y = 0.89$$

In a similar way, it is possible to find the value of E_Y for any colour bar shown in Fig. 12.13a (see the colour plate). The values of E_Y thus found are summarized in Table 12.1.

As is seen from the table, the signal E_Y takes on values from unity to zero, and the colour bars are displayed in descending order of luminance.

Table 12.1

Signal	Signal value, V, for different colours							
	white	yellow	cyan	green	magenta	red	blue	black
E_Y	1	0.89	0.67	0.59	0.41	0.3	0.11	0
E_{R-Y}	0	0.11	-0.67	-0.59	0.59	0.7	-0.11	0
E_{B-Y}	0	-0.89	0.33	-0.59	0.59	-0.3	0.89	0
E_{G-Y}	0	0.11	0.33	0.47	-0.41	-0.33	-0.11	0

The values of the chrominance (colour-difference) signals given in Table 12.1 have been found by Eqs. (11.23), (11.24) and (11.25). In contrast to the luminance signal, the chrominance signals can take both positive and negative values. Within white and black areas all colour-difference signals are zero.

The source signals for the colour-bar generator are symmetric square pulses (see Fig. 12.13*b*, *c* and *d* on the colour plate) produced by oscillators keyed by horizontal sync pulses (f_h). If we denote the scan duration of one bar as t_b , then the duration of E_R pulses (see Fig. 12.13*b* on the colour plate) will be $2t_b$, that of the E_G pulses (see Fig. 12.13*c* on the colour plate) will be $4t_b$, and that of the E_B pulses (see Fig. 12.13*d* on the colour plate) will be t_b .

From the oscillators, the E_R , E_G , and E_B signals are applied to the coding matrix. In the luminance matrix, the E_R , E_G and E_B signals are added together in proportions according to Eq. (11.21). During the transmission of white colour, the output signals of the E_R , E_G and E_B oscillators are the same (see Fig. 12.13*b*, *c* and *d* on the colour plate) and equal to unity. The matrix output signal is then

$$E_Y = 0.3 + 0.59 + 0.11 = 1$$

which corresponds to the value of E_Y in Table 12.1. When, say, magenta colour is transmitted, the output signals from the E_R , E_G and E_B oscillators respectively are 1, 0 and 1, and the luminance signal is $E_Y = 0.3 + 0.11 = 0.41$. By similar calculations it can be shown that the levels of E_Y at the matrix output always correspond to those given in the Table.

The colour-difference or chrominance signals are produced in a similar manner by the E_{R-Y} , E_{B-Y} and E_{G-Y} matrices. Oscillograms of these signals are shown in Fig. 12.13*f*, *g* and *h* (see the colour plate).

During alignment of a TV receiver, a composite colour signal must be used, that is the E_Y signal interleaved with the chrominance signals modulated onto the colour subcarrier. For this purpose, the colour bar generator incorporates the respective elements of the coder (see Sec. 11.14), namely: a subcarrier oscillator, an electronic line-by-line switch, l.f. and h.f. preemphasizers, and so on.

LARGE-SCREEN TELEVISION SYSTEMS

13.1. Brief Outline of Existing Systems

It has always been a challenge for TV engineers to design as large a TV screen as possible. However, there are some important factors to be reckoned with. For one thing, as practice has shown, the most convenient distance from an observer to the screen must be three to five times the screen height. At this distance, the observer will be least fatigued by watching a program, as he will not have to turn his head to see the whole of the picture because his angle of view is great enough. Nor has he to strain his eyes to make out fine detail. In an average living-room the observer will be able to seat at 3 to 5 m from his TV set, which means that the TV screen may be as large as 120 cm by 90 cm (or 150 cm diagonal). Existing direct-view picture tubes may have a diagonal of up to 65 to 70 cm, but they are heavy and bulky, and they are not at all easy to make. Also, public recreation centres, schools, hospitals and similar establishments need still larger screens approaching those used in the cinema.

Quite apart from a straightforward increase in the size of the picture tube, there is another and more promising approach to large-screen television. In fact, with this approach, there is no need to increase the tube size—the picture, however small on the tube, can be blown up to any dimensions by an optical projection system, much as this is done with motion pictures.

In principle, this can be done in two ways. The idea of the first method is illustrated in Fig. 13.1. A high-luminance picture is produced on a specially designed projection picture tube, *PT*. The high luminance is secured through the use of an increased anode voltage and beam current in comparison with a conventional picture tube. A highly efficient optical projection system, *PS*, throws an image of the picture from the picture tube onto a large screen, *LS*. In early large-screen systems, these were objective lenses, *OL*, similar to projection lenses used in the motion pictures (see Fig. 13.1*a*). Later, they gave way to a combination of a spherical mirror, *SM*, and a corrective lens, *CL*, having ten times higher efficiency and, as a consequence, producing an image of high brightness (see Fig. 13.1*b*).

The combination of a projection picture tube and a projection optical system offers a relatively simple answer to the problem of large-screen television, and it is used on a relatively wide scale. However, its limitations have spurred the search for the more attractive approaches. These limitations basically reduce to the following. Firstly, screens in excess of 10 m^2 require that the anode voltage of the projection picture tube be raised to 60 to 80 kV. Voltage of this magnitude is difficult to obtain and unsafe to the health and lives of attending personnel and viewers. Also, at this voltage, the projection picture tube would emit X-rays in excess of safe limits. Secondly, a projection picture tube using so high anode voltage and beam current would be short-lived. The life of phosphor would be cut down to a few tenths of that used in conventional picture tubes. To sum up, a large-screen television system using a projection picture tube would be justified for moderately sized viewing screens having an area of a few square metres.

The second method of large-screen television is shown in Fig. 13.2. The scanning beam, 9, produces a small picture on the screen, 3, of a specially designed picture tube, 6. The picture does not emit any light, but its elements differ in optical density, the light areas being more and the dark areas less transparent. In a way, the screen of the tube is not unlike a motion-picture frame or a transparency. The picture is then projected by highly efficient optical elements, 2 and 4, and a powerful light source, 1, onto a large viewing screen 5. In this system, there is nothing to limit the practical size of the viewing screen except the speed of the optical elements, the light output of the source, and the heat strength of the tube screen.

The large-screen television system just examined is called the light-modulator system because the picture-tube screen, 3, modulates light in proportion to the picture content.

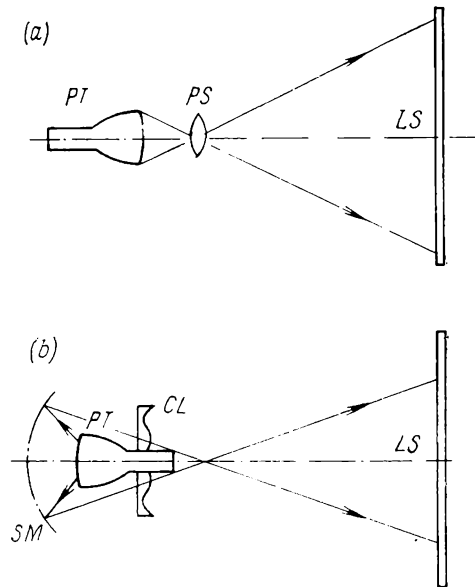


Fig. 13.1. Large-screen television system using (a) projection lens and (b) spherical mirror

A third promising approach to large-screen television has been taking shape since the advent of the laser. The idea of a laser large-screen television system is illustrated in Fig. 13.3. The light beam

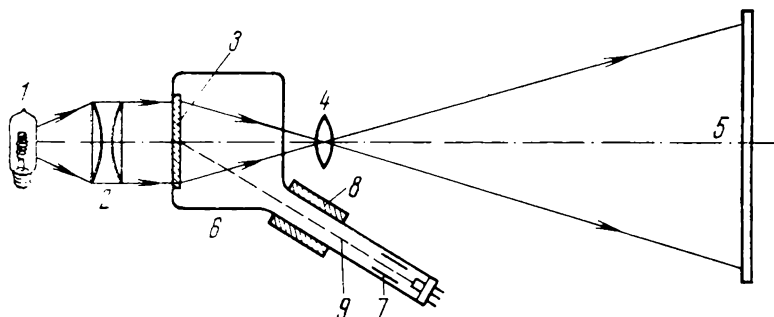


Fig. 13.2. Light-modulation large-screen television system
1—high-power light source; 2—condenser; 3—light-modulating plate; 4—projection lens; 5—large screen; 6—tube bulb; 7—electron gun; 8—deflection yoke; 9—electron beam

generated by a continuous-wave (CW) laser is directed first to a modulator where the television signal controls its intensity. Then

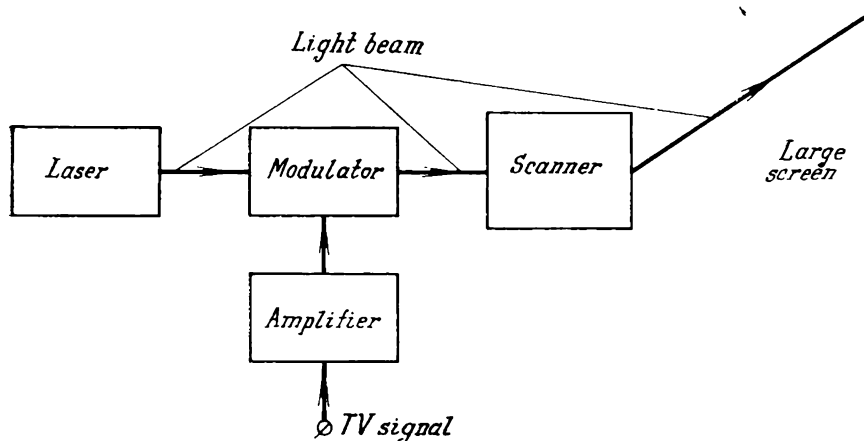


Fig. 13.3. Block diagram of a laser large-screen television system

the modulated laser beam is deflected by a scanning system horizontally and vertically so that, on reaching a large screen, it "paints" the picture there.

The technical difficulties arising in a laser large-screen television system may be summed up as follows. Firstly, the laser

beam, in distinction from the electron beam, cannot be deflected by electric or magnetic fields. In experimental set-ups it is made to deflect mechanically by rotating mirror drums. Since the speed of the line scan drum must be several hundred revolutions per minute, the arrangement of necessity becomes rather complicated. Secondly, because the laser beam has a very narrow emission spectrum, a single laser unit cannot produce a black-and-white picture. This can only be done by a combination of three lasers with beams of colours which can be combined to give the sensation of white.

13.2. Projection-Tube System

The widely employed large-screen television system using a projection picture tube and projection optics deserves a closer study. In our discussion we shall refer to the principles of illumination and optics set forth in Chapter 1.

An elementary optical system incorporating a projection lens is shown in Fig. 13.4a. The light emitted by the picture tube obeys

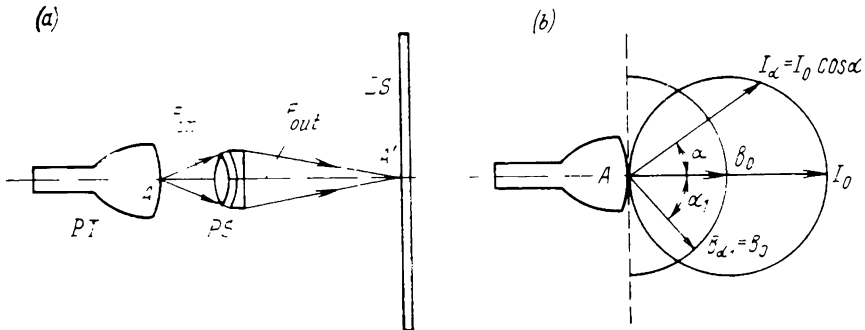


Fig. 13.4. Determining the efficiency of a projection-lens optical system
(a) optical train; (b) loci of brightness and light intensity

Lambert's law [see Sec. 1.2, Eqs. (1.13) and (1.14)], that is a luminous point on the picture tube screen is a perfectly diffuse radiator (Fig. 13.4b).

Therefore, in determining the light flux, F_{out} (Fig. 13.4a) we may use Eq. (1.22):

$$F_{out} = \tau F_{ln} = \pi I_0 (\tau/4) (D/f)^2$$

The efficiency of the projection system shown in Fig. 13.4a may be found by Eq. (1.25):

$$\eta = F_{out}/F_{tot} = (\tau/4) (D/f)^2$$

For a good-quality lens with an entrance pupil diameter to focal length ratio of $D/f = 1/2$, the transmission ratio is $\tau \approx 0.8$

so that the efficiency is

$$\eta = 0.8/4 (1/2)^2 = 0.05 = 5\%$$

Because the efficiency of the lens is extremely low (95% of light emitted by the screen of the projection picture tube does not contribute to the imagery on the large screen), the lens arrangement has been abandoned in favour of a more efficient system, known in astronomy as the Schmidt objective. In a fairly simple way, the

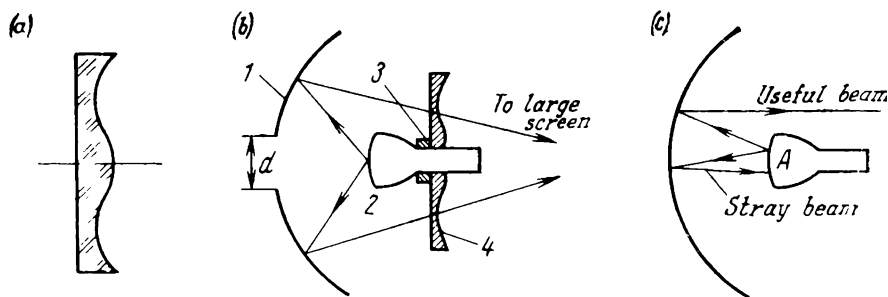


Fig. 13.5. Spherical-mirror optical system

(a) sketch of corrective lens; (b) sketch of projection optics; (c) stray illumination; 1—spherical mirror; 2—projection picture tube; 3—deflection yoke; 4—corrective lens

entrance diameter to focal length ratio of this system can be made equal to 1:0.6. Then, all other conditions being equal, the improvement in efficiency will, in accordance with Eq. (1.25), be:

$$\eta_{\text{Schmidt}}/\eta_{\text{lens}} = (D/f)_{\text{Schmidt}}^2/(D/f)_{\text{lens}}^2 = (1/0.6)^2/(1/2)^2 \approx 10 \text{ times}$$

that is,

$$\eta_{\text{Schmidt}} \simeq 10\eta_{\text{lens}} = 10 \times 0.05 = 50\%$$

The Schmidt objective, as originally designed for reflecting telescopes, consists of a spherical mirror. A major advantage of the Schmidt objective over, say, a simple lens, is that it effectively reduces spherical aberration (to one-tenth—one-thirtieth of that of a lens). A further important advantage of the spherical mirror is that it introduces practically no astigmatism, coma or distortion.

Although the spherical aberration of the spherical mirror is a split fraction of that possessed by lenses, it is objectionable when it comes to producing a clear and contrast image, and needs correction. This purpose is served by a suitably contoured corrective lens (Fig. 13.5a).

At its top, the spherical mirror has a round opening with a diameter d (Fig. 13.5b) approximately equal to that of the picture tube screen. This opening improves the contrast of the image. With-

For the practical directional screens used in television the directivity factor is 3 to 5. This implies that such screens can increase the visible brightness three to five times or, if the brightness be kept unchanged, make it possible to reduce the luminance of the projection picture tube to one-third to one-fifth or, all other conditions being equal, to increase the size of the screen in the same

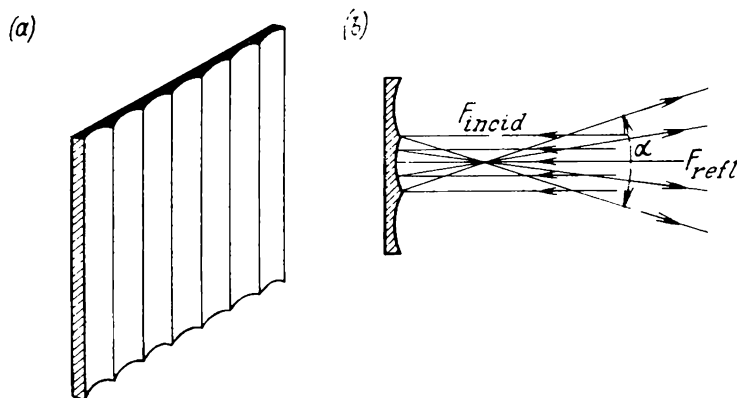


Fig. 13.7. Lobe-shaped brightness patterns of a viewing screen
(a) surface structure of a directional screen; (b) distribution of luminous flux reflected from a directional screen

proportion. The lobe-shaped brightness pattern is obtained by giving the screen an appropriate treatment. One such treatment consists in making narrow flutes on the surface of the screen (Fig. 13.7a). These flutes act like spherical mirrors. The light incident on them from a projection television system is reflected within a narrow angle α (Fig. 13.7b).

13.3. Light-Modulator Systems

Now we shall take a closer look at the light-modulator large-screen television system (see Fig. 13.2). In this system, the material deposited on the face of the cathode-ray tube and capable of varying its optical density according to the intensity of the electron beam might be potassium chloride. When bombarded by electrons, crystals of potassium chloride absorb light and produce dark spots or traces. This principle is utilized in a tube, called the skiatron or dark-trace tube, employed in radar to produce images of stationary or slow moving targets on a large screen. Unfortunately, dark-trace tubes with potassium-chloride scotophor (as the material deposited on the tube face is called in this case) cannot be used

in television. This is because, firstly, the crystals of potassium chloride take some time in recovering their transparency, the image persists for too long a time, and fast-moving objects appear smeared. Secondly, the image has insufficient contrast. Far better results have to date been obtained in light-modulator systems which operate by modulating the luminous flux as the surface of a thin

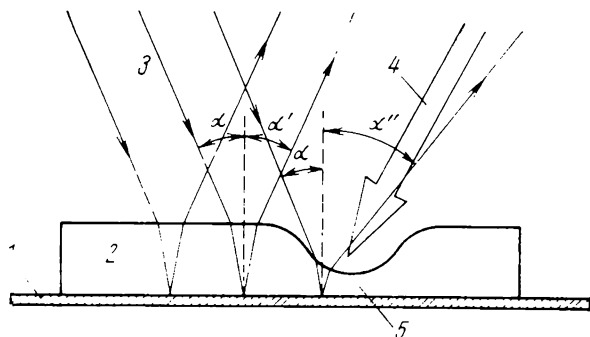


Fig. 13.8. Oil film deformed by the electron beam in a light-modulation television system

1—metal mirror; 2—oil film; 3—light rays; 4—electron beam; 5—deformation (ripple) on oil surface

layer of transparent oil is deformed by the electron beam. Systems of this type in operation both in the Soviet Union and abroad can produce black-and-white and colour pictures on a screen up to 100 square metres in area.

An idea about how an electron beam deforms the surface of oil can be gleaned from Fig. 13.8. A thin coat of oily fluid, 2, is applied to a metal mirror surface, 1. The light 3, coming from an external source and falling on the smooth surface of the fluid at an angle α is reflected from the fluid at an angle α' . Deflection coils cause the electron beam, 4, to graze and deform the surface of the fluid. The amount of deformation, 5, depends on the beam current. The light rays reflected from the mirror and passing twice through the deformed surface of the fluid emerge from this fluid at different angles α'' , determined by the amount of deformation at a given surface element.

Figure 13.9a shows how the deformation of a liquid surface is utilized in a mirror-and-slit projection television system. The light modulator is enclosed in an evacuated glass envelope. A thin coat, 1, of oil possessing the necessary mechanical and electrical properties is applied to the surface of a concave spherical mirror, 2. An electron gun, 3, produces an electron beam, 4, scanned horizontally and vertically by a deflection yoke, 5. In front of the window, 6, is placed a slit system 7 made up of mirror strips *a*, *b*, *c*,

..., arranged to make an angle of $\varphi = 45^\circ$ with the axis AB of the tube. The arrangement of the mirror slits is shown more clearly in Fig. 13.9b. The slits lie in the plane CD passing through the centre of curvature of the mirror, E .

Light rays from the source, 9, fall on mirror strips a, b, c, \dots , are reflected from them, strike the smooth surface of the oil, are

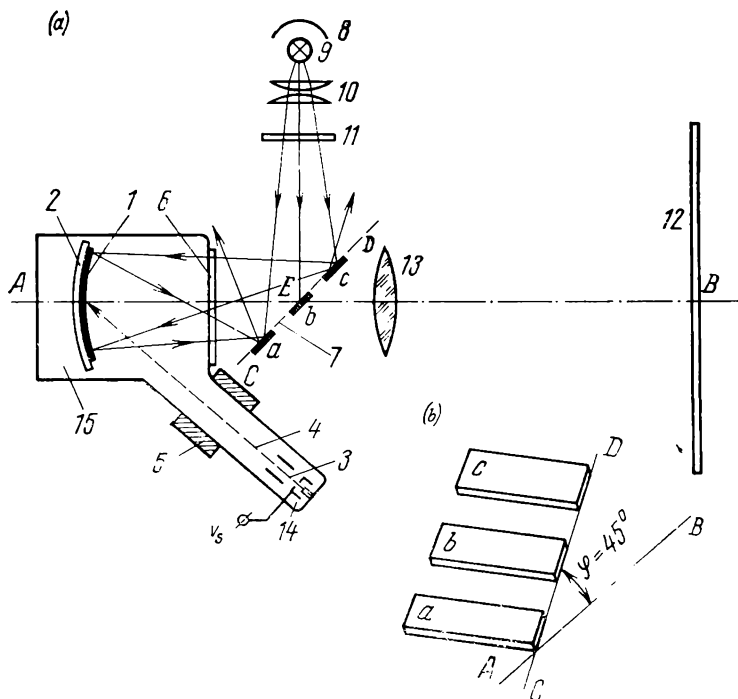


Fig. 13.9. ARISTON light-modulating large-screen television system
(a) overall arrangement; (b) mirror-slit system; 1—oil film; 2—spherical mirror; 3—electron gun; 4—electron beam; 5—deflection yoke; 6—tube faceplate; 7—mirror-slit system; 8—reflector; 9—light source; 10—condenser; 11—heat shield; 12—large screen; 13—projection lens; 14—control electrode

reflected towards and from the mirror slits again, and travel in the direction of the light source.

Thus, the slits and the spherical mirror are arranged so that the rays reflected from the mirror, 2, are not allowed to pass to the screen, 12, as long as the oil surface remains undeformed.

In the mirror-and-slit system being examined, light is produced by an illuminant which consists of a spherical reflector, 8, a high-power xenon lamp, 9, a condenser lens, 10, and a heat shield, 11, which blocks the passage of rays in the long-wave part of the light

spectrum, capable of heating the oil, 1, and evaporating it at a high rate.

When the electron beam, 4, deforms the surface of the oil, 1 (by producing tiny ripples on it) at some point, the rays of light passing through that point are displaced from their original position and are able to pass between the mirror slits towards the screen, 12. Collected by a lens, 13, these rays produce a luminous spot on the screen. The brightness of the spot is proportional to the amount of deformation in the oil film.

The amount of deformation in the oil film is controlled by the beam current which is in turn controlled by the television signal applied to the modulator, 14, of the electron gun, 3. Thus, as the electron beam is scanned, a latent intermediate image is formed on the oil surface. The light rays displaced from their original position by these deformations pass through the mirror slits, 7, and produce a bright television picture on the screen, 12. On making an "opening" for light in the oil film at a point corresponding to a picture element, the electron beam moves on, and the "opening" keeps passing light until the end of one picture period. This sort of "persistence" considerably enhancing the total luminous flux reaching the viewing screen is obtained through an appropriate choice of oil viscosity (density).

In the Soviet Union, the mirror-and-slit principle examined above has been embodied in the *Ariston* projection television system. It can produce sufficiently bright pictures on screens up to 100 m² in area.

Despite the high quality of the picture, the television projectors using oil as the light modulator suffer from serious drawbacks, both technological and operational. For one thing, the oil film enclosed in the evacuated envelope gradually evaporates, and one has to maintain vacuum by continually pumping the envelope as long as the tube is in operation, using a high-capacity vacuum pump. For another, because oil continually evaporates from the surface of the spherical mirror, 2, some means must be provided to restore the oil film during operation. For this purpose, the projector contains an oil reservoir and a mechanical system applying oil to the slowly rotating spherical mirror.

13.4. Laser Television Projectors

Special promise as regards large-scale television is held out by CW lasers. A laser generates a narrow, highly directional beam of high intensity. When efficient devices are developed to deflect and modulate it, the laser beam will be able to replace the electron beam used in picture tubes. This replacement will bring with it the following advantages. Firstly, the light beam and screen need

not be enclosed in an evacuated envelope. Secondly, the screen size will not be limited by that of the envelope (as is the case with conventional picture tubes). Thirdly, no phosphor need be applied to the viewing screen.

A laser television projector may be installed in any room, and the light beam will scan a screen differing but little from a motion-picture screen under the action of deflection systems. In block-diagram form, a laser colour-television projector is shown in Fig. 13.10. Three lasers, 1, 2 and 3, generate a red (R), a green (G) and

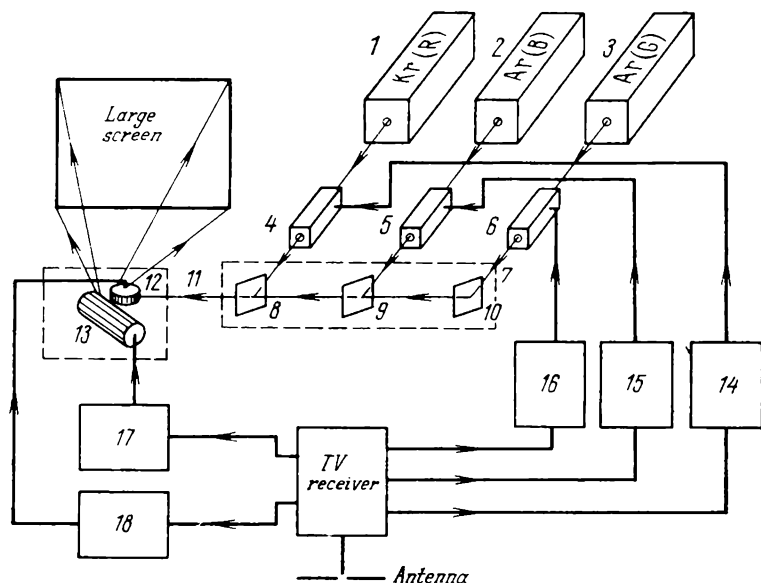


Fig. 13.10. Block diagram of a laser television projector

1, 2, 3—lasers; 4, 5, 6—laser-beam modulators; 7—light-beam mixer; 8, 9, 10—mirrors, 11—combined light beam; 12—line-scan mirror drum; 13—frame-scan mirror drum; 14, 15, 16—video amplifiers; 17, 18—mirror-drum mechanical synchronizer

a blue (B) beam. These beams are passed through the respective optical modulators, 4, 5 and 6, where they are intensity-modulated by video signals and combined in a mixer, 7, consisting of two dichroic mirrors, 8 and 9, and an ordinary mirror, 10, into a composite beam, 11.

The light beam is scanned by two rotating mirror drums, 12, horizontally, and 13 vertically. The video signals are applied to the optical modulators from amplifiers, 14, 15 and 16, which boost the signal to a peak-to-peak value of 500 to 700 V essential to the normal operation of the modulators. The vertical and horizontal

sync pulses are fed to devices 17 and 18 which control the rpm and phase of the scanning motors.

In comparison with the television projector using an oil modulator, the laser system is simpler in design and can produce images of higher resolution and sharpness. The laser beam is very small in diameter (1.5 to 3 mm), has a very small angular spread (1 to 1.5 minutes of arc), and shows an extremely high brightness ($B_{laser} = 10^{13}$ to 10^{15} candelas per square metre). The high brightness of the laser beam goes a long way towards producing a large and bright picture on the viewing screen.

Of the three gas lasers in the system under consideration, two use argon and the third uses krypton as the laser medium. In the argon lasers, the bulk of the radiation energy is divided between two wavelengths, blue ($\lambda_B = 488$ nm) and green ($\lambda_G = 515$ nm). The krypton laser mainly emits red ($\lambda_R = 647$ nm). Like the tricolour shadow-mask picture tube, the laser projector can reproduce black-and-white images as well.

The television signal intensity-modulates the laser beam on the basis of the Pockels effect which consists in the following. If a voltage is applied by means of two electrodes to a cubic crystal of, say, potassium dihydrogen phosphate (usually referred to as KDP), the plane-polarized rays passing through it will rotate their plane of polarization. The operation of the Pockels effect modulator is illustrated in Fig. 13.11a. The laser beam, 1, as it passes through a polarizer, 2 (the first Nicol prism), is polarized in a vertical plane, 3. Then the beam is passed through the modulating crystal, 4. If the voltage applied to its transparent electrodes, 5 and 6, is zero, the plane of polarization of the beam remains unchanged. Arranged at right angles to the plane of polarization of the polarizer is a second Nicol prism used as analyzer, 7. In the circumstances, the laser beam cannot pass through the analyzer. When a voltage is applied to the modulating crystal (electrodes 5 and 6), the plane of polarization of the laser beam in the modulating crystal is rotated through an angle ψ proportional to the applied voltage. The field intensity vector H of the laser beam after the rotation of its plane of polarization comes by a component, H' , which passes through the analyzer (Fig. 13.11b).

The manner in which the intensity of the light beam at the output from the electro-optical modulator depends on the applied voltage is shown in the plot of Fig. 13.11c. The appreciable non-linearity of this modulation characteristic has to be corrected by suitably predistorting the amplitude response of the video amplifiers.

The optical line scanner is the most complicated element of a laser television system. The electromagnetic and electrostatic deflection used to deflect the electron beam are useless in a laser sys-

tem. Electro-optical and ultrasonic deflection methods are still in the experimental stage. Therefore, the laser beam deflectors mostly used at present are rotating multi-sided mirror drums.

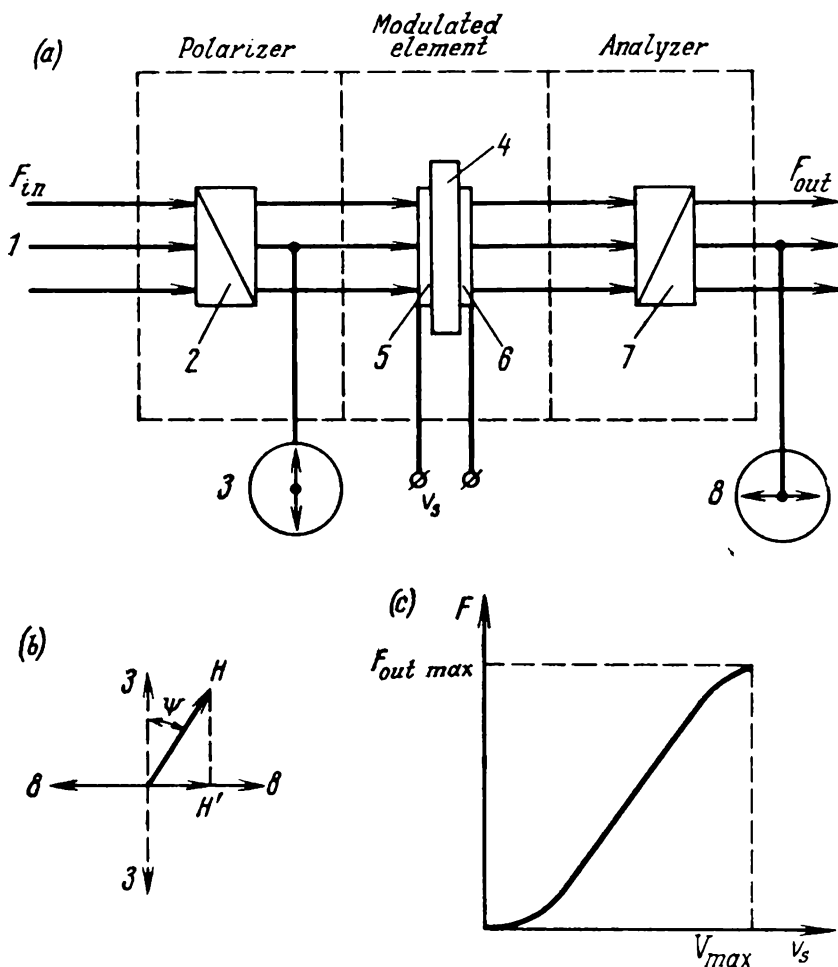


Fig. 13.11. Laser-beam modulator

(p) block diagram: 1—laser beam; 2—polarizer; 3—vertical polarization; 4—modulating crystal; 5, 6—modulating-crystal electrodes; 7—analyzer; 8—horizontal polarization; (b) chasor diagram of the laser modulator; (c) amplitude characteristic of the laser modulator

Each drum is mounted on the shaft of a synchronous motor and, in rotating, deflects the laser beam. According to the USSR standard, a 25-sided line scanner should run at 37,500 rpm to give a

line scan rate of 15,625 lines per second. An essential requirement for the line scanner, in addition to the high rotational speed, is speed stability.

To meet this requirement, the motor uses gas-lubricated bearings. Also, to maintain horizontal synchronization, suitable servos automatically control the phase of the motor.

The optical frame scanner, likewise using a rotating mirror drum, operates at a much slower speed, or frame scan rate, and entails no particular difficulties in realization.

CHAPTER FOURTEEN

INDUSTRIAL-INSTITUTIONAL TELEVISION

14.1. Tasks and Special Features of IIT

In the early days of television the primary objective was to build a broadcast television system capable of producing a high-quality picture on many millions of home TV receivers. Although industry was not slow in realizing the promise television held out as a means of measurement, monitoring, process control and similar applications, the state of the art was still insufficient to do these jobs. In the first place, pickup tubes were not sensitive and small enough for use in industrial and institutional television (IIT). Nor was the associated television apparatus suitable for uses other than TV broadcasts.

IIT made a rapid advance after the second world war, with the advent of new types of camera tubes, such as the image orthicon, the vidicon, etc. Today, IIT is gaining ever wider ground in science and technology. Several examples of the uses to which IIT is put follow.

Space exploration. Today we can hardly imagine a space probe carrying no television equipment. Television has proved indispensable as a means of keeping watch on the behaviour and condition of astronauts, visual examination of terrain at the destination, steering and handling of space vehicles. Space science owes a good deal of its advances to specialized TV systems.

Nuclear research. Contact with radioactive substances for scientific or technological purposes is fraught with danger to the health of personnel. This danger can be, and is, completely removed through the use of closed-circuit television (CCT). With it, processes in a nuclear reactor can safely be followed from a safe distance. When ganged up with manipulators, 3-D and colour closed-circuit systems extend, as it were, the reach of man's hands, and radioactive substances can be accurately handled under visual control from a safe distance.

Industrial quality control. Quite a number of factories use closed-circuit TV units to inspect their products for dimensions, configuration, structural flaws (such as blow holes in steel plate and sheet), etc. A very important feature of this form of quality control is that the inspector need not have direct contact with workpieces. In gauging the thickness of wire or sheet, no measuring tool has to

be applied to stop or delay the production process. The pickup tube of a closed-circuit television camera "looks" at the workpiece, and the video signal that it generates is then utilized for process control, actuating an alarm, or applying a corrective action.

Process control. Using a closed-circuit TV unit, a production process can readily be controlled visually from a central control room. TV supervision may be applied to assembly lines, sorting of railway cars on shunting yards, etc.

Educational television. Today television has become a widely used aid in teaching. Many TV centres broadcast educational programs on various subjects to a great number of TV viewers. These programs are conducted by highly qualified experts on the humanities, the life sciences, engineering disciplines, and foreign languages.

Also, there is a great number of specialized closed-circuit TV systems. At medical clinics, for example, they use large screens to demonstrate delicate surgical operations to numerous audiences of medical students and physicians (Fig. 14.1). These demonstrations are especially valuable because no operating room is large enough to accommodate many spectators.

TV-equipped class and lecture rooms have become a regular feature at many educational establishments (Fig. 14.2). A TV screen and a light pen have replaced the traditional blackboard and chalk. The lecturer displays the illustrative material (charts, equations, photographs, parts, etc.) in the sequence of his choosing by means of a TV camera, and the students can see them on the monitors conveniently disposed in the room and make their notes. The number of uses for closed-circuit TV might be multiplied, by reference to biology, medicine, astronomy, warfare, etc.

In most cases, a CCT system is not just a copy of a conventional TV broadcasting equipment as regards circuitry, parameters and design. The conditions under which CCT operates, the objects and scenes to be televised, the requirements for small size and light weight, enhanced reliability and ability to operate on a round-the-clock basis alleviate some specifications and make more stringent others.

In some cases, it will be enough to use a reduced resolution (for example, in a video telephone system where a closeup of the conversing parties is reproduced on the screen), and a reduced number of tonal gradations (as in the transmission of instrument dials, drawings, etc.). On the other hand, it is often required that a CCT camera be water or air tight (if it is to be used under water or in outer space) or heat-resistant (when it is used to watch a metal-making process).

In some cases, a colour CCT unit is required. In the above example of a surgical operation, the black-and-white picture would be

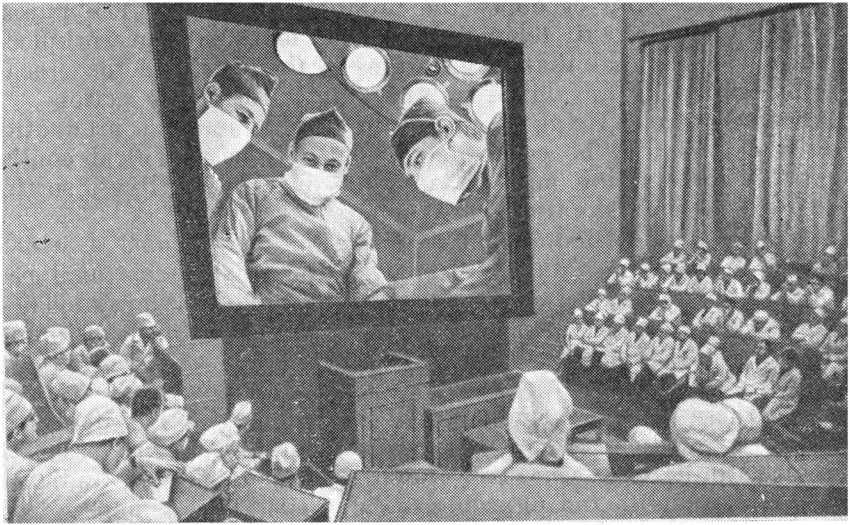


Fig. 14.1. Surgical operation demonstrated on a large TV screen

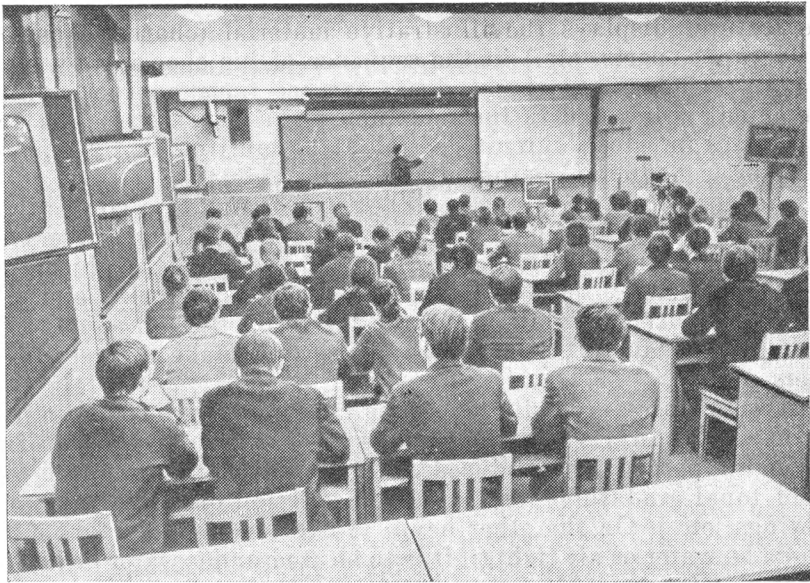


Fig. 14.2. TV-equipped lecture-room

fficult to make out, while a colour picture distinctly shows the d blood, the pink lungs, the blue-violet liver, etc.

Thus, in designing a CCT unit, one must consider the conditions under which it is to be used, as this may lead to a less expensive design and more lenient requirements for electrical and other characteristics.

The differences in electrical and functional parameters between closed-circuit and broadcast TV systems may be stated as follows: the number of scanning lines may be reduced in order to make use of a narrower frequency spectrum for the television signal and specify less stringent requirements for the communication link; the number of scanning lines may be increased so as to improve resolution;

a different aspect ratio may be used (for example, in a video telephone it is more convenient to have a picture height exceeding its width);

interlaced scanning may be abandoned so as to simplify the synchronizing circuits.

However, designers of quantity-produced CCT units often do not know where their products are to be used and how. In such cases, universal or standard CCT units are turned out, capable of handling a wide range of jobs.

In the Soviet Union, a considerable number of CCT types are available. Some of them meet the requirements of the USSR broadcast TV standard. This is done in order that use may be made of standard circuits, assemblies and units (such as camera and picture tubes, transformers, deflection coils, scan generators, and power units) whose manufacture has been well established. Also, such CCT systems may use ordinary TV receivers as picture monitors.

Functionally, closed-circuit and broadcast systems differ in a very important respect. In broadcast television, the bulk of programming apparatus (such as sync generators, signal correctors, video amplifiers, test equipment) is concentrated at the transmitting end (at a TV centre). The TV receiver is made functionally as simple as practicable. The viewer is not able technically to affect the performance of the equipment at the TV centre. Why this is so is clear—the average viewer has no technical training that would enable him to control a TV transmitter or camera intelligently. Also, the TV viewers are millions.

In a CCT system, the bulk of apparatus, including a picture monitor, is at the receiving end. Now the transmitting equipment consisting mainly of a pickup tube and an optical system is built into a light-weight, small-size camera of simple design, which needs no specialist attendance during operation. The camera is controlled (which includes focusing, supply of power and sawtooth currents for the deflection system, and main amplification of the

video signal) from the place where the picture monitor is set up. In fact, the same man who uses the monitor for his duties can at the same time operate and control the whole of the CCT system. The simple and light-weight camera can readily be installed under water, in a drill hole, in a missile, on a mast within a marshalling yard, or at a railway terminal.

The reason why industrial/institutional TV systems are also called "closed-circuit" is this. The television signals are not broadcast, but are transmitted over a closed circuit and received only

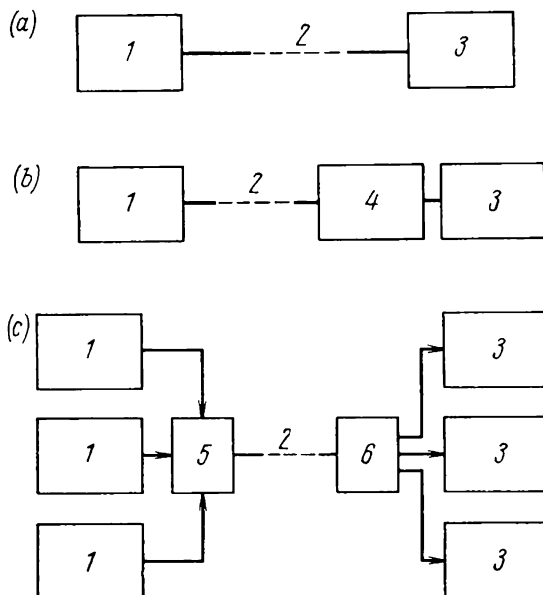


Fig. 14.3. Block diagrams of several CCT systems

(a) simple single-channel CCT without remote camera control; (b) single-channel dispatcher's CCT remotely controlled from a control unit at the video monitor; (c) multichannel dispatcher's CCT; 1—camera; 2—multicore cable; 3—video monitor; 4—channel unit; 5—switch; 6—switch

by a limited number of interconnected receivers. When the camera and the CCT receiver are connected by wires (by a special cable), the closed circuit is provided directly by the cable. Where use is made of a radio link, it is important to minimize interference with TV broadcasts. This is usually done, firstly, by reducing the level of the transmitted signal and, secondly, by suppressing the carrier modulated by the video signal; it may be supplied to the receiver over cable.

Soviet-made general-purpose CCT units are arranged as shown in the block diagram of Fig. 14.3. The camera tubes are the image

orthicon and the vidicon. An image orthicon CCT camera has ten times the sensitivity of a vidicon camera. In other words, given the same signal-to-noise ratio, the illumination of the scene for an image orthicon camera may be one-tenth of that for a vidicon camera (assuming that both cameras use similar lenses).

An example of a simple and inexpensive Soviet-made CCT system is the ИТТ-26 which is made up of a simplified vidicon camera

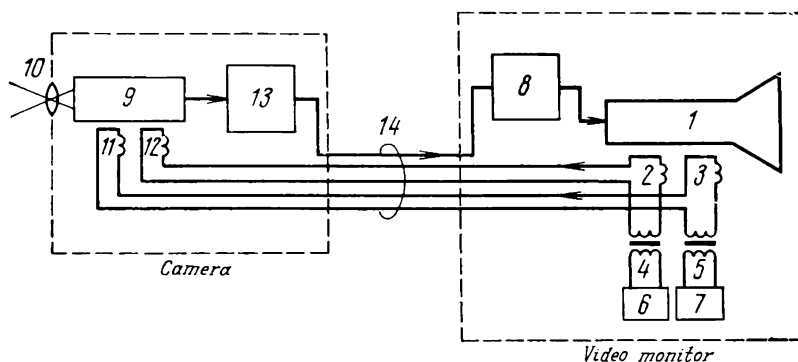


Fig. 14.4. Power supply for the deflection yoke of the camera tube from picture-tube scan generators

1—picture tube; 2—vertical deflection coils of picture tube; 3—horizontal deflection coils of picture tube; 4—vertical output transformer; 5—horizontal output transformer; 6—vertical scan generator; 7—horizontal scan generator; 8—video amplifier; 9—camera tube (vidicon); 10—lens; 11—horizontal deflection coils of vidicon; 12—vertical deflection coils of vidicon; 13—preamplifier; 14—multiconductor connecting cable

built into a dust and water proof case, a picture monitor, and a multiconductor connecting cable. The system is simple to operate and requires no skilled attendants. The ИТТ-26 has no controls for remote adjustment (from the monitor) of camera position, lens focus, etc. The camera is positioned as required before use, the lens is focused by hand, and these settings remain undisturbed in operation.

The circuitry of the ИТТ-26 has been simplified by omission of a separate scanning generator from the camera. The deflection coils of the vidicon are series-connected with those of the picture tube (Fig. 14.4). As a corollary, there is no need for a synchronizing generator. The ИТТ-26 uses progressive scanning at 50 frames/s and 300 lines per frame. The system is primarily intended for use in the metal-making, cement and other industries under arduous environmental conditions.

Another Soviet-made CCT system is the ИТТ-101 using an image orthicon. A block diagram of this system is shown in Fig. 14.5. This system operates by the USSR broadcast TV standard, that

is, 625 lines, 25 frames/s, and interlaced scanning. Therefore, its monitor may well be an ordinary TV receiver.

The camera 2 has been simplified to the utmost. In fact, it only houses the pickup tube, the focusing and deflection system, the optical head, and the preamplifier. The remaining elements ordinarily built into broadcast TV cameras are transferred into a camera control unit, 3, which may be set up at a distance of up to 25 m from the camera. The camera control unit houses the video

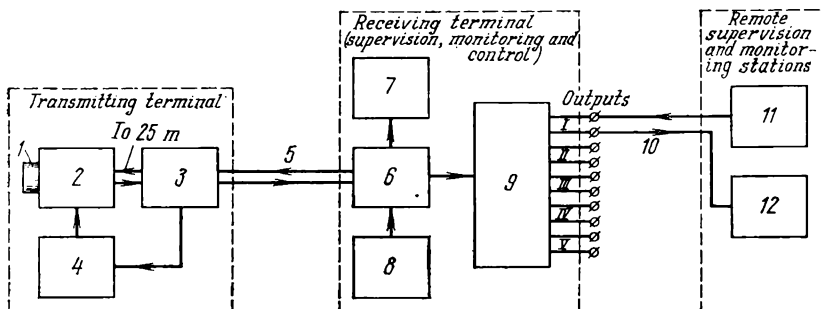


Fig. 14.5. Block diagram of PTV-101 industrial television system

1—lens; 2—camera; 3—camera control unit; 4—pan-tilt control; 5—main multiconductor cable up to 1000 m long; 6—channel unit; 7—video monitor; 8—control panel; 9—switch; 10—two-conductor cable, up to 1000 m long; 11—TV receiver; 12—remote control panel

amplifier and line scanning generator of the pickup tube. Control signals for the turret also come from the camera control unit 4.

After amplification, the video signal is channelled over a special cable (which may be up to 1 km long) to the channel section, 6, of the receiving equipment. The channel unit incorporates a synchronizing generator which supplies horizontal and vertical sync pulses, a television-signal final amplifier-shaper, and a VHF transmitter (tuned to operate on the 1st or 2nd broadcast channel) to relay television signals over special cables to conventional TV receivers. These receivers (as many as five sets) may be up to one kilometre distant from the channelling unit. The latter also houses the frame scanning generator of the image orthicon tube used in the camera. The generator supplies a saw-tooth current which is fed via the camera control unit to the vertical deflection coils of the camera tube.

The main picture monitor, 7, is set up close to the control console, 8. The control console enables the operator to make adjustments on the camera, the camera lens (its diaphragm and focus), and also to pan and tilt the camera.

The remote monitors, 11, enable up to five more persons to watch the scene being televised. The 1st or 2nd channel carrier modulated by the video signal is fanned out via a distributor-switcher, 9, and over cables to the antenna jacks of the remote monitors. It is possible to set up, next to each monitor, a control console, 12, from which the system can be controlled remotely (including adjustment of operating conditions, lens diaphragm and focus, pan and tilt motions).

14.2. Advantages of 3-D Television

Man sees the world around him in three dimensions. The perception of depth between objects and of the objects themselves as three-dimensional forms enables man to find his way in space.

For a long time, however, man had had to be content with two-dimensional pictures, until advances in engineering, photography, motion pictures and television made it possible to reproduce images in three dimensions, or stereoscopically. Apart from its artistic value, 3-D television can find uses in science, industry and warfare.

Among the tasks that can be handled more easily with 3-D television are remote control of moving objects (such as space craft at the time of approach and docking, manipulators handling radioactive substances, etc.), watch of the Earth's and other planets' surface from space vehicles, artillery fire control, and navigation.

14.3. Stereoscopic Effect

Normal vision is binocular, that is, with two eyes. It involves a number of factors such as perception of form, depth and distance, to name but a few.

In binocular vision, the retina of each eye forms an image of the object viewed. The two images merge into one in the mind. For this to happen, it is essential that the two images of a point fall on compare points on the retinas (compare points are those which are removed for the same distance and in the same direction from the fovea centralis). Each eye gets a slightly different view of the same object. When we close the left eye, the object appears to move to the left (that is, the right eye sees more of the right-hand surface of the object); when we close the right eye, the object appears to move to the right (that is, the left eye sees more of the left-hand surface of the object).

When the two images do not fall on compare points, we see two images. They will be perceived as a double image if the distance

between the excited points on the retinas are considerable. If the distance is small, we perceive both form and depth.

In viewing distant objects, the optic axes of the left and right eyes run practically parallel to each other (Fig. 14.6a). The distance, l , between the axes is called the interocular or interpupilar distance. It ranges from 52 to 76 mm in different persons, being 64 mm on the average. As the object being viewed approaches (or the observer approaches it, which is the same), the eyes turn involuntarily

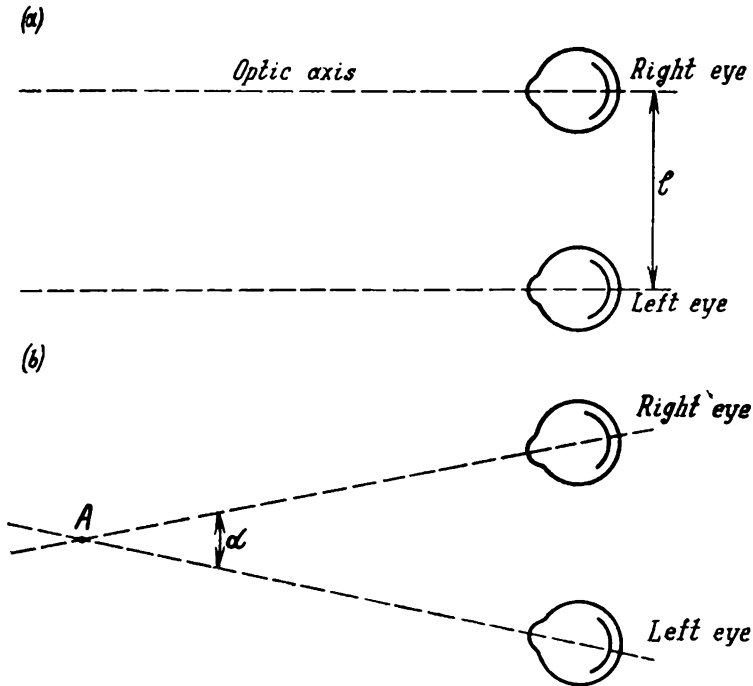


Fig. 14.6. Position of an observer's eyes
(a) looking at a distant object; (b) looking at a near object

so that the optic axes intersect on the object at an angle α (Fig. 14.6b), called the convergence angle. For each object there is a different convergence angle. Distance judgement is formed due to the difference in the effort the eye muscles apply in order to change the convergence angle. Depth perception, or stereoscopic vision, depends at least in part on the fact that each eye sees the same object a little differently. Suppose that the observer fixes his eyes on point A of a three-dimensional object, G (Fig. 14.7). Then the axes of sight passing through the centres of rotation of the eyeballs,

O_1 and O_2 , will intersect at point A . Images of the point will form at points a' and a'' , which are the centres of the macula lutea (the yellow spot) of the eyes where the acuity of vision is maximum.

In this position of the axes of sight, the image of point B at a viewing distance L will be formed at points b' and b'' on the retinas. It is seen from Fig. 14.7 that $a'b' = a''b''$, and points b' and b'' are displaced from points a' and a'' by the same amount. Thus, points A and B are projected on comparable points of the retinas.

Assuming that the axes of sight remain in the previous position, a projection of point C onto the retina of the right eye (point c') will coincide with point a' , and its projection on the retina of the left eye will coincide with point b' . It is an easy matter to show that

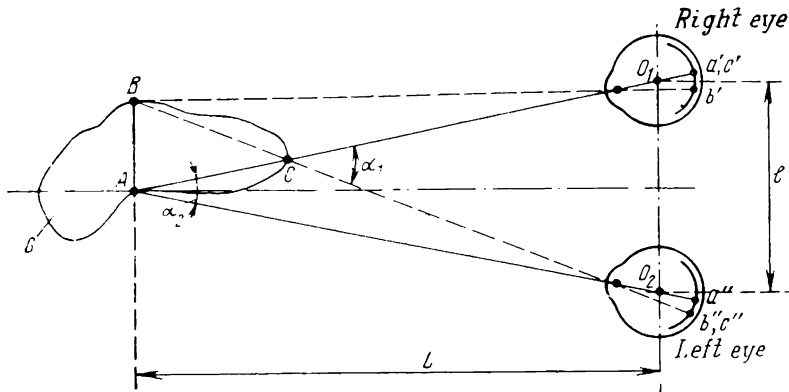


Fig. 14.7. Angular and linear parallax

point C is projected onto disparate (that is, unlike) points on the retina. This is so because point c' is coincident with point a' and it falls at the centre of the macula lutea in the right eye ($a' - c' = 0$). Point c'' is coincident with b'' , that is, it falls at a distance $a'' - c''$ from the centre of the macula lutea. Thus, $a' - c' \neq a'' - c''$, and this difference gives rise to depth perception, or stereoscopic vision. The disparateness of a pair of points may be expressed as the difference between segments $a'c'$ and $a''c''$, or as the difference of angles $\alpha_1 - \alpha_2$. The angle α_1 whose vertex lies at point C is called the parallax angle.

For points A and B the parallax angle is equal to the convergence angle, α_2 . The minimum value of $\Delta\alpha = \alpha_1 - \alpha_2$ at which depth perception is possible is called the threshold of depth vision. Its average value is $\Delta\alpha = 10''$ to $20''$.

14.4. Basic Arrangement of a Stereoscopic Television System

In order to reproduce TV pictures in three dimensions, a number of requirements should be satisfied. These requirements are:

1. Two images must be transmitted from two different positions so that some "interocular" distance is obtained.
2. The images transmitted should be reproduced so that they can separately be viewed by the right and left eye.

A simplified block diagram of a stereoscopic television system is shown in Fig. 14.8. The pickup tubes onto which images are projected by two lenses are spaced a distance l apart. The distance l is the "interocular" distance. After amplification, the video signals are sent into communication lines. In the general case, two communication lines would be needed. After amplification at the receiving end, the signals are reproduced on a stereo monitor which

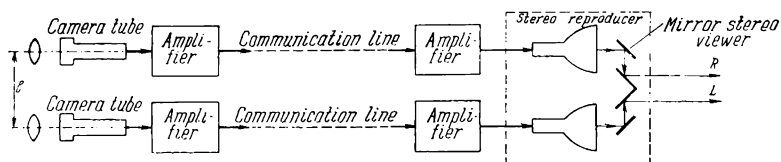


Fig. 14.8. Simplified block diagram of a stereo television system

has two picture tubes each reproducing the right-hand and left-hand images of the stereoscopic pair, respectively. A mirror stereoscope may be used to separate the images so that one will be visible to only the left eye and the other to only the right eye. The path of optical rays in a mirror stereoscope is shown in Fig. 14.8. As is seen, a double complement of equipment is required in order to transmit and reproduce 3-D pictures. A stereoscopic camera can be built up from the elements of a conventional black-and-white camera.

A mirror stereoscope as the reproducer suffers from a serious limitation—it can only be used by one person at a time. Therefore, this arrangement can only be useful in CCT systems where a single observer is often enough, such as in supervising the operation of nuclear manipulators, cranes, walking excavators, and the like.

Where 3-D pictures are to be shown to a group audience, use should be made of different reproducers. Figure 14.9 shows a stereo-monitor in which stereoscopic pairs are separated by a sheet or film polarizer. One form of film polarizers, known under the proprietary name of "Polaroid", consists of a multiplicity of micros-

copic crystals embedded in a gelatine substrate. The crystals which are a colloidal compound of iodine and quinine show a specific orientation of optic axes which make all crystals behave as a single entity. For their polarization effect the crystals used in film polarizers depend on the difference in the absorption of the ordinary and extraordinary rays.

A stereoscopic pair is separated as follows. Two cross-plane polarizers (or, simply, cross-polarizers), P_1 and P_2 , are placed in front of the picture tubes, 1 and 2. There is a semitransparent mirror, 3, to match the two images. The combined image is viewed by means of spectacles made from the same polarizer film. In the spectacles, the polarizer, P'_1 , for the left eye has its plane of polarization parallel to that of polarizer P_1 , while the plane of polarization of the polarizer P'_2 is parallel to that of the polarizer P_2 . Owing to this arrangement, the left eye sees the image reproduced on picture tube 2, and the right eye on picture tube 1. Image separation by polarizers is very convenient. A disadvantage of this method is that a

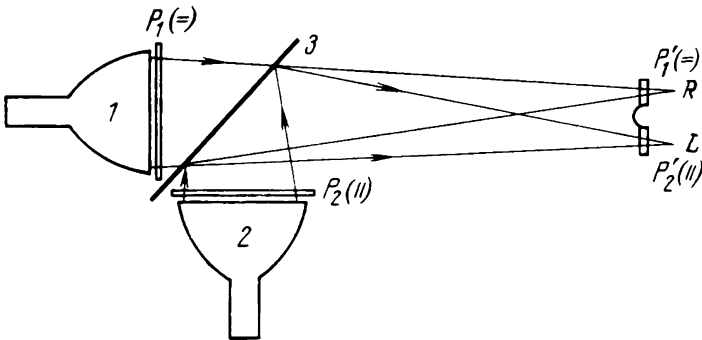


Fig. 14.9. Stereo viewer using film polarizers

good deal of light is lost in the film polarizers and also that the planes of polarization of the spectacles and of the respective polarizers in front of the picture tubes must be set precisely parallel. Because of the latter requirement, the viewer may tilt his head within only a very limited angle.

Stereo viewers based on the colour separation of stereoscopic pairs are built along similar lines. In this case, say, a red filter is placed in front of picture tube 1 (see Fig. 14.9) instead of a film polarizer, and a blue filter in front of picture tube 2. The two images are viewed through coloured spectacles made from a red and a blue filter so that the left eye sees through the blue filter and the right eye through the red filter. Light filters of two complementary colours enable the viewer to see the two components of a stereoscopic

pair separately. This happens as follows. Light from picture tube 1, on passing through the red filter installed in front of the picture tube and the red filter of the spectacles, can only be seen by the right eye. Blue light from picture tube 2 is fully cut out by red filter 1 and fails to reach the right eye. Similarly, the left eye sees the left-hand component of the stereoscopic pair in blue colour. The image as a whole is seen in black-and-white because the two colours seen by the right and left eyes are the complements of each other. In this case, binocular mixing of colours takes place. By the laws of colour mixing and matching, when the two complements are mixed in an appropriate proportion, their mixture is sensed as white.

14.5. Transmission of 3-D Television Signals over Communication Lines

As follows from Fig. 14.9, two communication channels are required to transmit 3-D television signals, because two cameras generate these signals. However, the use of two communication channels may be warranted only where a 3-D television picture is to be transmitted for a short distance over cable, as often is the case with closed-circuit systems.

Where long distances are involved, frequency interleaving or band sharing should preferably be used. Frequency interleaving

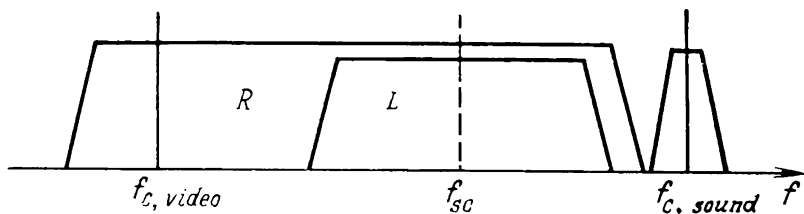


Fig. 14.10. Band-sharing by stereo signals

and band sharing for the transmission of 3-D TV signals is based on the fact that the signals representing the left-and right-hand images are practically identical and only differ in parallax. Experiments have shown that picture quality will suffer no degradation if the frequency spectrum of one of the stereoscopic components is reduced to 1 MHz, provided the other component is transmitted within the complete bandwidth of 6.5 MHz. The quality of the picture perceived visually will be that of the best of the two frames of the stereoscopic pair.

If one of the two images in a stereoscopic pair be transmitted within a reduced frequency band, use may be made of frequency

interleaving employed in colour television. The frequency spectrum for a stereoscopic image transmitted over a standard television channel is shown in Fig. 14.10. The video carrier is amplitude-modulated by the signal representing the right-hand image of the stereoscopic pair. The signal representing the left-hand image is transmitted within a reduced bandwidth and is modulated onto a subcarrier, f_{sc} . The subcarrier is an odd multiple of half the line frequency to secure proper frequency interleaving. In the USSR standard, the subcarrier may be equal to 4.3 MHz, that is, the same as for colour television. A major advantage of frequency interleaving is that a stereoscopic picture can be picked up by an ordinary TV receiver (in two dimensions, of course).

INDEX

- Aberration, spherical, 33
- Accommodation, 22
- Alignment, picture size and aspect, 379
- Amplifier-limiter, 154
- Amplitude separator, 165
- Analyzer, 14
- Aperture angle, 35
- Aperture compensation, 263
 - differentiating, 265
- Aperture corrector, delay line, 267
 - differentiating, 267
- Aperture distortion, 58
- Astigmatism, 33

- Band-sharing, colour-signal, 342
- Bandwidth of fine detail, 339
- Beam, high-velocity, 198
 - low-velocity, 197
- Beam convergence control, 335
- Beam deflection, 79
 - frame, 79
 - line, 79
- Beam defocusing, 79
- Beam focusing, 60
 - electromagnetic, 67
 - electrostatic, 61
- Beam lateral control, 336
- Beam lateral magnets, 335
- Beam modulation, 71
- Blanking pulses, frame, 138
 - line, 138
- Blocking oscillator, 121

- Camera, flying-spot, 186
- Camera tubes, 181
 - basic characteristics, 181
 - low-velocity-beam, 210
 - nonstorage, 185
 - storage type, 189
- Charge image, 16
- Chromaticity, 312
- Chromaticity coordinates, relative, 319
- Chrominance signals, 346
- CIE, 315
- CIE colour triangle, 317-8
- CIE primaries, 315
- CIE trichromatic coefficients, 316
- Cine camera, 277
- Closed-circuit television, 406, 410
 - Soviet equipment, 410
- Coder, PAL, 376
 - SECAM, 362
- Colorimetry, basic, 306
- Colour, attributes of, 312
- Colour-difference signals, 345
- Colour display, simultaneous, 323
- Colour identification circuit, 366
- Colour matching, 308
- Colour picture tubes, 330
 - shadow-mask, 330
- Colour purity control, 333
- Colour signal band-sharing, 342
- Colour television, 306
 - colour bar chart for, 389
 - compatible systems, 323
 - NTSC compatible system, 306, 347
 - block diagram, 351
 - receiving terminal, 352
 - PAL system, 306, 373
 - SECAM system, 306, 354
 - basic parameters, 357
 - sequential systems, 323
 - simultaneous systems, 326
- Colour triangle, 309
- Coma, 33
- Commission Internationale de l'Eclairage, 315
- Compatibility of television systems, 337
- Control room, 238
- Convergence, dynamic, 334
 - static, 334
- D.c. component, spectrum of, 135

- D.c. restoration, 257
D.c. restorer, gated, 262
 keyed, 262
 simple, 260
Decoder, PAL, 376
 SECAM, 362
Definition of television picture, 49
Deflection yoke, construction, 85
 electromagnetic, 81
Delay line, 371
Dichromic mirror, 328
Diffuser, ideal, 30
 perfect, 30
Dioptr, 32
Distortion, 33
 keystone, 205
Distribution coefficients, 319
Dynamic convergence magnets, 334

Einstein's law, 182
Electron gun, 15, 65
Equalizing pulses, 144
Equilibrium potential on insulated target, 194

F-number, reciprocal, 36
Flicker, 37
Flicker effect, 37
Flicker frequency, 36
Flip-flop, 148
Focal length, 31
Focal power, 31
Focus, virtual, 31
Fusion frequency, 36

Gamma correction, 270
Gamma corrector, 274
Gamma exponent, 270
Guard bands, 328

Halation, 75
Horizontal output stage, 98
Hue, 312
Human eye, 20

I-signal, 353-4
Iconoscope, 199
 light-transfer characteristic, 203-04
Illuminants, standard, 319
Illumination, 21, 24
Image-detail visibility, 50
Image dissector, 186
Image iconoscope, 207
 internal arrangement of, 207
Image orthicon, 216
Industrial-institutional television, 406
Insulated target, equilibrium potential of, 194
Interlaced scanning, 41
Ion spot, 89

Lambert's cosine law, 29
Lenses, aberrations of, 32
 aperture angle of, 35
 basic properties of, 30
Lenses, aberrations of
 multi-element, 34
 reciprocal f-number of, 36
 reciprocal relative aperture of, 36
 speed of, 35, 36
Line-by-line switch, 366, 370
Luminance, 24, 28, 312
Luminance signal, 336
Luminosity, relative, 24
Luminous efficiency, relative, 24
Luminous flux, 24, 25
Luminous intensity, 24, 26

Magnetic heads for television tape recording, 287
Matrix circuit, 338
Modulation, synchronous quadratic, 348
Modulator, synchronous quadratic, 352
Monoscope, 233
Multivibrator, single-shot, 153

Nipkow disc, 11, 186
Noise compensation, 249
NTSC compatible colour television system, 347

Operation, high-velocity-beam, 198
 low-velocity-beam, 197
Optics, 21
Output stage, horizontal, 98
 vertical, 114
 tube, 114

PAL coder, 376

- PAL colour television system, 373
 PAL decoder, 376
 Phosphors, persistence of, 77
 spectral emission characteristics of, 77
 Photocathodes, 15
 integral sensitivity of, 184
 spectral response of, 183
 Photoemission, 182
 Photometric quantities, 24
 Photometric units, 24
 Photometry, 21
 Picture contrast, 45
 factors affecting, 74
 Picture definition, 49
 Picture luminance, 43
 Picture resolution, factors affecting, 56
 Picture tubes, 59
 colour, 330
 construction, 59
 Plumbicon, 231
 Predistortion, 358
 Preemphasis, 358
 Preemphasiser, 359
 Pull-down, fast, 278
 Pulse shaper, 152

 Q-signal, 353-4

 Reciprocal f-number, 36
 Reciprocal relative aperture, 36
 Resolving power, 49

 Saturation, 312
 Sawtooth generator, 110
 Scanner, electronic, 15
 receiving, 14
 transmitting, 14
 Scanning, 10
 interlaced, 41
 electronic, 15
 Scanning generators, 92
 horizontal, 92
 transistor, 113
 synchronization of, 156
 vertical, 92, 113
 transistor, 126
 SECAM coder, 362
 SECAM colour television system, 354
 SECAM decoder, 362
 Secondary emission multiplier, 186
 Secondary emission ratio, 195
 Separation, horizontal from vertical
 sync pulses, 168
 Separation, sync pulses from video, 161
 Serrations, 142
 Shading effect, 205
 compensation, 205
 Shadow mask, 331
 Sharpness, 50
 Signal spectrum, SECAM-IIIB system, 362
 Static convergence magnets, 334
 Stoletov's law, 182
 Sweep driver, line, 110
 vertical, 118
 Sync signal generator, 144
 master oscillator of, 147
 pulse shaper of, 152
 timing system of, 144
 Synchronization, impulsive, 156, 159
 inertia-type, 175
 phase-lock, 174-5
 Synchronizing signal generator (see sync signal generator)
 Synchronous quadratic modulation, 348
 Synthesizer, 14

 Talbot law, 43
 Tape transport in video, tape recorder, 292
 Television, 3-D
 analysis and synthesis of information in, 9
 brief history of, 18-20
 closed circuit, 406, 410
 colour, 306
 definition, 9
 industrial-institutional, 406
 principles of, 10
 USSR standard, 17
 Television alignment procedures, 378
 Television broadcasting, 234
 Television cameras, 242
 Television film equipment, 246
 Television picture, 10
 Television recording, 275
 magnetic, 279
 longitudinal, 285
 transverse, 285
 optical, 276
 Television signal, spectrum of, 138
 r.f. spectrum for, 137
 Television spectrum, 128
 line structure of, 131
 Television system, electronic, 16
 block diagram of, 16
 parallel, 11

- satellite, 303
- sequential, 11
- cable relay, 297
- colour, 306
- compatible, 323
- large-screen, 392
 - laser, 394, 401-05
 - light-modulator, 394, 398-401
 - projection, 393
 - projection-tube, 395
 - spherical-mirror, 393
- radio relay, 296
- relay, 296
- Television system, electronic
 - satellite relay, 304
 - stereoscopic, 415-18
- Television tape recorder, design, 286
 - magnetic heads for, 287
- Television tests, 378
- Test signal, stair-step, 387
- Testing, amplitude linearity in video channel, 381
 - amplitude response, 382
 - colour bar chart, 389
 - frequency response, 382
 - interlaced scan, 381
 - low-frequency response, 381
 - luminance gradations, 381
 - picture resolution, 380
 - scan nonlinearity, 380
 - picture size and aspect, 379
 - transient response, 384
- Tonal gradations, 46
- Tracks, arrangement on video tape, 294
- Trichromatic coefficients, 312
- Tristimulus values, 308
- TV satellites, 303
- TV studio, 237
- Vertical oscillator, 122
- Video signal, amplification in TV camera, 249
 - generation in storage system, 194
 - standard waveform of, 138
- Video tape, arrangement of tracks on, 294
- Video tape recorder, head assembly and concave guide of, 293
 - tape transport, 292
- Vidicon, 224
 - aperture characteristic, 230
- Vision, 21
 - three-colour theory of, 307
- Weber-Fechner law, 48
- Weber's fraction, 47
- Weber's law, 47

TO THE READER

Mir Publishers would be grateful for your comments on the content, translation, and design of this book. We would also be pleased to receive any other suggestions you may wish to make.

Our address is: Mir Publishers, 2, Pervy Rizhsky Pereulok, 129820, Moscow I-110. GSP, USSR.

Printed in the Union of Soviet Socialist Republics

Professor V.F. Samoylov, D. Sc. (Tech.), is head of the chair of television at the Moscow Electrical Engineering Institute. Has been on the faculty staff in various capacities for 30 years. Has written over ten books (including monographs, texts and study aids) on television, some of which have been translated into European languages. Actively contributes to technical journals.

Professor B. P. Khromoy, Doctor of Technical Sciences, is with the Moscow Electrical Engineering Institute. Has been teaching for 14 years. Has written six books (a text, study aids and monographs) on television. Writes in technical journals.

This book presents a systematic and step-by-step approach to the theory and practice of television and associated equipment and includes separate sections on vision, photometry, and colorimetry. The subject-matter covers a wide range of circuits used in black-and-white, colour, large-screen and closed-circuit television. Ample space is devoted to the organization of TV centres, studios, and satellite links.

Intended as a text for college students, the book will undoubtedly be of value to practical engineers and technicians concerned with television.

